frontiers | Research Topics

Critical care cardiology for cardiovascular emergencies

Edited by
Keita Saku and Takahiro Nakashima

Published in
Frontiers in Cardiovascular Medicine

ISSN 1664-8714
ISBN 978-2-8325-6798-2
DOI 10.3389/978-2-8325-6798-2

Generative AI statement
Any alternative text (Alt text) provided alongside figures in the articles in this ebook has been generated by Frontiers with the support of artificial intelligence and reasonable efforts have been made to ensure accuracy, including review by the authors wherever possible. If you identify any issues, please contact us.

About Frontiers

Frontiers is more than just an open access publisher of scholarly articles: it is a pioneering approach to the world of academia, radically improving the way scholarly research is managed. The grand vision of Frontiers is a world where all people have an equal opportunity to seek, share and generate knowledge. Frontiers provides immediate and permanent online open access to all its publications, but this alone is not enough to realize our grand goals.

Frontiers journal series

The Frontiers journal series is a multi-tier and interdisciplinary set of open-access, online journals, promising a paradigm shift from the current review, selection and dissemination processes in academic publishing. All Frontiers journals are driven by researchers for researchers; therefore, they constitute a service to the scholarly community. At the same time, the *Frontiers journal series* operates on a revolutionary invention, the tiered publishing system, initially addressing specific communities of scholars, and gradually climbing up to broader public understanding, thus serving the interests of the lay society, too.

Dedication to quality

Each Frontiers article is a landmark of the highest quality, thanks to genuinely collaborative interactions between authors and review editors, who include some of the world's best academicians. Research must be certified by peers before entering a stream of knowledge that may eventually reach the public - and shape society; therefore, Frontiers only applies the most rigorous and unbiased reviews. Frontiers revolutionizes research publishing by freely delivering the most outstanding research, evaluated with no bias from both the academic and social point of view. By applying the most advanced information technologies, Frontiers is catapulting scholarly publishing into a new generation.

What are Frontiers Research Topics?

Frontiers Research Topics are very popular trademarks of the *Frontiers journals series*: they are collections of at least ten articles, all centered on a particular subject. With their unique mix of varied contributions from Original Research to Review Articles, Frontiers Research Topics unify the most influential researchers, the latest key findings and historical advances in a hot research area.

Find out more on how to host your own Frontiers Research Topic or contribute to one as an author by contacting the Frontiers editorial office: frontiersin.org/about/contact

Critical care cardiology for cardiovascular emergencies

Topic editors

Keita Saku — National Cerebral and Cardiovascular Center, Japan

Takahiro Nakashima — University of Michigan, United States

Citation

Saku, K., Nakashima, T., eds. (2025). *Critical care cardiology for cardiovascular emergencies*. Lausanne: Frontiers Media SA. doi: 10.3389/978-2-8325-6798-2

Table of contents

frontiers | Frontiers in Cardiovascular Medicine

TYPE Editorial
PUBLISHED 14 August 2025
DOI 10.3389/fcvm.2025.1668820

OPEN ACCESS

EDITED AND REVIEWED BY
Fabio Guarracino,
Azienda Ospedaliero Universitaria Pisana, Italy

*CORRESPONDENCE
Takahiro Nakashima
✉ n-takahiro@hotmail.co.jp

RECEIVED 18 July 2025
ACCEPTED 05 August 2025
PUBLISHED 14 August 2025

CITATION
Nakashima T and Saku K (2025) Editorial: Critical care cardiology for cardiovascular emergencies.
Front. Cardiovasc. Med. 12:1668820.
doi: 10.3389/fcvm.2025.1668820

Editorial: Critical care cardiology for cardiovascular emergencies

Takahiro Nakashima[1,2]* and Keita Saku[3]

[1]Department of Emergency Medicine and the Harry Max Weil Institute for Critical Care Research and Innovation, University of Michigan, Ann Arbor, MI, United States, [2]Department of Cardiovascular Medicine, Graduate School of Medical Sciences, Kumamoto University, Kumamoto, Japan, [3]Department of Cardiovascular Dynamics, National Cerebral and Cardiovascular Center, Suita, Japan

KEYWORDS

critical care cardiology, veno-arterial extracorporeal membrane oxygenation (V-A ECMO), intra-aortic balloon pump (IABP), microaxial flow-pumps, left ventricular assist device (LVAD), mechanical circulatory support (MCS)

Editorial on the Research Topic
Critical care cardiology for cardiovascular emergencies

In recent years, substantial evidence regarding cardiogenic shock and mechanical circulatory support (MCS) has been accumulated in the field of Critical Care Cardiology, contributing to the development of this emerging subspecialty (1). The patient population in cardiac care units (CCUs) has become increasingly complex and critically ill, raising concerns about whether these units can continue to manage high-acuity patients in the absence of intensivists (2). The necessity of critical care cardiologists has been acknowledged for over two decades. However, expert consensus statements on cardiogenic shock have only recently been published by professional societies in Europe, North America, and Japan (3–5). Given the heterogeneity of cardiogenic shock, which encompasses a variety of underlying etiologies, establishing it as a distinct academic field and generating robust evidence has remained a significant challenge. This special issue presents 18 contributions in the realm of critical care cardiology, including 9 original research articles, 3 reviews, 4 case reports, 1 brief research report, and 1 perspective piece (URL: https://www.frontiersin.org/research-topics/65741/critical-care-cardiology-for-cardiovascular-emergencies).

The growing use of LV-unloading devices has heightened the demand for noninvasive methods to assess left ventricular (LV) workload. Sato et al. evaluated the utility of the pressure-strain product (PSP), derived from echocardiographic strain and blood pressure, for estimating pressure-volume (PV) loop-based LV stroke work (LVSW) in a large animal model with a left ventricular assist device (LVAD). PSP demonstrated the strongest correlation with PV loop-derived LVSW, outperforming other parameters such as Echo-derived LV end-diastolic volume, Echo-LVSW, peak LV pressure, and global circumferential strain. Furthermore, PSP significantly correlated with LV myocardial oxygen consumption, pressure-volume area, coronary sinus oxygen saturation, and coronary vascular resistance. Although further clinical studies are warranted, PSP holds promise as a noninvasive biomarker for myocardial metabolic monitoring.

Right heart failure (RHF) following LVAD implantation remains a major clinical concern due to complex hemodynamic interactions that complicate its management. Nonaka et al. provided a comprehensive review of the current understanding of RHF

pathophysiology and evaluated existing predictive models for RHF after LVAD placement. The authors' discussion of current knowledge gaps is particularly valuable for improving future RHF management strategies. This review is expected to deepen readers' comprehension of RHF mechanisms.

With the increasing use of MCS, bedside explantation techniques are gaining attention. Xu et al. investigated the feasibility of a novel area-reduction post-closure technique for bedside explantation of veno-arterial extracorporeal membrane oxygenation (V-A ECMO). In their retrospective analysis of 18 patients, the procedure achieved a 100% technical success rate. The authors detailed the method, which notably included the use of an 8 Fr sheath to facilitate the deployment of the first Proglide device—an innovative and immediately applicable technique for clinical practice.

The 2025 ACC/AHA guidelines for acute coronary syndrome give a Class III recommendation against the routine use of intra-aortic balloon pump (IABP) in patients with myocardial infarction complicated by cardiogenic shock. However, the role of IABP remains controversial. Ota et al. presented an intriguing case highlighting the potential importance of aortic compliance in determining IABP efficacy. Their case involved an elderly patient with severe aortic stenosis and pneumonia who developed refractory cardiogenic shock and experienced a dramatic hemodynamic improvement following IABP insertion.

The use of MCS devices such as V-A ECMO and transvalvular micro-axial flow pumps (mAFP) significantly complicates brain death determination and organ donation procedures. Raimann and Willems addressed this challenging issue in patients receiving combined V-A ECMO and tMAFP support.

This issue also includes several additional studies offering valuable insights for clinicians engaged in critical care cardiology. We hope that critical care cardiologists worldwide will take the opportunity to explore these important contributions. As CCUs in developed countries evolve into cardiac intensive care units (CICUs), we are witnessing the dawn of the Critical Care Cardiology era. We look forward to continued advancements in the field, the generation of high-quality evidence, and, ultimately, improved outcomes for critically ill cardiovascular patients.

Author contributions

TN: Supervision, Writing – original draft, Writing – review & editing. KS: Writing – review & editing.

Conflict of interest

KS is a co-author of the papers by Sato et al. and Ota et al. cited in this editorial.

The remaining author declares that the research was conducted in the absence of any commercial or financial relationships that could be construed as a potential conflict of interest.

Generative AI statement

The author(s) declare that no Generative AI was used in the creation of this manuscript.

Any alternative text (alt text) provided alongside figures in this article has been generated by Frontiers with the support of artificial intelligence and reasonable efforts have been made to ensure accuracy, including review by the authors wherever possible. If you identify any issues, please contact us.

Publisher's note

References

1. Sinha SS, Geller BJ, Katz JN, Arslanian-Engoren C, Barnett CF, Bohula EA, et al. Evolution of critical care cardiology: an update on structure, care delivery, training, and research paradigms: a scientific statement from the American Heart Association. *Circulation.* (2025) 151:e687–707. doi: 10.1161/CIR.0000000000001300

2. Katz JN, Turer AT, Becker RC. Cardiology and the critical care crisis: a perspective. *J Am Coll Cardiol.* (2007) 49:1279–82. doi: 10.1016/j.jacc.2006.11.036

3. Møller JE, Sionis A, Aissaoui N, Ariza A, Bělohlávek J, De Backer D, et al. Step by step daily management of short-term mechanical circulatory support for cardiogenic shock in adults in the intensive cardiac care unit: a clinical consensus statement of the association for acute CardioVascular care of the European Society of Cardiology SC, the European society of intensive care medicine, the European branch of the extracorporeal life support organization, and the European association for cardio-thoracic surgery. *Eur Heart J Acute Cardiovasc Care.* (2023) 12:475–85. doi: 10.1093/ehjacc/zuad064

4. Sinha SS, Morrow DA, Kapur NK, Kataria R, Roswell RO. 2025 concise clinical guidance: an ACC expert consensus statement on the evaluation and management of cardiogenic shock: a report of the American College of Cardiology Solution Set Oversight Committee. *J Am Coll Cardiol.* (2025) 85:1618–41. doi: 10.1016/j.jacc.2025.02.018

5. Nakashima T, Kondo T, Nakata J, Saku K, Kawakami S, Kuwabara M, et al. Expert consensus statement on the evaluation, treatment, and transfer of cardiogenic shock using a Delphi method approach - a report of the Japan Critical Care Cardiology Committee (J4CS). *Circ J.* (2025) 89:998–1011. doi: 10.1253/circj.CJ-25-0192

frontiers | Frontiers in Cardiovascular Medicine

TYPE Original Research
PUBLISHED 18 November 2024
DOI 10.3389/fcvm.2024.1486697

OPEN ACCESS

EDITED BY
Keita Saku,
National Cerebral and Cardiovascular Center, Japan

REVIEWED BY
Yasunori Suematsu,
Fukuoka University Hospital, Japan
Cao Wenzhai,
Zigong First People's Hospital, China

*CORRESPONDENCE
Ying Liu
✉ liuyingwhu@126.com

RECEIVED 26 August 2024
ACCEPTED 23 October 2024
PUBLISHED 18 November 2024

CITATION
Liu Y (2024) Association between lactate/albumin ratio and 28-day mortality in ICU critical patients with coronary heart disease: a retrospective analysis of the MIMIC-IV database.
Front. Cardiovasc. Med. 11:1486697.
doi: 10.3389/fcvm.2024.1486697

Association between lactate/albumin ratio and 28-day mortality in ICU critical patients with coronary heart disease: a retrospective analysis of the MIMIC-IV database

Ying Liu[1,2,3]*

[1]Department of Radiology, The First Affiliated Hospital, Jiangxi Medical College, Nanchang University, Nanchang, Jiangxi, China, [2]Jiangxi Province Medical Imaging Research Institute, Nanchang, Jiangxi, China, [3]Clinical Research Center for Medical Imaging, Nanchang, Jiangxi, China

Background: The serum lactate/albumin ratio (LAR) is commonly employed for monitoring and evaluating the prognosis of critically ill patients. Both elevated lactate levels and decreased albumin levels may reflect the body's stress response and inflammatory reaction. Coronary heart disease (CHD), with common complications including myocardial infarction, arrhythmia, heart failure, is one of the leading causes of global death. Therefore, it is crucial to explore biomarkers that can predict the prognosis and mortality of CHD patients.
Methods: This is a retrospective study in which the data is from the MIMIC-IV database. Our study assessed the association between LAR value and mortality within 28 days of admission in a total of 1,902 CHD patients from the Beth Israel Deaconess Medical Center.
Results: The results demonstrated a significant increase in 28-day mortality among individuals with higher LAR values. Multivariate analysis by Cox proportional hazard model revealed an incremental rise in mortality across each quartile with the increase of LAR value. Furthermore, restricted cubic spline (RCS) Cox regression analysis further revealed that higher LAR values were associated with increased 28-day mortality in the CHD patients. And subgroup analysis confirmed that the LAR level could serve as an independent predictor of 28-day mortality with CHD patients.
Conclusions: Our study demonstrated that the LAR value can be an important risk predictor of 28-day mortality in patients with CHD, and a higher LAR associate with increased mortality rate.

KEYWORDS

lactate/albumin ratio, biomarker, coronary heart disease, 28-day mortality, MIMIC-IV database

1 Introduction

Coronary heart disease (CHD) is one of the most common cardiovascular diseases worldwide, particularly in developed countries and some developing countries where its incidence is relatively high. Additionally, CHD is one of the leading causes of global death (1, 2). According to the World Health Organization, over 17 million people die each year from cardiovascular diseases (including CHD) (3). Acute myocardial

infarction, arrhythmias, heart failure, and thrombosis resulting from CHD are major cause of death (4). Therefore, given the high incidence and mortality rates associated with CHD, it holds immense significance to explore biomarkers capable of predicting prognosis or mortality among hospitalized CHD patients.

Lactate is a product of cellular metabolism, particularly in hypoxic conditions. Elevated lactate levels typically indicate tissue hypoxia or hemodynamic disturbances, such as those seen in sepsis, shock, or heart failure (5). Serum albumin is a protein synthesized by the liver and is abundant in blood. It has antioxidant and anti-inflammatory properties, and primarily functions to maintain plasma colloid osmotic pressure, transport various substances such as hormones, fatty acids, and drugs. Low serum albumin levels (<3.5 g/dl) are often associated with poor prognosis, which may suggest malnutrition, chronic disease, acute inflammation or impaired liver function. Studies have revealed that low albumin levels are correlated with higher mortality rates, longer hospital stays, and increased complication rates (6–8). Serum albumin level is considered an important prognostic biomarker for ICU patients (9).

The serum lactate/albumin ratio (LAR) is a clinical indicator used to evaluate status of the patients, particularly those of critically ill patients. A higher ratio typically indicates a poorer prognosis. During acute illness or post-trauma, elevated lactate levels and decreased albumin levels may reflect the body's stress and inflammatory responses. The ratio combines information of both lactate and albumin levels, providing a more comprehensive evaluation of the patient's status (10).

Our study evaluated the relationship between the LAR level and 28-day mortality in CHD patients, and revealed that higher LAR levels associate with higher mortality rates. Therefore, LAR can serve as an independent predictor of higher 28-day mortality in CHD patients.

2 Methods

2.1 Data source

This is a retrospective study, data from the MIMIC-IV database (version 2.2). This database covers information on all patients admitted to the Beth Israel Deaconess Medical Center (BIDMC) during the years from 2008 to 2019, which includes comprehensive information on patients' hospital stay, laboratory tests, medication treatments, vital signs, and so no. To protect patient privacy, all personal information has been de-identified and replaced with random codes. Therefore, obtaining patients' informed consent or ethical approval was not necessary for this study. The MIMIC-IV (v.2.2) database can be downloaded from the online platform PhysioNet (https://physionet.org/content/mimiciv/2.2/). In order to gain access to this database and extract data, Ying Liu, the first author of this study, successfully completed the Collaborative Institutional Training Initiative (CITI) courses "Conflicts of Interest" and "Data or Specimens Only Research" (ID: 42343630). Consequently, we obtained the necessary qualifications for using the database and extract data.

2.2 Data selection criteria and exclusion criteria

From the MIMIC-IV database (v2.2), our analysis retrospectively included ICU patients diagnosed with CHD (the top 3 ranks) according to the International Classification of Diseases (ICD)-9 codes (410.xx–414.xx) (410.xx: Acute myocardial infarction; 411.xx: Other acute and subacute forms of ischemic heart disease; 412.xx: Old myocardial infarction; 413.xx: Angina pectoris; 414.xx: Other forms of chronic ischemic heart disease) and the ICD-10 codes (I20.x-I22.x, and I25.x) (I20.x: Angina pectoris; I21.x: Acute myocardial infarction; I22.x: Subsequent myocardial infarction; I25.x: Chronic ischemic heart disease). For patients with multiple ICU admissions, only data from the first admission were considered in our analysis. Patients meeting the following criteria will be excluded: (1) patients under 18 years old at the time of initial admission; (2) patients with multiple admissions for CHD, only data from the first admission will be retained; (3) patients with ICU stays of no more than 24 h; (4) patients with end-stage renal disease, liver cirrhosis, or malignant tumors; (5) patients without recorded blood lactate and serum albumin data within 24 h of admission (Figure 1).

2.3 Data extraction

We adopted Navicat Premium software (version 16.3.5) and used Structure Query Language (SQL) with PostgreSQL tools (v13.7.1) to extract the raw data of CHD patients within the first day after ICU admission. The data included demographic information (age, gender, race), vital signs (heart rate, SBP, DBP, temperature, respiratory rate), laboratory indicators (PH, PaO2, total CO2, total bilirubin, sodium, potassium, lactate, albumin, PTT, ALT, AST, PT, platelet, RBC, WBC), treatments (CRRT, ventilator), comorbidities (myocardial infarction, paraplegia, diabetes, rheumatic disease, congestive heart failure), and specific scores (SOFA score and GCS score).

For vital signs, laboratory tests, and specific scores that were measured multiple times during the ICU stay, we use the first measurement taken within the first 24 h of ICU admission.

2.4 Statistical analysis

Comparison of continuous variables was performed using the *t*-test or Kruskal–Wallis test, with results presented as mean ± standard deviation. Categorical variables were presented as percentages. Kaplan–Meier survival analysis was used to assess the incidence of 28-day mortality events between groups according to different levels of LAR. The hazard ratio (HR) and 95% confidence interval (CI) between LAR and primary endpoints were estimated using Cox proportional hazard models and adjusted for multiple models. Model 1 with no adjustments; Model 2 adjusted for gender, age, and race; and Model 3 adjusted for gender, age, race, pH, PaO2, total CO2, total

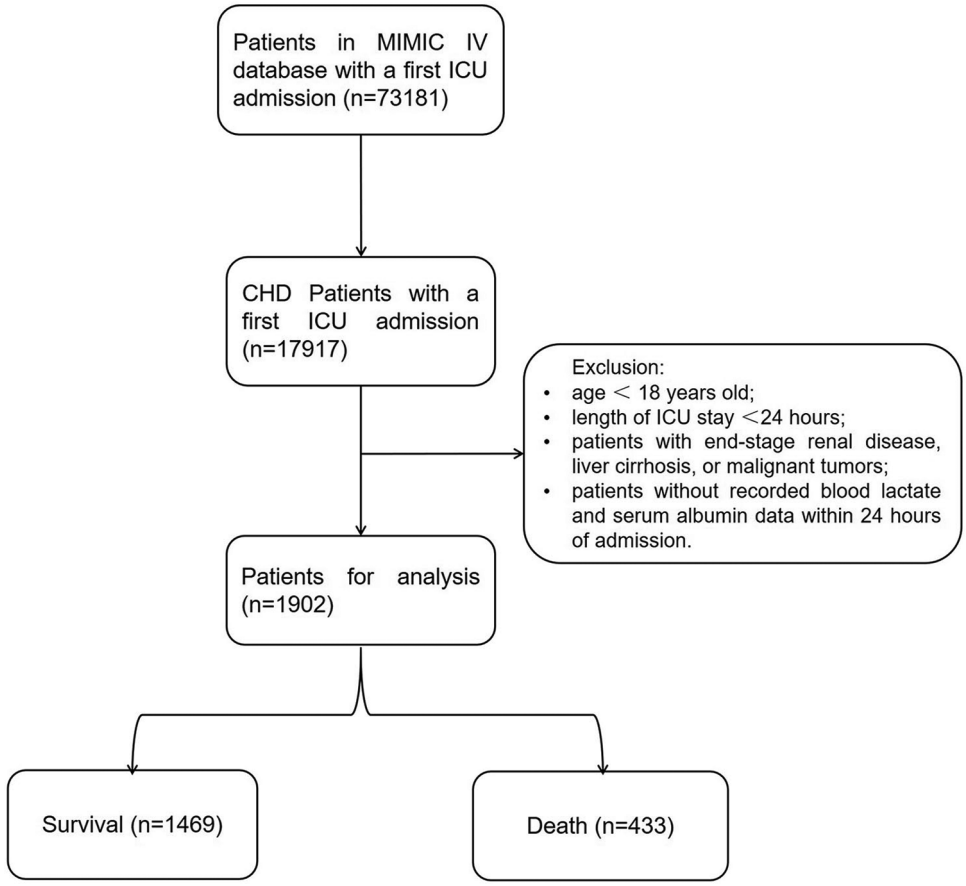

FIGURE 1
Inclusion and exclusion of patients.

bilirubin, potassium, PTT, PT, ALT, AST, RBC, WBC, heart rate, SBP, temperature, respiratory rate, SOFA, GCS, Charlson Comorbidity Index, myocardial infarction, paraplegia, rheumatic disease, and CRRT. When LAR was considered as a quartile variable, the lowest quartile was chosen as the reference group. Restricted cubic spline (RCS) Cox regression analysis was further used to determine if there was a potential non-linear relationship between LAR incidence and 28-day mortality in CHD patients, The optimal cut-off value of LAR was determined by the Youden index. Receiver Operating Characteristic (ROC) analysis was used to assess the predictive ability of Lactate, Albumin and LAR for predicting the 28-day mortality. All statistical analyses were performed using R software version 4.3.1. A two-tailed test indicating $P < 0.05$ is considered statistically significant.

3 Results

3.1 Baseline patient characteristics

A total of 1,902 patients with coronary artery disease meeting the inclusion criteria were included (1,156 females and 746 males), with an average age of 71.62 ± 13.26 years. The results showed statistically significant differences among the quartile groups (Q1–Q4) in age, PH, PaO2, total CO2, SBP, total bilirubin, potassium, lactate, albumin, PPT, PT, ALT, AST, WBC, heart rate, DBP, temperature, respiratory rate, SOFA score, GCS score, charlson comorbidity index, myocardial infarction, diabetes, CRRT, and 28-day mortality rate. Compared with the other three groups, Q4 group exhibited highest 28-day mortality rate, total bilirubin, potassium, lactate, PPT, PT, ALT, AST, WBC, heart rate, and respiratory rate. Q4 group also had higher prevalence of myocardial infarction, diabetes, and increased likelihood of receiving CRRT treatment compared with other three groups. Conversely, PH, PaO2, total CO2, albumin, and SBP levels were lowest in Q4 group. Please see details in Supplementary Table S1.

3.2 Association between LAR and 28-day mortality

The Kaplan-Meier survival curve revealed that individuals with high LAR had substantially poor 28-day survival, and the 28-day survival rates of Q1 patients is the highest compared to other quartiles ($P < 0.01$). With the increase of the LAR value, the

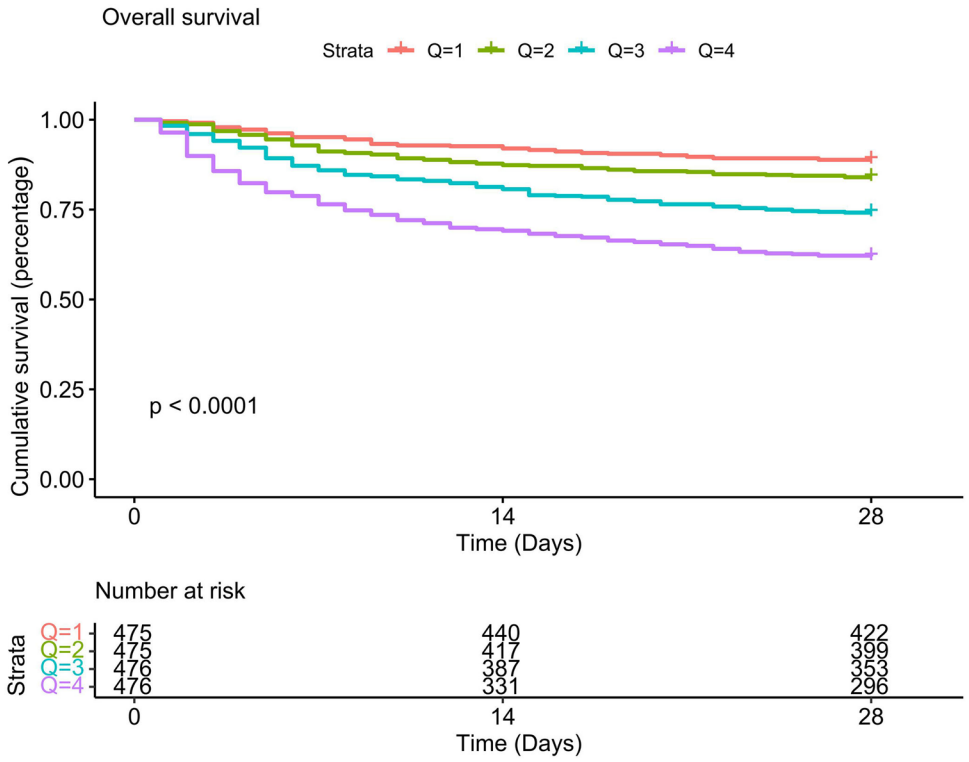

FIGURE 2
Kaplan-meier survival analysis curve for 28-day mortality.

cumulative 28-day mortality rate of each quartile decreased sequentially (see Figure 2). We further explored the association between the LAR value and 28-day mortality using multivariate Cox proportional hazards regression analyses. To minimize the impact of confounding factors, we constructed three models. In Model1, LAR was positively correlated with 28-day mortality [hazard ratio (HR) = 1.48 (95% CI: 1.39–1.58)]. When LAR was considered as a quartile variable (*P* for trend <0.001), the hazard ratio for 28-day mortality in the highest quartile (Q4) of LAR was 4.14 (95% CI: 3.05–5.63), which was significantly higher than that of Q1 ($P < 0.001$). In Models 2 and 3, we adjusted for different confounding factors (Model II adjusted for race, gender, and age; Model 3 adjusted for gender, age, race, pH, paO2, total CO2, total bilirubin, potassium, partial thromboplastin time, prothrombin time, ALT, AST, WBC, heart rate, respiratory rate, SOFA score, GCS score, Charlson comorbidity index, myocardial infarction, paraplegia, rheumatic disease, and CRRT factors), and this association between the LAR value and 28-day mortality remained the same (see Supplementary Table S2). Besides, results of single factor analysis on the difference analysis of various factors (gender, age, race, pH, paO2, total CO2, total bilirubin, potassium, partial thromboplastin time, prothrombin time, ALT, AST, WBC, heart rate, respiratory rate, SOFA score, GCS score, Charlson comorbidity index, myocardial infarction, paraplegia, rheumatic disease, and CRRT factors) between the death group and the non-death group were shown in Supplementary Table S3.

We further used restricted cubic splines to further evaluate whether there is a nonlinear relationship between LAR and 28-day mortality in CHD. We found that the relationship between LAR and 28-day mortality in coronary heart disease was approximately L type shaped (Figure 3). After adjusting for confounding factors, when LAR was higher than 0.56, the 28-day mortality in coronary heart disease increased with higher LAR value.

3.3 ROC curve analysis and prediction of mortality

ROC curves for LAR, albumin, and lactate were plotted to predict the 28-day mortality of patients with CHD (Figure 4). The results showed that the area under the curve (AUC) of LAR was 0.68 (95% CI: 0.65–0.71), which was superior to that of lactate 0.66 (95% CI: 0.64–0.69) and albumin 0.41 (95% CI: 0.38–0.44). The results showed that LAR was more effective in predicting 28-day mortality of CHD patients than albumin or lactate alone.

3.4 Subgroup analysis

Subgroup analysis was used to assess the association between LAR and 28-day mortality of CHD patients (Table 1). When

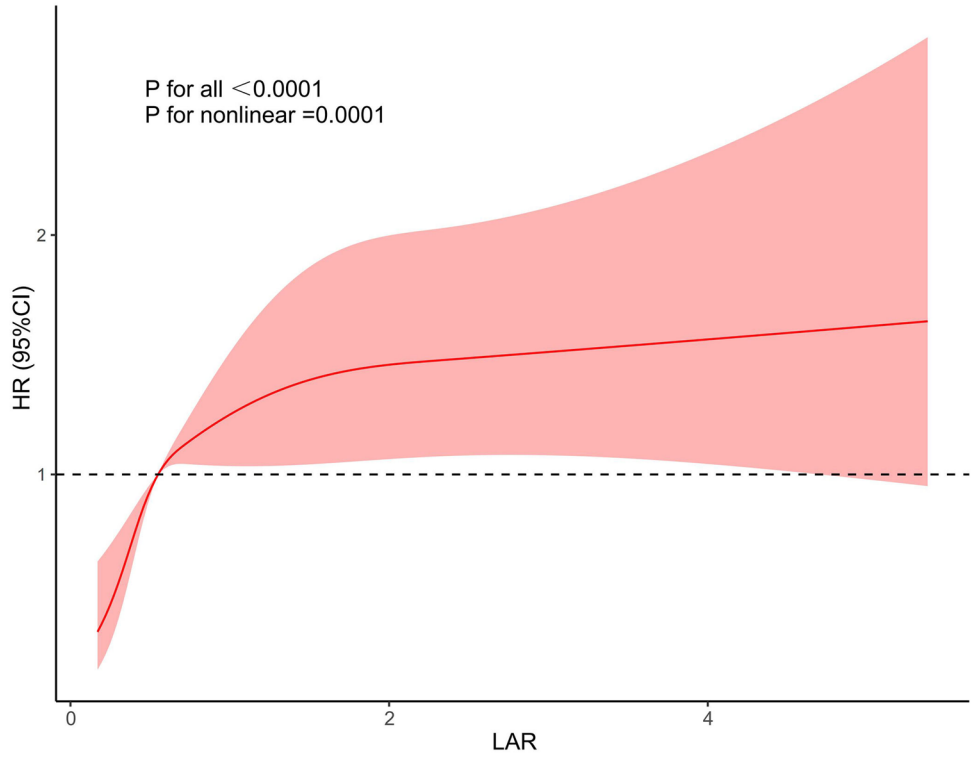

FIGURE 3
Restricted cubic spline model for association between the LAR and hazard ratio.

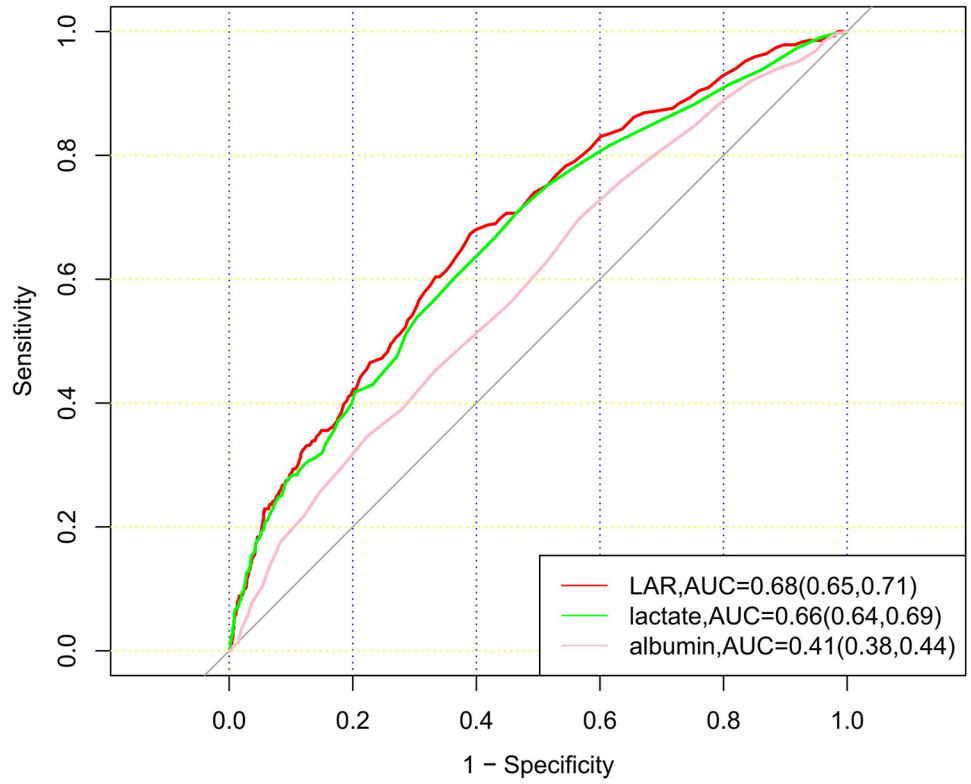

FIGURE 4
ROC curves for 3 indicators, LAR, lactate and albumin, to predict mortality.

TABLE 1 Subgroup analysis.

Variables	HR (95% CI)	*P* for interaction
Age		0.415
≥65	1.14 (1.01, 1.28)	
<65	1.21 (0.95, 1.54)	
Gender		0.346
Female	1.05 (0.91, 1.20)	
Male	1.41 (1.17, 1.70)	
Race		0.004
White	1.30 (1.12, 1.50)	
Other	1.08 (0.92, 1.28)	
Paralegia		0.25
Yes	1.14 (1.03, 1.27)	
No	6.84 (1.32, 35.46)	
Myocardial infarct		0.721
Yes	1.11 (0.90, 1.37)	
No	1.17 (1.04, 1.33)	
Rheumatic disease		0.07
Yes	2.16 (0.61, 7.67)	
No	1.14 (1.03, 1.27)	
CRRT		0.003
Yes	1.22 (0.95, 1.58)	
No	1.21 (1.06, 1.37)	

stratified for age, gender, race, paraplegia, myocardial infarct, rheumatic disease, CRRT. The results showed no significant interaction between LAR and most subgroups (*P* for interaction > 0.05). However, an interaction was observed between race and CRRT subgroups (*P* for interaction < 0.05).

4 Discussion

Our study used the publicly accessible MIMIC-IV database (v2.2) to assess the prognostic values of LAR level in patients with CHD. This retrospective analysis demonstrated a measurable association between elevated LAR levels and increased 28-day mortality in CHD patients. KM survival analysis indicated that patients with higher LAR levels had increased risk of death within 28 days of admission compared to those with lower LAR levels. The RCS curve revealed that when the LAR value exceeded 0.56, the mortality rate increased with rising LAR values. Subgroup analysis confirmed that the LAR level could serve as an independent predictor of 28-day mortality. Moreover, ROC curve analysis demonstrated that LAR had superior predictive performance for 28-day mortality compared to lactate or albumin alone.

4.1 The relationship between serum lactate, albumin, LAR and cardiovascular diseases

Lactate is a product of anaerobic metabolism, and it occurs when the body is under anoxic condition, leading to an increase in glycolysis. Elevated lactate levels reflect tissue hypoxia, metabolic disorders, and systemic inflammation, all of which are closely related to cardiovascular diseases (11, 12). Albumin is a protein synthesized by the liver, which plays a crucial role in maintaining blood osmotic pressure and transporting various substances such as fatty acids, hormones, and drugs. Albumin levels reflect nutritional status and liver function, and are also associated with inflammatory responses. Multiple studies have revealed that lactate and albumin can serve as prognostic and mortality predictors for cardiovascular diseases. Studies have found that elevated serum lactate levels and low albumin levels in patients with acute coronary syndrome (ACS) are associated with poorer outcomes, increased in-hospital and long-term mortality rates (8, 13, 14), indicating that lactate and albumin levels can serve as an effective predictor of prognosis in ACS patients. The serum lactate levels are also important prognostic indicators in heart failure patients. Heart failure patients with elevated lactate levels have a significantly increased risk of death both during hospitalization and after discharge (7, 15, 16). Besides, patients with low albumin levels have higher mortality rates during hospitalization and long-term follow-up (6, 17). In cardiac surgery, such as coronary artery bypass grafting or valve replacement, monitoring serum lactate levels help predict postoperative complications and mortality risk (18, 19). Persistent elevation of lactate levels and low albumin levels after surgery usually indicates a higher incidence of complications and poorer survival rates (19–22). The serum lactate and albumin levels in patients with cardiogenic shock are closely related to the severity of their condition and prognosis. Patients with high lactate levels generally have poorer prognosis and higher mortality rates (23, 24).

LAR reflect the metabolic load and nutritional status of patients, thereby providing a more comprehensive prognostic assessment. Numerous studies have demonstrated that LAR is more advantageous in predicting prognostic indicators such as mortality and complication rates in critical patients compared to relying solely lactate or albumin levels. High LAR values are often associated with poorer prognosis, making it a more sensitive and specific prognostic indicator (14, 25, 26). Additionally, LAR helps in better risk stratification, aiding clinicians in identifying high-risk patients for timely and targeted interventions. For patients with high LAR values, enhanced monitoring and more aggressive treatment strategies may be warranted.

LAR is an important indicator for predicting mortality in critical patients (27). It has shown good effectiveness in predicting prognosis and mortality in patients with cardiovascular diseases such as heart failure, myocardial infarction, and cardiac arrest. Studies have indicated that high LAR levels are independent risk factors for high mortality rates in patients with severe heart failure (28, 29). LAR can also predict the risk of readmission within three months for heart failure patients (30). Yang et al. (31) analyzed 2,816 hospitalized patients diagnosed with myocardial infarction and found that the LAR value was significantly higher in the death group compared to the survival group, demonstrating a significant independent predictive ability for increased all-cause mortality during hospitalization. Another study showed that the LAR ratio is significantly associated with 14-day, 28-day, and 90-day all-cause

mortality in critical AMI patients, with higher LAR being considered an independent risk factor for higher mortality in AMI patients (31). Haschemi et al. (32) demonstrated that LAR could predict 30-day survival after in-hospital cardiac arrest, with better prognostic performance for predicting 30-day survival compared to lactate or albumin alone. Additionally, LAR is significantly associated with poor prognosis in HF and CKD patients, and it may help identify HF and CKD patients with a high risk of all-cause mortality (33). Our study systematically revealed that the higher the LAR value, the higher the 28-day mortality rate with CHD patients, which will provide guidance for clinical treatment.

4.2 Mechanisms of increased LAR levels in CHD patients

CHD is often accompanied by coronary artery stenosis or obstruction, leading to decreased oxygen supply to myocardial cells. In hypoxic conditions, myocardial cells cannot produce enough energy through aerobic metabolism (oxidative phosphorylation) and instead rely on anaerobic metabolism (glycolysis) to generate energy. The end product of glycolysis is lactate, lactate accumulates and is released into the blood under ischemic conditions, leading to elevated blood lactate levels. Additionally, the ability of myocardial cells to clear lactate may also decrease, further contributing to the accumulation of lactate in the blood. Coronary artery disease patients often have endothelial dysfunction, which can reduce coronary blood flow and further decrease myocardial oxygen supply. Endothelial dysfunction may also affect lactate clearance and metabolism, which leads to increased blood lactate levels. Moreover, coronary artery disease patients often accompany with activation of the sympathetic nervous system, which increases the metabolic demand of the myocardium. When oxygen supply is insufficient, myocardial cells rely more on anaerobic metabolism, thus producing more lactate.

Liver is the main organ for synthesizing albumin. Patients with coronary artery disease may have mild to moderate liver function abnormalities, especially those with other chronic diseases (such as liver cirrhosis, hepatitis) or those using certain medications (such as statins). These factors can affect the liver's protein synthesis function, leading to reduced albumin synthesis. Furthermore, patients with coronary artery disease may have insufficient nutritional intake due to decreased appetite and gastrointestinal dysfunction, which can reduce the synthesis of plasma proteins (including albumin), leading to lower albumin levels. Coronary artery disease can also cause heart failure, which lead to hepatic congestion and renal insufficiency, thereby impacting albumin metabolism and contributing to decreased albumin levels.

Among our 1,902 CHD patients, primarily including those with myocardial infarction, ischemic heart disease, and angina, the possible mechanisms contributing to a higher LAR (lactate/albumin ratio) are as follows: In myocardial infarction and patients, insufficient blood supply to the heart prompts myocardial cells to undergo anaerobic metabolism, thus increasing lactate production. Besides, heart disease patients often accompany with renal dysfunction, which affects albumin metabolism and leads to decreased levels. During angina episodes, the temporary insufficiency of blood supply to the myocardium leads to an increase in anaerobic metabolism and a rise in lactate production. Prolonged ischemic conditions can impair the metabolic function of myocardial cells, resulting in lactate accumulation.

4.3 Study limitations

Despite significant progress in research on lactate as a prognostic and mortality predictor for cardiovascular diseases, there are still some limitations. Firstly, since the patients in our study were all admitted to the ICU, there were no stable CHD patients, which may result in our conclusions not being applicable to CHD patients in the general ward. Secondly, differences in lactate measurement methods and timing across studies may limit the comparability of results. What is more, more large-scale, multicenter prospective studies are needed to validate the predictive value of the LAR in coronary heart disease populations.

5 Conclusions

Our study demonstrated that the LAR value can be an important risk predictor of 28-day mortality in patients with CHD, and a higher LAR associate with increased mortality rate.

Data availability statement

The datasets presented in this study can be found in online repositories. The names of the repository/repositories and accession number(s) can be found below: https://physionet.org/content/mimiciv/2.2/.

Ethics statement

The studies involving humans were approved by The Institutional Review Board of the Massachusetts Institute of Technology and Beth Israel Deaconess Medical Center. The studies were conducted in accordance with the local legislation and institutional requirements. Written informed consent for participation was not required from the participants or the participants' legal guardians/next of kin in accordance with the national legislation and institutional requirements.

Author contributions

YL: Writing – original draft, Writing – review & editing.

Funding

The author(s) declare financial support was received for the research, authorship, and/or publication of this article. This study was supported by the National Natural Science Foundation of China (82201648) and the Clinical Research Center for Medical Imaging in Jiangxi Province (No. 20223BCG74001).

Conflict of interest

The author declares that the research was conducted in the absence of any commercial or financial relationships that could be construed as a potential conflict of interest.

Publisher's note

Supplementary material

The Supplementary Material for this article can be found online at: https://www.frontiersin.org/articles/10.3389/fcvm.2024.1486697/full#supplementary-material

References

1. Woodruff RC, Tong X, Khan SS, Shah NS, Jackson SL, Loustalot F, et al. Trends in cardiovascular disease mortality rates and excess deaths, 2010–2022. *Am J Prev Med*. (2024) 66:582–9. doi: 10.1016/j.amepre.2023.11.009

2. McGovern PG, Pankow JS, Shahar E, Doliszny KM, Folsom AR, Blackburn H, et al. Recent trends in acute coronary heart disease–mortality, morbidity, medical care, and risk factors. The Minnesota heart survey investigators. *N Engl J Med*. (1996) 334:884–90. doi: 10.1056/nejm199604043341403

3. Magnussen C, Ojeda FM, Leong DP, Alegre-Diaz J, Amouyel P, Aviles-Santa L, et al. Global effect of modifiable risk factors on cardiovascular disease and mortality. *N Engl J Med*. (2023) 389:1273–85. doi: 10.1056/NEJMoa2206916

4. Malakar AK, Choudhury D, Halder B, Paul P, Uddin A, Chakraborty S. A review on coronary artery disease, its risk factors, and therapeutics. *J Cell Physiol*. (2019) 234:16812–23. doi: 10.1002/jcp.28350

5. Wu Y, Ma W, Liu W, Zhang S. Lactate: a pearl dropped in the ocean-an overlooked signal molecule in physiology and pathology. *Cell Biol Int*. (2023) 47:295–307. doi: 10.1002/cbin.11975

6. Gotsman I, Shauer A, Zwas DR, Tahiroglu I, Lotan C, Keren A. Low serum albumin: a significant predictor of reduced survival in patients with chronic heart failure. *Clin Cardiol*. (2019) 42:365–72. doi: 10.1002/clc.23153

7. Ronit A, Kirkegaard-Klitbo DM, Dohlmann TL, Lundgren J, Sabin CA, Phillips AN, et al. Plasma albumin and incident cardiovascular disease: results from the CGPS and an updated meta-analysis. *Arterioscler Thromb Vasc Biol*. (2020) 40:473–82. doi: 10.1161/atvbaha.119.313681

8. Cheng CW, Lee CW, Chien SC, Yeh HI, Chen CY. Serum albumin was associated with a long term cardiovascular mortality among elderly patients with stable coronary artery disease. *Acta Cardiol Sin*. (2024) 40:87–96. doi: 10.6515/acs.202401_40(1).20230825a

9. Gremese E, Bruno D, Varriano V, Perniola S, Petricca L, Ferraccioli G. Serum albumin levels: a biomarker to be repurposed in different disease settings in clinical practice. *J Clin Med*. (2023) 12:6017. doi: 10.3390/jcm12186017

10. Gharipour A, Razavi R, Gharipour M, Mukasa D. Lactate/albumin ratio: an early prognostic marker in critically ill patients. *Am J Emerg Med*. (2020) 38:2088–95. doi: 10.1016/j.ajem.2020.06.067

11. Adeva-Andany M, López-Ojén M, Funcasta-Calderón R, Ameneiros-Rodríguez E, Donapetry-García C, Vila-Altesor M, et al. Comprehensive review on lactate metabolism in human health. *Mitochondrion*. (2014) 17:76–100. doi: 10.1016/j.mito.2014.05.007

12. Lin J, Ren J. Lactate-induced lactylation and cardiometabolic diseases: from epigenetic regulation to therapeutics. *Biochim Biophys Acta Mol Basis Dis*. (2024) 1870:167247. doi: 10.1016/j.bbadis.2024.167247

13. Kawase T, Toyofuku M, Higashihara T, Okubo Y, Takahashi L, Kagawa Y, et al. Validation of lactate level as a predictor of early mortality in acute decompensated heart failure patients who entered intensive care unit. *J Cardiol*. (2015) 65:164–70. doi: 10.1016/j.jjcc.2014.05.006

14. Zhu L, Chen M, Lin X. Serum albumin level for prediction of all-cause mortality in acute coronary syndrome patients: a meta-analysis. *Biosci Rep*. (2020) 40:BSR20190881. doi: 10.1042/bsr20190881

15. Bosso G, Mercurio V, Diab N, Pagano A, Porta G, Allegorico E, et al. Time-weighted lactate as a predictor of adverse outcome in acute heart failure. *ESC Heart Fail*. (2021) 8:539–45. doi: 10.1002/ehf2.13112

16. Chien SC, Chen CY, Lin CF, Yeh HI. Critical appraisal of the role of serum albumin in cardiovascular disease. *Biomark Res*. (2017) 5:31. doi: 10.1186/s40364-017-0111-x

17. Iskandarani E, El Kurdi B, Murtaza G, Paul TK, Refaat MM. Prognostic role of albumin level in heart failure: a systematic review and meta-analysis. *Medicine*. (2021) 100:e24785. doi: 10.1097/md.0000000000024785

18. Minton J, Sidebotham DA. Hyperlactatemia and cardiac surgery. *J Extra Corpor Technol*. (2017) 49:7–15. doi: 10.1051/ject/201749007

19. Hajjar LA, Almeida JP, Fukushima JT, Rhodes A, Vincent JL, Osawa EA, et al. High lactate levels are predictors of major complications after cardiac surgery. *J Thorac Cardiovasc Surg*. (2013) 146:455–60. doi: 10.1016/j.jtcvs.2013.02.003

20. Magovern JA, Sakert T, Magovern GJ, Benckart DH, Burkholder JA, Liebler GA, et al. A model that predicts morbidity and mortality after coronary artery bypass graft surgery. *J Am Coll Cardiol*. (1996) 28:1147–53. doi: 10.1016/s0735-1097(96)00310-5

21. Rich MW, Keller AJ, Schechtman KB, Marshall WG Jr., Kouchoukos NT. Increased complications and prolonged hospital stay in elderly cardiac surgical patients with low serum albumin. *Am J Cardiol*. (1989) 63:714–8. doi: 10.1016/0002-9149(89)90257-9

22. Xu R, Hao M, Zhou W, Liu M, Wei Y, Xu J, et al. Preoperative hypoalbuminemia in patients undergoing cardiac surgery: a meta-analysis. *Surg Today*. (2023) 53:861–72. doi: 10.1007/s00595-022-02566-9

23. Lindholm MG, Hongisto M, Lassus J, Spinar J, Parissis J, Banaszewski M, et al. Serum lactate and A relative change in lactate as predictors of mortality in patients with cardiogenic shock—results from the cardshock study. *Shock*. (2020) 53:43–9. doi: 10.1097/shk.0000000000001353

24. Schupp T, Behnes M, Rusnak J, Ruka M, Dudda J, Forner J, et al. Does albumin predict the risk of mortality in patients with cardiogenic shock? *Int J Mol Sci*. (2023) 24:7375. doi: 10.3390/ijms24087375

25. Ray CC, Pollack MM, Gai J, Patel AK. The association of the lactate-albumin ratio with mortality and multiple organ dysfunction in PICU patients. *Pediatr Crit Care Med*. (2023) 24:760–6. doi: 10.1097/pcc.0000000000003272

26. Zhang S, Chen N, Ma L. Lactate-to-albumin ratio: a promising predictor of 28-day all-cause mortality in critically ill patients with acute ischemic stroke. *J Stroke Cerebrovasc Dis*. (2024) 33:107536. doi: 10.1016/j.jstrokecerebrovasdis.2023.107536

27. Park JE, Chung KS, Song JH, Kim SY, Kim EY, Jung JY, et al. The C-reactive protein/albumin ratio as a predictor of mortality in critically ill patients. *J Clin Med*. (2018) 7:333. doi: 10.3390/jcm7100333

28. Chen Y, Yang K, Wu B, Lin W, Chen S, Xu X, et al. Association between lactate/albumin ratio and mortality in patients with heart failure after myocardial infarction. *ESC Heart Fail*. (2023) 10:1928–36. doi: 10.1002/ehf2.14359

29. Chen Y, Lai W, Yang K, Wu B, Xie D, Peng C. Association between lactate/albumin ratio and prognosis in patients with acute myocardial infarction. *Eur J Clin Invest*. (2024) 54:e14094. doi: 10.1111/eci.14094

30. Sun H, Wang B, An G, Zhang Y, Ma L. Association of lactate/albumin ratio with 3-month readmission risk in heart failure patients: a retrospective study. *ESC Heart Fail*. (2024) 11:2182–90. doi: 10.1002/ehf2.14788

31. Wang D, Luo C, Li Q, Zheng T, Gao P, Wang B, et al. Association between lactate/albumin ratio and all-cause mortality in critical patients with acute myocardial infarction. *Sci Rep*. (2023) 13:15561. doi: 10.1038/s41598-023-42330-8

32. Haschemi J, Müller CT, Haurand JM, Oehler D, Spieker M, Polzin A, et al. Lactate to albumin ratio for predicting clinical outcomes after in-hospital cardiac arrest. *J Clin Med*. (2023) 12:4136. doi: 10.3390/jcm12124136

33. Chen Y, Ba J, Peng C, Peng H, Li S, Lai W. Impact of lactate/albumin ratio on prognostic outcomes in patients with concomitant heart failure and chronic kidney disease. *Intern Emerg Med*. (2024) 19:1625–36. doi: 10.1007/s11739-024-03656-x

frontiers | Frontiers in Cardiovascular Medicine

TYPE Review
PUBLISHED 29 November 2024
DOI 10.3389/fcvm.2024.1483482

OPEN ACCESS

EDITED BY
Keita Saku,
National Cerebral and Cardiovascular Center, Japan

REVIEWED BY
Hisayoshi Murai,
Kanazawa University, Japan
Jun Nakata,
Nippon Medical School Hospital, Japan

*CORRESPONDENCE
Yue Liu
liuyueheart@hotmail.com
Min Yang
yangmin@ahmu.edu.cn

RECEIVED 20 August 2024
ACCEPTED 18 November 2024
PUBLISHED 29 November 2024

CITATION
Qi C, Wang W, Liu Y, Hua T, Yang M and Liu Y (2024) Heart-brain interactions: clinical evidence and mechanisms based on critical care medicine.
Front. Cardiovasc. Med. 11:1483482.
doi: 10.3389/fcvm.2024.1483482

Heart-brain interactions: clinical evidence and mechanisms based on critical care medicine

Chuyao Qi[1], Wenting Wang[2], Yanfei Liu[2], Tianfeng Hua[1], Min Yang[1]* and Yue Liu[2]*

[1]Laboratory of Cardiopulmonary Resuscitation and Critical Care, The Second Affiliated Hospital of Anhui Medical University, Hefei, Anhui, China, [2]National Clinical Research Center for TCM Cardiology, Xiyuan Hospital of China Academy of Chinese Medical Sciences, Beijing, China

In this review paper, we search the recent literature regarding the application of the heart-brain interaction theories in the field of intensive care unit. Simultaneously, we methodically summarize the clinical evidence supporting its application in intensive care unit treatment, based on clinical randomized trials and clinical case studies. We delve into how it's applied in treating severely ill patients and in researching animal models for cardio-cerebral comorbidities, aiming to supply benchmarks for subsequent clinical trials and studies on mechanisms.

KEYWORDS

heart-brain interaction, critical care medicine, intensive care unit, clinical evidence, mechanism, progress

1 Introduction

According to the World Health Organization, cardio-cerebrovascular diseases, such as stroke and myocardial infarction, have remained the primary reason for mortality and disability worldwide for the last 15 years (1). Growing studies in the field of cardio-cerebrovascular diseases have revealed a significant connection between cardiovascular diseases and neurological conditions, leading to a new discipline known as "Neurocardiology". A research indicates that a 50%–100% surge in both stroke survivors and patients over the past 25 years, with a notable rise in the disease burden of patients (2, 3), potentially linked to cardiac issues caused by stroke. Stroke ranks as the second most prevalent cause of mortality globally (4). A range of new-onset cardiovascular complications, such as arrhythmias and takotsubo cardiomyopathy, may occur subsequent to a stroke (5). The cardiac death rate is elevated (19.4% of all deaths) during the initial 4 weeks after stroke (6). Concurrently, the management of neurological disorders like acute ischemic stroke (AIS) faces significant hurdles due to cardiac complications (7, 8). Meanwhile, heart failure (HF) represents a significant health challenge globally and ranks as a primary reason for unfavorable outcomes and death rates (9).

Historically, academic studies have concentrated on the distinct therapeutic approaches of cardiology and neurology for cardio-cerebrovascular diseases management. Consequently, a deficit exists in the systematic and uniform interdisciplinary foundational and clinical studies across various disciplines concerning cardio-cerebrovascular disorders. Furthermore, the engagement of intensive care physicians is essential for patients in critical conditions (10). This review searches both fundamental and clinical researches concerning the use of heart-brain interaction

theories in critical care, aiming to encapsulate the latest clinical research findings on its application in preventing and treating severe cardio-cerebrovascular diseases, along with its effect mechanisms, to guide future pertinent studies.

2 The theories of heart-brain interaction

Numerous theories regarding heart-brain interaction have emerged over the past hundred years, influenced by clinical symptoms and the progression of pathological alterations (Figure 1). This section will present the heart-brain interaction concepts from two perspectives: fundamental scientific research experiments and clinical case studies. In 1959, Selye (11) developed an animal model of subarachnoid hemorrhage (SAH) and used drugs like reserpine, which block catecholamine release, to avert myocardial damage. This research indicated that cardiac necrosis following SAH is attributable to catecholamine toxicity. Furthermore, it demonstrated that catecholamines released directly into the heart via the nervous system exhibit significantly greater toxicity compared to those that arrive at the heart through the bloodstream. Subsequently, Masuda et al. (12) observed that in the acute phase of SAH (180 min after SAH), heightened sympathetic nervous system (SNS) activity has been associated with myocardial injury and contributes to the development of cardiac dysfunction. Thackeray et al. (13) employed serial noninvasive whole-body positron emission tomography to concurrently interrogate the heart and the brain. The positron emission tomography imaging agents utilized in this study were specifically designed to target the 18-kDa mitochondrial translocator protein, which is known to be upregulated in activated microglia and in systemic monocytes. Inflammatory responses are observed in both the brain and the heart one week following an acute myocardial infarction (AMI).

A research in 2014 revealed that intense intracranial hypertension, such as SAH, excessively stimulates the SNS (Figure 2), leading to the development of serious cardiac arrhythmia in patients (14). Following this, Silvani et al. (15) found that the brain innervates the heart via the sympathetic and parasympathetic pathways of the autonomic nervous system (ANS), and neurological conditions may disrupt the central autonomic regulation of the cardiovascular system, resulting in grave outcomes like myocardial injury, arrhythmia, and potentially abrupt mortality. During the year 2018, Doehner and colleagues (16) clearly suggested that the heart and the brain

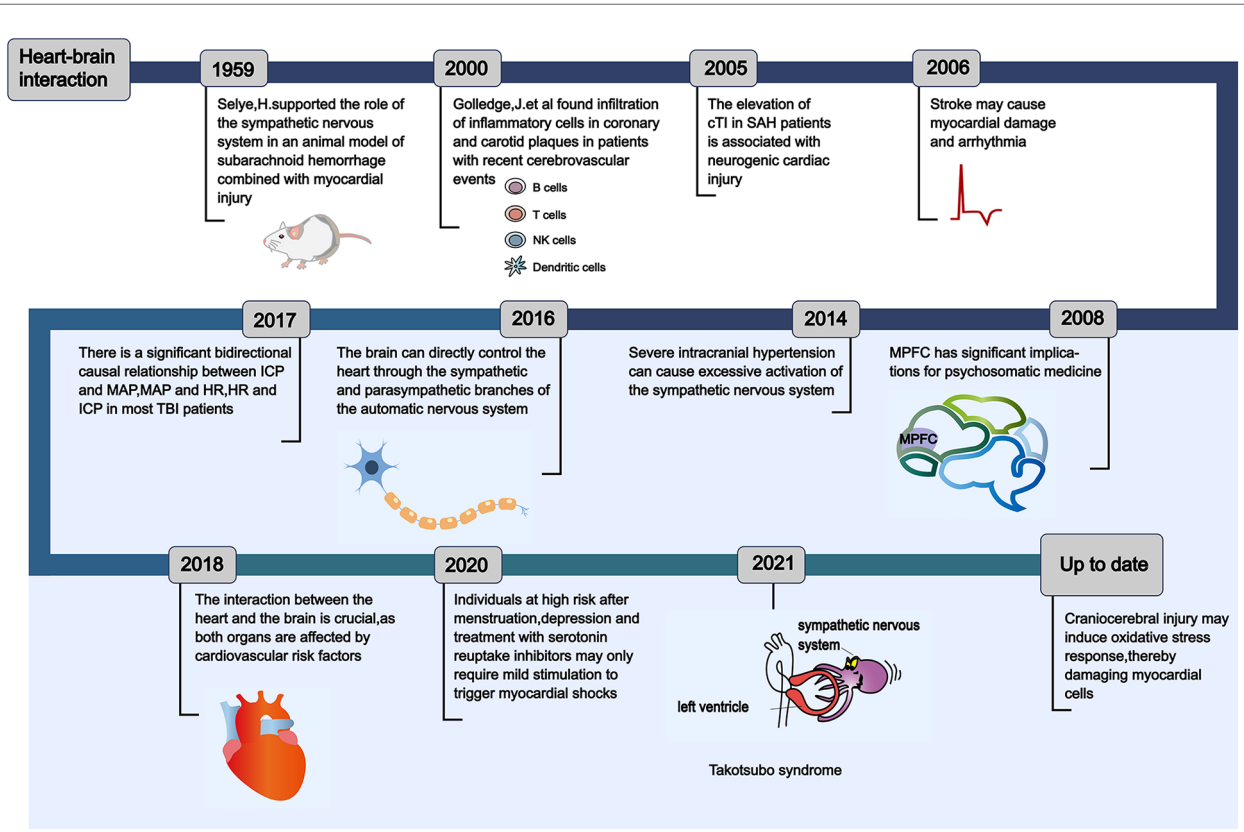

FIGURE 1
The historical evolution of the concept of heart-brain interaction. This reveals the evolution process of the theories of heart-brain interaction, which has been understood and discovered by scholars from different perspectives from ancient times to the present. Understanding the evolution of the theories of heart-brain interaction can provide important insights for the prevention of critical cardio-cerebrovascular diseases in intensive care unit. cTI, cardiac tropnin I; SAH, subarachnoid hemorrhage; MPFC, medial prefrontal cortex; ICP, intracranial pressure; MAP, mean arterial pressure; HR, heart rate; TBI, traumatic brain injury.

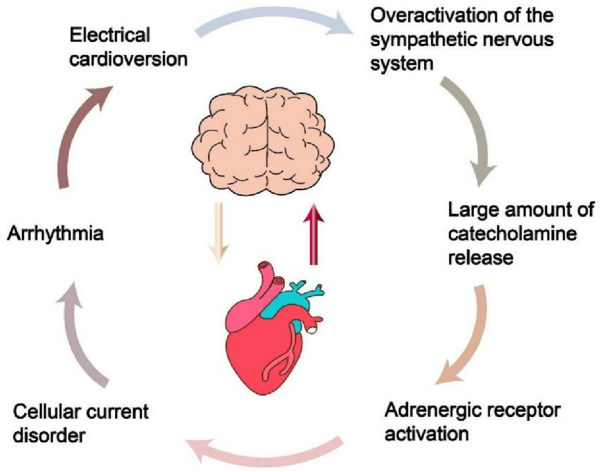

FIGURE 2
The process of intracranial hypertension leading to heart damage. Understanding this process can provide a basis for preventing cardiovascular complications in patients with traumatic brain injury in intensive care unit.

interact in two directions. For instance, individuals diagnosed with severe HF exhibit a diminished left ventricular ejection fraction (LVEF), which correlates with an elevated annual stroke risk estimated at 4%. In contrast, patients experiencing mild to moderate HF have an approximate annual stroke risk of 1.5%. A sympathetic-vagal imbalance due to stroke may lead to a decrease in myocardial contractility and trigger the lysis of myocardial cells. The aforementioned studies indicate that the central nervous system (CNS)' s control over heart function is attainable via the outflow of cardiac motor sympathetic and parasympathetic signals to both the cardiac conduction system and the myocardium. Conversely, impairments in heart performance may impact the health of the brain, including neuroinflammation and the deterioration of cognitive functions. Neuroinflammation is characterized as the immune response elicited by the CNS in reaction to localized injury or systemic infection. Microglia is the main agonist of neuroinflammation and it is present in significant quantities within the brain (17). In addition, following heart transplantation or cardiac resynchronization therapy (CRT), there is an observed increase in cerebral blood flow and an enhancement in cognitive function among patients with severe HF. This observation suggests that the cognitive impairments observed in individuals with severe HF may be linked to the underlying mechanisms associated with impaired cardiac systolic function, which leads to a reduction in cardiac output. Such a decrease in output may result in diminished cerebral blood flow and subsequent cerebral ischemia due to insufficient cerebral perfusion (18–20).

To sum up, numerous academics have explored the heart-brain interaction through diverse viewpoints, formulated several innovative theories, and unearthed a plethora of fresh research findings, laying a robust groundwork for averting secondary brain injuries in patients with severe cardiovascular conditions (such as severe HF or cardiac dysfunction requiring mechanical cardiac support leading to cognitive impairment) or secondary cardiac issues in those with critical neurological conditions (such as severe stroke causing myocardial injury, arrhythmia, and potentially abrupt mortality) within intensive care unit (ICU). In the subsequent chapters, we will respectively elaborate on the application of the heart-brain interaction concepts within the contexts of clinical practice and fundamental scientific research experiments.

3 Heart-brain interactions: clinical evidence

3.1 Heart to brain: heart failure on cognitive function

Cardio-cerebrovascular diseases have consistently been a primary reason for hospital admissions, illness and death globally (1). The cardiovascular system plays a crucial role in circulating blood throughout the body, brain included. HF can result in neurological disorders like stroke, with Table 1 encapsulating the risk factors linked to stoke, HF included. Furthermore, it's proposed that diminished cardiac output could primarily lead to prolonged cerebral hypoperfusion and cognitive deterioration in patients suffering from HF (26, 27).

Given that a malfunctioning heart can impair the standard structure and functionality of the brain and prompt treatment of the heart performance in severe HF patients can avert neurological conditions like stroke (28). The Montreal Cognitive Assessment serves as a diagnostic instrument for identifying cognitive impairment. Bhat et al. (29) conducted a follow-up study on patients with end-stage HF who had undergone implantation of left ventricular assist devices for a duration of eight months. The study revealed notable enhancements in the patients' The Montreal Cognitive Assessment total score, visuospatial, executive, and delayed recall cognitive domains. These findings indicated that improvements in cardiac function, characterized by reductions in mitral and tricuspid regurgitation and decreased serum levels of B-type natriuretic peptide, are associated with positive effects on cognitive function in the brain. Research conducted by Lee and colleagues also showed that individuals with advanced HF exhibit atypical brain metabolism, characterized by significantly reduced creatine levels in the

TABLE 1 Heart related risk factors for stroke.

Factors	Characteristic	Ref.
HF (heart failure)	There is an interaction between HF and stroke, and stroke increases the incidence rate and mortality of HF patients	(21)
Atrial fibrosis	Atrial fibrosis is the main cardiac risk factor for stroke	(22)
Hypertension	Hypertension is a common risk factor for recurrent stroke	(23)
Rheumatic heart disease	Rheumatic heart disease is one of the main causes of stroke in middle-and low-income countries	(24)
Valvular heart disease	American residents with valvular heart disease have a higher risk of experiencing stroke	(25)

parietal white matter compared to control subjects. Notably, these cerebral metabolic abnormalities can be ameliorated following an enhancement in LVEF subsequent to heart transplantation (30). Bommel et al. (31) conducted a thorough investigation into how cardiovascular system operations impact the nervous system. Patients with HF were randomly divided into two groups. Patients in the control group received medication and lifestyle enhancements due to their unsuitability for CRT, in contrast to the treatment group who underwent a 6-month CRT. The results showed that enhanced systolic function in the left ventricle of the treated group leads to a rise in cerebral blood circulation and better cognitive abilities in the patients. A clinical trial was conducted involving patients with life-threatening, terminal HF. The researchers objectively assessed neurocognitive function by utilizing cognitive P300 auditory evoked potentials. The results demonstrated that after the successful implantation of a ventricular assist device, there was a notable increase in the P300 evoked potential in patients suffering from severe HF, alongside an enhancement in neurocognitive function (32). Additionally, a separate investigation into patient suffering from severe HF revealed that enhancements in LVEF achieved via CRT are associated with improvements in cognitive impairment among patients, specifically in the executive functioning, global cognition, and visuospatial functioning (33).

To sum up, for severe HF patients, ameliorating heart performance proactively averts neurological disorders. Facing with complications like stroke or cognitive impairment, concurrent treatments of the heart and the brain are crucial for ameliorating the function of patients' heart and brain.

3.2 Brain to heart

3.2.1 ANS dysfunction in takotsubo cardiomyopathy

Disorders related to neurology, such as AIS, SAH represent a primary contributing factor to the development of takotsubo cardiomyopathy (34). A substantial body of evidence indicates that takotsubo cardiomyopathy is associated with the heart-brain axis (35–37). Researchers administered β- blockers to patients with aneurysmal subarachnoid hemorrhage (aSAH) prior to their admission and utilized echocardiography to assess any impairment in ventricular systolic function. The findings indicated that the intervention group exhibited a significantly reduced incidence of takotsubo cardiomyopathy following aSAH in comparison to the control group. This study primarily examined the application of β- blockers in patients with aSAH prior to hospital admission, focusing on preventive measures. However, there exists a paucity of clinical research data on this topic. The relationship between the risk of hypotension associated with β- blocker use and the objectives of SAH management post-aneurysm repair is inconsistent. Specifically, the management protocols may permit or, in certain instances, necessitate hypertension to mitigate the risk of cerebral vasospasm, which can lead to infarction. Consequently, it remains unclear whether the administration of β- blockers within 3 days after admission to reduce cardiac output in aSAH patients is harmful to the patients or beneficial in the pathogenesis of takotsubo cardiomyopathy caused by aSAH. Furthermore, the use of β- blockers is contraindicated in patients with acute and severe HF who exhibit low LVEF, hypotension, and in those with bradycardia (38).

Table 2 encapsulates the progress made in studying the link between takotsubo cardiomyopathy and CNS disorders. Scholars have discovered that enhancements in cardiac function, including improvements in cardiac contraction, can lead to amelioration of cognitive impairments. Conversely, the restoration of CNS function, exemplified by the inhibition of excessive SNS activation, has been shown to positively influence cardiac function. This includes benefits such as improved myocardial remodeling, a reduction in arrhythmias and the prevention of sudden cardiac death. Research indicates that alterations in ECG among patients with takotsubo cardiomyopathy frequently manifest within 10 h following AIS events. Notably, the majority of these ECG changes (including ST-segment elevation and negative giant T waves) are not associated with cardiac symptoms, which are typically absent upon admission. Additionally, echocardiographic assessments reveal localized dysfunction in LV motility, particularly in the apical region (43). The ANS, which includes nucleus ambiguus, the nucleus tractus solitarius, the dorsal motor nucleus of the vagus, and the rostral ventrolateral medulla, receives regulatory information from the CNS and exerts control over the heart, blood vessels, and adrenal glands via pressure receptors. Consequently, this study posits that significant ischemia in the brainstem may result in disorders of the ANS, potentially contributing to the development of takotsubo cardiomyopathy. Patients with takotsubo cardiomyopathy who present with elevated intraventricular pressure gradients (PG)

TABLE 2 Central nervous system disorders and takotsubo cardiomyopathy: a historical perspective.

Year	Author	Description	Ref.
1991	Dote, K. et al.	First report takotsubo cardiomyopathy	(39)
1998	Brandspiegel, H.	Takotsubo cardiomyopathy is mainly caused by psychological factors	(40)
2005	Wittstein, I. S. et al.	The main reason may be overstimulation of the sympathetic nervous system	(41)
2007	Dorfman, T. et al.	Takotsubo cardiomyopathy maybe is induced by multiple sources of physical stress	(42)
2008	Yoshimura, S. et al.	Takotsubo cardiomyopathy can be caused by acute ischemic stroke	(43)
2014	Suzuki, H. et al.	The role of brain cardiac axis in the pathogenesis of takotsubo cardiomyopathy is crucial	(44)
2015	Templin, C. et al.	Takotsubo cardiomyopathy is induced by acute, past, or chronic neurological or psychiatric disorders	(36)
2016	Ghadri, J. R. et al.	Neurological disorders may lead to morphological changes in the heart	(45)
2020	Amin, H. Z. et al.	High levels of catecholamines play a crucial role in the pathogenesis and pathophysiology of takotsubo cardiomyopathy	(46)
2022	Matta, A. et al.	Sympathetic nerve stimulation and catecholamine storm play a central role in the development of takotsubo cardiomyopathy	(47)

attributed to heightened SNS activation in a clinical trial were divided into two distinct groups. Participants in the intervention group received propranolol, a β-blocker more than 24 h following the onset of the condition. Meanwhile, those in the control group complied with clinical treatment guidelines, such as lifestyle enhancements. Results suggested that the intervention group experienced a reduction in the intraventricular PG alongside an enhancement in LVEF. This suggests that β-blockers may confer cardioprotective effects by counteracting the overactivation of the SNS, diminishing the release of catecholamines and mitigating their deleterious effects on cardiac function (48). Nevertheless, several studies indicate that the intravenous administration of propranolol requires meticulous monitoring due to numerous contraindications associated with the use of β-blockers. These contraindications include conditions such as asthma, respiratory failure, diabetic coma, decompensated HF, vasospasm, and bradyarrhythmia (49).

Currently, there is a lack of targeted intervention strategies for the management of takotsubo cardiomyopathy in patients suffering from severe cerebrovascular conditions, including aSAH, and AIS. Consequently, it is prudent to conduct further investigations into the incidence of takotsubo cardiomyopathy both prior to and following hospital admission, as well as to determine the optimal timing for interventions, appropriate dosages, and the impact of such treatments on cardiac and neurological function in this patient population, particularly with respect to the use of β-blockers. Future clinical randomized controlled trials may provide valuable insights that could enhance cardiac function—addressing issues such as left ventricular outflow tract obstruction, cardiogenic shock, and arrhythmias—by facilitating the recovery of compromised CNS functions, which may include addressing cerebral tissue ischemic infarction, secondary cerebral vasospasm resulting from elevated intracranial pressure, acute cerebral edema, and extensive neuronal death.

3.2.2 Systematic immunity

The pathological mechanisms of heart dysfunction caused by acute cerebrovascular disorders remain unelucidated, potentially linked to malfunctions in the ANS, intestinal microbiota, inflammation, microvesicles and microRNAs (Figure 3). Intervening in the aforementioned mechanisms can avert cardiovascular complications in patients suffering from severe cerebrovascular accidents. The benefits and drawbacks of intervening in ANS dysfunction resulting from acute cerebrovascular accidents (including aSAH and AIS) to prevent or address cardiac dysfunction (such as reduced ventricular

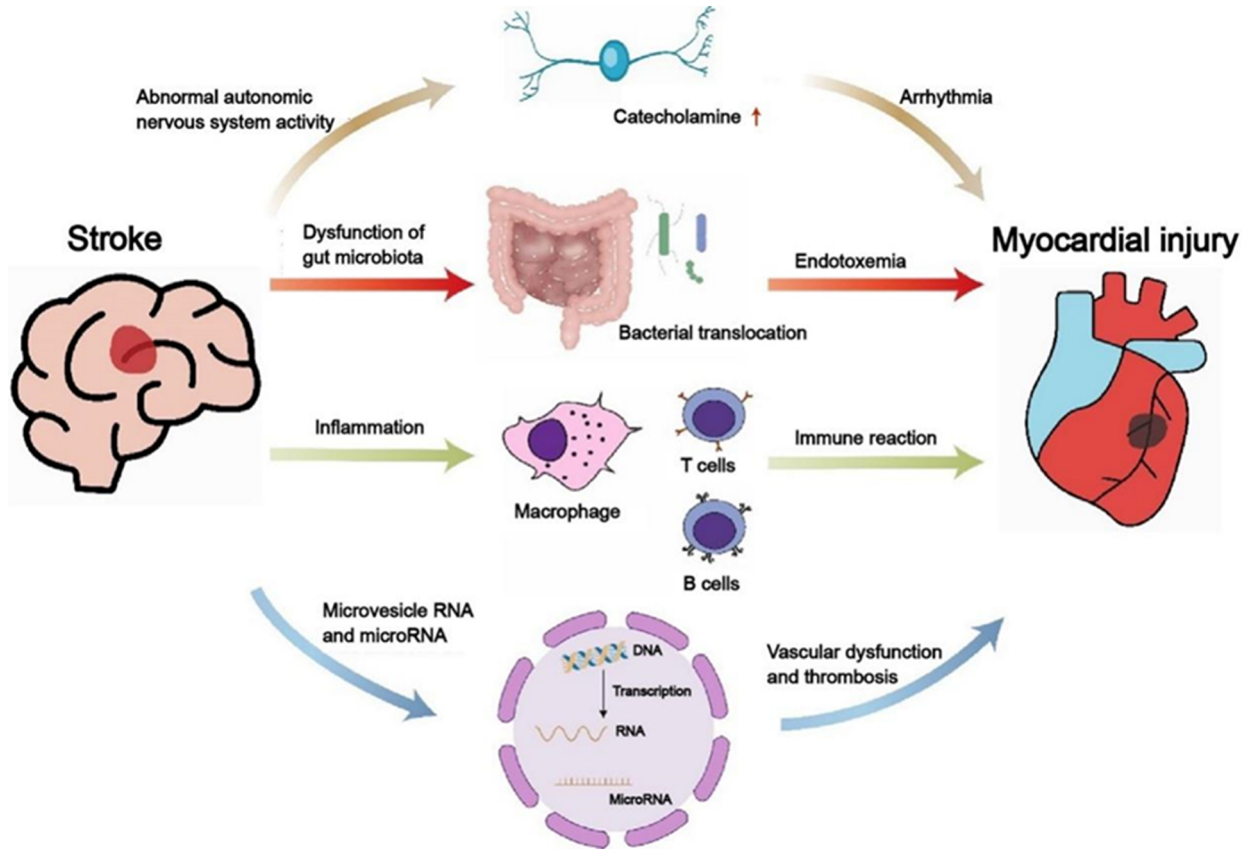

FIGURE 3
The relationship between stroke and cardiac dysfunction. Displayed the mechanisms of the activity of the autonomic sympathetic nervous system, immune system, gut microbiome, and microRNA and microvesicle RNA. Clarifying the interaction between heart and brain will help develop more appropriate and effective treatment strategies for severely ill patients with cardio- cerebrovascular diseases.

systolic function and LVEF) in patients have been thoroughly examined in previous literature. Consequently, this discussion will primarily concentrate on the local and systemic inflammatory responses observed in both the brain and the heart. Bilt and colleagues (50) discovered that patients with SAH exhibit myocardial damage and neutrophils are present in this region. Levels of Tumor Necrosis Factor-alpha (TNF-α) escalate in correlation with the severity of cardiovascular diseases. Research has demonstrated that anti-TNF-α therapy can enhance cardiac function in patients with HF. This improvement is attributed to the phenomenon whereby stress-activated cytokines in cardiac tissue surpass the capacity of local cell receptors involved in autocrine and paracrine signaling, subsequently entering the systemic circulation as hematogenous cytokines. These cytokines, being large molecules, typically face challenges in crossing the blood-brain barrier. However, in instances where the blood-brain barrier surrounding the periventricular organs is compromised or absent, these cytokines can infiltrate the brain via saturable or passive transport mechanisms. Once in the brain, they may act as mediators of inflammation and stimulate the SNS. Nevertheless, existing research has yet to elucidate the precise mechanisms underlying the interplay between cardiac injury and neuroinflammation. Consequently, additional experimental studies and clinical trials are warranted to further investigate and validate these interactions in the future.

4 The animal models for cardio-cerebral co-morbidities

The preceding section has provided an overview of the utilization of the heart-brain interaction concepts in the prevention and management of critically ill patients suffering from cardio-cerebrovascular diseases within clinical settings. This section will concentrate on presenting certain heart-brain interaction concepts that have been identified through animal studies but have not been implemented in actual clinical practice. Chen and colleagues (51) developed a test model for AIS using adult mice free from primary heart conditions or pre-existing vascular lesions. The results indicated that mice exhibit heart irregularities, including a decrease in cardiac ejection fraction, enlargement of cardiomyocytes and myocardial fibrosis. Subsequently, Bieber and colleagues (52) observed a reduction in heart rate, an enhancement in ejection fraction, and a notable decline in plasma brain natriuretic peptide levels in AIS mice following the administration of β- blockers. These findings indicate that β-blockade may mitigate the progression of chronic cardiac dysfunction by decelerating cardiac remodeling and suppressing sympathetic nerve activity linked to chronic autonomic dysfunction. Another study revealed that in a traumatic brain injury model, mice brain tissues produce microvesicles, potentially linked to increased blood coagulation (53). Research indicates that following injury to the left insular cortex in murine models, there is a notable decrease in both left ventricular systolic pressure and left ventricular end diastolic pressure, accompanied by elevated levels of norepinephrine in both plasma and myocardial tissues. These findings imply that focal ischemia in the left hemisphere of the brain may contribute to cardiac dysfunction, with the extent of this dysfunction correlating with the severity of damage to the insular cortex. Furthermore, the excessive release of catecholamines may play a mediating role in the observed cardiac dysfunction (54). Following a successful induction of selective insular cortex AIS in rats over a period of 28 days, Balint et al. (55) conducted a histological analysis that revealed a pronounced severity of endothelial dysfunction, inflammation, and fibrosis in the left atrial tissue adjacent to the pulmonary vein. This region is characterized by the highest concentration of sympathetic nerve processes within the atrial myocardium. This study posited that excessive activation of endothelial cells within the brain may facilitate the swift infiltration of neutrophils into myocardial tissue via the vascular endothelium, highlighting the possible involvement of autonomic dysfunction in the onset of cardiac injury. Nevertheless, additional research is warranted to uncover novel targets aimed at preventing structural alterations in the left atrium resulting from stroke, as well as addressing potential post-stroke cardiovascular complications, including arrhythmias and sudden cardiac death. Future investigations should also concentrate on the temporal evolution of left atrial heart disease triggered by ischemic strokes, alterations in the ventricles and right atrium, and myocardial changes that occur following infarcts of comparable size in other cerebral regions.

Francis et al. (56) observed an elevation in the synthesis of TNF-α within the brain, heart, and plasma of rats following AMI. This finding implies that AMI may trigger the production of pro-inflammatory cytokines in the hypothalamus. Concurrently, Meissner et al. (57) proposed that the administration of pharmacological agents that inhibit pro-inflammatory TNF-α in HF murine models markedly mitigated the reduction in dendritic spine density and the associated memory deficits induced by HF. Research has demonstrated that anti-TNF-α therapy can enhance cardiac function in rats with HF. This improvement is attributed to the phenomenon whereby stress-activated cytokines in cardiac tissue surpass the capacity of local cell receptors involved in autocrine and paracrine signaling, subsequently entering the systemic circulation as hematogenous cytokines. These cytokines, being large molecules, typically face challenges in crossing the blood-brain barrier. However, in instances where the blood-brain barrier surrounding the periventricular organs is compromised or absent, these cytokines can infiltrate the brain via saturable or passive transport mechanisms. Once in the brain, they may act as mediators of inflammation and stimulate the SNS. Consequently, anti-TNF-α therapy may enhance LVEF by mitigating the levels of cytokines and oxidative stress within the brain, ultimately leading to improved cardiac function in rats (58). Currently, numerous innovative strategies have emerged for the prevention and treatment of myocardial inflammation, particularly concerning injury and repair mechanisms. Among these is the identification of a novel specific myocardial cell within the damaged heart, as well as the Ym-1hi Neu subpopulation of cardiac neutrophils, which exhibit functional heterogeneity (59). Table 3 provides a summary of various animal models along with their respective features.

TABLE 3 Preparation of animal models for cardio-cerebrovascular diseases.

Animal model	Examples	Characteristic
Traumatic brain injury	Mouse model of fluid percussion injury (60)	With the heads of mice unconstrained, rapidly injecting saline into the closed skull cavity of the mice's heads under controlled pressure of 1.9 ± 0.1 atmospheres Effective, reliable, easy to operate, and clinically relevant
	Extraluminal Permanent distal middle cerebral artery occlusion Model (51)	A midline incision is opened between the orbit and the ear Clear penumbra can be seen around the infarcted core Animals have a longer survival time and small infarct area (61–63)
Acute myocardial infarction	The model of acute myocardial infarction in rats by ligation of coronary artery (64)	Ligation of the left anterior descending branch of the left coronary artery in rats Similar to the actual pathogenesis of myocardial infarction
Takotsubo cardiomyopathy	Rat model of takotsubo cardiomyopathy *in vivo* (65)	Injecting adrenaline into the external jugular vein Easy to operate

5 Conclusion and perspective

Managing cardio-cerebrovascular diseases clinically stands as a significant worldwide issue in public health (66). Approximately 1.6% of patients suffering from AIS experience cardiac complications like AMI, leading to a significant rise in both the hospital mortality rate and healthcare expenses for these patients (67). Meanwhile, HF poses a major risk for the emergence of AIS. Strategies like intensive heart rate management and antithrombotic interventions markedly lower stroke occurrences in HF patients, leading to a substantial decrease in hospital admissions and death rates (68). The central autonomic network can link with the intracardiac nervous system through the exogenous CNS, issuing instructions to the cardiac conduction system that are subsequently relayed to the myocardium (69). Yet, in states of sleep or emotional stimulation, the central autonomic network stimulates the heart through sympathetic and vagal nerves and is modulated by responses from myocardial and cardiovascular stress receptors (70).

The effect mechanisms of averting cardio-cerebrovascular diseases in severely ill patients, steered by the theories of heart-brain interaction, is linked to enhancing heart performance, improving ANS dysfunction and immune system regulation. Consequently, it acts as a directive for the prevention and management of severely ill patients suffering from takotsubo cardiomyopathy due to cerebrovascular diseases, severe HF coupled with neurological disorders. Concurrently, there are certain constraints associated with the outcomes of this review: regarding clinical evidence, the majority of literature fail to explicitly mention the individualized care of acute cardio-cerebrovascular patients within ICU. This includes considerations such as the adverse cardiac events associated with aSAH and the potential application of β- blockers during the acute phase of takotsubo cardiomyopathy resulting from acute cerebrovascular incidents. Further investigation is required into how ICU, the department of cardiovascular medicine and neurology department collaborate on cardio-cerebrovascular diseases. Moreover, there's a scarcity of clinical randomized controlled trials in ICU focusing on heart-brain interaction theories to direct the prevention and treatment of diverse cardio-cerebrovascular diseases, and the overall quality is subpar, missing in comprehensive, multi-center, large-sample randomized controlled trials. Regarding the study of effect mechanisms, the research on how the theories of heart-brain interaction guide the treatment of severely ill patients with cardio-cerebrovascular diseases is limited and there is a single research method.

In summary, prior research in ICU has laid a theoretical groundwork for preventing and treating acute cardio-cerebrovascular diseases, a frequent clinical crisis. A thorough examination of the theoretical underpinnings of these diseases can lead to innovative approaches in managing and preventing acute cardio-cerebrovascular diseases in severely ill patients. In my opinion, future research should prioritize the execution of fundamental experiments and the accumulation of clinical evidence to elucidate the interactions between the autonomic nervous system and cardiac function, as well as the relationship between cardiac injury and neuroinflammation. Furthermore, it is essential to enhance collaboration among the ICU, the Department of Cardiovascular Medicine and Neurology Department in the management and prevention of acute cardio-cerebrovascular diseases. The adoption of more advanced and precise technological methodologies is also recommended to thoroughly investigate potential novel mechanisms underlying the interaction between the heart and the brain. This will establish a link between fundamental principles and clinical practice, and lay the groundwork for the uniform application of heart-brain interaction theories in both preventing and treating severely ill patients.

Author contributions

CQ: Funding acquisition, Methodology, Resources, Supervision, Writing – original draft. WW: Formal Analysis, Investigation, Methodology, Writing – original draft. YL: Investigation, Methodology, Writing – review & editing. TH: Investigation, Methodology, Writing – review & editing. MY: Conceptualization, Funding acquisition, Writing – review & editing. YL: Conceptualization, Supervision, Writing – review & editing.

Funding

The author(s) declare financial support was received for the research, authorship, and/or publication of this article. This article was funded by The National Natural Science Foundation of China (No. 82072134), Anhui Province Key Research and Development Plan High-tech Special Project (No. 202304a05020071) and the Research Fund of Anhui Institute of translational medicine (No. 2023zhyx-C64 and 2022zhyx-C76).

Conflict of interest

The authors declare that the research was conducted in the absence of any commercial or financial relationships that could be construed as a potential conflict of interest.

The author(s) declared that they were an editorial board member of Frontiers, at the time of submission. This had no impact on the peer review process and the final decision.

Publisher's note

References

1. Méloux A, Béjot Y, Rochette L, Cottin Y, Vergely C. Brain-Heart interactions during ischemic processes: clinical and experimental evidences. *Stroke*. (2020) 51:679–86. doi: 10.1161/STROKEAHA.119.027732

2. Feigin VL, Norrving B, Mensah GA. Global burden of stroke. *Circ Res*. (2017) 120:439–48. doi: 10.1161/CIRCRESAHA.116.308413

3. Virani SS, Alonso A, Benjamin EJ, Bittencourt MS, Callaway CW, Carson AP, et al. Heart disease and stroke statistics—2020 update: a report from the American Heart Association. *Circulation*. (2020) 141:e139–596. doi: 10.1161/CIR.0000000000000757

4. Vos T, Lim SS, Abbafati C, Abbas KM, Abbasi M, Abbasifard M, et al. Global burden of 369 diseases and injuries in 204 countries and territories, 1990–2019: a systematic analysis for the global burden of disease study 2019. *Lancet*. (2020) 396:1204–22. doi: 10.1016/S0140-6736(20)30925-9

5. Mathias TL, Albright KC, Boehme AK, Monlezun D, George AJ, Jones E, et al. The impact of myocardial infarction vs. Pneumonia on outcome in acute ischemic stroke. *J Cardiovasc Dis*. (2014) 2:1–3.

6. Prosser J, MacGregor L, Lees KR, Diener H-C, Hacke W, Davis S. Predictors of early cardiac morbidity and mortality after ischemic stroke. *Stroke*. (2007) 38:2295–302. doi: 10.1161/STROKEAHA.106.471813

7. Sörös P, Hachinski V. Cardiovascular and neurological causes of sudden death after ischaemic stroke. *Lancet Neurol*. (2012) 11:179–88. doi: 10.1016/S1474-4422(11)70291-5

8. Kumar S, Selim MH, Caplan LR. Medical complications after stroke. *Lancet Neurol*. (2010) 9:105–18. doi: 10.1016/S1474-4422(09)70266-2

9. Benjamin EJ, Virani SS, Callaway CW, Chamberlain AM, Chang AR, Cheng S, et al. Heart disease and stroke statistics—2018 update: a report from the American Heart Association. *Circulation*. (2018) 137:e67–492. doi: 10.1161/CIR.0000000000000558

10. Tahsili-Fahadan P, Geocadin RG. Heart-brain axis effects of neurologic injury on cardiovascular function. *Circ Res*. (2017) 120:559–72. doi: 10.1161/CIRCRESAHA.116.308446

11. Selye H. The chemical prevention of cardiac necrosis. *Am J Med Sci*. (1959) 238:130. doi: 10.1097/00000441-195907000-00030

12. Masuda T, Sato K, Yamamoto S, Matsuyama N, Shimohama T, Matsunaga A, et al. Sympathetic nervous activity and myocardial damage immediately after subarachnoid hemorrhage in a unique animal model. *Stroke*. (2002) 33:1671–6. doi: 10.1161/01.STR.0000016327.74392.02

13. Thackeray JT, Hupe HC, Wang Y, Bankstahl JP, Berding G, Ross TL, et al. Myocardial inflammation predicts remodeling and neuroinflammation after myocardial infarction. *J Am Coll Cardiol*. (2018) 71:263–75. doi: 10.1016/j.jacc.2017.11.024

14. Wybraniec MT, Miziastec K, Krzych Ł. Neurocardiogenic injury in subarachnoid hemorrhage: a wide spectrum of catecholamin-mediated brain-heart interactions. *Cardiol J*. (2014) 21:220–8. doi: 10.5603/CJ.a2014.0019

15. Silvani A, Calandra-Buonaura G, Dampney RAL, Cortelli P. Brain–heart interactions: physiology and clinical implications. *Philos Trans A Math Phys Eng Sci*. (2016) 374:20150181. doi: 10.1098/rsta.2015.0181

16. Doehner W, Ural D, Haeusler KG, Čelutkienė J, Bestetti R, Cavusoglu Y, et al. Heart and brain interaction in patients with heart failure: overview and proposal for a taxonomy. A position paper from the study group on heart and brain interaction of the heart failure association. *Eur J Heart Fail*. (2018) 20:199–215. doi: 10.1002/ejhf.1100

17. Rivest S. Regulation of innate immune responses in the brain. *Nat Rev Immunol*. (2009) 9:429–39. doi: 10.1038/nri2565

18. Roman DD, Kubo SH, Ormaza S, Francis GS, Bank AJ, Shumway SJ. Memory improvement following cardiac transplantation. *J Clin Exp Neuropsychol*. (1997) 19:692–7. doi: 10.1080/01688639708403754

19. Bornstein RA, Starling RC, Myerowitz PD, Haas GJ. Neuropsychological function in patients with end-stage heart failure before and after cardiac transplantation. *Acta Neurol Scand*. (1995) 91:260–5. doi: 10.1111/j.1600-0404.1995.tb07001.x

20. Dixit NK, Vazquez LD, Cross NJ, Kuhl EA, Serber ER, Kovacs A, et al. Cardiac resynchronization therapy: a pilot study examining cognitive change in patients before and after treatment. *Clin Cardiol*. (2010) 33:84–8. doi: 10.1002/clc.20710

21. Kristensen SL, Jhund PS, Køber L, Preiss D, Kjekshus J, McKelvie RS, et al. Comparison of outcomes after hospitalization for worsening heart failure, myocardial infarction, and stroke in patients with heart failure and reduced and preserved ejection fraction. *Eur J Heart Fail*. (2015) 17:169–76. doi: 10.1002/ejhf.211

22. Emmett ES, Douiri A, Marshall IJ, Wolfe CDA, Rudd AG, Bhalla A. A comparison of trends in stroke care and outcomes between in-hospital and community-onset stroke—the South London stroke register. *PLoS One*. (2019) 14:e0212396. doi: 10.1371/journal.pone.0212396

23. Xia X, Yue W, Chao B, Li M, Cao L, Wang L, et al. Prevalence and risk factors of stroke in the elderly in northern China: data from the national stroke screening survey. *J Neurol*. (2019) 266:1449–58. doi: 10.1007/s00415-019-09281-5

24. Karthikeyan G, Connolly SJ, Yusuf S. Overestimation of stroke risk in rheumatic mitral stenosis and the implications for oral anticoagulation. *Circulation*. (2020) 142:1697–9. doi: 10.1161/CIRCULATIONAHA.120.050347

25. Meschia JF, Bushnell C, Boden-Albala B, Braun LT, Bravata DM, Chaturvedi S, et al. Guidelines for the primary prevention of stroke. *Stroke*. (2014) 45:3754–832. doi: 10.1161/STR.0000000000000046

26. Pullicino PM, Hart J. Cognitive impairment in congestive heart failure? *Neurology*. (2001) 57:1945–6. doi: 10.1212/WNL.57.11.1945

27. Gaviria M, Pliskin N, Kney A. Cognitive impairment in patients with advanced heart failure and its implications on decision-making capacity. *Congest Heart Fail*. (2011) 17:175–9. doi: 10.1111/j.1751-7133.2011.00242.x

28. McDonagh TA, Metra M, Adamo M, Gardner RS, Baumbach A, Böhm M, et al. 2021 ESC guidelines for the diagnosis and treatment of acute and chronic heart failure: developed by the task force for the diagnosis and treatment of acute and chronic heart failure of the European Society of Cardiology (ESC) with the special contribution of the heart failure association (HFA) of the ESC. *Eur Heart J*. (2021) 42:3599–726. doi: 10.1093/eurheartj/ehab368

29. Bhat G, Yost G, Mahoney E. Cognitive function and left ventricular assist device implantation. *J Heart Lung Transplant*. (2015) 34:1398–405. doi: 10.1016/j.healun.2015.05.015

30. Lee CW, Lee J-H, Kim J-J, Park S-W, Hong M-K, Kim S-T, et al. Cerebral metabolic abnormalities in congestive heart failure detected by proton magnetic resonance spectroscopy. *J Am Coll Cardiol*. (1999) 33:1196–202. doi: 10.1016/S0735-1097(98)00701-3

31. van Bommel RJ, Marsan NA, Koppen H, Delgado V, Borleffs CJW, Ypenburg C, et al. Effect of cardiac resynchronization therapy on cerebral blood flow. *Am J Cardiol*. (2010) 106:73–7. doi: 10.1016/j.amjcard.2010.02.015

32. Zimpfer D, Wieselthaler G, Czerny M, Fakin R, Haider D, Zrunek P, et al. Neurocognitive function in patients with ventricular assist devices: a comparison of pulsatile and continuous blood flow devices. *ASAIO J*. (2006) 52:24–7. doi: 10.1097/01.mat.0000191334.51375.7e

33. Hoth KF, Poppas A, Ellison KE, Paul RH, Sokobin A, Cho Y, et al. Link between change in cognition and left ventricular function following cardiac resynchronization therapy. *J Cardiopulm Rehabil Prev*. (2010) 30:401–8. doi: 10.1097/HCR.0b013e3181e1739a

34. Porto I, Bona RD, Leo A, Proietti R, Pieroni M, Caltagirone C, et al. Stress cardiomyopathy (tako-tsubo) triggered by nervous system diseases: a systematic review of the reported cases. *Int J Cardiol*. (2013) 167:2441–8. doi: 10.1016/j.ijcard.2013.01.031

35. Samuels MA. The brain–heart connection. *Circulation*. (2007) 116:77–84. doi: 10.1161/CIRCULATIONAHA.106.678995

36. Templin C, Ghadri JR, Diekmann J, Napp LC, Bataiosu DR, Jaguszewski M, et al. Clinical features and outcomes of takotsubo (stress) cardiomyopathy. *N Engl J Med*. (2015) 373:929–38. doi: 10.1056/NEJMoa1406761

37. Ghadri JR, Sarcon A, Diekmann J, Bataiosu DR, Cammann VL, Jurisic S, et al. Happy heart syndrome: role of positive emotional stress in takotsubo syndrome. *Eur Heart J*. (2016) 37:2823–9. doi: 10.1093/eurheartj/ehv757

38. Ghadri J-R, Wittstein IS, Prasad A, Sharkey S, Dote K, Akashi YJ, et al. International expert consensus document on takotsubo syndrome (part II): diagnostic workup, outcome, and management. *Eur Heart J*. (2018) 39:2047–62. doi: 10.1093/eurheartj/ehy077

39. Dote K, Sato H, Tateishi H, Uchida T, Ishihara M. Myocardial stunning due to simultaneous multivessel coronary spasms: a review of 5 cases. *J Cardiol*. (1991) 21:203–14.

40. Brandspiegel H, Marinchak R, Rials S, Kowey P. A broken heart. *Circulation*. (1998) 98:1349. doi: 10.1161/01.CIR.98.13.1349

41. Wittstein IS, Thiemann DR, Lima JAC, Baughman KL, Schulman SP, Gerstenblith G, et al. Neurohumoral features of myocardial stunning due to sudden emotional stress. *N Engl J Med*. (2005) 352:539–48. doi: 10.1056/NEJMoa043046

42. Dorfman T, Aqel R, Allred J, Woodham R, Iskandrian AE. Takotsubo cardiomyopathy induced by treadmill exercise testing: an insight into the pathophysiology of transient left ventricular apical (or midventricular) ballooning in the absence of obstructive coronary artery disease. *J Am Coll Cardiol*. (2007) 49:1223–5. doi: 10.1016/j.jacc.2006.12.033

43. Yoshimura S, Toyoda K, Ohara T, Nagasawa H, Ohtani N, Kuwashiro T, et al. Takotsubo cardiomyopathy in acute ischemic stroke. *Ann Neurol*. (2008) 64:547–54. doi: 10.1002/ana.21459

44. Suzuki H, Matsumoto Y, Kaneta T, Sugimura K, Takahashi J, Fukumoto Y, et al. Evidence for brain activation in patients with takotsubo cardiomyopathy. *Circ J*. (2014) 78:256–8. doi: 10.1253/circj.CJ-13-1276

45. Ghadri JR, Cammann VL, Napp LC, Jurisic S, Diekmann J, Bataiosu DR, et al. Differences in the clinical profile and outcomes of typical and atypical takotsubo syndrome: data from the international takotsubo registry. *JAMA Cardiol*. (2016) 1:335–40. doi: 10.1001/jamacardio.2016.0225

46. Amin HZ, Amin LZ, Pradipta A. Takotsubo cardiomyopathy: a brief review. *J Med Life*. (2020) 13:3–7. doi: 10.25122/jml-2018-0067

47. Matta A, Delmas C, Campelo-Parada F, Lhermusier T, Bouisset F, Elbaz M, et al. Takotsubo cardiomyopathy. *Rev Cardiovasc Med*. (2022) 23:38. doi: 10.31083/j.rcm2301038

48. Yoshioka T, Hashimoto A, Tsuchihashi K, Nagao K, Kyuma M, Ooiwa H, et al. Clinical implications of midventricular obstruction and intravenous propranolol use in transient left ventricular apical ballooning (tako-tsubo cardiomyopathy). *Am Heart J*. (2008) 155:526.e1–7. doi: 10.1016/j.ahj.2007.10.042

49. Kyuma M, Tsuchihashi K, Shinshi Y, Hase M, Nakata T, Ooiwa H, et al. Effect of intravenous propranolol on left ventricular apical ballooning without coronary artery stenosis (ampulla cardiomyopathy): three cases. *Circ J*. (2002) 66:1181–4. doi: 10.1253/circj.66.1181

50. Bilt IACVD, Vendeville JP, Hoef TPVD, Begieneman MPV, Niessen HWM. Myocarditis in patients with subarachnoid hemorrhage: a histopathologic study. *J Crit Care*. (2016) 32:196–200. doi: 10.1016/j.jcrc.2015.12.005

51. Chen J, Cui C, Yang X, Xu J, Venkat P, Zacharek A, et al. MiR-126 affects brain-heart interaction after cerebral ischemic stroke. *Transl Stroke Res*. (2017) 8:374–85. doi: 10.1007/s12975-017-0520-z

52. Bieber M, Werner RA, Tanai E, Hofmann U, Higuchi T, Schuh K, et al. Stroke-induced chronic systolic dysfunction driven by sympathetic overactivity. *Ann Neurol*. (2017) 82:729–43. doi: 10.1002/ana.25073

53. Tian Y, Salsbery B, Wang M, Yuan H, Yang J, Zhao Z, et al. Brain-derived microparticles induce systemic coagulation in a murine model of traumatic brain injury. *Blood*. (2015) 125:2151–9. doi: 10.1182/blood-2014-09-598805

54. Min J, Farooq MU, Greenberg E, Aloka F, Bhatt A, Kassab M, et al. Cardiac dysfunction after left permanent cerebral focal ischemia. *Stroke*. (2009) 40:2560–3. doi: 10.1161/STROKEAHA.108.536086

55. Balint B, Jaremek V, Thorburn V, Whitehead SN, Sposato LA. Left atrial microvascular endothelial dysfunction, myocardial inflammation and fibrosis after selective insular cortex ischemic stroke. *Int J Cardiol*. (2019) 292:148–55. doi: 10.1016/j.ijcard.2019.06.004

56. Francis J, Chu Y, Johnson AK, Weiss RM, Felder RB. Acute myocardial infarction induces hypothalamic cytokine synthesis. *American Journal of Physiology-Heart and Circulatory Physiology*. (2004) 286:H2264–71. doi: 10.1152/ajpheart.01072.2003

57. Meissner A, Visanji NP, Momen MA, Feng R, Francis BM, Bolz S-S, et al. Tumor necrosis factor-α underlies loss of cortical dendritic spine density in a mouse model of congestive heart failure. *J Am Heart Assoc*. (2015) 4:e001920. doi: 10.1161/JAHA.115.001920

58. Guggilam A, Haque M, Kerut EK, McIlwain E, Lucchesi P, Seghal I, et al. TNF-α blockade decreases oxidative stress in the paraventricular nucleus and attenuates sympathoexcitation in heart failure rats. *Am J Physiol Heart Circ Physiol*. (2007) 293:H599–609. doi: 10.1152/ajpheart.00286.2007

59. Dong Y, Kang Z, Zhang Z, Zhang Y, Zhou H, Liu Y, et al. Single-cell profile reveals the landscape of cardiac immunity and identifies a cardio-protective ym-1hi neutrophil in myocardial ischemia–reperfusion injury. *Sci Bull*. (2024) 69:949–67. doi: 10.1016/j.scib.2024.02.003

60. Dong J, Tian Y, Salsbery B, Yuan H, Wang M, Wu X, et al. Brain-derived microparticles induce systemic coagulation associated with traumatic brain injury. *Blood*. (2014) 124:1497. doi: 10.1182/blood.V124.21.1497.1497

61. Fluri F, Schuhmann MK, Kleinschnitz C. Animal models of ischemic stroke and their application in clinical research. *Drug Des Devel Ther*. (2015) 9:3445–54. doi: 10.2147/DDDT.S56071

62. Hermann DM, Popa-Wagner A, Kleinschnitz C, Doeppner TR. Animal models of ischemic stroke and their impact on drug discovery. *Expert Opin Drug Discov*. (2019) 14:315–26. doi: 10.1080/17460441.2019.1573984

63. Gao X, Zhang X, Cui L, Chen R, Zhang C, Xue J, et al. Ginsenoside Rb1 promotes motor functional recovery and axonal regeneration in post-stroke mice through cAMP/PKA/CREB signaling pathway. *Brain Res Bull*. (2020) 154:51–60. doi: 10.1016/j.brainresbull.2019.10.006

64. Yu Y, Zhang Z-H, Wei S-G, Serrats J, Weiss RM, Felder RB. Brain perivascular macrophages and the sympathetic response to inflammation in rats after myocardial infarction. *Hypertension*. (2010) 55:652–9. doi: 10.1161/HYPERTENSIONAHA.109.142836

65. Couch LS, Fiedler J, Chick G, Clayton R, Dries E, Wienecke LM, et al. Circulating microRNAs predispose to takotsubo syndrome following high-dose Adrenaline exposure. *Cardiovasc Res*. (2021) 118:1758–70. doi: 10.1093/cvr/cvab210

66. Joseph P, Leong D, McKee M, Anand SS, Schwalm J-D, Teo K, et al. Reducing the global burden of cardiovascular disease, part 1. *Circ Res*. (2017) 121:677–94. doi: 10.1161/CIRCRESAHA.117.308903

67. Alqahtani F, Aljohani S, Tarabishy A, Busu T, Adcock A, Alkhouli M. Incidence and outcomes of myocardial infarction in patients admitted with acute ischemic stroke. *Stroke*. (2017) 48:2931–8. doi: 10.1161/STROKEAHA.117.018408

68. Oladiran O, Nwosu I. Stroke risk stratification in atrial fibrillation: a review of common risk factors. *J Community Hosp Intern Med Perspect*. (2019) 9:113–20. doi: 10.1080/20009666.2019.1593781

69. Witt CM, Bolona L, Kinney MO, Moir C, Ackerman MJ, Kapa S, et al. Denervation of the extrinsic cardiac sympathetic nervous system as a treatment modality for arrhythmia. *EP Europace*. (2017) 19:1075–83. doi: 10.1093/europace/eux011

70. Benarroch EE. The central autonomic network: functional organization, dysfunction, and perspective. *Mayo Clin Proc*. (1993) 68:988–1001. doi: 10.1016/s0025-6196(12)62272-1

frontiers | Frontiers in Cardiovascular Medicine

TYPE Original Research
PUBLISHED 09 December 2024
DOI 10.3389/fcvm.2024.1513212

OPEN ACCESS

EDITED BY
Keita Saku,
National Cerebral and Cardiovascular Center, Japan

REVIEWED BY
Daisuke Onohara,
The Research Institute at Nationwide Children's Hospital, United States
Junya Matsuda,
Nippon Medical School, Japan

*CORRESPONDENCE
Peng Nie
✉ gshlsh20012005@hotmail.com
Lei Huang
✉ gshlsh2001005@126.com

†These authors have contributed equally to this work

RECEIVED 18 October 2024
ACCEPTED 21 November 2024
PUBLISHED 09 December 2024

CITATION
Qu X, Liu Y, Nie P and Huang L (2024) Association of cardiovascular-kidney-metabolic index with all-cause mortality during hospitalization in critically ill patients: a retrospective cohort study from MIMIC IV2.2. Front. Cardiovasc. Med. 11:1513212. doi: 10.3389/fcvm.2024.1513212

Association of cardiovascular-kidney-metabolic index with all-cause mortality during hospitalization in critically ill patients: a retrospective cohort study from MIMIC IV2.2

Xiaolong Qu[1†], Yuping Liu[2†], Peng Nie[1*] and Lei Huang[3*]

[1]Department of Cardiovascular Medicine, Renji Hospital, Shanghai Jiaotong University School of Medicine, Shanghai, China, [2]Department of Nutrition, Gongli Hospital of Shanghai Pudong New Area, Shanghai, China, [3]Department of Cardiology, Renji Hospital Ningbo Branch, Shanghai Jiao Tong University School of Medicine, Ningbo, China

Background: The cardiovascular-kidney-metabolic index (CKMI), a novel functional indicator proposed in this study, aims to accurately reflect the functional status of the heart, kidneys, and metabolism. However, its ability to predict mortality risk in critically ill patients during their stay in the intensive care unit (ICU) remains uncertain. Therefore, this study aims to validate the correlation between the CKMI during hospitalization and all-cause mortality.
Methods: The study utilized the Medical Information Mart for Intensive Care IV 2.2 (MIMIC-IV) dataset for a retrospective analysis of cohorts. The cohorts were divided into quartiles based on CKMI index levels. The primary endpoint was all-cause mortality during ICU and hospital stay, while secondary endpoints included the duration of ICU stay and overall hospitalization period. We established Cox proportional hazards models and employed multivariable Cox regression analysis and restricted cubic spline (RCS) regression analysis to explore the relationship between CKMI index and all-cause mortality during hospitalization in critically ill patients. Additionally, subgroup analyses were conducted based on different subgroups.
Results: The study enrolled 1,576 patients (male 60.79%). In-patient and ICU mortality was 11.55% and 6.73%. Multivariate COX regression analysis demonstrated a significant negative correlation between CKMI index and the risk of hospital death [HR, 0.26 (95% CI 0.07–0.93), $P = 0.038$] and ICU mortality [HR, 0.13 (95% CI 0.03–0.67), $P = 0.014$].RCS regression model revealed that in-hospital mortality (P-value =0.015, P-Nonlinear =0.459) and ICU mortality (P-value =0.029, P-Nonlinear =0.432) increased linearly with increasing CKMI index. Subgroup analysis confirmed consistent effect size and direction across different subgroups, ensuring stable results.
Conclusion: Our research findings suggest that a higher CKMI index is associated with a significant reduction in both in-hospital and ICU mortality among critically ill patients. Therefore, CKMI index emerges as a highly valuable prognostic indicator for predicting the risk of in-hospital death in this population. However, to strengthen the validity of these results, further validation through larger-scale prospective studies is imperative.

KEYWORDS

cardiovascular-kidney-metabolic index, in-hospital mortality, intensive care unit, MIMIC-IV database, retrospective cohort study

Introduction

The intricate interplay and significant impact of cardiovascular, renal, and metabolic functions on patient outcomes make them pivotal in critically ill individuals (1–3). Throughout the entire duration of Intensive Care Unit (ICU) stay, a comprehensive evaluation of various biomarkers and indices is regularly conducted to ascertain prognosis and guide treatment decisions. Conventional markers such as left ventricular ejection fraction (LVEF), estimated glomerular filtration rate (eGFR), and triglyceride-glucose index (TyG) have been linked to adverse outcomes in critically ill patients (4–6).

LVEF is a critical indicator of cardiac function, reflecting the proportion of blood expelled by the left ventricle with each heartbeat. As an established marker of cardiovascular health, it has demonstrated associations with mortality in various patient populations (7). The eGFR is considered to be a more precise indicator of renal function than the creatinine level alone. In patients with chronic kidney disease, a decreased eGFR is linked to adverse cardiovascular outcomes and increased mortality (8). The TyG, which represents the degree of insulin resistance, has been associated with elevated cardiovascular risk and increased mortality in individuals diagnosed with metabolic syndrome (9, 10).

In our study, we aimed to integrate three key indicators, namely LVEF, eGFR, and TyG, into a novel comprehensive index known as the Cardiovascular- Kidney- Metabolic index (CKMI). This comprehensive index is specifically designed for a thorough evaluation of cardiovascular, kidney, and metabolic functions in critically ill patients, as well as assessing the prognostic value of CKMI in predicting overall mortality during ICU hospitalization. To the best of our knowledge, this pioneering research represents the first attempt to amalgamate these three indicators into a unified index and evaluate its prognostic utility in critically ill patients. The CKMI is not simply a simplistic scoring system for physiological indicators, but rather an all-encompassing and systematic assessment tool for evaluating physiological stress and multi-organ function. It integrates crucial health indicators from the cardiovascular, renal, and metabolic systems. This interdisciplinary approach surpasses conventional scoring systems like APACHE II and SOFA (11, 12), which typically focus solely on acute physiological changes and organ failure while neglecting to fully consider the significant impact of cardiac, renal, and metabolic systems on patients' overall physiological state. By comprehensively considering multiple key physiological parameters, the CKMI can accurately identify high-risk patients and provide robust support for clinical decision-making. In comparison to traditional scoring systems, the CKMI exhibits substantial improvements in predictive accuracy and clinical applicability, thereby offering a reliable scientific foundation for patient treatment and prognosis management.

The primary objective of this retrospective cohort study is to investigate the association between serum creatine kinase levels during hospitalization and overall mortality in critically ill patients. Data analysis was conducted using the Medical Information Mart for Intensive Care IV 2.2 (MIMIC-IV) database. By utilizing this innovative biomarker to identify high-risk patients, clinicians may be able to personalize treatment strategies more effectively and enhance the prognosis of critically ill individuals.

Methods

Data source

The present study is a retrospective observational investigation, utilizing data obtained from the online international database MIMC-IV (version 2.2) (https://mimic.mit.edu). MIMC-IV represents a longitudinal single-center repository established by the Computational Physiology Laboratory at Massachusetts Institute of Technology(MIT), Beth Israel Deaconess Medical Center at Harvard Medical School(BIDMC), and Philips Medical (13). This comprehensive database encompasses information pertaining to patients admitted to BIDMC between 2008 and 2019.This dataset has undergone examination and certification to grant author (X.Q.) access (Record ID 62252237), and it is responsible for data extraction. The project has received approval from the Institutional Review Board of MIT and BIDMC. As patient health information remains anonymous in the database, individual consent is not required.

Population selection

The inclusion criteria for this study were as follows: (1) 18 years aged 80 years; (2) admission to the ICU; (3) availability of CKMI index calculation for patients; (4) ICU stay exceeding 24 h. In total, 1,576 patients were enrolled in the study and divided into four groups based on the CKMI index quartile. Please refer to Figure 1 for a detailed explanation of the research methodology.

Data extraction

The baseline patient characteristics were obtained utilizing Structured Query Language (SQL) along with PostgreSQL (version 14.2). These attributes included patient demographic details comprising of age, gender, body mass index (BMI) as well as ethnicity. Additionally, vital signs like heart rate (HR), systolic blood pressure (SBP), diastolic blood pressure (DBP), mean arterial pressure (MAP), arterial oxygen saturation (SpO2), and body temperature (T) were recorded. The severity upon admission was evaluated based on the Sequential Organ Failure Assessment (SOFA) score, Acute Physiological Score III (APS III), systemic Inflammatory response syndrome (SIRS) score, Simplified Acute Physiological Score II (SAPSII), Oxford Acute Disease Severity Score (OASIS score), and Glasgow Coma Scale (GCS score). Intravenous vasoactive agents, including dobutamine, dopamine, and norepinephrine, are utilized. Laboratory test results encompass red blood cell (RBC), white blood cell (WBC), platelet, hemoglobin level, albumin concentration, serum creatinine (Scr) level as

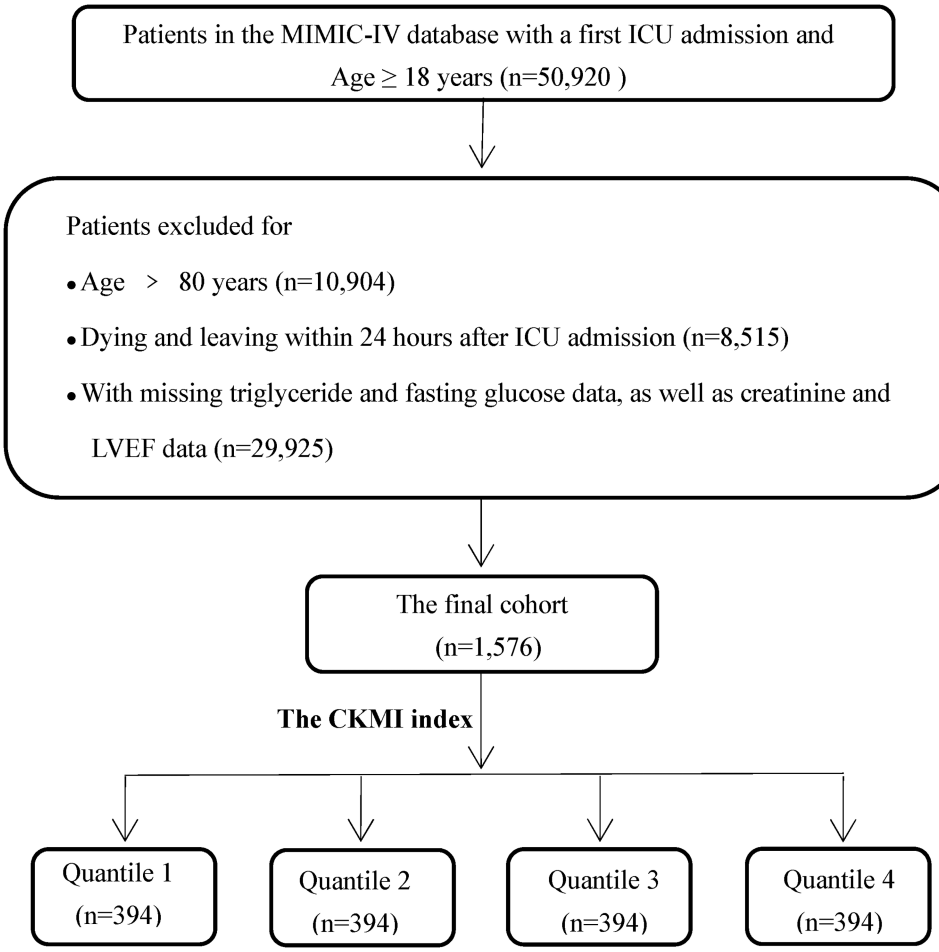

FIGURE 1
Flow chart of study participants.

well as sodium, potassium and calcium ion concentrations. Additionally included are fasting blood glucose (FBG) value; glycated hemoglobin (HbA1c) level; anion gap; triglyceride (TG); total cholesterol (TC); high-density lipoprotein cholesterol (HDL-C); low-density lipoprotein cholesterol (LDL-C); alanine aminotransferase (ALT), and aspartate aminotransferase (AST). Cardiac ultrasonography findings represent the mean values of left ventricular ejection fraction (LVEF) during intensive care unit stay.Additionally, the following comorbidities were extracted from the MIMIC-IV database: coronary heart disease (CHD), congestive heart failure (CHF), myocardial infarction (MI), hypertension, diabetes, hyperlipidemia, chronic kidney disease (CKD), acute kidney injury (AKI), chronic obstructive pulmonary disease (COPD), respiratory failure (RF), stroke, liver disease (LD), pneumonia, sepsis and cancer.

The CKMI index is calculated using the following formula:

CKMI index = In [LVEF(%) × eGFR(ml/min/1.732)/2]/ TyG Index.

The TyG index was calculated by employing the following formula, which takes into account levels of TG and FBG (14):

TyG Index = ln [TG (mg/dl) × FBG (mg/dl)/2]

Notably, the CKD-EPl equation for estimating GFR, developed in 2021 (in ml/min/1.73 m^2), does not incorporate a race coefficient (15): Female and SCr ≤0.7 mg/dl: $143 \times (SCr/0.7)^{-0.241} \times 0.9938^{age\ in\ years}$ Female and SCr >0.7 mg/dl: $143 \times (SCr/0.7)^{-1.200} \times 0.9938^{age\ in\ years}$ Male and SCr ≤0.9 mg/dl: $142 \times (SCr/0.9)^{-0.302} \times 0.9938^{age\ in\ years}$ Male and SCr >0.9 mg/dl: $142 \times (SCr/0.9)^{-1.200} \times 0.9938^{age\ in\ years}$

Primary outcomes and secondary outcomes

The primary outcomes measure of this study was the occurrence of all-cause mortality during hospitalization, encompassing both the ICU and general ward settings. Secondary outcomes included the duration of ICU stay and overall hospitalization period.

Statistical analysis

To provide a comprehensive and easily understandable representation of data distribution, we conducted an extensive

review of relevant literature and categorized CKMI into four groups based on quartiles (16). Continuous variables were reported as mean ± standard deviation (SD) or median quartile range (IQR), while categorical variables were presented as total and frequency (%). Pairwise comparison of continuous variables was conducted using Student's *t*-test, and multi-group comparison was performed using one-way ANOVA. Chi-square test was applied for pairwise comparison of categorical variables. After screening, more than 10% of variables with missing values are excluded from the analysis. For variables with missing values less than 10%, we employ multiple interpolation techniques to process and impute the missing data using the most appropriate dataset. Additionally, for variables exhibiting outliers, we apply a screening method based on the 1st and 99th percentile cutoff points. The Kaplan-Meier (K-M) curve and Cox proportional risk model were employed to assess the association between the CKMI index and the risk of in-hospital mortality. Only those variables exhibiting a significance level of $p < 0.05$ among the CKMI quartile groups were included in the multivariate model, considering baseline variables. Furthermore, multicollinearity was assessed using the variance inflation factor (VIF) to ensure independence of selected variables, with a proposed VIF value of 5 adopted based on previous research experience (17). Based on clinical expertise and relevant literature, we meticulously selected covariates that are closely associated with the research outcomes and further identified statistically significant covariates through univariate Cox regression analysis. Subsequently, three Cox proportional hazards models were constructed using the aforementioned approach: Model A, which included no adjustments; Model B, adjusted for age and BMI; and Model C, which further incorporated comorbidities such as CHD, CHF, hypertension, diabetes, stroke, sepsis, along with laboratory parameters including WBC, RBC, hemoglobin, albumin, HbA1c, and ALT in addition to the adjustments made in Model B. The association between the CKMI index and in-hospital mortality across various subgroups was examined through subgroup analysis. Additionally, the dose-response relationship between the CKMI index and mortality was investigated using restricted cubic splines (RCSs). Finally, receiver operating characteristic (ROC) curve analysis was performed to evaluate predictive ability alongside sensitivity and specificity. In addition, the effectiveness and robustness of the prediction model were evaluated through stepwise regression analysis, cross-validation analysis, as well as assessment of parameter correlation and interaction.

Results

A total of 1,576 patients were included in the study. The mean age of enrolled patients was 60.00 ± 13.45 years, with a majority being males (958; 60.79%). The mean CKMI index value for all participants was determined to be 0.81 ± 0.12 (Figure 2). In-hospital and ICU mortality rates were observed at rates of 11.55% and 6.73%, respectively.

Baseline characteristics

The baseline characteristics of the patients enrolled in this study are presented in Table 1. Patients were stratified into

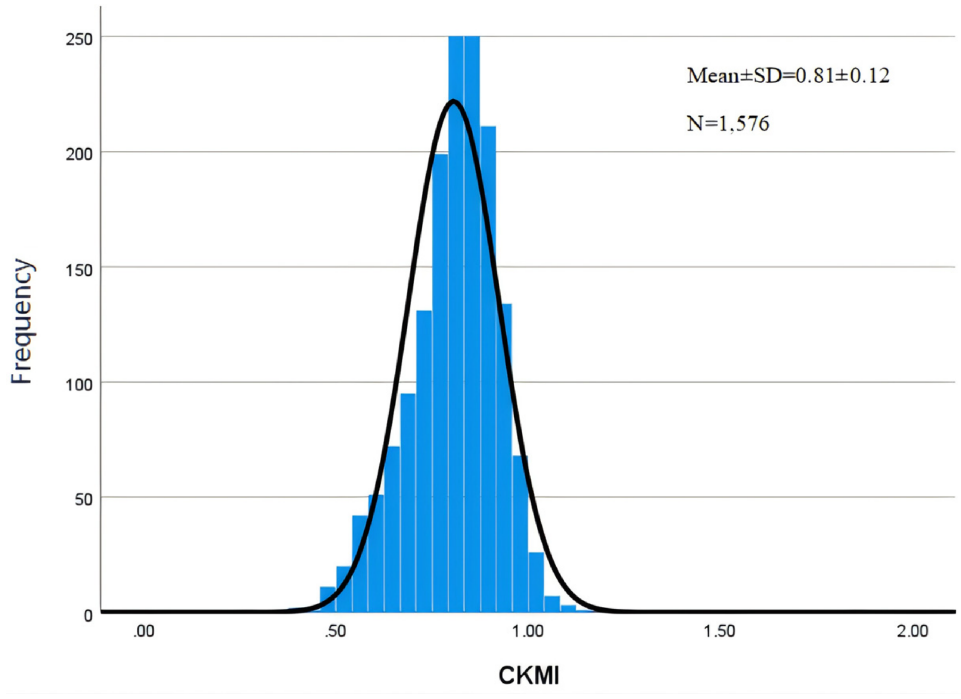

FIGURE 2
Histogram of CKMI.

10.3389/fcvm.2024.1513212

TABLE 1 Baseline characteristics of the critically ill patients stratifed by the CKMI index quartiles.

Characteristic	CKMI				*p*-value
	Q1 [0.29,0.74], *N* = 394	Q2 [0.74,0.82], *N* = 394	Q3 [0.82,0.89], *N* = 394	Q4 [0.89,1.85], *N* = 394	
Demographic					
Age, years, *n* (%)					<0.001
<60	142 (36.0%)	171 (43.4%)	171 (43.4%)	204 (51.8%)	
≥60	252 (64.0%)	223 (56.6%)	223 (56.6%)	190 (48.2%)	
Gender, *n* (%)					0.712
Female	157 (39.8%)	145 (36.8%)	160 (40.6%)	156 (39.6%)	
Male	237 (60.2%)	249 (63.2%)	234 (59.4%)	238 (60.4%)	
Ethnicity, *n* (%)					0.393
White	230 (58.4%)	256 (65.0%)	236 (59.9%)	259 (65.7%)	
Black	45 (11.4%)	30 (7.6%)	38 (9.6%)	28 (7.1%)	
Asian	8 (2.0%)	7 (1.8%)	10 (2.5%)	13 (3.3%)	
Hispanic/Latino	13 (3.3%)	15 (3.8%)	17 (4.3%)	12 (3.0%)	
Other	98 (24.9%)	86 (21.8%)	93 (23.6%)	82 (20.8%)	
Weight, kg, median [IQR]	91 (75, 107)	89 (74, 107)	81 (71, 95)	80 (67, 95)	<0.001
Height, cm, median [IQR]	170 (163, 178)	173 (163, 178)	171 (163, 176)	172 (164, 177)	0.431
BMI, kg/cm^2, *n* (%)					<0.001
<28	134 (34.0%)	148 (37.6%)	196 (49.7%)	213 (54.1%)	
≥28	260 (66.0%)	246 (62.4%)	198 (50.3%)	181 (45.9%)	
Vital signs					
HR, bpm, *n* (%)					<0.001
<80	98 (24.9%)	111 (28.2%)	149 (37.8%)	183 (46.4%)	
80–100	140 (35.5%)	157 (39.8%)	143 (36.3%)	134 (34.0%)	
≥100	156 (39.6%)	126 (32.0%)	102 (25.9%)	77 (19.5%)	
SBP, mmHg, median [IQR]	121 (104, 140)	125 (110, 144)	130 (109, 147)	130 (112, 149)	<0.001
DBP, mmHg, median [IQR]	67 (55, 80)	72 (60, 86)	72 (62, 84)	73 (63, 84)	<0.001
MBP, mmHg, median [IQR]	79 (68, 93)	85 (73, 98)	86 (75, 100)	87 (75, 99)	<0.001
SpO_2, %, median [IQR]	97.0 (94.0, 99.0)	97.0 (94.3, 100.0)	98.0 (95.0, 100.0)	98.0 (95.0, 100.0)	0.088
Severity scores					
SOFA score, median [IQR]	7.0 (4.0, 11.0)	4.0 (2.0, 8.0)	3.0 (1.0, 6.0)	2.0 (1.0, 5.0)	<0.001
APSIII score, median [IQR]	59 (44, 77)	43 (32, 59)	36 (27, 50)	33 (24, 45)	<0.001
SIRS score, median [IQR]	3.00 (2.00, 4.00)	3.00 (2.00, 3.00)	3.00 (2.00, 3.00)	2.00 (2.00, 3.00)	<0.001
SAPSII score, median [IQR]	43 (33, 54)	32 (25, 43)	29 (22, 38)	27 (20, 35)	<0.001
OASIS score, median [IQR]	35 (29, 43)	31 (26, 37)	30 (24, 37)	28 (23, 34)	<0.001
GCS score, median [IQR]	15.00 (14.00, 15.00)	15.00 (14.00, 15.00)	15.00 (14.00, 15.00)	15.00 (13.00, 15.00)	0.068
Comorbidities					
CHD, *n* (%)					0.026
No	342 (86.8%)	350 (88.8%)	361 (91.6%)	365 (92.6%)	
Yes	52 (13.2%)	44 (11.2%)	33 (8.4%)	29 (7.4%)	
CHF, *n* (%)					<0.001
No	215 (54.6%)	267 (67.8%)	285 (72.3%)	345 (87.6%)	
Yes	179 (45.4%)	127 (32.2%)	109 (27.7%)	49 (12.4%)	
MI, *n* (%)					<0.001
No	314 (79.7%)	312 (79.2%)	329 (83.5%)	352 (89.3%)	
Yes	80 (20.3%)	82 (20.8%)	65 (16.5%)	42 (10.7%)	
Hypertension, *n* (%)					<0.001
No	276 (70.1%)	207 (52.5%)	187 (47.5%)	211 (53.6%)	
Yes	118 (29.9%)	187 (47.5%)	207 (52.5%)	183 (46.4%)	
Diabetes, *n* (%)					<0.001
No	203 (51.5%)	256 (65.0%)	302 (76.6%)	352 (89.3%)	
Yes	191 (48.5%)	138 (35.0%)	92 (23.4%)	42 (10.7%)	
Hyperlipemia, *n* (%)					0.601
No	256 (65.0%)	253 (64.2%)	259 (65.7%)	270 (68.5%)	
Yes	138 (35.0%)	141 (35.8%)	135 (34.3%)	124 (31.5%)	
CKD, *n* (%)					<0.001
No	269 (68.3%)	341 (86.5%)	367 (93.1%)	384 (97.5%)	
Yes	125 (31.7%)	53 (13.5%)	27 (6.9%)	10 (2.5%)	

(*Continued*)

TABLE 1 Continued

Characteristic	CKMI				*p*-value
	Q1 [0.29,0.74], *N* = 394	Q2 [0.74,0.82], *N* = 394	Q3 [0.82,0.89], *N* = 394	Q4 [0.89,1.85], *N* = 394	
AKI, *n* (%)					<0.001
No	110 (27.9%)	206 (52.3%)	283 (71.8%)	339 (86.0%)	
Yes	284 (72.1%)	188 (47.7%)	111 (28.2%)	55 (14.0%)	
COPD, *n* (%)					0.235
No	363 (92.1%)	360 (91.4%)	373 (94.7%)	370 (93.9%)	
Yes	31 (7.9%)	34 (8.6%)	21 (5.3%)	24 (6.1%)	
RF, *n* (%)					<0.001
No	166 (42.1%)	224 (56.9%)	249 (63.2%)	284 (72.1%)	
Yes	228 (57.9%)	170 (43.1%)	145 (36.8%)	110 (27.9%)	
Stroke, *n* (%)					0.016
No	355 (90.1%)	354 (89.8%)	346 (87.8%)	329 (83.5%)	
Yes	39 (9.9%)	40 (10.2%)	48 (12.2%)	65 (16.5%)	
HD, *n* (%)					0.990
No	355 (90.1%)	357 (90.6%)	357 (90.6%)	355 (90.1%)	
Yes	39 (9.9%)	37 (9.4%)	37 (9.4%)	39 (9.9%)	
Pneumonia, *n* (%)					<0.001
No	225 (57.1%)	237 (60.2%)	255 (64.7%)	285 (72.3%)	
Yes	169 (42.9%)	157 (39.8%)	139 (35.3%)	109 (27.7%)	
Sepsis, *n* (%)					<0.001
No	249 (63.2%)	315 (79.9%)	322 (81.7%)	345 (87.6%)	
Yes	145 (36.8%)	79 (20.1%)	72 (18.3%)	49 (12.4%)	
Cancer, *n* (%)					0.458
No	361 (91.6%)	348 (88.3%)	352 (89.3%)	356 (90.4%)	
Yes	33 (8.4%)	46 (11.7%)	42 (10.7%)	38 (9.6%)	
Laboratory tests					
WBC, K/ul, median [IQR]	13 (9, 19)	12 (8, 16)	11 (8, 14)	10 (7, 13)	<0.001
RBC, m/ul, median [IQR]	3.56 (3.05, 4.21)	3.90 (3.30, 4.44)	4.04 (3.43, 4.50)	4.03 (3.48, 4.50)	<0.001
Platelet, K/ul, median [IQR]	198 (136, 261)	204 (154, 266)	209 (158, 265)	207 (159, 266)	0.067
Hemoglobin, g/dl, median [IQR]	10.50 (9.10, 12.70)	11.70 (9.80, 13.30)	12.00 (10.20, 13.60)	12.20 (10.50, 13.60)	<0.001
Albumin, g/dl, median [IQR]	3.00 (2.60, 3.50)	3.20 (2.70, 3.61)	3.36 (2.82, 3.78)	3.50 (3.00, 3.87)	<0.001
Sodium, mEq/L, median [IQR]	138.0 (134.3, 140.0)	138.0 (136.0, 141.0)	139.0 (136.0, 142.0)	139.0 (136.0, 141.0)	<0.001
Potassium, mEq/L, median [IQR]	4.40 (3.90, 4.90)	4.10 (3.70, 4.50)	4.00 (3.70, 4.30)	3.90 (3.60, 4.20)	<0.001
Calcium, mg/dl, median [IQR]	8.20 (7.60, 8.80)	8.30 (7.73, 8.90)	8.50 (7.90, 8.90)	8.50 (8.03, 9.00)	<0.001
Glucose, mg/dl, median [IQR]	172 (121, 244)	144 (116, 193)	121 (103, 147)	106 (93, 126)	<0.001
HbA1c,%,median [IQR]	6.50 (5.90, 7.63)	6.10 (5.79, 6.98)	5.86 (5.66, 6.20)	5.70 (5.50, 5.90)	<0.001
Aniongap, mEq/L, median [IQR]	18.0 (15.0, 21.0)	15.0 (13.0, 17.0)	14.0 (12.0, 16.0)	14.0 (12.0, 15.8)	<0.001
TG, mg/dl, median [IQR]	207 (131, 343)	162 (119, 230)	129 (100, 175)	84 (65, 109)	<0.001
TC, mg/dl, median [IQR]	128 (110, 158)	140 (119, 174)	146 (121, 186)	143 (123, 175)	<0.001
HDL-C, mg/dl, median [IQR]	31 (24, 38)	35 (29, 41)	37 (30, 44)	43 (35, 54)	<0.001
LDL-C, mg/dl, median [IQR]	67 (55, 84)	72 (59, 102)	77 (60, 112)	77 (60, 103)	<0.001
LT, IU/L, median [IQR]	43 (22, 102)	38 (21, 94)	34 (21, 72)	31 (18, 65)	<0.001
AST, IU/L, median [IQR]	70 (32, 186)	57 (28, 159)	47 (27, 111)	41 (24, 92)	<0.001
Creatinine, mg/dl, median [IQR]	2.00 (1.30, 3.60)	1.00 (0.80, 1.40)	0.90 (0.70, 1.10)	0.70 (0.60, 0.90)	<0.001
eGFR, ml/min/1.73^2, *n* (%)					<0.001
Stage5 <15	282 (71.6%)	82 (20.8%)	27 (6.9%)	9 (2.3%)	
Stage4 15–30	94 (23.9%)	205 (52.0%)	209 (53.0%)	136 (34.5%)	
Stage3 30–60	18 (4.6%)	105 (26.6%)	157 (39.8%)	243 (61.7%)	
Stage2 60–90	0 (0.0%)	2 (0.5%)	1 (0.3%)	5 (1.3%)	
Stage1 ≥90	0 (0.0%)	0 (0.0%)	0 (0.0%)	1 (0.3%)	
LVEF, %, *n* (%)					<0.001
<50	158 (40.1%)	103 (26.1%)	71 (18.0%)	36 (9.1%)	
≥50	236 (59.9%)	291 (73.9%)	323 (82.0%)	358 (90.9%)	
Treatment measures					
Ventilation, *n* (%)					<0.001
No	63 (16.0%)	69 (17.5%)	88 (22.3%)	117 (29.7%)	
Yes	331 (84.0%)	325 (82.5%)	306 (77.7%)	277 (70.3%)	

(*Continued*)

TABLE 1 Continued

Characteristic	CKMI				*p*-value
	Q1 [0.29,0.74], *N* = 394	Q2 [0.74,0.82], *N* = 394	Q3 [0.82,0.89], *N* = 394	Q4 [0.89,1.85], *N* = 394	
CRRT, *n* (%)					<0.001
No	294 (74.6%)	365 (92.6%)	379 (96.2%)	388 (98.5%)	
Yes	100 (25.4%)	29 (7.4%)	15 (3.8%)	6 (1.5%)	
Dobutamine, *n* (%)					<0.001
No	355 (90.1%)	383 (97.2%)	387 (98.2%)	393 (99.7%)	
Yes	39 (9.9%)	11 (2.8%)	7 (1.8%)	1 (0.3%)	
Dopamine, *n* (%)					<0.001
No	358 (90.9%)	373 (94.7%)	378 (95.9%)	382 (97.0%)	
Yes	36 (9.1%)	21 (5.3%)	16 (4.1%)	12 (3.0%)	
Norepinephrine, *n* (%)					<0.001
No	200 (50.8%)	275 (69.8%)	290 (73.6%)	339 (86.0%)	
Yes	194 (49.2%)	119 (30.2%)	104 (26.4%)	55 (14.0%)	
Events					
LOS Hospital, days, median [IQR]	17 (8, 28)	12 (6, 26)	10 (4, 21)	9 (5, 20)	<0.001
LOS ICU, days, median [IQR]	7 (3, 13)	4 (2, 10)	3 (1, 9)	3 (2, 5)	<0.001
Hospital mortality, *n* (%)					<0.001
No	317 (80.5%)	348 (88.3%)	360 (91.4%)	369 (93.7%)	
Yes	77 (19.5%)	46 (11.7%)	34 (8.6%)	25 (6.3%)	
ICU mortality, *n* (%)					<0.001
No	344 (87.3%)	366 (92.9%)	380 (96.4%)	380 (96.4%)	
Yes	50 (12.7%)	28 (7.1%)	14 (3.6%)	14 (3.6%)	

CKMI, cardiovascular-kidney-metabolic index; BMI, body mass index; HR, heart rate; SBP, systolic blood pressure; DBP, diastolic blood pressure; MBP, mean blood pressure; SOFA, sequential organ failure assessment; APSIII, acute physiology score III; SIRS, systemic infammatory response syndrome; SAPSII, simplifed acute physiological score II; OASIS, oxford acute severity of illness score; GCS, Glasgow coma scale; CHD, Coronary Heart Disease; CHF, congestive heart failure; MI, myocardial infarction; CKD, chronic renal failure; AKI, acute kidney injury; COPD, chronic obstructive pulmonary disease; RF, respiratory failure; HD, hepatic disease; WBC, white blood cell; RBC, red blood cell; HbA1c, hemoglobin A1c; TG, triglyceride; TC, total cholesterol; HDL, high density lipoprotein; LDL, low density lipoprotein; ALT, alanine aminotransferase; AST, aspartic transaminase; eGFR, estimated glomerular filtration rate; CRRT, continuous renal replacement therapy; LOS, length of stay; ICU, Intensive Care Unit.

quartiles based on their admission CKMI index(Q1: 0.29–0.74; Q2: 0.74–0.82; Q3: 0.82–0.89; Q4: 0.89–1.85), with mean CKMI levels for each group being 0.65 ± 0.07, 0.78 ± 0.02, 0.85 ± 0.02, and 0.94 ± 0.06, respectively. Compared to the high-value group, patients with a lower CKMI index generally exhibit advanced age and higher BMI. In terms of vital signs upon admission, they present with an elevated heart rate, decreased blood pressure, and reduced SpO2 levels. The severity of disease at admission is also heightened, accompanied by an increased incidence of complications such as CHD, CHF, MI, diabetes, CKD, AKI, RF, pneumonia, sepsis, etc. Furthermore, there are significant elevations in WBC, serum potassium, Serum creatinine concentration, and FBG level; HbA1c content and anion gap are also notably increased. TC levels and ALT/AST enzyme activities are all elevated. Mechanical ventilation demand and CRRT treatment requirement escalate while rescue drug application frequency rises accordingly. However, these patients demonstrate a decreasing trend in the incidence of hypertension and stroke accidents. Additionally noted trends include decreased RBC, platelet, hemoglobin as well as albumin content reduction. Simultaneously observed are lower serum sodium concentration and serum calcium level along with diminished TC levels including HDL-C and LDL-C, finally yet importantly worth mentioning is the decrease in eGFR and LVEF. Moreover, with an increase in the CKMI index, there is a gradual decrease observed in the duration of ICU stay (7 days vs. 4 days vs. 3 days vs. 3 days, $P < 0.001$), length of hospitalization (17 days vs. 12 days vs. 10 days vs. 9 days, $P < 0.001$), all-cause ICU mortality (12.7% vs. 7.1% vs. 3.6% vs. 3.6%, $P < 0.001$) and in-hospital mortality (19.5% vs. 11.7% vs. 8.6% vs. 6.3%, $p < 0.001$).

Primary outcomes

In this study, we constructed three Cox proportional hazards models to investigate the association between the CKMI index and in-hospital mortality as well as ICU mortality. The results demonstrated significant negative correlations between the continuous CKMI index and both in-hospital mortality [Model A: HR, 0.25 [95% CI 0.08–0.77], $P = 0.016$; Model B: HR, 0.25 [95% CI 0.08–0.76], $P = 0.015$; Model C: HR, 0.26 [95% CI 0.07–0.93], $P = 0.038$] and ICU mortality [Model A: HR, 0.14 [95% CI 0.03–0.59], $P = 0.008$; Model B: HR, 0.15 [95% CI 0.03–0.62], $P = 0.009$; Model C: HR, 0.13 [95% CI 0.03–0.67], $P = 0.014$] across all three models, unadjusted Model A, partially adjusted Model B, and fully adjusted Model C. Notably, in model C where adjustments were made for variables related to population characteristics and confounding factors, each one-standard-deviation increase in CKMI led to a remarkable 74% reduction in in-hospital mortality and 87% reduction in ICU mortality.

When considering the CKMI index as a categorical variable, there was no significant association observed between the CKMI index and hospitalization or ICU mortality in Group Q2 compared to the lowest quartile (Group Q1) across all three Cox proportional risk models. However, a significant correlation was found in Groups Q3 and Q4, indicating that higher quartile arrays were associated with lower risks when compared to lower quartile arrays. In Model C, following comprehensive adjustment for potential confounders, CKMI index Q3 and Q4 exhibited a significantly decreased risk of hospital mortality compared to CIMI index Q1 [Q1 vs. Q3: HR, 0.71 [95% CI 0.45–0.91], $P = 0.023$; Q4: HR, 0.53 [95% CI 0.32–0.87], $P = 0.012$]. Furthermore, there was an inverse correlation between the increase in CKMI index value and the escalation of risk level. Cox proportional hazards analysis was employed to investigate the association between CKMI index and ICU mortality, yielding consistent findings [Q1 vs. Q3: HR, 0.42 [95% CI 0.22–0.79], $P = 0.007$; Q4: HR, 0.44 [95% CI 0.23–0.85], $P = 0.014$] (refer to Table 2).

The incidence of major outcomes in each group, based on the CKMI index quartile, was analyzed using Kaplan-Meier survival analysis curve as depicted in Figure 3. Patients with a higher CKMI index exhibited a decreased risk of hospitalization and ICU mortality.

In the fully adjusted model C, a restricted cubic spline regression model was employed to demonstrate a consistent linear decline in both hospital mortality (P-value = 0.015, P-Nonlinear = 0.459) and ICU mortality (P-value = 0.029, P-Nonlinear = 0.432) as the CKMI index increased (Figure 4).

ROC analysis of the CKMI index and its comparison with established severity scores

The clinical efficacy of the CKMI index was evaluated using ROC analysis, revealing that the CKMI index exhibited a certain predictive value (AUC for in-hospital death: 0.635; AUC for ICU death: 0.658). The cutoff values for the CKMI index were determined as 0.825 and 0.794 for hospital deaths and ICU deaths respectively (Figure 5).

In order to conduct a more rigorous evaluation of the predictive performance of CKMI, we compared ROS analysis with established severity scoring tools such as SOFA, APSIII, and SIRS. In terms of predicting mortality in the ICU, CKMI exhibited a lower AUC value compared to established severity scores such as SOFA [0.759 (95% CI 0.716–0.802), $P < 0.001$], APSIII [0.796 (95% CI 0.753–0.839), $P < 0.001$], and SAPSII [0.775 (95% CI 0.732–0.818), $P < 0001$]. However, it demonstrated a significantly higher AUC value than OASIS [0.621 (95% CI 0.581–0.670), $P = 0.043$] and GCS 0.476 (95% CI 0.423–0.530, $P < 0001$)], while showing no statistical difference with SIRS [0.654 (95% CI 0.607–0.702), $p = 0.923$] (refer to Table 3).

In the prediction of hospital mortality rate, CKMI exhibited a lower AUC value compared to established severity scores such as SOFA [0.728 (95% CI 0.692–0.764), $P < 0.001$], APSIII [0.766 (95% CI 0.732–0.801), $P < 0.001$], and SAPSII [0.774 (95% CI 0.742–0.805), $P < 0001$]. However, it demonstrated a significantly higher AUC value than OASIS [0.605 (95% CI 0.545–0.659), $P = 0.039$] and GCS [0.459 (0.418–0.500), $P < 0001$], with no statistically significant difference observed when compared to SIRS [0.624 (95% CI 0.585–0662), $P = 0.698$] (refer to Table 3).

Secondary outcomes

The results of multiple linear regression analysis revealed a significant negative correlation between the CKMI index and the length of stay in both ICU and general wards, even when not adjusting for confounding factors (LOS Hospital: $\beta = -24.05$, $P < 0.001$; LOS ICU: $\beta = -14.51$, $P < 0.001$) (refer to Table 4). This association remained consistent among hospitalized patients, even after partial (LOS Hospital: $\beta = -25.99$, $P < 0.001$; LOS ICU: $\beta = -14.69$, $P < 0.001$) or complete adjustment for confounders (LOS Hospital: $\beta = -9.40$, $P = 0.031$; LOS ICU: $\beta = -7.83$, $P < 0.001$) (refer to Table 4). These findings suggest that higher levels of CKMI may be indicative of longer hospital stays, thereby highlighting its potential as an effective indicator for assessing resource utilization in ICUs or hospitals, particularly in predicting critically ill patients who require extended periods of hospitalization.

TABLE 2 Cox proportional hazard ratios (HR) for all-cause mortality.

Variables	Q1		Q2		Q3		Q4		CKMI	
	HR (95% CI)	*p*-value	HR (95% CI)	*p*-value	HR (95% CI)	*p*-value	HR (95% CI)	*p*-value	HR (95% CI)	*p*-value
Hospital mortality										
Model A	Ref.	–	0.75 (0.52, 1.08)	0.127	0.71 (0.47, 0.95)	0.035	0.58 (0.37, 0.91)	0.017	0.25 (0.08,0.77)	0.016
Model B	Ref.	–	0.74 (0.51, 1.06)	0.102	0.67 (0.45, 0.97)	0.042	0.54 (0.34, 0.85)	0.008	0.25 (0.08,0.76)	0.015
Model C	Ref.	–	0.75 (0.51, 1.11)	0.150	0.71 (0.45, 0.91)	0.023	0.53 (0.32, 0.87)	0.012	0.26 (0.07,0.93)	0.038
ICU mortality										
Model A	Ref.	–	0.72 (0.45, 1.15)	0.166	0.46 (0.25, 0.83)	0.010	0.52 (0.29, 0.93)	0.029	0.14 (0.03,0.59)	0.008
Model B	Ref.	–	0.71 (0.45, 1.13)	0.151	0.44 (0.24, 0.81)	0.008	0.49 (0.27, 0.88)	0.018	0.15 (0.03,0.62)	0.009
Model C	Ref.	–	0.74 (0.45, 1.21)	0.234	0.42 (0.22, 0.79)	0.007	0.44 (0.23, 0.85)	0.014	0.13 (0.03,0.67)	0.014

HRs, hazard ratios; CI, confidence interval; CKMI, cardiovascular-kidney-metabolic index; ICU, intensive care unit; BMI, body mass index; CHD, coronary heart disease; CHF, congestive heart failure; WBC, white blood cell; RBC, red blood cell; HbA1c, hemoglobin A1c; ALT, alanine aminotransferase. Model A: unadjusted covariates. Model B: adjusted by age and BMI. Model C: adjusted by age, BMI, CHD, CHF, hypertension, diabetes, stroke, sepsis, WBC, RBC, hemoglobin, albumin, HbA1c, and ALT.

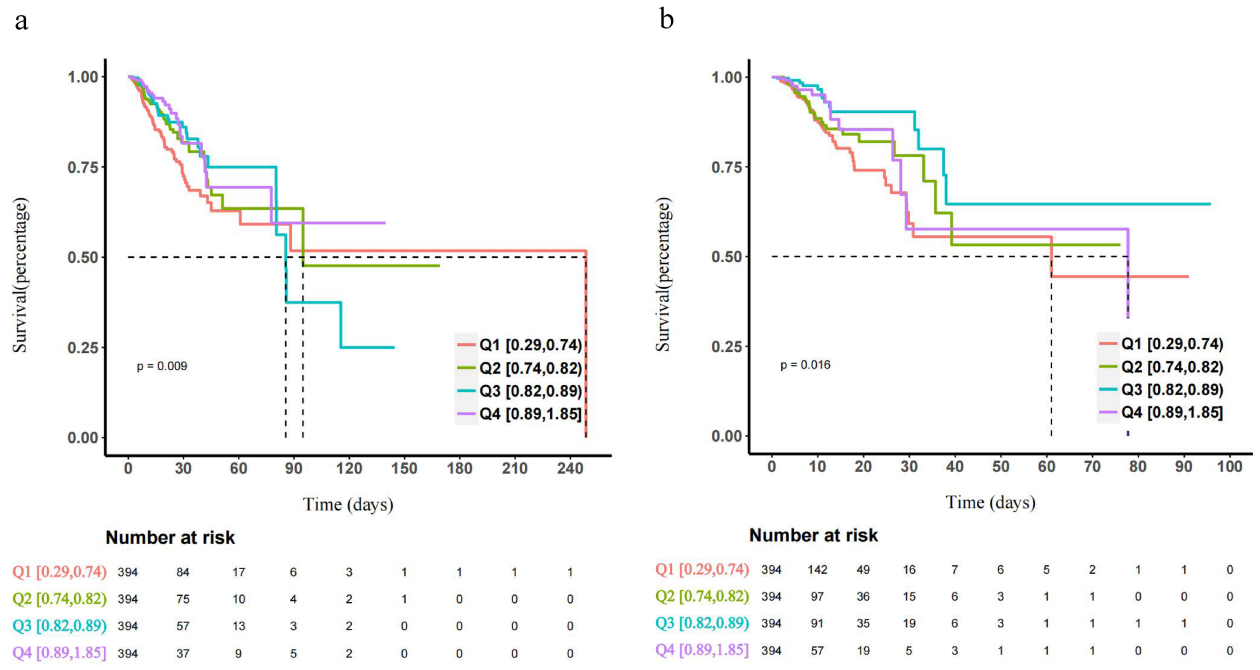

FIGURE 3
The Kaplan-Meier survival analysis curves depict the cumulative probability of all-cause mortality in quartile groups within the hospital (**a**), and ICU (**b**).

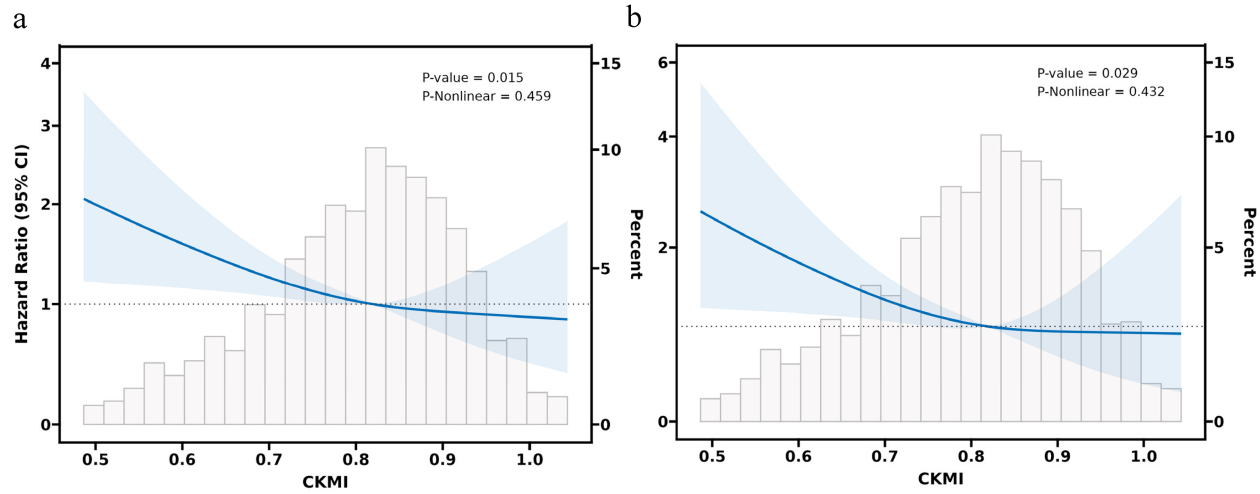

FIGURE 4
RCS analysis was conducted to examine the association between CKMI and all-cause mortality in both hospital and ICU settings. (**a**) The RCS curve illustrates the relationship between CKMI and all-cause hospital mortality. (**b**) The RCS curve demonstrates the correlation between CKMI and ICU mortality.

Subgroup analysis

To further investigate potential disparities within the specific population, we conducted Cox regression analysis on various subgroups, encompassing crucial variables including age, gender, ethnicity, BMI ≥28, hypertension, diabetes, CHD, and CHF. By constructing subgroup forest plots, several noteworthy findings were revealed:

Upon further examination of the relationship between the CKMI index and ICU mortality, we observed a significant inverse association in specific subgroups including individuals aged ≥60 years [HR, 0.06 (95% CI 0.02–0.18), $P = 0.001$], females [HR, 0.04 (95% CI 0.01–0.62), $P = 0.021$], white ethnicity [HR, 0.35 (95% CI 0.21–0.82), $P = 0.027$], diabetic patients [HR, 0.05 (95% CI 0.02–0.27), $P = 0.008$], and those with CHD [HR, 0.11 (95% CI 0.02–0.63), $P = 0.014$]. In contrast, no such correlation

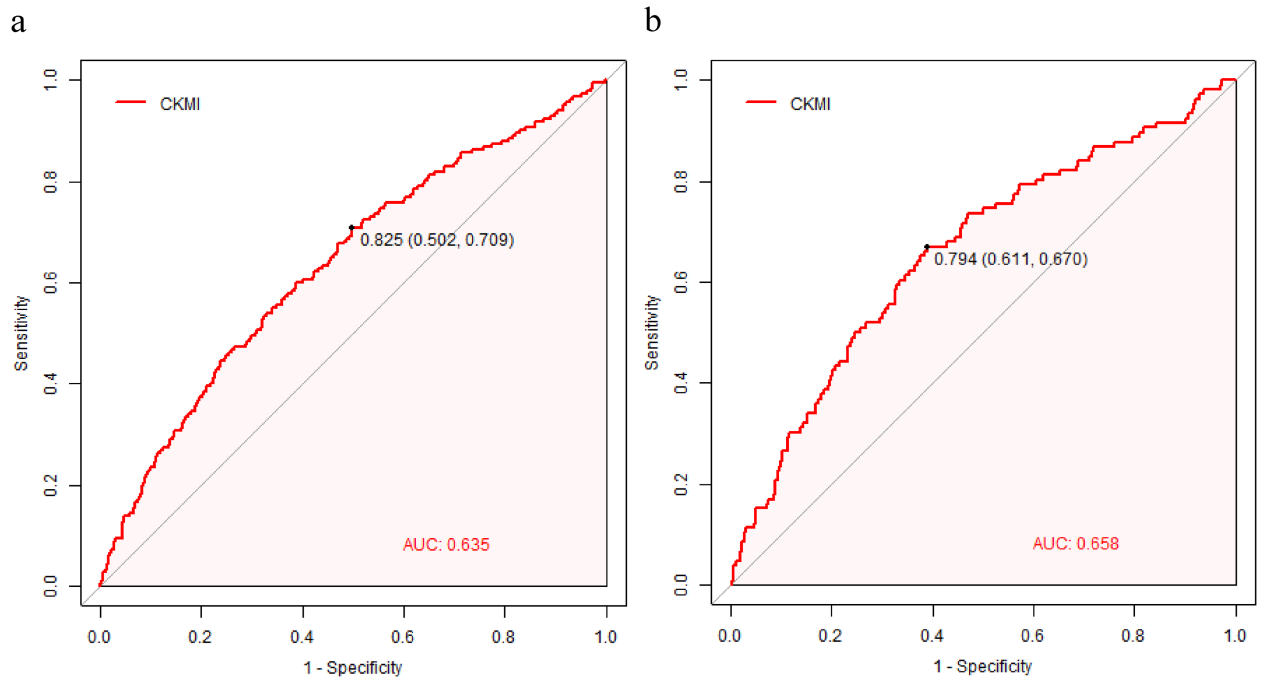

FIGURE 5
The CKMI correlation ROC curve for predicting in-hospital (a) and ICU mortality (b).

TABLE 3 ROC analysis of the CKMI index and its comparison with established severity scores.

Predictor	ICU mortality AUC (95% CI)	The *p*-value compared to CKMI	Hospital mortality AUC (95% CI)	The *p*-value compared to CKMI
CKMI	0.658 (0.602–0.714)	–	0.635 (0.591–0.679)	–
SOFA	0.759 (0.716–0.802)	$P < 0.001$	0.728 (0.692–0.764)	$P < 0.001$
APSIII	0.796 (0.753–0.839)	$P < 0.001$	0.766 (0.732–0.801)	$P < 0.001$
SIRS	0.654 (0.607–0.702)	$P = 0.923$	0.624 (0.585–0.662)	$P = 0.698$
SAPSII	0.775 (0.732–0.818)	$P < 0.001$	0.774 (0.742–0.805)	$P < 0.001$
OASIS	0.621 (0.581–0.670)	$P = 0.043$	0.605 (0.545–0.659)	$P = 0.039$
GCS	0.476 (0.423–0.530)	$P < 0.001$	0.459 (0.418–0.500)	$P < 0.001$

TABLE 4 The correlation between the CKMI index and length of hospital stay (LOS).

Characteristic	β	95% CI	*p*-value
LOS Hospital			
Model A	−24.05	−32.01, −16.10	<0.001
Model B	−25.99	−34.05, −17.93	<0.001
Model C	−9.40	−17.95, −0.85	0.031
LOS ICU			
Model A	−14.51	−18.62, −10.40	<0.001
Model B	−14.69	−18.83, −10.56	<0.001
Model C	−7.83	−12.32, −3.34	<0.001

CI, confidence interval; CKMI, cardiovascular-kidney-metabolic index; ICU, intensive care unit; BMI, body mass index; CHD, coronary heart disease; CHF, congestive heart failure; WBC, white blood cell; RBC, red blood cell; HbA1c, hemoglobin A1c; ALT, alanine aminotransferase. Model A: unadjusted covariates. Model B: adjusted by age and BMI. Model C: adjusted by age, BMI, CHD, CHF, hypertension, diabetes, stroke, sepsis, WBC, RBC, hemoglobin, albumin, HbA1c, and ALT.

was detected when comparing diabetic vs. non-diabetic patients, patients with BMI <28 vs. ≥28, hypertensive vs. non-hypertensive patients, and those with CHF compared to those without (Figure 6).

Among subgroups of individuals aged ≥60 years [HR, 0.04 (95% CI 0.01–0.27), $P = 0.001$], females [HR, 0.12 (95% CI 0.01–0.92), $P = 0.042$], white ethnicity [HR, 0.36 (95% CI 0.09–0.76), $P = 0.043$], those with a BMI ≥28 [HR, 0.17 (95% CI 0.03–0.99), $P = 0.048$], hypertensive patients [HR, 0.07 (95% CI 0.02–0.94), $P = 0.045$], diabetic patients [HR, 0.05 (95% CI 0.01–0.16), $P = 0.001$], and patients with CHF [HR, 0.14 (95% CI 0.03–0.70), $P = 0.016$], a significant inverse correlation was observed between the CKMI index and hospital mortality. However, it is important to note that no association between the CKMI index and hospital mortality was found when comparing patients with and without CHD (Figure 6).

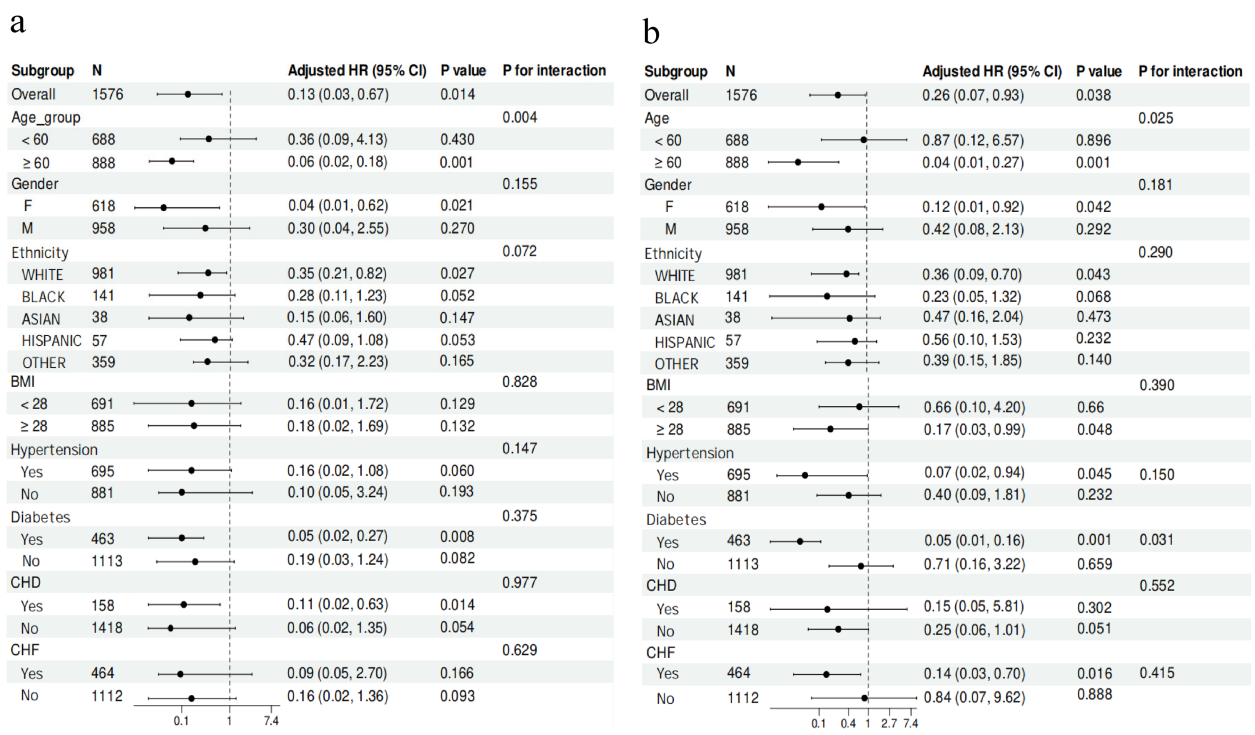

FIGURE 6
Subgroup analysis for the correlation between the CKMI index and the risk of ICU (**a**) and in-hospital (**b**) mortality in critically ill patients.

Additionally, our study has revealed significant interactions between the CKMI index and other variables. Specifically, in terms of influencing hospital mortality, the CKMI index demonstrated noteworthy interactions with age (*P* for interaction = 0.025) and diabetes (*P* for interaction = 0.031). Similarly, when investigating factors impacting ICU mortality, a substantial interaction between the CKMI index and age (*P* for interaction = 0.004) was also observed (Figure 6).

In summary, this study provides robust evidence for comprehending the relationship between the CKMI index, diverse patient characteristics, and their clinical outcomes through meticulous subgroup analysis and exploration of interactions.

The assessment of model value

We utilized stepwise regression analysis and cross-validation to assess the model, yielding a coefficient of determination (R-squared) of 0.9157, indicating that the model can account for 91.57% of the variability in the data. This outcome holds great significance, suggesting a robust fit and effective explanation of CKMI variations by the model. The mean squared error (MSE) was determined to be 0.0012, signifying minimal deviation between predicted values and actual values, thereby demonstrating high predictive accuracy. The stepwise regression analysis identified eGFR, TyG, and LVEF as pivotal variables within the model with statistically significant effects on CKMI (p-value < 0.05). Further cross-validation analysis revealed that among all tested models, the combination of three variables—LVEF + eGFR + TyG—achieved an exceptional R-squared score of 0.9038, indicating superior predictive performance compared to single parameter prediction models (LVEF, eGFR, TyG) or simple combination prediction models (LVEF + eGFR, LVEF + Tyg, eGFR + TyG). Moreover, it was observed that eGFR and TyG made substantial contributions towards predicting CKMI while LVEF played a relatively smaller role.

Discussion

In this study, we introduced the CKMI as a novel functional indicator and validated its predictive validity for in-hospital and ICU all-cause mortality in critically ill patients using the extensive clinical database MIMIC-IV. CKMI, encompassing LVEF, eGFR, and metabolic index TyG, aims to comprehensively reflect the status of heart, kidney, and metabolic functions. The findings demonstrated a significant inverse correlation between CKMI and both in-hospital and ICU mortality, highlighting its potential as an important prognostic marker for predicting the risk of in-hospital mortality among critically ill patients.

As a crucial component of the CKMI index, LVEF serves as a pivotal indicator for assessing cardiac systolic function. Its decline typically heralds CHF or cardiac dysfunction, which are significant contributors to heightened in-hospital mortality (18). Numerous studies have demonstrated a strong association between reduced

LVEF and the risk of cardiovascular events such as heart failure and myocardial infarction (7, 19). In critically ill patients, impaired cardiac function often results in inadequate circulating blood volume, subsequently compromising organ perfusion throughout the body and escalating the likelihood of death (20–22). Consequently, evaluating cardiac function through LVEF can indirectly reflect circulatory status and mortality risk among critically ill patients. A higher CKMI index signifies that individuals with superior cardiac function can endure greater physiological stress levels, thereby reducing hospitalization-related mortality.

As another crucial component of the CKMI index, eGFR is considered the gold standard for evaluating renal filtration function, and its decline often indicates renal function impairment (23). The kidney not only plays a pivotal role in waste excretion and fluid balance regulation but also actively participates in various physiological activities, including hormone secretion and blood pressure regulation (24–26). In critically ill patients, AKI is a common complication closely associated with mortality. AKI not only leads to the accumulation of metabolic waste and toxins in the body but also gives rise to significant issues such as electrolyte imbalances and acid-base disturbances, further exacerbating the patient's condition (27–29). Therefore, utilizing the CKMI index to assess renal function through eGFR can effectively predict the risk of death resulting from impaired renal function in critically ill patients.

The TyG index is a novel metabolic indicator that integrates levels of TG and FPG to assess insulin resistance and the risk of metabolic syndrome (30). In critically ill patients, metabolic dysfunction is a prevalent pathophysiological state closely associated with mechanisms such as inflammatory response and oxidative stress (31, 32). The TyG index serves as a valuable tool for evaluating metabolic status, with recent studies demonstrating its significant association with cardiovascular diseases (33), strokes (34), kidney diseases (35), and other pathological conditions (36–38). Moreover, emerging evidence suggests that the TyG index holds promise in predicting overall mortality and cardiovascular disease-specific mortality among the general population and critically ill patients (14, 39–41). A high CKMI index indicates a relatively favorable metabolic condition in patients, thereby reducing the likelihood of complications arising from metabolic abnormalities and consequently lowering in-hospital mortality.

The CKMI index is a comprehensive physiological health evaluation system that assesses cardiac function, renal function, and metabolic status in a holistic manner. In critically ill patients, these three aspects of functional status are intricately interconnected and mutually influential, collectively determining the prognosis of patients (4–6). CHF can result in circulatory disorders, which subsequently impact renal perfusion and metabolite clearance (42). Renal insufficiency may lead to toxin accumulation in the body, thereby increasing the burden on the heart and causing metabolic disturbances (43). Metabolic abnormalities can accelerate the progression of cardiovascular and renal diseases (44). Therefore, by simultaneously considering the key systems of the heart, kidney, and metabolism, the CKMI index achieves a comprehensive assessment of overall bodily function. In critically ill patients specifically, interdependencies among these three systems often exist and jointly determine patient outcomes. Consequently, utilizing the CKMI index enables a more comprehensive reflection of a patient's physiological state while enhancing prediction accuracy.

Currently, the prediction of in-hospital mortality for critically ill patients primarily relies on various models such as APACHE II score, SAPS II score, and SOFA score (45–47). However, these models predominantly rely on physiological parameters and medical history information for prediction. For instance, the APACHE II score focuses on assessing acute physiological status and chronic health conditions (45), while SOFA specifically evaluates sequential organ failure but often overlooks a comprehensive assessment of cardiac, renal, and metabolic states (47). CKMI offers a more comprehensive perspective by integrating indicators of cardiac, renal, and metabolic health to evaluate the physiological stress and multi-organ functional status of ICU patients. It may possess unique advantages in predicting ICU and in-hospital mortality rates. Metabolic status is a crucial indicator that reflects the body's energy metabolism and substance metabolism, which is closely associated with the development of various diseases. Previous studies have demonstrated that metabolic abnormalities, such as hyperglycemia and hypoalbuminemia, play a significant role in predicting adverse outcomes among ICU and hospitalized patients (48, 49). Therefore, incorporating metabolic status into scoring models aids in accurately assessing overall patient health and predicting unfavorable results. By comparing and analyzing different approaches, CKMI stands out for its uniqueness and innovation in integrating biological indicators like metabolic status. Traditional models often overlook these essential metabolic markers; however, they hold great significance when considering overall patient health and forecasting adverse outcomes. CKMI can more precisely reflect the comprehensive metabolic status of patients by including these metabolic indicators, thereby greatly contributing to clinical treatment guidance and patient prognosis assessment. In comparison to traditional scoring systems, CKMI provides a more comprehensive framework that assists clinicians in early identification of high-risk patients while developing personalized treatment plans. Moreover, the multidimensional comprehensive evaluation offered by CKMI may contribute to enhancing risk stratification and management strategies within complex ICU environments encompassing multiple variables.

Additionally, our study revealed a significant inverse correlation between CKMI levels and LOS in both the ICU and general wards, suggesting that patients with lower CKMI levels may necessitate prolonged hospitalization. The significant association between CKMI and LOS provides valuable insights into the utilization of ICU or hospital resources. Initially, patients exhibiting reduced levels of CKMI might require extended hospitalization and continuous monitoring, which could consequently increase the utilization of ICU or hospital resources. Consequently, by monitoring CKMI levels, we can promptly identify individuals who may require additional

resources to ensure timely and effective treatment interventions. Secondly, the correlation between CKMI and LOS also implies that optimizing treatment strategies could potentially mitigate the adverse impact of CKMI on LOS, thus reducing patients' length of stay in hospitals and minimizing resource utilization.

Finally, we observed overlapping Kaplan-Meier curves between Q2 and Q3, as well as between Q3 and Q4. After a thorough examination of the data and analysis process, we posit that the overlap of the curves may be attributed to several key factors: firstly, due to limited research resources in the database study, there might not be an adequate sample size to fully demonstrate significant differences in survival rates among different CKMI quartiles (Q1-Q4), despite efforts made to include a sufficient number of patients. The small sample size could result in less distinct differences between survival curves leading to overlapping phenomena. Secondly, heterogeneity exists within the patient population studied in terms of age, gender, underlying diseases, etc., which may cause variations in response to CKMI index among different patients and partially mask its predictive effect on survival rates for specific patient subgroups. Furthermore, the duration of follow-up can also impact the degree of separation between survival curves. If the follow-up time is insufficiently long enough, it may fail to capture significant differences in patient survival rates particularly at early stages. It should be emphasized that despite this phenomenon of overlap occurring; however,the CKMI index still retains certain predictive value especially for specific patient populations.

Moreover, in the subgroup analysis, a significant inverse association between CKMI and mortality risk was observed among female patients., while this correlation was not evident in male patients. Although the specific mechanisms are not fully understood, it is speculated that they may be attributed to several factors. Firstly, fluctuations in levels of sex hormones such as estrogen in women may exert profound effects on metabolic processes (50). estrogen exhibits anti-inflammatory, antioxidant, and cardiovascular protective effects which could potentially influence the relationship between CKMI and mortality risk among women (51). Secondly, females typically possess higher metabolism rates and distinct patterns of fat distribution which might contribute to more rapid elimination of metabolic waste and toxins from the body thereby alleviating metabolic stress; consequently impacting the association between CKMI and mortality risk (52). Additionally,females exhibit different biological characteristics and prognosis disparities compared to males when it comes to certain severe illnesses; these differences might result in a higher predictive value for CKMI among women (53, 54). In summary, an elevated CKMI during early stages reflects compensatory capacity of the body; whereas an elevation during later stages primarily indicates degree of organ failure. This variation could lead to gender-specific differences regarding predictive value of CKMI.Additionally, In order to investigate the disparities in metabolic capacity and predictive ability across different racial groups, we conducted a subgroup analysis based on the racial composition of the population. The findings revealed that CKMI exhibited a significant prognostic capability for mortality risk among Caucasians, while its efficacy was not observed in other ethnicities. Several potential factors may account for this discrepancy: firstly, substantial genetic and biological variations exist among diverse races, which could influence the association between CKMI and mortality risk (55); secondly, disparities in environmental factors and lifestyles might also impact the predictive performance of CKMI (56); additionally, critically ill patients from different racial backgrounds may exhibit distinct disease characteristics and patterns of complications, thereby affecting the applicability of CKMI as a prognostic indicator (57). It is important to note that due to relatively small sample sizes within other ethnic groups, statistical power is limited. Consequently, it is possible that statistically significant associations may go undetected even if they do indeed exist.

The CKMI index holds significant clinical application value, providing crucial prognostic information for patients in the early stages of ICU admission. For individuals with a low CKMI index, doctors can promptly implement intervention measures such as adjusting treatment plans and enhancing monitoring to mitigate the risk of mortality. Moreover, the CKMI index effectively reflects patient-specific differences and serves as a foundation for formulating personalized treatment strategies. Additionally, it allows dynamic adjustments based on changes in a patient's condition, offering an ongoing evaluation framework for physicians. Regular monitoring of the CKMI index enables timely modifications to treatment plans, ensuring optimal therapeutic outcomes for patients.

Limitations

Despite the positive findings obtained in this study, several limitations should be acknowledged. Firstly, it is important to note that this study employed a retrospective analysis approach, which may introduce potential selection bias and information bias. Secondly, the accuracy of indicators such as LVEF, eGFR, and TyG upon which the calculation of CKMI index relies can be influenced by various factors. Moreover, it is worth mentioning that this study did not account for the impact of underlying diseases and treatment interventions on both CKMI index and in-hospital mortality.

Based on previous literature, we excluded patients aged ≥80 years due to potential physiological changes and differences in drug metabolism that may impact the interpretation of CKMI in elderly patients. Additionally, patients with ICU stays of less than 24 h were also excluded to mitigate the risk of missing data or inaccurate measurement of CKMI associated with shorter ICU stays. However, it is acknowledged that these exclusion criteria may limit the generalizability of our findings. Future studies are planned to investigate the performance of CKMI across different age groups and in patients experiencing rapid deterioration or early death within 24 h of ICU admission, aiming to enhance its applicability in diverse ICU patient populations.

Furthermore,we acknowledge the significance of dissecting the constituents of CKMI-related mortality rates to augment the

efficacy of this study. This not only facilitates deeper insights but also fosters a comprehensive comprehension of the correlation between CKMI and mortality rates. Nevertheless, a major constraint of this study lies in our inability to procure specific cause-of-death information from the MIMIC database. This limitation curtails our capacity to conduct meticulous analyses on mortality rates associated with distinct components of CKMI (cardiovascular-related deaths, renal failure-related deaths, metabolic disease-related deaths). In prospective clinical studies, we intend to incorporate more participants who can furnish detailed records regarding causes of death so as to further investigate the relationship between CKMI and various causes of death.

To further validate the predictive efficacy of the CKMI index, future research should consider adopting a prospective design, increasing sample size, and incorporating additional influencing factors. Moreover, it is worth exploring the predictive value of the CKMI index in various disease types and age groups of patients, as well as investigating its potential synergistic effects when combined with other prediction models. Furthermore, studying the role of the CKMI index in informing treatment decision-making for critically ill patients can optimize clinical management plans.

Conclusion

In summary, this study utilized the MIMIC-IV database to comprehensively investigate the efficacy of the CKMI index in predicting overall mortality during hospitalization for critically ill patients. The findings demonstrate a significant inverse association between the CKMI index and all-cause mortality within both hospitalization and ICU settings, suggesting its potential as a robust tool for prognosticating in-hospital death risk among critically ill patients. By integrating comprehensive assessments of cardiac function, renal function, and metabolic status, the CKMI index establishes a holistic physiological health evaluation system that offers clinicians more precise predictive evidence and personalized treatment guidance. However, further prospective studies with larger sample sizes are warranted to validate its predictive efficacy and clinical applicability.

Data availability statement

Publicly available datasets were analyzed in this study. This data can be found here: https://mimic.mit.edu/.

Ethics statement

The studies involving humans were approved by the Computational Physiology Laboratory at Massachusetts Institute of Technology (MIT), Beth Israel Deaconess Medical Center at Harvard Medical School (BIDMC). The studies were conducted in accordance with the local legislation and institutional requirements. The participants provided their written informed consent to participate in this study.

Author contributions

XQ: Conceptualization, Data curation, Formal Analysis, Writing – original draft. YL: Formal Analysis, Investigation, Methodology, Project administration, Visualization, Writing – review & editing. PN: Data curation, Methodology, Project administration, Investigation, Resources, Visualization, Writing – review & editing. LH: Data curation, Supervision, Validation, Investigation, Resources, Software, Writing – review & editing.

Funding

The author(s) declare that no financial support was received for the research, authorship, and/or publication of this article.

Acknowledgments

The authors express their gratitude to the MIMIC for their contribution in study design and data sharing, as well as to all investigators and participants.

Conflict of interest

The authors declare that the research was conducted in the absence of any commercial or financial relationships that could be construed as a potential conflict of interest.

Generative AI statement

The author(s) declare that no Gen AI was used in the creation of this manuscript.

Publisher's note

All claims expressed in this article are solely those of the authors and do not necessarily represent those of their affiliated organizations, or those of the publisher, the editors and the reviewers. Any product that may be evaluated in this article, or claim that may be made by its manufacturer, is not guaranteed or endorsed by the publisher.

References

1. Zampieri FG, Serpa-Neto A, Wald R, Bellomo R, Bagshaw SM. Hierarchical endpoints in critical care: a post-hoc exploratory analysis of the standard versus accelerated initiation of renal-replacement therapy in acute kidney injury and the intensity of continuous renal- replacement therapy in critically ill patients trials. *J Crit Care*. (2024) 82:154767. doi: 10.1016/j.jcrc.2024.154767

2. Yan F, Chen X, Quan X, Wang L, Wei X, Zhu J. Association between the stress hyperglycemia ratio and 28-day all-cause mortality in critically ill patients with sepsis: a retrospective cohort study and predictive model establishment based on machine learning. *Cardiovasc Diabetol*. (2024) 23:163. doi: 10.1186/s12933-024-02265-4

3. Russotto V, Tassistro E, Myatra SN, Parotto M, Antolini L, Bauer P, et al. Peri-intubation cardiovascular collapse in patients who are critically ill: insights from the intube study. *Am J Respir Crit Care Med*. (2022) 206:449–58. doi: 10.1164/rccm.202111-2575OC

4. Cheng L, Zhang F, Xue W, Yu P, Wang X, Wang H, et al. Association of dynamic change of triglyceride-glucose index during hospital stay with all-cause mortality in critically ill patients: a retrospective cohort study from mimic iv2.0. *Cardiovasc Diabetol*. (2023) 22:142. doi: 10.1186/s12933-023-01874-9

5. Ransley DG, See EJ, Mizrahi A, Robbins R, Bellomo R. Inpatient and outpatient nephrology management of critically ill patients with acute kidney injury. *Nephrology (Carlton)*. (2021) 26:319–27. doi: 10.1111/nep.13838

6. Varudo R, Gonzalez FA, Leote J, Martins C, Bacariza J, Fernandes A, et al. Machine learning for the real-time assessment of left ventricular ejection fraction in critically ill patients: a bedside evaluation by novices and experts in echocardiography. *Crit Care*. (2022) 26:386. doi: 10.1186/s13054-022-04269-6

7. Chen L, Huang Z, Zhao X, Liang J, Lu X, He Y, et al. Predictors and mortality for worsening left ventricular ejection fraction in patients with HFpEF. *Front Cardiovasc Med*. (2022) 9:820178. doi: 10.3389/fcvm.2022.820178

8. Vinnakota S, Scott CG, Rodeheffer RJ, Chen HH. Estimated glomerular filtration rate, activation of cardiac biomarkers and long-term cardiovascular outcomes: a population-based cohort. *Mayo Clin Proc*. (2019) 94:2189–98. doi: 10.1016/j.mayocp.2019.03.033

9. Zhou Z, Liu Q, Zheng M, Zuo Z, Zhang G, Shi R, et al. Comparative study on the predictive value of TG/HDL-C, TyG and TyG-BMI indices for 5-year mortality in critically ill patients with chronic heart failure: a retrospective study. *Cardiovasc Diabetol*. (2024) 23:213. doi: 10.1186/s12933-024-02308-w

10. Zhang R, Shi S, Chen W, Wang Y, Lin X, Zhao Y, et al. Independent effects of the triglyceride-glucose index on all-cause mortality in critically ill patients with coronary heart disease: analysis of the mimic-III database. *Cardiovasc Diabetol*. (2023) 22:10. doi: 10.1186/s12933-023-01737-3

11. Chlabicz M, Laguna W, Kazimierczyk R, Kazimierczyk E, Lopatowska P, Gil M, et al. Value of APACHE II, SOFA and CardShock scoring as predictive tools for cardiogenic shock: a single-centre pilot study. *ESC Heart Fail*. (2024) 8:13. doi: 10.1002/ehf2.15020

12. Shahi S, Paneru H, Ojha R, Karn R, Rajbhandari R, Gajurel BP. SOFA And APACHE II scoring systems for predicting outcome of neurological patients admitted in a tertiary hospital intensive care unit. *Ann Med Surg (Lond*. (2024) 86 (4):1895–900. doi: 10.1097/MS9.0000000000001734

13. Johnson A, Bulgarelli L, Shen L, Gayles A, Shammout A, Horng S, et al. Mimic-iv, a freely accessible electronic health record dataset. *Sci Data*. (2023) 10:1. doi: 10.1038/s41597-022-01899-x

14. Zheng R, Qian S, Shi Y, Lou C, Xu H, Pan J. Association between triglyceride-glucose index and in-hospital mortality in critically ill patients with sepsis: analysis of the mimic-iv database. *Cardiovasc Diabetol*. (2023) 22:307. doi: 10.1186/s12933-023-02041-w

15. Gansevoort RT, Anders HJ, Cozzolino M, Fliser D, Fouque D, Ortiz A, et al. What should European nephrology do with the new CKD-EPI equation? *Nephrol Dial Transplant*. (2023) 38:1–6. doi: 10.1093/ndt/gfac254

16. Chung HS, Lee JS, Kim JA, Roh E, Lee YB, Hong SH, et al. Variability in total cholesterol concentration is associated with the risk of dementia: a nationwide population-based cohort study. *Front Neurol*. (2019) 10:441. doi: 10.3389/fneur.2019.00441

17. Gonzalez AA, Navas GF, Leon JJ, Arando AA, Delgado BJ, Camacho VM. Data mining as a tool to infer chicken carcass and meat cut quality from autochthonous genotypes. *Animals (Basel)*. (2022) 12. doi: 10.3390/ani12192702

18. Stewart S, Playford D, Scalia GM, Currie P, Celermajer DS, Prior D, et al. Ejection fraction and mortality: a nationwide register-based cohort study of 499 153 women and men. *Eur J Heart Fail*. (2021) 23:406–16. doi: 10.1002/ejhf.2047

19. Liu Y, Song J, Wang W, Zhang K, Qi Y, Yang J, et al. Association of ejection fraction with mortality and cardiovascular events in patients with coronary artery disease. *ESC Heart Fail*. (2022) 9:3461–8. doi: 10.1002/ehf2.14063

20. Blixt PJ, Nguyen M, Cholley B, Hammarskjold F, Toiron A, Bouhemad B, et al. Association between left ventricular systolic function parameters and myocardial injury, organ failure and mortality in patients with septic shock. *Ann Intensive Care*. (2024) 14:12. doi: 10.1186/s13613-023-01235-5

21. Jentzer JC, Reddy YN, Rosenbaum AN, Dunlay SM, Borlaug BA, Hollenberg SM. Outcomes and predictors of mortality among cardiac intensive care unit patients with heart failure. *J Card Fail*. (2022) 28:1088–99. doi: 10.1016/j.cardfail.2022.02.015

22. Jentzer JC, Wiley BM, Gersh BJ, Borlaug BA, Oh JK, Anavekar NS. Myocardial contraction fraction by echocardiography and mortality in cardiac intensive care unit patients. *Int J Cardiol*. (2021) 344:230–9. doi: 10.1016/j.ijcard.2021.09.040

23. Lees JS, Welsh CE, Celis-Morales CA, Mackay D, Lewsey J, Gray SR, et al. Glomerular filtration rate by differing measures, albuminuria and prediction of cardiovascular disease, mortality and end-stage kidney disease. *Nat Med*. (2019) 25:1753–60. doi: 10.1038/s41591-019-0627-8

24. Pickkers P, Darmon M, Hoste E, Joannidis M, Legrand M, Ostermann M, et al. Acute kidney injury in the critically ill: an updated review on pathophysiology and management. *Intensive Care Med*. (2021) 47:835–50. doi: 10.1007/s00134-021-06454-7

25. Jhee JH, Park JY, An JN, Kim DK, Joo KW, Oh YK, et al. Cumulative fluid balance and mortality in elderly patients with acute kidney injury requiring continuous renal-replacement therapy: a multicenter prospective cohort study. *Kidney Res Clin Pract*. (2020) 39:414–25. doi: 10.23876/j.krcp.20.089

26. Griffin BR, Vaughan-Sarrazin M, Shi Q, Ten EP, Reisinger HS, Kennelty K, et al. Blood pressure, readmission, and mortality among patients hospitalized with acute kidney injury. *JAMA Netw Open*. (2024) 7:e2410824. doi: 10.1001/jamanetworkopen.2024.10824

27. Mccoy I, Brar S, Liu KD, Go AS, Hsu RK, Chinchilli VM, et al. Achieved blood pressure post-acute kidney injury and risk of adverse outcomes after aki: a prospective parallel cohort study. *BMC Nephrol*. (2021) 22:270. doi: 10.1186/s12882-021-02480-1

28. Czopek A, Moorhouse R, Gallacher PJ, Pugh D, Ivy JR, Farrah TE, et al. Endothelin blockade prevents the long-term cardiovascular and renal sequelae of acute kidney injury in mice. *Sci Transl Med*. (2022) 14:eabf5074. doi: 10.1126/scitranslmed.abf5074

29. Liang Z, Yue S, Zhong J, Wu J, Chen C. Associations of systolic blood pressure and in-hospital mortality in critically ill patients with acute kidney injury. *Int Urol Nephrol*. (2023) 55:2099–109. doi: 10.1007/s11255-023-03510-7

30. Ramdas NV, Satheesh P, Shenoy MT, Kalra S. Triglyceride glucose (TyG) index: a surrogate biomarker of insulin resistance. *J Pak Med Assoc*. (2022) 72:986–8. doi: 10.47391/JPMA.22-63

31. Feng F, Yang H, Yang W, Chen Y. Metabolic resuscitation therapy in critically ill patients with sepsis and septic shock: a pilot prospective randomized controlled trial. *Open Med (Wars)*. (2023) 18:20230637. doi: 10.1515/med-2023-0637

32. Kobayashi H, Amrein K, Mahmoud SH, Lasky-Su JA, Christopher KB. Metabolic phenotypes and vitamin d response in the critically ill: a metabolomic cohort study. *Clin Nutr*. (2024) 43:10–9. doi: 10.1016/j.clnu.2024.09.030

33. Cui C, Liu L, Qi Y, Han N, Xu H, Wang Z, et al. Joint association of TyG index and high sensitivity c-reactive protein with cardiovascular disease: a national cohort study. *Cardiovasc Diabetol*. (2024) 23:156. doi: 10.1186/s12933-024-02244-9

34. Huo RR, Liao Q, Zhai L, You XM, Zuo YL. Interacting and joint effects of triglyceride- glucose index (TyG) and body mass index on stroke risk and the mediating role of tyg in middle-aged and older Chinese adults: a nationwide prospective cohort study. *Cardiovasc Diabetol*. (2024) 23:30. doi: 10.1186/s12933-024-02122-4

35. Ren X, Jiang M, Han L, Zheng X. Association between triglyceride-glucose index and chronic kidney disease: a cohort study and meta-analysis. *Nutr Metab Cardiovasc Dis*. (2023) 33:1121–8. doi: 10.1016/j.numecd.2023.03.026

36. Zeng Y, Yin L, Yin X, Zhao D. Association of triglyceride-glucose index levels with gestational diabetes mellitus in the US pregnant women: a cross-sectional study. *Front Endocrinol (Lausanne)*. (2023) 14:1241372. doi: 10.3389/fendo.2023.1241372

37. Chen T, Qian Y, Deng X. Triglyceride glucose index is a significant predictor of severe disturbance of consciousness and all-cause mortality in critical cerebrovascular disease patients. *Cardiovasc Diabetol*. (2023) 22:156. doi: 10.1186/s12933-023-01893-6

38. Tian N, Song L, Hou T, Fa W, Dong Y, Liu R, et al. Association of triglyceride-glucose index with cognitive function and brain atrophy: a population-based study. *Am J Geriatr Psychiatry*. (2024) 32:151–62. doi: 10.1016/j.jagp.2023.09.007

39. Chen J, Wu K, Lin Y, Huang M, Xie S. Association of triglyceride glucose index with all-cause and cardiovascular mortality in the general population. *Cardiovasc Diabetol*. (2023) 22:320. doi: 10.1186/s12933-023-02054-5

40. Yang Z, Gong H, Kan F, Ji N. Association between the triglyceride glucose (TyG) index and the risk of acute kidney injury in critically ill patients with heart failure: analysis of the mimic-iv database. *Cardiovasc Diabetol*. (2023) 22:232. doi: 10.1186/s12933-023-01971-9

41. Cai W, Xu J, Wu X, Chen Z, Zeng L, Song X, et al. Association between triglyceride-glucose index and all-cause mortality in critically ill patients with ischemic stroke: analysis of the mimic-iv database. *Cardiovasc Diabetol*. (2023) 22:138. doi: 10.1186/s12933-023-01864-x

42. Mullens W, Damman K, Testani JM, Martens P, Mueller C, Lassus J, et al. Evaluation of kidney function throughout the heart failure trajectory - a position statement from the heart failure association of the European Society of Cardiology. *Eur J Heart Fail*. (2020) 22(4):584–603. doi: 10.1002/ejhf.1697

43. Ostrominski JW, Thierer J, Claggett BL, Miao ZM, Desai AS, Jhund PS, et al. Cardio-Renal-Metabolic overlap, outcomes, and dapagliflozin in heart failure with mildly reduced or preserved ejection fraction. *JACC Heart Fail*. (2023) 11 (11):1491–503. doi: 10.1016/j.jchf.2023.05.015

44. Kadowaki T, Maegawa H, Watada H, Yabe D, Node K, Murohara T, et al. Interconnection between cardiovascular, renal and metabolic disorders: a narrative review with a focus on Japan. *Diabetes Obes Metab*. (2022) 24(12):2283–96. doi: 10.1111/dom.14829

45. Tian Y, Yao Y, Zhou J, Diao X, Chen H, Cai K, et al. Dynamic APACHE II score to predict the outcome of intensive care unit patients. *Front Med (Lausanne)*. (2021) 8:744907. doi: 10.3389/fmed.2021.744907

46. Hou N, Li M, He L, Xie B, Wang L, Zhang R, et al. Predicting 30-days mortality for MIMIC-III patients with sepsis-3: a machine learning approach using XGboost. *J Transl Med*. (2020) 18(1):462. doi: 10.1186/s12967-020-02620-5

47. Elias A, Agbarieh R, Saliba W, Khoury J, Bahouth F, Nashashibi J, et al. SOFA score and short-term mortality in acute decompensated heart failure. *Sci Rep*. (2020) 10(1):20802. doi: 10.1038/s41598-020-77967-2

48. Niu M, Chen J, Hou R, Sun Y, Xiao Q, Pan X, et al. Emerging healthy lifestyle factors and all-cause mortality among people with metabolic syndrome and metabolic syndrome-like characteristics in NHANES. *J Transl Med*. (2023) 21(1):239. doi: 10.1186/s12967-023-04062-1

49. Mayen AL, Sabra M, Aglago EK, Perlemuter G, Voican C, Ramos I, et al. Hepatic steatosis, metabolic dysfunction and risk of mortality: findings from a multinational prospective cohort study. *BMC Med*. (2024) 22(1):221. doi: 10.1186/s12916-024-03366-3

50. Oh ES, Steele CN, You Z, Nowak KL, Jovanovich AJ. Sex hormones and the risk of cardiovascular disease and mortality in male and female patients with chronic kidney disease: a systematic review and meta-analysis. *Physiol Rep*. (2022) 10(22): e15490. doi: 10.14814/phy2.15490

51. Donald DM, McDonnell T, O'Reilly MW, Sherlock M. Replacement with sex steroids in hypopituitary men and women: implications for gender differences in morbidities and mortality. *Rev Endocr Metab Disord*. (2024) 25(5):839–54. doi: 10.1007/s11154-024-09897-7

52. Longpre-Poirier C, Dougoud J, Jacmin-Park S, Moussaoui F, Vilme J, Desjardins G, et al. Sex and gender and allostatic mechanisms of cardiovascular risk and disease. *Can J Cardiol*. (2022) 38(12):1812–27. doi: 10.1016/j.cjca.2022.09.011

53. Honarvar M, Mehran L, Masoumi S, Agahi S, Khalili S, Azizi F, et al. Independent association between age- and sex-specific metabolic syndrome severity score and cardiovascular disease and mortality. *Sci Rep*. (2023) 13(1):14621. doi: 10.1038/s41598-023-41546-y

54. Beltrame A, Salguero P, Rossi E, Conesa A, Moro L, Bettini LR, et al. Association between sex hormone levels and clinical outcomes in patients with COVID-19 admitted to hospital: an observational, retrospective, cohort study. *Front Immunol*. (2022) 13:834851. doi: 10.3389/fimmu.2022.834851

55. Galiatsatos P, Brems H, Myers CN, Montemayor K. Race, ethnicity, and gender disparities in management and outcomes of critically ill adults with sepsis. *Crit Care Clin*. (2024) 40(4):741–52. doi: 10.1016/j.ccc.2024.06.001

56. Ho S, Phua HP, Lim WY, Mahalingam N, Tan G, Puah SH, et al. Sepsis, cardiovascular events and short-term mortality risk in critically ill patients. *Ann Acad Med Singap*. (2022) 51(5):272–82. doi: 10.47102/annals-acadmedsg.202220

57. Erickson SE, Vasilevskis EE, Kuzniewicz MW, Cason BA, Lane RK, Dean ML, et al. The effect of race and ethnicity on outcomes among patients in the intensive care unit: a comprehensive study involving socioeconomic status and resuscitation preferences. *Crit Care Med*. (2011) 39(3):429–35. doi: 10.1097/CCM.0b013e318206b3af

frontiers | Frontiers in Cardiovascular Medicine

TYPE Original Research
PUBLISHED 23 December 2024
DOI 10.3389/fcvm.2024.1508766

OPEN ACCESS

EDITED BY
Keita Saku,
National Cerebral and Cardiovascular Center, Japan

REVIEWED BY
Masafumi Ueno,
Kindai University Hospital, Japan
Tatsuhiro Shibata,
Kurume University, Japan

*CORRESPONDENCE
Cheng Jiang
chengjiang@whu.edu.cn
Yan Zhao
doctoryanzhao@whu.edu.cn

†These authors have contributed equally to this work and share first authorship

RECEIVED 09 October 2024
ACCEPTED 13 November 2024
PUBLISHED 23 December 2024

CITATION
Wu M, Li S, Yu H, Jiang C, Dai S, Jiang S and Zhao Y (2024) Extension of an ICU-based noninvasive model to predict latent shock in the emergency department: an exploratory study.
Front. Cardiovasc. Med. 11:1508766.
doi: 10.3389/fcvm.2024.1508766

Extension of an ICU-based noninvasive model to predict latent shock in the emergency department: an exploratory study

Mingzheng Wu†, Shaoping Li†, Haibo Yu†, Cheng Jiang*, Shuai Dai, Shan Jiang and Yan Zhao*

Emergency Center, Hubei Clinical Research Center for Emergency and Resuscitaion, Zhongnan Hospital of Wuhan University, Wuhan, Hubei, China

Background: Artificial intelligence (AI) has been widely adopted for the prediction of latent shock occurrence in critically ill patients in intensive care units (ICUs). However, the usefulness of an ICU-based model to predict latent shock risk in an emergency department (ED) setting remains unclear. This study aimed to develop an AI model to predict latent shock risk in patients admitted to EDs.

Methods: Multiple regression analysis was used to compare the difference between Medical Information Mart for Intensive Care (MIMIC)-IV-ICU and MIMIC-IV-ED datasets. An adult noninvasive model was constructed based on the MIMIC-IV-ICU v3.0 database and was externally validated in populations admitted to an ED. Its efficiency was compared with efficiency of testing with noninvasive systolic blood pressure (nSBP) and shock index.

Results: A total of 50,636 patients from the MIMIC-IV-ICU database was used to develop the model, and a total of 2,142 patients from the Philips IntelliSpace Critical Care and Anesthesia (ICCA)-ED and 425,087 patients from the MIMIC-IV-ED were used for external validation. The modeling and validation data revealed similar non-invasive feature distributions. Multiple regression analysis of the MIMIC-IV-ICU and MIMIC-IV-ED datasets showed mostly similar characteristics. The area under the receiver operating characteristic curve (AUROC) of the noninvasive model 10 min before the intervention was 0.90 (95% CI: 0.84–0.96), and the diagnosis accordance rate (DAR) was above 80%. More than 80% of latent shock patients were identified more than 70 min earlier using the noninvasive model; thus, it performed better than evaluating shock index and nSBP.

Conclusion: The adult noninvasive model can effectively predict latent shock occurrence in EDs, which is better than using shock index and nSBP.

KEYWORDS

shock, emergency department, intensive care unit, artificial intelligence, model

1 Introduction

Latent shock is characterized by the presence of circulatory failure and is a common occurrence in critical illness. Approximately 30% of intensive care unit (ICU) patients suffer hemodynamic change, and the mortality rate is above 40% (1, 2). Most cases of latent shock can be reversed in the early stage of circulatory failure, especially prior to ICU transfer. However, timely identification of latent shock remains a great challenge.

Unlike the ICU, the emergency department (ED) manages a wide array of illnesses with unknown origins. Patients deemed to be in critical condition are promptly cared for by continuous monitoring of their circulatory function. The low nurse-to-patients ratios make manual assessments in Eds difficult, thus there is an excessive reliance on alarms for physiological measurements to identify individuals at risk of circulatory deterioration. These signals fail to incorporate comprehensive patient information, possibly causing non-specific alarms that contribute to alarm fatigue (3–5). Emergency physicians are engaged in the subsequent diagnostic and therapeutic processes, such as documenting medical records, conducting ultrasound examinations, or carrying out other invasive operations. Therefore, changes in monitoring data and laboratory results may not sent, interpreted, or acted upon by physicians in a timely manner (6, 7). A single measurement cannot fully describe the entire patient state and may lead to misunderstanding of the circulatory function. Integrated evidence analysis potentially decreases the incidence of misdiagnosis and adverse events, thereby improving patient safety and outcomes. In a high-paced environment like an ED, quickly filtering the important information from the vast amounts of data is necessary but increasingly hard for emergency health workers.

Machine-learning (ML) models utilize algorithms to learn from larger datasets and make predictions or decisions based on new data. Multiple parameter systems were developed as a method to identify patients at risk of delayed septic shock in EDs (8). The newly proposed hemodynamic stability index (HSI) model has outperformed against every single parameter for risk prediction in both adults and pediatrics (9, 10). The model consisted of more than thirty input features, including vital signs, laboratory measurements, and ventilation settings. Most of the variables are not routinely measured in EDs, and variables collected before ICU admission and in the first 6 h after ICU transfer were also excluded in these studies. More than 7,000 ICU transfers from the ED in Zhongnan Hospital of Wuhan University were retrospectively reviewed. It was found that the median interval from ED admission to ICU transfer was 5 h, with cases of latent shock mostly receiving fluid resuscitation within 6 h. How to quickly predict latent shock in cases within the ED remains a challenge.

The ICU-based noninvasive model for predicting latent shock risk has not yet been generalized to the ED. Non-invasive features that are easy to acquire in a short time should be considered. The study aimed to develop an adult noninvasive model in order to provide an earlier warning of latent shock risk, which is good for pre-hospital triage to the ICU.

2 Materials and methods

2.1 Definition of latent shock

Latent shock was defined as patients who were administrated with vasoactives and had a mean arterial pressure of below 65 mmHg (11). Fluid resuscitation was not included because most of the patients had a shorter ED stay once latent shock was identified. ED physicians are also more likely to use vasoactives than fluid resuscitation to improve the mean arterial pressure (MAP) before the underlying reasons for the condition are ascertained. Blood transfusion is time-consuming and rarely applied in the ED. More evidence of latent shock definition is described in the Supplementary Materials. Detailed categories or quantification of these definitions are listed in Supplementary Table S1.

2.2 Dataset selection

Medical Information Mart for Intensive Care (MIMIC) and eICU are two public datasets that are frequently used for ML research. Variables in the eICU dataset such as medicines or fluid administration are not labeled with the specific time. This makes it inconvenient for researchers to calculate the total volume of fluid infusion throughout a specific duration. Therefore, the Mimic-IV-ICU v3.0 dataset was used for model establishment between 2008 and 2022. In addition, data for external validation were extracted from two databases: the Philips IntelliSpace Critical Care and Anesthesia (ICCA) systems from the ED of Zhongnan Hospital of Wuhan University from December 2022 to July 2023 and the MIMIC-IV-ED between 2008 and 2022. Patients of an age ≥18 years were retrospectively included. Based on the unique patient number, in cases where the same patient is admitted repeatedly, only the first admission number was selected. Patients younger than 18 years of age, those with missing age values, those with stays of less than 30 min, or those with latent shock occurring within 30 min were excluded. All records in this study were strictly privacy-protected, and the use of the database was approved by the Beth Israel Deaconess Medical Center (BIDMC) Institutional Review Committee, Massachusetts Institute of Technology (CITI certificate number: 55436196) and Ethics Committee of Zhongnan Hospital of Wuhan University (2024066K).

2.3 Data processing and feature selection

Patients who received clinical intervention were placed in the unstable group. The start time of treatment was used as the time of diagnosis. The most recent feature values prior to the diagnosis of latent shock were extracted. For patients in the ED, missing values were filled in with the most recent data values. If clinical interventions were not received, patients were placed in the stable group, and any value that could be the result of the first measurement was extracted.

Features were screened based on missing values being less than 20%. The selected features were present in both databases, and the unit conversion was based on the ICCA system data. All variables were subjected to a rationality filter (Supplementary Table S2) to check whether their values were within the physiological validity range and to exclude outliers. By using random forests, the importance of model features in predicting latent shock was

calculated. Features were input into the XGBoost classifier to get the SHAP value and force plot.

2.4 Algorithm selection

For the training set, 70% of the sample was randomly selected; the remaining 30% was used as the test set. The parameters were iteratively adjusted to achieve the best performance of the model. Several commonly used algorithms include random forest, logistic regression, adaptive boosting (AdaBoost), extreme gradient boosting (XGBoost), and neural networks. The parameters of these algorithms were iteratively tuned on the training set using five-fold internal cross-validation. The AUROC performance of these five algorithms was compared on the training set and the test set respectively.

2.5 Model development and external validation

A noninvasive model was constructed using features of greater than 0.01 importance that met the criteria. In EDs, identifying individuals at a high risk of latent shock without performing time-consuming laboratory tests is critical. Hence, noninvasive features were also included to build a noninvasive prediction model. After training, validating, and testing through common algorithms, the dataset was further divided through random sampling without replacement at a ratio of 7:3. The algorithm that worked best was selected to build the model and complete the external validation. The predictive accuracy of the model was interpreted based on the results of the calibration curve. If the calibration curve was close to the diagonal line, it indicated that the predicted probability of the model was consistent with the actual probability, and the model had a good calibration degree.

2.6 Statistical analysis

Continuous variables were presented as mean (standard deviation, SD) or median (interquartile range, IQR). Categorical variables were summarized by number (proportion). The unpaired *t*-test or the Mann–Whitney *U* test was used for continuous variables, and the Chi-square test or the Fisher exact test was used for categorical variables, as appropriate. In Python, functions were implemented to compute 95% confidence intervals (CI) for various metrics, including diagnosis accordance rate(DAR), area under the receiver operating characteristic curve (AUROC), sensitivity, specificity, F1 score, positive predictive value (PPV), and negative predictive value (NPV). For the shock index and the systolic blood pressure, the AUC was calculated using a binary logistic regression model. One-way analysis of variance was used to compare the AUC values of three models. Multiple regression analysis was used to compare the difference between the MIMIC-IV-ICU and MIMIC-IV-ED data sets. All statistical analyses were performed using the EmpowerStats statistical package (http://www.empowerstats.com, X&Y Solutions, Inc., Boston, MA) and R version 3.6.0. A two-sided $P < 0.05$ was considered statistically significant.

3 Results

3.1 Study population

A total of 94,458 patients were extracted from MIMIC-IV-ICU. A total of 43,822 patients were excluded, for reasons including repeated admission (23,686), ICU stay time <30 min or latent shock occurring <30 min (10,352), missing values (9,729), or abnormal values (55). Finally, 50,636 patients with latent shock (21,175) and non-latent shock (29,461) were included for model establishment. 425,087 patients were also extracted from the MIMIC-IV-ED. Ultimately, a total of 48,410 patients including latent shock (1,074) and non-latent shock group (47,336) were included for external validation on zero minute. 3,039 patients were also extracted from the ICCA system. Ultimately, a total of 2,142 patients including latent shock (78) and non-latent shock group (1,964) were included for external validation every 10 min (Figure 1). The modeling and validation data showed that the non-invasive feature distribution of the unstable group and the stable group were roughly similar (Table 1). The results of the multiple regression analysis between the MIMIC-IV-ICU and MIMIC-IV-ED datasets showed that most of the characteristics were similar (Supplementary Table S3). With an alert every 10 min, the 2,042 patients' vital signs were constantly changing. Patient information and characteristics of externally validated data on minute 0 are presented in Supplementary Table S4.

3.2 Feature selection

Blood gas analysis features missing more than 60% were not collected. Finally, eight noninvasive features with relatively complete information were collected (Table 1). Temperature was not included in the external validation data due to this not being present in ED data. By using a random forest, Figure 2 shows the importance of the features (>0.01) of the model for predicting latent shock, finding that the gender of the patient has very little effect and blood pressure has the greatest influence on predicting latent shock. The higher the ranking, the more important the feature. The dot to the left of the digital baseline represents a negative contribution to experiencing latent shock, while the dot to the right represents a positive contribution. The farther away from the baseline, the greater the effect. Red stripes represent positive contributions and blue stripes represent negative contributions. The wider the stripes, the greater the contribution.

3.3 XGBoost algorithm

On the test set, Figure 3 shows that XGBoost is the best algorithm for constructing the prediction model of latent shock (AUC = 0.94). On the external validation, XGBoost algorithm was used to validate

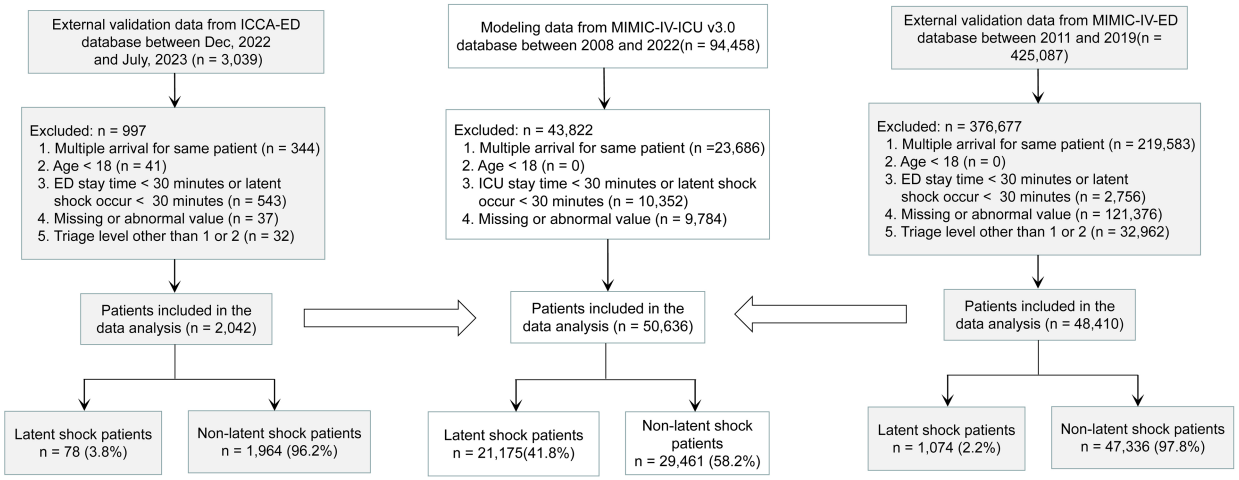

FIGURE 1
Study Flowchart. The stability and generalization ability of the model were verified externally several times. First, the MIMIC-IV-ED dataset is used for the first external validation, and then the ICCA-ED dataset is used for dynamic external validation every 10 minutes. MIMIC-IV-ICU, Medical Information Mart for Intensive Care IV in Intensive Care Unit; MIMIC-IV-ED, Medical Information Mart for Intensive Care IV in Emergency Department; ICCA-ED, IntelliSpace Critical Care and Anesthesia in Emergency Department; ICU, Intensive Care Unit; ED, Emergency Department.

TABLE 1 Feature comparison between MIMIC-IV-ICU and MIMIC-IV-ED.

	Latent shock	Non-latent shock	*P*-values
MIMIC-IV-ICU			
Patients, *N* (%)	29,461 (41.8%)	21,175 (58.2%)	
Age, year, Median (Q1, Q3)	69.9 (57.3, 81.2)	63.3 (50.9, 75.0)	<0.001
Gender (Male), *N* (%)	10,589 (50.0%)	17,165 (58.3%)	<0.001
heart rate (HR, beats per minute), Median (Q1, Q3)	82.0 (70.0, 96.0)	85.0 (73.0, 100.0)	<0.001
Respiration rate (RR, beats per minute), Median (Q1, Q3)	19.0 (15.0, 22.0)	18.0 (15.0, 22.0)	<0.001
Transcutaneous Oxygen Saturation (SpO_2,%), Median (Q1, Q3)	97.0 (95.0, 99.0)	98.0 (95.0, 100.0)	<0.001
Non, invasive systolic blood pressure (nSBP, mmHg), Median (Q1, Q3)	98.0 89.0, 109.0)	130.0 (116.0, 46.0)	<0.001
<90, *N* (%)	5,431 (25.6%)	485 (1.6%)	<0.001
≥90, *N* (%)	15,744 (74.4%)	28,976 (98.4%)	
Non, invasive diastolic blood pressure (nDBP, mmHg), Median (Q1, Q3)	49.0 (44.0, 54.0)	75.0 (65.0, 85.0)	<0.001
<60, *N* (%)	18,369 (86.7%)	3,878 (13.2%)	<0.001
≥60, *N* (%)	2,806 (13.3%)	25,583 (86.8%)	
Non, invasive mean blood pressure (nMBP, mmHg), Median (Q1, Q3)	61.0 (57.0, 64.0)	89.0 (79.0, 100.0)	<0.001
< 65, *N* (%)	17,788 (84.0%)	790 (2.7%)	<0.001
≥65, *N* (%)	3,387 (16.0%)	28,671 (97.3%)	
Shock index, Median (Q1, Q3)	0.8 (0.7, 1.0)	0.7 (0.5, 0.8)	<0.001
MIMIC-IV-ED			
Patients, *N* (%)	1,074 (2.2%)	47,336 (97.8%)	
Age, year, Median (Q1, Q3)	69.0 (55.0, 80.0)	63.0 (47.0, 76.0)	<0.001
Gender (Male), *N* (%)	479 (44.6%)	24,660 (52.1%)	<0.001
Heart rate (HR, beats per minute), Median (Q1, Q3)	83.0 (68.0, 98.0)	82.0 (70.0, 96.0)	0.475
Respiration rate (RR, beats per minute), Median (Q1, Q3)	18.0 (16.0, 22.0)	18.0 (16.0, 19.0)	<0.001
Transcutaneous Oxygen Saturation (SpO_2,%), Median (Q1, Q3)	98.0 (96.0, 100.0)	98.0 (97.0, 100.0)	<0.001
Non, invasive systolic blood pressure (nSBP, mmHg), Median (Q1, Q3)	91.0 (84.0, 98.0)	132.0 (117.0, 148.0)	<0.001
<90, *N* (%)	457 (42.6%)	463 (1.0%)	<0.001
≥90, *N* (%)	617 (57.4%)	46,873 (99.0%)	
Non, invasive diastolic blood pressure (nDBP, mmHg), Median (Q1, Q3)	45.0 (41.0, 49.0)	75.0 (66.0, 85.0)	<0.001
<60, *N* (%)	1,039 (96.7%)	6,350 (13.4%)	<0.001
≥60, *N* (%)	35 (3.3%)	40,986 (86.6%)	
Non, invasive mean blood pressure (nMBP, mmHg), Median (Q1, Q3)	61.0 (57.0, 63.0)	94.0 (84.0, 105.0)	<0.001
<65, *N* (%)	955 (88.9%)	637 (1.3%)	<0.001
≥65, *N* (%)	119 (11.1%)	46,699 (98.7%)	
Shock index, Median (Q1, Q3)	0.9 (0.7, 1.1)	0.6 (0.5, 0.8)	<0.001

MIMIC-IV-ICU v3.0 database is from to 2008 to 2022. MIMIC-IV-ED database is from 2008 to 2019. Q1: the first quartile; Q3: the third quartile; *P*-values was calculated using non, parametric tests or Chi, square tests based on variable type.

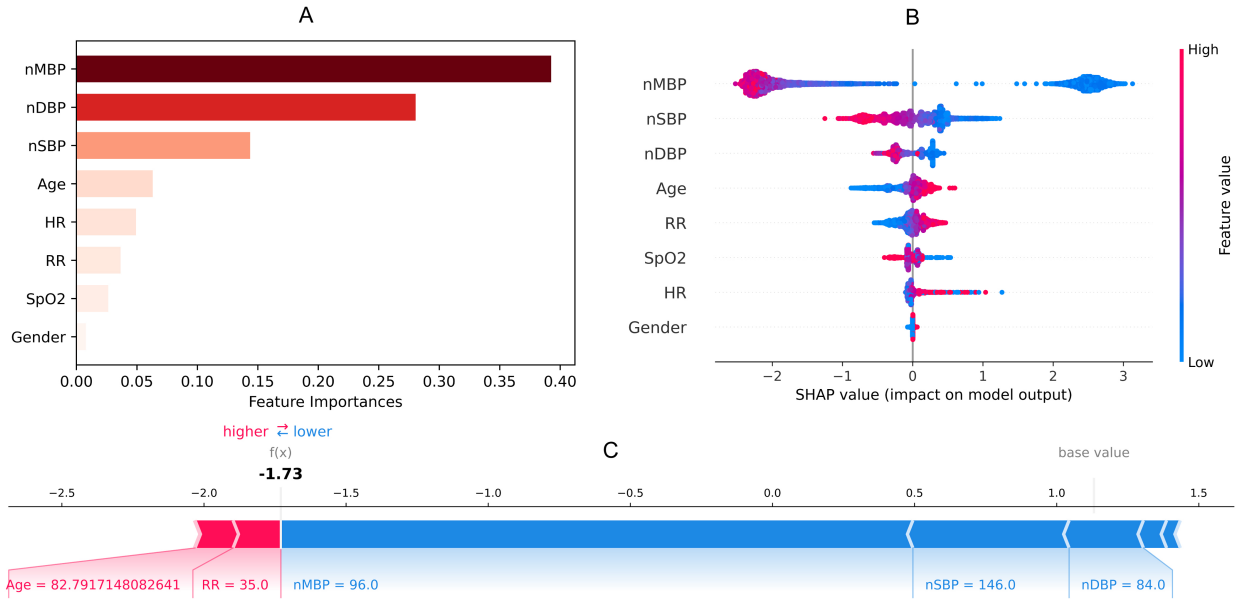

FIGURE 2
Feature importance (A), SHAP value (B) and force plot (C) of noninvasive model for predicting latent shock. We found that the gender of the patient has very little effect and blood pressure has the greatest influence on noninvasive model. nSBP, noninvasive systolic blood pressure; nDBP, noninvasive diastolic blood pressure; nMBP, noninvasive mean blood pressure; HR, heart rate; RR, respiratory rate; SpO2, saturation of peripheral oxygen; SHAP, SHapley additive exPlanations.

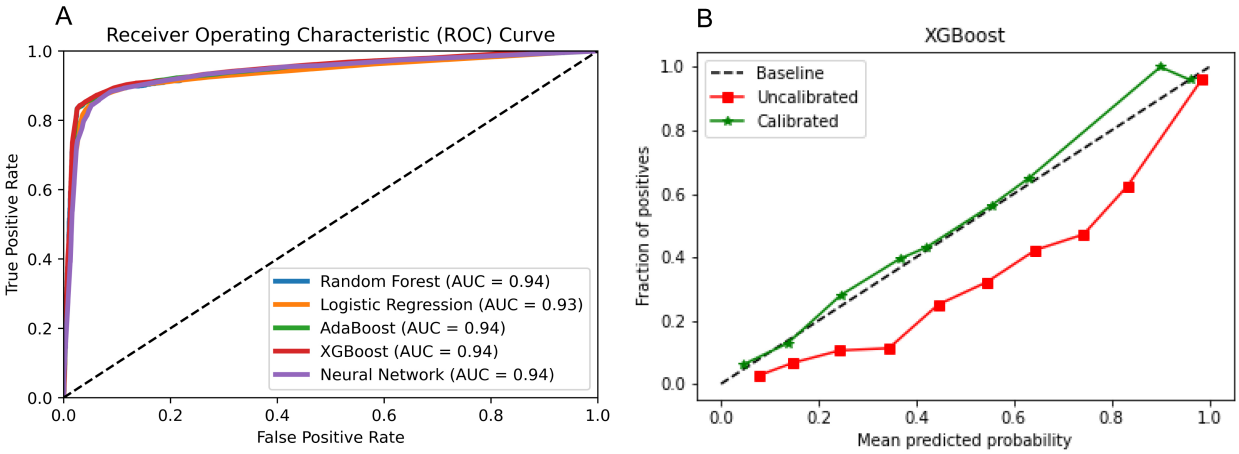

FIGURE 3
Algorithm selection. (A) Five algorithms for constructing the prediction model of latent shock; (B) The noninvasive model has a good calibration degree with XGBoost algorithm.

the performance of the noninvasive model. Figure 3 shows that the noninvasive model has a good calibration degree with XGBoost algorithm, which allows missing values in external validation.

3.4 Model performance over time

Different thresholds cause model effects to vary. The results of model performance over time when the threshold is 0.2 or 0.4 are shown in Table 2. External validation results of the two datasets show that AUROC of the non-invasive model is as high as 0.99 at 0 min. AUROC of the noninvasive model 10 min before the intervention was 0.90 (95% CI: 0.84–0.96), and the DAR was more than 80%. The calibration plot also indicated that when the threshold was set to 0.2, more than 80% of latent shock patients could be identified more than 70 min earlier (Figure 4). A logistic regression model was used to calculate the area under the

10.3389/fcvm.2024.1508766

TABLE 2 Performance of noninvasive model for predicting latent shock, mean (95% CI).

Minutes before the intervention	Threshold	DAR	AUROC	Recall	Specificity	NPV	PPV	F1-score
MIMIC-IV-ED[a]								
0	0.4	0.97 (0.97–0.98)	0.99 (0.98–0.99)	0.96 (0.95–0.97)	0.97 (0.97–0.98)	1.00 (1.00–1.00)	0.46 (0.44–0.47)	0.62 (0.60–0.64)
ICCA-ED[b]								
0	0.2	0.85 (0.79–0.92)	0.99 (0.97–1.00)	0.98 (0.96–1.00)	0.85 (0.79–0.91)	1.00 (0.99–1.00)	0.16 (0.12–0.20)	0.27 (0.22–0.33)
10	0.2	0.86 (0.78–0.93)	0.90 (0.84–0.96)	0.86 (0.79–0.93)	0.86 (0.78–0.93)	1.00 (0.98–1.00)	0.11 (0.08–0.15)	0.20 (0.15–0.25)
20	0.2	0.84 (0.78–0.91)	0.86 (0.80–0.92)	0.74 (0.66–0.82)	0.85 (0.78–0.91)	0.99 (0.97–1.00)	0.12 (0.09–0.15)	0.20 (0.16–0.25)
30	0.2	0.85 (0.78–0.91)	0.86 (0.79–0.92)	0.69 (0.61–0.76)	0.85 (0.79–0.92)	0.99 (0.97–1.00)	0.12 (0.09–0.15)	0.20 (0.16–0.25)
40	0.2	0.84 (0.77–0.91)	0.86 (0.79–0.93)	0.73 (0.64–0.81)	0.84 (0.77–0.91)	0.99 (0.97–1.00)	0.11 (0.08–0.14)	0.19 (0.14–0.23)
50	0.2	0.84 (0.76–0.92)	0.85 (0.78–0.93)	0.75 (0.66–0.84)	0.84 (0.77–0.92)	0.99 (0.97–1.00)	0.11 (0.08–0.14)	0.19 (0.14–0.24)
60	0.2	0.83 (0.75–0.92)	0.81 (0.72–0.90)	0.63 (0.56–0.76)	0.84 (0.75–0.92)	0.99 (0.97–1.00)	0.09 (0.06–0.12)	0.16 (0.11–0.21)
70	0.2	0.84 (0.74–0.93)	0.80 (0.70–0.90)	0.56 (0.44–0.67)	0.84 (0.75–0.94)	0.99 (0.96–1.00)	0.07 (0.04–0.10)	0.12 (0.08–0.17)
80	0.2	0.83 (0.73–0.93)	0.85 (0.76–0.94)	0.77 (0.66–0.88)	0.83 (0.73–0.93)	0.99 (0.97–1.00)	0.09 (0.06–0.13)	0.17 (0.11–0.22)
90	0.2	0.83 (0.72–0.94)	0.80 (0.68–0.92)	0.70 (0.57–0.83)	0.84 (0.73–0.95)	0.99 (0.97–1.00)	0.08 (0.04–0.11)	0.14 (0.09–0.20)
100	0.2	0.83 (0.71–0.95)	0.80 (0.67–0.93)	0.65 (0.50–0.79)	0.83 (0.71–0.95)	0.99 (0.96–1.00)	0.07 (0.04–0.10)	0.12 (0.07–0.18)
110	0.2	0.82 (0.67–0.97)	0.80 (0.65–0.95)	0.58 (0.41–0.75)	0.82 (0.68–0.97)	0.99 (0.96–1.00)	0.05 (0.02–0.08)	0.09 (0.04–0.14)
120	0.2	0.82 (0.62–1.00)	0.73 (0.52–0.95)	0.57(0.35–0.79)	0.82(0.63–1.00)	0.99(0.96–1.00)	0.03(0.01–0.05)	0.06(0.02–0.10)

[a]The noninvasive model of potential shock was externally validated on 0 min with the data set derived from MIMIC-IV-ED.
[b]The noninvasive model of potential shock was externally validated every 10 min with the data set derived from ICCA in ED.

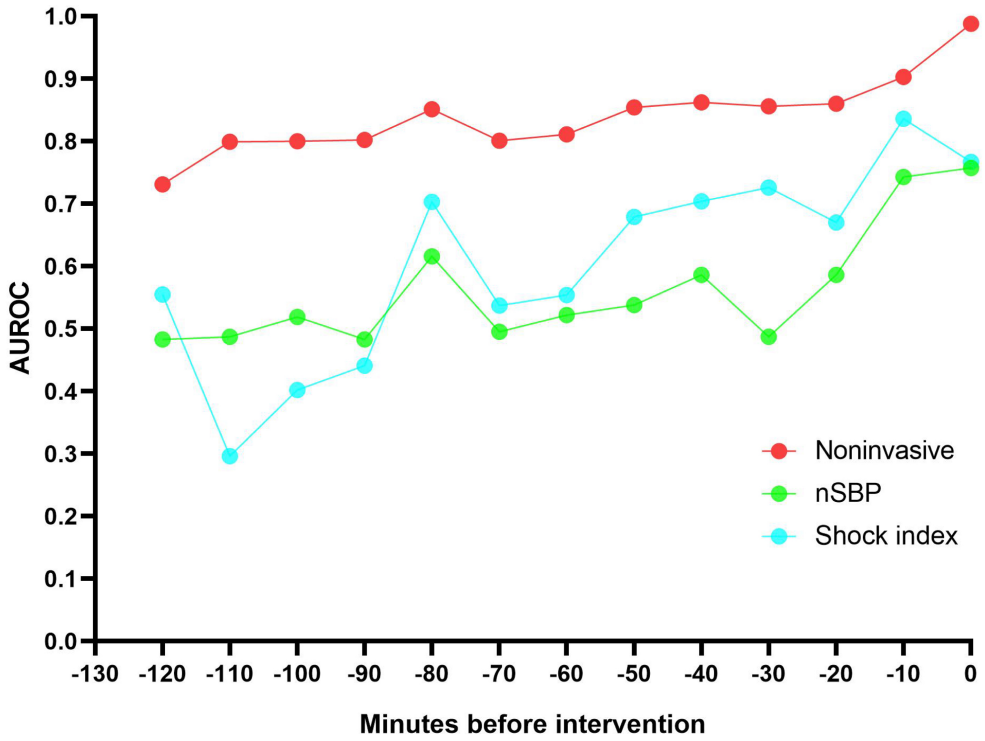

FIGURE 4
The non-invasive models had a higher AUROC 120 minutes before intervention than the shock index and noninvasive systolic blood pressure (nSBP). More than 80% of latent shock patients could be identified more than 70 minutes earlier.

AUROC curve for shock index and noninvasive systolic blood pressure (nSBP). The non-invasive models had higher AUROC than the shock index and nSBP models. There were statistically significant differences in the AUC per 10 min of external validation among the three models ($P < 0.05$).

4 Discussion

Notably, the modeling and validation data revealed similar non-invasive feature distributions. Multiple regression analysis of MIMIC-IV-ICU and MIMIC-IV-ED datasets showed mostly

similar characteristics. Blood pressure was identified as the most influential feature in predicting latent shock. Furthermore, our noninvasive model demonstrated AUROC and DAR of above 0.80 for predicting latent shock 70 min before intervention, outperforming both the single shock index and nSBP models, with statistically significant differences observed in the AUC per 10 min of external validation. This study has important clinical significance for pre-hospital care and for ED to triage of ICU.

In the ED, not all patients are referred to the ICU. Doctors classify the severity of patients' conditions, especially those with latent shock. The triage and acuity scale is called the Emergency Severity Index (ESI) Five Level triage system (12). Level 1 and level 2 patients are likely to be admitted to the ICU (13). This study found that the noninvasive model was a model that could be useful. The AUROC of our noninvasive model is similar to models from Chiang Dung-Hung et al. (9) (AUROC = 0.81) and Potes Cristhia et al. (10) (AUROC = 0.76). According to Table 1, Supplementary Tables S3, S4, the differences in most features between the MIMIC-IV-ICU and ED datasets are not significant. Thus, it can be seen that it is theoretically feasible for us to use the data of latent shock patients in the ICU to establish a noninvasive predictive model and adjust the model parameters based on the severity of the disease to provide an earlier warning of latent shock patients in the ED.

Clinically, vital signs are important disease information. Our study classifies vital signs as noninvasive and found that blood pressure is the most influential feature in predicting latent shock. Noninvasive features are also covered, such as age, gender, saturation of peripheral oxygen (SpO_2), and GCS. Systolic blood pressure features are most important in models predicting latent shock, which is consistent with the reported importance of features (9, 10). Chang, H et al. (11) used six noninvasive indicators (nSBP, nDBP, RR, pulse rate, temperature, and SpO_2) to establish an emergency department latent shock warning model. At 3 h before latent shock, the predictive AUROC values of RNN, MLP, RF, and LR methods were 0.822, 0.841, 0.852, and 0.830, respectively. Our study shows that more than 80% of latent shock patients could be identified more than 70 min earlier. And the noninvasive model is better than the shock index or nSBP. Therefore, an ICU-based noninvasive model for identifying latent shock risk in the ED is theoretically feasible.

Laboratory measurements and respiratory setting indicators are mostly invasive. Combining the model with laboratory measurements and respiratory setting indicators is conducive to improving its sensitivity, specificity, and accuracy (2, 14). But as the waiting time is long and cost high for invasive features. sequential organ failure assessment(SOFA) score was also confirmed as a predictor of mortality in ICU patients (15). The SOFA score exhibited the highest accuracy in predicting hospital mortality of septic latent shock at 0.880, followed closely by the SOS score (0.878), modified early warning score (MEWS) (0.858), quick sequential organ failure assessment (qSOFA) score (0.847), and NEWS score (0.833) (16). But the SOFA score contains invasive features. So, our ICU-based noninvasive model is a model that can be chosen but needs further study.

This study demonstrates that the non-invasive model can provide an early warning of latent shock risk in the emergency department, 70 min ahead of the current time, which holds significant value as a reference for early diagnosis and treatment. When Philips' ICCA system issues an alert for latent shock risk during the rescue and observation process, medical staff can immediately prioritize the patient's condition and initiate corresponding diagnostic and treatment protocols. This facilitates rapid identification and management of latent shock symptoms, thereby reducing the incidence of misdiagnosis and missed diagnoses. Patients can receive treatment earlier, alleviating their pain and discomfort. Consequently, this approach enhances patient satisfaction and trust, fostering improved doctor-patient relationships. Future research should explore the integration of our model with other noninvasive indicators to further enhance prediction accuracy, while also considering the balance between invasiveness, cost, and practicality in clinical settings. Ultimately, our study contributes to the ongoing effort to optimize triage and management strategies for latent shock patients in the ED.

5 Limitations

This study has limitations. First, while common clinical indicators were used as features, other factors such as a patient's temperature and Glasgow score (GCS) may also have provided useful features. Second, other important features need to be added, and the noninvasive model needs to be continually optimized. Third, when interpreting blood pressure data within the model, it is essential to fully consider the patient's underlying conditions and reasons for admission. For instance, blood pressure levels may differ between elderly and younger patients, potentially impacting the model's predictive performance across different age groups. Fourth, given the limited number of cases in the current study, a substantial amount of external validation set data is planned to be collected in the future. This will enable us to conduct analyses on various patient subgroups, allowing for separate modeling and external validation tailored to each subgroup. Fifth, in the process of promoting the model, the differences in ICU and ED data from different sources may affect the stability and generalization ability of the model, which requires multi-center external validation. Sixth, the significant imbalance in sample size between the stable and unstable groups within the external validation set has led to prediction biases, risks of overfitting, distorted evaluation metrics, and decreased statistical significance. In our future prospective studies, the sample size of the unstable group within the external validation set will be increased to mitigate the issue of sample imbalance. Therefore, these predictive models require further optimization and prospective study. Seventh, there was no analysis of the potential impact on model

performance evaluation, clinical alert accuracy, and patient treatment outcomes based on different underlying disease subgroups of patients. In the later stage, we will establish subgroup analysis for different underlying diseases, integrate it into the ICCA system, and intelligently match early warning models for different types of patients.

6 Conclusion

This study found that ICU-based noninvasive model can effectively predict latent shock risk in ED, which is better than using the simple shock index and nSBP. Further prospective multicenter studies are needed to generalize these models.

Data availability statement

The raw data supporting the conclusions of this article will be made available by the authors, without undue reservation.

Ethics statement

The studies involving humans were approved by Medical Ethics Committee, Zhongnan Hospital of Wuhan University. The studies were conducted in accordance with the local legislation and institutional requirements. The participants provided their written informed consent to participate in this study. Written informed consent was not obtained from the individual(s) for the publication of any potentially identifiable images or data included in this article because This is a retrospective study, which has been approved by the Medical Ethics Committee of Zhongnan Hospital of Wuhan University to use the data.

Author contributions

MZW: Writing – original draft. SL: Writing – review & editing. HBY: Formal Analysis, Writing – original draft. CJ: Project administration, Supervision, Writing – review & editing. SD: Writing – review & editing, Formal Analysis, Methodology. SJ: Formal Analysis, Methodology, Writing – review & editing. YZ: Conceptualization, Project administration, Supervision, Writing – original draft.

Funding

The author(s) declare that no financial support was received for the research, authorship, and/or publication of this article.

Acknowledgments

We thank all the patients of this study for their participation.

Conflict of interest

The authors declare that the research was conducted in the absence of any commercial or financial relationships that could be construed as a potential conflict of interest.

Generative AI statement

The author(s) declare that no Generative AI was used in the creation of this manuscript.

Publisher's note

Supplementary material

The Supplementary Material for this article can be found online at: https://www.frontiersin.org/articles/10.3389/fcvm.2024.1508766/full#supplementary-material

References

1. Cecconi M, De Backer D, Antonelli M, Beale R, Bakker J, Hofer C, et al. Consensus on circulatory shock and hemodynamic monitoring. Task Force of the European Society of Intensive Care Medicine. *Intensive Care Med*. (2014) 40(12):1795–815. doi: .org/10.1007/s00134-014-3525-z

2. Chang Y, Antonescu C, Ravindranath S, Dong J, Lu M, Vicario F, et al. Early prediction of cardiogenic shock using machine learning. *Front Cardiovasc Med*. (2022) 9:9862424. doi: 10.3389/fcvm.2022.862424

3. Duke G, Green J, Briedis J. Survival of critically ill medical patients is time-critical. *Crit Care Resusc*. (2004) 6(4):261–7.

4. Ruppel H, De Vaux L, Cooper D, Kunz S, Duller B, Funk M. Testing physiologic monitor alarm customization software to reduce alarm rates and improve nurses' experience of alarms in a medical intensive care unit. *PLoS One*. (2018) 13(10): e0205901. doi: 10.1371/journal.pone.0205901

5. Graham KC, Cvach M. Monitor alarm fatigue: standardizing use of physiological monitors and decreasing nuisance alarms. *Am J Crit Care*. (2010) 19(1):28–35. doi: .org/10.4037/ajcc2010651

6. Fackler JC, Watts C, Grome A, Miller T, Crandall B, Pronovost P. Critical care physician cognitive task analysis: an exploratory study. *Crit Care*. (2009) 13(2):R33. doi: .org/10.1186/cc7740

7. Wright MC, Dunbar S, Macpherson BC, Moretti EW, Del Fiol G, Bolte J, et al. Toward designing information display to support critical care. A qualitative contextual evaluation and visioning effort. *Appl Clin Inform*. (2016) 7(4):912–29. doi: 10.4338/ACI-2016-03-RA-0033

8. Wardi G, Carlile M, Holder A, Shashikumar S, Hayden SR, Nemati S. Predicting progression to septic shock in the emergency department using an externally generalizable machine-learning algorithm. *Ann Emerg Med*. (2021) 77(4):95–406. doi: 10.1016/j.annemergmed.2020.11.007

9. Dung-Hung C, Cong T, Zeyu J, Yu-Shan OY, Yung-Yan L. External validation of a machine learning model to predict hemodynamic instability in intensive care unit. *Crit Care*. (2022) 26(1):215. doi: 10.1186/s13054-022-04088-9

10. Potes C, Conroy B, Xu-Wilson M, Newth C, Inwald D, Frassica J. A clinical prediction model to identify patients at high risk of hemodynamic instability in the pediatric intensive care unit. *Crit Care*. (2017) 21(1):1–8. doi: 10.1186/s13054-017-1874-z

11. Chang H, Jung W, Ha J, Yu JY, Heo S, Lee GT, et al. Early prediction of unexpected latent shock in the emergency department using vital signs. *Shock*. (2023) 60(3):373–8. doi: 10.1097/SHK.0000000000002181

12. Daş M, Bardakci O, Siddikoglu D, Akdur G, Yilmaz MC, Akdur O, et al. Prognostic performance of peripheral perfusion index and shock index combined with ESI to predict hospital outcome. *Am J Emerg Med*. (2020) 38(10):2055–9. doi: 10.1016/j.ajem.2020.06.084

13. Nguyen M, Corbin CK, Eulalio T, Ostberg NP, Machiraju G, Marafino BJ, et al. Developing machine learning models to personalize care levels among emergency room patients for hospital admission. *J Am Med Inform Assoc*. (2021) 28 (11):2423–32. doi: 10.1093/jamia/ocab118

14. Rahman A, Chang Y, Dong J, Conroy B, Natarajan A, Kinoshita T, et al. Early prediction of hemodynamic interventions in the intensive care unit using machine learning. *Crit Care*. (2021) 25(1):388. doi: 10.1186/s13054-021-03808-x

15. Raith EP, Udy AA, Bailey M, McGloughlin S, MacIsaac C, Bellomo R, et al. Prognostic accuracy of the SOFA score, SIRS criteria, and qSOFA score for in-hospital mortality among adults with suspected infection admitted to the intensive care unit. *JAMA*. (2017) 317(3):290–300. doi: 10.1001/jama.2016.20328

16. Khwannimit B, Bhurayanontachai R, Vattanavanit V. Comparison of the accuracy of three early warning scores with SOFA score for predicting mortality in adult sepsis and septic shock patients admitted to intensive care unit. *Heart Lung*. (2019) 48(3):240–4. doi: 10.1016/j.hrtlng.2019.02.005

frontiers | Frontiers in Cardiovascular Medicine

TYPE Original Research
PUBLISHED 07 January 2025
DOI 10.3389/fcvm.2024.1499324

OPEN ACCESS

EDITED BY
Keita Saku,
National Cerebral and Cardiovascular Center, Japan

REVIEWED BY
Hiroki Matsushita,
National Cerebral and Cardiovascular Center, Japan
Yuki Ikeda,
Kitasato University, Japan
Naofumi Yoshida,
National Cerebral and Cardiovascular Center, Japan

*CORRESPONDENCE
Shengqing Song
✉ 2802605743@qq.com
Yu Xia
✉ 3028461168@qq.com

†These authors have contributed equally to this work and share first authorship

RECEIVED 20 September 2024
ACCEPTED 16 December 2024
PUBLISHED 07 January 2025

CITATION
Cai Y, Zhang Y, Zhou N, Tang Y, Zheng H, Liu H, Liang J, Zeng R, Song S and Xia Y (2025) Association between red blood cell distribution width-to-albumin ratio and prognosis in post-cardiac arrest patients: data from the MIMIC-IV database.
Front. Cardiovasc. Med. 11:1499324.
doi: 10.3389/fcvm.2024.1499324

Association between red blood cell distribution width-to-albumin ratio and prognosis in post-cardiac arrest patients: data from the MIMIC-IV database

Yinhe Cai[1,2†], Yao Zhang[1,2†], Ningzhi Zhou[1,2], Yong Tang[1,2], Haixia Zheng[1,2], Hong Liu[1,2], Jiahua Liang[3], Ruixiang Zeng[4], Shengqing Song[5*] and Yu Xia[1,2*]

[1]Department of Cardiology, The Third Affiliated Hospital of Guangzhou University of Chinese Medicine, Guangzhou, China, [2]Guangzhou University of Chinese Medicine, Guangzhou, China, [3]The Department of Cardiovascular Disease, Meizhou Hospital of Traditional Chinese Medicine, Meizhou, China, [4]Department of Critical Care Medicine, Guangdong Provincial Hospital of Chinese Medicine, Guangzhou, China, [5]The Third Affiliated Hospital of Guangzhou University of Chinese Medicine, Guangzhou, China

Background: Cardiac arrest (CA) triggers a systemic inflammatory response, resulting in brain and cardiovascular dysfunction. The red blood cell distribution width (RDW)-to-albumin ratio (RAR) has been widely explored in various inflammation-related diseases. However, the predictive value of RAR for the prognosis of CA remains unclear. We aimed to explore the correlation between the RAR index and the 30- and 180-day mortality risks in post-CA patients.

Methods: Clinical data were extracted from the MIMIC-IV database. The enrolled patients were divided into three tertiles based on their RAR levels (<3.7, 3.7–4.5, >4.5). Restricted cubic spline, Kaplan–Meier (K-M) survival curves, and Cox proportional hazards regression model were used to explicate the relationship between the RAR index and all-cause mortality risk. Subgroup analyses were also conducted to increase stability and reliability. The receiver operator characteristic (ROC) analysis was used to assess the predictive ability of the RAR index, red blood cell distribution width, and serum albumin for 180-day all-cause mortality.

Results: A total of 612 patients were eligible, including 390 men, with a mean age of 64.1 years. A non-linear relationship was observed between the RAR index and 180-day all-cause mortality, with a hazards ratio (HR) >1 when the RAR level exceeded 4.54. The K-M survival curve preliminarily indicated that patients in higher tertiles (T2 and T3) of the RAR index presented lower 30- and 180-day survival rates. An elevated RAR index was significantly associated with an increased 30-day [adjusted HR: 1.08, 95% confidence interval (CI): 1.01–1.15] and 180-day (adjusted HR: 1.09, 95% CI: 1.03–1.16) mortality risk. According to the ROC curve analysis, the RAR index outperformed the RDW and albumin in predicting all-cause 180-day mortality [0.6404 (0.5958–0.6850) vs. 0.6226 (0.5774–0.6679) vs. 0.3841 (0.3390–0.4291)]. The prognostic value of the RAR index for 180-day mortality was consistent across subgroups, and a significant interaction was observed in patients who were white, those with chronic pulmonary disease, or those without cerebrovascular disease.

Conclusion: The RAR index is an independent risk factor for 30- and 180-day all-cause mortality in post-CA patients. The higher the RAR index, the higher the mortality. An elevated RAR index may be positively associated with adverse prognosis in post-CA patients, which can remind clinicians to quickly assess these patients.

KEYWORDS

all-cause mortality, cardiac arrest, red blood cell distribution width, albumin, MIMIC-IV database

Introduction

Cardiac arrest (CA) is one of the leading fatal diseases, characterized by the sudden cessation of cardiac ejection due to various causes (1). Only 25% of patients survive after experiencing CA, and more than 300,000 inpatients suffer from CA each year in the United States (2). Hence, early and accurate prediction associated with death in CA patients is particularly significant, contributing to stratifying high-risk patients swiftly and helping clinicians take more appropriate treatments in clinical practice.

Red blood cell distribution width (RDW) is a commonly used indicator in routine clinical hematology. Existing evidence indicates that RDW has been a novel and easily convenient marker of systemic inflammation. It has been reported that higher RDW levels are associated with worse prognoses in cardiovascular diseases (3, 4), ischemic stroke (5), kidney disease (6), and various infectious diseases (7). However, the RDW level is known to be unstable, as it is susceptible to other factors such as senescence, oxidative stress, malnutrition, or renal impairment (8). Furthermore, serum albumin (ALB) is an indicator of systemic nutritional status, and it can reduce the systemic inflammatory response by inhibiting oxidative stress and accelerating endothelial apoptosis (9, 10). Previous studies have identified low levels of serum albumin as an independent risk factor for increased cardiovascular mortality (11, 12). However, serum albumin levels are also susceptible to other factors such as chronic diseases, nutritional risk, malnutrition, and inflammation (13). Several studies have suggested that the combined marker—RDW-to-albumin ratio (RAR)—is a novel biomarker associated with the prognosis of circulation system diseases, such as stroke (9), acute myocardial infarction (14), and atrial fibrillation (15). Compared to other inflammatory markers, the RAR index being rapid, reproducible, and easy to acquire means it could be used for routine screening in clinical practice through laboratory testing. The RAR index serves as a composite marker that combines both nutritional status (ALB) and inflammatory status (RDW), and it reflects a better correlation with the inflammatory response and identification of high-risk patients compared to other single-identified markers. It has been reported that post-CA patients with high levels of inflammatory response face higher mortality rates and/or worse neurologic consequences (16, 17). However, whether the RAR index can more accurately assess the prognosis of post-CA patients has not yet been evaluated.

In this study, we aimed to explore the correlation between the RAR index and 30- and 180-day mortality in post-CA patients enrolled in the intensive care unit (ICU).

Materials and methods

Sources of data

All data were collected from the Medical Information Mart for Intensive Care IV (MIMIC-IV; version 2.0) database, a large and open critical care database approved by the Beth Israel Deaconess Medical Center and the Massachusetts Institute of Technology. This database contains records from 76,540 ICU patients admitted between 2008 and 2019. The longest follow-up period for each patient in the database was 1 year after their last discharge, providing available data support for clinical research. The personal information of all included patients was de-identified to ensure privacy of patients. Therefore, the informed consent of patients was exempt for this study.

Sample size and power analysis

The sample size was predetermined due to the retrospective design of the study (18). A *post-hoc* power analysis was performed using PASS 24.0 software to assess the study's statistical power, which was calculated to exceed 90%.

Study population

Patients who met the following criteria were enrolled: (1) patients diagnosed with CA based on the International Classification of Diseases versions 9 and 10 (ICD-9 and 10)

Abbreviations

RAR, red blood cell distribution width-to-albumin ratio; RDW, red blood cell distribution width; CA: cardiac arrest; MIMIC, Medical Information Mart for Intensive Care; ICU, intensive care unit; SOFA, Sequential Organ Failure Assessment; SAPSII, Simplified Acute Physiology Score II; BUN, blood urea nitrogen; INR, international normalized ratio; ALT, alanine aminotransferase; ALP, alkaline phosphatase; AST, aspartate aminotransferase; SBP, systolic blood pressure; DBP, diastolic blood pressure; SpO_2, pulse oxygen saturation; WBC, white blood cell; RBC, red blood cell; SD, standard deviation; HR, hazards ratio; CI, confidence interval; RCS, restricted cubic spline.

diagnosis codes ("4,275," "I46," "I,462," "I,468," and "I,469"); (2) only the first ICU admission during the initial hospitalization was considered; and (3) age 18 years and above. Exclusion criteria were as follows: (1) patients without recorded RDW or albumin levels; and (2) ICU length of stay <24 h.

Data extraction

Data were extracted from the MIMIC-IV database based on three parts: (1) baseline characteristics, including sex, age, ethnicity [white, or others (Asian, Black, unknown)], weight, comorbidities (cardiovascular disease, congestive heart failure, chronic lung disease, diabetes, peripheral vascular disease, and cerebrovascular disease), the Sequential Organ Failure Assessment (SOFA) score, the Simplified Acute Physiology Score II (SAPSII), and norepinephrine use; (2) vital signs, including systolic blood pressure (SBP), diastolic blood pressure (DBP), heart rate, respiratory rate, and pulse oxygen saturation (SpO_2); and (3) laboratory biomarkers, including RDW, red blood cell (RBC) count, white blood cell (WBC) count, platelet (PLT) count, hemoglobin, albumin, creatinine, blood urea nitrogen (BUN), glucose, international normalized ratio (INR), anion gap, alanine aminotransferase (ALT), aspartate aminotransferase (AST), alkaline phosphatase (ALP), total sodium, and potassium. All data were extracted within the first 24 h after admission to the ICU, excluding variables with ≥10% missing values. For continuous variables with less than 5% missing data, we imputed with the median of non-missing values. Variables with 5%–10% missing data were filled with multiple imputations. Data were obtained using Navicat Premium version 15.0.

Groups and outcomes

The exposure factor, RAR index, was calculated as RDW (%) divided by albumin (g/dl) (19). Violin plots and histogram density plots were prepared to visualize the fundamental characteristics of the RAR index. A total of 612 patients were enrolled in our study and divided into three groups based on the tertiles of the RAR index (20): T1 (<3.7, $n = 139$), T2 (3.7–4.5, $n = 150$), and T3 (>4.5, $n = 323$).

The endpoints of this study were 30- and 180-day all-cause mortality.

Statistical analysis

Continuous data that conformed to normal distribution are presented as the mean ± standard deviation (SD) and were analyzed using one-way ANOVA; data with a skewed distribution are presented as the median and quartile spacing [M (Q1, Q3)] and were analyzed using the Kruskal–Wallis test. Categorical variables are presented as n (%), with the analysis of the chi-square test (or Fisher's exact test).

The cumulative probability of 30- and 180-day all-cause mortality was visualized across the RAR index tertiles (T1, T2, T3) using Kaplan–Meier (K-M) curves with the log-rank test. Univariate and multivariate Cox proportional hazards regression models were used to evaluate the prognostic values of the RAR index for 30- and 180-day all-cause mortality, and hazards ratios (HRs) and 95% confidence intervals (CIs) were presented. Model 1 was adjusted for age, sex, weight, and race. Model 2 was adjusted for age, sex, weight, race, SOFA score, SAPSII score, cardiovascular disease, chronic pulmonary disease, diabetes, cerebrovascular disease, peripheral vascular disease, norepinephrine use, creatinine, SBP, DBP, ALT, ALP, and AST. In addition, subgroup analyses were also conducted based on different strata, such as demographic characteristics (sex, age, and race), comorbidities (cardiovascular disease, chronic pulmonary disease, diabetes, cerebrovascular disease, and peripheral vascular disease), and norepinephrine use.

Restricted cubic spline (RCS) analysis, based on the Cox model, was utilized to elucidate the dose–response relationship between the RAR index and 180-day all-cause mortality in post-CA patients. Receiver operating characteristic (ROC) analysis was performed to predict 180-day mortality in CA patients among RDW, albumin, RAR index, SOFA score, and SAPSII score. The above statistical analyses were performed using Stata 15.0 and SPSS 23.0 software. P-values <0.05 were considered statistically significant.

Results

Clinical characteristics of patients

We included data of 612 eligible CA patients from the MIMIC-IV database (see Figure 1). In general, 318 patients (51.96%) and 362 patients (59.15%) died of various causes within 30 and 180 days after admission. According to Table 1, the average age of the included patients was 64.1 ± 17.6 years, of whom 390 were men and 222 were women. The median overall RAR index was 4.61 (3.82–5.7), and its distribution is displayed in Figure 2. Using the RAR T1 group as the reference, an increase in RAR index was associated with a higher proportion of patients admitted to ICU, an increased likelihood of women patients, older age, lower body weight, reduced SBP and DBP, higher levels of RDW, creatinine, and BUN, and lower levels of albumin and platelets. The SOFA and SAPSII scores were worse, and the prevalence of diabetes and peripheral vascular disease was higher. The proportion of patients with cerebrovascular disease was lower.

Associations between the RAR index and mortality risk in post-CA patients

When considering the RAR index as a continuous variable, Cox regression analysis revealed that an elevated RAR index was significantly associated with higher 30- and 180-day mortality in both the unadjusted model (30-day: HR: 1.14; 95% CI: 1.08–1.21;

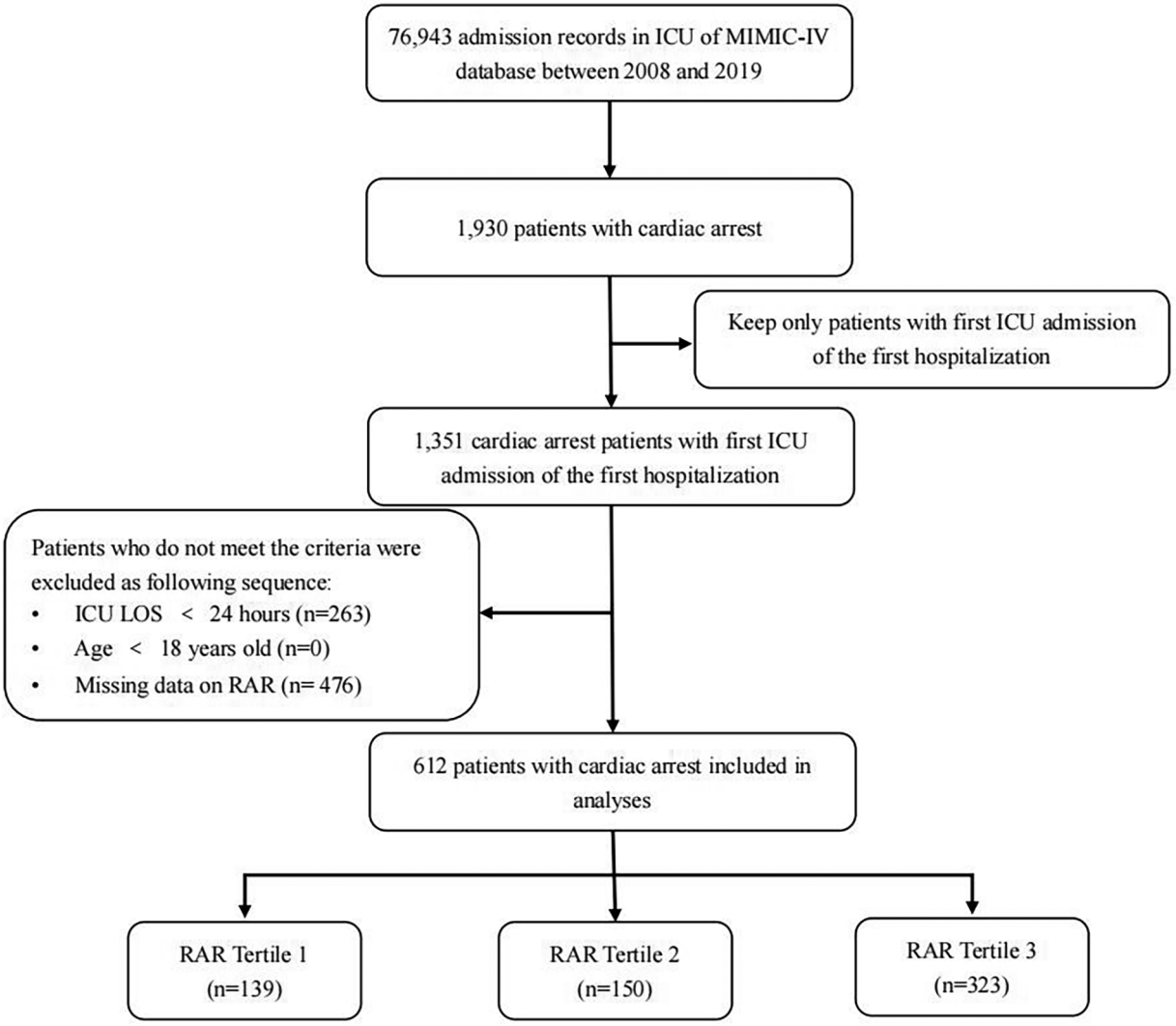

FIGURE 1
Flowchart of patient screening.

180-day: HR: 1.16; 95% CI: 1.10–1.22) and the fully adjusted model (30-day: HR: 1.08; 95% CI: 1.01–1.15; 180-day: HR: 1.09; 95% CI: 1.03–1.16). When analyzing the RAR index as a categorized variable, Cox proportional hazards analysis revealed that the highest tertile (T3) of the RAR index was also significantly correlated with increased 180-day mortality in both the unadjusted model (HR: 2.07; 95% CI: 1.57–2.79) and the adjusted model (Model 1: HR: 2.00; 95% CI: 1.48–2.72; Model 2: HR: 1.74; 95% CI: 1.26–2.42) (Table 2). Similar results were also observed between the highest tertile (T3) of the RAR index and 30-day all-cause mortality (unadjusted: HR: 1.90; 95% CI: 1.39–2.60; Model 1: HR: 1.83; 95% CI: 1.33–2.52; Model 2: HR: 1.60; 95% CI: 1.13–2.25).

RCS analysis indicated a non-linear relationship between the RAR index and 180-day mortality in patients with CA (Figure 3). The risk of mortality increased with increasing RAR levels, and its HR was always >1 when the RAR level exceeded 4.54. The cumulative 30-day and 180-day mortality across RAR index groups is shown in Kaplan–Meier analysis (30-day: T1: 50, 35.97%; T2: 78, 52%; T3: 190, 58.82%; 180-day: T1: 55, 39.57%; T2: 90, 60%; T3: 217, 67.18%) (see Figure 4). The analysis revealed that the cumulative incidence of 30- and 180-day death increased with elevating quartiles of the RAR index (log-rank test, $p < 0.001$).

ROC curve analysis of the RAR index

ROC curve analyses were conducted for the RAR index, RDW, albumin, SOFA score, SAPSII score, and SAPSII combined RAR to predict 180-day mortality in patients with CA (Figure 5). It was observed that the RAR index [0.640 (0.596–0.685)] outperformed the RDW [0.623 (0.577–0.668)], albumin [0.384 (0.339–0.429)], and SOFA score [0.601 (0.556–0.646)] in predicting all-cause 180-day mortality, both with $p < 0.001$. In addition, the RAR index showed no significant superiority over the SAPSII score [0.677 (0.634–0.720)] for CA patients. Further analysis of the

TABLE 1 Comparisons of the baseline characteristics categorized by the RAR index.

Variables	Total overall, *N* = 612	RAR tertile 1 (*N* = 139)	RAR tertile 2 (*N* = 150)	RAR tertile 3 (*n* = 323)	*P*-value
RAR index	4.61 (3.82–5.7)	3.4 (3.16–3.55)	4.15 (3.93–4.32)	5.6 (4.98–6.61)	<0.001
Age, years	64.1 ± 17.6	56.8 ± 17.6	65.3 ± 17.9	66.6 ± 16.6	<0.001
Sex, male, *n* (%)	390 (63.73)	106 (76.26)	93 (62.00)	191 (59.13)	0.002
Weight, kg	86.4 ± 23.5	92.2 ± 21.5	86.2 ± 22.2	84.5 ± 25.0	0.006
Race, *n* (%)					0.703
White	329 (53.8)	71 (51.08)	84 (56.00)	174 (53.87)	
Other	283 (46.2)	68 (48.92)	66 (44.00)	149 (46.13)	
SBP, mmHg	114.7 ± 15.8	117.7 ± 16.3	117.8 ± 16.0	112.0 ± 15.1	<0.001
DBP, mmHg	64.0 ± 11.2	68.7 ± 11.1	65.0 ± 11.6	61.5 ± 10.3	<0.001
Heart rate, beats/min	84.93 ± 19.13	79.1 ± 16.9	81.7 ± 19.4	88.9 ± 19.0	<0.001
Respiratory rate, times/min	21.3 ± 4.7	21.1 ± 4.5	21.2 ± 4.3	21.5 ± 5.0	0.608
SpO_2, %	97.7 (96.0–99.1)	97.9 (96.3–99.3)	98.0 (96.1–99.4)	97.5 (95.8–98.9)	0.012
Comorbidities, *n* (%)					
Cardiovascular disease	151 (24.67)	36 (25.9)	39 (26.0)	76 (23.53)	0.786
Chronic pulmonary disease	165 (26.96)	30 (21.58)	45 (30.00)	90 (27.86)	0.237
Diabetes	190 (31.03)	23 (16.55)	48 (32.00)	119 (36.84)	<0.001
Cerebrovascular disease	90 (14.71)	25 (17.99)	29 (19.33)	36 (11.15)	0.030
Peripheral vascular disease	87 (14.22)	11 (7.91)	18 (12.00)	58 (17.96)	0.012
Congestive heart failure	231 (37.75)	46 (33.09)	61 (40.67)	124 (38.39)	0.390
Norepinephrine use, *n* (%)	405 (66.18)	86 (61.87)	94 (62.67)	225 (69.66)	0.155
Scoring systems					
SOFA	8.7 ± 4.1	7.3 ± 3.8	7.8 ± 3.7	9.5 ± 4.1	<0.001
SAPSII	49.1 ± 17.0	40.8 ± 17.0	46.8 ± 15.5	53.8 ± 16.1	<0.001
Laboratory tests					
ALT, IU/L	72 (32–221)	98 (40–303)	76 (34–201)	61 (28–217)	0.038
AST, IU/L	118 (49–357)	118 (50–374)	118 (51–275)	118 (47–367)	0.910
ALP, IU/L	86 (62–124)	75 (61–97)	81 (62–113)	95 (61–134)	<0.001
RDW, %	14.6 (13.6–16.0)	13.2 (12.6–13.8)	14.2 (13.5–15.0)	15.6 (14.5–17.3)	<0.001
Albumin, g/dl	3.3 (2.7–3.7)	4.0 (3.8–4.2)	3.4 (3.2–3.7)	2.8 (2.4–3.1)	<0.001
WBC, 10^9/L	13.4 (9.4–17.8)	13.7 (11.1–18.4)	12.9 (9.6–16.7)	13.3 (8.8–18.0)	0.181
RBC, 10^{12}/L	3.8 (3.2–4.5)	4.5 (4.0–4.8)	4.0 (3.5–4.5)	3.4 (3.0–4.1)	<0.001
Platelets, 10^9/L	188 (141–249)	203 (172–247)	182 (146–232)	181 (122–260)	0.010
Hemoglobin, g/dl	11.6 ± 2.4	13.6 ± 1.9	12.3 ± 1.9	10.4 ± 2.1	<0.001
Anion gap, mmol/L	16.7 (14.3–19.7)	16.3 (14–18.8)	16.5 (14.5–18.8)	17 (14.3–20.2)	0.223
Potassium, mg/dl	4.2 (3.9–4.7)	4.17 (3.9–4.7)	4.2 (3.9–4.5)	4.2 (3.8–4.8)	0.523
Sodium, mg/dl	139.0 (136.4–141.7)	139.6 (137.8–142.0)	138.4 (136.2–141.4)	138.8 (136.0–141.7)	0.031
Creatinine, mg/dl	1.4 (0.9–2.2)	1.1 (0.9–1.6)	1.3 (0.9–2.0)	1.7 (1.0–2.6)	<0.001
BUN, mg/dl	25.2 (17.2–40.6)	20.0 (15.0–26.5)	24.3 (17.5–37.0)	30.3 (18.5–52.3)	<0.001
Glucose, mg/dl	186.0 ± 83.0	184.2 ± 77.2	185.1 ± 76.4	187.3 ± 8.4	0.922
INR	1.3 (1.2–1.71)	1.16 (1.1–1.3)	1.2 (1.1–1.5)	1.5 (1.2–1.9)	<0.001
30-day mortality, *n* (%)	318 (51.96)	50 (35.97)	78 (52)	190 (58.82)	<0.001
180-day mortality, *n* (%)	362 (59.15)	55 (39.57)	90 (60.00)	217 (67.18)	<0.001

RAR, ratio of RDW to albumin; SBP systolic blood pressure; DBP, diastolic blood pressure; SOFA, Sequential Organ Failure Assessment; SAPSII, Simplified Acute Physiology Score II; ALT, alanine aminotransferase; AST, aspartate aminotransferase; ALP, alkaline phosphatase; RDW, red blood cell distribution width; WBC, white blood cell; RBC, red blood cell; BUN, blood urea nitrogen; INR, international normalized ratio.

combined RAR index and SAPSII score for prognostic assessment in CA patients showed a better predictive capability [0.698 (0.655–0.740)] compared to the RAR index and SAPSII score alone.

Subgroup analyses

After adjusting for all covariates, we conducted subgroup analyses based on demographics and several comorbidities. As shown in Table 3, the positive association between the RAR index and 180-day mortality remained generally consistent across subgroups. An interaction was found in the strata of race (p for interaction = 0.025), chronic pulmonary disease (p for interaction = 0.005), and cerebrovascular disease (p for interaction = 0.010). Patients with higher RAR levels were related to higher mortality among white patients, those with chronic pulmonary disease, or those without cerebrovascular disease.

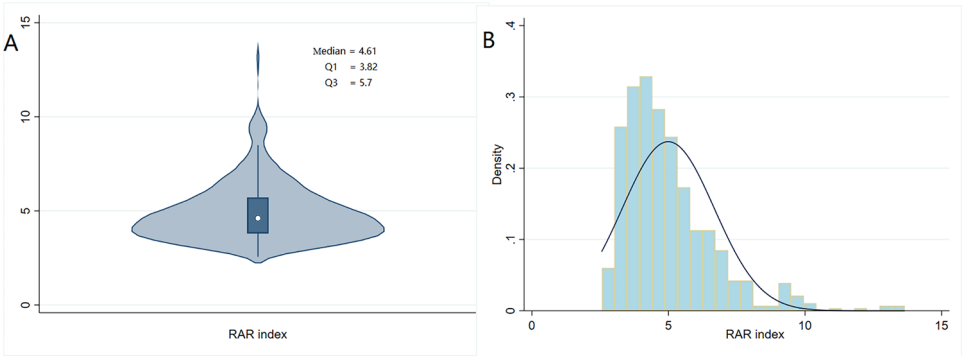

FIGURE 2
Violin plot (A) and histogram density plot (B) displaying the distribution of the RAR index.

TABLE 2 Cox proportional hazards analysis of 30- and 180-day all-cause mortality in post-CA patients.

Outcomes	Groups	Non-adjusted		Model 1[a]		Model 2[b]	
		HR (95% CI)	*P*	HR (95% CI)	*P*	HR (95% CI)	*P*
30-day mortality	Continuous	1.14 (1.08–1.21)	0.0001	1.15 (1.08–1.22)	0.0001	1.08 (1.01–1.15)	0.0016
	T1 (<3.7; *N* = 135)	1		1		1	
	T2 (3.7–4.5; *N* = 155)	1.58 (1.10–2.25)	0.012	1.55 (1.08–2.22)	0.018	1.45 (1.00–2.09)	0.045
	T3 (>4.5; *N* = 322)	1.90 (1.39–2.60)	0.0001	1.83 (1.33–2.52)	0.0001	1.60 (1.13–2.25)	0.008
180-day mortality	Continuous	1.16 (1.10–1.22)	0.0001	1.16 (1.10–1.23)	0.0001	1.09 (1.03–1.16)	0.003
	T1 (<3.7; *N* = 135)	1		1		1	
	T2 (3.7–4.5; *N* = 155)	1.71 (1.23–2.40)	0.002	1.69 (1.20–2.37)	0.003	1.59 (1.12–2.25)	0.009
	T3 (>4.5; *N* = 322)	2.07 (1.54–2.79)	0.0001	2.00 (1.48–2.72)	0.0001	1.74 (1.26–2.42)	0.001

Models 1 and 2 were derived from Cox proportional hazards regression models.
[a]Model 1 covariates were adjusted for age, race, weight, and sex.
[b]Model 2 covariates were adjusted for age, race, weight, sex, SOFA score, SAPSII score, cardiovascular disease, chronic pulmonary disease, diabetes, cerebrovascular disease, peripheral vascular disease, norepinephrine use, creatinine, SBP, DBP, ALT, ALP, and AST.

Discussion

Recently, mortality in CA patients has been gradually found to be associated with an anion gap, albumin-corrected anion gap (21), INR (22), and the stress hyperglycemia ratio (23), which reflects tissue hypoxia, abnormalities in the coagulation–fibrinolysis system, and electrolyte disturbances. However, few studies have explored the predictive power of inflammatory indicators in determining mortality among CA patients. To our knowledge, this study is the first to underscore that elevated RAR levels, a novel inflammatory biomarker, are associated with higher 30- and 180-day all-cause mortality in post-CA patients admitted to the ICU, both as a continuous and nominal variable. First, we used RCS analysis to investigate the potential correlation between the RAR index and 180-day prognosis. There was a corresponding increase in all-cause mortality with an increased RAR index. When RAR was >4.54, the risk of all-cause death was increased. The K-M survival curve and Cox regression analysis further indicated that the 30- and 180-day mortality risks were noticeably higher in CA patients with an elevated RAR index, which was still robust in the subgroup analyses. Therefore, our findings could help clinicians initially predict the prognosis of CA patients within 180 days using an easily accessible index.

Post-CA patients suffer from systemic ischemia/reperfusion injury (24), which triggers the activation of systemic inflammation, contributes to hemodynamic instability, and exacerbates injury to the brain and myocardium (25). Previous studies have shown that high levels of inflammatory response in CA patients are associated with higher mortality and/or worse neurologic consequences (16, 17). It is significant for clinicians to identify effective biomarkers that can reflect systemic inflammation and predict the mortality of patients after CA.

RDW measures the degree of heterogeneity in RBC volume, as detected by a blood analysis, and a high RDW reflects severe erythrocyte homeostasis deregulation caused by various metabolic abnormalities, such as inflammation (26). Previous studies have demonstrated that high RDW is associated with all-cause mortality in patients with cardiovascular disease, diabetes, cancer, liver and kidney failure, and other diseases (27). Similarly, albumin levels are usually utilized to analyze the nutritional status of patients (28) and have now been proposed as an inflammation biomarker of prognosis in critically ill patients (29). It has been shown that the synthesis rate of albumin is negatively associated with

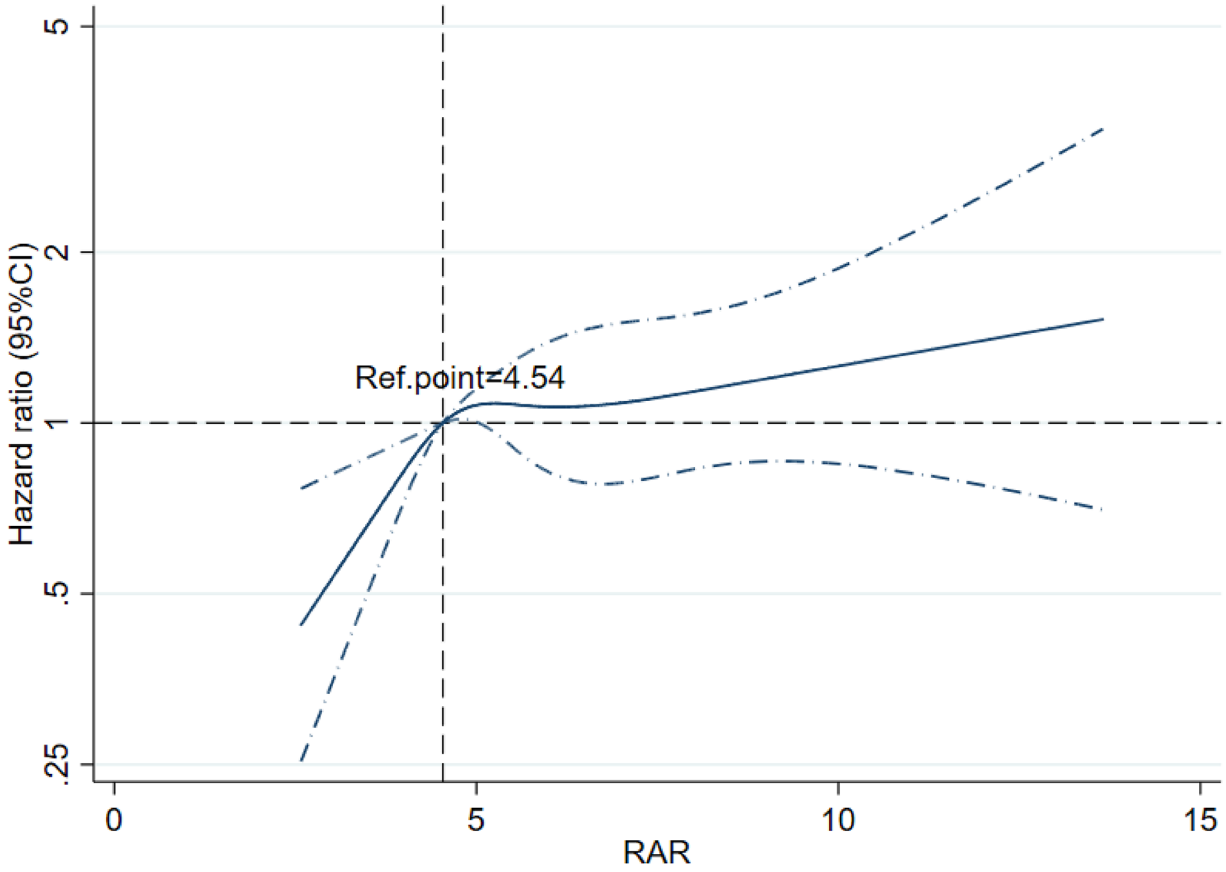

FIGURE 3
Restricted cubic spline regression analysis of the RAR index for 180-day mortality among post-CA patients.

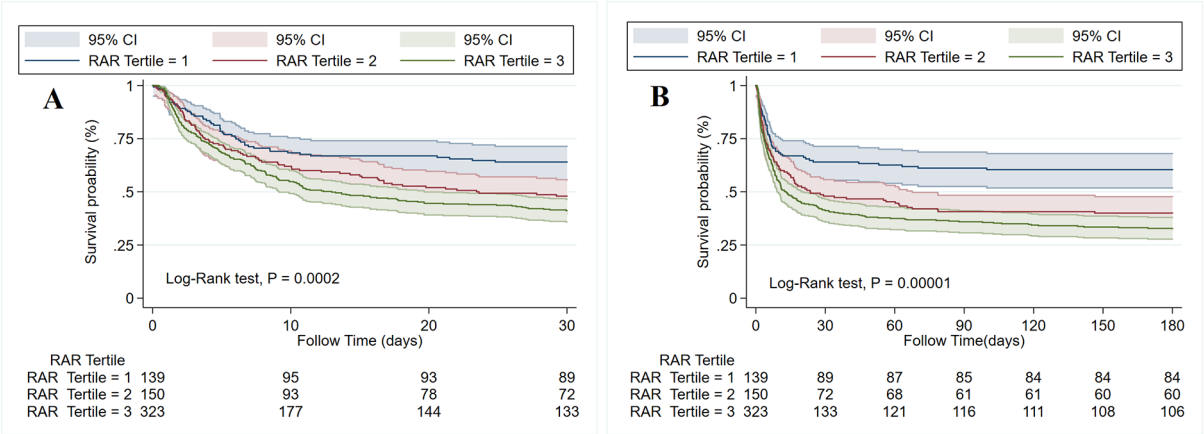

FIGURE 4
Kaplan–Meier survival curve of the cumulative survival rate among three tertiles of the RAR index within 30-day **(A)** and 180-day **(B)** follow-ups.

inflammatory activity (30), and low albumin levels in the early phase play a pro-inflammatory role and are positively correlated with hospitalization mortality of patients after CA (31).

Currently, the RAR index has emerged as a rapid, reproducible, and easily accessible composite marker that combines both nutritional status (ALB) and inflammatory status (RDW), and it may be a better tool to reflect the inflammatory response and identify high-risk patients compared to other single-identified markers (RDW and albumin). Xu et al. revealed that the RAR index is a potential prognostic indicator for sepsis patients, and a

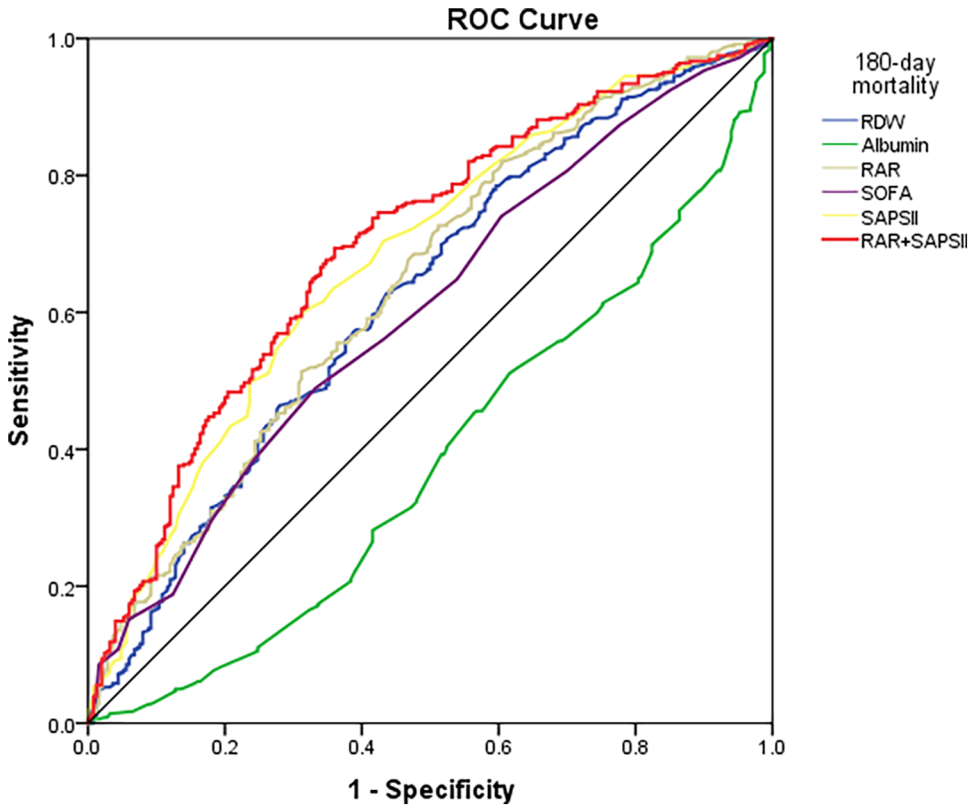

FIGURE 5
ROC curves predicting 180-day mortality in CA patients.

higher RAR index indicates worse clinical prognosis (19). Li and Xu reported that a high RAR index is a potential marker of increased mortality in AMI patients (14). However, no studies have explored the relationship between the RAR index and CA patients. Remarkably, this study indicated that after adjusting for age, race, weight, sex, SOFA score, SAPSII score, cardiovascular disease, chronic pulmonary disease, diabetes, cerebrovascular disease, peripheral vascular disease, norepinephrine use, creatinine, SBP, DBP, ALT, ALP, and AST, the RAR index was positively correlated with increased 180-day mortality in patients with CA. It is suggested that a higher RAR level is associated with worse prognosis in post-CA patients.

In our study, the RAR index is an independent predictor of 180-day mortality in CA patients. It showed superior predictive value compared to standalone markers, such as RDW, albumin, or SOFA scores. This indicates that the RAR index may be an available supplementary measure to clinical decision-making for prognostic assessment in CA patients. For ICU patients, particularly those with CA, routine monitoring of RAR may be advisable to remind clinicians to quickly identify high-risk patients. In addition, combining RAR with the SAPSII score may improve predictive significance.

The mechanisms by which the RAR level influences 180-day mortality in CA patients remain elusive but are hypothetically related to chronic inflammation and nutritional deficiencies. Cardiac arrest-induced inflammation could lead to increased RDW elevation and decreased albumin levels, which causes a significant increase in RAR. However, our study was unable to assess the indirect effect of inflammatory markers [such as C-reactive protein, hypersensitive C-reactive protein, erythrocyte sedimentation rate (ESR), and ferritin] on the association between the RAR level and the likelihood of 180-day mortality through mediation analysis because of the high number of missing values. Gaining insight into these underlying mechanisms is propitious to ascertain potential interventions that focus on regulating the inflammatory environment and improving outcomes in patients with CA.

Our study indicated that the cutoff value of the RAR index for predicting 180-day mortality is 4.54. The RAR index combines both nutritional status (ALB) and inflammatory status (RDW); the elevation in RAR often stems from higher RDW and/or lower albumin levels. We hypothesized that when the RAR index exceeds 4.54, post-CA patients may have developed severe inflammation and/or poor nutritional status, which is difficult to reverse. Several previous reports have also shown a similar finding. A study conducted on patients with coronary heart disease and diabetes mellitus demonstrated that individuals with a RAR cutoff value >4.26 exhibited significantly higher 1-year mortality compared to those with a RAR cutoff value <4.26 [area under curve (AUC) 0.68] (32). Similarly, another study focusing on patients with sepsis and

TABLE 3 Subgroup analyses of the association between the RAR index and 180-day all-cause mortality.

Variables	No. of patients	RAR index			*P* for interaction
		T1 (3.7)	T2 (3.7–4.5)	T3(>4.5)	
Sex					0.404
Male	390	1.0	1.51 (0.99–2.32)	2.04 (1.37–3.04)	
Female	222	1.0	1.39 (0.73–2.67)	1.06 (0.58–1.95)	
Age					0.116
<60	219	1.0	1.54 (0.90–2.62)	1.51 (0.92–2.45)	
≥60	393	1.0	1.75 (1.06–2.88)	2.15 (1.33–3.46)	
Race					0.025
White	329	1.0	1.75 (1.06–2.88)	2.15 (1.33–3.46)	
Other	283	1.0	1.54 (0.90–2.62)	1.51 (0.92–22.45)	
Cardiovascular disease					0.531
No	461	1.0	1.55 (1.04–2.30)	1.71 (1.18–2.48)	
Yes	151	1.0	1.64 (0.76–3.53)	1.77 (0.84–3.75)	
Diabetes					0.721
No	422	1.0	1.63 (1.10–2.43)	1.94 (1.34–2.81)	
Yes	190	1.0	1.54 (0.66–3.56)	1.41 (0.65–3.07)	
Chronic pulmonary disease					0.210
No	447	1.0	1.44 (0.98–2.13)	1.52 (1.06–2.18)	
Yes	165	1.0	3.72 (1.48–9.32)	3.33 (1.30–8.53)	
Cerebrovascular disease					0.005
No	522	1.0	1.42 (0.95–2.13)	1.90 (1.31–2.76)	
Yes	90	1.0	3.63 (1.63–8.09)	1.31 (0.56–3.05)	
Peripheral vascular disease					0.010
No	525	1.0	1.42 (0.98–2.05)	1.80 (1.28–2.53)	
Yes	87	1.0	5.59 (1.68–18.62)	1.13 (0.33–3.83)	
Norepinephrine use					0.781
No	207	1.0	1.48 (0.77–2.85)	1.24 (0.65–2.37)	
Yes	405	1.0	1.61 (1.05–2.46)	1.84 (1.24–2.72)	

HRs (95% CIs) were derived from Cox regression models. Covariates were adjusted as in model 2 (Table 2).

atrial fibrillation revealed that the optimal cutoff value of RAR for predicting in-hospital mortality was 4.882 (15).

Furthermore, subgroup analyses showed a significant interaction among patients with chronic pulmonary disease. This may be attributed to hypoxic conditions and inflammation responses, as acute hypoxia and inflammatory responses could promote an increase in serum erythropoietin and lead to greater variability in red blood cells, which is reflected by elevated RDW (33). However, enlarged red blood cells in the circulatory system would lead to inferior capabilities of transport oxygen, which likely exacerbates hypoxia (34).

Nevertheless, our study has some drawbacks. First, we used a retrospective study design, and the selection bias and confounding bias of the retrospective study itself cannot be ignored, although we adjusted for potential confounding confounders and performed subgroup analyses. Future prospective cohort studies are needed to validate our outcomes. Second, we tested RAR only at the time of ICU admission without dynamically supervising the RAR index, which may change over time or in response to the condition of the patients after CA. Third, due to the limitation of the database, some variables, including cardiac function classification, echocardiography results, care conditions out of hospital, and therapy (potential confounders), were unavailable, which might impact our results. Finally, the potential mechanism between a higher RAR index and elevated mortality in post-CA patients remains unclear, warranting further research. In addition, since ischemia–reperfusion injury and inflammatory responses play key roles in the pathophysiology of cardiac arrest, it may be worth exploring the association between other inflammatory or hypoxic indicators and mortality among CA patients.

Conclusion

Our study identified the RAR index as an independent prognostic marker for post-CA patients, and an increased RAR index was associated with higher 180-day mortality in post-CA patients. The RAR index is expected to be an available and effective prognostic evaluation indicator in post-CA patients.

Data availability statement

Publicly available datasets were analyzed in this study. This data can be found here: https://physionet.org/content/mimiciv/2.0/.

Ethics statement

Ethical approval was not required for the study involving humans in accordance with the local legislation and institutional requirements. Written informed consent to participate in this study was not required from the participants or the participants' legal guardians/next of kin in accordance with the national legislation and the institutional requirements.

Author contributions

YC: Conceptualization, Data curation, Investigation, Methodology, Visualization, Writing – original draft. YZ: Conceptualization, Data curation, Methodology, Visualization, Writing – original draft. NZ: Data curation, Formal Analysis, Investigation, Validation, Writing – original draft. YT: Investigation, Validation, Writing – review & editing. HZ: Methodology, Resources, Software, Validation, Visualization, Writing – review & editing. HL: Supervision, Validation, Writing – review & editing. JL: Data curation, Methodology, Software, Validation, Writing – review & editing. RZ: Conceptualization, Methodology, Resources, Validation, Writing – review & editing. SS: Conceptualization, Project administration, Supervision, Writing – review & editing. YX: Conceptualization, Project administration, Writing – review & editing.

Funding

The author(s) declare financial support was received for the research, authorship, and/or publication of this article. This study was financially supported by the Administration of Traditional Chinese Medicine of Guangdong Province (202304292145498460).

Conflict of interest

The authors declare that the research was conducted in the absence of any commercial or financial relationships that could be construed as a potential conflict of interest.

Publisher's note

References

1. Tsao CW, Aday AW, Almarzooq ZI, Anderson C, Arora P, Avery CL, et al. Heart disease and stroke statistics—2023 update: a report from the American Heart Association. *Circulation*. (2023) 147:e93–621. doi: 10.1161/CIR.0000000000001123

2. Jacobs I, Nadkarni V, Bahr J, Berg RA, Billi JE, Bossaert L, et al. Cardiac arrest and cardiopulmonary resuscitation outcome reports: update and simplification of the Utstein templates for resuscitation registries: a statement for healthcare professionals from a task force of the international liaison committee on resuscitation (American Heart Association, European Resuscitation Council, Australian Resuscitation Council, New Zealand Resuscitation Council, Heart and Stroke Foundation of Canada, InterAmerican Heart Foundation, Resuscitation Councils of Southern Africa). *Circulation*. (2004) 110:3385–97. doi: 10.1161/01.CIR.0000147236.85306.15

3. Ji X, Ke W. Red blood cell distribution width and all-cause mortality in congestive heart failure patients: a retrospective cohort study based on the Mimic-III database. *Front Cardiovasc Med*. (2023) 10:1126718. doi: 10.3389/fcvm.2023.1126718

4. Zhang B, Xu Y, Huang X, Sun T, Ma M, Chen Z, et al. Red blood cell distribution width: a risk factor for prognosis in patients with ischemic cardiomyopathy after percutaneous coronary intervention. *J Clin Med*. (2023) 12:1584. doi: 10.3390/jcm12041584

5. Xue J, Zhang D, Zhang XG, Zhu XQ, Xu XS, Yue Y. Red cell distribution width is associated with stroke severity and unfavorable functional outcomes in ischemic stroke. *Front Neurol*. (2022) 13:938515. doi: 10.3389/fneur.2022.938515

6. Hua R, Liu X, Yuan E. Red blood cell distribution width at admission predicts outcome in critically ill patients with kidney failure: a retrospective cohort study based on the MIMIC-IV database. *Ren Fail*. (2022) 44:1182–91. doi: 10.1080/0886022X.2022.2098766

7. Wu H, Liao B, Cao T, Ji T, Huang J, Ma K. Diagnostic value of RDW for the prediction of mortality in adult sepsis patients: a systematic review and meta-analysis. *Front Immunol*. (2022) 13:997853. doi: 10.3389/fimmu.2022.997853

8. Lippi G, Turcato G, Cervellin G, Sanchis-Gomar F. Red blood cell distribution width in heart failure: a narrative review. *World J Cardiol*. (2018) 10:6–14. doi: 10.4330/wjc.v10.i2.6

9. Zhao N, Hu W, Wu Z, Wu X, Li W, Wang Y, et al. The red blood cell distribution width-albumin ratio: a promising predictor of mortality in stroke patients. *Int J Gen Med*. (2021) 14:3737–47. doi: 10.2147/IJGM.S322441

10. Wang X, Wang J, Wu S, Ni Q, Chen P. Association between the neutrophil percentage-to-albumin ratio and outcomes in cardiac intensive care unit patients. *Int J Gen Med*. (2021) 14:4933–43. doi: 10.2147/IJGM.S328882

11. Grimm G, Haslacher H, Kampitsch T, Endler G, Marsik C, Schickbauer T, et al. Sex differences in the association between albumin and all-cause and vascular mortality. *Eur J Clin Invest*. (2009) 39:860–5. doi: 10.1111/j.1365-2362.2009.02189.x

12. Xia M, Zhang C, Gu J, Chen J, Wang LC, Lu Y, et al. Impact of serum albumin levels on long-term all-cause, cardiovascular, and cardiac mortality in patients with first-onset acute myocardial infarction. *Clin Chim Acta*. (2018) 477:89–93. doi: 10.1016/j.cca.2017.12.014

13. Eckart A, Struja T, Kutz A, Baumgartner A, Baumgartner T, Zurfluh S, et al. Relationship of nutritional status, inflammation, and serum albumin levels during acute illness: a prospective study. *Am J Med*. (2020) 133:713–22.e7. doi: 10.1016/j.amjmed.2019.10.031

14. Li H, Xu Y. Association between red blood cell distribution width-to-albumin ratio and prognosis of patients with acute myocardial infarction. *BMC Cardiovasc Disord*. (2023) 23:66. doi: 10.1186/s12872-023-03094-1

15. Gu YL, Yang D, Huang ZB, Chen Y, Dai ZS. Relationship between red blood cell distribution width-to-albumin ratio and outcome of septic patients with atrial fibrillation: a retrospective cohort study. *BMC Cardiovasc Disord*. (2022) 22:538. doi: 10.1186/s12872-022-02975-1

16. Peberdy MA, Andersen LW, Abbate A, Thacker LR, Gaieski D, Abella BS, et al. Inflammatory markers following resuscitation from out-of-hospital cardiac arrest—a prospective multicenter observational study. *Resuscitation*. (2016) 103:117–24. doi: 10.1016/j.resuscitation.2016.01.006

17. Oda Y, Tsuruta R, Kasaoka S, Inoue T, Maekawa T. The cutoff values of intrathecal interleukin 8 and 6 for predicting the neurological outcome in cardiac arrest victims. *Resuscitation*. (2009) 80:189–93. doi: 10.1016/j.resuscitation.2008.10.001

18. Gauss T, Ageron FX, Devaud ML, Debaty G, Travers S, Garrigue D, et al. Association of prehospital time to in-hospital trauma mortality in a physician-staffed emergency medicine system. *JAMA Surg*. (2019) 154:1117–24. doi: 10.1001/jamasurg.2019.3475

19. Xu W, Huo J, Chen G, Yang K, Huang Z, Peng L, et al. Association between red blood cell distribution width to albumin ratio and prognosis of patients with sepsis: a retrospective cohort study. *Front Nutr*. (2022) 9:1019502. doi: 10.3389/fnut.2022.1019502

20. Weng Y, Peng Y, Xu Y, Wang L, Wu B, Xiang H, et al. The ratio of red blood cell distribution width to albumin is correlated with all-cause mortality of patients after percutaneous coronary intervention—a retrospective cohort study. *Front Cardiovasc Med*. (2022) 9:869816. doi: 10.3389/fcvm.2022.869816

21. Chen J, Dai C, Yang Y, Wang Y, Zeng R, Li B, et al. The association between anion gap and in-hospital mortality of post-cardiac arrest patients: a retrospective study. *Sci Rep*. (2022) 12:7405. doi: 10.1038/s41598-022-11081-3

22. Tang Y, Sun J, Yu Z, Liang B, Peng B, Ma J, et al. Association between prothrombin time-international normalized ratio and prognosis of post-cardiac arrest patients: a retrospective cohort study. *Front Public Health*. (2023) 11:1112623. doi: 10.3389/fpubh.2023.1112623

23. Lian LY, Xue WH, Lu JJ, Zheng RJ. Impact of stress hyperglycemia ratio on mortality in patients with cardiac arrest: insight from American MIMIC-IV database. *Front Endocrinol (Lausanne)*. (2024) 15:1383993. doi: 10.3389/fendo.2024.1383993

24. Nolan JP, Neumar RW, Adrie C, Aibiki M, Berg RA, Böttiger BW, et al. Post-cardiac arrest syndrome: epidemiology, pathophysiology, treatment, and prognostication. A Scientific Statement from the International Liaison Committee on Resuscitation; the American Heart Association Emergency Cardiovascular Care Committee; the Council on Cardiovascular Surgery and Anesthesia; the Council on Cardiopulmonary, Perioperative, and Critical Care; the Council on Clinical Cardiology; the Council on Stroke. *Resuscitation*. (2008) 79:350–79. doi: 10.1016/j.resuscitation.2008.09.017

25. Bro-Jeppesen J, Johansson PI, Hassager C, Wanscher M, Ostrowski SR, Bjerre M, et al. Endothelial activation/injury and associations with severity of post-cardiac arrest syndrome and mortality after out-of-hospital cardiac arrest. *Resuscitation*. (2016) 107:71–9. doi: 10.1016/j.resuscitation.2016.08.006

26. Ananthaseshan S, Bojakowski K, Sacharczuk M, Poznanski P, Skiba DS, Prahl WL, et al. Red blood cell distribution width is associated with increased interactions of blood cells with vascular wall. *Sci Rep*. (2022) 12:13676. doi: 10.1038/s41598-022-17847-z

27. Salvagno GL, Sanchis-Gomar F, Picanza A, Lippi G. Red blood cell distribution width: a simple parameter with multiple clinical applications. *Crit Rev Clin Lab Sci*. (2015) 52:86–105. doi: 10.3109/10408363.2014.992064

28. Alcorta MD, Alvarez PC, Cabetas RN, Martín MA, Valero M, Candela CG. The importance of serum albumin determination method to classify patients based on nutritional status. *Clin Nutr ESPEN*. (2018) 25:110–3. doi: 10.1016/j.clnesp.2018.03.124

29. Lee JH, Kim J, Kim K, Jo YH, Rhee J, Kim TY, et al. Albumin and C-reactive protein have prognostic significance in patients with community-acquired pneumonia. *J Crit Care*. (2011) 26:287–94. doi: 10.1016/j.jcrc.2010.10.007

30. Arques S. Human serum albumin in cardiovascular diseases. *Eur J Intern Med*. (2018) 52:8–12. doi: 10.1016/j.ejim.2018.04.014

31. Lee H, Lee J, Shin H, Lim TH, Jang BH, Cho Y, et al. Association between early phase serum albumin levels and outcomes of post-cardiac arrest patients: a systematic review and meta-analysis. *J Pers Med*. (2022) 12:1787. doi: 10.3390/jpm12111787

32. Chen S, Guan S, Yan Z, Ouyang F, Li S, Liu L, et al. Prognostic value of red blood cell distribution width-to-albumin ratio in ICU patients with coronary heart disease and diabetes mellitus. *Front Endocrinol (Lausanne)*. (2024) 15:1359345. doi: 10.3389/fendo.2024.1359345

33. Yčas JW, Horrow JC, Horne BD. Persistent increase in red cell size distribution width after acute diseases: a biomarker of hypoxemia? *Clin Chim Acta*. (2015) 448:107–17. doi: 10.1016/j.cca.2015.05.021

34. Friedman JS, Lopez MF, Fleming MD, Rivera A, Martin FM, Welsh ML, et al. SOD2-deficiency anemia: protein oxidation and altered protein expression reveal targets of damage, stress response, and antioxidant responsiveness. *Blood*. (2004) 104:2565–73. doi: 10.1182/blood-2003-11-3858

frontiers | Frontiers in Cardiovascular Medicine

TYPE Review
PUBLISHED 08 January 2025
DOI 10.3389/fcvm.2024.1520596

OPEN ACCESS

EDITED BY
Keita Saku,
National Cerebral and Cardiovascular Center, Japan

REVIEWED BY
Cheng Jiang,
Wuhan University, China
Masafumi Fukumitsu,
National Cerebral and Cardiovascular Center, Japan

*CORRESPONDENCE
Pengfei Pan
ppfswh@126.com
Xiangyou Yu
yu2796@163.com

†These authors have contributed equally to this work

RECEIVED 31 October 2024
ACCEPTED 16 December 2024
PUBLISHED 08 January 2025

CITATION
Du X, Xiong F, Hou Y, Yu X and Pan P (2025) Levosimendan for sepsis-induced myocardial dysfunction: friend or foe?
Front. Cardiovasc. Med. 11:1520596.
doi: 10.3389/fcvm.2024.1520596

Levosimendan for sepsis-induced myocardial dysfunction: friend or foe?

Xinxin Du[1,2†], Fang Xiong[3†], Yafei Hou[4], Xiangyou Yu[2*] and Pengfei Pan[3*]

[1]Cardiac Intensive Care Center, Zhongshan Hospital, Fudan University, Shanghai, China, [2]Department of Critical Care Medicine, The First Affiliated Hospital of Xinjiang Medical University, Urumqi, Xinjiang, China, [3]Department of Critical Care Medicine, Chongqing University Three Gorges Hospital, Wanzhou, Chongqing, China, [4]Shanghai Institute of Immunology, Shanghai Jiao Tong University School of Medicine, Shanghai, China

Sepsis-induced myocardial dysfunction (SIMD) involves reversible myocardial dysfunction. The use of inotropes can restore adequate cardiac output and tissue perfusion, but conventional inotropes, such as dobutamine and adrenaline, have limited efficacy in such situations. Levosimendan is a novel inotrope that acts in a catecholamine-independent manner. However, study results regarding the treatment of SIMD with levosimendan are inconsistent, and the use of levosimendan is highly controversial. In this review, we summarized the therapeutic mechanisms of levosimendan in SIMD and considered recent research on how to improve the efficacy of levosimendan in SIMD. We also analyzed the potential and limitations of levosimendan for the treatment of SIMD to provide ideas for future clinical trials and the clinical application of levosimendan in SIMD.

KEYWORDS

levosimendan, inotropes, sepsis, sepsis-induced myocardial cardiac dysfunction, organ protection

1 Introduction

Sepsis is characterized by life-threatening organ dysfunction caused by a dysregulated host response to infection (1). Despite the significant advances in the past few decades, sepsis and septic shock remain the leading causes of death in intensive care units (ICUs). In addition to the distributive shock caused by vascular hyporesponsiveness and autonomic nervous dysfunction, sepsis can induce myocardial depression and consequently reduce cardiac pumping and cardiac output (CO), which is manifested as treatment-resistant hypotension that responds poorly to fluid resuscitation and vasoactive agents. This acute reversible myocardial depression secondary to sepsis is known as sepsis-induced cardiac dysfunction (SIMD) or sepsis-induced cardiomyopathy (SICM). The use of inotropes can restore sufficient CO and peripheral blood oxygen delivery in SIMD patients (2). Digitalis, catecholamines, and phosphodiesterase (PDE) inhibitors increase myocardial contractility by increasing the levels of intracellular cyclic adenosine monophosphate and Ca^{2+}. However, elevated intracellular Ca^{2+} levels increase myocardial oxygen consumption and predispose to arrhythmias.

Levosimendan is a distinctive inodilator that combines calcium sensitization, PDE inhibition, and vasodilatory properties through the opening of adenosine triphosphate (ATP)-dependent K^+ channels (3). In 2000, it was first approved in Sweden for the short-term treatment of acutely decompensated severe chronic heart failure when

conventional therapy is not effective and in cases where inotropic support is required (3). An increasing number of studies have shown that levosimendan improves cardiac function without affecting myocardial oxygen consumption and has protective effects on other organs. Therefore, levosimendan is an ideal treatment choice for sepsis complicated by myocardial depression. However, the use or non-use of levosimendan during sepsis and septic shock remains controversial. The current Surviving Sepsis Campaign (SSC) guidelines do not recommend levosimendan for the treatment of septic shock for several reasons: it is expensive, ineffective, not easily available, and can lead to hypotension and arrhythmias (4). Previous studies have shown conflicting results regarding the use of levosimendan in SIMD, and the timing and methods of its application also need to be investigated further. Whether levosimendan can be used in the treatment of SIMD is full of controversy, and many questions need to be answered regarding levosimendan in the treatment of SIMD.

2 SIMD: a significant global challenge

SIMD or SICM is a reversible myocardial dysfunction that occurs as part of multiple organ failure caused by sepsis and septic shock (5). There is no objective definition of SIMD. Although the definition of SIMD is based on left ventricular systolic dysfunction, both ventricles may be affected (6). Martin et al. (7) defined SIMD as an acute cardiac dysfunction syndrome associated with sepsis that is unrelated to myocardial ischemia, with one or more of the main clinical features: (1) left ventricular dilation with normal or reduced filling pressure; (2) reduced ventricular contractility; and (3) right ventricular diastolic dysfunction or left ventricular (systolic or diastolic) dysfunction with reduced volume responsiveness. For patients with sepsis-related organ dysfunction, particularly those with septic shock who require vasopressors, the possibility of SIMD should be considered (8). Based on the clinical and echocardiographic parameters, Geri et al. (9) classified septic shock into five phenotypes: (1) well resuscitated; (2) left ventricular systolic dysfunction; (3) hyperkinetic state; (4) right ventricular failure; and (5) hypovolemic. Patients with different echocardiographic manifestations may require different treatments and have different clinical outcomes. Zhang et al. (10) found that according to LVEF, patients with sepsis were divided into high LVEF group (LVEF higher than or equal to 70%), normal LVEF group (LVEF higher than or equal to 50% and less than 70%), and low LVEF group (LVEF less than 50%), and patients with low LVEF had the highest in-hospital mortality and 28-day mortality.

The epidemiology of SIMD remains elusive due to the lack of a consensus on its definition. According to previous studies, the prevalence of SIMD in sepsis and septic shock ranges from 18% to 40%, while in some reports it can reach as high as 70% (11). SIMD is increasingly recognized as a major and severe complication of sepsis and septic shock, posing a significant challenge globally. Patients with SIMD have a mortality rate of 70%–90%, which is 2–3-fold higher than that of non-cardiac affected septic patients (12). In a meta-analysis involving 1,373 patients with sepsis and septic shock, the incidence of right ventricular dysfunction was 35%, and the occurrence of right ventricular dysfunction was associated with higher short- and long-term mortality (13). With appropriate treatment, myocardial dysfunction may recover within 7–10 days (14).

Over the past 20 years, the mechanism of SIMD has been extensively studied in various fields, including proteomics and genomics (15). The pathophysiology of SIMD is complex, and its exact mechanisms need further investigation. The pathological mechanisms of SIMD include the release of bacterial endotoxins, mitochondrial dysfunction, and increased levels of cytokines, inflammatory mediators, nitric oxide (NO), and reactive oxygen species (16). These mechanisms decrease the intrinsic contractility of the heart in septic patients. In another review, Bi et al. (15) found that mechanisms such as cell apoptosis, mitochondrial damage, autophagy, excessive inflammatory response, oxidative stress, and pyroptosis are involved in sepsis-induced myocardial injury. Sepsis-induced myocardial cell death involves cell apoptosis, necrosis, mitochondrial-mediated necrosis, pyroptosis, iron necrosis, and autophagy (17). Recent studies have shown that non-coding RNAs (including microRNA, long-chain non-coding RNA, and cyclic RNA) play a crucial role in the development of myocardial dysfunction after sepsis (12).

Echocardiography is the preferred method for the diagnosis of myocardial dysfunction due to sepsis. SIMD is characterized by reduced left ventricular contractility eventually associated with left ventricular dilatation with or without right ventricle failure (11). Systolic function [i.e., left ventricular ejection fraction (LVEF)] is the first parameter affected in the diagnosis of SIMD. An LVEF of ≤50% and the presence of left ventricle dilatation are generally used as diagnostic criteria for SIMD (18). In addition to impaired left ventricular systolic function, left ventricular diastolic function and right ventricle are also involved in SIMD patients. Some echocardiographic parameters, such as LVEF, depend on the load conditions of the cardiovascular system, particularly the afterload, making it difficult to determine whether the observed cardiac dysfunction is due to myocardial dysfunction or due to hemodynamic disturbances occurring during septic shock (19). The global longitudinal strain measured by speckle echocardiography is more sensitive and specific than LVEF for the diagnosis of myocardial dysfunction. Cardiac biomarkers are also used to evaluate cardiac involvement in sepsis. Troponin I is a highly sensitive marker for myocardial injury, which can be elevated without evidence of myocardial ischemia (16). The other biomarkers include troponin T, brain natriuretic peptides (B-type natriuretic peptide and N-terminal pro-B-type natriuretic peptide), and others.

Despite extensive research on SIMD, there is a lack of guidelines for its treatment that can improve the prognosis of sepsis. The recommended treatment options include fluid resuscitation, vasoactive drugs (including dobutamine), β-blockers, levosimendan, and aortic balloon counter pulsation (16). Inotropes have the same hypothetical benefits as vasopressors for increasing CO, which can improve oxygen delivery to peripheral tissues (20). When low CO manifestations caused by myocardial dysfunction are identified, it is at the

discretion of the physician to decide whether or not to use inotropes. In septic shock, inotropes should not be used as first-line therapy (21). Inotrope use is indicated only in patients with signs of tissue hypoperfusion due to a low CO induced by impaired cardiac function (22). Salvage, optimization, stabilization, and de-escalation have been introduced to describe the different phases of shock resuscitation, and inotropes should mainly be used in the optimization stage. As for the choice of inotropes, Backer et al. (22) recommended using a limited dose of dobutamine, followed by substituting or adding enoximone or milrinone, as appropriate, and then substituting or adding in cases of severe impairment. Heart rate control may be an option for certain patients (8). The key to successful treatment of septic shock is the early identification of hemodynamic changes. Bedside echocardiography can guide fluid resuscitation and hemodynamic optimization. After initial fluid resuscitation, the amount and speed of fluid replenishment should be dynamically adjusted based on the volume responsiveness. If hypotension persists, timely vasopressor therapy should be initiated with vasopressor and/or inotropic therapy adjusted according to the measures of CO and tissue perfusion (19). In a retrospective study conducted by Lan et al. (23), the use of echocardiography in patients with septic shock improved outcomes at 28 days. A study by Fu et al. (24) in 2022 also reported similar findings. Finally, SIMD patients who do not respond to medical management should be promptly provided with mechanical circulatory support, including veno-arterial extracorporeal membrane oxygenation (25).

3 Basic pharmacology and mechanism of levosimendan

Levosimendan is a novel calcium sensitizer and ATP-dependent K^+ channel activator that is useful for the treatment of patients with acute decompensated heart failure and those requiring inotropic therapy. From a pharmacodynamic standpoint, levosimendan possesses a triple mechanism of action: (1) calcium sensitization by selective binding to Ca^{2+}-saturated cardiac troponin C; (2) opening of ATP-dependent K^+ channels in the cardiomyocyte mitochondria; and (3) opening of ATP-dependent K^+ channels in vascular smooth muscle cells (3). The pharmacological mechanism of levosimendan is illustrated in Figure 1.

As a calcium sensitizer, levosimendan binds directly to troponin C, stabilizing the Ca^{2+}-bound conformation of troponin, thus prolonging the actin-myosin interaction without

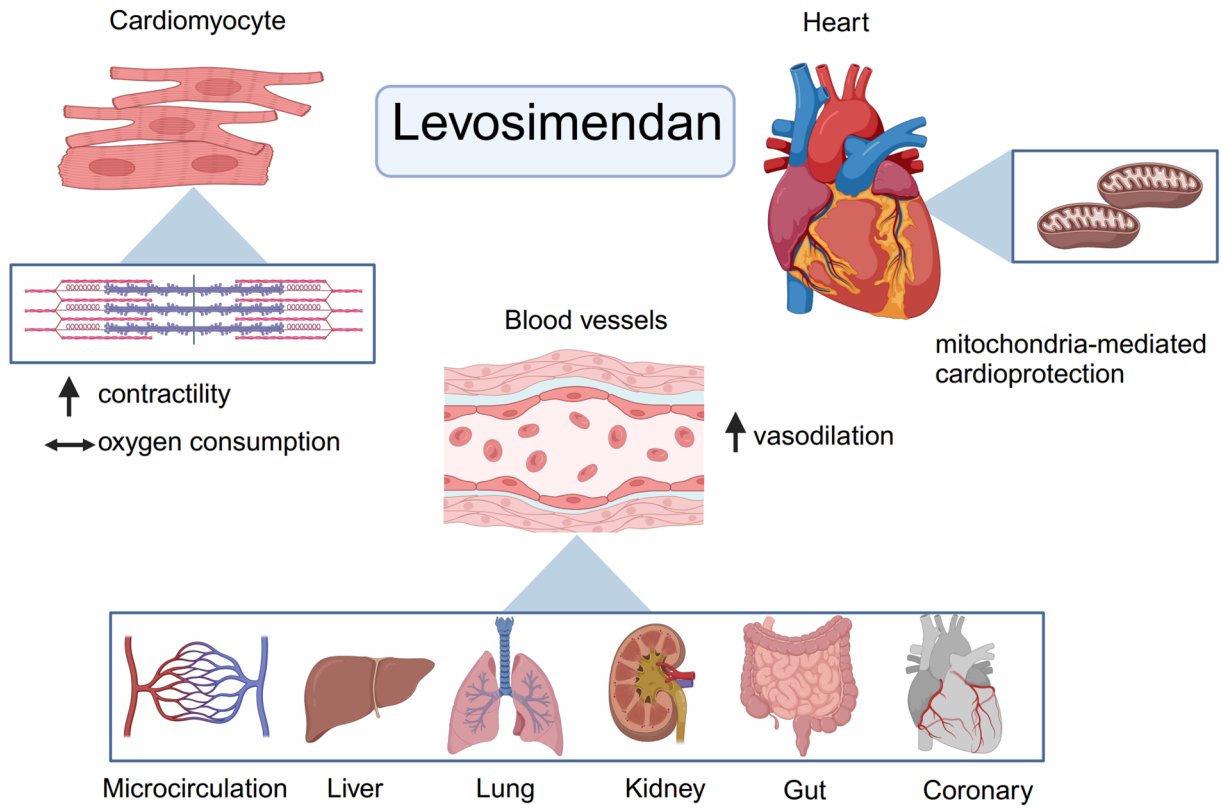

FIGURE 1
Basic pharmacology and mechanism of levosimendan. From a pharmacodynamic point of view, levosimendan has a threefold mechanism of action. First, as a calcium sensitizer, levosimendan can enhance myocardial contractility without increasing myocardial oxygen consumption. Then, levosimendan could open ATP- dependent K^+ channels in the mitochondrial and cytoplasmic membranes of cardiomyocytes and thus has a cardioprotective effect. Finally, levosimendan could open ATP- dependent potassium channels in vascular smooth muscle cells to dilate blood vessels in other organs and improve organ perfusion such as kidneys, gut and so forth. (Created with BioRender.com).

altering cross-bridge cycling (26). This potentiating effect increases the interaction of actin and myosin at any given intracellular Ca^{2+} concentration, without significantly increasing the myocardial oxygen consumption. Levosimendan promotes the cardiac contractile force without an increase in the amplitude of intracellular Ca^{2+} transient (27). Furthermore, it exerts inotropic effects in a Ca^{2+}-dependent manner. The gradual decline in intracellular Ca^{2+} concentration during diastole decreases the calcium-sensitizing effect of the drug, thereby preventing a postulated adverse influence on myocardial relaxation (28). In addition, levosimendan selectively inhibits PDE III, which has a positive lusitropic effect; this antagonizes the negative lusitropic effect of calcium sensitization (29). Overall, levosimendan enhances myocardial contractility without increasing myocardial oxygen consumption and improves diastolic function, which is theoretically superior to other inotropes such as dobutamine. Dobutamine and levosimendan exert their effects on the heart through distinct mechanisms. Dobutamine, a β1-AR agonist, increases cAMP production via adenylyl cyclase activation, leading to PKA-mediated enhancement of calcium handling and contractility. However, prolonged β1-AR activation also triggers harmful downstream effects, including hypertrophy, apoptosis, and arrhythmias, mediated by CaMKII and GRK2 pathways. The pharmacological differences between levosimendan and dobutamine are shown in Figure 2.

Levosimendan opens ATP-dependent K^+ channels in the mitochondrial and cytoplasmic membranes of cardiomyocytes and thus has a cardioprotective effect in the presence of myocardial ischemia. The heart is highly dependent on high ATP levels to maintain its systolic and diastolic functions (30). Levosimendan improves mitochondrial Ca^{2+} overload, preserves high-energy phosphate, regulates the mitochondrial number, reduces infarct size, and mitigates myocardial ischemia/reperfusion injury (31, 32).

Levosimendan and its long-acting active metabolite OR-1896 activate multiple vasodilatory mechanisms, which involve the opening of ATP-sensitive K^+ channels and other K^+ channels as well as highly selective inhibition of the PDE III enzyme. Importantly, levosimendan does not inhibit PDE IV at low doses (33). Levosimendan increases myocardial oxygen supply by dilating coronary resistance vessels and improves tissue perfusion and oxygen metabolism in other organs by causing arterial and venous vasodilation. Notably, the plasma concentration at which levosimendan exerts its vasodilatory effects is far higher than that at which it exerts its inotropic effects.

In addition to its inotropic, cardioprotective, and vasodilatory effects, levosimendan may have protective effects on kidneys, liver, lungs, and gastrointestinal and central nervous systems through its anti-inflammatory, antioxidant, anti-apoptotic, and other effects (28).

The abovementioned pharmacological properties of levosimendan allow it to be widely used in critical illnesses in the ICU. In addition to acute decompensated heart failure,

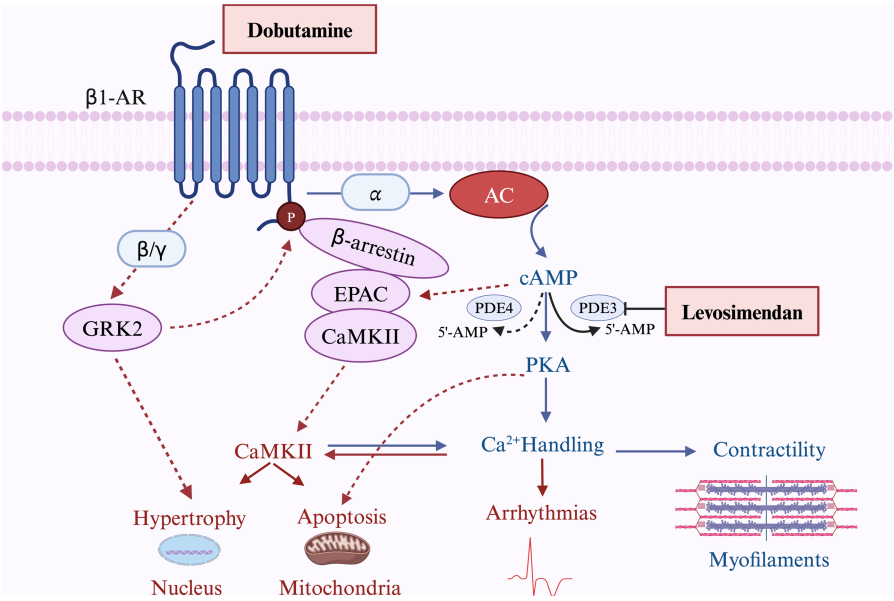

FIGURE 2
The pharmacological difference between levosimendan and dobutamine. The figure illustrates the distinct mechanisms of action of dobutamine and levosimendan. Dobutamine mainly activates β1-AR, leading to both beneficial effects (blue lines) through increased cAMP production, PKA activation, and enhanced calcium handling to improve contractility, and harmful effects (red lines) via CaMKII-mediated pathways promoting hypertrophy, apoptosis, and arrhythmias. Levosimendan enhances the cAMP-PKA pathway by inhibiting PDE3, amplifying beneficial effects. Solid lines represent direct actions, while dashed lines indicate indirect or secondary effects. β1-AR, Beta-1 Adrenergic Receptor; AC, Adenylyl Cyclase; cAMP, Cyclic Adenosine Monophosphate; PDE, Phosphodiesterase; PDE3, Phosphodiesterase 3; PDE4, Phosphodiesterase 4; PKA, Protein Kinase A; EPAC, Exchange Protein Activated by cAMP; CaMKII, Calcium/Calmodulin-Dependent Protein Kinase II; GRK2, G Protein-Coupled Receptor Kinase 2; 5′-AMP, 5′-Adenosine Monophosphate (Created with BioRender.com).

levosimendan is useful for chronic heart failure, perioperative prophylaxis of cardiac surgery, ventilator evacuation, and subarachnoid hemorrhage.

4 The rationale for levosimendan in the treatment of SIMD

Septic shock involves a complex interaction between abnormal vasodilation, relative or absolute hypovolemia, myocardial dysfunction, and altered blood flow distribution to the tissues (29). Early recognition and rapid reversal of tissue perfusion deficits due to infection are critical in the treatment of septic shock. Fluid administration, vasopressors, and inotropes aim to restore impaired tissue perfusion during septic shock. SIMD is mediated by multiple factors. However, regardless of the mechanisms, myocardial dysfunction is the main reason for the use of inotropes during septic shock. Dobutamine and other inotropes have typically been used to increase CO and oxygen transport, aiming to restore cell respiration and aerobic metabolism (29). According to the 2016 SSC guidelines, the use of inotropes, such as dobutamine (up to 20 $\mu g/kg \cdot min^{-1}$), should be considered in patients with myocardial dysfunction (manifested as low CO, increased filling pressures, and persistent tissue hypoperfusion) after adequate fluid resuscitation and use of vasopressors (34). The current SSC guidelines recommend the use of norepinephrine and dobutamine or adrenaline alone for patients with sufficient volume and blood pressure but persistently insufficient tissue perfusion (4). However, the use of dobutamine in SIMD remains controversial. Although dobutamine leads to an increase in cardiac index, myocardial oxygen demand also increases, thus increasing the risk of myocardial ischemia and tachyarrhythmias (35). The new inotrope levosimendan is a calcium sensitizer, which can improve myocardial function without affecting calcium ion flow. Unlike other inotropic agents, the positive inotropic effect of levosimendan is independent of ATP production; therefore, it can minimize oxygen demand, arrhythmias, and catecholamine resistance (36). Although the current SSC guidelines do not recommend the use of levosimendan, it has shown potential advantages in the treatment of SIMD.

Levosimendan can increase myocardial contractility. The CO level is normal or even high in septic patients after initial fluid resuscitation, but myocardial contractility may be impaired in a significant proportion of septic patients. During sepsis or under lipopolysaccharide (LPS) exposure, the Ca^{2+} homeostasis of myocardial cells is usually altered, leading to a decrease in myocardial contractility. Reduced systolic force limits the ability of the ventricle to reach a low end-systolic volume, resulting in a decrease in stroke volume. Nevertheless, the decrease in the stroke volume may be compensated by the increased end-diastolic volume achieved through adequate fluid resuscitation and by the decreased afterload due to arterial vasodilation (29). As a new calcium sensitizer, levosimendan increases the sensitivity of cardiomyocytes by altering the structure of troponin C, which can enhance myocardial contractility without increasing the intracellular calcium load or intracellular ATP level (18). Previous studies have shown that levosimendan increases myocardial contractility and CO, and improves tissue perfusion in septic patients (37). The use of other positive inotropic drugs is associated with side effects, including increased myocardial oxygen consumption, while levosimendan acts in a catecholamine-independent manner without increasing the myocardial oxygen consumption and heart rate.

Levosimendan can improve ventricular diastolic function. Diastolic dysfunction also occurs during sepsis and septic shock, which affects ventricular filling (38). Unlike the ATP-dependent inotropes milrinone and dobutamine, which can only improve the systolic function, levosimendan does not cause ventricular diastolic dysfunction due to Ca^{2+} overload and can improve ventricular diastolic function by improving the diastolic velocity ratio, shortening the diastolic phase, and improving the diastolic filling. In the experimental model of sepsis, Barraud et al. (39) found that levosimendan was superior to dobutamine and milrinone in restoring the ventricular systolic and diastolic functions of LPS-treated rabbits.

Levosimendan has several beneficial effects on hemodynamic parameters. Cardiovascular failure due to sepsis also involves peripheral vascular dysfunction. Abnormalities in the distribution of vital blood flow to the tissues may persist after the optimization of the CO. Levosimendan is a new positive inotropic drug with vasodilatory effects. Most previous studies have shown that levosimendan has beneficial effects on the macro-hemodynamics and tissue perfusion indices. Compared with dobutamine, levosimendan provides a favorable hemodynamic response without increasing the cardiac oxygen demand (40). Meng et al. (41) explored the effects of levosimendan on myocardial injury and systemic hemodynamic biomarkers in patients with septic shock. Compared with dobutamine, levosimendan reduced the biomarkers of myocardial injury, improved systemic hemodynamics in patients with septic shock, and reduced the duration of mechanical ventilation and ICU stay. The beneficial effect of levosimendan on microvascular distribution is independent of its effect on CO. Levosimendan can improve the sublingual microcirculation blood flow in patients with septic shock (42).

Apart from its direct effect on cardiac function, levosimendan also demonstrates multifaceted effects targeting specific pathological physiological mechanisms associated with SIMD. Levosimendan has anti-inflammatory and anti-apoptosis effects, improves myocardial ischemia, increases the synthesis of NO, protects vascular endothelial cells, and inhibits the expression of the hypoxia-inducible factor-1a (18). Moreover, levosimendan reduces the inflammatory response by downregulating nuclear factor-κB-dependent transcription, inhibiting inducible NO promoter activity, and reducing NO expression *in vitro* (43). Sepsis can cause structural damage to myocardial mitochondria and loss of mitochondrial function. In a mouse model of myocardial injury caused by an intraperitoneal injection of LPS, Shi et al. (44) found that levosimendan inhibited inflammation and oxidative stress, and protected against LPS-induced cardiac dysfunction through mitophagy and the PINK-1-Parkin signaling pathway.

5 Application and limitations of levosimendan in septic shock and SIMD

After more than 20 years, the clinical applications of levosimendan in the field of emergency and critical care medicine have expanded considerably and now include various cardiac diseases (such as cardiogenic shock, Takotsubo cardiomyopathy, advanced heart failure, right ventricular failure, pulmonary hypertension, and cardiac surgery) and non-cardiac diseases (such as amyotrophic lateral sclerosis) (32).

In the clinical research on the use of levosimendan for septic shock and SIMD, early randomized controlled trials (RCTs) had small sample sizes. In 2015, a meta-analysis was conducted by Zandrillo et al. (45), which included 7 RCTs and 246 patients with severe sepsis or septic shock. Compared with conventional inotropes (mainly dobutamine), levosimendan significantly reduced the mortality, increased the cardiac index, and reduced the blood lactate level, but there was no difference in the mean arterial pressure or norepinephrine dose between the two groups. However, the data on the use of levosimendan in definite SIMD remains limited. Gordon et al. (46) published the results of a multicenter, randomized, double-blind, placebo-controlled clinical trial (LeoPARDS study) in The New England Journal of Medicine in 2016. The study had the largest sample size to date of any studies conducted on this topic. In this study, 516 patients with septic shock were randomly divided into the levosimendan and placebo groups. The results showed that levosimendan did not reduce the Sequential Organ Failure Assessment score and the 28-day mortality rate during hospitalization, but was associated with high risks of supraventricular tachyarrhythmia and ventilator weaning failure. Following that, Antcliffe et al. (47) conducted a subgroup analysis of the LeoPARDS study according to the levels of cardiac troponin I and NT pro-brain natriuretic peptide and failed to observe any benefit of levosimendan or decrease in the levels of inflammatory biomarkers in any subgroup. However, these research findings do not definitively refute the effectiveness of levosimendan in SIMD. As described in the LeoPARDS study, the cases selected did not undergo cardiac ultrasound and the proportion of patients with cardiac dysfunction was low, which may explain the lack of positive results (48). Putzu et al. (49) believe that the subjects included in the LeoPARDS study were low-risk patients in the relatively late stages of septic shock, who were not confirmed to have concomitant cardiac dysfunction, and who developed hypotension and supraventricular tachycardia after receiving high doses of levosimendan, up to 0.2 μg/(kg·min). Cardiac ultrasound examination or hemodynamic monitoring was not performed during the study, and no effective fluid resuscitation was performed before the administration of levosimendan. Overall, the LeoPARDS study tells us that septic patients with reduced systemic vascular resistance but no clinical signs of myocardial dysfunction do not benefit from levosimendan.

In a meta-analysis of 10 studies and 1,036 patients with sepsis and septic shock, levosimendan was more effective in reducing lactate levels (37). Compared with dobutamine, patients who received levosimendan reported significantly higher cardiac index (37). In another meta-analysis, levosimendan could reduce serum lactate levels more effectively and improve cardiac function (50). However, statistical significance in mortality was obscured after the LeoPARDS study was included. Interestingly, patients who received levosimendan also received significantly more fluid than their counterparts probably due to the vasodilatory effect of levosimendan. To sum up, these benefits have not been translated to the clinical endpoints in the two studies above.

Based on the results of the LeoPARDS study, the latest SSC guideline panel issued a weak recommendation against the use of levosimendan because of its lack of clinical benefits (4). The other reasons for not recommending its use include its safety profile, cost, and limited availability (4). However, these reasons should not negate the clinical application of this drug. The first concern with the use of levosimendan is its clinical benefit. The current SSC guidelines were directly influenced by the LeoPARDS study. As mentioned above, there are many concerns regarding the results of the LeoPARDS study, and the presence of clear evidence of myocardial dysfunction is required for levosimendan use. The second concern is drug safety. Levosimendan has a predictable safety profile, with the most common adverse events being hypotension, headache, and atrial arrhythmias (3). The 2021 European Society of Cardiology guidelines on chronic and acute heart failure suggest that in patients treated with β-blockers, levosimendan or a phosphodiesterase type 3 inhibitor may be superior to dobutamine because they act through independent mechanisms (51). Excessive peripheral vasodilatation and hypotension may be major limitations of levosimendan, especially when high doses are administered and/or bolus doses are initiated. However, at therapeutic doses, levosimendan is less likely to cause ventricular arrhythmias and can improve myocardial injury caused by sepsis (18). Hypotension associated with vasodilation can be prevented by adequate fluid resuscitation before levosimendan use, avoidance of loading doses, and concomitant use of vasopressors (2). The third issue is the cost of levosimendan. Levosimendan has a prolonged duration of action, with the drug effect lasting for over 7 days when the drug is administered intravenously for 24 h, whereas the other inotropes have a short duration of action. A prolonged duration (5–7 days) of intravenous administration of dobutamine is not associated with a lesser cost than 24 h of intravenous administration of levosimendan. The final issue is drug accessibility. The limited availability of the drug is not a valid reason for not recommending its use. With economic development, levosimendan is increasingly available even in low-income countries and regions.

A meta-analysis of 6 RCTs and 192 patients showed that, compared with dobutamine, the administration of levosimendan for 24 h significantly improved the cardiac index and left ventricular beat index, as well as significantly decreased the blood lactate level, in patients with SIMD, although there was no effect on the mortality rate or LVEF (31). In our previous meta-analysis, which included 10 RCTs and 543 patients with SIMD (defined as LVEF $\leq$ 50%), levosimendan increased the LVEF, decreased the cardiac troponin I and blood lactate levels, and reduced the mortality rate compared to dobutamine (52). In a recent

10.3389/fcvm.2024.1520596

TABLE 1 Main randomized controlled trials on the use of levosimendan in sepsis-induced myocardial dysfunction.

Study	Year	Participants	Sample size (L/C)	Levosimendan therapy	Control therapy	Hemodynamic improvement	Mortality outcome	Potential adverse events	Conclusion
Morelli (56)	2005	Septic shock with LVEF ≤ 45% and PAOP ≥ 12 mmHg	15/13	Levosimendan (0.2 μg/kg·min^{-1}) without a bolus loading dose for 24 h	Dobutamine (5 μg/kg·min^{-1}) for 24 h	Improved	No reduction	Not reported	Favors levosimendan
Vaitsis (57)	2009	Severe sepsis or septic shock with CI < 2.2 or LVEF < 35%	23/19	Levosimendan (0.1 μg/kg·min^{-1}) without a bolus loading dose for 24 h	Dobutamine (5–10 μg/kg·min^{-1}) for 24 h	Improved	Reduced	Not reported	Favors levosimendan
Fang (58)	2014	Septic shock with LVEF ≤ 45%	18/18	Dobutamine (5 μg/kg·min^{-1}) for 24 h; levosimendan (0.2 μg/kg·min^{-1}) without a bolus loading dose for 24 h subsequently	Dobutamine (5 μg/kg·min^{-1}) for 24 h	Improved	No reduction	Not reported	Favors levosimendan
Meng (41)	2016	Septic shock with LVEF ≤ 45%	19/19	Levosimendan (0.2 μg/kg·min^{-1}) without a bolus loading dose for 24 h	Dobutamine (5 μg/kg·min^{-1}) for 24 h	Improved	No reduction	Not reported	Favors levosimendan
Xu (59)	2018	Septic shock with LVEF ≤ 50%	15/15	Levosimendan (0.2 μg/kg·min^{-1}) without a bolus loading dose for 24 h	Dobutamine (5 μg/kg·min^{-1}) for 24 h	Improved	No reduction	Not reported	Favors levosimendan
Sun (53)	2023	severe SIMD (LVEF ≤ 35%)	15/15	Levosimendan (0.2 μg/kg·min^{-1}) without a bolus loading dose for 24 h	Dobutamine (5 μg/kg·min^{-1}) for 24 h	Improved	No reduction	Not reported	Favors levosimendan
Sun (60)	2024	Sepsis with LVEF ≤ 45%	20/20	Levosimendan (0.2 μg/kg·min^{-1}) without a bolus loading dose for 24 h	Dobutamine (5 μg/kg·min^{-1}) for 24 h	Improved	Not reported	Not reported	Favors levosimendan

CI, cardiac index; L/C, levosimendan group/control group; LVEF, left ventricular ejection fraction; PAOP, pulmonary arterial occlusion pressure; SIMD, sepsis-induced myocardial dysfunction.

prospective, single-blind, RCT, Sun et al. (53) enrolled 30 patients with severe SIMD (LVEF ≤ 35%) and compared the hemodynamic and clinical outcomes of patients treated with fixed doses of levosimendan (0.2 μg/kg·min^{-1}) or dobutamine (5 μg/kg·min^{-1}) for 24 h. The results showed that at 24 h, the cardiac index, LVEF, stroke volume index, and fluid volume were higher, whereas the norepinephrine dose was lower, in the levosimendan group than in the dobutamine group. On the third day, the cardiac troponin I level was lower in the levosimendan group than in the dobutamine group. There were no significant differences in terms of the 28-day mortality rate, length of ICU stay, and cost of ICU stay between the two groups, although the ventilator time was significantly shorter in the levosimendan group. A meta-analysis published in 2023 indicates that levosimendan is safe and effective in treating sepsis and septic cardiomyopathy (54). Recent evidence suggests that levosimondan significantly improves CI and lactate levels in patients with sepsis (55). However, due to the small sample sizes, inconsistent diagnostic criteria as well as high heterogeneity in the clinical studies included in the meta-analysis, conclusions drawn from it should be approached with caution. Most importantly, well-designed clinical trials are needed to determine the value of levosimendan in septic shock and SIMD. Main randomized controlled trials on the use of levosimendan in SIMD are reported in Table 1. It is noteworthy that no adverse events associated with levosimendan were reported in these RCTs. Upon detailed examination of the original studies, the absence of adverse events appears to reflect the actual trial outcomes rather than an omission or lack of data collection. The lack of adverse events in these RCTs may be attributed to factors such as stringent patient selection criteria or well-controlled dosing regimens. However, it is important to interpret this finding with caution. The relatively small sample sizes and the specific characteristics of the study populations may limit the generalizability of these results.

6 Conclusions and perspectives

As one of the most serious complications of sepsis, SIMD has received extensive attention in recent years. Despite the SSC guideline recommends against the use of levosimendan for sepsis patients with cardiac dysfunction under certain conditions, it is crucial to recognize that recommendations should not override a clinician's individualized decision-making for specific cases. What's more, the guidelines do not explicitly oppose the administration of levosimendan in septic shock patients with confirmed low cardiac output syndrome (LCOS) by echocardiography, pulmonary artery catheter, or pulse index continuous cardiac output (61). In addition, as Vincent points out, a balance should be maintained between SSC guidelines and individualized care (62). With the development of precision medicine, identifying SIMD patients with certain treatable characteristics and giving targeted treatment may help to find patients who can benefit from levosimendan.

In conclusion, the present comprehensive review has highlighted key findings and insights into levosimendan for SIMD. The accumulated evidence underscores the significance of

indications and timing of levosimendan administration. Moving forward, several avenues for future research merit attention. Exploring the pathogenesis of SIMD, establishing the gold standard for the diagnosis, and identifying subgroups of patients with different clinical manifestations of SIMD will contribute to a deeper understanding of SIMD. Furthermore, it is essential to integrate treatment and monitoring, and to equilibrate a delicate balance between clinical guidelines and the unique needs of individual patients. Embracing these future directions promises to advance the field and provide valuable implications for the application of levosimendan in SIMD.

Author contributions

XD: Writing – original draft. FX: Data curation, Writing – review & editing. YH: Data curation, Writing – review & editing. XY: Conceptualization, Supervision, Writing – review & editing. PP: Conceptualization, Funding acquisition, Writing – review & editing.

Funding

The author(s) declare financial support was received for the research, authorship, and/or publication of this article. This study was supported by grants from the Chongqing Medical Scientific Research Project (a joint project of the Chongqing Health Commission and Science and Technology Bureau) (2020FYYX133), the joint medical scientific research project of the Health Commission and Science and Technology Bureau in Wanzhou Chongqing (wzstc- kw2021001) and the National Natural Science Foundation of China (NSFC 82160360).

Acknowledgments

We thank LetPub (www.letpub.com) for its linguistic assistance during the preparation of this manuscript.

Conflict of interest

The authors declare that the research was conducted in the absence of any commercial or financial relationships that could be construed as a potential conflict of interest.

Generative AI statement

The author(s) declare that no Generative AI was used in the creation of this manuscript.

Publisher's note

References

1. Singer M, Deutschman CS, Seymour CW, Shankar-Hari M, Annane D, Bauer M, et al. The third international consensus definitions for sepsis and septic shock (sepsis-3). *JAMA*. (2016) 315(8):801–10. doi: 10.1001/jama.2016.0287

2. Herpain A, Bouchez S, Girardis M, Guarracino F, Knotzer J, Levy B, et al. Use of levosimendan in intensive care unit settings: an opinion paper. *J Cardiovasc Pharmacol*. (2019) 73(1):3–14. doi: 10.1097/FJC.0000000000000636

3. Conti N, Gatti M, Raschi E, Diemberger I, Potena L. Evidence and current use of levosimendan in the treatment of heart failure: filling the gap. *Drug Des Devel Ther*. (2021) 15:3391–409. doi: 10.2147/DDDT.S295214

4. Evans L, Rhodes A, Alhazzani W, Antonelli M, Coopersmith CM, French C, et al. Surviving sepsis campaign: international guidelines for management of sepsis and septic shock 2021. *Intensive Care Med*. (2021) 47(11):1181–247. doi: 10.1007/s00134-021-06506-y

5. Lima MR, Silva D. Septic cardiomyopathy: a narrative review. *Rev Port Cardiol*. (2023) 42(5):471–81. doi: 10.1016/j.repc.2021.05.020

6. Zhang H, Liu D. Sepsis-related cardiomyopathy: not an easy task for ICU physicians. *J Intensive Med*. (2022) 2(4):257–9. doi: 10.1016/j.jointm.2022.05.005

7. Martin L, Derwall M, Al Zoubi S, Zechendorf E, Reuter DA, Thiemermann C, et al. The septic heart: current understanding of molecular mechanisms and clinical implications. *Chest*. (2019) 155(2):427–37. doi: 10.1016/j.chest.2018.08.1037

8. Boissier F, Aissaoui N. Septic cardiomyopathy: diagnosis and management. *J Intensive Med*. (2022) 2(1):8–16. doi: 10.1016/j.jointm.2021.11.004

9. Geri G, Vignon P, Aubry A, Fedou AL, Charron C, Silva S, et al. Cardiovascular clusters in septic shock combining clinical and echocardiographic parameters: a *post hoc* analysis. *Intensive Care Med*. (2019) 45(5):657–67. doi: 10.1007/s00134-019-05596-z

10. Zhang L, Qi D, Peng M, Meng B, Wang X, Zhang X, et al. Decoding molecular signature on heart of septic mice with distinct left ventricular ejection fraction. *iScience*. (2023) 26(10):107825. doi: 10.1016/j.isci.2023.107825

11. Carbone F, Liberale L, Preda A, Schindler TH, Montecucco F. Septic cardiomyopathy: from pathophysiology to the clinical setting. *Cells*. (2022) 11(18):2833. doi: 10.3390/cells11182833

12. Liu S, Chong W. Roles of LncRNAs in regulating mitochondrial dysfunction in septic cardiomyopathy. *Front Immunol*. (2021) 12:802085. doi: 10.3389/fimmu.2021.802085

13. Vallabhajosyula S, Shankar A, Vojjini R, Cheungpasitporn W, Sundaragiri PR, DuBrock HM, et al. Impact of right ventricular dysfunction on short-term and long-term mortality in sepsis: a meta-analysis of 1,373 patients. *Chest*. (2021) 159(6):2254–63. doi: 10.1016/j.chest.2020.12.016

14. L'Heureux M, Sternberg M, Brath L, Turlington J, Kashiouris MG. Sepsis-induced cardiomyopathy: a comprehensive review. *Curr Cardiol Rep*. (2020) 22(5):35. doi: 10.1007/s11886-020-01277-2

15. Bi CF, Liu J, Yang LS, Zhang JF. Research progress on the mechanism of sepsis induced myocardial injury. *J Inflamm Res*. (2022) 15:4275–90. doi: 10.2147/JIR.S374117

16. Khalid N, Patel PD, Alghareeb R, Hussain A, Maheshwari MV. The effect of sepsis on myocardial function: a review of pathophysiology, diagnostic criteria, and treatment. *Cureus*. (2022) 14(6):e26178. doi: 10.7759/cureus.26178

17. Zhang G, Dong D, Wan X, Zhang Y. Cardiomyocyte death in sepsis: mechanisms and regulation (review). *Mol Med Rep*. (2022) 26(2):257. doi: 10.3892/mmr.2022.12773

18. Yang F, Zhao LN, Sun Y, Chen Z. Levosimendan as a new force in the treatment of sepsis-induced cardiomyopathy: mechanism and clinical application. *J Int Med Res*. (2019) 47(5):1817–28. doi: 10.1177/0300060519837103

19. Tullo G, Candelli M, Gasparrini I, Micci S, Franceschi F. Ultrasound in sepsis and septic shock: from diagnosis to treatment. *J Clin Med*. (2023) 12(3):1185. doi: 10.3390/jcm12031185

20. Ehrman RR, Sullivan AN, Favot MJ, Sherwin RL, Reynolds CA, Abidov A, et al. Pathophysiology, echocardiographic evaluation, biomarker findings, and prognostic

implications of septic cardiomyopathy: a review of the literature. *Crit Care*. (2018) 22(1):112. doi: 10.1186/s13054-018-2043-8

21. Heringlake M, Alvarez J, Bettex D, Bouchez S, Fruhwald S, Girardis M, et al. An update on levosimendan in acute cardiac care: applications and recommendations for optimal efficacy and safety. *Expert Rev Cardiovasc Ther*. (2021) 19(4):325–35. doi: 10.1080/14779072.2021.1905520

22. De Backer D, Cecconi M, Chew MS, Hajjar L, Monnet X, Ospina-Tascón GA, et al. A plea for personalization of the hemodynamic management of septic shock. *Crit Care*. (2022) 26(1):372. doi: 10.1186/s13054-022-04255-y

23. Lan P, Wang TT, Li HY, Yan RS, Liao WC, Yu BW, et al. Utilization of echocardiography during septic shock was associated with a decreased 28-day mortality: a propensity score-matched analysis of the MIMIC-III database. *Ann Transl Med*. (2019) 7(22):662. doi: 10.21037/atm.2019.10.79

24. Fu H, Hu Z, Gong J, Li N, Na L, Zhang Q, et al. The relationship between transthoracic echocardiography and mortality in adult patients with multiple organ dysfunction syndrome: analysis of the MIMIC-III database. *Ann Transl Med*. (2022) 10(6):310. doi: 10.21037/atm-22-717

25. Radosevich M, Couture EJ, Nabzdyk C. Levosimendan and septic cardiomyopathy: a key that may have found its lock? *J Cardiothorac Vasc Anesth*. (2023) 37(3):350–2. doi: 10.1053/j.jvca.2022.12.012

26. Pan J, Yang YM, Zhu JY, Lu YQ. Multiorgan drug action of levosimendan in critical illnesses. *Biomed Res Int*. (2019) 2019:9731467. doi: 10.1155/2019/9731467

27. Papp Z, Edes I, Fruhwald S, De Hert SG, Salmenpera M, Leppikangas H, et al. Levosimendan: molecular mechanisms and clinical implications: consensus of experts on the mechanisms of action of levosimendan. *Int J Cardiol*. (2012) 159(2):82–7. doi: 10.1016/j.ijcard.2011.07.022

28. Farmakis D, Alvarez J, Gal TB, Brito D, Fedele F, Fonseca C, et al. Levosimendan beyond inotropy and acute heart failure: evidence of pleiotropic effects on the heart and other organs: an expert panel position paper. *Int J Cardiol*. (2016) 222:303–12. doi: 10.1016/j.ijcard.2016.07.202

29. Ospina-Tascón GA, Calderon-Tapia LE. Inodilators in septic shock: should these be used? *Ann Transl Med*. (2020) 8(12):796. doi: 10.21037/atm.2020.04.43

30. Habimana R, Choi I, Cho HJ, Kim D, Lee K, Jeong I. Sepsis-induced cardiac dysfunction: a review of pathophysiology. *Acute Crit Care*. (2020) 35(2):57–66. doi: 10.4266/acc.2020.00248

31. Liu DH, Ning YL, Lei YY, Chen J, Liu YY, Lin XF, et al. Levosimendan versus dobutamine for sepsis-induced cardiac dysfunction: a systematic review and meta-analysis. *Sci Rep*. (2021) 11(1):20333. doi: 10.1038/s41598-021-99716-9

32. Papp Z, Agostoni P, Alvarez J, Bettex D, Bouchez S, Brito D, et al. Levosimendan efficacy and safety: 20 years of SIMDAX in clinical use. *J Cardiovasc Pharmacol*. (2020) 76(1):4–22. doi: 10.1097/FJC.0000000000000859

33. Burkhoff D, Rich S, Pollesello P, Papp Z. Levosimendan-induced venodilation is mediated by opening of potassium channels. *ESC Heart Fail*. (2021) 8(6):4454–64. doi: 10.1002/ehf2.13669

34. Rhodes A, Evans LE, Alhazzani W, Levy MM, Antonelli M, Ferrer R, et al. Surviving sepsis campaign: international guidelines for management of sepsis and septic shock: 2016. *Intensive Care Med*. (2017) 43(3):304–77. doi: 10.1007/s00134-017-4683-6

35. Sato R, Nasu M. Time to re-think the use of dobutamine in sepsis. *J Intensive Care*. (2017) 5:65. doi: 10.1186/s40560-017-0264-6

36. Guo J, Zhang X, Zhu Y, Cheng Q. Comparison of dobutamine and levosimendan for treatment of sepsis-induced cardiac dysfunction: a protocol for systematic review and meta-analysis. *Medicine (Baltimore)*. (2022) 101(11):e29092. doi: 10.1097/MD.0000000000029092

37. Chang W, Xie JF, Xu JY, Yang Y. Effect of levosimendan on mortality in severe sepsis and septic shock: a meta-analysis of randomised trials. *BMJ Open*. (2018) 8(3):e019338. doi: 10.1136/bmjopen-2017-019338

38. Sanfilippo F, Corredor C, Arcadipane A, Landesberg G, Vieillard-Baron A, Cecconi M, et al. Tissue Doppler assessment of diastolic function and relationship with mortality in critically ill septic patients: a systematic review and meta-analysis. *Br J Anaesth*. (2017) 119(4):583–94. doi: 10.1093/bja/aex254

39. Barraud D, Faivre V, Damy T, Welschbillig S, Gayat E, Heymes C, et al. Levosimendan restores both systolic and diastolic cardiac performance in lipopolysaccharide-treated rabbits: comparison with dobutamine and milrinone. *Crit Care Med*. (2007) 35(5):1376–82. doi: 10.1097/01.CCM.0000261889.18102.84

40. Ravikumar N, Sayed MA, Poonsuph CJ, Sehgal R, Shirke MM, Harky A. Septic cardiomyopathy: from basics to management choices. *Curr Probl Cardiol*. (2021) 46(4):100767. doi: 10.1016/j.cpcardiol.2020.100767

41. Meng JB, Hu MH, Lai ZZ, Ji CL, Xu XJ, Zhang G, et al. Levosimendan versus dobutamine in myocardial injury patients with septic shock: a randomized controlled trial. *Med Sci Monit*. (2016) 22:1486–96. doi: 10.12659/MSM.898457

42. Morelli A, Donati A, Ertmer C, Rehberg S, Lange M, Orecchioni A, et al. Levosimendan for resuscitating the microcirculation in patients with septic shock: a randomized controlled study. *Crit Care*. (2010) 14(6):R232. doi: 10.1186/cc9387

43. Wang Q, Yokoo H, Takashina M, Sakata K, Ohashi W, Abedelzaher LA, et al. Anti-inflammatory profile of levosimendan in cecal ligation-induced septic mice and in lipopolysaccharide-stimulated macrophages. *Crit Care Med*. (2015) 43(11):e508–20. doi: 10.1097/CCM.0000000000001269

44. Shi J, Chen Y, Zhi H, An H, Hu Z. Levosimendan protects from sepsis-inducing cardiac dysfunction by suppressing inflammation, oxidative stress and regulating cardiac mitophagy via the PINK-1-parkin pathway in mice. *Ann Transl Med*. (2022) 10(4):212. doi: 10.21037/atm-22-483

45. Zangrillo A, Putzu A, Monaco F, Oriani A, Frau G, Luca MD, et al. Levosimendan reduces mortality in patients with severe sepsis and septic shock: a meta-analysis of randomized trials. *J Crit Care*. (2015) 30(5):908–13. doi: 10.1016/j.jcrc.2015.05.017

46. Gordon AC, Perkins GD, Singer M, McAuley DF, Orme RM, Santhakumaran S, et al. Levosimendan for the prevention of acute organ dysfunction in sepsis. *N Engl J Med*. (2016) 375(17):1638–48. doi: 10.1056/NEJMoa1609409

47. Antcliffe DB, Santhakumaran S, Orme RML, Ward JK, Al-Beidh F, O'Dea K, et al. Levosimendan in septic shock in patients with biochemical evidence of cardiac dysfunction: a subgroup analysis of the LeoPARDS randomised trial. *Intensive Care Med*. (2019) 45(10):1392–400. doi: 10.1007/s00134-019-05731-w

48. Hamzaoui O, Teboul JL. Levosimendan in sepsis. *N Engl J Med*. (2017) 376(8):799. doi: 10.1056/NEJMc1616632

49. Putzu A, Belletti A, Zangrillo A. Levosimendan in sepsis. *N Engl J Med*. (2017) 376(8):798–9. doi: 10.1056/NEJMc1616632

50. Bhattacharjee S, Soni KD, Maitra S, Baidya DK. Levosimendan does not provide mortality benefit over dobutamine in adult patients with septic shock: a meta-analysis of randomized controlled trials. *J Clin Anesth*. (2017) 39:67–72. doi: 10.1016/j.jclinane.2017.03.011

51. McDonagh TA, Metra M, Adamo M, Gardner RS, Baumbach A, Böhm M, et al. 2021 ESC guidelines for the diagnosis and treatment of acute and chronic heart failure. *Eur Heart J*. (2021) 42(36):3599–726. doi: 10.1093/eurheartj/ehab368

52. Yang C, Pan P, Du X, Wang Y, Yu X. Clinical effect of levosimendan on the patients with septic cardiomyopathy: a meta-analysis of randomized controlled trials. *Chin J Crit Care Med*. (2022) 5:406–11. doi: 10.3969/i.issn.1002-1949.2022.05.006

53. Sun T, Zhang N, Cui N, Wang SH, Ding XX, Li N, et al. Efficacy of levosimendan in the treatment of patients with severe septic cardiomyopathy. *J Cardiothorac Vasc Anesth*. (2023) 37(3):344–9. doi: 10.1053/j.jvca.2022.10.032

54. Guan Q, Zhang C, Li B, Huang D, Li A, Qin J, et al. Meta-analysis of the efficacy of levosimendan in the treatment of severe sepsis complicated with septic cardiomyopathy. *Heart Surg Forum*. (2023) 26(5):E609–e20. doi: 10.59958/hsf.6439

55. Tan R, Guo H, Yang Z, Yang H, Li Q, Zhu Q, et al. Efficacy and safety of levosimendan in patients with sepsis: a systematic review and network meta-analysis. *Front Pharmacol*. (2024) 15:1358735. doi: 10.3389/fphar.2024.1358735

56. Morelli A, De Castro S, Teboul JL, Singer M, Rocco M, Conti G, et al. Effects of levosimendan on systemic and regional hemodynamics in septic myocardial depression. *Intensive Care Med*. (2005) 31(5):638–44. doi: 10.1007/s00134-005-2619-z

57. Vaitsis J, Michalopoulou H, Thomopoulos C, Massias S, Stamatis P. Use of levosimendan in myocardial dysfunction due to sepsis. *Crit Care*. (2009) 13(Suppl 1):165. doi: 10.1186/cc7329

58. Fang M, Dong S. Effects of levosimendan on hemodynamics and cardiac function in patients with septic shock. *Zhonghua Wei Zhong Bing Ji Jiu Yi Xue*. (2014) 26(10):692–6. doi: 10.3760/cma.j.issn.2095-4352.2014.10.002

59. Xu CX, Li L, Gong SJ, Yu YH, Yan J. The effects of levosimendan on the cardiac function and prognosis in elderly patients with septic shock and myocardial contractility impairment. *Zhonghua Nei Ke Za Zhi*. (2018) 57(6):423–8. doi: 10.3760/cma.j.issn.0578-1426.2018.06.006

60. Sun T, Sun QL, Liu Y, Zhang YY, Sheng P, Cui N, et al. The efficacy of levosimendan and dobutamine on reducing peripheral blood interleukin-6 levels and improving cardiac function in patients with septic cardiomyopathy: a comparative study. *J Physiol Pharmacol*. (2024) 75(4). doi: 10.26402/jpp.2024.4.05

61. Girardis M, Bettex D, Bojan M, Demponeras C, Fruhwald S, Gál J, et al. Levosimendan in intensive care and emergency medicine: literature update and expert recommendations for optimal efficacy and safety. *J Anesth Analg Crit Care*. (2022) 2(1):4. doi: 10.1186/s44158-021-00030-7

62. Vincent JL, Singer M, Einav S, Moreno R, Wendon J, Teboul JL, et al. Equilibrating SSC guidelines with individualized care. *Crit Care*. (2021) 25(1):397. doi: 10.1186/s13054-021-03813-0

frontiers | Frontiers in Cardiovascular Medicine

TYPE Original Research
PUBLISHED 09 January 2025
DOI 10.3389/fcvm.2024.1502173

OPEN ACCESS

EDITED BY
Takahiro Nakashima,
University of Michigan, United States

REVIEWED BY
Hideaki Nonaka,
The University of Queensland, Australia
Masaaki Hino,
TMG Asaka Medical center, Japan

*CORRESPONDENCE
Aydın Nadir
✉ aydin_nadir@yahoo.com

RECEIVED 08 November 2024
ACCEPTED 17 December 2024
PUBLISHED 09 January 2025

CITATION
Nadir A, Kara D and Turkoz A (2025) The effect of thermoelectric craniocerebral cooling device on protecting brain functions in post-cardiac arrest syndrome.
Front. Cardiovasc. Med. 11:1502173.
doi: 10.3389/fcvm.2024.1502173

The effect of thermoelectric craniocerebral cooling device on protecting brain functions in post-cardiac arrest syndrome

Aydın Nadir[1]*, Deniz Kara[2] and Ayda Turkoz[2]

[1]Department of Cardiology, Faculty of Medicine, Bezmialem Vakif University, Istanbul, Türkiye, [2]Department of Anesthesiology and Reanimation, Faculty of Medicine, Bezmialem Vakif University, Istanbul, Türkiye

Aim: This study aimed to protect brain functions in patients who experienced in-hospital cardiac arrest through the application of local cerebral hypothermia. By utilizing a specialized thermal hypothermia device, this approach sought to mitigate ischemic brain injury associated with post-cardiac arrest syndrome, enhance survival rates, and improve neurological outcomes as measured by standardized scales.

Methods: A prospective, single-center cohort study was conducted involving patients aged ≥18 years who experienced in-hospital cardiac arrest and achieved return of spontaneous circulation (ROSC). Patients were cooled using a hypothermia helmet to achieve a target temperature of 32°C–34°C, maintained for 36–72 h, followed by controlled rewarming and normothermia for 72 h. Neurological recovery was assessed using the Cerebral Performance Category (CPC) scale, where CPC 1–2 denotes good recovery and CPC 3–5 indicates poor outcomes. Body temperature, hemodynamic parameters, biochemical changes, and survival data were meticulously recorded and analyzed. Statistical analysis included paired *t*-tests to compare pre- and post-treatment data.

Results: Of 116 cardiac arrest cases, 30 (25.86%) were in-hospital, and 16 (53.33%) of these achieved ROSC. Among the patients, 62.5% underwent emergency coronary angiography due to ST-elevation myocardial infarction (STEMI). The mean time to hypothermia initiation was 32.9 ± 13.5 min, with hypothermia maintained for 58 ± 6.4 h. Neurological outcomes were favorable, with 62.5% of patients achieving CPC scores of 1 or 2, indicating functional recovery and independence. In contrast, CPC scores of 3 or higher were observed in 37.5% of patients, reflecting varying degrees of disability. Biochemical analysis revealed significant decreases in sodium, potassium, calcium, and magnesium levels, alongside increased urea and creatinine concentrations. Hemodynamic improvements included elevated systolic blood pressure and heart rate, while left ventricular ejection fraction remained stable. Overall survival was 75%, and the majority (62.5%) of survivors were discharged without significant neurological deficits.

Conclusion: The findings suggest that early and targeted application of craniocerebral thermal hypothermia has the potential to improve survival and preserve neurological function in post-cardiac arrest syndrome. The high rates of favorable outcomes, as reflected by CPC scores, underscore the neuroprotective effects of localized hypothermia. Further large-scale, multicenter trials are recommended to validate these promising results and refine protocols for optimal clinical application.

KEYWORDS

cardiac arrest, hypothermia, neurological outcomes, post-resuscitation care, target temperature management

Introduction

According to the American Heart Association's 2019 updated statistics, approximately 565,000 cardiac arrest cases occur worldwide. Of these cases, 356,000 are out-of-hospital, while 209,000 are in-hospital. According to United States data, the survival rate is 12% for out-of-hospital cardiac arrest and 25% for in-hospital cardiac arrest. The survival rate with good neurological outcomes is 8% (1). Most of the poor outcomes and deaths of cardiac arrest survivors are attributed to widespread brain damage (2).

Therapeutic hypothermia was first applied in Russia in 1803 by covering the body with snow during the resuscitation of patients who developed cardiac arrest. In the 1958s, hypothermia was attempted by immersing the body in cold water during open heart, brain, and spinal cord surgeries. To increase the rate of sequela-free discharge of cardiac arrest survivors who can achieve rhythm with cardiac massage and to reduce brain damage, more modern, practical, fast, and easily applicable hypothermia devices are needed.

Organizations such as the International Liaison Committee on Resuscitation (ILCOR), American Heart Association (AHA), and European Resuscitation Council (ERC) state in their basic recommendations that "Adult patients showing ventricular fibrillation as the initial rhythm due to out-of-hospital sudden cardiac arrest should be cooled between 32°C and 34°C for 12–24 h" (3–5). Such a cooling method can also be beneficial in malignant arrhythmias such as VT/VF that primarily affect hemodynamics, post-CPR, and in-hospital sudden cardiac arrest patients. Today, hypothermia is accepted by medical science as a treatment method.

According to the guidelines published in 2022 by the European Resuscitation Council (ERC) and the European Society of Intensive Care Medicine (ESICM), adults who are unconscious after cardiac arrest should be treated with fever management and avoidance of fever. However, many questions about the optimal target temperature, cooling methods, and optimal duration still await answers (6).

In recent years, the use of therapeutic hypothermia in post-cardiac arrest patients has been a focus of clinical research. This study aims to contribute to the growing body of evidence regarding the potential benefits of craniocerebral hypothermia devices, which may offer a non-invasive and controlled method of cooling the brain following a cardiac arrest.

The aim of this study was to assess the safety, feasibility, and effectiveness of using craniocerebral thermal hypothermia as a treatment for patients with post-cardiac arrest syndrome. By utilizing a thermoelectric hypothermia helmet, the research sought to determine the device's ability to induce and maintain target temperature cooling (32°C–34°C) and its potential impact on improving neurological outcomes in this high-risk patient population.

Methods

This study was a prospective, single-center cohort study conducted to assess the safety, feasibility, and potential impact of craniocerebral thermal hypothermia in patients with post-cardiac arrest syndrome. The cohort consisted of adult patients (≥18 years) who experienced in-hospital cardiac arrest and achieved return of spontaneous circulation (ROSC). The study spanned a period of 12 months, from January to December 2023.

Study design

This study utilized a single-arm observational cohort design, aimed at evaluating the effects of a thermoelectric hypothermia device on targeted temperature management (TTM) and neurological recovery in patients following in-hospital cardiac arrest. Due to the absence of a control group, no comparative analysis was conducted. Instead, the The primary focus of this study was to evaluate the safety and feasibility of the intervention.

Inclusion criteria

- Adults (≥18 years) with in-hospital cardiac arrest of cardiac origin (e.g., ventricular fibrillation, ventricular tachycardia, asystole, or unknown causes).
- Patients who achieved ROSC and spontaneous circulation.
- Glasgow Coma Scale (GCS) ≤9 upon admission.
- Patients who were intubated and eligible for therapeutic hypothermia.

Exclusion criteria

- Age <18 years.
- Consciousness (GCS >9) at the time of admission.
- Active cancer treatment or severe comorbidities (e.g., acute stroke, advanced dementia, pregnancy).
- Body temperature <30°C at the time of arrival.

The primary objective of this study was to evaluate the effectiveness of craniocerebral hypothermia in improving neurological outcomes in post-cardiac arrest patients. Descriptive analysis of neurological recovery was performed using the Cerebral Performance Category (CPC) scale, assessed at multiple time points during and after treatment.

Due to the single-arm design, a comparative analysis against other interventions could not be performed. The study focused on describing changes in neurological status, including CPC scores correlated with different treatment phases: cooling, rewarming, and post-recovery.

Additionally, clinical parameters such as survival rates, time to normothermia, and biomarkers were tracked to further evaluate the potential impact of hypothermia on patient outcomes.

For patients who developed cardiac arrest, advanced life support protocols were promptly initiated, including intubation and cardiac resuscitation. Body temperature was continuously monitored using transnasal esophageal probes and axillary probes after intubation. Initial body temperature, hypothermia onset, duration, and time to normothermia were systematically recorded.

FIGURE 1
Thermoelectric hypothermia helmet.

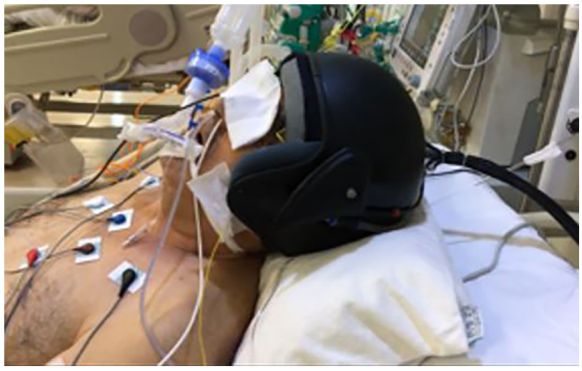

FIGURE 2
Example of thermohypothermia application in a patient.

The Turkish-patented thermoelectric hypothermia helmet used in this study was specifically designed for craniocerebral hypothermia (CSH) (7) (Figures 1, 2). Informed consent was obtained from all patients' families before initiating treatment.

Safety and Complications: The safety of the thermoelectric hypothermia device was closely monitored throughout the study, with particular focus on potential therapeutic hypothermia (TTM)-related complications.

Other potential complications associated with TTM, such as hypotension, electrolyte imbalances, and skin injuries (e.g., pressure sores from prolonged cooling), were closely monitored. Blood pressure, electrolyte levels, and skin integrity were regularly assessed, and corrective interventions were implemented when necessary. Arterial blood gases and fingertip blood glucose were monitored hourly to assess metabolic and respiratory status, ensuring the safe management of hypotension and other complications.

As a therapeutic hypothermia protocol, patients were gradually cooled at 0.5°C in 2 h to reach the target body temperature of 32°C–34°C in 2–4 h, and hypothermia was applied continuously for 36–72 h. Appropriate sedation was provided to patients during hypothermia. For sedation, Propofol and Remifentanil (Propofol 1 mg/kg bolus followed by 0.3–4.0 mg/kg/h, Remifentanil 0.05–0.1 mg/kg/min) were used according to the patient's weight. After therapeutic hypothermia, patients were started to be rewarmed at a rate of 0.25–0.50°C/h, and controlled normothermia was maintained for 72 h, followed by prognosis evaluation.

Glasgow Coma Scale and Cerebral Performance Category scale were used to evaluate patients' consciousness (8). Hourly arterial blood gas and fingertip blood sugar monitoring were performed during hypothermia. Patients' hemodynamic changes, recurrent arrhythmias, death, or discharge data were recorded. Hospital stay duration was recorded from the time of admission until discharge. The CPC score assessment was performed regularly during the hospital stay and at discharge to evaluate the neurological recovery process of the patients.

Fluid management strategies were employed to prevent hypotension during cooling and to ensure adequate organ perfusion. Adverse events, including complications arising from cooling and rewarming, were systematically recorded, and the safety profile of the device was assessed based on the incidence and management of these complications.

Treatment timeline

1. Hypothermia Initiation (Time 0): Immediate initiation following cardiac arrest
2. Cooling Phase (36–72 h): Continuous hypothermic treatment
3. End of Cooling (72nd hour): Completion of cooling phase
4. Rewarming Phase (72 h): Gradual rewarming with maintained normothermia

Smart thermoelectric hypothermia helmet

The Thermohypotherm system, developed in Austria and patented by the Turkish Patent Institute (Figures 1, 3), is the first and only system of its kind, designed to induce both superficial and deep craniocerebral hypothermia. The thermoelectric micromodule, which is integrated into the helmet, facilitates external cooling of the head, thereby allowing the target brain temperature to be achieved by adjusting the applied DC current. By increasing the current, the cooling effect is intensified, and conversely, by reversing the direction of the current, the micromodule can act as a heater, enabling a controlled transition from hypothermia to normothermia once the desired cooling is achieved.

This system is integrated with both esophageal temperature and in-helmet temperature sensors, enabling continuous monitoring and automatic adjustment of the patient's body temperature. Through the device's digital interface, clinicians can set the target body temperature, define the maximum temperature drop allowed in the helmet, and control the

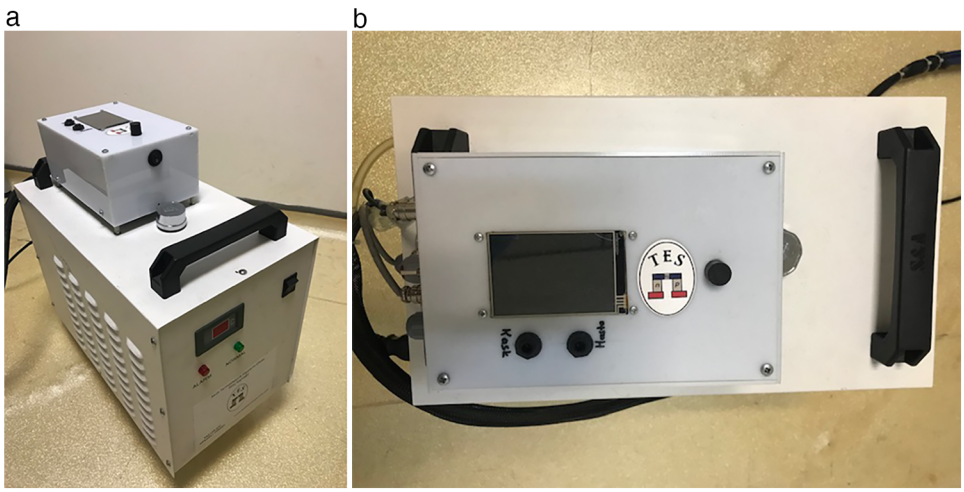

FIGURE 3
Thermohypothermia device. **(a)** Front view of the thermohypothermia device. **(b)** Top view of the thermohypothermia device.

duration of the hypothermic phase. In this study, the maximum temperature reduction achievable by the device was set at 20°C.

The thermoelectric hypothermia helmet employed in this study was designed to achieve controlled cooling specifically targeting the head region in patients with post-cardiac arrest syndrome. The in-helmet temperature represents the temperature measured within the space between the patient's skin and the helmet, influenced by the cooling effect of the integrated thermoelectric micromodule. While this measurement reflects the cooling efficiency of the helmet, it does not directly correlate with the brain temperature. Instead, it serves as an indirect indicator of the cooling effect on the brain. To standardize temperature management and align with conventional practices, esophageal temperature was utilized as the target body temperature in this study. This approach is consistent with widely recognized temperature management systems, such as Thermogard and Arctic Sun, which rely on continuous core body temperature monitoring as a standard for guiding therapeutic hypothermia. These systems ensure precise control over the cooling process, reducing variability and optimizing patient outcomes. Since direct measurement of brain temperature was not conducted, the expected brain temperature was inferred based on the combined analysis of in-helmet temperature and esophageal temperature, reflecting the potential impact of localized head cooling on cerebral thermoregulation.

Cerebral performance category

It is a scale categorized between 1 and 5 points to evaluate patients' cerebral performance after CPR (8). Table 1 contains explanations about CPC. A CPC score of 1 or 2 was considered as survival with appropriate neurological function.

Table 1 Cerebral performance category (CPC).

CPC Description:

TABLE 1 Basic clinical and demographic characteristics of patients at the time of admission.

Parameter	Patients
Age	49.4 ± 7.3
Gender M, (*n*, %)	10 (62.5)
Obesity (*n*, %)	8 (50)
Hypertension (*n*, %)	8 (50)
Hyperlipidemia (*n*, %)	10 (62.5)
Diabetes (*n*, %)	4 (25)
Smoker (*n*, %)	10 (62.5)
Family history (*n*, %)	6 (37.5)
BMI (kg/m^2)	23 5.2
ECG findings - NSR (*n*, %) - AF (*n*, %)	16 (100) 0 (–)

1. Return to normal cerebral functions and normal life
2. Independent daily life with limitations in brain functions
3. Inability to maintain daily life independently with severe effects on brain functions
4. Coma
5. Brain death

Statistical analysis

Statistical analysis was performed using SPSS (Statistical Package for the Social Sciences) version 25.0. Continuous variables were expressed as means ± standard deviations (SD) and categorical variables as frequencies and percentages. Paired *t*-tests or Wilcoxon signed-rank tests were used to compare pre- and post-treatment biochemical markers and hemodynamic parameters. Survival analysis was performed using Kaplan-Meier curves to estimate overall survival and neurological recovery. A

p-value < 0.05 was considered statistically significant for all analyses.

Ethical considerations

The study was approved by the institutional ethics committee (approval number: 71306642-050.01.04/2020). Informed consent was obtained from all patients or their legal representatives prior to enrollment. This study adhered to ethical principles outlined in the Declaration of Helsinki.

Results

During the 1-year study period, a total of 116 cardiac arrest cases were admitted to our clinic. Of the admitted patients, 86 (74.14%) were out-of-hospital arrests, and 30 (25.86%) were in-hospital arrests. Of the in-hospital arrests, 22 (73.33%) were cardiac, and 8 (26.67%) were respiratory in origin. Of the in-hospital cardiac arrests, 16 (72.73%) responded to CPR and sinus rhythm was achieved, while 6 (27.27%) patients did not respond to CPR and were lost.

Of the patients who achieved sinus rhythm, 10 (62.5%) had ST elevation on ECG [4 patients with inferior myocardial infarction (MI), 6 patients with anterior MI].These patients were taken for emergency coronary angiography. 6 (37.5%) patients had no ST elevation and did not undergo emergency coronary angiography.

A total of 16 cases, 10 (62.5%) of whom were male, were included in this study. All of the cardiac arrests occurred in the emergency department, and the cause of arrest was cardiac in all [2 patients with asystole (12.5%), 10 patients with ventricular tachycardia (62.5%), 4 patients with VF (25%)]. The basic clinical and demographic characteristics of the patients, characteristics and procedures related to cardiac arrest at admission are shown in Table 2.

10 (87.5%) patients in the angiography laboratory underwent interventional procedures. As a result of coronary angiography, critical lesions were detected in the right coronary artery (RCA) in 3 patients, in the circumflex coronary artery (Cx) in 1 patient, and in the left anterior descending artery (LAD) in 6 patients. TIMI III flow was achieved in all patients after the procedure.

TABLE 2 Characteristics and procedures related to cardiac arrest.

Parameter	*n*/Time
Cause of the cardiac arrest (*n*)	16
Cardiac (*n*)	16
Asystole (*n*)	2 (12.5)
Ventricular tachycardia (*n*)	10 (62.5)
Ventricular fibrillation (*n*)	4 (25)
Respiratory insufficiency (*n*)	–
Unknown	–
Cardiopulmonary resuscitation time (min)	16.3 ± 8.7
Hypothermia onset time (min)	32.9 ± 13.5
Time to reach target temperature 32–34°C (min)	214 ± 28.4
Duration of hypothermia <36°C (hours)	58 ± 6.4

TABLE 3 Coronary angiography and clinical parameters.

Parameter	Value (*n*, % or Mean ± SD)
Coronaryangiography	–
Electively (*n*, %)	10 (100)
Urgent (*n*, %)	–(0)
Diagnostic (*n*, %)	10 (100)
Interventional (*n*, %)	3 (30)
Inferior myocardial infarction	1 (10)
Right coronary artery (RCA)	6 (60)
Circumflex coronary artery (Cx)	
Anterior myocardial infarction	
Left anterior descending (LAD)	
Systolic blood pressure (mmHg)	143.8 ± 86.5
Diastolic blood pressure (mmHg)	78.3 ± 9.2
Heart rate (beats/min):	78.2 ± 11.2
Procedure time (min)	36.2 ± 8.6
Unfractionated heparin dose (U)	9,000 ± 1,000

Table 3 shows the demographic characteristics of patients during the angiography laboratory.

The mean CPR duration of the patients was recorded as 16.3 ± 8.7 min. The time to start hypothermia was determined as 32.9 ± 13.5 min, the time to reach the targeted body temperature was 214 ± 28.4 min, and the duration of hypothermia was 58 ± 6.4 h. Temperature changes during hypothermic therapy are shown in Figure 4. Figure 4 illustrates the temperature dynamics observed during hypothermic therapy in post-cardiac arrest patients, with measurements recorded hourly and daily at multiple sites, including the intensive care unit, helmet, axillary, and esophageal regions. This comprehensive monitoring allowed for a detailed evaluation of temperature changes throughout the course of therapy.

A significant temperature decrease was observed in both axillary and esophageal temperature follow-ups with the thermoelectric hypothermia device. The hypothermia helmet was found to be effective ($p < 0.005$). During hypothermia application, while a statistically significant decrease was observed in sodium, potassium, calcium, and magnesium levels in biochemical parameters, a statistically significant increase was observed in urea and creatinine values. Additionally, a statistically significant increase in systolic blood pressure and heart rate was determined with hypothermia. There was no statistically significant change in left ventricular Ejection fraction. (Table 4).

Two patients lost their lives due to cardiogenic shock and re-arrest in the first hour of hospitalization. Hypothermia was terminated early in 6 patients due to GCS being above 9 in the first 24 h of hypothermia, and they were extubated by providing normothermia (GCS 15 and CPC 1). At the end of the 72nd hour, hypothermia was terminated for the remaining patients and status evaluation was made. Four patients demonstrated spontaneous breathing and a Glasgow Coma Scale (GCS) score above 9. Following clinical assessment and evaluation, extubation was performed on these selected patients after blood gas analysis and appropriate adjustment of ventilator settings. After extubation, the patients were evaluated with a GCS of 15 and a cerebral performance category (CPC) score of 4. Four patients

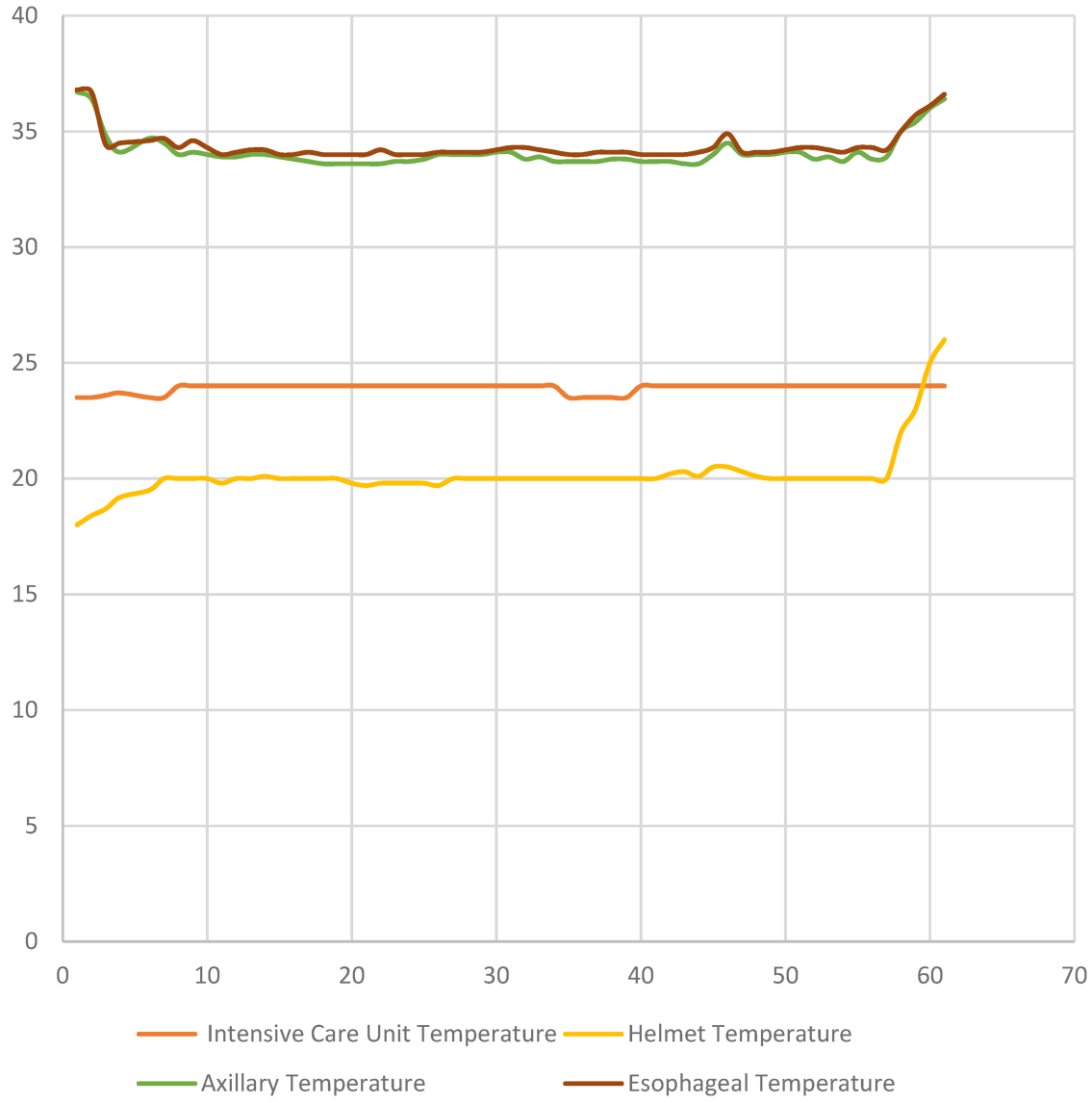

FIGURE 4
Temperature dynamics during hypothermic therapy in post-cardiac arrest patients are shown in Figure 4. The graph depicts temperature changes at various measurement sites (Intensive Care Unit, Helmet, Axillary, and Esophageal temperatures) over time, with measurements taken hourly and daily during the course of the therapy.

could not be extubated as their GCS was below 9. In further follow-ups, 2 patients were lost due to pneumonia, and two patients were discharged with GCS 9 after tracheostomy was performed (Table 5).

As a result, with early hypothermia application, the survival rate was 75%, while the rate of remaining without sequelae was 62.5%. The average hospital stay for surviving patients was 13 ± 7 days.

Study population characteristics

The study included 16 patients, with 10 (62.5%) being male. All cardiac arrests occurred in the emergency department with the following rhythms:

- Asystole: 2 patients (12.5%)
- Ventricular tachycardia: 10 patients (62.5%)
- Ventricular fibrillation: 4 patients (25%)

Coronary intervention outcomes

Among patients in the angiography laboratory:

- 10 patients (87.5%) underwent interventional procedures
- Critical lesions were identified in:
  - Right coronary artery (RCA): 3 patients
  - Circumflex coronary artery (Cx): 1 patient
  - Left anterior descending artery (LAD): 6 patients
- TIMI III flow was achieved in all patients post-procedure

TABLE 4 Comparison of variables before and during hypothermia therapy.

Variable	Pre-HT (Mean ± SD)	During HT (Mean ± SD)	*p*-value
Sodium (mM/L)	134 ± 4.65	135 ± 3.98	0.103
Potassium (mM/L)	4.23 ± 0.65	3.96 ± 0.47	0.064
Calcium (mg/L)	7.83 ± 0.65	7.48 ± 0.58	0.075
Magnesium (mg/L)	2.14 ± 0.16	2,08 ± 0.13	0.087
Hemoglobin (g/dl)	12.8 ± 1.97	12,6 ± 1.69	0.308
Hematocrit (%)	39.1 ± 6.23	38,9 ± 5.04	0.174
Plt (103/ul)	310 ± 83	312 ± 87	0.751
Urea (g/L)	23.3 ± 8.7	25.7 ± 10.8	0.068
Creatinin (mg/dl)	1.06 ± 0.29	1.14 ± 0.38	0.074
Hs-CRP(mg/L)	14.83 ± 15.39	13.72 ± 13.4	0.589
Systolic BP(mmHg)	106.1 ± 13.01	114.4 ± 13.75	0.001
Diastolic BP (mmHg)	67.92 ± 10.19	70.88 ± 9.7	0.062
Mean arterial pressure (MAP)	80.64 ± 11.56	85.38 ± 11.72	0.031
Axillary temperature (C°)	36.2 ± 1.04	33.6 ± 1.06	0.001
Esophagus temperature (C°)	36.6 ± 1.12	34.1 ± 1.08	0.003
Temperature inside the helmet (C°)	20 ± 1.14	19 ± 1.17	0.084
Heart rate(beat/min)	116 ± 11	93 ± 10	0.034
EF%	58 ± 3.5	60 ± 2.1	0.291

"During HT" refers to the entire period of hypothermic therapy (HT), from the initiation of cooling to the end of the cooling phase. The mean and standard deviation (SD) values represent the data collected over this entire period.

Effectiveness of hypothermia helmet

The effectiveness of the thermoelectric hypothermia helmet was primarily evaluated based on its ability to achieve and maintain the target temperature range of 32°C–34°C for the prescribed duration of therapy. A statistically significant decrease in body temperature was observed following the initiation of hypothermia treatment. The device effectively reduced body temperature, achieving the target range within an average of 214 ± 28.4 min, and maintained this temperature for 58 ± 6.4 h. The *p*-value of <0.005 was derived from a paired *t*-test comparison of pre-treatment baseline temperatures and post-treatment temperatures. This demonstrated that the helmet was statistically effective in reducing the core body temperature compared to baseline values.

Furthermore, the device demonstrated excellent control over temperature fluctuations during both the cooling and rewarming phases, with minimal variation from the target temperature. The controlled temperature regulation was essential in minimizing the risk of complications associated with uncontrolled hypothermia or hyperthermia.

Lactate levels and cohort severity

Lactate levels, an important indicator of tissue hypoxia and severity of metabolic acidosis, were elevated upon admission for most patients, which is consistent with severe ischemia and shock at the time of cardiac arrest. Although lactate levels were not part of the routine study protocol, early lactate monitoring was conducted in a subset of patients, showing levels greater than 6 mmol/L in several cases. These elevated lactate levels gradually decreased with clinical stabilization and initiation of hypothermia treatment, reflecting improved tissue perfusion and metabolic recovery.

Complications and device safety

No adverse events or device-related complications were reported throughout the study period, highlighting the safety of the thermoelectric hypothermia helmet in the clinical setting. Importantly, no skin injuries or pressure sores were observed, even after prolonged periods of hypothermia therapy. Continuous monitoring of the patients' body temperature ensured that the cooling process was precisely controlled, preventing the risk of overcooling or rebound hyperthermia. Furthermore, the helmet's low invasiveness was a key feature, as it did not require invasive procedures beyond routine clinical care, such as temperature monitoring via esophageal probes and arterial blood gases.

TABLE 5 Clinical outcomes of hypothermia treatment in post-cardiac arrest patients.

Patient group	Initial clinical presentation (first 24 hours)	Clinical status after 72 hours of hypothermia	Extubation process	Final outcomes
Deceased patients	2 patients experienced cardiogenic shock followed by re-arrest and death			Mortality occurred within the first 24 h due to cardiogenic shock
Early termination of hypothermia	6 patients demonstrated GCS >9 within the first 24 h, hypothermia was terminated early, normothermia achieved (GCS 15, SPS 1)		Early extubation performed after reaching normothermia (GCS 15, CPC 4)	Successful recovery from hypothermia and extubation, no further complications noted
Gradual extubation group		4 patients exhibited spontaneous respiration and GCS >9 after 72 h of hypothermia	Gradual extubation performed post-hypothermia (GCS 15, CPC 4)	Successful extubation, with GCS 15, CPC 4; patients remained stable post-extubation
Non-extubation group		4 patients had GCS <9 after 72 h, failed to demonstrate spontaneous respiration	Extubation not performed due to poor neurological status	2 patients died from pneumonia; 2 patients discharged with tracheostomy and GCS 9

GCS, Glasgow coma scale score; CPC, cerebral performance category scale.

The safety profile of the device is a significant advantage, particularly in critically ill patients where the risk of complications from invasive procedures is high. The absence of complications associated with the device, combined with its ability to effectively induce and maintain hypothermia, suggests that the device could be a valuable tool in clinical practice for post-cardiac arrest care.

Survival and neurological outcomes

- Survival rate: Overall, 75% of patients who achieved ROSC survived to discharge.
- Neurological outcomes: Among survivors, 62.5% had favorable neurological outcomes, with a Cerebral Performance Category (CPC) score of 1 or 2, indicating full or near-full recovery. These patients were able to return to independent daily living with minimal to no functional impairments. In contrast, 37.5% of survivors had a CPC score of 3 or higher, indicating moderate to severe neurological impairment. These patients were unable to perform activities of daily living independently and had ongoing cognitive or motor deficits.

Discussion

In this study, we sought to investigate the neuroprotective effects of craniocerebral thermal hypothermia in patients who developed post-cardiac arrest syndrome. Our results indicated that early application of hypothermia led to a survival rate of 75%, with 62.5% of patients remaining without significant sequelae. These findings suggest that craniocerebral hypothermia may represent an effective strategy in mitigating brain damage following cardiac arrest.

The neuroprotective effects of mild hypothermia, particularly in alleviating global cerebral hypoxia and ischemic injury, have been well-documented in the literature (9, 10). Studies have consistently shown that therapeutic hypothermia improves neurological outcomes in patients post-cardiac arrest. The favorable survival and low sequelae rates observed in our cohort further substantiate these findings. Hypothermia exerts a protective effect by reducing cerebral oxygen consumption, which is critical in mitigating the deleterious consequences of hypoxia. A decrease of 1°C in body temperature results in approximately a 6% reduction in cerebral metabolic rate (11), thereby attenuating the formation of excitotoxic amino acids and free radicals. Moreover, hypothermia inhibits the release of intracellular excitotoxins and diminishes the inflammatory cascade that contributes to post-cardiac arrest syndrome (7, 12).

Although the systemic application of hypothermia has been associated with a range of complications, including arrhythmias, coagulopathies, and infections (13), our approach of local cerebral hypothermia seeks to minimize these risks. The craniocerebral thermal hypothermia device utilized in our study is an original, patented technology in Turkey (14), offering a more efficient and controlled cooling method compared to conventional systemic cooling techniques. In support of our clinical findings, animal studies have demonstrated favorable outcomes with similar hypothermia interventions. For instance, a study conducted on rodents revealed a dramatic 80% reduction in mortality following hypothermic treatment (15). While these results align with the positive outcomes observed in our clinical cohort, caution is warranted in extrapolating animal model data to human physiology due to inherent differences between species. Timing is a critical factor in the effectiveness of hypothermia in post-cardiac arrest patients. The literature emphasizes that early initiation of hypothermic therapy significantly improves neurological outcomes (16, 17).

Our study is a single-arm, non-randomized investigation, which is a key limitation when interpreting the results. The absence of a control group means that we cannot definitively attribute the observed outcomes solely to the device. However, the findings, particularly the neurological outcomes measured by the Cerebral Performance Category (CPC) scale, provide valuable insight into the potential benefits of localized hypothermia. Among survivors, 62.5% achieved CPC scores of 1 or 2, indicating favorable neurological recovery with minimal cognitive or motor impairment. These results suggest that localized cooling may contribute to preserving brain function following cardiac arrest, as supported by similar findings in other studies investigating hypothermic therapies.

The craniocerebral thermal hypothermia device also demonstrated an excellent safety profile. No adverse events related to the device, such as skin injuries, pressure sores, or hypothermic complications, were reported, supporting the non-invasive nature of the device. This is consistent with findings from other studies that have highlighted the low risk of complications associated with localized cooling techniques compared to more invasive cooling methods.

In our study, hypothermia was initiated on average within 32.9 ± 13.5 min after cardiac arrest, a factor we believe contributed significantly to the favorable results observed. The average duration of hypothermia in our cohort was 58 ± 6.4 h, which aligns with the 24–72 h duration recommended in prior studies (18, 19). However, further investigation is required to determine the optimal duration of hypothermia for maximal neuroprotection. Recent randomized controlled trials, such as the TTM2 trial, have raised questions regarding the precise temperature target for therapeutic hypothermia post-cardiac arrest (20). For example, the TTM2 study could not show a clear difference in whether target temperature management is more effective at 33°C or 37°C (21). However, local cerebral hypothermia applications like our study can add a new dimension to these discussions. Local application can provide deeper and more sustainable hypothermia in brain tissue while reducing systemic side effects. The findings from this study suggest that craniocerebral thermal hypothermia is a feasible and safe method for achieving controlled hypothermia in patients with post-cardiac arrest syndrome. However, it is important to note that due to the single-arm design and absence of a control group, this study was not designed to assess the definitive efficacy of the device on survival rates or neurological recovery.

Therefore, conclusions regarding the device's effectiveness in improving outcomes should be made cautiously.

The primary objective of this study was to evaluate the safety, feasibility, and efficacy in achieving targeted hypothermia using the thermoelectric hypothermia helmet. The device successfully achieved and maintained the target temperature range of 32°–34°C, which is critical for neuroprotection in post-cardiac arrest syndrome. The precise and controlled temperature regulation within the helmet and systemically is a significant advantage, as it minimizes the risk of complications associated with more invasive cooling methods. In this cohort, patients were cooled effectively, with an average time of 214 ± 28.4 min to reach the target temperature, and cooling was maintained for 58 ± 6.4 h.

The favorable neurological outcomes, as measured by the Cerebral Performance Category (CPC) scale, showed that 62.5% of survivors achieved CPC scores of 1 or 2, indicating favorable neurological recovery with minimal cognitive or motor impairment. However, 37.5% of patients exhibited moderate to severe neurological impairments (CPC scores of 3 or higher), which is consistent with the known challenges of post-cardiac arrest syndrome.

It is important to emphasize that the absence of a control group limits our ability to directly attribute these positive neurological outcomes to the device alone. The observed results may also be influenced by the clinical interventions provided, the timing of resuscitation, and other patient-specific factors such as comorbidities and the severity of initial cardiac arrest.

The safety profile of the device is a key finding in this study. No adverse events related to the device, such as skin injuries, pressure sores, or hypothermic complications, were observed. This highlights the low invasiveness of the device, as it does not require invasive monitoring beyond standard clinical care procedures. The absence of any significant complications suggests that craniocerebral thermal hypothermia could be a promising non-invasive treatment method for post-cardiac arrest care, particularly in settings where other forms of therapeutic hypothermia might pose higher risks or be less feasible.

Despite these promising findings, it is essential to acknowledge the study's limitations. The small sample size, single-arm design, and lack of long-term follow-up restrict the ability to generalize the results. Therefore, the conclusions drawn from this study should be considered preliminary. Further large-scale, multi-center randomized controlled trials are needed to rigorously assess the device's impact on neurological recovery, long-term survival, and quality of life. Additionally, studies evaluating optimal cooling duration, cooling rate, and patient subgroups that may benefit most from this approach are warranted.

In conclusion, this study demonstrates that craniocerebral thermal hypothermia, using a thermoelectric hypothermia helmet, is a safe and feasible intervention for inducing controlled hypothermia in post-cardiac arrest syndrome. While the results suggest the device's potential for achieving the target temperature safely, the impact on neurological outcomes, as indicated by CPC scores, remains an important area for future investigation.

Limits of the study

First, our number of patients is relatively small and there is no control group. This limits the generalizability of our results. Also, long-term follow-up results have not yet been obtained. Longer follow-up is required for a full assessment of neurological recovery.

In the future, the craniocerebral thermal hypothermia device should be further developed and its widespread use in ambulances and intensive care units should be targeted. This technology can be evaluated as a potential treatment method not only after cardiac arrest but also for traumatic brain injury, stroke, and other neurological emergencies.

Conclusion

The results of this study suggest that craniocerebral thermal hypothermia is a potentially effective and safe intervention for achieving targeted therapeutic hypothermia in patients with post-cardiac arrest syndrome. While the study demonstrated favorable survival rates and promising neurological outcomes, the single-arm desig Primary focus was on n, lack of a control group, and relatively small sample size limit the ability to draw definitive conclusions regarding the device's impact on clinical outcomes. Therefore, caution is warranted when interpreting these findings as conclusive evidence of the device's efficacy in improving neurological recovery or long-term survival.

The primary strength of this study lies in its demonstration of the feasibility and safety of utilizing the thermoelectric hypothermia device in a clinical setting. The device successfully achieved the target temperature range (32°–34°C) in a controlled and sustained manner, which is essential for mitigating ischemic injury and reducing the effects of post-cardiac arrest syndrome. However, the observed improvements in survival and neurological recovery should be considered preliminary and indicative of the device's potential, rather than definitive evidence of its clinical efficacy.

Given the inherent limitations of the study, including the absence of a control group and the lack of long-term follow-up data, future research should prioritize the design of large-scale, multi-center randomized controlled trials (RCTs). These trials would provide a more comprehensive understanding of the device's clinical efficacy, specifically assessing long-term neurological recovery, survival rates, and any potential adverse effects. Further investigations are also needed to determine the optimal duration of hypothermia therapy and identify specific patient subgroups that may benefit the most from this approach.

In this study, patients who survived cardiac arrest and achieved favorable neurological outcomes were initially described as having recovered without sequelae. However, this term can be ambiguous and subject to interpretation. To provide greater clarity, we used the Cerebral Performance Category (CPC) scale to more precisely assess neurological outcomes. A CPC score of 1 or 2 indicates favorable recovery, with CPC 1 representing full recovery or mild impairments, and CPC 2 indicating moderate disability that does

not hinder independent living. Therefore, rather than using the imprecise expression "without sequelae," we now refer to CPC scores for a more specific and reliable evaluation of neurological function.

In conclusion, while this study contributes to the growing body of evidence supporting the use of localized craniocerebral hypothermia, further rigorous research is necessary to fully assess its role as a standard treatment for post-cardiac arrest syndrome.

Data availability statement

The original contributions presented in the study are included in the article/Supplementary Material, further inquiries can be directed to the corresponding author.

Ethics statement

The studies involving humans were approved by Ethics Committee Approval: This study was conducted in accordance with the principles of the Declaration of Helsinki and was approved by the Ethics Committee of Bezmialem Vakif University (No.23.12.2021-44371). The studies were conducted in accordance with the local legislation and institutional requirements. The participants provided their written informed consent to participate in this study. Written informed consent was obtained from the individual(s) for the publication of any potentially identifiable images or data included in this article.

Author contributions

AN: Writing – original draft, Writing – review & editing. DK: Writing – review & editing. AT: Writing – review & editing.

Funding

The author(s) declare that no financial support was received for the research, authorship, and/or publication of this article.

Conflict of interest

The authors declare that the research was conducted in the absence of any commercial or financial relationships that could be construed as a potential conflict of interest.

Generative AI statement

The authors declare that no Generative AI was used in the creation of this manuscript.

Publisher's note

References

1. Benjamin EJ, Muntner P, Alonso A, Bittencourt MS, Callaway CW, Carson AP, et al. Heart disease and stroke statistics-2019 update: a report from the American Heart Association. *Circulation*. (2019) 139(10):e56–528. doi: 10.1161/CIR.0000000000000659

2. Geocadin RG, Callaway CW, Fink EL, Golan E, Greer DM, Ko NU, et al. Standards for studies of neurological prognostication in comatose survivors of cardiac arrest: a scientific statement from the American Heart Association. *Circulation*. (2019) 140(9):e517–42. doi: 10.1161/CIR.0000000000000702

3. Nolan JP, Soar J, Cariou A, Cronberg T, Moulaert VR, Deakin CD, et al. European Resuscitation Council and European Society of intensive care medicine guidelines for post-resuscitation care 2015: section 5 of the European resuscitation council guidelines for resuscitation 2015. *Resuscitation*. (2015) 95:202–22. doi: 10.1016/j.resuscitation.2015.07.018

4. Callaway CW, Donnino MW, Fink EL, Geocadin RG, Golan E, Kern KB, et al. Part 8: post-cardiac arrest care: 2015 American Heart Association guidelines update for cardiopulmonary resuscitation and emergency cardiovascular care. *Circulation*. (2015) 132(18 Suppl 2):S465–82. doi: 10.1161/CIR.0000000000000262

5. Donnino MW, Andersen LW, Berg KM, Reynolds JC, Nolan JP, Morley PT, et al. Temperature management after cardiac arrest: an advisory statement by the advanced life support task force of the international liaison committee on resuscitation and the American Heart Association emergency cardiovascular care committee and the council on cardiopulmonary, critical care, perioperative and resuscitation. *Circulation*. (2015) 132(25):2448–56. doi: 10.1161/CIR.0000000000000313

6. Nolan JP, Sandroni C, Böttiger BW, Cariou A, Cronberg T, Friberg H, et al. European Resuscitation Council and European Society of intensive care medicine guidelines 2021: post-resuscitation care. *Intensive Care Med*. (2021) 47(4):369–421. doi: 10.1007/s00134-021-06368-4

7. Kapıdere M, Ahiska R, Güler İ. Mikrodenetleyici kontrollü termohipoterm tıp cihazı. In *Biyomut, Biyomedikal Mühendisliği Ulusal Toplantısı*. Ankara, Türkiye: BIYOMUT (2002). p. 209–14.

8. Safar P. Resuscitation after brain ischemia. In: Grenvik A, Safar P, editors. *Brain Failure and Resuscitation*. New York: Churchill Livingstone (1981). p. 155–84.

9. Hypothermia after Cardiac Arrest Study Group. Mild therapeutic hypothermia to improve the neurologic outcome after cardiac arrest. *N Engl J Med*. (2002) 346(8):549–56. doi: 10.1056/NEJMoa012689

10. Arrich J, Holzer M, Havel C, Müllner M, Herkner H. Hypothermia for neuroprotection in adults after cardiopulmonary resuscitation. *Cochrane Database Syst Rev*. (2016) 2(2):CD004128. doi: 10.1002/14651858.CD004128.pub4

11. Geocadin RG, Wijdicks E, Armstrong MJ, Damian M, Mayer SA, Ornato JP, et al. Practice guideline summary: reducing brain injury following cardiopulmonary resuscitation: report of the guideline development, dissemination, and implementation subcommittee of the American Academy of Neurology. *Neurology*. (2017) 88(22):2141–9. doi: 10.1212/WNL.0000000000003966

12. Dankiewicz J, Cronberg T, Lilja G, Jakobsen JC, Levin H, Ullén S, et al. Hypothermia versus normothermia after out-of-hospital cardiac arrest. *N Engl J Med*. (2021) 384(24), 2283–94. doi: 10.1056/NEJMoa2100591

13. Ovul I, Nadirzade RS, Oner K, Nadirzade SM. A method for monitoring intracerebral temperature in neurosurgical patients. *Technol Surg Approach*. (1997) 3:354.

14. Ovul I, Nadirzade RS, Oner K, Nadirzade SM. A new technique for brain hypothermia. *Technol Surg Approach*. (1997) 3:353.

15. Demirel H, Ahıska R. Microcontrolled based rat termohypotherm system, 3. *International Advanced Technologies Syposium*; Ankara (2003). p. 165–73

16. Bernard SA, Gray TW, Buist MD, Jones BM, Silvester W, Gutteridge G, et al. Treatment of comatose survivors of out-of-hospital cardiac arrest with induced hypothermia. *N Engl J Med*. (2002) 346(8):557–63. doi: 10.1056/NEJMoa003289

17. Polderman KH. Mechanisms of action, physiological effects, and complications of hypothermia. *Crit Care Med*. (2009) 37(7 Suppl):S186–202. doi: 10.1097/CCM.0b013e3181aa5241

18. Polderman KH, Herold I. Therapeutic hypothermia and controlled normothermia in the intensive care unit: practical considerations, side effects, and cooling methods. *Crit Care Med*. (2009) 37(3):1101–20. doi: 10.1097/CCM.0b013e3181962ad5

19. Clifton GL, Jiang JY, Lyeth BG, Jenkins LW, Hamm RJ, Hayes RL. Marked protection by moderate hypothermia after experimental traumatic brain injury. *J Cereb Blood Flow Metab*. (1991) 11(1):114–21. doi: 10.1038/jcbfm.1991.13

20. Mellergard P, Nordstrom CH, Christensson M. A method for monitoring intracerebral temperature in neurosurgical patients. *Neurosurgery*. (1990) 27(4):654–7. doi: 10.1227/00006123-199010000-00029

21. Roedl K, Wolfrum S, Kluge S. Vorgehen nach erfolgreicher Reanimation – kühlen oder nicht mehr kühlen [Procedure after successful cardiopulmonary resuscitation-cooling or no more cooling]. *Inn Med (Heidelb)*. (2023). doi: 10.1007/s00108-023-01582-2

frontiers | Frontiers in Cardiovascular Medicine

TYPE Original Research
PUBLISHED 15 January 2025
DOI 10.3389/fcvm.2024.1522789

OPEN ACCESS

EDITED BY
Keita Saku,
National Cerebral and Cardiovascular Center, Japan

REVIEWED BY
Junya Matsuda,
Nippon Medical School, Japan
Naoki Tadokoro,
National Cerebral and Cardiovascular Center, Japan

*CORRESPONDENCE
Yi-qi Jin
jinyiqi2022@163.com

†These authors have contributed equally to this work

RECEIVED 05 November 2024
ACCEPTED 31 December 2024
PUBLISHED 15 January 2025

CITATION
Xu C, Xu G-x, Cao Y-f, Chen L and Jin Y-q (2025) Feasibility of the area reduction post-closure technique for bedside weaning of veno-arterial extracorporeal membrane oxygenation.
Front. Cardiovasc. Med. 11:1522789.
doi: 10.3389/fcvm.2024.1522789

Feasibility of the area reduction post-closure technique for bedside weaning of veno-arterial extracorporeal membrane oxygenation

Chen Xu[1†], Guo-xiong Xu[1†], Yi-fei Cao[2], Lei Chen[1] and Yi-qi Jin[1*]

[1]Department of Vascular and Endovascular Surgery, The Affiliated Suzhou Hospital of Nanjing Medical University, Suzhou, China, [2]Department of Critical Care Medicine, The Affiliated Suzhou Hospital of Nanjing Medical University, Suzhou, China

Objective: To evaluate the safety and efficacy of the area reduction post-closure technique for bedside weaning of veno-arterial extracorporeal membrane oxygenation (V-A ECMO).

Methods: A retrospective study was conducted from December 2022 to November 2023, analyzing data from patients who underwent V-A ECMO weaning at our center. The area reduction post-closure technique, utilizing two ProGlide devices (Abbott Vascular, Santa Clara, CA), was adopted as a standard practice. The technical success was defined as achieving complete hemostasis without a bailout open repair. The complications associated with access included hemorrhagic events, pseudoaneurysm formation, limb ischemia, distal embolization, and wound infections.

Results: A total of 18 patients were included. The median age of the cohort was 72.0 years [interquartile range (IQR), 57.5–81.5 years], with a male-to-female ratio of 2:1. The median size of arterial sheath utilized was 18.0 Fr (IQR, 17.0–20.0 Fr). The median duration of the procedure was 10.0 min (IQR, 9.0–13.0 min), and the median length of total hospital stay was 31.0 days (IQR, 25.5–39.0 days). Furthermore, the technique demonstrated a success rate of 100%. One patient (5.6%) experienced minor bleeding, which was successfully managed through compression. No additional complications associated with access were observed after the procedure.

Conclusions: The post-closure area reduction technique emerges as a viable option for bedside weaning of V-A ECMO. Nonetheless, it is essential that this technique be validated through larger comparative studies.

KEYWORDS

the area reduction post-closure technique, bedside weaning, veno-arterial extracorporeal membrane oxygenation, ProGlide devices, access bleeding

Introduction

The global adoption of percutaneous mechanical circulatory support (MCS) devices has experienced a consistent upward trend over the past decade (1). Veno-arterial extracorporeal membrane oxygenation (V-A ECMO) is primarily utilized for patients exhibiting unstable hemodynamics and significant gas exchange impairments, and it can be rapidly implemented in emergency situations (2–4). However, the large arterial cannula size has raised concerns regarding access-related complications after V-A

ECMO decannulation (5, 6). Compared with the open repair, the percutaneous removal technique utilizing Proglide devices (Abbott Vascular, Santa Clara, California, USA) has demonstrated improved patient comfort and a reduced procedure duration (7).

The pre-closure technique has been widely reported for weaning process of V-A ECMO (8, 9). However, this technique can prolong the time needed for the insertion of V-A ECMO. The presence of indwelling sutures may increase the risk of wound infections and vascular injury, while also enhancing the care requirement. Recent studies have investigated the feasibility of post-closure techniques during V-A ECMO decannulation (10–12). However, the existing data remains limited, and the challenges related to effectively capturing vascular wall tissue within the large arterial cannula hole are concerning. Therefore, this study aimed to evaluate the safety and efficacy of the area reduction post-closure technique for bedside weaning of V-A ECMO.

Methods

Study population

This study involved all patients who underwent bedside weaning of V-A ECMO at our center from December 2022 to November 2023. Patients treated with the area reduction post-closure technique were included. Exclusion criteria included severe vascular calcification, advanced vascular stenosis, coagulation disorders, the need for an open repair approach due to active bleeding or infected access sites, central V-A ECMO, and mortality before decannulation (Figure 1). V-A ECMO was utilized in cases where patients in shock did not demonstrate a favorable response to vasopressor therapy, coupled with the acute cardiopulmonary failure. The institutional committee approved this study including any relevant details, and the informed consent requirement was waived due to the retrospective and anonymous nature of the analysis.

Technique details

The area reduction post-closure technique involves a double-wire approach to deploy two Proglide devices gradually reducing the area of the large arterial cannula hole during weaning process of V-A ECMO at the patient's bedside, therefore achieving complete hemostasis (Figure 2). All procedures were performed by the same team. Two operators were recommended to finish the procedure at least: one performing the percutaneous closure, another performing bedside ultrasound and controlling bleeding. Notably, a large sheath with size up to 12–16 Fr was prepared for standby insertion to control the bleeding in case of

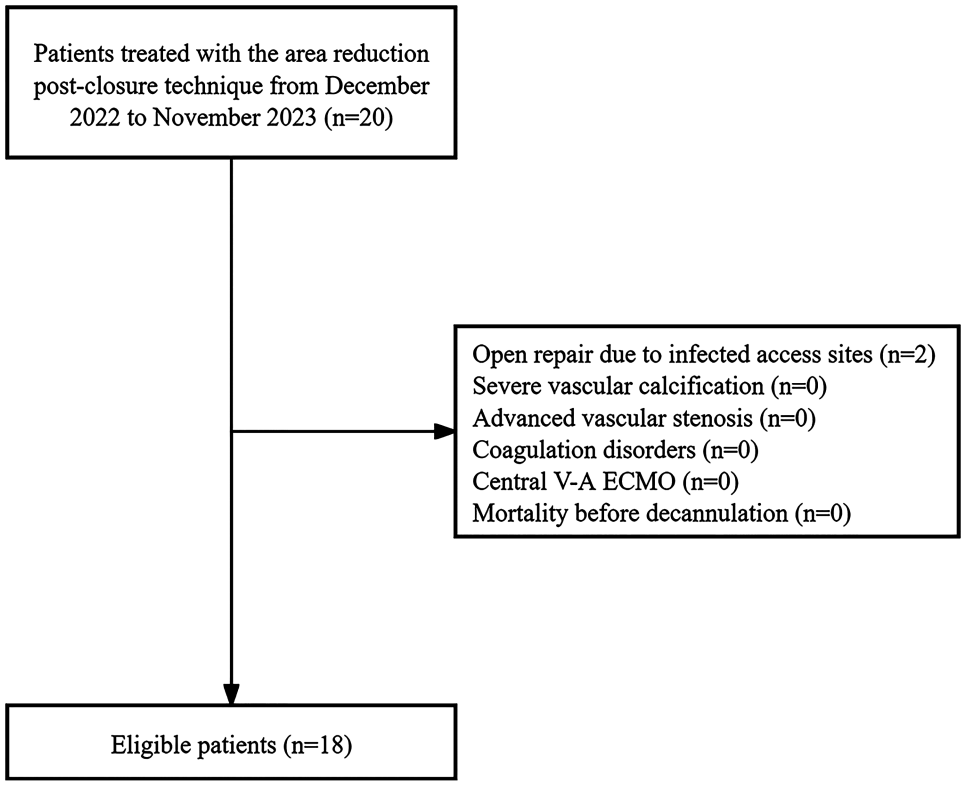

FIGURE 1
The study flowchart.

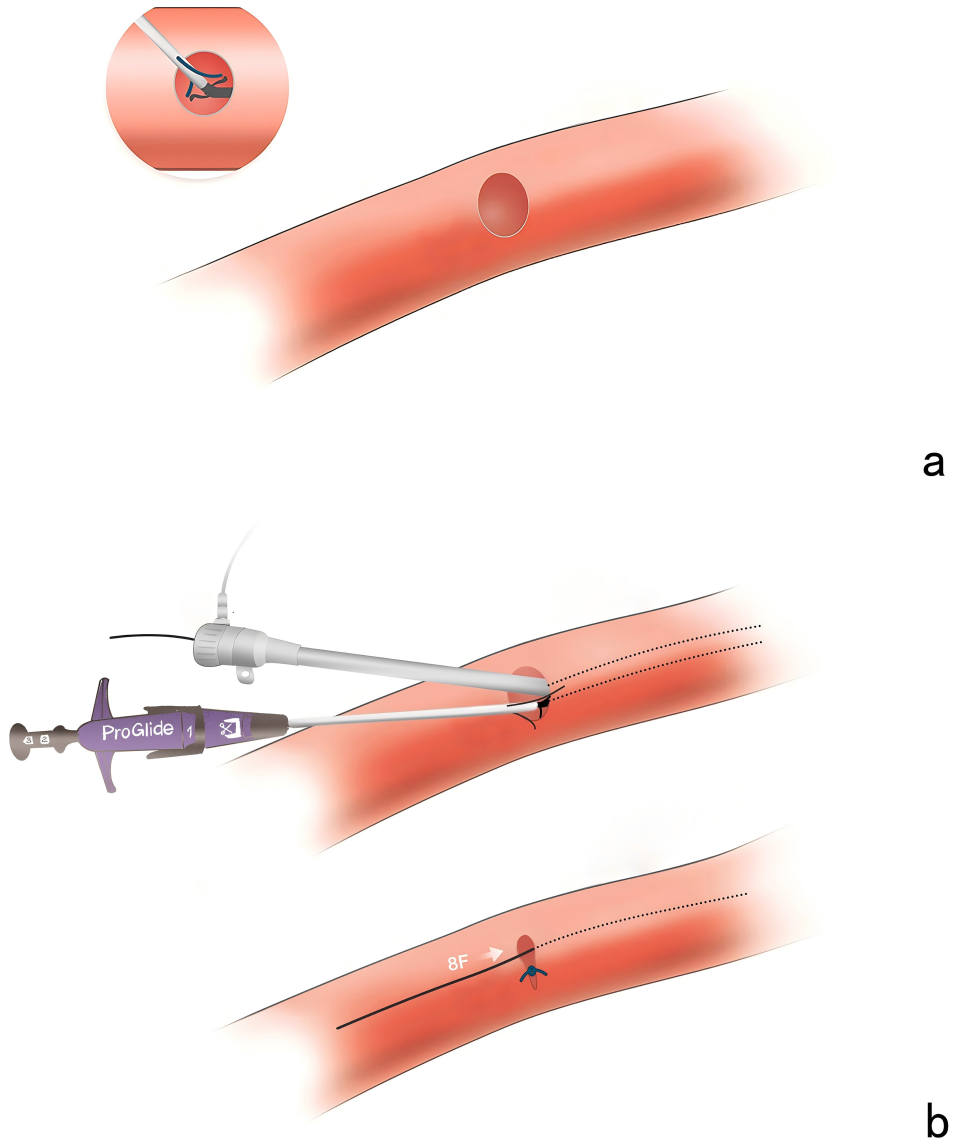

FIGURE 2
The area reduction post-closure technique. **(a)** The inability to capture a sufficient portion of the vascular wall tissue to allow adequate sealing. **(b)** The large arterial cannula hole was shrunk to 8 Fr in diameter after suturing the first Proglide device.

closure failure. During the procedure, it is essential to incorporate volume management strategies alongside the evaluation of the patient's circulatory status and tissue perfusion. It is advisable to meticulously regulate fluid intake, promptly manage any instances of volume overload, sustain a relatively low volume status, diminish both preload and post-load on the heart, reduce venous pressure, improve organ perfusion, and utilize continuous renal replacement therapy when indicated. The administration of heparin was discontinued 30–60 min before decannulation, and a brief monitoring period was required to confirm stable hemodynamic conditions.

Figure 3 illustrates the details of the technique. After disinfection, the arterial cannula was clamped with two forceps (Maquet, Germany, 20 cm), and the V-A ECMO flow was halted as expected. A direct puncture was performed in the proximal section of the arterial cannula with the Seldinger technique. The first guidewire (0.035-inch, Terumo, Tokyo, Japan) was inserted, and an 8 Fr sheath (Terumo, Somerset, NJ) was introduced. The second guidewire was inserted through the 8 Fr sheath. While one operator applied manual compression to the access, the 8 Fr sheath and V-A ECMO arterial cannula were carefully removed, ensuring the guidewire remained in position. The 8 Fr sheath was reintroduced over the first guidewire. The first Proglide device was deployed over the second guidewire at a 10 o'clock angle, and the suturing was carried out to control bleeding. Subsequently, the large arterial cannula hole was shrunk to 8 Fr in diameter. After removing the sheath, the second Proglide device was deployed over the first guidewire at a 2 o'clock angle

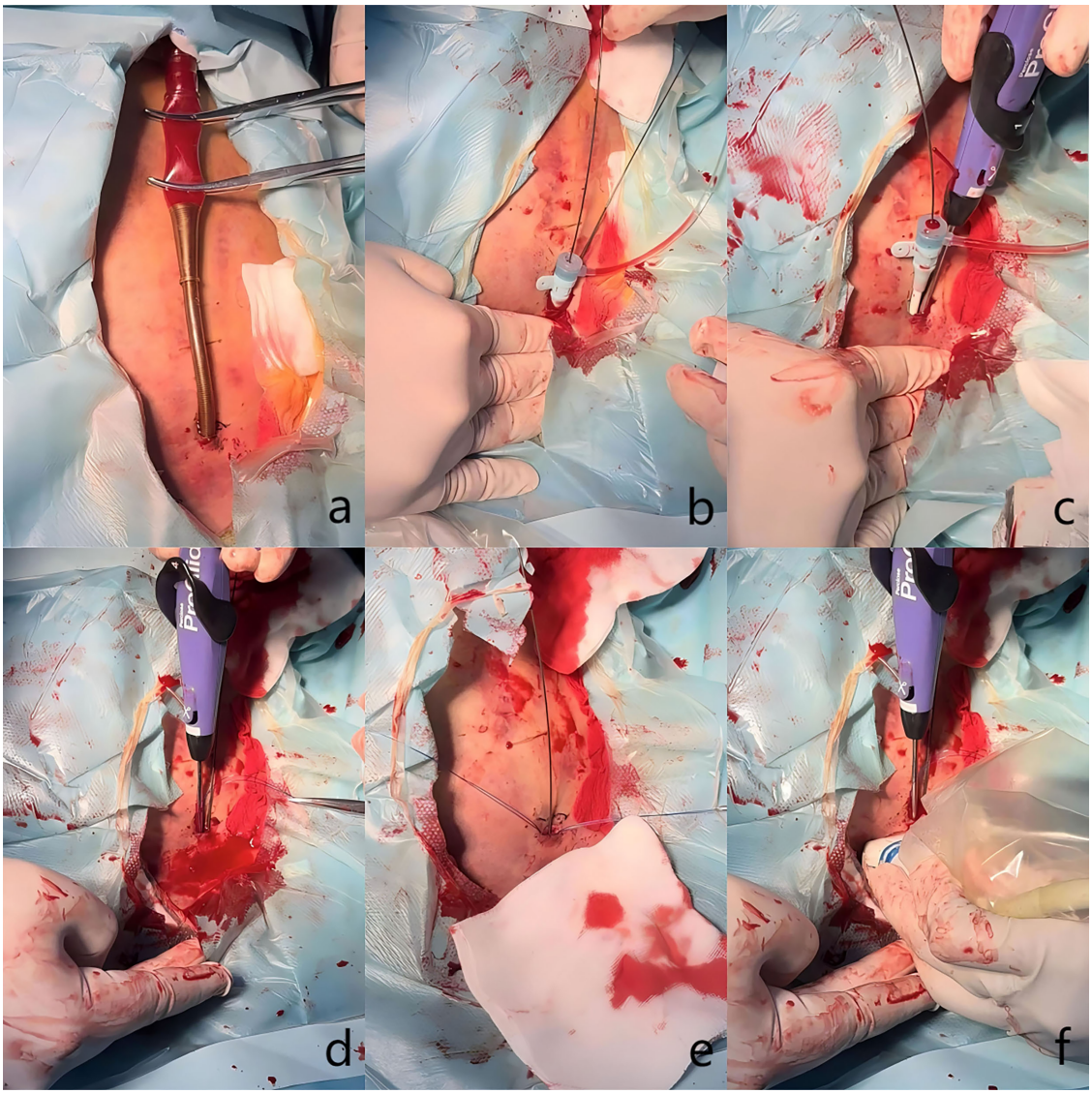

FIGURE 3
Clinical details of the technique. **(a)** The arterial cannula was clamped with two forceps. **(b)** Two guidewires were advanced and an 8 Fr sheath was introduced. **(c)** The first Proglide device was deployed to control bleeding. **(d)** The second Proglide device was deployed to control bleeding. **(e)** Hemostasis was achieved. **(f)** Proper position of the device's foot pedal was confirmed through ultrasound examination.

to achieve further hemostasis. The first guidewire remained in place until complete hemostasis was conformed. If significant bleeding occurs, a third Proglide device will be deployed at a 12 o'clock angle over the safety guidewire. If hemostasis is not achieved after that, the procedure is considered unsuccessful, and a large sheath should be inserted to control bleeding. Emergency open repair should be arranged quickly in the operating room. Notably, an ultrasound examination was utilized at the operator's discretion during the deployment of Proglide device to confirm that the foot pedal are correctly positioned against the vessel wall rather than the adjacent soft tissue (Figure 4).

Finally, the manual compression was performed for several minutes. All access were examined right after the procedure and again 24 h later, utilizing ultrasound to detect any access-related complications.

Definitions and follow-up

The primary outcome was the technical success, which was defined as achieving complete hemostasis without the need for an emergency open repair. The secondary outcome was the access-related complications, including hemorrhagic events, pseudoaneurysm formation, limb ischemia, distal embolization, and wound infections. Minor bleeding encompassed skin bruising and hematomas. Major bleeding was considered as a

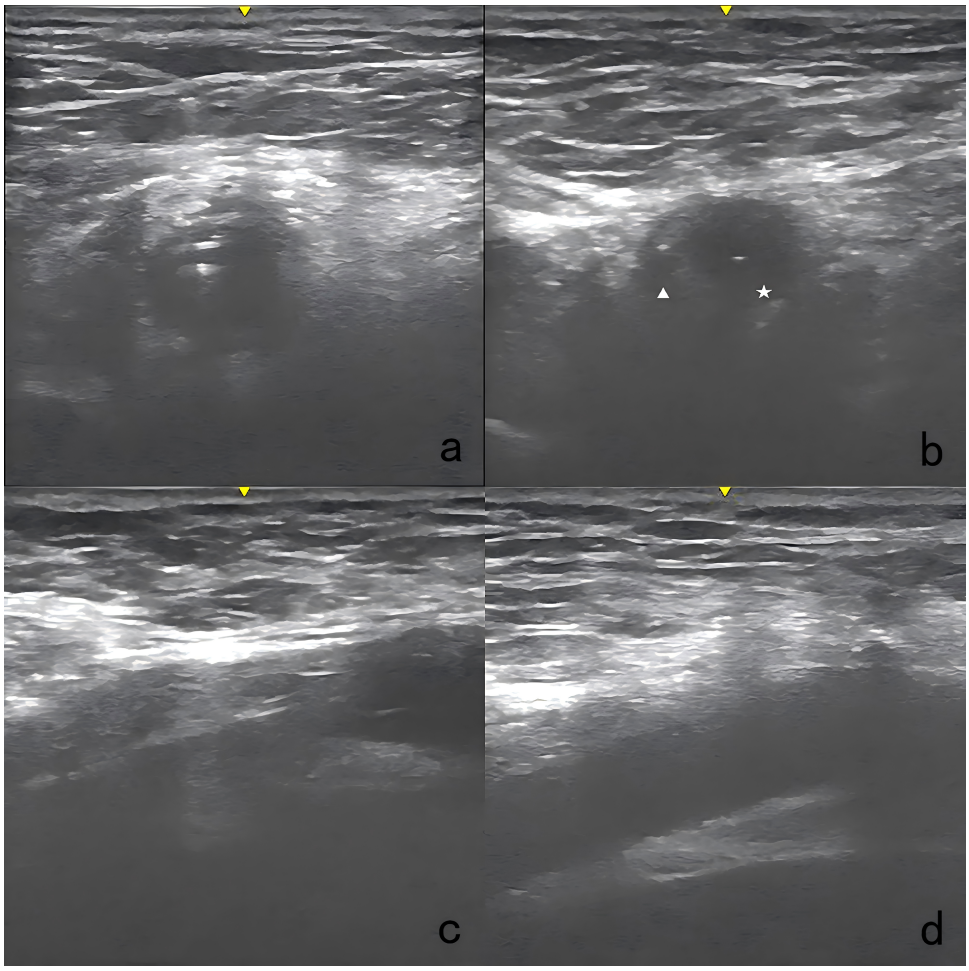

FIGURE 4
Ultrasound images of the technique. **(a)** Two guidewires were advanced in the arterial cannula. **(b)** An 8 Fr sheath was introduced over the first guide wire, positioned parallel to the second guidewire. Pentacle: the 8 Fr sheath; triangle: the remaining vascular lumen. **(c)** The foot pedal of the Proglide device was confirmed to be abutting the vessel wall. **(d)** The access site was examined right after the procedure with ultrasound to detect any potential complications.

significant drop in hemoglobin levels that required a blood transfusion. Furthermore, the additional ues of Proglide device, the duration of the procedure, the duration of V-A ECMO support, the duration of intensive care unit (ICU) stay after weaning, the length of total hospital stay, the need for V-A ECMO reinsertion, and in-hospital mortality were recorded and analyzed. The follow-up ultrasound was utilized before discharge to evaluate any complications related to the access. Detailed clinical data were obtained from the online clinical and standard operative records.

Statistical analysis

The distributed data is presented as the interquartile range (IQR). Categorical data is represented as counts and percentages. Statistical analyses were conducted using SPSS software (version 19.0; SPSS Inc., Chicago, IL, USA).

Results

Baseline characteristics

Two patients required open repair for V-A ECMO decannulation due to infected access sites. Subsequently, 18 patients utilizing the area reduction post-closure technique were included. Table 1 presents the baseline characteristics. The median age of the cohort was 72.0 years (IQR, 57.5–81.5 years), with a male-to-female ratio of 2:1. The median size of arterial sheath utilized was 18.0 Fr (IQR, 17.0–20.0 Fr).

Clinical outcomes

Table 2 presents the clinical outcomes. The technical success rate was 100%. Two patients (11.1%) accepted additional Proglide deployment, with one device utilized for each patients.

TABLE 1 Baseline characteristics ($n = 18$).

Age, years	72.0 (57.5, 81.5)
Sex, male	12 (66.7)
Body mass index, kg/m^2	23.9 (20.9, 29.3)
Comorbidities	
Hypertension	10 (55.6)
Diabetes mellitus	8 (44.4)
Coronary artery disease	8 (44.4)
Chronic kidney disease	4 (22.2)
Current smoking	5 (27.8)
Indication	
Cardiogenic failure	15 (83.3)
Respiratory failure	2 (11.1)
Septic shock	1 (5.6)
Arterial cannula size, Fr	
16	2 (11.1)
17	6 (33.3)
18	4 (22.2)
20	6 (33.3)
Median size of arterial sheathe, Fr	18.0 (17.0, 20.0)
Ipsilateral venous cannula	16 (88.9)
Cardiopulmonary resuscitation at insertion	10 (55.6)
Continuous renal replacement therapy	4 (22.2)
Anticoagulant treatment	18 (100.0)
Antiplatelet treatment	
SAPT	3 (16.7)
DAPT	8 (44.4)
Previous open repair or vascular closure device use	8 (44.4)

INR, International normalized ratio; SAPT, single antiplatelet therapy; DAPT, dual antiplatelet therapy.
Values are median with interquartile ranges (IQR) or number (%).

TABLE 2 Clinical outcomes ($n = 18$).

Technical success	100%
Additional use of Proglide device	2 (11.1)
Access-related complications	
Minor bleeding	1 (5.6)
Major bleeding	0
Other	0
Duration of procedure, min	10.0 (9.0, 13.0)
Duration of V-A ECMO support, days	7.0 (6.0, 9.5)
Duration of ICU stay after weaning, days	15.0 (13.0, 19.5)
Length of hospital stay, days	31.0 (25.5, 39.0)
Need for ECMO reinsertion	0
In-hospital mortality	3 (16.7)

V-A ECMO, veno-arterial extracorporeal membrane oxygenation; ICU, intensive care unit.
Values are median with interquartile ranges (IQR) or number (%).

One patient experienced (5.6%) minor bleeding that was successfully managed with manual compression, and there were no other access-related complications during the study period. The total access-related complication rate was 5.6%. Furthermore, the median duration of the procedure was 10.0 min (IQR, 9.0–13.0 min). No instances of V-A ECMO reinsertion were observed, and the in-hospital mortality rate was recorded at 16.7%.

Discussion

This single-center study evaluated the safety and efficacy of the area reduction post-closure technique for bedside weaning of V-A ECMO. The initial results indicated that the technical success rate was 100%, and the total access-related complication rate was 5.6%. Overall, this technique was a feasible and safe strategy and may be considered as a viable option.

The Proglide-assisted pre-closure technique has gained considerable attention and application for weaning process of V-A ECMO (8, 9). However, this technique may not be applicable to all cases of V-A ECMO, particularly in urgent situations such as cardiac arrest or cardiogenic shock, where the timely insertion is critical. Furthermore, the large arterial cannula system is typically not removed immediately, which may elevate the risk of wound infections and vascular injury, while also increase the care requirement. Recently, Hwang et al. (7) have reported a standard post-closure technique utilizing two Proglide devices. Their findings indicate that post-closure removal is not inferior to surgical removal in terms of the procedural outcomes and complications. A significant distinction between their technique and the area reduction technique lies in the size of the cannula utilized. The present study predominantly utilizes the 20 Fr cannulas. Theoretically, there is a concern of the capacity to obtain an adequate segment of the vascular wall tissue directly through a single Proglide in a large arterial cannula hole, which may hinder effective sealing. Hayakawa et al. (10) have described a post-closure technique that involves access to the contralateral femoral artery. This technique requires inserting and inflating a balloon while deploying two Proglide devices to achieve hemostasis. However, the contralateral femoral access and additional balloon insertion may increase the technical complexity.

This study presents the area reduction post-closure technique for the bedside weaning of V-A ECMO. The area was significantly reduced through the advancement of an 8 Fr sheath, which facilitated the effective deployment of the first Proglide device. Subsequently, the closure of the remaining 8 Fr hole can be achieved through the second Proglide device. Notably, the potential applicability of this technique to larger cannula sizes would further evaluate its advantages in comparison to the standard post-closure method. Furthermore, the access-related complication rate was 5.6%, aligning with conventional pre-closure studies that reported ranging from 4.8% to 28.6% (8, 9, 13).

In this study, an 8 Fr sheath was routinely utilized to reduce the cross-sectional area of the large cannula. However, it is conceivable that the application of an 8 Fr sheath may not completely preclude the placement of a ProGlide device at the center. In cases where larger cannula sizes are employed, such as a 24 Fr cannula, a sheath size ranging from 10 to 12 Fr may be required. Further studies is warranted to determine whether the cannula size for ECMO affects the appropriate sheath size. Additionally, the lack of fluoroscopy can be considered as a disadvantage that affects the technical reliability. However, there are advantages to weaning patients from V-A ECMO at the bedside. Firstly, it reduces the risk of complications that can arise during the transport of critically ill patients, which often involves moving a

large amount of equipment and infusion lines, making the process more complex. Secondly, it can be performed at any time without the need for prior coordination with surgical team, allowing for a more prompt procedure for the patient. Further studies are need to evaluate the safety and efficacy of beside decannulation compared to that performed in the operating room under fluoroscopy.

This study is subject to several limitations, notably its relatively small sample size and its single-center design. It is important to highlight that the lack of a comparison group may affect the reliability of the results. Furthermore, patients deemed suitable for an open repair, such as those requiring infection debridement, hemostasis, or embolectomy were excluded from the study. This exclusion effectively restricts the study population to patients with lower risk profiles, where the effectiveness of percutaneous vascular closure devices (VCDs) is expected to be greater. Overall, there is a need for larger prospective studies that include an appropriate comparison group.

Conclusion

The area reduction post-closure technique was a feasible and safe strategy for bedside weaning of V-A ECMO, and may be considered as a viable option.

Data availability statement

The raw data supporting the conclusions of this article will be made available by the authors, without undue reservation.

Ethics statement

The studies involving humans were approved by The Ethics Committee of Suzhou Hospital Affiliated to Nanjing Medical University. The studies were conducted in accordance with the local legislation and institutional requirements. Written informed consent for participation was not required from the participants or the participants' legal guardians/next of kin in accordance with the national legislation and institutional requirements.

Author contributions

CX: Data curation, Writing – original draft. GX: Data curation, Methodology, Writing – review & editing. YC: Formal Analysis, Project administration, Resources, Writing – review & editing. LC: Resources, Supervision, Validation, Writing – review & editing. YJ: Conceptualization, Project administration, Resources, Supervision, Writing – review & editing.

Funding

The author(s) declare that no financial support was received for the research, authorship, and/or publication of this article.

Conflict of interest

The authors declare that the research was conducted in the absence of any commercial or financial relationships that could be construed as a potential conflict of interest.

Generative AI statement

The author(s) declare that no Generative AI was used in the creation of this manuscript.

Publisher's note

Supplementary material

The Supplementary Material for this article can be found online at: https://www.frontiersin.org/articles/10.3389/fcvm.2024.1522789/full#supplementary-material

References

1. Stretch R, Sauer CM, Yuh DD, Bonde P. National trends in the utilization of short-term mechanical circulatory support: incidence, outcomes, and cost analysis. *J Am Coll Cardiol.* (2014) 64(14):1407–15. doi: 10.1016/j.jacc.2014.07.958

2. Ganslmeier P, Philipp A, Rupprecht L, Diez C, Arlt M, Mueller T, et al. Percutaneous cannulation for extracorporeal life support. *Thorac Cardiovasc Surg.* (2011) 59:103–7. doi: 10.1055/s-0030-1250635

3. JhandA, Shabbir MA, Um J, Velagapudi P. Veno-arterial extracorporeal membrane oxygenation for cardiogenic shock. *J Vis Exp.* (2023) (199):e62052. doi: 10.3791/62052

4. Broman LM, Taccone FS, Lorusso R, Malfertheiner MV, Pappalardo F, Di Nardo M, et al. The ELSO Maastricht treaty for ECLS nomenclature: abbreviations for cannulation configuration in extracorporeal life support—a position paper of the extracorporeal life support organization. *Crit Care.* (2019) 23(1):36. doi: 10.1186/s13054-019-2334-8

5. Singh V, Singh G, Arya RC, Kapoor S, Garg A, Ralhan S, et al. Vascular access complications in patients undergoing veno-arterial ecmo and their impact on survival in patients with refractory cardiogenic shock: a retrospective 8-year study. *Ann Card Anaesth.* (2022) 25(2):171–7. doi: 10.4103/aca.aca_22_22

6. Laimoud M, Saad E, Koussayer S. Acute vascular complications of femoral veno-arterial ECMO: a single-centre retrospective study. *Egypt Heart J*. (2021) 73(1):15. doi: 10.1186/s43044-021-00143-y

7. Hwang JW, Yang JH, Sung K, Song YB, Hahn JY, Choi JH, et al. Percutaneous removal using Perclose ProGlide closure devices versus surgical removal for weaning after percutaneous cannulation for venoarterial extracorporeal membrane oxygenation. *J Vasc Surg*. (2016) 63(4):998–1003.e1. doi: 10.1016/j.jvs.2015.10.067

8. Chandel A, Desai M, Ryan LP, Clevenger L, Speir AM, Singh R. Preclosure technique versus arterial cutdown after percutaneous cannulation for venoarterial extracorporeal membrane oxygenation. *JTCVS Tech*. (2021) 10:322–30. doi: 10.1016/j.xjtc.2021.08.030

9. Xu X, Liu Z, Han P, He M, Xu Y, Yin L, et al. Feasibility and safety of total percutaneous closure of femoral arterial access sites after veno-arterial extracorporeal membrane oxygenation. *Medicine (Baltimore)*. (2019) 98(45):e17910. doi: 10.1097/MD.0000000000017910

10. Hayakawa N, Tobita K, Kodera S, Ishibashi N, Kasai Y, Arakawa M, et al. An effective method for percutaneous removal of venoarterial extracorporeal membrane oxygenation by a combination of balloon dilatation in endovascular therapy and the perclose proglide closure device. *Ann Vasc Surg*. (2021) 73:532–7. doi: 10.1016/j.avsg.2020.12.028

11. Tian L, Zhang L, Zhang N, Xu X, Xu Y, Liu Z, et al. Case report: total percutaneous post-closure of femoral arterial access sites after veno-arterial extracorporeal membrane oxygenation. *Front Med*. (2022) 9:980122. doi: 10.3389/fmed.2022.980122

12. Au SY, Chan KS, Fong KM, Leung PWR, George Ng WY, Leung KHA. Bedside decannulation of peripheral V-A ECMO using percutaneous perclose ProGlide post-close technique. *J Emerg Crit Care Med*. (2020) 4:4. doi: 10.21037/jeccm.2019.09.08

13. Liu Z, Xu Y, Xu X, He M, Han P, Shao C, et al. Comparison of success rate and complications of totally percutaneous decannulation in patients with veno-arterial extracorporeal membrane oxygenation and endovascular aneurysm repair. *Front Med*. (2021) 8:72442. doi: 10.3389/fmed.2021.724427

frontiers | Frontiers in Cardiovascular Medicine

TYPE Brief Research Report
PUBLISHED 16 January 2025
DOI 10.3389/fcvm.2024.1509162

OPEN ACCESS

EDITED BY
Takahiro Nakashima,
University of Michigan, United States

REVIEWED BY
Luca Baldetti,
Cardiac Intensive Care Unit (Cardiovascular Department), San Raffaele Scientific Institute (IRCCS), Italy
Masahiro Yamamoto,
Kumamoto University, Japan

*CORRESPONDENCE
Marina Pieri
pieri.marina@hsr.it

RECEIVED 10 October 2024
ACCEPTED 27 December 2024
PUBLISHED 16 January 2025

CITATION
Pieri M, Iannaccone M, Burzotta F, Botti G, Aurigemma C, Trani C, Ajello S, Altizio S, Sanna T, Romagnoli E, Paraggio L, Cappannoli L, Scandroglio AM and Chieffo A (2025) Can a mechanical circulatory support comprehensive approach to cardiogenic shock at referral centers reduce 30-day mortality?
Front. Cardiovasc. Med. 11:1509162.
doi: 10.3389/fcvm.2024.1509162

Can a mechanical circulatory support comprehensive approach to cardiogenic shock at referral centers reduce 30-day mortality?

Marina Pieri[1,2]*, Mario Iannaccone[3], Francesco Burzotta[4,5], Giulia Botti[2,6], Cristina Aurigemma[7], Carlo Trani[4,5], Silvia Ajello[1], Savino Altizio[1], Tommaso Sanna[4,5], Enrico Romagnoli[5], Lazzaro Paraggio[5], Luigi Cappannoli[5], Anna Mara Scandroglio[1] and Alaide Chieffo[2,6]

[1]Department of Anesthesia and Intensive Care, IRCCS San Raffaele Scientific Institute, Milan, Italy, [2]School of Medicine, Vita-Salute San Raffaele University, Milan, Italy, [3]Department of Cardiology, San Giovanni Bosco Hospital, ASL Città di Torino, Turin, Italy, [4]School of Medicine, Università Cattolica del Sacro Cuore, Rome, Italy, [5]Department of Cardiovascular Sciences, Fondazione Policlinico Universitario Agostino Gemelli IRCCS, Università Cattolica del Sacro Cuore, Rome, Italy, [6]Interventional Cardiology Unit, IRCCS San Raffaele Scientific Institute, Milan, Italy, [7]Dipartimento CUORE, Fondazione Policlinico Univeristario A. Gemelli IRCCS Roma, Rome, Italy

Although mortality risk prediction in cardiogenic shock (CS) is possible, assessing the impact of the multitude of therapeutic efforts on outcomes is not straightforward. We assessed whether a temporary mechanical circulatory support comprehensive approach to the treatment of CS may reduce 30-day mortality as compared to expected mortality predicted by the recently proposed Cardiogenic Shock Score (CSS). Consecutive CS patients supported by pVAD Impella (Abiomed, Danvers, MA) at two national referral centers were included. 170 patients were included: age was 65 ± 13 years, and 75.9% were male and acute myocardial infarction was the prevalent cause of shock (71.1%). Expected mortality according to CSS was higher than observed (51.8% vs. 41.5%, $p < 0.001$), this trend being particularly evident for CSS > 4. The AUC ROC curve confirmed poor diagnostic accuracy in this population (AUC 0.53 CI: 0.23–0.82, $p = 0.83$). The lower observed mortality compared to the expected mortality in critical cardiogenic shock population underscores the role of a comprehensive approach to acute cardiac care patients at referral centers, which should consider including temporary mechanical circulatory support.

KEYWORDS

cardiogenic shock, mortality, risk score, mechanical circulatory support, Impella, inotropes

Introduction

Despite significant advancements in the treatment of cardiogenic shock (CS), including mechanical circulatory support, its mortality has remained high (1). Therefore, the stratification of patients' mortality risk is of great clinical interest to guarantee to each patient the most appropriate type and timing of treatments (2). Recently, the novel Cardiogenic Shock Score (CSS) has emerged as a powerful and easily implemented tool (3) to predict the outcome of patients irrespective of the cause of CS and the type of treatment received, showing superior predictive ability compared to established scores (4, 5). Although CS outcome prediction is possible, assessing the

10.3389/fcvm.2024.1509162

impact of the multitude of therapeutic efforts on outcomes remains challenging in critically ill patients.

The present study aimed to assess whether a mechanical circulatory support comprehensive approach to the treatment of CS with percutaneous ventricular assist devices (pVAD) may reduce 30-day mortality compared to the expected mortality predicted by the recently proposed CSS.

Methods

Consecutive patients with CS (6) treated with Impella 2.5, Impella CP, Impella 5.0, or Impella RP in IRCCS San Raffaele Scientific Institute, Milan, Italy and Institute of Cardiology and Fondazione Policlinico Universitario A. Gemelli IRCCS, Rome; Italy from 2013 to 2018 were included. Briefly, data related to medical history, procedural characteristics, 30-day and one-year outcomes were collected from each centre and included in a pre-specified structured data set. Adverse events were then adjudicated by two independent cardiologists using source documents provided by each center. The collection of data at each participating site was performed according to the policies of the local institutional review board/ethics committee.

The primary objective of the study was to assess the effect of a comprehensive approach to cardiogenic shock at referral centers, encompassing temporary mechanical circulatory support (tMCS), on 30-day mortality risk, as assessed by the novel CSS. In addition, the composite of all-cause death, rehospitalization for heart failure, left ventricle assist device implantation, or heart transplantation (HT), overall referred to as major adverse cardiac events (MACE) was evaluated at 1 year.

Categorical variables are reported as counts and percentages, whereas continuous variables as mean and standard deviation or median and interquartile range (IQR). Gaussian or non-Gaussian distribution was evaluated with the Kolmogorov-Smirnov test. The *t*-test was used to assess differences between normally distributed continuous variables, paired or unpaired according to the tested variable, the Mann-Whitney *U* test for non-Gaussian variables, the χ^2 test for categorical variables (expected vs. observed mortality), and Fisher exact test for 2×2 tables. The distribution of the population and predicted and observed mortality within risk categories were calculated and evaluated by XY correlation.

The discriminative ability of the risk prediction model was assessed by the area under the receiver operating characteristic (ROC) curve (AUC) or c-statistic. A two-sided *p*-value <0.05 was regarded as statistically significant. Analyses were performed with SPSS® Statistics v24 and STATA v17 (StataCorp, College Station, Texas).

TABLE 1 Patients' characteristics.

Parameter	Value
Baseline characteristics	
Age, years	65.3 ± 13.0
Male gender, *n*	129 (75.9)
BMI	26.2 ± 4.6
Smoking, *n*	68 (40.0)
Hypertension, *n*	76 (44.7)
Dyslipidemia, *n*	62 (36.5)
Diabetes Mellitus, *n*	47 (27.6)
Prior Myocardial infarction, *n*	52 (30.6)
Prior TIA or Stroke, *n*	9 (5.3)
Prior PCI, *n*	54 (31.8)
Prior CABG, *n*	9 (5.3)
PAD, *n*	21 (12.4)
Chronic heart failure, *n*	45 (26.5)
Atrial fibrillation, *n*	16 (9.4)
Chronic Kidney Disease, *n*	33 (19.4)
Baseline Lactates, mmol/L	6.6 ± 5.4
Lactates >2 mmol/L, *n*	106 (62.4)
Baseline Creatinine, mg/dl	1.6 ± 1.3
Baseline Haemoglobin, g/dl	12.2 ± 2.3
Glucose level at presentation, mg/dl	215.3 ± 91.8
Ejection Fraction, %	23.7 ± 12.1
Heart Rate, bpm	95 ± 25
MAP, mmHg	64.9 ± 19.9
Inotropic therapy, *n*	131 (77.1)
>1 inotrope, *n*	101 (59.4)
Mechanical Ventilation, *n*	132 (77.6)
Etiology of Cardiogenic Shock	
STEMI, *n*	90 (52.9)
NSTEMI, *n*	31 (18.2)
Acute Myocarditis, *n*	10 (5.8)
VT Ablation, *n*	9 (5.3)
Other, n	30 (17.8)
Other MCS support	
IABP, *n*	66 (38.8)
ECMO, *n*	58 (34.1)
Treatment Escalation	
ECMO, *n*	24 (14.1)
VAD, *n*	10 (5.8)
Heart Transplantation, *n*	2 (1.2)
ECMO + VAD, *n*	5 (2.9)
ECMO + VAD + Heart Transplantation, *n*	3 (1.8)
CCS Score	
≤4	44 (25.8)
5–8	81 (47.6)
≥9	45 (26.5)

Values are expressed as number (percentage) or mean ± standard deviation.
BMI, body mass index; TIA, transient ischemic attack; PCI, percutaneous coronary intervention; CABG, coronary artery bypass graft; PAD, peripheral artery disease; MAP, mean arterial pressure; OHCA, out-of-hospital cardiac arrest; CPR, cardiopulmonary resuscitation; STEMI, ST-elevation myocardial infarction; NSTEMI, non-ST-Elevation myocardial infarction; VT, ventricular tachycardia; IABP, intra-aortic balloon pump; ECMO, extracorporeal membrane oxygenator; VAD, ventricular assist device.

Results

One hundred and seventy patients were included in the analysis: the mean age was 65 ± 13 years, and 75.9% were male. Patients' characteristics are shown in Table 1. Acute myocardial infarction was the prevalent cause of shock, accounting for 71.1% of cases. Mean arterial pressure at presentation at implantation was 64.9 ± 19.9 mmHg, mean heart rate was 95 ± 25 bpm. Mean lactates were 6.6 ± 5.4 mg/dl, mean baseline creatinine was 1.6 ± 1.3 mg/dl and mean blood glucose was 215.3 ± 91.8 mg/dl.

The prevalent etiology of CS was ischemic due to acute ST-elevation myocardial infarction 52.9%; 24.7% of the patients experienced out-of-hospital cardiac arrest and 77.6% required mechanical ventilation. Pharmacological support with catecholamines was needed in 77.1% of patients. Cardiopulmonary resuscitation (CPR) was rapidly effective (<30 min) in 20% of patients, whereas 6% required extensive CPR (>30 min) and 14.7% experienced refractory cardiac arrest. Mean duration of Impella support was 96 ± 154 h, 34.1% of patients were previously or concomitantly supported with veno-arterial extracorporeal membrane oxygenation (VA ECMO), 38.8% patients received intra-aortic balloon pump before Impella support, and 59.4% were treated with more than 1 inotrope. The most used device was Impella 2.5, in 66.5% of cases. After the implantation of the Impella device, escalation of mechanical circulatory support or heart transplantation was performed in one quarter of patients (24 patients were upgraded to VA ECMO support, 10 patients eventually received a durable left ventricular assist device, 2 patients underwent cardiac transplantation, and 8 patients required a combination of advanced support techniques).

Regarding the calculation of the CCS score, the population was distributed as follows: 25.8% of the patients had a CSS ≤ 4, 47.6% scored between 5 and 8, and 26.5% of patients scored ≥ 9. Expected 30-day mortality according to CSS was higher than observed (51.8% vs. 41.5%, $p < 0.001$—Figure 1A), this trend being particularly evident for score values > 4 (Figure 1B). The AUC ROC curve confirmed poor diagnostic accuracy in this population (AUC 0.53 CI: 0.23–0.82, $p = 0.83$).

Discussion

Our findings draw attention on the relevance of the approach to CS by clinicians and the need to quantify the impact of the implemented therapeutic efforts on mortality risk. The principal finding of our study was that we observed a statistically significant reduction of recorded mortality compared to what was expected according to CSS. Such results in the authors' opinion should be ascribed to the following elements: patients were treated at national referral centers for CS; management of CS patients oversaw a multidisciplinary shock team; a comprehensive approach to CS with tMCS support was adopted. Our findings are in line with existing literature showing improved outcomes in high-volume shock centers (7, 8), where patients are treated according to dedicated shock protocols and shock teams (9), and with a robust MCS program in place (10). With reference to MCS therapy, on one hand the association of hospital volume with outcome is not a new finding (11, 12), given that in the present year for the first time a randomized controlled trial has also shown significant survival benefits in a population of acute myocardial infarction CS patients treated with microaxial flow pumps (13) compared to standard therapy, further corroborating our findings. On top of this, our study presented an innovative approach (i.e., comparing observed vs. expected mortality risk with a robust statical analysis) that may help to document and quantify the impact on major clinical outcomes in a context of lack or biased randomized control trial due to logistic and ethical reasons. The choice of CSS among the multiple existing mortality risk prediction in CS (above all IABP-SHOCK II and CardShock

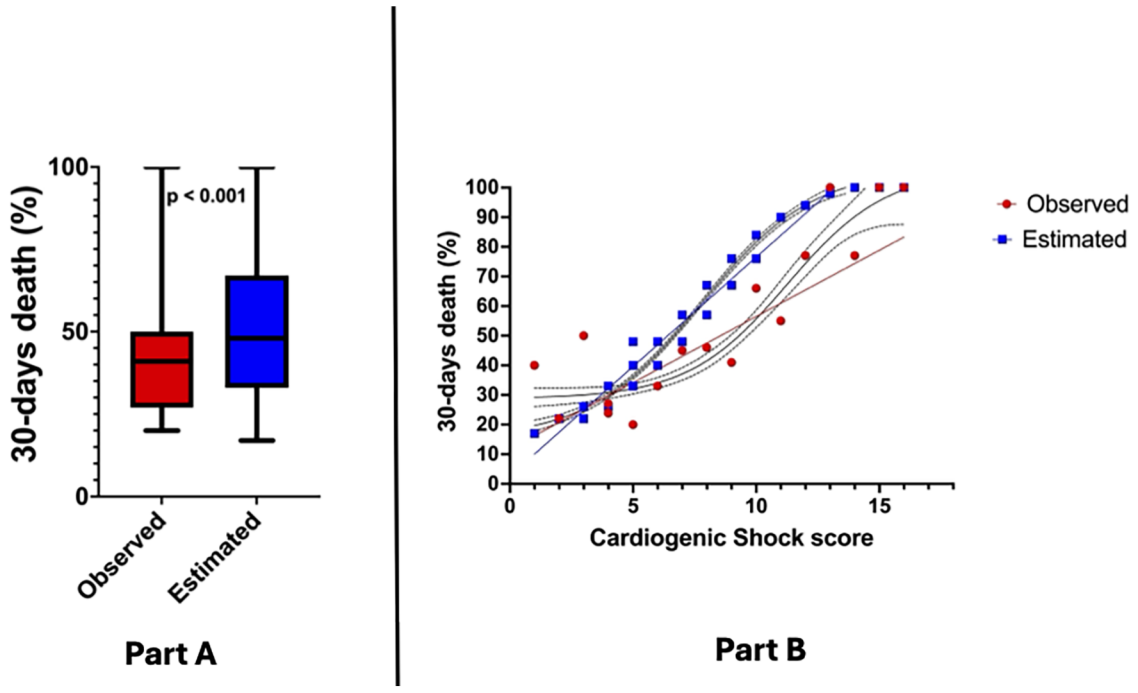

FIGURE 1
(Part A) Observed vs. expected 30-day mortality in study population; (Part B) association between cardiogenic shock score and 30-day mortality.

risk scores (4, 5) was dictated by several considerations. First, CSS was developed and validated in large populations of patients compared to the other two scores. Furthemore, CSS was developed on a mixed population of CS with a 1:1 ratio between AMI related and non ischemic CS: this makes the CSS particularly valid to test mortality risk in all real clinical life CS patients. Although the majority of the patients of the present study had AMI related CS, making them suitable also for mortality risk prediction with CardShock score (developed in a population with >80% AMI CS incidence) (5) and IABP-SHOCK II (developed only in AMI CS patients) (4), we favoured CSS because he shows superior predictive ability when directly compared to IABP-SHOCK II and CardShock scores (3). Finally, CSS includes simple, quick and easy-to-collect at bedside parameters: since it does not require coronary angiography data, it can be calculated immediately upon patient admission, thus providing prompt information that may guide early clinical management of critically ill patients. It would also be relevant from a clinical point of view to assess wether the reduction in mortality observed in the present study is confirmed also with different strategies of MCS, including VA ECMO and IABP. While literature comparing different MCS approaches in CS is growing (14, 15), it is difficult to identify large homogenous patients'population for comparison and the present study itself was not powered to assess this outcome. We also acknowledge the limitations of our approach, that might have influenced the results, especially the limited sample size, the bicentric rather then multicentric approach and the lack of a comparison group not receiving MCS. Indeed, since all patients received mAFP support, discriminating if the survival benefit was due to MCS, to the referral center or to the team is not straightforward. Furthermore, we are aware that the complexity of critically ill CS patients is only partially captured by a score, even if the most valid available, and that this may at least partially affect results. Finally, in the era of DangerShock Trial, we have learnt that complications in MCS patients are frequent, with possible negative implications on outcomes (13). The burden of complications in MCS patients therefore makes the applicability of predictive models more complex.

In conclusion, the main result of this multicenter study was that the mortality rate observed in a population of critically ill CS patients admitted to national referral centers for CS with a dedicated multidisciplinary shock team using a comprehensive approach to the treatment of CS, encompassing temporary mechanical circulatory support with pVAD, was lower than expected according to the CSS, a well-established prognostic score in this field.

Data availability statement

As per institutional policy dataset will be made available upon motivated request to the corresponding author. Requests to access these datasets should be directed to pieri.marina@hsr.it.

Ethics statement

Ethical approval was not required for the studies involving humans because fully anonymized data was already collected institutional registries were used to perform this study. The studies were conducted in accordance with the local legislation and institutional requirements. The participants provided their written informed consent to participate in this study. Written informed consent was not obtained from the individual(s) for the publication of any potentially identifiable images or data included in this article due to the retrospective collection of fully anonymized data.

Author contributions

MP: Conceptualization, Data curation, Formal Analysis, Methodology, Validation, Visualization, Writing – original draft, Writing – review & editing. MI: Formal Analysis, Methodology, Resources, Software, Visualization, Writing – original draft, Writing – review & editing. FB: Data curation, Validation, Visualization, Writing – review & editing. GB: Validation, Visualization, Writing – review & editing, Data curation, Formal Analysis, Writing – original draft. CA: Investigation, Supervision, Visualization, Writing – review & editing, Validation. CT: Data curation, Investigation, Supervision, Visualization, Writing – review & editing, Methodology. SiA: Data curation, Supervision, Visualization, Writing – review & editing, Conceptualization, Investigation, Writing – original draft. SaA: Data curation, Supervision, Validation, Visualization, Writing – review & editing, Methodology. TS: Data curation, Validation, Visualization, Writing – review & editing, Supervision. ER: Validation, Visualization, Writing – review & editing, Data curation, Investigation, Project administration. LP: Validation, Visualization, Writing – review & editing, Software, Supervision. LC: Conceptualization, Data curation, Investigation, Validation, Visualization, Writing – review & editing. AS: Investigation, Resources, Validation, Visualization, Writing – original draft, Writing – review & editing, Conceptualization, Data curation. AC: Formal Analysis, Validation, Visualization, Writing – original draft, Writing – review & editing, Investigation, Methodology, Project administration, Resources, Supervision.

Funding

The author(s) declare financial support was received for the research, authorship, and/or publication of this article. We thank Abiomed Europe GmbH for providing economic support for publication (payment of journal APC).

Conflict of interest

The authors declare that the research was conducted in the absence of any commercial or financial relationships that could be construed as a potential conflict of interest.

The reviewer LB declared a shared affiliation with the authors MP, GB, SA, SA, AMS and AC to the handling editor at the time of review.

Generative AI statement

The author(s) declare that no Generative AI was used in the creation of this manuscript.

Publisher's note

References

1. Tehrani BN, Truesdell AG, Psotka MA, Rosner C, Singh R, Sinha SS, et al. A standardized and comprehensive approach to the management of cardiogenic shock. *JACC Heart Fail.* (2020) 8(11):879–91. doi: 10.1016/j.jchf.2020.09.005

2. Kapur NK, Kanwar M, Sinha SS, Thayer KL, Garan AR, Hernandez-Montfort J, et al. Criteria for defining stages of cardiogenic shock severity. *J Am Coll Cardiol.* (2022) 80(3):185–98. doi: 10.1016/j.jacc.2022.04.049

3. Beer BN, Jentzer JC, Weimann J, Dabboura S, Yan I, Sundermeyer J, et al. Early risk stratification in patients with cardiogenic shock irrespective of the underlying cause—the cardiogenic shock score. *Eur J Heart Fail.* (2022) 24(4):657–67. doi: 10.1002/ejhf.2449

4. Pöss J, Köster J, Fuernau G, Eitel I, de Waha S, Ouarrak T, et al. Risk stratification for patients in cardiogenic shock after acute myocardial infarction. *J Am Coll Cardiol.* (2017) 69:1913–20; 22. doi: 10.1016/j.jacc.2017.02.027

5. Harjola VP, Lassus J, Sionis A, Køber L, Tarvasmäki T, Spinar J, et al. Clinical picture and risk prediction of short-term mortality in cardiogenic shock. *Eur J Heart Fail.* (2015) 17:501–9. doi: 10.1002/ejhf.260

6. Naidu SS, Baran DA, Jentzer JC, Hollenberg SM, van Diepen S, Basir MB, et al. SCAI SHOCK stage classification expert consensus update: a review and incorporation of validation studies: this statement was endorsed by the American college of cardiology (ACC), American college of emergency physicians (ACEP), American heart association (AHA), European society of cardiology (ESC) association for acute cardiovascular care (ACVC), international society for heart and lung transplantation (ISHLT), society of critical care medicine (SCCM), and society of thoracic surgeons (STS) in December 2021. *J Am Coll Cardiol.* (2022) 79(9):933–46. doi: 10.1016/j.jacc.2022.01.018

7. Vallabhajosyula S, Dunlay SM, Barsness GW, Rihal CS, Holmes DR Jr., Prasad A. Hospital-level disparities in the outcomes of acute myocardial infarction with cardiogenic shock. *Am J Cardiol.* (2019) 124(4):491–8. doi: 10.1016/j.amjcard.2019.05.038

8. Chieffo A, Ancona MB, Burzotta F, Pazzanese V, Briguori C, Trani C, et al. Observational multicentre registry of patients treated with IMPella mechanical circulatory support device in ITaly: the IMP-IT registry. *EuroIntervention.* (2020) 15(15):e1343–50. doi: 10.4244/EIJ-D-19-00428

9. Tehrani BN, Truesdell AG, Sherwood MW, Desai S, Tran HA, Epps KC, et al. Standardized team- based care for cardiogenic shock. *J Am Coll Cardiol.* (2019) 73:1659–69. doi: 10.1016/j.jacc.2018.12.084

10. Chieffo A, Dudek D, Hassager C, Combes A, Gramegna M, Halvorsen S, et al. Joint EAPCI/ACVC expert consensus document on percutaneous ventricular assist devices. *Eur Heart J Acute Cardiovasc Care.* (2021) 10(5):570–83. doi: 10.1093/ehjacc/zuab015

11. Watanabe A, Miyamoto Y, Ueyama HA, Gotanda H, Jentzer JC, Kapur NK, et al. Impacts of hospital volume and patient-hospital distances on outcomes of older adults receiving percutaneous microaxial ventricular assist devices for cardiogenic shock. *Circ Cardiovasc Interv.* (2024) 17(12):e014738. doi: 10.1161/CIRCINTERVENTIONS.124.014738

12. Araki T, Kondo T, Imaizumi T, Sumita Y, Nakai M, Tanaka A, et al. Relationship between the volume of cases and in-hospital mortality in patients with cardiogenic shock receiving short-term mechanical circulatory support. *Am Heart J.* (2023) 261:109–23. doi: 10.1016/j.ahj.2023.03.017

13. Møller JE, Engstrøm T, Jensen LO, Eiskjær H, Mangner N, Polzin A, et al. Microaxial flow pump or standard care in infarct-related cardiogenic shock. *N Engl J Med.* (2024) 390(15):1382–93. doi: 10.1056/NEJMoa2312572

14. Ardito V, Sarucanian L, Rognoni C, Pieri M, Scandroglio AM, Tarricone R. Impella versus VA-ECMO for patients with cardiogenic shock: comprehensive systematic literature review and meta-analyses. *J Cardiovasc Dev Dis.* (2023) 10(4):158. doi: 10.3390/jcdd10040158

15. Ahmad S, Ahsan MJ, Ikram S, Lateef N, Khan BA, Tabassum S, et al. Impella versus extracorporeal membranous oxygenation (ECMO) for cardiogenic shock: a systematic review and meta-analysis. *Curr Probl Cardiol.* (2023) 48(1):101427. doi: 10.1016/j.cpcardiol.2022.101427

frontiers | Frontiers in Medicine

TYPE Case Report
PUBLISHED 29 January 2025
DOI 10.3389/fmed.2025.1530566

OPEN ACCESS

EDITED BY
Takahiro Nakashima,
University of Michigan, United States

REVIEWED BY
Pauline Yeung Ng,
The University of Hong Kong, Hong Kong SAR, China
Maria Paparoupa,
University Medical Center Hamburg-Eppendorf, Germany

*CORRESPONDENCE
Jihong Zhang
✉ alihealth@sina.cn

RECEIVED 19 November 2024
ACCEPTED 08 January 2025
PUBLISHED 29 January 2025

CITATION
Zhu G, Yue W, Li Y, Wang H, Li J, Zhou X, Zhang Q and Zhang J (2025) Successful resuscitation of acute type A aortic dissection with pulmonary embolism using long-term venoarterial extracorporeal membrane oxygenation: a case report. *Front. Med.* 12:1530566. doi: 10.3389/fmed.2025.1530566

Successful resuscitation of acute type A aortic dissection with pulmonary embolism using long-term venoarterial extracorporeal membrane oxygenation: a case report

Guiwei Zhu[1], Wenhui Yue[2], Yanmin Li[3], Haiqing Wang[1], Jianqiang Li[1], Xin Zhou[3], Qinghai Zhang[1] and Jihong Zhang[1]*

[1]Department of Critical Care Medicine, Weifang People's Hospital, Weifang, Shandong, [2]Department of Hand and Foot Orthopedic Surgery, Weifang People's Hospital, Weifang, Shandong, China, [3]Office of Medical Affairs, Weifang People's Hospital, Weifang, Shandong, China

Acute aortic dissection (AAD) and pulmonary embolism (PE) are two critical and potentially fatal causes of chest pain. The simultaneous occurrence of these conditions is exceptionally rare; however, when they co-occur, the conflicting therapeutic strategies required significantly elevate mortality rates. While venoarterial extracorporeal membrane oxygenation (VA-ECMO) has been extensively reported as a life-saving intervention for high-risk pulmonary embolism, its application in the management of AAD remains highly debated. Recently, our institution successfully employed VA-ECMO to treat a patient with acute type A aortic dissection (ATAAD) complicated by PE. This case highlights that VA-ECMO may serve as a crucial life-saving measure for patients with AAD who present with hemodynamic instability or cardiac arrest.

KEYWORDS

acute type A aortic dissection, pulmonary embolism, veno-arterial extracorporeal membrane oxygenation, cardiopulmonary arrest, hemodynamic instability, case report

Introduction

Acute aortic dissection (AAD) is characterized by a disruption of the tunica intima, allowing blood to enter the tunica media, which can propagate along the length of the aorta and extend into its branch vessels. For patients with acute type A aortic dissection (ATAAD) managed conservatively, the 24-h mortality rate is approximately 60% (1). Pulmonary embolism (PE) is the third leading cause of cardiovascular death, with 30-day and 6-month all-cause mortality rates of 9.1 and 19.6%, respectively, in the Medicare population (2). The simultaneous occurrence of AAD and PE is exceedingly rare; however, their concurrent presentation significantly amplifies mortality due to conflicting therapeutic strategies. While venoarterial extracorporeal membrane oxygenation (VA-ECMO) is well-documented as a life-saving intervention for high-risk PE (3), its application in AAD remains highly debated, as AAD is considered a relative contraindication for VA-ECMO (4). To date, only one case has been reported in which VA-ECMO was utilized in

the management of a type B aortic dissection complicated by PE (5), and no cases have been documented for ATAAD with concurrent PE.

Here, we present the case of a patient with a malignant tumor in the upper lobe of the left lung (pT1N0M0, stage IA). On the first postoperative day following lobectomy, the patient experienced cardiopulmonary arrest during ambulation. Despite cardiopulmonary resuscitation, stable autonomous cardiac rhythm could not be achieved, necessitating the initiation of VA-ECMO therapy. Comprehensive diagnostic evaluation subsequently revealed ATAAD complicated by PE. Following 27 h of intensive management, VA-ECMO support was successfully weaned, and the patient underwent surgical intervention for ATAAD. The patient achieved full recovery, with no residual symptoms observed. This case represents the first successful use of VA-ECMO in the management of a patient with ATAAD complicated by PE.

Case description

A 60-year-old female (height: 165 cm, weight: 64.5 kg) underwent a routine chest CT scan 2 years and 5 months prior, revealing ground-glass nodules in the right upper lobe and bilateral lower lobes. No specific treatment was administered at the time. However, a follow-up chest CT scan conducted 15 days before admission identified a mixed ground-glass nodule in the apicoposterior segment of the left upper lobe, prompting her presentation to our hospital for further evaluation and management. The patient reported no symptoms such as persistent or irritative cough, sputum production, hemoptysis, fever, night sweats, or fatigue. She denied chest pain, tightness, dyspnea, hoarseness, or dysphagia. Her past medical history was unremarkable, with no history of occupational or toxic substance exposure, and no history of smoking, alcohol use, or drug abuse.

On physical examination, vital signs were stable, including a temperature of 36°C, pulse of 76 beats per minute, respiratory rate of 19 breaths per minute, and blood pressure of 120/99 mmHg. There was no palpable lymphadenopathy in the supraclavicular regions, and the thorax appeared symmetrical with normal bilateral respiratory movement. Percussion revealed resonance bilaterally, and auscultation noted clear breath sounds without adventitious sounds. Cardiovascular examination showed a regular heart rate of 76 beats per minute with no pathological murmurs in any valve region. The remainder of the systemic examination was unremarkable.

Upon admission, comprehensive diagnostic tests were performed. Echocardiography revealed mild tricuspid regurgitation but no other abnormalities. Venous ultrasonography of the bilateral common iliac, internal and external iliac, femoral, popliteal, anterior and posterior tibial, and intermuscular veins showed no evidence of thrombus. Contrast-enhanced chest CT demonstrated a ground-glass nodule in the left upper lobe, raising suspicion for a neoplastic lesion, along with bilateral ground-glass micronodules, solid micronodules, and a calcified nodule in the right upper lobe.

On the second day of hospitalization, the patient underwent a "right lung nodule microwave ablation," with an uneventful postoperative course. On the sixth day of hospitalization, she underwent a "thoracoscopic resection of LS(1+2)(a+b)+3c segments with lymphadenectomy." Postoperative histopathological examination of the lung tissue revealed a moderately differentiated invasive adenocarcinoma, with no evidence of lymph node metastasis. On the first postoperative day (seventh day of hospitalization) at 14:30, during her initial ambulation attempt, the patient experienced transient syncope characterized by pallor, diaphoresis, and dyspnea. She remained responsive. Oxygen therapy at 6 L/min via a face mask was immediately initiated, and peripheral blood glucose measured 7.3 mmol/L. Cardiac monitoring showed a heart rate of 123 beats per minute, respiratory rate of 36 breaths per minute, oxygen saturation of 85%, and blood pressure of 82/43 mmHg. Auscultation revealed coarse bilateral breath sounds. Intravenous access was established, and 500 mL of lactated Ringer's solution was administered. The patient's condition rapidly deteriorated, and at 14:40, cardiac monitoring revealed pulseless electrical activity. Immediate chest compressions were initiated, followed by intravenous epinephrine administration, bedside endotracheal intubation, and manual ventilation. Spontaneous cardiac activity resumed at 14:45; however, hemodynamic stability could not be achieved despite high-dose norepinephrine (1.68 μg/kg/min). Bedside ultrasonography revealed right ventricular dilation and global hypokinesia. Considering that the patient was on the first postoperative day after a lung lobectomy and had contraindications to thrombolytic therapy, we opted to initiate VA-ECMO to stabilize her circulation. Ultrasound-guided cannulation of the left femoral vein and right femoral artery was performed, with successful puncture of both vessels on the first attempt. VA-ECMO was successfully commenced at 15:41. Under VA-ECMO support, computed tomography angiography (CTA) identified ATAAD with concurrent PE (Figures 1A, B). Multidisciplinary discussion determined that, due to the small size of the PE, thrombolysis was unnecessary. Anticoagulation therapy was initiated with a target activated clotting time of 180–220 s. VA-ECMO flow was progressively reduced while monitoring hemoglobin levels and coagulation parameters. As the hospital lacked surgical capacity for ATAAD, and the risks of transporting the unstable patient were significant, arrangements were made with the family to transfer the patient to a higher-level facility once her vital signs stabilized.

After 27 h on VA-ECMO, the patient regained consciousness, achieved hemodynamic stability, and no longer required vasopressor support. VA-ECMO was successfully weaned and explanted, and she was transferred to a higher-level hospital on the same day. At the receiving facility, the patient underwent a "aortic valve repair, partial ascending aortic resection with graft replacement, total aortic arch replacement, and stented elephant trunk procedure (Sun's procedure)." Intraoperative findings revealed the dissection tear on the lesser curvature of the aortic arch. Cardiopulmonary bypass was discontinued without complications.

The patient's postoperative course was favorable, and she was discharged in stable condition. At her 9-month follow-up visit, she exhibited no neurological deficits, all organ functions were normal, and pulmonary CTA showed no evidence of thrombus formation (Figure 2).

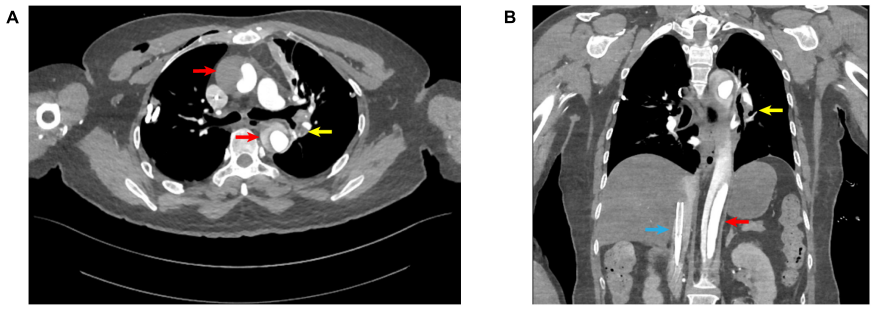

FIGURE 1
(A) Transverse view; **(B)** coronal view; red arrows: aortic dissection; yellow arrows: pulmonary embolism; blue arrows: V-A ECMO venous drainage cannula.

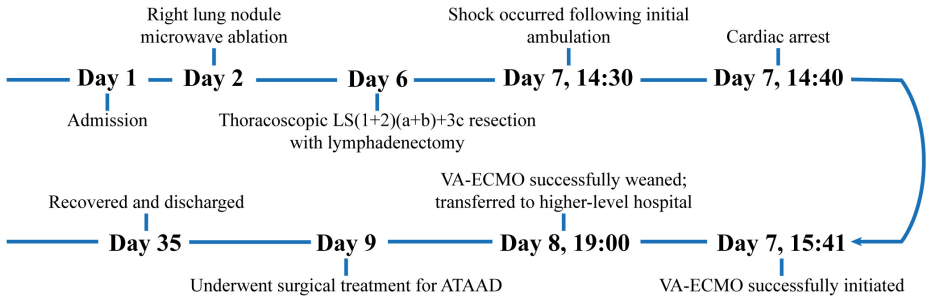

FIGURE 2
The timeline of the patient's disease progression.

Discussion

Acute aortic dissection is characterized by a disruption of the tunica intima, allowing blood to enter the tunica media, which can propagate along the entire length of the aorta and its branch vessels. The incidence of AAD is estimated to be 5–30 cases per million individuals annually. ATAAD involves the ascending aorta, is highly fatal if left untreated, with a 24-h mortality rate of approximately 60% in conservatively managed cases. Mortality increases substantially when complications such as cardiac tamponade (with or without cardiogenic shock), acute myocardial ischemia or infarction, stroke, or malperfusion of vital organs occur (1). PE is the third leading cause of cardiovascular death, with 30-day and 6-month all-cause mortality rates of 9.1 and 19.6%, respectively, in the Medicare population (2). The simultaneous occurrence of AAD and PE is exceedingly rare; however, when these conditions co-occur, the conflicting management strategies significantly increase mortality. VA-ECMO has been extensively reported as a rescue therapy for high-risk PE (3), but its use in AAD remains controversial due to the risk of exacerbating the dissection, AAD is generally considered a relative contraindication for VA-ECMO (4). To date, only one case has been reported describing VA-ECMO use in type B aortic dissection complicated by PE (5), with no documented cases involving ATAAD with concurrent PE. At our institution, VA-ECMO was successfully utilized to manage a patient with ATAAD complicated by PE. This represents the first documented case of successful VA-ECMO intervention in a patient with ATAAD and concurrent PE.

The precise temporal relationship and potential interactions between ATAAD and PE in this case remain challenging to ascertain. Aoki et al. previously reported a case of ATAAD caused by adjustments to the position of the VA-ECMO return cannula (6). However, in our patient, the dissection tear was located on the lesser curvature of the aortic arch, making VA-ECMO cannulation an unlikely cause of the ATAAD.

One of the primary concerns regarding VA-ECMO use in patients with ATAAD is the risk of arterial cannulation inadvertently entering the false lumen. Current protocols for arterial cannulation during cardiopulmonary bypass in ATAAD include options such as the ascending aorta, innominate artery, axillary artery, central artery, and femoral artery. While the axillary artery is preferred for its ability to maintain adequate cerebral perfusion, femoral artery cannulation remains the first choice for hemodynamically unstable patients due to its ease and rapid accessibility (7). Data from the German Registry for Acute Aortic Dissection Type A (GERAADA) indicate that only 50.1% of ATAAD cases involve the descending aorta, with 37.9% involving the abdominal aorta and 24.8% involving the pelvic arteries (8). Therefore, in at least 75% of cases, femoral artery cannulation for VA-ECMO is unlikely to result in false lumen perfusion. Furthermore, ultrasound-guided puncture can minimize cannulation errors, making it a safe and feasible option for hemodynamically unstable patients. Concerns about potential cannulation into the false lumen should not preclude the use of this life-saving intervention.

For high-risk PE, current guidelines recommend anticoagulation combined with thrombolytic or thrombectomy therapy (2). However, in this case, the concurrent ATAAD

posed a significant bleeding risk. Given the small burden of PE on pulmonary CTA, thrombolysis or thrombectomy was deemed unnecessary. Anticoagulation therapy in patients with combined AAD and PE lacks standardized protocols. We opted for unfractionated heparin, given its ability to be rapidly neutralized with protamine, targeting an activated clotting time ACT of 180–220 s. Platelet counts were maintained within normal limits, and hemoglobin levels were closely monitored. To prevent retrograde VA-ECMO flow from exacerbating hematoma expansion or causing rupture of the dissection, blood pressure was meticulously controlled within a target range of 100–120 mmHg during VA-ECMO support. VA-ECMO flow was gradually reduced as the patient's hemodynamics stabilized. No expansion of the dissection hematoma was observed, and VA-ECMO was successfully weaned without complications.

ATAAD necessitates urgent surgical intervention, with literature indicating an approximately 1–2% increase in mortality per hour without surgery, reaching up to 60% within 24 h (1). However, due to the lack of surgical capabilities at our facility, emergency surgery could not be performed, and VA-ECMO was utilized for 27 h. This represents the longest documented duration of VA-ECMO support for a patient with AAD. Malperfusion of the heart and visceral organs in aortic dissection is associated with poor outcomes, as irreversible organ damage significantly increases mortality. Recent studies suggest that restoring end-organ perfusion through endovascular techniques prior to aortic repair may improve outcomes (7). Hiroyuki Ohbe et al. demonstrated that extracorporeal cardiopulmonary resuscitation can improve outcomes in some patients with AAD complicated by refractory cardiac arrest (9). Although current evidence remains insufficient to overturn the contraindication of VA-ECMO in AAD, further clinical studies are needed to evaluate its viability as a rescue therapy in this population. In cases of refractory cardiac arrest of unknown origin, VA-ECMO should be promptly considered when patients meet specific criteria (10).

Conclusion

For patients with AAD presenting with hemodynamic instability or cardiac arrest, VA-ECMO may serve as a critical life-saving intervention.

Data availability statement

The original contributions presented in this study are included in this article/Supplementary material, further inquiries can be directed to the corresponding author.

Ethics statement

Ethical approval was not required for the studies involving humans because this case report was conducted with strict adherence to safeguarding the patient's privacy and rights. The studies were conducted in accordance with the local legislation and institutional requirements. The participants provided their written informed consent to participate in this study. Written informed consent was obtained from the individual(s) for the publication of any potentially identifiable images or data included in this article. Written informed consent has been obtained from the participant(s) for the publication of this case report.

Author contributions

GZ: Writing – original draft. WY: Writing – review and editing. YL: Resources, Writing – review and editing. HW: Software, Writing – review and editing. JL: Software, Writing – review and editing. XZ: Resources, Writing – review and editing. QZ: Funding acquisition, Writing – review and editing. JZ: Supervision, Writing – review and editing.

Funding

The author(s) declare that financial support was received for the research, authorship, and/or publication of this article. This article was supported by the Wu Jieping Medical Foundation (Grant no. 320.6750.2024-18-77).

Conflict of interest

The authors declare that the research was conducted in the absence of any commercial or financial relationships that could be construed as a potential conflict of interest.

Generative AI statement

The authors declare that no Generative AI was used in the creation of this manuscript.

Publisher's note

Supplementary material

The Supplementary Material for this article can be found online at: https://www.frontiersin.org/articles/10.3389/fmed.2025.1530566/full#supplementary-material

References

1. Malaisrie S, Szeto W, Halas M, Girardi L, Coselli J, Sundt T III, et al. The American association for thoracic surgery expert consensus document: Surgical treatment of acute type A aortic dissection. *J Thorac Cardiovasc Surg.* (2021) 162(3), 735–58.e2. doi: 10.1016/j.jtcvs.2021.04.053

2. Ortel T, Neumann I, Ageno W, Beyth R, Clark N, Cuker A, et al. American society of hematology 2020 guidelines for management of venous thromboembolism: Treatment of deep vein thrombosis and pulmonary embolism. *Blood Adv.* (2020) 4(19):4693–738.

3. Kobayashi T, Pugliese S, Sethi S, Parikh S, Goldberg J, Alkhafan F, et al. Contemporary management and outcomes of patients with high-risk pulmonary embolism. *J Am Coll Cardiol.* (2024) 83(1):35–43.

4. Tsangaris A, Alexy T, Kalra R, Kosmopoulos M, Elliott A, Bartos J, et al. Overview of veno-arterial extracorporeal membrane oxygenation (VA-ECMO) support for the management of cardiogenic shock. *Front Cardiovasc Med.* (2021) 8:686558. doi: 10.3389/fcvm.2021.686558

5. Maybauer M, El Banayosy A, Koerner M, Hooker R, Swant L, Mihu M, et al. Mechanical cardiopulmonary resuscitation for venoarterial ECMO implantation in pulmonary embolism complicated by type B aortic dissection and retroperitoneal hemorrhage. *J Card Surg.* (2020) 35(10):2821–4. doi: 10.1111/jocs.14782

6. Aoki M, Senoo S, Mori T, Fukada T, Kawai Y, Kazamaki T, et al. Stanford type a aortic dissection caused by veno-arterial extracorporeal membrane oxygenation. *Am J Emerg Med.* (2021) 49, 438.e1-.e3.

7. Isselbacher E, Preventza O, Hamilton Black J III, Augoustides J, Beck A, Bolen M, et al. 2022 ACC/AHA guideline for the diagnosis and management of aortic disease: A report of the american heart association/american college of cardiology joint committee on clinical practice guidelines. *Circulation.* (2022) 146(24):e334–482.

8. Conzelmann L, Weigang E, Mehlhorn U, Abugameh A, Hoffmann I, Blettner M, et al. Mortality in patients with acute aortic dissection type A: analysis of pre- and intraoperative risk factors from the german registry for acute aortic dissection type A (GERAADA). *Eur J Cardiothorac Surg.* (2016) 49(2):e44–52. doi: 10.1093/ejcts/ezv356

9. Ohbe H, Ogura T, Matsui H, Yasunaga H. Extracorporeal cardiopulmonary resuscitation for acute aortic dissection during cardiac arrest: A nationwide retrospective observational study. *Resuscitation.* (2020) 156:237–43. doi: 10.1016/j.resuscitation.2020.08.001

10. Richardson A, Tonna J, Nanjayya V, Nixon P, Abrams D, Raman L, et al. Extracorporeal cardiopulmonary resuscitation in adults. interim guideline consensus statement from the extracorporeal life support organization. *ASAIO J.* (2021) 67(3):221–8. doi: 10.1097/MAT.0000000000001344

frontiers | Frontiers in Medicine

TYPE Perspective
PUBLISHED 20 March 2025
DOI 10.3389/fmed.2025.1569951

OPEN ACCESS

EDITED BY
Takahiro Nakashima,
University of Michigan, United States

REVIEWED BY
Cale Kassel,
University of Nebraska Medical Center,
United States

*CORRESPONDENCE
Florian J. Raimann
✉ Raimann@med.uni-frankfurt.de

RECEIVED 02 February 2025
ACCEPTED 06 March 2025
PUBLISHED 20 March 2025

CITATION
Raimann FJ and Willems LM (2025) Diagnosis of brain death and consecutive donor management under combined circulatory support with ECMELLA therapy.
Front. Med. 12:1569951.
doi: 10.3389/fmed.2025.1569951

Diagnosis of brain death and consecutive donor management under combined circulatory support with ECMELLA therapy

Florian J. Raimann[1]* and Laurent M. Willems[2]

[1]Department of Anesthesiology, Intensive Care Medicine and Pain Therapy, University Hospital, Goethe University Frankfurt, Frankfurt, Germany, [2]Department of Neurology and Epilepsy Center Frankfurt Rhine-Main, University Hospital, Goethe University Frankfurt, Frankfurt, Germany

Background: Managing brain death determination (BDD) in potential organ donors is a challenging aspect of modern intensive care medicine. In critically ill patients with implanted circulatory or left ventricular support devices, standard recommendations for BDD are often no longer applicable.

Methods/results: The available recommendations and evidence for BDD and organ procuring under ECMELLA therapy—a combined circulatory support using a veno-arterial extracorporeal membrane oxygenation (vaECMO) and an invasive left ventricular support device (Impella® CP)—are discussed based on a clinical case. To the authors' knowledge, this is the first report of BDD under ECMELLA therapy.

Conclusion: Although BDD in patients with multimodal invasive circulatory support, such as ECMELLA therapy, is demanding and time-intensive, it can still be performed safely and based on evidence. Given the continuing low numbers of organ donors, these insights may help to facilitate organ donation in patients with combined invasive mechanical circulatory support.

KEYWORDS

ECMO, impella, critical care, cardiac arrest, intensive care, organ donation

Background

Brain death determination (BDD) is a central yet challenging aspect of modern interdisciplinary intensive care medicine. National and international guidelines strictly regulate BDD, providing clear instructions for the procedure and interpretation of findings in most cases (1). The use of extracorporeal support devices can sometimes make the diagnosis of BDD considerably more difficult or even impossible. Over the last few years, extracorporeal cardiopulmonary resuscitation (eCPR) and extracorporeal life support (ECLS) have been increasingly implemented in CPR and post-resuscitation care. Moreover, invasive short-term cardiac assist devices, such as micro-axial flow pumps (e.g., the Impella CP®), have been established to bridge patients with insufficient or critical cardiac function after the return of spontaneous circulation (ROSC). Both procedures significantly complicate BDD and donation after brain death (DBD) considerably and are often not adequately addressed in guidelines (2, 3).

This brief perspective illustrates and discusses the implications and potential pitfalls of a combined vaECMO (CardioHelp®; Getinge Deutschland GmbH, Rastatt, Germany) and Impella® + SmartAssist (Abiomed Europe, Aachen, Germany) (ECMELLA) therapy on BDD and DBD based on the case of a 54-year-old man who developed low cardiac output after

complex Tirone-David operation (aortocoronary bypass + aortic valve replacement). In addition to an intraoperative epicardial pacer, the patient consecutively received a vaECMO [ELSO Maastricht nomenclature: V23/55frivc-A17/15fldt (4)] under transient cardiopulmonary resuscitation (CPR) as well as an Impella® CP due to ongoing cardiac failure (Figure 1). Due to inadequate clinical awakening and signs of brainstem dysfunction, a cranial CT was performed, revealing global hypoxic brain damage with generalized cerebral edema. The unfavorable prognosis and the patient's family's willingness for DBD were discussed with the legal representative, and BDD was initiated according to the national guidelines, as the concept of donation after cardiac death (DCD) has not been approved in Germany (1, 5). A schematic overview of the clinical and device instead of aparitive setting on intensive care unit is given in Figure 1.

Results

Implications of ECMELLA on brain death determination

The German guidelines specify a strictly regulated two-step process for BDD, comprising primarily the clinical confirmation of the loss of brain functions and secondary proof of irreversibility for donation after brain death (DBD) (1, 6). To avoid false high CO_2 values due to a Harlequin effect under vaECMO samples for arterial blood gas analysis (BGA) were drawn from both brachial arteries following national and international recommendations. In the present case, the Harlequin effect was further enhanced by the orthogonal flow of the Impella® device, and both Impella® and vaECMO settings had to be adjusted in multiple small steps to facilitate bilateral CO_2 values of 35 to 45 mmHg as basic requirements for conducting the apnea test. Once the initial $paCO_2$ values were within the specified range, the vaECMO and Impella flow rates were carefully and gradually reduced. An increase in CO_2 to >60 mmHg could only be achieved through a gradual reduction in O_2 admixture and flow. Due to the increased risk of organ hypoxemia after more than 9 min, a minimal FiO_2 had to be maintained during this procedure. Due to the high risk of clotting in the oxygenator during flow reduction, the flow could only be reduced carefully while on standby for manual operation. After adjusting the $paCO_2$ to >60 mmHg in both BGAs obtained from the brachial artery lines, the apnea test was performed. Notably, the apnea test had to be discontinued several times due to cardio-circulatory insufficiency caused by hypercapnic acidosis. The presented approach was orientated on the "Guidance for the Diagnosis of Death using Neurological Criteria when the patient is supported with extracorporeal membrane oxygenation" (7). Furthermore, after pausing the epicardial pacemaker [heart rate: 90–100 beats*min^{-1}, AV delay 140 ms, atrial pacing 10 V, ventricular pacing 12 V (transcutaneous pacer)], asystole was observed. Given this and the

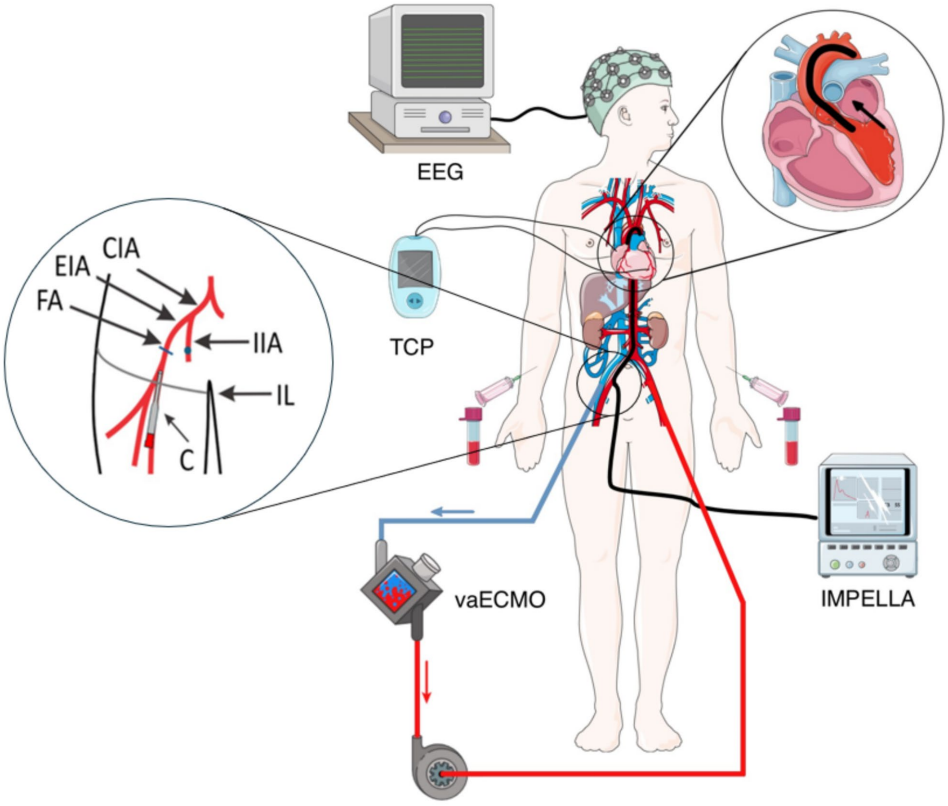

FIGURE 1
Schematic overview of brain death determination (BDD) in the described patient with multimodal cardiocirculatory support and transcutaneous pacer (TCP). CIA = common iliac artery, EIA = external iliac artery, FA = femoral artery, IIA = internal iliac artery, IL inguinal, and C = (arterial return) cannula [figure based on images from Servier Medical ART, licensed under CC BY 4.0, https://smart.servier.com].

TABLE 1 Dis–/advantages of perfusion procedures.

Option	Advantage	Disadvantage
1	• Rapid application of the perfusion solution	• Necessity to install a 3/8′-3/8' LuerLock T-piece (see Figure 1) • Short-term clamping of the connecting tube between the drainage cannula and oxygenator • Insufficient lumen of the LuerLock
2	• Rapid application of the perfusion solution	• Need to install a 3/8′-1/4′ adapter (see Figure 1) • Stopping the vaECMO and cutting the tube between the oxygenator and the return cannula • Ligature around the drainage cannula at a length of 15 cm and deep seat in the area of the inguinal ligament
3	• Parallel set-up of all materials required for perfusion. • No ligature around the return cannula • Perfusion procedure already familiar to all team members	• Slower application of the perfusion solution

absence of blood pressure autoregulation under ECMELLA therapy [Impella CP: Flow Control P3, Purge Flow 16.5 mL*h^{-1}, Purge Pressure 400–450 mmHg, Impella Flow 1.6 L*min^{-1}; vaECMO: 3000RPM, 2.8 LPM, FiO2 0.9, SweepGas Flow 2.0 L*min^{-1}], the assessment of a vegetative reaction to painful stimuli, such as an increase in heart rate or systolic blood pressure, was deemed unreliable. Consequently, observation of vegetative response to nociceptive stimuli was reduced to potential motor reactions, facial grimacing or increased sweating. Finally, the clinical loss of brain function was identified.

Under vaECMO therapy, and therefore also under ECMELLA, confirmation of the irreversibility of brain function loss was accessed by electroencephalography (EEG). Following national and international guidelines, proof of irreversibility through cerebral circulatory arrest was not permissible due to the low mean systolic pressure under mechanic circulatory support, as a mean arterial pressure of >90 mmHg is required as a fundamental prerequisite (1). Alternatively, confirmation of irreversibility by means of a second clinical protocol with an apnea test after >72 h was not considered feasible due to the patient's instability and the abovementioned significantly complicated procedure. For these reasons, irreversibility was determined by EEG in the present case. Due to multiple sources of electrical interference and fields under ECMELLA, as well as the cardiac pacer and other electrical devices within the ICU environment, EEG sampling using Ag/AgCl-surface electrodes was not feasible for technical reasons. Consequently, platinum needle electrodes were inserted into the scalp according to the 10–20 system (8). To further reduce artifacts caused by cables and supply lines in the bed, the electrodes were routed to hang freely at the head end of the bed, ensuring the cables make contact with the bed or the patient, except at their tips. As a result of these measures, an artifact-free recording was achieved, producing an isoelectric EEG < 2 μV without evidence of brain activity thus confirming brain death (1).

Implications of ECMELLA on organ donation management

For the perfusion of the abdominal organs, 8 L (800 mL/min application rate) of a Custodiol® solution (Dr. Franz Köhler Chemie GmbH, Bensheim, Germany) was used. Based on the ECMELLA treatment, three different perfusion scenarios were discussed in advance between the anesthesiology team, cardio-technicians, and visceral surgeons.

1. Active perfusion via vaECMO over the draining cannula (see Figure 1 – return cannula)
2. Passive, gravity-following perfusion via the arterial return cannula (17 Fr) (see Figure 1 – return cannula)
3. Passive, gravity-following perfusion via the external iliac artery (see Figure 1 – blue dot)

Option 3, described in Table 1, was selected as the primary route to organ perfusion after interdisciplinary discussion as all team members are familiar with this procedure and it represents the lowest risk of complications. Option 2 was defined as the relapse option as the perfusion speed is higher here compared to option 3. During organ and vessel preparation, it was noticed that the return cannula, around which a ligature would have to be placed, extends too short into the abdomen from the intra-abdominal area.

Discussion

This complex scenario of brain death diagnostics and intraoperative management under ECMELLA therapy is rare. Due to its infrequency and the unique challenges posed by the therapy, physicians face significant difficulties. Not only is a high level of expertise in brain death diagnosis essential but also extensive knowledge in managing vaECMO and Impella is highly relevant. These challenges persist throughout the organ donation process. For instance, explantation surgeons must have a thorough knowledge of the perfusion cannula position and its resulting implications. In our view, an interdisciplinary preliminary discussion and dedicated planning of both BDD and explantation are crucial to avoiding complications. In the context of BDD under vaECMO therapy, the adjustment of guideline-compliant paCO2 partial pressures for the correct performance of the apnea test poses a particular challenge (9–11), as attention must be paid to the occurrence of Harlequin syndrome. The Harlequin effect is a condition that can occur with

peripheral cannulation during veno-arterial extracorporeal membrane oxygenation (VA-ECMO). In cases of poor lung function coupled with residual cardiac contractility, deoxygenated blood enters the aortic arch, leading to reduced perfusion in the upper extremities as hypoxemic blood reaches the upper half of the body. This occurs due to antegrade (hypoxemic) blood flow, which flows against the retrograde blood flow generated by the ECMO. The IMPELLA placed over the aortic valve can enhance the Harlequin effect by artificially increasing the antegrade flow, even in the absence of residual myocardial contractility. Bilateral blood gas analyses on both upper extremities are necessary, requiring distinct knowledge of ECMO and IMPELLA operation. Another complicating factor is that physiological parameters continue to change under combined therapy with Impella® CP. Among other things, the localization of the support devices as well as of their cannulation is crucial here (12). Although reviews on brain death diagnostics under vaECMO already exist (11, 13, 14), there are currently no guidelines or procedural instructions for managing brain death diagnosis under ECMELLA therapy. To our knowledge, the procedure presented here is the first description of brain death diagnostics under ECMELLA therapy. We hope that our approach, experiences, and thoughts will help others in improving BDD under ECLS with ECMO and IMPELLA devices.

Data availability statement

The original contributions presented in the study are included in the article/supplementary material, further inquiries can be directed to the corresponding author.

Ethics statement

The studies involving humans were approved by Institutional ethics committee of University Hospital Frankfurt. The studies were conducted in accordance with the local legislation and institutional requirements. Written informed consent for participation in this study was provided by the participants' legal guardians/next of kin.

Author contributions

FR: Conceptualization, Data curation, Formal analysis, Funding acquisition, Investigation, Methodology, Project administration, Resources, Software, Supervision, Validation, Visualization, Writing – original draft, Writing – review & editing. LW: Conceptualization, Data curation, Formal analysis, Funding acquisition, Investigation, Methodology, Project administration, Resources, Software, Supervision, Validation, Visualization, Writing – original draft, Writing – review & editing.

Funding

The author(s) declare that no financial support was received for the research and/or publication of this article.

Conflict of interest

The authors declare that the research was conducted in the absence of any commercial or financial relationships that could be construed as a potential conflict of interest.

Generative AI statement

The author(s) declare that no Gen AI was used in the creation of this manuscript.

Publisher's note

References

1. Angstwurm H, Bartenstein PA, Brandt S, Clusmann H, Emami P, Förderreuther S. German guideline for brain death diagnosis (5th updated version) In: Official announcement of the FMA. Berlin, Germany: German Federal Medical Association (2022). 1–31.

2. Sandroni C, D'Arrigo S. Brain death is common after extracorporeal cardiopulmonary resuscitation (eCPR): an undesired outcome with potential benefits. *Resuscitation*. (2024) 200:110246. doi: 10.1016/j.resuscitation.2024.110246

3. Rajsic S, Treml B, Innerhofer N, Eckhardt C, Radovanovic Spurnic A, Breitkopf R. Organ donation from patients receiving extracorporeal membrane oxygenation: a systematic review. *J Cardiothorac Vasc Anesth*. (2024) 38:1531–8. doi: 10.1053/j.jvca.2024.03.020

4. Broman LM, Taccone FS, Lorusso R, Malfertheiner MV, Pappalardo F, Di Nardo M, et al. The ELSO Maastricht treaty for ECLS nomenclature: abbreviations for cannulation configuration in extracorporeal life support—a position paper of the extracorporeal life support organization. *Crit Care Med*. (2019) 23. doi: 10.1186/s13054-019-2334-8

5. Eden J, Dutkowski P, Schlegel A. Reply to: "how many liver grafts could be recovered after implementation of donation after cardiac death in Germany?". *J Hepatol*. (2023) 79:e120–1. doi: 10.1016/j.jhep.2023.05.014

6. Hoffmann O, Salih F, Masuhr F. Diagnosis of brain death in Germany-implementation of the guidelines of the German Medical association. *Nervenarzt*. (2023) 94:1129–38. doi: 10.1007/s00115-023-01520-5

7. Meadows CIS, Toolan M, Slack A, Newman S, Ostermann M, Camporota L, et al. The Faculty of Intensive Care Medicine. Supplementary guidance for the diagnosis of death using neurological criteria when the patient is supported by extracorporeal membrane oxygenation In: Diagnosing death using neurological criteria. London: FICM (2021).

8. Walte U, Loewenbrück KF, Dodel R, Storch A, Trenkwalder C, Höglinger G. Recommendations of the German Society for Clinical Neurophysiology and Functional Imaging for the diagnosis of irreversible loss of brain function. *Klinische Neurophys*. (2019) 50:17–22. doi: 10.1055/a-2069-3379

9. Bein T, Muller T, Citerio G. Determination of brain death under extracorporeal life support. *Intensive Care Med*. (2019) 45:364–6. doi: 10.1007/s00134-018-05510-z

10. Lie SA, Hwang NC. Challenges of brain death and apnea testing in adult patients on extracorporeal membrane oxygenation-a review. *J Cardiothorac Vasc Anesth*. (2019) 33:2266–72. doi: 10.1053/j.jvca.2019.01.042

11. Sady ERR, Junqueira L, Veiga VC, Rojas SSO. Apnea test for brain death diagnosis in adults on extracorporeal membrane oxygenation: a review. *Rev Bras Ter Intensiva*. (2020) 32:312–8. doi: 10.5935/0103-507x.20200048

12. Thevathasan T, Füreder L, Donker DW, Nix C, Wurster TH, Knie W, et al. Case report: refractory cardiac arrest supported with veno-arterial-venous extracorporeal membrane oxygenation and left-ventricular Impella CP((R))-physiological insights and pitfalls of ECMELLA. *Front Cardiovasc Med*. (2022) 9:1045601. doi: 10.3389/fcvm.2022.1045601

13. Migdady I, Stephens RS, Price C, Geocadin RG, Whitman G, Cho SM. The use of apnea test and brain death determination in patients on extracorporeal membrane oxygenation: a systematic review. *J Thorac Cardiovasc Surg*. (2021) 162:e861:867–877.e1. doi: 10.1016/j.jtcvs.2020.03.038

14. Salih F, Lambeck J, Günther A, Ferse C, Hoffmann O, Dimitriadis K, et al. Brain death determination in patients with veno-arterial extracorporeal membrane oxygenation: a systematic study to address the harlequin syndrome. *J Crit Care*. (2024) 81:154545. doi: 10.1016/j.jcrc.2024.154545

frontiers | Frontiers in Cardiovascular Medicine

TYPE Case Report
PUBLISHED 28 April 2025
DOI 10.3389/fcvm.2025.1567723

OPEN ACCESS

EDITED BY
Fabio Guarracino,
Azienda Ospedaliero Universitaria Pisana, Italy

REVIEWED BY
Daisuke Onohara,
The Research Institute at Nationwide Children's Hospital, United States
Hayato Hosoda,
Chikamori Hospital, Japan

*CORRESPONDENCE
Yuta Nakamura
✉ nakamurasanchinokazoku@gmail.com

RECEIVED 27 January 2025
ACCEPTED 14 April 2025
PUBLISHED 28 April 2025

CITATION
Nakamura Y, Saku K, Homma S, Midorikawa Y, Yamabe T and Ota T (2025) Pulmonary artery rupture by pulmonary artery catheter in cardiac surgery: a case report and review of literature.
Front. Cardiovasc. Med. 12:1567723.
doi: 10.3389/fcvm.2025.1567723

Pulmonary artery rupture by pulmonary artery catheter in cardiac surgery: a case report and review of literature

Yuta Nakamura[1,2]*, Keita Saku[2], Suzu Homma[1], Yoko Midorikawa[1], Tsuyoshi Yamabe[3] and Takashi Ota[1]

[1]Department of Anesthesiology, Shonan Kamakura General Hospital, Kamakura, Japan, [2]Department of Cardiovascular Dynamics, National Cerebral and Cardiovascular Center Research Institute, Suita, Japan, [3]Department of Cardiovascular Surgery, Shonan Kamakura General Hospital, Kamakura, Japan

The pulmonary artery catheter (PAC) is widely used in cardiac surgery for monitoring hemodynamics and cardiovascular function. Complications including pulmonary artery injury causing massive intratracheal hemorrhage are rare but can be life-threatening. We report a case of intratracheal bleeding (3,000 ml) caused by PAC-induced pulmonary artery injury during cardiac surgery and after weaning from cardiopulmonary bypass (CPB). During surgery for acute type A aortic dissection followed by CPB weaning, pulsatile bleeding from the endotracheal tube and desaturation were observed. We reinstituted CPB and placed a right-sided double-lumen tube to compress the injured site of the lung and protect the contralateral site. Following initial bleeding control, we conducted coil embolization to treat tracheal obstruction by a pseudoaneurysm on day 7. A review of 21 recent cases of pulmonary artery injury during cardiac surgery showed that most cases occurred during CPB weaning, manifested hemoptysis, and were treated by coil embolization. This case underscores the importance of enhanced PAC monitoring even after CPB weaning and the need for prompt evaluation and intervention when pulmonary artery injury is suspected during cardiac surgery.

KEYWORDS

cardiovascular anesthesia, pulmonary artery catheter, pulmonary artery rupture, aortic dissection, extracorporeal membrane oxygenation, coil embolization, intensive care

1 Introduction

The use of pulmonary artery catheter (PAC) in critical care, major non-cardiac surgeries, and acute coronary syndrome patients has been extensively studied. However, evidence has shown that PAC use in these settings does not improve outcomes and is associated with a higher incidence of complications (1, 2). In contrast, recent reports highlight the utility of PAC in the management of cardiogenic shock, particularly in the context of initiation and management of mechanical circulatory support (MCS) (3). Furthermore, PAC continues to be used in more than one-third of all cardiac surgeries (4, 5). Patients undergoing cardiac surgery often have severe cardiac diseases with increased risk of hemodynamic instability and cardiac dysfunction, and use of PAC is likely beneficial in this patient population. However, PAC has the risk of highly fatal complications such as pulmonary artery injury causing massive intratracheal hemorrhage, with a reported incidence of 0.1%–0.8% and mortality rate of 45%–60%

(6, 7). Therefore, it is recommended to carefully select cases in which intraoperative PAC placement is likely to be beneficial.

We encountered a case of pulmonary artery injury associated with PAC use, resulting in intratracheal bleeding of approximately 3,000 ml, during surgery for acute type A aortic dissection followed by weaning from cardiopulmonary bypass (CPB). Comprehensive management including CPB reinstitution to stabilize hemodynamics and limit pulmonary blood flow, placement of a right-sided double-lumen tube to compress the injured site and protect the contralateral lung, and coil embolization for a pseudoaneurysm successfully resolved the condition without the need for pulmonary resection.

We also reviewed 21 recent cases of pulmonary artery injury during cardiac surgery to gain better understanding of PAC-induced pulmonary artery injury. This case and literature review underscore the importance of enhanced PAC monitoring even after CPB weaning and the need for prompt evaluation and intervention when pulmonary artery injury is suspected during cardiac surgery.

2 Case report

A 64-year-old man was transported to our emergency department due to sudden onset of chest and back pain at rest, followed by weakness and left-sided hemiparesis. He had hypertension managed with amlodipine, but no history of smoking, diabetes mellitus and cardiovascular diseases. On admission, his vital signs were stable except for blood pressure discrepancies. Right gaze deviation, dysarthria, and incomplete paralysis of the left upper and lower limbs were present. Transthoracic echocardiography showed no abnormalities in contraction, pericardial effusion, and aortic valve regurgitation. Contrast-enhanced computed tomography (CT) of the chest identified aortic dissection extending from the sinus of Valsalva to the common iliac arteries. The dissection was categorized as type A according to Stanford classification, type I according to DeBakey classification, and AE2M2 + M3- according to TEM classification. The diagnosis was acute type A aortic dissection requiring emergent total arch replacement with frozen elephant trunk placement.

Anesthesia was induced uneventfully with propofol, fentanyl, and rocuronium, and was followed by endotracheal intubation with a single-lumen tube. Anesthesia was maintained with continuous propofol infusion. Invasive blood pressure monitoring was established via bilateral radial arteries and the left dorsalis pedis artery. A PAC was placed via the right internal jugular vein under transesophageal echocardiography (TEE) guidance. The catheter was positioned 3 cm proximal to the wedge position at a depth of 55 cm without complications. The central venous pressure (CVP) and pulmonary artery pressure (PAP) waveforms were appropriate. Anesthesia was maintained without complications. CPB was established by inserting a 21-Fr arterial cannula into the left femoral artery, and 24-Fr and 32-Fr venous cannulas into the superior and inferior vena cava, respectively. After achieving high-moderate hypothermia at 26°C, circulatory arrest with selective cerebral perfusion was established. The procedure, including arch branch reconstruction, progressed smoothly up until the stage immediately prior to weaning from CPB.

2.1 Timeline

The timeline after occurrence of PAC-induced pulmonary artery injury is shown below (Figure 1).

2.2 Diagnostic assessment of event

A flat PAP waveform and a right ventricular pattern on the CVP waveform were observed prior to weaning from CPB, as shown in the timeline. The catheter depth migrated deeper from 55 to 56 cm. The PAC was retracted to 30 cm with the balloon deflated and readjusted, but the flat PAP waveform remained unchanged. After CPB weaning, a gradual decrease in peripheral oxygen saturation (SpO_2) was observed immediately before protamine administration, although other vital signs remained stable. During protamine infusion, pulsatile bleeding from the endotracheal tube (ETT) was noted. Even after ETT suctioning, hemostasis could not be achieved, and the patient's blood pressure began to fall. CPB was re-established to provide hemodynamic support and regulate pulmonary artery blood flow.

The surgeons checked the surgical site, the lungs, and the peri-airway area at our request, but no abnormalities were found. The ETT was blindly advanced deeper into the trachea to achieve single-lung intubation. Pulsatile bleeding continued within the ETT alone, with no oral bleeding. Withdrawal of the ETT under suction confirmed that the bleeding originated from the right bronchus. Based on these clinical findings, pulmonary artery injury was strongly suspected as the source of hemorrhage.

2.3 Interventions

The single-lumen ETT was replaced with a 37-Fr right-sided double-lumen tube (DLT), positioned distally in the right upper lobe bronchus. Only the right bronchial lumen of the DLT was clamped, achieving compressive hemostasis and tamponade of the bleeding sites in the right middle and lower lobes. Adequate ventilation was subsequently achieved, and the vital signs stabilized. To prevent alveolar collapse in the unaffected lung while oxygenation and ventilation were supported by CPB, PEEP was maintained at 10 cmH_2O and recruitment maneuvers were applied using an airway pressure of 30 cmH_2O sustained for 10 s. The patient was switched from CPB to venoarterial extracorporeal membrane oxygenation (VA-ECMO) for transfer to the intensive care unit (ICU). A small dose of protamine was administered to maintain the activated clotting time (ACT) between 150 and 200 s. Coagulation was further optimized with transfusions of platelets and fresh frozen plasma, along with careful regulation of body temperature and calcium levels. Total

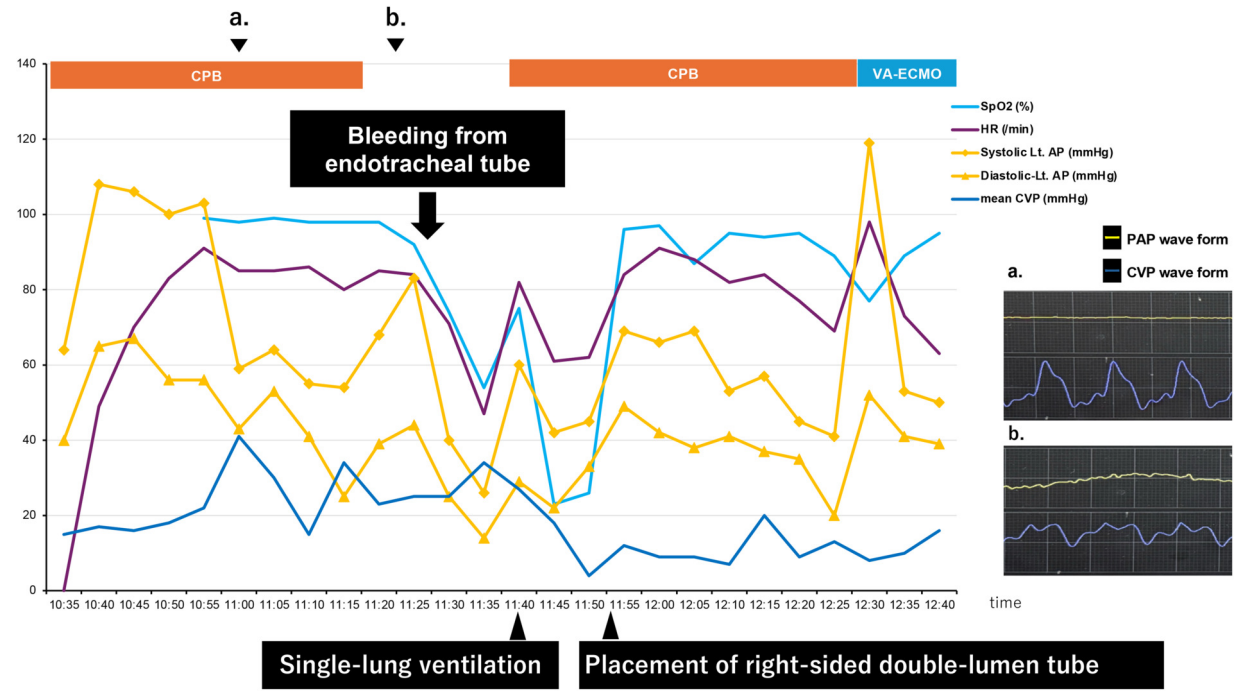

FIGURE 1
Timeline.

anesthesia time was 7 h and 8 min; surgical duration was 5 h and 50 min; and estimated blood loss was 5,815 ml, including approximately 3,000 ml from ETT bleeding. Postoperative coagulation status was corrected with transfusions, electrolytes, and coagulation factors. Hemostasis was achieved within 3 h after ICU admission.

2.4 Follow-up and outcomes

Within the first postoperative day, the patient was successfully weaned off VA-ECMO with stable hemodynamics. However, intermittent decline in oxygenation was observed due to persistent minor tracheal bleeding and blood clots causing bronchial obstruction. On postoperative day 7, pulmonary artery angiography revealed a pseudoaneurysm in the right middle lobe branch and surrounding atelectasis (Figure 2). Coil embolization was performed successfully, resolving the pseudoaneurysm and preventing further bleeding (Figure 3). Following embolization, the tracheal bleeding was resolved, and the patient's respiratory condition improved gradually. A tracheostomy was required on postoperative day 11 due to prolonged intubation. No additional surgical complications were found.

3 Discussion

We report a case of pulmonary artery injury associated with PAC use, which resulted in intratracheal bleeding of 3,000 ml after weaning from CPB. The condition was successfully managed without the need for pulmonary resection, through comprehensive management including reinstitution of CPB to stabilize hemodynamics and limit pulmonary blood flow, placement of a right-sided double-lumen tube to compress the injured site and protect the contralateral lung, and coil embolization of a pseudoaneurysm.

Massive intratracheal bleeding during cardiac surgery is rare but carries a high risk of mortality. The causes can be categorized into three main types: underlying pulmonary disease, surgical trauma, and PAC-related injury. In this case, surgical exploration under bloodless conditions during CPB detected no surgical trauma, visceral pleural injury, and hematoma. When pulmonary blood flow was restricted, adjustment of the single-lumen ETT from a bilateral ventilation position to a single-lung ventilation position revealed active bleeding from the right lung. Prior to CPB weaning, a flattened PAP waveform and a CVP waveform indicative of right ventricular pressure suggested that the PAC had migrated too distally during CPB. These clinical findings strongly suggested PAC-induced pulmonary artery injury, particularly given that over 90% of such injuries originate from the right lung (7).

PAC-related pulmonary artery injury is a rare complication, with an incidence of 0.1%–0.8% (7). Although the extent of bleeding varies, the reported mortality rate is as high as 45%–60% (7). Risk factors include advanced age, female sex, pulmonary hypertension, hypothermia-induced catheter stiffness, over-insertion, and anticoagulation therapy (7, 8). Especially, deeper hypothermia may further increase PAC stiffness, leading

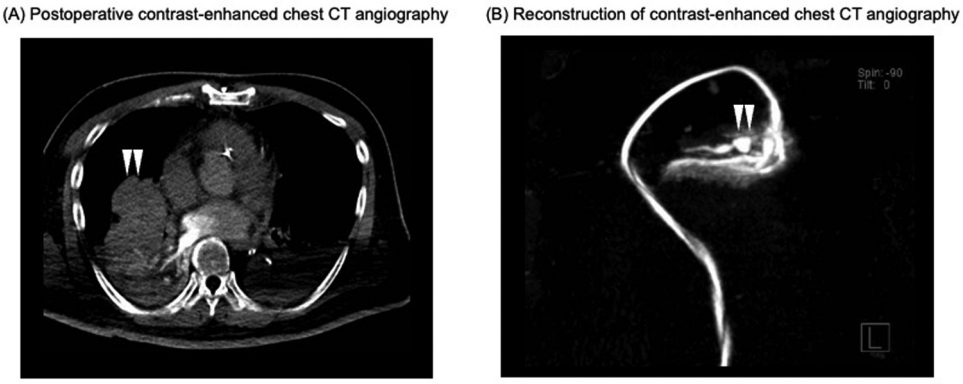

FIGURE 2
Postoperative contrast-enhanced chest CT angiography on POD 7. **(A)** Postoperative contrast-enhanced chest CT angiogram. The white arrows indicate atelectasis surrounding a pseudoaneurysm in the right middle lobe branch. **(B)** Reconstruction of contrast-enhanced chest CT angiogram at the site of the pseudoaneurysm and surrounding vessels. The white arrows indicate the site of the pseudoaneurysm. CT, computed tomography; POD, postoperative day.

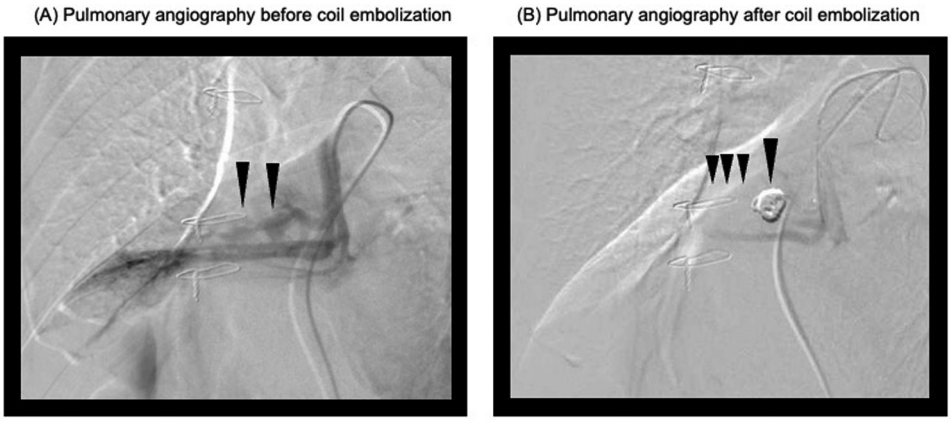

FIGURE 3
Pulmonary angiograms before and after coil embolization. **(A)** Pulmonary angiogram before coil embolization. The black arrows indicate the target pulmonary artery branch planned for embolization. **(B)** Pulmonary angiogram after coil embolization. The black arrows indicate the successfully occluded pulmonary artery branch.

to a higher risk of PAC-induced pulmonary artery injury (9). In the present case, hypothermia and over-insertion likely contributed to the complication. Furthermore, several mechanisms for PAC-induced pulmonary artery injury have been proposed, including balloon overinflation, eccentric balloon inflation caused by damage to the catheter tip, peripheral wedging of the catheter tip, and rapid distal migration with catheter tip impact leading to pulmonary artery trauma. Preventive methods include withdrawing the catheter by 3–5 cm after insertion and prior to CPB initiation, limiting balloon inflation, avoiding inflation during wedging, and positioning the PAC near the proximal pulmonary artery (8). The importance of appropriately positioning the PAC in the proximal right pulmonary artery under TEE guidance has been well discussed in previous studies. Adding pressure waveform analysis can further enhance the accuracy of catheter placement (10, 11). In the present case, the PAC was advanced into the pulmonary artery under TEE guidance, and its position was adjusted by monitoring the pressure waveform. Once the catheter reached the wedge position, it was withdrawn by 3 cm while monitoring the pressure waveform and secured at 55 cm. To ensure appropriate placement, it would have been preferable to confirm the catheter balloon's position in the proximal right pulmonary artery under TTE guidance after identifying the wedge position and gradually withdrawing the catheter. This adjustment could have also helped eliminate slack in the catheter. If slack had remained in the PAC, the slack itself might have contributed to unintended distal migration of the catheter. In such a case, the catheter could have been fixed at the superior vena cava by the venous cannulation tourniquet, and intracardiac collapse or surgical manipulation

TABLE 1 Demographics, clinical course, and outcome of the reviewed cases.

First author (year)	No. of cases	Age and sex	Risk factors*	Indications for PAC	Onset timing of PA injury symptoms	MCS device use	Initial evidence of PA injury	Duration between PAC insertion and initial evidence of PA injury (days)	Site of pseudo-aneurysm	Treatment	Outcome	References No.
De Lima (1994)	1	76F	1,2,3	MVR	On weaning from CPB	-	Hemoptysis	0	RML	No treatment	Discharged	(8)
Cicenia (1996)	1	69F	1,2	CABG	No trigger	-	Hemoptysis	0	RUL	Coil embolization	Discharged	(9)
Feritti (1996)	5	69M	NA	CABG	NA	-	Hemoptysis	5	RLL	Coil embolization	Discharged	(10)
		74F	NA	CABG	NA	-	Hemoptysis	19	RML	Coil embolization	Discharged	(10)
		75F	NA	MVR	NA	-	Hemoptysis	0	RML	Coil embolization	Discharged	(10)
		81F	NA	CABG	NA	-	Hemoptysis	0	RML	Coil embolization	Discharged	(10)
		67F	NA	CABG	NA	-	Hemoptysis	2	RLL	Coil embolization	Discharged	(10)
Mullerworth (1998)	3	83F	NA	CABG	On weaning from CPB	-	Hemoptysis	0	NA	No treatment	Discharged	(11)
		84F	NA	AVR	Continuous wedged	-	Hemoptysis	2	NA	NA	Died from exsanguination	(11)
		71F	NA	CABG	On weaning from CPB	ECMO	Hemoptysis, hypotension, hypoxemic	0	RML	PAC withdrawn only	Discharged	(11)
Laureys (2004)	1	75F	1,2,4	AVR + MVR	Thoracic closure	-	Hypotension, CXR	0	RML	Coil embolization	Discharged	(12)
Sidery (2004)	1	71F	1,2,4	CABG	No trigger	-	CXR	10	RLL	No treatment	Discharged	(13)
Bossert (2006)	2	64M	no	CABG	PCWP measurement	-	Hemoptysis	0	RLL	Intraluminal vasopressin and assisted ventilation with PEEP of 15 cm H_2O	Discharged	(14)
		80F	1,2	CABG	NA	-	VF, Hemoptysis	0	RML	Lobectomy	Discharged	(14)
Bianchini (2007)	1	75F	1,2	AVR + MVR	After weaning from CPB	ECMO/ IABP	Hypotension, Hypoxia, Hemoptysis	0	RLL	Coil embolization	Discharged	(15)
Burrel (2010)	3	77M	no	AVR	No trigger	-	Hemoptysis	1	RML	Plug	Discharged	(16)
		75F	1,2,3,4	AVR + MVR	No trigger	-	Hemoptysis	14	RML	Plug	Died from cerebral hematoma	(16)
		77F	1,2,3	AVR + MVR	No trigger	-	Hemoptysis	1	RML	Plug	Discharged	(16)
Rudziński (2016)	2	55M	NA	AVR	No trigger	-	Hemoptysis	7	RLL	Coil embolization	Discharged	(17)
		68M	NA	AVR	No trigger	-	CXR	0	RLL	Plug	Discharged	(17)
Russo (2024)	1	82F	1,2	MVR + TVR	Balloon deflation		Hemoptysis	0	RML	Coil embolization	Discharged	(18)

MVR, mitral valve replacement; CABG, coronary artery bypass graft; AVR, aortic valve replacement; TVR, tricuspid valve replacement; CPB, cardiopulmonary bypass; NA, data not applicable; ECMO, extracorporeal membrane oxygenation; IABP, intra-aortic balloon pumping; CXR, chest x-ray; VF, ventricular fibrillation; RML, right middle lobe; RUL, right upper lobe; RLL, right lower lobe; PAC, pulmonary artery catheter; PEEP, Positive End-Expiratory Pressure.

*Risk factors: 1. age > 60 years, 2. female sex, 3. pulmonary hypertension, 4. systemic anticoagulation, 5. long-term steroid use, and 6. surgically induced hypothermia.

10.3389/fcvm.2025.1567723

might have caused it to advance further into the pulmonary artery. Furthermore, verifying the absence of slack during initial placement using C-arm fluoroscopy, or withdrawing the PAC by approximately 3 cm after CPB initiation, might have helped prevent this advancement.

Prior to CPB weaning, the PAC was found to have migrated deeper from 55 to 56 cm, prompting an attempt to reposition it by withdrawing to 30 cm. However, proper waveforms could not be obtained. This observation suggests that the catheter tip had advanced distally during CPB, potentially causing trauma to the pulmonary artery. Examination of the PAC upon removal showed no damage, suggesting that the injury was caused by the catheter tip impacting the distal pulmonary artery wall.

Management of massive intratracheal bleeding begins with securing ventilation. Minor bleeding can be effectively managed with frequent suctioning. However, significant bleeding requires a more aggressive approach, including isolation of the injured lung and protection of the unaffected lung using a bronchial blocker or DLT. In cases of massive intratracheal bleeding, such as the 3,000 ml volume in the present case, identifying the affected lung can be challenging. Restricting pulmonary blood flow may facilitate identification of the affected lung and subsequent protection. Approximately 65% of PAC-related pulmonary artery injuries occur during CPB weaning (8), whereas symptoms appeared after CPB weaning in the present case. We reinstituted CPB to restrict pulmonary blood flow and adjusted the single-lumen ETT to provide single-lung ventilation, allowing bronchoscopic identification of the affected lung. A right-sided DLT was then positioned distal to the right upper lobe branch, achieving targeted isolation and tamponade of the injured area and simultaneously ensuring adequate ventilation. To prevent alveolar collapse in the unaffected lung while oxygenation and ventilation were supported by CPB, PEEP was maintained at 10 cmH_2O and recruitment maneuvers were applied using an airway pressure of 30 cmH_2O sustained for 10 s.

While emergency pulmonary resection is an option for uncontrolled massive intratracheal bleeding, the procedure is associated with increased mortality during cardiac surgery (7). After consultation with the thoracic surgery team, we determined that resection was not warranted, as there was no evidence of diffuse parenchymal hemorrhage, visceral pleural rupture, or central pulmonary artery damage. Active bleeding subsided within three hours postoperatively, permitting bilateral lung ventilation and VA-ECMO removal on postoperative day 1. Postoperative rebleeding is reported in 45% of cases within 48 h to 14 days. In the present case, despite frequent suctioning and hemostatic management, minor hemoptysis persisted, and intermittent hypoxemia occurred during position changes. Pulmonary angiography on postoperative day 7 revealed a pseudoaneurysm in the right middle lobe branch and surrounding atelectasis, which was successfully treated with coil embolization.

We conducted a literature search and reviewed all reported cases of PAC-induced pulmonary artery injury published between 1990 and 2024 (Table 1) (12–22). A comprehensive search on PubMed® used the keywords "pulmonary artery catheter," "Swan-Ganz catheter," "cardiac surgery," "complications," "pulmonary artery rupture," "pulmonary artery injury," "intrapulmonary artery injury," "vascular perforation," and "hemorrhage". All the identified review articles, randomized-control trials and metanalysis were hand-searched for additional references, and reference lists for identified studies were snowballed for additional articles (1, 2, 23, 24). As a result, 23 articles were identified. After excluding duplicates, non-English publications, and inaccessible full-text articles, 11 articles documenting 21 cases were reviewed. The patient population consisted of 16 females aged between 67 and 84 years (mean: 76 years) and 5 males aged between 55 and 77 years (mean: 67 years). The surgeries comprised 11 valve replacements and 10 CABG procedures. Hemoptysis was the initial sign of injury in 86% of the cases, and most pseudoaneurysms (90%) were located in the right pulmonary artery. Coil embolization was the most common treatment (48%), with surgical intervention required in one case. Mortality was reported in two cases. The present case uniquely occurred after CPB weaning, whereas most injuries in the review occurred during CPB weaning (33%). Furthermore, although the literature review identified only two cases in which MCS was used, this case highlights the effectiveness of pulmonary blood flow restriction via CPB resumption in controlling massive intratracheal bleeding and facilitating the identification of the injury site. These findings highlight the unique aspects of this case report and underscore the importance of vigilance throughout the perioperative period and the potential role of MCS in managing PAC-induced pulmonary artery injury.

4 Conclusion

We report a case of massive intratracheal bleeding caused by PAC-induced pulmonary artery injury, which was successfully managed through comprehensive treatment without the need for pulmonary resection. This case provides two important lessons. First, restricting pulmonary blood flow during massive intratracheal bleeding is effective not only for stabilizing hemodynamic but also for identifying the cause and site of injury. Second, precise localization and control of the injured area combined with a multidisciplinary approach to comprehensive management can avoid pulmonary resection and achieve successful outcomes. We hope this report serves as a valuable reference for the management of similar complications in the future.

Data availability statement

The original contributions presented in the study are included in the article/Supplementary Material, further inquiries can be directed to the corresponding author.

Ethics statement

The requirement of ethical approval was waived by ethics committee of Shonan Kamakura General Hospital for the studies involving humans because ethics committee of Shonan Kamakura General Hospital. The studies were conducted in accordance with the local legislation and institutional requirements. The participants provided their written informed consent to participate in this study. Written informed consent was obtained from the individual(s) for the publication of any potentially identifiable images or data included in this article.

Author contributions

YN: Conceptualization, Data curation, Formal analysis, Investigation, Methodology, Project administration, Writing – original draft, Writing – review & editing. KS: Conceptualization, Funding acquisition, Investigation, Supervision, Writing – original draft, Writing – review & editing. SH: Data curation, Methodology, Writing – original draft, Writing – review & editing. YM: Data curation, Methodology, Writing – original draft, Writing – review & editing. TY: Data curation, Methodology, Writing – original draft, Writing – review & editing. TO: Supervision, Writing – original draft, Writing – review & editing.

Funding

The author(s) declare that financial support was received for the research and/or publication of this article. The comprehensive literature search in this report was partly supported by the Intramural Research Fund for Cardiovascular Diseases of National Cerebral and Cardiovascular Centre (24-B-7) and the research program of the Japan Agency for Medical Research and Development (24uk1024007h0003/25uk1024007h0004).

Acknowledgments

We would like to express our gratitude to Dr, Motoki Nagatsuka for their invaluable contributions to the surgical procedure. We also thank Teresa Nakatani for their assistance in proofreading and English language editing.

Conflict of interest

KS received research funding from Abiomed Inc., NTT Research, Inc., Asahi Kasei ZOLL Medical Corporation, Neuroceuticals Inc., and Zeon Medical Inc., and honoraria from Abiomed Japan KK and Mallinckrodt Pharma KK.

The remaining authors declare that the research was conducted in the absence of any commercial or financial relationships that could be construed as a potential conflict of interest.

Generative AI statement

The author(s) declare that no Generative AI was used in the creation of this manuscript.

Publisher's note

References

1. Binanay C, Califf RM, Hasselblad V, O'Connor CM, Shah MR, Sopko G, et al. Evaluation study of congestive heart failure and pulmonary artery catheterization effectiveness: the ESCAPE trial. *JAMA*. (2005) 294:1625–33. doi: 10.1001/jama.294.13.1625

2. Sandham JD, Hull RD, Brant RF, Knox L, Pineo GF, Doig CJ, et al. A randomized, controlled trial of the use of pulmonary-artery catheters in high-risk surgical patients. *N Engl J Med*. (2003) 348:5–14. doi: 10.1056/NEJMoa021108

3. Garan AR, Kanwar M, Thayer KL, Whitehead E, Zweck E, Hernandez-Montfort J, et al. Complete hemodynamic profiling with pulmonary artery catheters in cardiogenic shock is associated with lower in-hospital mortality. *JACC Heart Failure*. (2020) 8:903–13. doi: 10.1016/j.jchf.2020.08.012

4. Judge O, Ji F, Fleming N, Liu H. Current use of the pulmonary artery catheter in cardiac surgery: a survey study. *J Cardiothorac Vasc Anesth*. (2015) 29:69–75. doi: 10.1053/j.jvca.2014.07.016

5. Brovman EY, Gabriel RA, Dutton RP, Urman RD. Pulmonary artery catheter use during cardiac surgery in the United States, 2010 to 2014. *J Cardiothorac Vasc Anesth*. (2016) 30:579–84. doi: 10.1053/j.jvca.2015.11.012

6. Joseph C, Garrubba M, Smith JA, Melder A. Does the use of a pulmonary artery catheter make a difference during or after cardiac surgery? *Heart Lung Circ*. (2018) 27:952–60. doi: 10.1016/j.hlc.2018.02.004

7. Urschel JD, Myerowitz PD. Catheter induced pulmonary artery rupture in the setting of cardiopulmonary bypass. *Ann Thorac Surg*. (1993) 56:585–9. doi: 10.1016/0003-4975(93)90912-2

8. Kearney TJ, Shabot MM. Pulmonary artery rupture associated with the swan-ganz catheter. *Chest*. (1995) 108:1349–52. doi: 10.1378/chest.108.5.1349

9. Cohen JA, Blackshear RH, Gravenstein N, Woeste J. Increased pulmonary artery perforating potential of pulmonary artery catheters during hypothermia. *J Cardiothorac Vasc Anesth*. (1991) 5:234–6. doi: 10.1016/1053-0770(91)90280-7

10. Cronin B, Robbins R, Maus T. Pulmonary artery catheter placement using transesophageal echocardiography. *J Cardiothorac Vasc Anesth*. (2017) 31:178–83. doi: 10.1053/j.jvca.2016.07.012

11. Cronin B, Kolotiniuk N, Youssefzadeh K, Newhouse B, Schmidt U, O'Brien EO, et al. Pulmonary artery catheter placement aided by transesophageal echocardiography versus pressure waveform transduction. *J Cardiothorac Vasc Anesth*. (2018) 32:2578–82. doi: 10.1053/j.jvca.2018.05.018

12. DeLima LG, Wynands JE, Bourke ME, Walley VM. Catheter-induced pulmonary artery false aneurysm and rupture: case report and review. *J Cardiothorac Vasc Anesth*. (1994) 8:70–5. doi: 10.1016/1053-0770(94)90016-7

13. Cicenia J, Shapira N, Jones M. Massive hemoptysis after coronary artery bypass grafting. *Chest*. (1996) 109:267–70. doi: 10.1378/chest.109.1.267

14. Ferretti GR, Thony F, Link KM, Durand M, Wollschläger K, Blin D, et al. False aneurysm of the pulmonary artery induced by a swan-ganz catheter: clinical presentation and radiologic management. *AJR Am J Roentgenol*. (1996) 167:941–5. doi: 10.2214/ajr.167.4.8819388

15. Mullerworth MH, Angelopoulos P, Couyant MA, Horton AM, Robinson SM, Petring OU, et al. Recognition and management of catheter-induced pulmonary artery rupture. *Ann Thorac Surg*. (1998) 66:1242–5. doi: 10.1016/s0003-4975(98)00593-1

16. Laureys M, Golzarian J, Antoine M, Desmet JM. Coil embolization treatment for perioperative pulmonary artery rupture related to swan-ganz catheter placement. *Cardiovasc Intervent Radiol*. (2004) 27:407–9. doi: 10.1007/s00270-004-0164-8

17. Sidery M, Cahir J, Screaton NJ, Vuylsteke A. Computed tomography reveals an unusual complication in a patient having undergone coronary artery bypass surgery. *J Cardiothorac Vasc Anesth*. (2004) 18:668–70. doi: 10.1053/j.jvca.2004.07.020

18. Bossert T, Gummert JF, Bittner HB, Barten M, Walther T, Falk V, et al. Swan-Ganz catheter-induced severe complications in cardiac surgery: right ventricular perforation, knotting, and rupture of a pulmonary artery. *J Card Surg*. (2006) 21:292–5. doi: 10.1111/j.1540-8191.2006.00235.x

19. Bianchini R, Melina G, Benedetto U, Rossi M, Fiorani B, Iasenzaniro M, et al. Extracorporeal membrane oxygenation for Swan-Ganz induced intraoperative hemorrhage. *Ann Thorac Surg*. (2007) 83:2213–4. doi: 10.1016/j.athoracsur.2007.01.023

20. Burrel M, Real MI, Barrufet M, Arguis P, Sánchez M, Berrocal L, et al. Pulmonary artery pseudoaneurysm after swan-ganz catheter placement: embolization with vascular plugs. *J Vasc Interv Radiol*. (2010) 21:577–81. doi: 10.1016/j.jvir.2009.12.399

21. Rudziński PN, Henzel J, Dzielińska Z, Lubiszewska BM, Michałowska I, Szymański P, et al. Pulmonary artery rupture as a complication of swan-ganz catheter application. Diagnosis and endovascular treatment: a single centre's experience. *Postepy Kardiol Interwencyjnej*. (2016) 12:135–9. doi: 10.5114/aic.2016.59364

22. Russo R, Calzolari A, Salice V, Micieli C, Castiglioni C, Gomarasca M, et al. Pulmonary artery pseudoaneurysm due to pulmonary artery catheter placement: a new minimally invasive approach to solve a life-threatening complication. *J Cardiothorac Vasc Anesth*. (2025) 39:215–9. doi: 10.1053/j.jvca.2024.10.017

23. Rong LQ, Luhmann G, Di Franco A, Dimagli A, Perry LA, Martinez AP, et al. Pulmonary artery catheter use and in-hospital outcomes in cardiac surgery: a systematic review and meta-analysis. *Interdiscip Cardiovasc Thorac Surg*. (2024) 39: ivae129. doi: 10.1093/icvts/ivae129

24. Nellaiyappan M, Omar HR, Justiz R, Sprenker C, Camporesi EM, Mangar D. Pulmonary artery pseudoaneurysm after swan-ganz catheterization: a case presentation and review of literature. *Eur Heart J Acute Cardiovasc Care*. (2014) 3:281–8. doi: 10.1177/2048872613520252

frontiers | Frontiers in Cardiovascular Medicine

TYPE Original Research
PUBLISHED 29 April 2025
DOI 10.3389/fcvm.2025.1538395

OPEN ACCESS

EDITED BY
Keita Saku,
National Cerebral and Cardiovascular Center, Japan

REVIEWED BY
Toshinobu Kazui,
University of Arizona Medical Center, United States
Andrea Farina,
Alessandro Manzoni Hospital, Italy
Shuai Fu,
Wuhan First Hospital, China

*CORRESPONDENCE
Meilin Liu
✉ liumeilin@pku.edu.cn

RECEIVED 02 December 2024
ACCEPTED 04 April 2025
PUBLISHED 29 April 2025

CITATION
Fang D, Chen H, Geng H, Chen X and Liu M (2025) Development and validation of a nomogram for predicting survival in patients with cardiogenic shock.
Front. Cardiovasc. Med. 12:1538395.
doi: 10.3389/fcvm.2025.1538395

Development and validation of a nomogram for predicting survival in patients with cardiogenic shock

Dingfeng Fang[1,2], Huihe Chen[3], Hui Geng[1], Xiahuan Chen[1] and Meilin Liu[1]*

[1]Department of Geriatrics, Peking University First Hospital, Beijing, China, [2]Peking University Health Science Center, Beijing, China, [3]Department of Sports Medicine and Cardiopulmonary Rehabilitation Center, Jiangbin Hospital of Guangxi Zhuang Autonomous Region, Nanning, China

Background: There is currently a lack of easy-to-use tools for assessing the severity of cardiogenic shock (CS) patients. This study aims to develop a nomogram for evaluating severity in CS patients regardless of the underlying cause.

Methods and results: The MIMIC-IV database was used to identify 1,923 CS patients admitted to the ICU. A multivariate Cox model was developed in the training cohort (70%) based on LASSO regression results. Factors such as age, systolic blood pressure, arterial oxygen saturation, hemoglobin, serum creatinine, blood glucose, arterial pH, arterial lactate, and norepinephrine use were incorporated into the final model. This model was visualized as a Cardiogenic Shock Survival Nomogram (CSSN) to predict 30-day survival rates. The model's c-statistic was 0.75 (95% CI: 0.73–0.77) in the training cohort and 0.73 (95% CI: 0.70–0.77) in the validation cohort, demonstrating good predictive accuracy. The AUC of the CSSN for 30-day survival probabilities was 0.76 in the training cohort and 0.73 in the validation cohort. Calibration plots showed strong concordance between predicted and actual survival rates, and decision curve analysis (DCA) affirmed the model's clinical utility. The CSSN outperformed the Cardiogenic Shock Score (CSS) in various metrics, including c-statistic, time-dependent ROC, calibration plots, and DCA (c-statistic: 0.75 vs. 0.72; AUC: 0.76 vs. 0.73, $P < 0.01$ by Delong test). Subgroup analysis confirmed the model's robustness across both AMI-CS and non-AMI-CS subgroups.

Conclusions: The CSSN was developed to predict 30-day survival rates in CS patients irrespective of the underlying cause, showing good performance and potential clinical utility in managing CS.

KEYWORDS

nomogram, survival, cardiogenic shock, mortality, mechanical circulatory support

Introduction

Cardiogenic shock (CS) is a life-threatening medical emergency with a high mortality rate of 40% to 60%, despite advancements in medical care, leading to prolonged suffering for affected patients and significant healthcare costs (1–4). The causes and severity of CS can vary widely, which results in different treatment approaches and prognoses (3, 5, 6). Early identification of high-risk patients can help promptly implement reasonable and practical treatment measures. Thus, assessing the severity of the condition is essential,

as it directly influences clinical decisions, such as whether to administer mechanical circulatory support (MCS). Several risk assessment tools for CS have been developed, with the most widely accepted being the IABP-SHOCK II Score (7), CardShock risk Score (8), and Cardiogenic Shock Score (CSS) (9). However, these models are primarily presented as scoring systems, which are relatively complex and thus less frequently used in clinical practice. Nomograms are graphical representations of mathematical models employed to forecast outcomes by assessing clinical events and incorporating key prognostic factors across various diseases (10, 11). They offer intuitive, fast, straightforward, and user-friendly advantages. Currently, no predictive model for CS uses a nomogram presentation available for clinical use.

Moreover, the SHOCK II Score and CardShock Risk Score mainly target the AMI-CS population, which may not apply to non-AMI-CS patients. Recent epidemiological studies have found that AMI as a cause of CS has decreased to approximately 30%, indicating that AMI is no longer the predominant cause of cardiogenic shock (3, 12). The Society for Cardiovascular Angiography and Intervention (SCAI) classification appears to be the most widely used risk assessment tool, but it is more focused on staging the progression of CS rather than providing a specific and easy-to-use risk scoring system (6, 13). Given these reasons, our study aims to develop an easy-to-use predictive model for CS, irrespective of the underlying cause, in the emergency setting, which accounts for survival assessments. This model will be presented as a Cardiogenic Shock Survival Nomogram (CSSN) to enhance clinical applicability. The establishment of this model will aid physicians in timely assessing the severity of CS, thereby making appropriate clinical decisions to improve patient survival rates.

Methods

Data source and study participants

This study utilized the MIMIC-IV database, a comprehensive repository of critical care data (14–16). MIMIC-IV is a collection of clinical records from patients treated in intensive care units (ICU) at the Beth Israel Deaconess Medical Center. The first author of this study, Dingfeng Fang, has completed the Collaborative Institutional Training Initiative (CITI) program course of Massachusetts Institute of Technology Affiliates (Human Research, Data or Specimens Only Research, and Refresher Course), granting access to the MIMIC-IV database (Record ID: 50924352). Data retrieval from the database was conducted using Structured Query Language (SQL). For this study, all patients who experienced cardiogenic shock (CS) during their hospital stay and subsequently received further treatment in the ICU were included. Patients for this cohort were identified by querying the MIMIC-IV database for instances of the International Classification of Diseases, Ninth Revision (ICD-9) code 785.51, and the Tenth Revision (ICD-10) code R57.0, both denoting cardiogenic shock. To reduce survival and treatment biases caused by readmissions, only patients admitted to the ICU for the first time were included in the analysis.

Data collection

Demographic, vital signs, laboratory, clinical, and outcome data, procedures, and therapies performed during the ICU and hospital stay were collected from the MIMIC-IV database. Radiographic, invasive hemodynamic, and physical examination data were not available. Baseline characteristics included gender, age, admission diagnosis (CS, AMI), comorbidities (previous MI, hypertension, diabetes, renal impairment), and smoking history. Systolic blood pressure (SBP), diastolic blood pressure (DBP), mean arterial pressure (MAP), arterial oxygen saturation (SpO_2), and partial pressure of oxygen (PaO_2) were all recorded from the lowest values within the first 24 h of admission. The serum creatinine level was recorded as the maximum value within the first 24 h of admission. Other laboratory tests were defined by the first recorded value after ICU admission or the value closest to ICU admission. Laboratory tests included blood assays (hemoglobin, leukocytes, platelets), arterial blood gas analysis [pH, PaO_2, partial pressure of carbon dioxide ($PaCO_2$), lactate, base excess, total carbon dioxide], coagulation profile, liver function, renal function, serum albumin, electrolyte measurements, blood glucose, low-density lipoprotein cholesterol (LDL-C), and cardiac enzymes [troponin T, N-terminal pro-b-type natriuretic peptide (NT-proBNP)]. Critical respiratory and cardiovascular treatments administered to the patients, such as norepinephrine, dopamine, dobutamine, epinephrine infusions, invasive mechanical ventilation, IABP, and continuous renal replacement therapy (CRRT), were also recorded. The primary outcome was all-cause mortality within 30 days. The database determined the date of death based on state records and hospital documentation. In cases where data from both sources are available, the hospital records take precedence (14–16). All patients had access to complete follow-up data for one year. Survival duration was calculated from the time of hospital admission until death.

Statistical analysis

Data analysis was performed using R version 4.3.3. A significance level of less than 0.05 was considered statistically significant for all analyses. Variables with more than 20% missing values were excluded. For variables with less than 20% missing values, missing data were imputed using multiple imputations with random forests, implemented through the mice package in R. The data were randomly split into training (70%)

Abbreviations

CS, cardiogenic shock; CSS, cardiogenic shock score; CSSN, cardiogenic shock survival nomogram; CRRT, continuous renal replacement therapy; LASSO, least absolute shrinkage and selection operator; MCS, mechanical circulatory support; MIMIC-IV, medical information mart for intensive Care IV; SCAI, society for cardiovascular angiography and intervention.

and validation (30%) sets for subsequent analysis. Continuous variables were reported as the median and interquartile range (IQR), while categorical variables were presented as frequencies and percentages. Differences between groups were compared using chi-square tests for categorical variables and Wilcoxon rank-sum tests for continuous variables.

In the training cohort, LASSO regression was employed to identify predictors of 30-day mortality in patients with CS. Potential variables for model construction were based on readily available point-of-care parameters and previous studies. The most parsimonious set of variables selected by LASSO regression was used to develop a multivariate Cox proportional hazards model. Multicollinearity was evaluated using the variance inflation factor (VIF). Harrell's Concordance Index (c-statistic) assessed the model's predictive accuracy. Factors with prognostic significance in the multivariate Cox regression analysis were used to construct 30-day survival prediction models (1—mortality), visualized using a nomogram. Factors with prognostic significance in the multivariate Cox regression analysis were used to construct 30-day survival prediction models (1—mortality), visualized using a nomogram. The nomogram predicted the 30-day mortality risk for all patients, categorizing them into four risk groups: low risk (0%–15%), moderate risk (16%–49%), high risk (50%–84%), and very high risk (85%–100%). These thresholds were determined based on the distribution of predicted probabilities in the training cohort. The Kaplan–Meier plotter was used to perform 1-year survival analysis for the four patient groups, which confirmed significant differences in survival outcomes across the four groups (Figure 2).

Time-dependent Receiver Operating Characteristic (ROC) curves and Area Under the Curve (AUC) were used to evaluate the discriminative power of the nomogram. The DeLong test is used to compare the discriminatory performance between models. Calibration curves assessed the difference between the actual and nomogram-predicted event-free survival rates using bootstrap (500 resamplings). The multivariate Cox proportional hazards model was similarly established in the validation cohort, and the c-statistic was calculated to evaluate its predictive accuracy. In the validation cohort, the performance of the nomogram was similarly evaluated using ROC curves, AUC, and calibration curves. Finally, decision curve analysis (DCA) was conducted to evaluate the clinical utility of the prediction models over 30 days. DCA assesses the net benefit across a range of threshold probabilities, comparing the benefits of correctly identifying high-risk patients with the harms of unnecessary interventions in low-risk patients, helping to determine the optimal decision threshold. Additionally, this study compared the accuracy and discrimination of our model with that of the Cardiogenic Shock Score (CSS).

Subgroup analysis were conducted in two ways: (1) performing multivariate Cox regression analysis using the variables from the nomogram on all AMI-CS patients and calculating the c-statistic and AUC to evaluate the predictive accuracy in AMI-CS patients; (2) performing multivariate Cox regression analysis using the variables from the nomogram on all non-AMI-CS patients and calculating the c-statistic and AUC to evaluate its predictive accuracy in non-AMI-CS patients.

Results

Study population and baseline characteristics

A total of 2,216 patients with admission diagnosis of CS based on ICD-9 code 785.51 and ICD-10 code R57.0. Of these, 152 were readmissions, and 141 did not require ICU admission; these patients were excluded from this study. The final cohort included 1,923 patients, with 1,346 randomly assigned to the training cohort and 577 to the validation cohort. Variables with over 20% missing data (albumin, troponin T, NT-proBNP, D-dimer, and LDL-C) were excluded. Variables with less than 20% missing data were imputed using the "mice" package in R, utilizing random forest-based multiple imputation, resulting in 89 imputed datasets.

Of the 1,923 patients, the median age was 70 (IQR 60–79), and 40.46% were female. Acute myocardial infarction-related cardiogenic shock (AMI-CS) was present in 28.13% of patients. Medical history included 14.25% of patients with previous myocardial infarction, 26.94% with hypertension, 40.04% with diabetes, and 46.33% with renal impairment. During the first 24 h after ICU admission, the median minimum values for key vital signs were 79 mmHg (IQR 68.75–87) for SBP and 91% (IQR 87%–94%) for SpO2. Abnormal laboratory findings included a median, minimum oxygen partial pressure of 46 mmHg (IQR 33–79), a median maximum serum creatinine of 159.12 μmol/L (IQR 106.08–247.52), and a median arterial lactate level of 3.3 mmol/L (IQR 1.90–6.40 mmol/L). Arterial blood gas pH was below 7.0 in 81 patients (4.21%).

Treatment and outcome

As shown in Table 1, patients received various treatments during hospitalization, including vasopressors, respiratory and circulatory support, and renal replacement therapy. Treatments included dopamine ($n = 465$, 24.18%), dobutamine ($n = 481$, 25.01%), norepinephrine ($n = 1,351$, 70.25%), epinephrine ($n = 469$, 24.39%), intra-aortic balloon pump (IABP) ($n = 319$, 16.59%), mechanical ventilation ($n = 1,111$, 57.77%), and continuous renal replacement therapy (CRRT) ($n = 306$, 15.91%). During the one-month follow-up, 1,097 patients survived (57.05%), and 826 patients died (42.95%).

Predictor selection and nomogram construction

LASSO regression was used to identify predictors of 30-day mortality in CS patients from the training cohort (Supplementary Figure S1). Potential variables for model construction were based on readily available point-of-care parameters and previous studies, including gender, age, admission diagnosis of AMI, admission of cardiac arrest, comorbidities (previous MI,

10.3389/fcvm.2025.1538395

TABLE 1 Baseline characteristics, treatment, and outcomes of the study population.

Group	All	Training cohort	Validation cohort	P[a]
Number	1,923	1,346	577	
Age, year	70.00 (60.00–79.00)	70.00 (60.00–78.75)	71.00 (60.00–80.00)	0.179
Female	778 (40.46%)	540 (40.12%)	238 (41.25%)	0.644
Etiology				
AMI				0.712
non-AMI	1,382 (71.87%)	960 (71.32%)	422 (73.14%)	
NSTEMI	406 (21.11%)	289 (21.47%)	117 (20.28%)	
STEMI	135 (7.02%)	97 (7.21%)	38 (6.59%)	
Cardiac arrest, *n* (%)	238 (12.38%)	163 (12.11%)	75 (13.00%)	0.588
Comorbidities				
Previous MI, *n* (%)	274 (14.25%)	184 (13.67%)	90 (15.60%)	0.268
Hypertension, *n* (%)	518 (26.94%)	363 (26.97%)	155 (26.86%)	0.962
Diabetes, *n* (%)	770 (40.04%)	540 (40.12%)	230 (39.86%)	0.916
Renal impairment, *n* (%)	891 (46.33%)	619 (45.99%)	272 (47.14%)	0.642
Smoker, *n* (%)	206 (10.71%)	141 (10.48%)	65 (11.27%)	0.608
Vital signs				
SBP, mmHg	79.00 (68.75–87.00)	79.00 (68.12–87.00)	79.00 (69.00–87.00)	0.57
DBP, mmHg	39.00 (31.00–46.00)	39.75 (31.00–46.00)	39.00 (31.00–46.00)	0.675
MAP, mmHg	51.00 (42.00–59.00)	51.00 (42.00–59.00)	51.00 (42.00–58.50)	0.418
SpO2, %	91.00 (87.00–94.00)	92.00 (87.25–94.00)	91.00 (86.00–94.00)	0.105
GCS	15.00 (15.00–15.00)	15.00 (15.00–15.00)	15.00 (15.00–15.00)	0.759
Laboratory findings at admission				
Hemoglobin, g/dl	11.20 (9.50–12.85)	11.20 (9.60–12.90)	11.10 (9.30–12.80)	0.226
Aspartate aminotransferase, U/L	70.00 (32.00–245.00)	70.50 (32.00–238.00)	69.00 (32.00–270.00)	0.993
Alanine aminotransferase, U/L	45.00 (22.00–149.50)	45.00 (21.25–147.50)	44.00 (22.00–151.00)	0.869
Serum creatinine, umol/L	159.12 (106.08–247.52)	159.12 (106.08–238.68)	159.12 (106.08–247.52)	0.804
Serum sodium, mmol/L	138.00 (134.00–141.00)	138.00 (134.00–141.00)	137.00 (135.00–140.00)	0.662
Serum potassium, mmol/L	4.30 (3.80–4.80)	4.30 (3.80–4.80)	4.20 (3.80–4.80)	0.302
Serum calcium, mg/dl	8.50 (7.90–8.90)	8.50 (7.90–8.90)	8.50 (8.00–8.90)	0.925
Blood glucose				0.281
<11.1 mmol/L	1,452 (75.51%)	1,007 (74.81%)	445 (77.12%)	
≥11.1 mmol/L	471 (24.49%)	339 (25.19%)	132 (22.88%)	
Arterial blood gas				
pH				0.228
<7.0	81 (4.21%)	55 (4.09%)	26 (4.51%)	
7.0–7.35	1,310 (68.12%)	933 (69.32%)	377 (65.34%)	
>7.35	532 (27.67%)	358 (26.60%)	174 (30.16%)	
PaO_2, mmHg	46.00 (33.00–79.00)	46.00 (33.00–79.00)	47.00 (33.00–79.00)	0.833
$PaCO_2$, mmHg	40.00 (34.00–47.00)	41.00 (35.00–47.75)	39.00 (34.00–46.00)	0.049
lactate, mmol/L	3.30 (1.90–6.40)	3.40 (2.00–6.50)	3.00 (1.90–5.80)	0.068
Treatments				
Dopamine, *n* (%)	465 (24.18%)	318 (23.63%)	147 (25.48%)	0.385
Dobutamine, *n* (%)	481 (25.01%)	356 (26.45%)	125 (21.66%)	0.026
Norepinephrine, *n* (%)	1,351 (70.25%)	960 (71.32%)	391 (67.76%)	0.118
Epinephrine, *n* (%)	469 (24.39%)	339 (25.19%)	130 (22.53%)	0.214
IABP, *n* (%)	319 (16.59%)	227 (16.86%)	92 (15.94%)	0.619
Invasive ventilation, *n* (%)	1,111 (57.77%)	792 (58.84%)	319 (55.29%)	0.148
CRRT, *n* (%)	306 (15.91%)	219 (16.27%)	87 (15.08%)	0.512
Outcomes				
Death during 1-month	826 (42.95%)	591 (43.91%)	235 (40.73%)	0.197
Death during 1-year	1,106 (57.51%)	776 (57.65%)	330 (57.19%)	0.852

[a]Comparison between the training and validation cohort.

Data are presented as median (interquartile range) unless otherwise indicated.

AMI, acute myocardial infarction; Previous MI, previous myocardial infarction; NSTEMI, non-ST-elevation myocardial infarction; STEMI, ST-elevation myocardial infarction; SBP, systolic blood pressure; DBP, diastolic blood pressure; MAP, mean arterial pressure; SPO_2, arterial oxygen saturation; GCS, Glasgow Coma Scale; PaO_2, Partial pressure of oxygen; $PaCO_2$, partial pressure of carbon dioxide; IABP, intra-aortic balloon pump; CRRT, continuous renal replacement therapy.

hypertension, diabetes, renal impairment), smoking history, SBP, heart rate, SpO_2, Glasgow Coma Scale (GCS), hemoglobin, alanine aminotransferase (ALT), aspartate aminotransferase (AST), serum creatinine, serum sodium, serum potassium, serum calcium, serum chloride, blood glucose, arterial blood gas (pH, partial pressure of oxygen, lactate), and treatments (dopamine, dobutamine, norepinephrine, epinephrine, IABP, invasive ventilation, CRRT). The lambda.1se ($\lambda = 0.0621$) was used to obtain the simplest model with nine predictors: Age, SBP, SpO_2, hemoglobin, serum creatinine, blood glucose, pH, arterial lactate, and norepinephrine. These predictors were used to develop a multivariate Cox proportional hazards model, and the result is shown in Table 2. Higher age, serum creatinine, blood glucose, arterial lactate, norepinephrine use, and lower SBP, SpO_2, hemoglobin, and pH were associated with increased mortality. Multicollinearity was assessed, and variance inflation factor (VIF) values were below the threshold, indicating no significant multicollinearity issues. The model demonstrated good discriminative ability, as evidenced by a c-statistic of 0.75 (95% CI: 0.73–0.77) and an area under the curve (AUC) of 0.76. Additionally, external validation using CSS data from the training set yielded a c-statistic of 0.72 (95% CI: 0.70–0.74) with an AUC of 0.73. A nomogram was constructed using the multivariate Cox model to predict 30 survival rates (1—mortality rate) (Figure 1).

The nomogram stratified all patients into four risk categories for 30-day mortality: low risk (0%–15%), moderate risk (16%–49%), high risk (50%–84%), and very high risk (85%–100%). Using Kaplan–Meier curves, a one-year survival analysis was conducted across these four groups, revealing significant differences in mortality within the first year (Figure 2).

Performance and validation of the model

The performance of the CSSN was evaluated using multiple metrics, including the c-statistic, AUC, calibration plots, and DCA. The c-statistic for the predictive model was 0.75 (95% CI: 0.73–0.77) in the training cohort and 0.733 (95% CI: 0.70–0.77) in the validation cohort, indicating good predictive accuracy. ROC curves for 30-day survival predictions yielded corresponding AUC values (Figure 3). In the training cohort, the AUC for CSSN predicting 30-day survival was 0.76, compared to 0.73 for the CSS. In the validation cohort, CSSN had an AUC of 0.73, while the CSS had an AUC of 0.72, demonstrating superior discriminative power by CSSN ($P < 0.01$ by Delong test). Calibration plots (Figure 4, panels A and B) revealed strong agreement between nomogram-predicted and actual survival probabilities, indicating better model calibration than CSS. DCA also demonstrated the superior performance of the CSSN over the CSS (Figure 5, panels A and B).

Subgroup analysis

Subgroup analysis were conducted to verify the robustness of the model, as detailed in Table 3: (1) In the subset of patients with AMI-CS, the model demonstrated a c-statistic of 0.77 (95% CI: 0.74–0.80) and an AUC of 0.77 for CSSN. (2) In the subset of non-AMI-CS patients, the model showed a c-statistic of 0.73 (95% CI: 0.71–0.76) and an AUC of 0.73 for CSSN. These analyses confirmed the predictive capability and reliability of the nomogram across different patient subsets, with the highest accuracy observed in patients with AMI-CS.

Discussion

In this study, we developed a predictive model for assessing the survival rates of CS patients at 30-day intervals to evaluate the risk of death. Our model, constructed using easily accessible variables from the emergency setting, demonstrated better performance than CSS. Visualized as a Cardiogenic Shock

TABLE 2 Multivariate Cox analysis of potential prognostic factors identified by LASSO regression.

Variables	VIF	Coefficients	HR (95%CI)	*P*
Age, year	1.042	0.031	1.032 (1.025, 1.039)	<0.0001
SBP, mmHg	1.285	−0.013	0.988 (0.982 0.993)	<0.0001
SpO_2, %	1.263	−0.013	0.987 (0.981, 0.993)	<0.0001
Hemoglobin, g/dl	1.019	−0.088	0.916 (0.871, 0.964)	0.0007
Serum creatinine, umol/L	1.096	0.001	1.001 (1.001, 1.002)	0.0024
Blood glucose	1.098			
<11.1 mmol/L		Reference		
≥11.1 mmol/L		0.406	1.501 (1.254, 1.796)	<0.0001
pH (Arterial blood gas)	1.455			
<7.1		Reference		
7.1–7.35		−0.731	0.481 (0.342, 0.677)	<0.0001
>7.35		−0.978	0.376 (0.249, 0.567)	<0.0001
Arterial lactate, mmol/L	1.657	0.059	1.061 (1.038, 1.084)	<0.0001
Norepinephrine	1.062	0.791	2.205 (1.747, 2.74)	<0.0001

This multivariate Cox proportional hazards model was performed to predict 30-day mortality in patients with CS in the training cohort ($N = 1,346$). The Harrell's concordance index (c-statistic) is 0.75 (95% CI: 0.73–0.77).

Multicollinearity among variables was evaluated by calculating the variance inflation factor (VIF). A VIF greater than 10 indicates the presence of multicollinearity.

HR, hazard ratio; CI, confidence interval; SBP, systolic blood pressure; SpO_2, peripheral oxygen saturation.

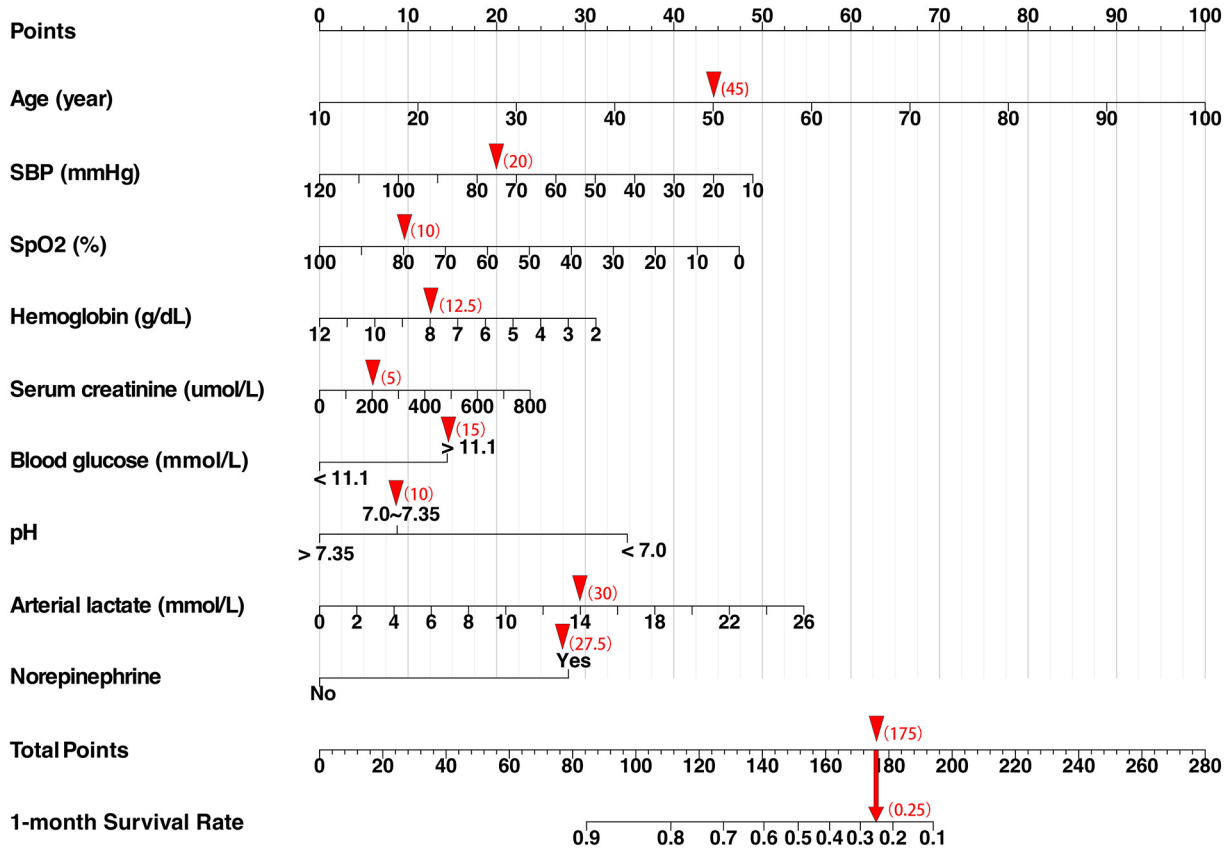

FIGURE 1
Cardiogenic shock survival nomogram (CSSN). The nomogram predicts the 30-day survival rates for patients with CS. SBP, systolic blood pressure; SpO_2, peripheral oxygen saturation. When using the nomogram, clinicians should locate the score for each patient's parameters on the corresponding axis, sum the scores of all variables to obtain the total score, and then determine the patient's 30-day survival probability based on the total score axis. For example, a male patient with acute myocardial infarction complicated by cardiogenic shock: Age: 50 years (score: 45), Initial arterial blood pressure: 75/54 mmHg (score: 20), SpO_2: 81% (score: 10), Hemoglobin: 7.7 g/dl (score: 12.5), Serum creatinine: 200.8 μmol/L (score: 5), Blood glucose: 13.5 mmol/L (score: 15), Arterial pH: 7.227 (score: 10), Arterial lactate: 14 mmol/L (score: 30), Norepinephrine use: yes (score: 27.5), Total score: 175 (30-day survival probability: 25%).

Survival Nomogram (CSSN), our model is simple and user-friendly. Furthermore, this is the first prognostic model for cardiogenic shock mortality risk presented as a nomogram, enhancing its clinical applicability and facilitating timely and appropriate clinical decision-making.

The importance of risk assessment in CS patients

Risk assessment in CS patients is crucial for guiding physicians in making more appropriate treatment strategies, particularly in deciding whether to use mechanical circulatory support (MCS). MCS can somewhat mitigate the issue of insufficient cardiac output in CS patients, but insufficient evidence remains to prove its efficacy in reducing mortality rates (2, 17–21). This is primarily due to the many complications associated with MCS use, such as vascular complications, thrombosis, limb ischemia, infection, and fatal hemorrhage (2, 20, 22). Inappropriate use of MCS can lead to an imbalance of risks and benefits. For example: (1) Using MCS in low-risk patients may alleviate their insufficient cardiac output, but its complications might outweigh the benefits, potentially reducing the patient's quality of life and survival rate. High-risk patients might be misclassified as low-risk, thereby missing the opportunity for timely MCS intervention, leading to adverse outcomes. (3) For patients with highly severe conditions (meager survival rates), using MCS may not provide enough survival benefits and could impose a heavy medical burden. Thus, timely and accurate risk assessment and appropriate treatment strategies are critical challenges clinicians face and are crucial to benefiting patients. The CSSN stratifies patients into four groups: low risk (0%–15% mortality), moderate risk (16%–49% mortality), high risk (50%–84% mortality), and very high risk (85%–100% mortality). This stratification may guide MCS decision-making as follows: (1) Low-risk patients: The complications of MCS may outweigh its benefits; thus, pharmacological support should be prioritized. (2) Moderate- to high-risk patients: Individualized assessment is required, integrating clinical context and hemodynamic status, as MCS may improve outcomes. (3) Very high-risk patients: MCS may

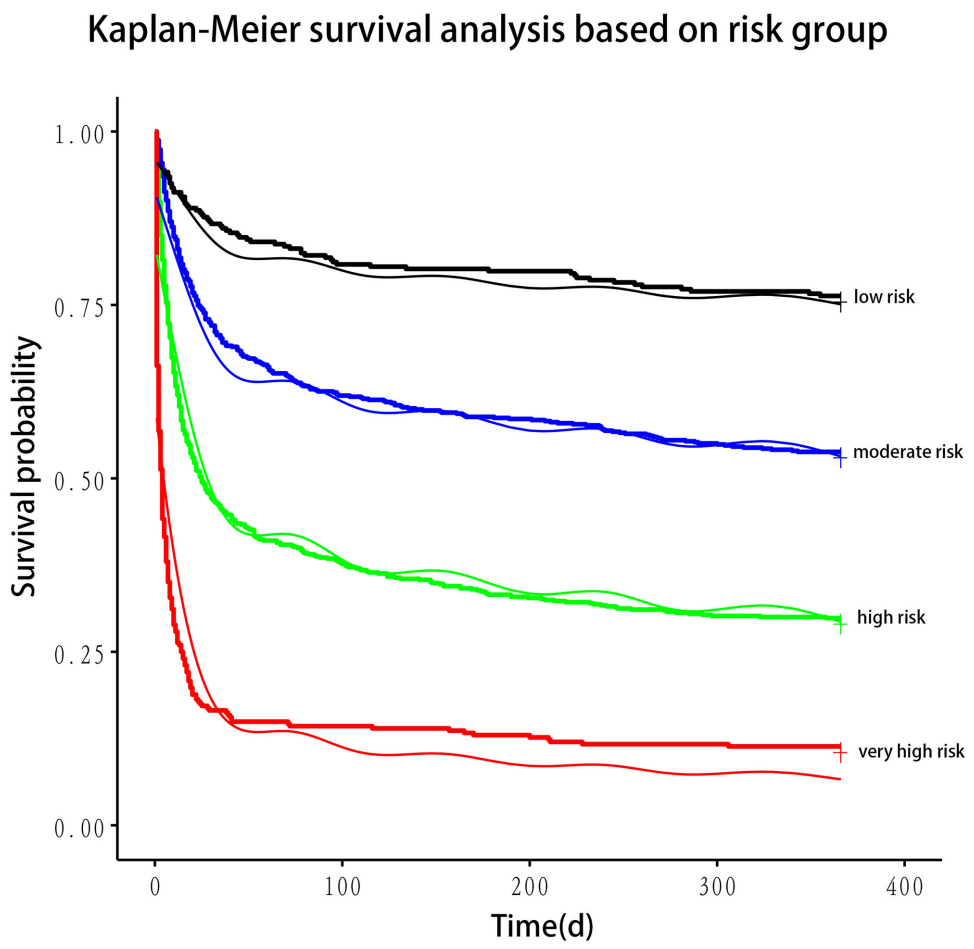

FIGURE 2
Kaplan–meier plotter for risk stratification based on nomogram.

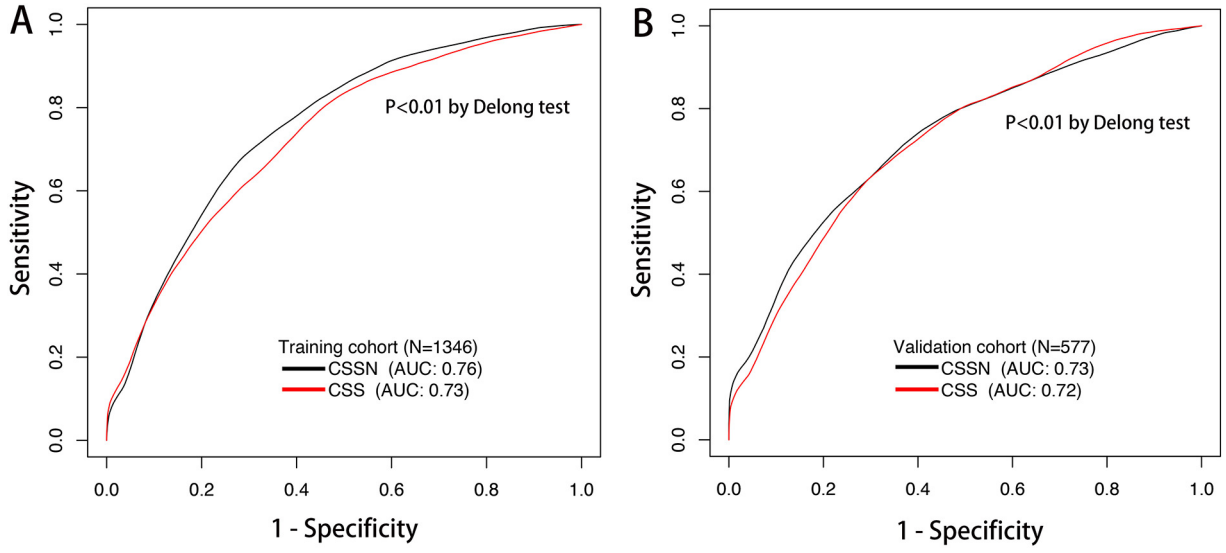

FIGURE 3
The time-dependent ROC curve and AUC of the CSSN and CSS in the training (Panel A) and validation (Panel B) cohorts. AUC, the area under the ROC curve; ROC, receiver operating characteristic; CSSN, cardiogenic shock survival nomogram; CSS, cardiogenic shock score.

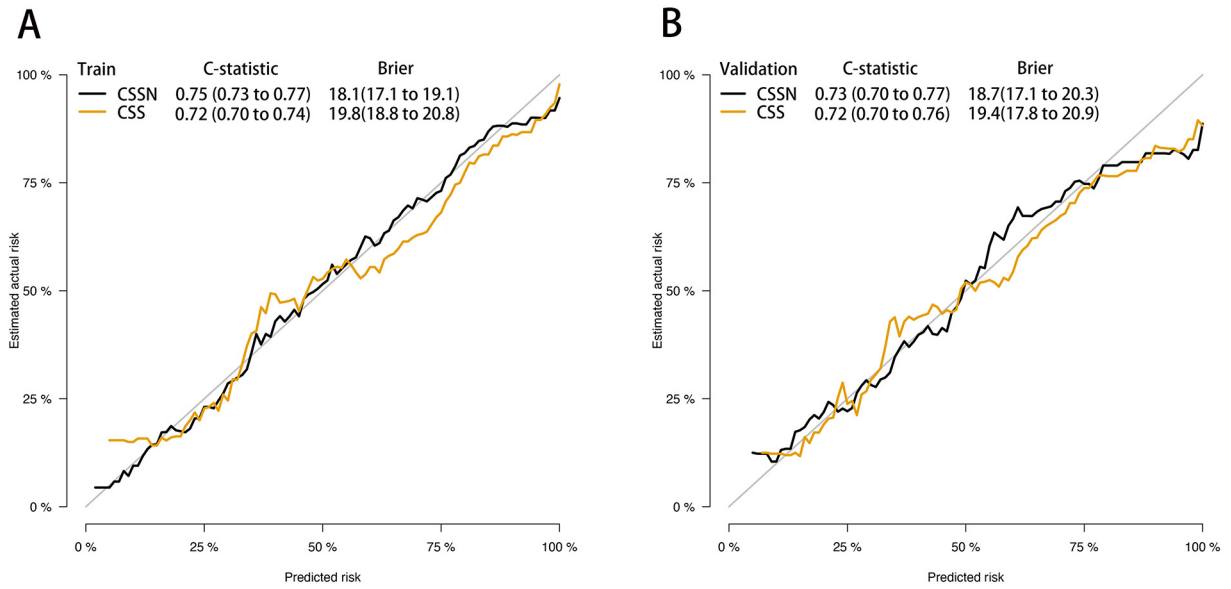

FIGURE 4
Calibration plot of the CSSN and CSS in the training and validation cohort. Panels **(A)** demonstrate the calibration plots for predicting 30-day survival in the training cohort, while panel **(B)** illustrates the calibration plots for predicting 30-day in the validation cohort.

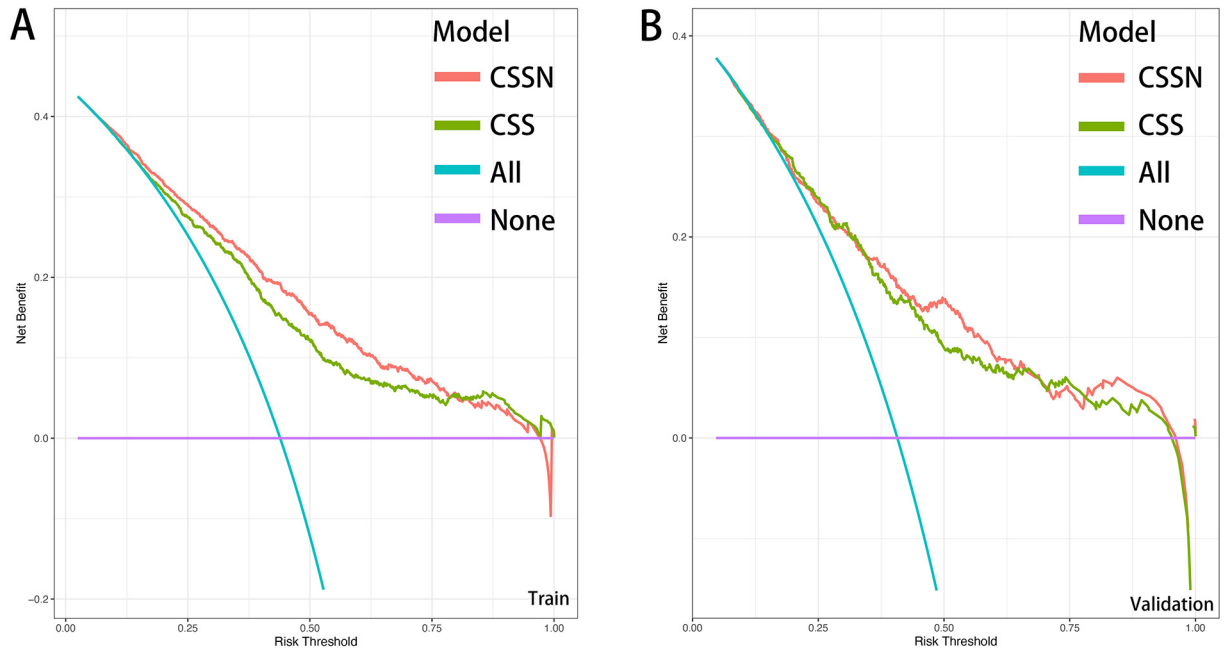

FIGURE 5
Decision curve analysis of CSSN and CSS in the training (Panel A) and validation (Panel B) cohorts.

fail to reverse outcomes, necessitating careful consideration of resource allocation and patient preferences. However, as this study is still in the model development phase, clinical application research will be the focus of subsequent work. Therefore, these hypotheses lack evidence-based medical validation and require further confirmation in future studies.

Risk assessment of CS patients also aids in guiding the implementation of clinical trials. Previously, several randomized trials investigating the use of MCS in CS patients failed to demonstrate survival benefits. For instance, the large randomized trial, IABP-SHOCK II, did not show that intra-aortic balloon pump (IABP) could lower the 30-day, 1-year, and 6-year

TABLE 3 Subgroup analysis.

	AMI cases		non-AMI cases	
Number	(*N* = 541)		(*N* = 1,143)	
c-statistic	0.768 (0.737, 0.798)		0.734 (0.713, 0.755)	
AUC	0.768		0.732	
Variables	HR (95%CI)	*P*	HR (95%CI)	*P*
Age, year	1.040 (1.029, 1.052)	<0.0001	1.030 (1.024, 1.037)	<0.0001
SBP, mmHg	0.980 (0.971, 0.989)	<0.0001	0.993 (0.988, 0.999)	0.0161
SpO_2, %	0.987 (0.976, 0.996)	0.0167	0.983 (0.978, 0.989)	<0.0001
Hemoglobin, g/dl	0.929 (0.855, 1.009)	0.0814	0.940 (0.893, 0.989)	0.0164
Serum creatinine, umol/L	1.001 (1.001, 1.002)	0.024	1.001 (1.001, 1.001)	0.0008
Blood glucose				
<11.1 mmol/L	Reference		Reference	
≥11.1 mmol/L	1.530 (1.177, 1.989)	0.0015	1.294 (1.067, 1.569)	0.0088
pH (Arterial blood gas)				
<7.1	Reference		Reference	
7.1–7.35	0.424 (0.258, 0.697)	0.0007	0.535 (0.374, 0.766)	0.0006
>7.35	0.263 (0.141, 0.481)	<0.0001	0.525 (0.344, 0.780)	0.0027
Arterial lactate, mmol/L	1.085 (1.051, 1.119)	<0.0001	1.078 (1.054, 1.103)	<0.0001
Norepinephrine	1.645 (1.178, 2.298)	0.0035	2.012 (1.607, 2.519)	<0.0001

Multivariate Cox proportional hazards model for 30-day mortality in AMI and non-AMI cases.
HR, hazard ratio; CI, confidence interval; SBP, systolic blood pressure; SpO_2, peripheral oxygen saturation.

mortality rates in patients with CS complicating acute myocardial infarction (AMI) undergoing early revascularization (17, 21, 23). Similarly, previous ECMO and Impella trials failed to demonstrate survival improvements in CS (1, 19, 20, 24). However, the latest randomized trial published by Møller and colleagues in the New England Journal of Medicine (NEJM) has changed this perspective (25). In this trial, 360 AMI-CS patients were randomly assigned to either the Impella or the standard treatment group, with all patients undergoing revascularization. Results showed that the 180-day mortality rate in the Impella group was 45.8%, significantly lower than the 58.5% in the standard treatment group (hazard ratio = 0.74; 95% CI: 0.55–0.99; $P = 0.04$). This marks the first MCS device proven to reduce mortality in CS patients in an RCT since the 1999 SHOCK trial. Notably, this trial differed from previous ones: (1) The trial excluded patients in SCAI-CSWG stages A and B, avoiding the imbalance of risks and benefits from using Impella in low-risk patients. (2) Patients who had been resuscitated from out-of-hospital cardiac arrest and remained comatose upon arrival at the cardiac catheterization laboratory were excluded. This likely excluded extremely critical patients who might not benefit neurologically or survive from MCS. (3) The trial's follow-up period was 180 days, whereas previous studies typically had 30-day follow-ups. The SHOCK trial indicated that PCI's effect on 30-day mortality in AMI-CS patients was neutral, but benefits were seen at 180 days (26). Therefore, 30 days as a primary endpoint may be too early to assess the intervention's effects adequately. These findings highlight the importance of considering both short-term and long-term outcomes, not just short-term ones.

In summary, risk assessment and stratification of CS patients are essential for guiding physicians in patient management and facilitating the successful implementation of clinical trials. Developing a simple and easy-to-use predictive model that considers both short-term and long-term outcomes of CS will be of significant clinical value.

Previous models

Currently, three primary models are used to predict the prognosis of CS patients: IABP-SHOCK II risk score (7), CardShock risk Score (8), and Cardiogenic Shock Score (CSS) (9). These models provide tools for the management of CS patients and the conduct of clinical trials. However, they have not been widely used in clinical practice, possibly due to limitations in population applicability, easy-to-use, and consideration of long-term outcomes. Population applicability may be the primary factor limiting the practical utility of these models. The IABP-SHOCK II risk score was developed for AMI-CS patients and requires post-PCI TIMI flow grades, making it unsuitable for non-AMI-CS patients. The CardShock score was developed in 2015 for all CS patients but included most AMI-CS patients (81%). In addition, the sample size was only 219, which may limit the applicability of the results to non-AMI-CS patients. Historically, AMI has been the primary cause of CS, constituting the majority of cases (>80%) (8). However, recent epidemiological surveys indicate that the proportion of AMI-CS in CS gradually decreases, now accounting for about 30% (3, 12). In the 2017–2018 North American CCCTN study, only 30% of CS cases were related to AMI, and among non-AMI-CS patients, approximately two-thirds had a history of heart failure (12). Therefore, models unsuitable for non-AMI-CS patients may limit their clinical application.

Secondly, the simplicity of the model and its consideration of long-term outcomes also determine whether clinicians will use them in practice. The CSS, a recent score system developed to predict 30-day mortality in CS, has better population applicability than the IABP-SHOCK II and CardShock risk scores, covering all causes of CS (9). The CSS includes nine easily obtainable parameters (age, sex, AMI-CS, systolic blood pressure, heart rate, pH, lactate, glucose, and cardiac arrest) and demonstrates good accuracy (c-statistic = 0.74). However, the CSS only focuses on the 30-day mortality of CS patients and does not consider long-term outcomes. In reality, the recovery of CS patients within one year after discharge is not optimistic, and survival rates continue to decline (4, 27). Currently, the in-hospital mortality rate of CS patients is about 30%–40%, and the one-year mortality rate can reach 50%–60% (3). Once again, the latest Impella trial successfully demonstrated that the Impella microaxial pump could reduce mortality in CS patients, and the follow-up period for this trial was 180 days (6 months) rather than 30 days (25). This indicates that the long-term outcomes of CS patients are also worthy of our attention. This study compared the performance of the CSS and the newly developed CSSN using c-statistic, time-dependent ROC, calibration plots, and decision curve analysis (DCA), indicating higher accuracy of the CSSN. Furthermore, the study employed CSSN to predict 30-day mortality risk for all patients, grouping them based on risk levels. Significant differences were observed in survival curves among the groups over one year.

CSSN and its clinical contributions

A growing body of evidence suggests that several clinical indicators can be used to predict the severity and outcomes of patients with CS (7–9, 28). Based on the previous model, the CSSN was developed, including the IABP-SHOCK II risk (7), CardShock risk score (8), and CSS (9). In this study, we used LASSO regression and the multivariable Cox model to screen and confirm easily obtainable parameters in emergency settings and those widely recognized in previous studies. Consequently, age, SBP, SpO_2, hemoglobin, serum creatinine, blood glucose, pH, arterial lactate, and norepinephrine were identified and used to develop the prognostic nomogram in our study. This nomogram demonstrated good discrimination and calibration in predicting patients' 30-day probability of survival with CS, as assessed by the c-statistic, AUC value, calibration plots, and clinical decision curve analysis indicating good performance and high value for clinical use.

Based on previous models and after multiple refinements and optimizations, our nomogram has several advantages (7–9): (1) Comprehensive Application: Our model is designed for CS resulting from any cause, and we have confirmed its accuracy in both AMI-CS and non-AMI-CS through subgroup analysis. (2) Simplicity and Accessibility: Our model includes only nine parameters that are easily accessible in emergency settings, and it is presented in the form of a nomogram, making it simple and easy to use. Clinicians can quickly assess a patient's risk using our nomogram. (3) Holistic Approach: Our model performs well even one year after discharge, enabling clinicians to provide more appropriate treatment measures by weighing risks and benefits.

Furthermore, our model can be used with SCAI classification, allowing physicians to assess a patient's survival rates accurately. SCAI divides cardiogenic shock into five stages (A-E), corresponding to "at risk" for CS, "beginning" shock, "classic" CS, "deteriorating", and "extremis", respectively (12). This staging is based on a comprehensive evaluation of blood pressure, heart rate, lactate levels, urine output, serum creatinine, vasopressor dose and duration, and blood pressure response to vasopressors. Through SCAI classification, clinicians can roughly understand the patient's disease progression stage and provide appropriate treatment strategies (6). Our nomogram can complement SCAI classification for a more precise assessment. For example, age is a critical factor influencing the prognosis of CS patients, and patients at the same SCAI stage may face different risks due to age differences (29, 30). Combining CSSN with SCAI staging can enable a more precise assessment. Moreover, our study incorporates continuous variables into the model as much as possible to achieve more refined predictive capabilities, greatly enhancing its usability.

Limitations

Despite the large sample size and thorough evaluation and validation, our study has several limitations inherent to retrospective research. The primary limitation is the inability to rule out unknown confounding factors, a common issue in retrospective studies. These unknown factors could potentially influence our predictive model's outcomes and accuracy. The 7:3 random division (training-validation sets) used in this study is an internal validation method, which cannot fully demonstrate the model's generalizability in independent external populations. Secondly, the CSSN is based on the MIMIC database, and all patients received ICU hospitalization, which may introduce bias when applied to patients in other regions. Additionally, because the MIMIC database does not include etiological diagnoses of CS, we could not obtain specific causes of CS in patients; the diagnosis of AMI-CS was based on the admission diagnosis. Although this study is based on a large database, all patients were from ICUs in a single region, and their treatment strategies and population characteristics may differ from those in other regions. Future multicenter and multi-regional prospective studies are needed to further validate the generalizability of the CSSN. Despite these limitations, we believe the CSSN remains a valuable tool for clinicians in managing cardiogenic shock. The model's ability to predict outcomes of CS, combined with its simplicity, makes it a practical addition to current clinical decision-making processes. Future prospective studies and validation in diverse patient populations are needed further to enhance the robustness and applicability of the CSSN.

Conclusion

In this study, we developed a prognostic model for predicting survival rates in patients with cardiogenic shock, known as the

Cardiogenic Shock Survival Nomogram (CSSN). The CSSN is constructed using easily obtainable parameters in an emergency setting. This model is straightforward, intuitive, and easy to use. Utilizing the CSSN aids physicians in the early risk assessment of CS patients and helps formulate targeted treatment strategies, potentially improving patient outcomes.

Data availability statement

Publicly available datasets were analyzed in this study. This data can be found here: the MIMIC-IV database hosted on PhysioNet (https://physionet.org/content/mimiciv). However, access to the raw data requires completion of the CITI Program training (https://www.citiprogram.org) (Human Research, Data or Specimens Only Research) and formal registration on PhysioNet (https://physionet.org/register/). These steps are mandated to ensure compliance with ethical standards and patient privacy regulations. Once approved, researchers may freely download and analyze the data.

Ethics statement

The studies involving humans were approved by The Institutional Review Board at the Beth Israel Deaconess Medical Center. The studies were conducted in accordance with the local legislation and institutional requirements. Written informed consent for participation was not required from the participants or the participants' legal guardians/next of kin in accordance with the national legislation and institutional requirements.

Author contributions

DF: Conceptualization, Data curation, Formal analysis, Investigation, Methodology, Project administration, Resources, Software, Supervision, Validation, Visualization, Writing – original draft, Writing – review & editing. HC: Methodology, Software, Supervision, Writing – review & editing. HG: Investigation, Methodology, Project administration, Validation, Writing – review & editing. XC: Supervision, Validation, Visualization, Writing – review & editing. ML: Conceptualization, Data curation, Formal analysis, Funding acquisition, Investigation, Methodology, Project administration, Resources, Supervision, Writing – review & editing.

Funding

The author(s) declare that financial support was received for the research and/or publication of this article. This work was funded by Project 2019BD019, supported by the PKU-Baidu Fund and the Special Project of the National Health Commission (2024ZD01), which facilitated the completion of this study.

Acknowledgments

The authors thank the original study group for providing data for the current analysis.

Conflict of interest

The authors declare that the research was conducted in the absence of any commercial or financial relationships that could be construed as a potential conflict of interest.

Generative AI statement

The author(s) declare that no Generative AI was used in the creation of this manuscript.

Publisher's note

Supplementary material

The Supplementary Material for this article can be found online at: https://www.frontiersin.org/articles/10.3389/fcvm.2025.1538395/full#supplementary-material

References

1. Banning AS, Sabaté M, Orban M, Gracey J, López-Sobrino T, Massberg S, et al. Venoarterial extracorporeal membrane oxygenation or standard care in patients with cardiogenic shock complicating acute myocardial infarction: the multicentre, randomised euro shock trial. *EuroIntervention*. (2023) 19(6):482–92. doi: 10.4244/eij-d-23-00204

2. Thiele H, Zeymer U, Akin I, Behnes M, Rassaf T, Mahabadi AA, et al. Extracorporeal life support in infarct-related cardiogenic shock. *N Engl J Med*. (2023) 389(14):1286–97. doi: 10.1056/NEJMoa2307227

3. Berg DD, Bohula EA, Morrow DA. Epidemiology and causes of cardiogenic shock. *Curr Opin Crit Care*. (2021) 27(4):401–8. doi: 10.1097/mcc.0000000000000845

4. Aissaoui N, Puymirat E, Tabone X, Charbonnier B, Schiele F, Lefèvre T, et al. Improved outcome of cardiogenic shock at the acute stage of myocardial infarction: a report from the usik 1995, usic 2000, and fast-mi French nationwide registries. *Eur Heart J*. (2012) 33(20):2535–43. doi: 10.1093/eurheartj/ehs264

5. Hernandez-Montfort J, Sinha SS, Thayer KL, Whitehead EH, Pahuja M, Garan AR, et al. Clinical outcomes associated with acute mechanical circulatory support utilization in heart failure related cardiogenic shock. *Circ Heart Fail*. (2021) 14(5): e007924. doi: 10.1161/circheartfailure.120.007924

6. Jentzer JC, van Diepen S, Barsness GW, Henry TD, Menon V, Rihal CS, et al. Cardiogenic shock classification to predict mortality in the cardiac intensive care unit. *J Am Coll Cardiol*. (2019) 74(17):2117–28. doi: 10.1016/j.jacc.2019.07.077

7. Pöss J, Köster J, Fuernau G, Eitel I, de Waha S, Ouarrak T, et al. Risk stratification for patients in cardiogenic shock after acute myocardial infarction. *J Am Coll Cardiol*. (2017) 69(15):1913–20. doi: 10.1016/j.jacc.2017.02.027

8. Harjola VP, Lassus J, Sionis A, Køber L, Tarvasmäki T, Spinar J, et al. Clinical picture and risk prediction of short-term mortality in cardiogenic shock. *Eur J Heart Fail*. (2015) 17(5):501–9. doi: 10.1002/ejhf.260

9. Beer BN, Jentzer JC, Weimann J, Dabboura S, Yan I, Sundermeyer J, et al. Early risk stratification in patients with cardiogenic shock irrespective of the underlying cause—the cardiogenic shock score. *Eur J Heart Fail*. (2022) 24(4):657–67. doi: 10.1002/ejhf.2449

10. Hwang HK, Wada K, Kim HY, Nagakawa Y, Hijikata Y, Kawasaki Y, et al. A nomogram to preoperatively predict 1-year disease-specific survival in resected pancreatic cancer following neoadjuvant chemoradiation therapy. *Chin J Cancer Res*. (2020) 32(1):105–14. doi: 10.21147/j.issn.1000-9604.2020.01.12

11. Zhou Q, Li AB, Lin ZQ, Zhang HZ. A nomogram and a risk classification system predicting the cancer-specific survival of patients with initially-diagnosed osseous spinal and pelvic tumors. *Spine*. (2020) 45(12):E713–e20. doi: 10.1097/brs.0000000000003404

12. Berg DD, Bohula EA, van Diepen S, Katz JN, Alviar CL, Baird-Zars VM, et al. Epidemiology of shock in contemporary cardiac intensive care units. *Circ Cardiovasc Qual Outcomes*. (2019) 12(3):e005618. doi: 10.1161/circoutcomes.119.005618

13. Baran DA, Grines CL, Bailey S, Burkhoff D, Hall SA, Henry TD, et al. Scai clinical expert consensus statement on the classification of cardiogenic shock: this document was endorsed by the American college of cardiology (acc), the American Heart Association (aha), the society of critical care medicine (sccm), and the society of thoracic surgeons (Sts) in April 2019. *Catheter Cardiovasc Interv*. (2019) 94(1):29–37. doi: 10.1002/ccd.28329

14. Goldberger AL, Amaral LA, Glass L, Hausdorff JM, Ivanov PC, Mark RG, et al. Physiobank, physiotoolkit, and physionet: components of a new research resource for complex physiologic signals. *Circulation*. (2000) 101(23):E215–20. doi: 10.1161/01.cir.101.23.e215

15. Johnson A, Bulgarelli L, Pollard T, Horng S, Celi LA, Mark R. MIMIC-IV (version 2.2). *PhysioNet*. (2023). doi: 1013026/6mm1-ek67

16. Johnson AEW, Bulgarelli L, Shen L, Gayles A, Shammout A, Horng S, et al. Mimic-Iv, a freely accessible electronic health record dataset. *Sci Data*. (2023) 10(1):1. doi: 10.1038/s41597-022-01899-x

17. Thiele H, Zeymer U, Thelemann N, Neumann FJ, Hausleiter J, Abdel-Wahab M, et al. Intraaortic balloon pump in cardiogenic shock complicating acute myocardial infarction: long-term 6-year outcome of the randomized iabp-shock ii trial. *Circulation*. (2019) 139(3):395–403. doi: 10.1161/circulationaha.118.038201

18. Fang D, Yu D, Xu J, Ma W, Zhong Y, Chen H. Effects of intra-aortic balloon pump on in-hospital outcomes and 1-year mortality in patients with acute myocardial infarction complicated by cardiogenic shock. *BMC Cardiovasc Disord*. (2023) 23(1):425. doi: 10.1186/s12872-023-03465-8

19. Ostadal P, Rokyta R, Karasek J, Kruger A, Vondrakova D, Janotka M, et al. Extracorporeal membrane oxygenation in the therapy of cardiogenic shock: results of the ecmo-cs randomized clinical trial. *Circulation*. (2023) 147(6):454–64. doi: 10.1161/circulationaha.122.062949

20. Schrage B, Ibrahim K, Loehn T, Werner N, Sinning JM, Pappalardo F, et al. Impella support for acute myocardial infarction complicated by cardiogenic shock. *Circulation*. (2019) 139(10):1249–58. doi: 10.1161/circulationaha.118.036614

21. Thiele H, Zeymer U, Neumann FJ, Ferenc M, Olbrich HG, Hausleiter J, et al. Intra-aortic balloon counterpulsation in acute myocardial infarction complicated by cardiogenic shock (Iabp-Shock Ii): final 12 month results of a randomised, open-label trial. *Lancet*. (2013) 382(9905):1638–45. doi: 10.1016/s0140-6736(13)61783-3

22. Lemor A, Dabbagh MF, Cohen D, Villablanca P, Tehrani B, Alaswad K, et al. Rates and impact of vascular complications in mechanical circulatory support. *Catheter Cardiovasc Interv*. (2022) 99(5):1702–11. doi: 10.1002/ccd.30150

23. Thiele H, Zeymer U, Neumann FJ, Ferenc M, Olbrich HG, Hausleiter J, et al. Intraaortic balloon support for myocardial infarction with cardiogenic shock. *N Engl J Med*. (2012) 367(14):1287–96. doi: 10.1056/NEJMoa1208410

24. Ouweneel DM, Eriksen E, Sjauw KD, van Dongen IM, Hirsch A, Packer EJ, et al. Percutaneous mechanical circulatory support versus intra-aortic balloon pump in cardiogenic shock after acute myocardial infarction. *J Am Coll Cardiol*. (2017) 69(3):278–87. doi: 10.1016/j.jacc.2016.10.022

25. Møller JE, Engstrøm T, Jensen LO, Eiskjær H, Mangner N, Polzin A, et al. Microaxial flow pump or standard care in infarct-related cardiogenic shock. *N Engl J Med*. (2024) 390(15):1382–93. doi: 10.1056/NEJMoa2312572

26. Hochman JS, Sleeper LA, Webb JG, Sanborn TA, White HD, Talley JD, et al. Early revascularization in acute myocardial infarction complicated by cardiogenic shock. Shock investigators. Should we emergently revascularize occluded coronaries for cardiogenic shock. *N Engl J Med*. (1999) 341(9):625–34. doi: 10.1056/nejm199908263410901

27. Shah RU, de Lemos JA, Wang TY, Chen AY, Thomas L, Sutton NR, et al. Post-hospital outcomes of patients with acute myocardial infarction with cardiogenic shock: findings from the NCDR. *J Am Coll Cardiol*. (2016) 67(7):739–47. doi: 10.1016/j.jacc.2015.11.048

28. Jentzer JC, Schrage B, Patel PC, Kashani KB, Barsness GW, Holmes DR Jr., et al. Association between the acidemia, lactic acidosis, and shock severity with outcomes in patients with cardiogenic shock. *J Am Heart Assoc*. (2022) 11(9):e024932. doi: 10.1161/jaha.121.024932

29. Kanwar M, Thayer KL, Garan AR, Hernandez-Montfort J, Whitehead E, Mahr C, et al. Impact of age on outcomes in patients with cardiogenic shock. *Front Cardiovasc Med*. (2021) 8:688098. doi: 10.3389/fcvm.2021.688098

30. Blumer V, Kanwar MK, Barnett CF, Cowger JA, Damluji AA, Farr M, et al. Cardiogenic shock in older adults: a focus on age-associated risks and approach to management: a scientific statement from the American heart association. *Circulation*. (2024) 149(14):e1051–e65. doi: 10.1161/cir.0000000000001214

frontiers | Frontiers in Cardiovascular Medicine

TYPE Case Report
PUBLISHED 22 May 2025
DOI 10.3389/fcvm.2025.1583801

OPEN ACCESS

EDITED BY
Andreea Calin,
Carol Davila University of Medicine and Pharmacy, Romania

REVIEWED BY
Satoshi Miyashita,
Cleveland Clinic, United States
Raviteja Guddeti,
Christ Hospital, United States

*CORRESPONDENCE
Jun Nakata
jun-nakata@nms.ac.jp

RECEIVED 26 February 2025
ACCEPTED 05 May 2025
PUBLISHED 22 May 2025

CITATION
Watanabe Y, Nakata J, Matsushita H, Saku K, Mozawa K, Seki T, Tokita Y, Izumi Y, Tsutsumi M, Hoshika Y, Kimura T, Hino M, Shiomura R, Sangen H, Yamamoto T and Asai K (2025) Case Report: Balloon aortic valvuloplasty with subsequent Impella support as bridge therapy to transcatheter aortic valve replacement in cardiogenic shock with severe aortic stenosis.
Front. Cardiovasc. Med. 12:1583801.
doi: 10.3389/fcvm.2025.1583801

Case Report: Balloon aortic valvuloplasty with subsequent Impella support as bridge therapy to transcatheter aortic valve replacement in cardiogenic shock with severe aortic stenosis

Yukihiro Watanabe[1], Jun Nakata[1]*, Hiroki Matsushita[2], Keita Saku[2], Kosuke Mozawa[3], Toshiki Seki[3], Yukichi Tokita[3], Yuki Izumi[3], Masayuki Tsutsumi[1], Yu Hoshika[1], Tokuhiro Kimura[1], Masaaki Hino[1], Reiko Shiomura[1], Hideto Sangen[1], Takeshi Yamamoto[1] and Kuniya Asai[3]

[1]Division of Cardiovascular Intensive Care, Nippon Medical School Hospital, Tokyo, Japan, [2]Department of Cardiovascular Dynamics, National Cerebral and Cardiovascular Center Research Institute, Osaka, Japan, [3]Department of Cardiovascular Medicine, Nippon Medical School, Tokyo, Japan

Introduction: Cardiogenic shock (CS) with severe aortic stenosis (AS) is a drug-resistant hemodynamically unstable condition with high mortality. We report three cases of CS with severe AS that were successfully managed with balloon aortic valvuloplasty (BAV), followed by left ventricular (LV) unloading using Impella as a bridge therapy for transcatheter aortic valve replacement (TAVR). We call this therapeutic approach "BAV-PELLA-TAVR".

Case presentation: Case 1: A 92-year-old Japanese female presented with CS due to low-flow, low-gradient severe AS and multivessel coronary artery disease. After emergent BAV and Impella 2.5 support, the patient's hemodynamics stabilized. Percutaneous coronary intervention was performed on the right coronary and left anterior descending arteries with Impella 2.5 support. Subsequently, her heart failure (HF) improved and elective TAVR was performed. Case 2: An 89-year-old Japanese female presented with CS due to severe AS. Despite administration of high-dose catecholamines, the patient developed exacerbation of CS due to reduced cardiac output, corresponding to Stage D according to the Society for Cardiovascular Angiography and Interventions (SCAI) classification. Consequently, BAV was performed, which reduced the aortic valve pressure gradient (PG). However, due to persistent hemodynamic instability, Impella 2.5 support was initiated. This procedure resulted in hemodynamic improvement and elective TAVR was performed. Case 3: An 86-year-old Japanese female developed CS with pulmonary edema due to severe AS. Emergent BAV was performed. However, there was no improvement in the PG and hemodynamics, and the initial mild aortic regurgitation worsened to a moderate degree. Therefore, an Impella CP was implanted, which resulted in improved hemodynamics. Following the removal of the Impella CP device, and sub-emergent TAVR was successfully performed.

10.3389/fcvm.2025.1583801

Discussion: In all cases, emergent BAV and subsequent hemodynamic support from the Impella were provided as the initial treatment for CS at Stage C/D according to the SCAI classification. This approach improved CS, enabling interventions for concomitant ischemic heart disease, multidisciplinary heart team evaluation, and TAVR with reduced perioperative risk.

KEYWORDS

severe aortic stenosis, cardiogenic shock, balloon aortic valvuloplasty, impella, transcatheter aortic valve replacement, BAV-PELLA-TAVR

1 Introduction

Cardiogenic shock (CS) is a life-threatening condition characterized by tissue hypoperfusion due to low cardiac output (CO) (1). CS is caused by diseases involving impaired function of the myocardium, valve, conduction system, or pericardium, either in isolation or in combination (2). The incidence of aortic stenosis (AS) has been increasing worldwide with an aging population (3), and it is one of the major causes of CS and acute decompensated heart failure (ADHF). Furthermore, CS with severe AS is associated with high mortality and morbidity (4).

In recent years, transcatheter aortic valve replacement (TAVR) has become an established standard treatment for high-risk patients with severe AS (5, 6). However, in the setting of CS, TAVR is generally not indicated due to uncertain benefits and a high risk of complications. In a multicenter retrospective observational study, patients with decompensated AS who underwent emergency TAVR had poor outcomes, with a 30-day mortality of 24% and a high incidence of complications (vascular complications: 22%; stroke: 9%). Meanwhile, a staged treatment approach involving emergency balloon aortic valvuloplasty (BAV) followed by elective TAVR has also been widely adopted; however, this strategy similarly resulted in poor outcomes (7). Therefore, current therapeutic options have limited effectiveness, highlighting the need to establish effective treatment strategies for this condition.

We successfully performed BAV with subsequent hemodynamic support using Impella (Abiomed, Danvers, MA) as bridge therapy for TAVR. Several recent reports have supported this approach as a feasible and effective therapeutic option (8–11). We call this approach "BAV-PELLA-TAVR" and propose it as the optimal therapeutic strategy for CS with severe AS. The combination of aortic valve pressure gradient (PG) reduction by BAV and left ventricular (LV) unloading with Impella could stabilize hemodynamics and enable TAVR with reduced perioperative risk. This report presents three cases treated with BAV-PELLA-TAVR and discusses the hemodynamic advantages of this therapeutic approach.

2 Case presentation

2.1 Case 1: Low flow, low gradient (LF-LG) severe AS with multivessel coronary artery disease

A 92-year-old Japanese female with a medical history of hypertension and diabetes was admitted to our cardiovascular intensive care unit for ADHF. On admission, her vital signs were as follows: blood pressure, 103/65 mmHg; heart rate, 160 beats/min; and peripheral oxygen saturation, 95%, while receiving supplemental oxygen at 10 L/min. Blood tests showed an elevated high-sensitivity troponin T level of 0.243 ng/ml. Chest radiography revealed a cardiothoracic ratio of 66% and pulmonary congestion. Electrocardiography (ECG) showed atrial fibrillation with a heart rate of 150 beats/min and poor R-wave progression. Echocardiography revealed diffuse hypokinesis with a reduced left ventricular ejection fraction (LVEF) of 38%, aortic valve calcification, and severe mitral regurgitation (MR). The aortic valve peak velocity was 3.3 m/s, and the mean PG was 29 mmHg; however, the aortic valve area (AVA) was markedly low at 0.39 cm^2 (calculated using the continuity equation), and the stroke volume index was also low at 20 ml/m^2, suggesting LF-LG severe AS (Figure 1A).

Non-invasive positive pressure ventilation and intravenous furosemide administration were initiated. Landiolol was administered to manage tachycardic atrial fibrillation; however, as rate control remained inadequate, electrical cardioversion was performed, which successfully restored the sinus rhythm. Despite these initial treatments, the patient's blood pressure decreased to 77/37 mmHg, and the serum lactate level was elevated to 2.2 mmol/L, indicating Stage C according to the Society for Cardiovascular Angiography and Interventions classification (SCAI). Subsequently, mechanical ventilation was initiated, and norepinephrine at 0.3 γ and dobutamine at 3 γ were administered, resulting in an increase in blood pressure to 99/50 mmHg. Cardiac catheterization was performed to evaluate hemodynamics and coronary arteries. Right heart catheterization demonstrated the following hemodynamic parameters: pulmonary capillary wedge pressure (PCWP) of 23 mmHg, pulmonary artery pressure (PAP) of 50/20 mmHg, central venous pressure (CVP) of 13 mmHg, CO of 2.7 L/min (measured by the Fick method), and cardiac index (CI) of 1.9 $L/min/m^2$. Coronary angiography (CAG) revealed multivessel coronary artery disease with 90% stenosis in the proximal and mid-right coronary artery, 90% stenosis in the proximal and mid-left anterior descending artery, and 75% stenosis in the proximal and mid-circumflex artery.

The cause of CS was considered to be non-ST-elevation myocardial infarction associated with LF-LG severe AS, severe MR, and ischemic heart disease. Consequently, we planned to improve hemodynamics through an intervention for severe AS by performing BAV using an 18-mm Tyshak balloon (Cardinal Health Japan, Tokyo, Japan). Immediately after the procedure, the patient experienced cardiac arrest owing to pulseless electrical activity. Cardiopulmonary resuscitation was promptly initiated, and an Impella 2.5 device was implanted, resulting in the

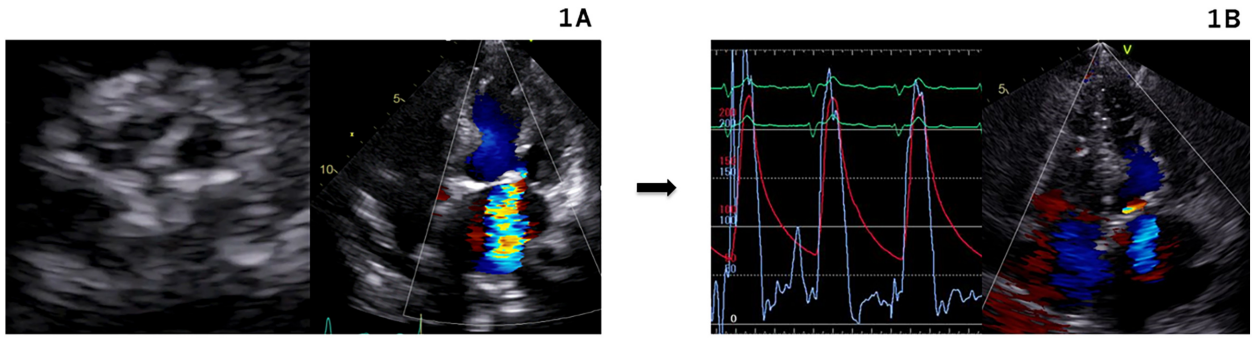

FIGURE 1
Hemodynamics and images in Case 1. **(A)** Echocardiography on admission (Case 1). **(B)** Hemodynamic improvement after BAV and Impella support (Case 1). AS, aortic stenosis; AV, aortic valve; AVA, aortic valve area; BAV, balloon aortic valvuloplasty; BP, blood pressure; EF, ejection fraction; ERO, effective regurgitant orifice; LF-LG, low flow low gradient; LVOT-VTI, left ventricular outflow tract velocity time integral; MR, mitral regurgitation; PG, pressure gradient; RV, regurgitant volume; SVi, stroke volume index.

stabilization of blood pressure at 115/56 mmHg. These procedures led to a reduction in the aortic valve PG from 29 to 13 mmHg, and the MR improved significantly (Figure 1B). Subsequently, percutaneous coronary intervention (PCI) was performed and drug-eluting stents (Xience Alpine; Abbott Vascular, Santa Clara, CA) were implanted into the right coronary artery and left anterior descending artery. These interventions stabilized the patient's hemodynamics, allowing discontinuation of catecholamines. The Impella device was removed on day 5, and the patient was extubated on day 9. Thereafter, the patient maintained compensated heart failure (HF) and stable hemodynamics with oral therapy alone. The heart team evaluation deemed the patient to be at a high surgical risk (STS score: 12.8%, Clinical Frailty Scale score: 4, Katz Index: 4), and TAVR was recommended. Elective TAVR with a 23-mm SAPIEN 3 valve (Edwards Lifesciences, Irvine, CA) was successfully performed on day 19.

2.2 Case 2: reduced cardiac output due to severe AS

An 89-year-old Japanese female with a history of hypertension and dyslipidemia was admitted to another hospital for ADHF. Owing to worsening hemodynamics, she was transferred to our hospital for advanced intensive care. On admission, the patient was intubated and on mechanical ventilation, with continuous infusions of norepinephrine at 0.3 γ and dopamine at 4 γ. Her vital signs were as follows: blood pressure, 94/61 mmHg; heart rate, 100 beats/min; and peripheral oxygen saturation, 100%, while receiving an FiO2 of 0.4. Chest radiography revealed pleural effusion, slight pulmonary congestion and a cardiothoracic ratio of 62%. ECG revealed atrial fibrillation with a heart rate of 129 beats/min and ST-segment depression in leads V4-V6. Echocardiography demonstrated a reduced LVEF of 37% and severe AS, with an aortic valve peak velocity of 5.8 m/s, a mean PG of 82 mmHg, and an AVA of 0.31 cm^2. In addition, a septal e' velocity of 3.2 cm/s, an E/e' ratio of 23.8, and a left atrial volume index of 113 ml/m^2 were suggestive of LV diastolic dysfunction.

Electrical cardioversion was performed to manage atrial fibrillation and successfully restore the sinus rhythm. Despite the administration of high-dose catecholamines, hemodynamics remained unstable, and the serum lactate level was elevated at 2.4 mmol/L, indicating SCAI SHOCK Stage D. Right heart catheterization demonstrated the following hemodynamic parameters: PCWP of 10 mmHg, PAP of 25/12 mmHg, CVP of 5 mmHg, CO of 1.6 L/min (measured by the Fick method), and CI of 1.2 $L/min/m^2$. CAG revealed no significant stenosis.

The pathology was considered CS associated with reduced cardiac output due to severe AS. Emergent BAV was performed using an 18-mm Z-Med balloon (NuMED, Inc., Hopkinton, NY), resulting in a reduction in the aortic valve PG from 102 to 56 mmHg. However, low cardiac output persisted with a CO of 1.8 L/min and a CI of 1.4 $L/min/m^2$. Subsequently, an Impella 2.5 device was implanted, selected because of poor vascular access and small body surface area of 1.2 m^2. These interventions resulted in an increase in CO to 2.3 L/min, CI to 1.7 $L/min/m^2$, and blood pressure to 138/62 mmHg (Figure 2). As the patient's cardiac function showed gradual improvement and hemodynamic parameters stabilized, the Impella device was removed on day 6. In the multidisciplinary heart team discussion, it was determined that the patient was at high surgical risk (STS score:

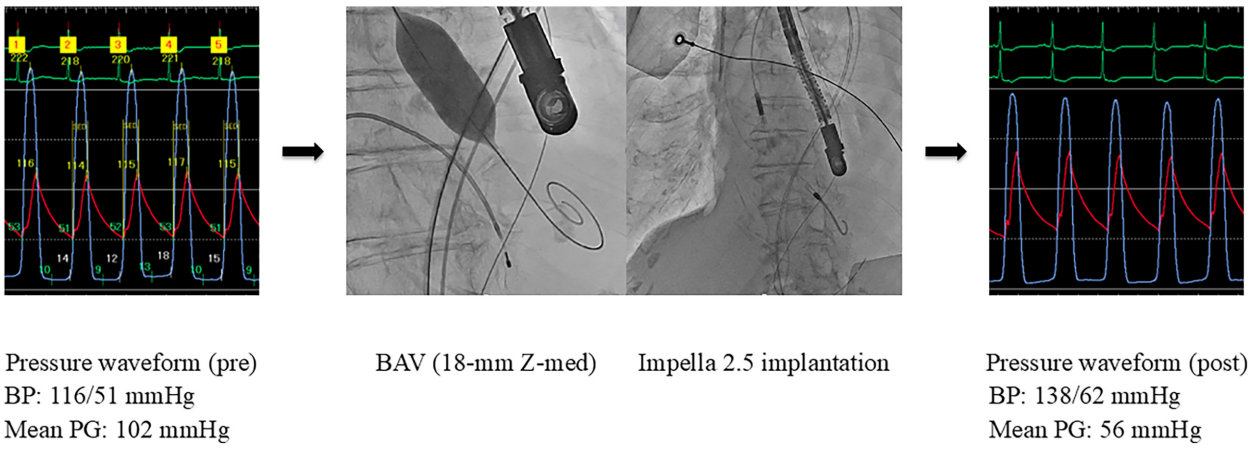

FIGURE 2
Hemodynamic improvement after BAV and Impella support (Case 2). BAV, balloon aortic valvuloplasty; BP, blood pressure; PG, pressure gradient.

32.2%, Clinical Frailty Scale score: 2, Katz Index: 5), and TAVR was planned. On day 9, elective TAVR with a 23-mm SAPIEN 3 valve was successfully performed.

2.3 Case 3: cardiogenic pulmonary edema due to severe AS

An 86-year-old Japanese female with a history of hypertension was admitted to our cardiovascular intensive care unit for ADHF. On admission, her vital signs were as follows: blood pressure, 165/87 mmHg; heart rate, 85 beats/min; and peripheral oxygen saturation, 97%, while receiving 6 L/min of supplemental oxygen. Chest radiography revealed a cardiothoracic ratio of 60%, pulmonary congestion, and pleural effusion. ECG showed sinus rhythm with a heart rate of 88 beats/min and ST-segment depression in leads V4-V6. An echocardiogram demonstrated a LVEF of 55%, mild aortic regurgitation (AR), and severe AS, with an aortic valve peak velocity of 4.7 m/s, a mean PG of 63 mmHg, and an AVA of 0.21 cm^2.

After initiating mechanical ventilation, the blood pressure decreased, and the serum lactate level was elevated at 2.0 mmol/L, indicating SCAI SHOCK Stage C. Administration of norepinephrine at 0.1 γ was initiated immediately. Right heart catheterization demonstrated the following hemodynamic parameters: PCWP of 42 mmHg, PAP of 51/37 mmHg, CVP of 17 mmHg, CO of 3.7 L/min (measured by the Fick method), and CI of 2.6 L/min/m^2. CAG showed no significant stenosis. The peak-to-peak gradient between the left ventricle and aorta (LV-Ao) was 100 mmHg.

The pathology was CS with pulmonary edema caused by severe AS. Emergent BAV was performed using a 16-mm Z-Med balloon. However, the LV-Ao PG remained high at 80 mmHg, and the PCWP was high at 42 mmHg. Furthermore, the severity of AR worsened from mild to moderate; thus, an additional oversized BAV was determined to carry a high risk of further AR exacerbation. Consequently, an Impella CP device was implanted, which led to an increase in the blood pressure, allowing for the discontinuation of catecholamines, and a reduction in PCWP to 15 mmHg. The heart team evaluation determined that the patient was at a high surgical risk (STS score: 22.2%, Clinical Frailty Scale score: 4, Katz Index: 4), and TAVR was planned. Preoperative computed tomography performed under Impella CP support demonstrated the following measurements: an aortic valve annulus with diameters of 16.3 × 23.3 mm, a perimeter of 63.2 mm, and an area of 303 mm^2. On day 7, following the removal of the Impella CP device, sub-emergent TAVR with a 20-mm SAPIEN 3 valve was successfully performed, reducing the aortic valve PG from 81 to 8 mmHg (Figure 3). Subsequently, adequate diuresis was achieved, pulmonary congestion improved, and the patient was extubated on day 9. HF remained compensated with oral medications alone. Cardiac rehabilitation was carried out, resulting in improved activities of daily living, and the patient was discharged home on day 28.

3 Discussion

Patients with severe AS often develop ADHF and CS, resulting in poor prognosis (12, 13). Several case series have demonstrated the value of BAV in achieving hemodynamic stability before definitive therapy (14, 15). However, BAV has intrinsic risks, and its efficacy is modest, with a risk of significant AR.

On the other hand, emergent or urgent TAVR can be an optional therapy (16). Classically, patients with CS are not considered candidates for TAVR because of concerns regarding the feasibility of a standard pre-procedural evaluation including computed tomography and the consequent risks of inaccurate transcatheter aortic valve sizing, improper assessment of periprocedural complications, and unsuitability of iliofemoral access, as well as the risk of complications associated with the procedure itself (7). Nonetheless, in light of the results of a substudy of the Society of Thoracic Surgeons and the American College of Cardiology Transcatheter Valve Therapy registry, "primary" TAVR has demonstrated a high procedural success rate in patients with CS (17). Despite this, the 30-day mortality rate remains high at 19.1%,

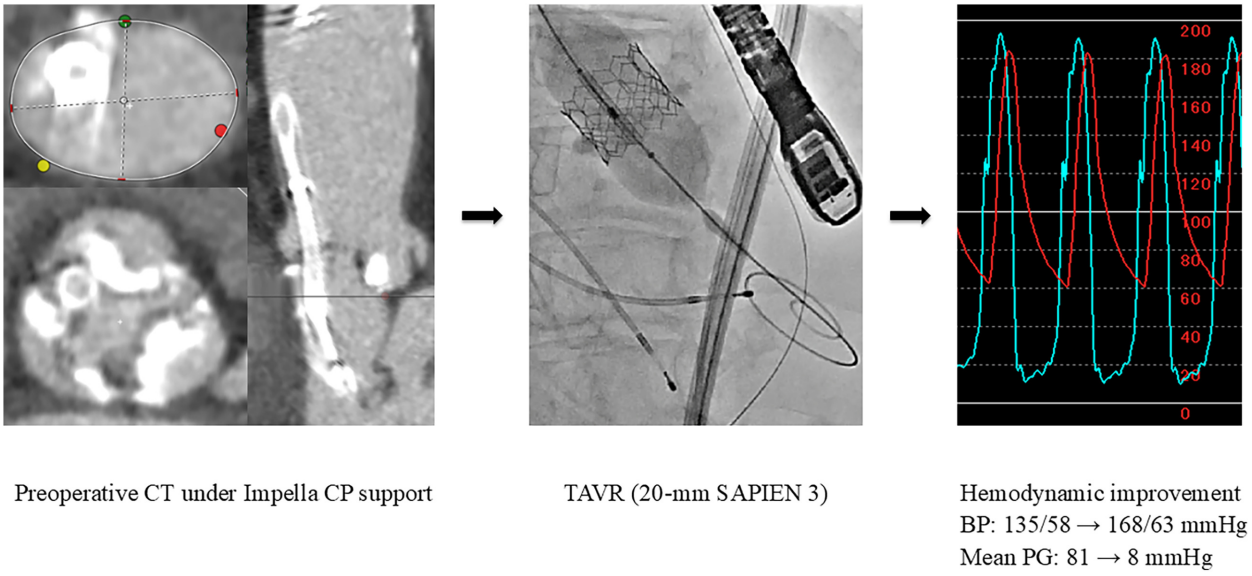

FIGURE 3
Preoperative CT imaging and urgent TAVR (Case 3). BP, blood pressure; CT, computed tomography; PG, pressure gradient; TAVR, transcatheter aortic valve replacement.

suggesting that primary TAVR alone may not lead to sufficient improvement in clinical outcomes. In contrast, BAV, as a bridge to definitive therapy, may be considered in hemodynamically unstable patients who are at high risk for surgery (5, 15). Thus, emergent BAV with subsequent hemodynamic support by mechanical circulatory support, followed by elective or urgent TAVR after hemodynamic stabilization, is essentially an ideal approach for CS with severe AS.

According to the Japanese Circulation Society (JCS)/Japanese Society for Cardiovascular Surgery (JSCVS)/Japanese College of Cardiology (JCC)/Japanese Association of Cardiovascular Intervention and Therapeutics (CVIT) 2023 guidelines focused on the indication and operation of percutaneous cardiopulmonary support (PCPS)/extracorporeal membrane oxygenation (ECMO)/Impella, intravenous inotropic drugs are recommended to be administered first for patients with SCAI SHOCK Stages C and D. Coronary revascularization, such as PCI, should be performed if necessary, and Impella should be used if hypoperfusion persists, accompanied by elevated left ventricular end-diastolic pressure (LVEDP) (18). Physiologically, patients with severe AS are not eligible for Impella because the insertion of the device through the stenotic valve orifice is technically challenging. However, emergent BAV with a small balloon to achieve the minimum diameter makes it possible to insert an Impella device. We measured the aortic annulus diameter using transesophageal echocardiography prior to BAV and selected a balloon size that did not exceed the measured value. This allowed for successful Impella insertion across the aortic valve in all cases. Thus, "BAV-PELLA," which refers to BAV and hemodynamic support with Impella, may be an ideal option as a reasonable and safe intervention for CS caused by severe AS.

The treatment sequence of BAV-PELLA-TAVR is recommended for AS patients with impaired cardiac function in whom congestion and low CO are likely to persist even after BAV. Figure 4 illustrates the hemodynamics of LF-LG AS with impaired LV function and the treatment process of BAV-PELLA-TAVR using our previously developed cardiovascular simulator (19, 20). Figure 4A shows the hemodynamics and pressure-volume (PV) loops of a normal heart, AS, and LF-LG AS. AS causes a significant increase in the PG and an upward shift in the PV loop, suggesting an increase in LV mechanical work. However, in patients with normal LV function, changes in CO, atrial pressure, and left ventricular end-diastolic volume (LVEDV) remain within acceptable ranges without major circulatory collapse. In contrast, with impaired LV systolic and diastolic functions, the PV loop shifts downward and the PG also significantly decreases. Figure 4B shows BAV in a LF-LG AS patient with low LV function. Although BAV significantly reduces PG, the resulting increase in stroke volume is limited, and congestive HF may not be sufficiently improved. Using Impella in such cases can significantly improve hemodynamics while reducing the LV load. In some cases, Impella-mediated HF management can even improve LV function. As shown in Figure 4C transitioning to TAVR with well-managed HF enables the safe radical treatment of AS.

Case 1 most closely resembles the simulation shown in Figure 4. Impella-mediated HF management and PCI may contribute to improved LV function. In Case 2, cardioversion was promptly performed for atrial fibrillation after transfer, successfully restoring sinus rhythm. The recovery of atrial function can increase the inflow from the left atrium to the LV. However, in this case with severe AS and LV diastolic dysfunction, the increased LV inflow due to sinus rhythm restoration may not have contributed to an increase in CO and could have exacerbated LV load. Although severe AS may have contributed to the reduced CO, the use of vasopressors and diuretics for congestion relief and blood pressure maintenance might have caused a significant preload reduction and afterload increase, potentially leading to a persistently low CO after BAV. Impella

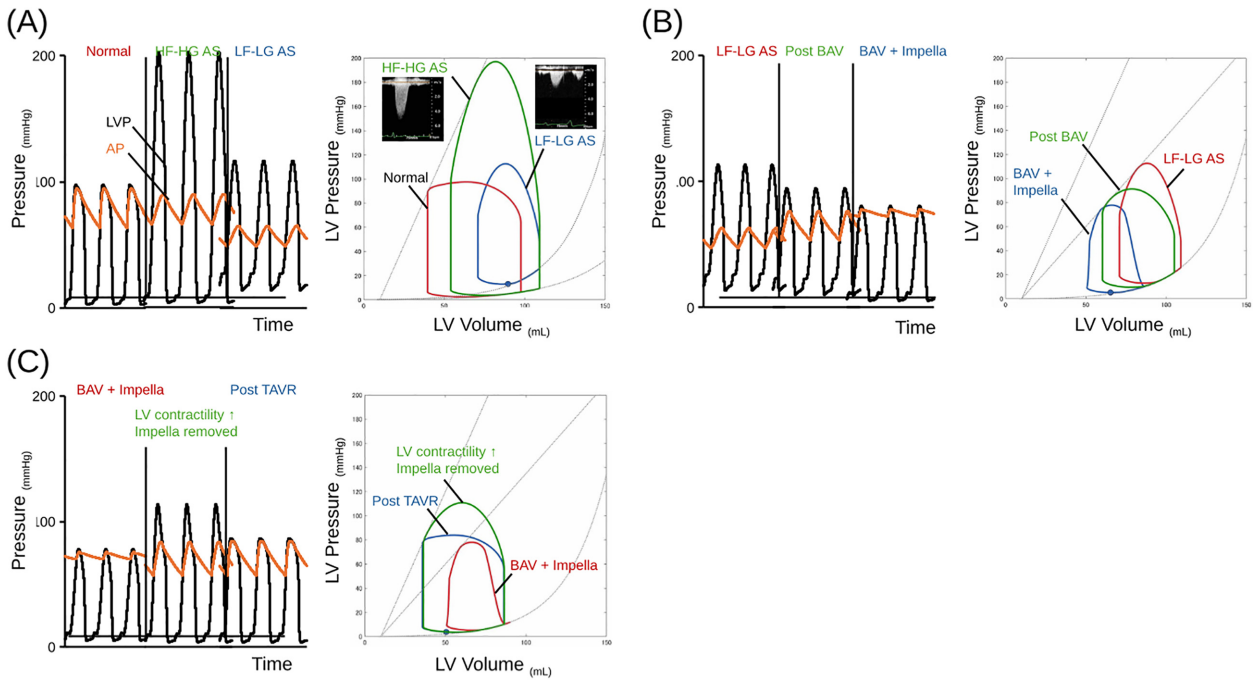

FIGURE 4
The schema of trends in hemodynamics and PV loop in LF-LG AS case treating BAV-PELLA-TAVR. **(A)** Hemodynamics and PV loops of a normal heart, AS, and LF-LG AS patients. The schema of hemodynamics and PV loops were illustrating by hemodynamic simulator. The AS causes a significant upward shift in the PV loop (green line) from the baseline (red line). Impaired LV systolic and diastolic function shifts the PV loop downward (blue line). The details of the simulation model can be found in reference (17). In the simulation, each ventricular valve was modeled as a one-way valve based on Bernoulli's theorem, while AS was simulated by varying the AVA from 4.0 to 0.4 cm^2/s. **(B)** Hemodynamics and PV loops of BAV in an LF-LG AS patient with low LV function followed by Impella support. BAV significantly reduces the PG, while the increase of stroke volume is limited, and congestive HF is not sufficiently improved (green line). Impella significantly improves hemodynamics while reducing the LV load (blue line). **(C)** Hemodynamics and PV loops in a LF-LG AS patient transitioning to TAVR. Impella support after BAV provides stable hemodynamics, contributes to improved LV contractility (green line), and allows TAVR (blue line) to be performed in a stable condition. AP, aortic pressure; AS, aortic stenosis; BAV, balloon aortic valvuloplasty; AVA, aortic valve area; HF, heart failure; HF-HG, high flow high gradient; LF-LG, low flow low gradient; LV, left ventricular; LVP, left ventricular pressure; PG, pressure gradient; PV loop, pressure-volume loop; TAVR, transcatheter aortic valve replacement.

support promptly improved hemodynamics and enabled stable medication adjustment and pre-TAVR HF management. Case 3 had severe AS with preserved LV function. As BAV treatment was limited owing to worsening AR, Impella was used for HF management, enabling a stable transition to TAVR. Despite differences in LV function, AS severity, and HF status, all three cases shared the common feature that Impella-mediated HF management after BAV facilitated a stable transition to TAVR treatment. In addition, BAV-PELLA-TAVR provided sufficient time to discuss the optimal strategy for severe AS in the heart team meeting.

4 Conclusions

"BAV-PELLA-TAVR," which stabilizes hemodynamics and improves ADHF, may be one of the optimal therapeutic options for the sickest patients with CS due to severe AS.

Data availability statement

The datasets presented in this article are not readily available because the raw data supporting the conclusions of this article are not publicly available due to concerns regarding patient confidentiality. Relevant information has been anonymized and summarized in the article. Further details may be provided upon reasonable request, contingent on approval by the institutional ethics board. Requests to access the datasets should be directed to Jun Nakata, jun-nakata@nms.ac.jp.

Ethics statement

Written informed consent was obtained from the participant/patient(s) for the publication of this case report.

Author contributions

YW: Writing – original draft, Writing – review & editing. JN: Conceptualization, Writing – original draft, Writing – review & editing. HM: Investigation, Writing – original draft, Writing – review & editing. KS: Conceptualization, Investigation, Writing – original draft, Writing – review & editing. KM: Supervision, Writing – review & editing. TS: Supervision, Writing – review & editing. YT: Supervision, Writing – review & editing. YI: Supervision, Writing – review & editing. MT: Supervision, Writing – review & editing. YH: Supervision, Writing – review &

editing. TK: Supervision, Writing – review & editing. MH: Supervision, Writing – review & editing. RS: Supervision, Writing – review & editing. HS: Supervision, Writing – review & editing. TY: Supervision, Writing – review & editing. KA: Supervision, Writing – review & editing.

Funding

The author(s) declare that financial support was received for the research and/or publication of this article. The simulation study in this report was partly supported by the grant from ABIOMED, Inc. The funder was not involved in the study design, collection, analysis, interpretation of data, the writing of this article, or the decision to submit it for publication.

Conflict of interest

JN received honoraria from Abiomed Japan K.K. and Mallinckrodt Pharma K.K. KS received research funding from Abiomed Inc., NTT Research, Inc., Asahi Kasei ZOLL Medical Corporation, Neuroceuticals Inc., and Zeon Medical Inc., and honoraria from Abiomed Japan K.K. and Mallinckrodt Pharma K.K.

The remaining authors declare that the research was conducted in the absence of any commercial or financial relationships that could be construed as a potential conflict of interest.

Generative AI statement

The author(s) declare that no Generative AI was used in the creation of this manuscript.

Publisher's note

References

1. Lüsebrink E, Binzenhöfer L, Adamo M, Lorusso R, Mebazaa A, Morrow DA, et al. Cardiogenic shock. *Lancet*. (2024) 404:2006–20. doi: 10.1016/s0140-6736(24)01818-x

2. Nakata J, Yamamoto T, Saku K, Ikeda Y, Unoki T, Asai K. Mechanical circulatory support in cardiogenic shock. *J Intensive Care*. (2023) 11:64. doi: 10.1186/s40560-023-00710-2

3. d'Arcy JL, Coffey S, Loudon MA, Kennedy A, Pearson-Stuttard J, Birks J, et al. Large-scale community echocardiographic screening reveals a major burden of undiagnosed valvular heart disease in older people: the OxVALVE population cohort study. *Eur Heart J*. (2016) 37:3515–22. doi: 10.1093/eurheartj/ehw229

4. Nair RM, Chawla S, Abdelghaffar B, Alkhalaieh F, Bansal A, Puri R, et al. Comparison of contemporary treatment strategies in patients with cardiogenic shock due to severe aortic stenosis. *J Am Heart Assoc*. (2024) 13:e033601. doi: 10.1161/jaha.123.033601

5. Otto CM, Nishimura RA, Bonow RO, Carabello BA, Erwin JP 3rd, Gentile F, et al. 2020 ACC/AHA guideline for the management of patients with valvular heart disease: a report of the American College of Cardiology/American Heart Association Joint Committee on clinical practice guidelines. *Circulation*. (2021) 143:e72–e227. doi: 10.1161/cir.0000000000000923

6. Izumi C, Eishi K, Ashihara K, Arita T, Otsuji Y, Kunihara T, et al. JCS/JSCS/JATS/JSVS 2020 guidelines on the management of valvular heart disease. *Circ J*. (2020) 84:2037–119. doi: 10.1253/circj.CJ-20-0135

7. Bongiovanni D, Kühl C, Bleiziffer S, Stecher L, Poch F, Greif M, et al. Emergency treatment of decompensated aortic stenosis. *Heart*. (2018) 104:23–9. doi: 10.1136/heartjnl-2016-311037

8. Johnson DW, Erwin IJ. Use of Impella 5.0 prior to transcatheter aortic valve replacement in a patient with severe aortic stenosis and cardiogenic shock. *J Heart Valve Dis*. (2017) 26:485–7.

9. Burzotta F, Nerla R, Trani C. Bail-ouse of impella CP as a bridge to TAVI in a cardiogenic shock patient: the "pump-rewiring" technique. *J Invasive Cardiol*. (2016) 28:E1–5.

10. Panoulas V, Greenough N, Sulemane S, Monteagudo-Vela M, Lees N. The role of mechanical circulatory support in patients with severe left ventricular impairment treated with transcatheter aortic valve implantation and percutaneous coronary intervention. *Cardiovasc Revasc Med*. (2021) 28s:169–75. doi: 10.1016/j.carrev.2021.03.020

11. Abraham J, Wang L, Kumar V, Kirker EB, Spinelli KJ. Axillary transvalvular microaxial pump as extended bridge to transcatheter aortic valve replacement in cardiogenic shock with severe aortic stenosis. *J Heart Lung Transplant*. (2022) 41:434–7. doi: 10.1016/j.healun.2021.12.010

12. Miura S, Arita T, Kumamaru H, Domei T, Yamaji K, Soga Y, et al. Causes of death and mortality and evaluation of prognostic factors in patients with severe aortic stenosis in an aging society. *J Cardiol*. (2015) 65:353–9. doi: 10.1016/j.jjcc.2015.02.011

13. Goel K, Shah P, Jones BM, Korngold E, Bhardwaj A, Kar B, et al. Outcomes of transcatheter aortic valve replacement in patients with cardiogenic shock. *Eur Heart J*. (2023) 44:3181–95. doi: 10.1093/eurheartj/ehad387

14. Eugène M, Urena M, Abtan J, Carrasco JL, Ghodbane W, Nataf P, et al. Effectiveness of rescue percutaneous balloon aortic valvuloplasty in patients with severe aortic stenosis and acute heart failure. *Am J Cardiol*. (2018) 121:746–50. doi: 10.1016/j.amjcard.2017.11.048

15. Debry N, Kone P, Vincent F, Lemesle G, Delhaye C, Schurtz G, et al. Urgent balloon aortic valvuloplasty in patients with cardiogenic shock related to severe aortic stenosis: time matters. *EuroIntervention*. (2018) 14:e519–e25. doi: 10.4244/eij-d-18-00029

16. Kitahara H, Kumamaru H, Kohsaka S, Yamashita D, Kanda T, Matsuura K, et al. Clinical outcomes of urgent or emergency transcatheter aortic valve implantation-insights from the nationwide registry of Japan transcatheter valve therapies. *Circ J*. (2024) 88:439–47. doi: 10.1253/circj.CJ-22-0536

17. Masha L, Vemulapalli S, Manandhar P, Balan P, Shah P, Kosinski AS, et al. Demographics, procedural characteristics, and clinical outcomes when cardiogenic shock precedes TAVR in the United States. *JACC Cardiovasc Interv*. (2020) 13:1314–25. doi: 10.1016/j.jcin.2020.02.033

18. Nishimura T, Hirata Y, Ise T, Iwano H, Izutani H, Kinugawa K, et al. JCS/JSCVS/JCC/CVIT 2023 guideline focused update on indication and operation of PCPS/ECMO/IMPELLA. *J Cardiol*. (2024) 84:208–38. doi: 10.1016/j.jjcc.2024.04.006

19. Hiraoka A, Saku K, Nishikawa T, Sunagawa K. A case report of unexpected right-to-left shunt under mechanical support for post-infarction ventricular septal defect: evaluation with haemodynamic simulator. *Eur Heart J Case Rep*. (2021) 5:ytab209. doi: 10.1093/ehjcr/ytab209

20. Yokota S, Nishikawa T, Saku K. Impella as an optimizing tool for heart failure interventions. *J Coron Artery Dis*. (2024) 30:127–37. doi: 10.7793/jcad.30.23-00021

frontiers | Frontiers in Cardiovascular Medicine

TYPE Review
PUBLISHED 22 May 2025
DOI 10.3389/fcvm.2025.1586389

OPEN ACCESS

EDITED BY
Keita Saku,
National Cerebral and Cardiovascular Center, Japan

REVIEWED BY
Naoki Tadokoro,
National Cerebral and Cardiovascular Center, Japan
Ikuko Shibasaki,
Dokkyo Medical University, Japan

*CORRESPONDENCE
Hideaki Nonaka
✉ hideaki54nonaka@gmail.com

†These authors share last authorship

RECEIVED 02 March 2025
ACCEPTED 26 March 2025
PUBLISHED 22 May 2025

CITATION
Nonaka H, Lu LY, Obonyo NG, Suen JY, McGiffin DC, Fanning JP and Fraser JF (2025) Right heart failure after left ventricular assist device implantation: latest insights and knowledge gaps on mechanism and prediction.
Front. Cardiovasc. Med. 12:1586389.
doi: 10.3389/fcvm.2025.1586389

Right heart failure after left ventricular assist device implantation: latest insights and knowledge gaps on mechanism and prediction

Hideaki Nonaka[1,2]*, Lawrence Y. Lu[1,3], Nchafatso G. Obonyo[1,2,4,5], Jacky Y. Suen[1,2,6], David C. McGiffin[1,7,8], Jonathon P. Fanning[1,2,9†] and John F. Fraser[1,2,10†]

[1]Critical Care Research Group, The Prince Charles Hospital, Brisbane, QLD, Australia, [2]Institute for Molecular Bioscience, University of Queensland, Brisbane, QLD, Australia, [3]Division of Surgery, Princess Alexandra Hospital, Brisbane, QLD, Australia, [4]Wellcome Trust Centre for Global Health Research, Imperial College London, London, United Kingdom, [5]Initiative to Develop African Research Leaders/KEMRI-Wellcome Trust Research Programme, Kilifi, Kenya, [6]School of Pharmacy and Medical Sciences, Griffith University, Southport, QLD, Australia, [7]Cardiothoracic Surgery and Transplantation, The Alfred Hospital, Melbourne, VIC, Australia, [8]Department of Surgery, Monash University, Melbourne, VIC, Australia, [9]Anesthesia & Perfusion Services, The Prince Charles Hospital, Brisbane, QLD, Australia, [10]Intensive Care Unit, St Andrews War Memorial Hospital, Brisbane, QLD, Australia

Heart failure is a global health concern, with many patients being unresponsive to medical therapies. In end-stage disease, left ventricular assist devices (LVADs) offer an alternative to transplantation, yet their clinical course remains unfavorable, with up to one in four patients dying within a year. Although LVAD implantation aims to alleviate left-sided congestion and reduce right ventricular burden, a significant proportion of patients develop RHF, which is a major driver of morbidity and mortality. The underlying mechanisms leading to RHF remain a subject of debate, with no definitive conclusions reached. Due to the heterogeneity of heart failure pathophysiology, clinical data varies, and the translation of preclinical findings into effective bedside management remains challenging. These factors collectively hinder the precise characterization of RHF mechanisms, with some proposed explanations remaining speculative. Assessing the risk of RHF development based on pathophysiological insights is essential. However, predicting the progression of RHF following LVAD implantation remains difficult due to complex hemodynamic interactions and the lack of established guidelines, often leading to missed opportunities for timely right ventricular (RV) support device implantation. To reduce the incidence of RHF, this review aims to provide insights into RV failure mechanisms and propose a refined predictive approach. Although data in this field is rapidly evolving, explanations and assessment methods have not been significantly updated. This paper consolidates recent findings, presents updated perspectives, and identifies remaining gaps in knowledge.

KEYWORDS

LVAD, left ventricular twist, pressure-volume loop, PV loop, RHF, right ventricle, RVF, score

1 Introduction

Heart failure (HF) affects more than 65 million worldwide, with many patients being unresponsive to medical therapies (1). For those with end-stage HF, mechanical circulatory support (MCS), in the form of left ventricular assist devices (LVADs), has emerged as a bridge to transplantation, to a decision, or to myocardial recovery, as well as destination therapy in patients in whom cardiac transplantation is contraindicated (2).

Despite advances in LVAD indications, the incidence of right heart failure (RHF) after LVAD implantation remains a major concern, where the dysfunctional right ventricle (RV) undermines hemodynamic stability and is a driver of morbidity and mortality (3, 4). Previous studies report that 10%–35% of patients experience RHF within one month following LVAD placement (5–8) and the in-hospital mortality rate of LVAD recipients requiring right ventricular assist device (RVAD) was up to 50%, while patients undergoing planned biventricular assist device (BiVAD) placement face a mortality rate of 30% (6).

Considering that LVADs relieve congestion in the left-side heart and, consequently, the right side, the underlying mechanism of RHF is challenging to fully elucidate. Several contributing factors have been discussed in previous reviews, including excessive LVAD suction disrupting ventricular interdependence and increased LVAD flow elevating RV preload, yet adequate evidence supporting some of these phenomena is lacking, with speculative components included. Additionally, it remains unclear which mechanisms are well supported by firm evidence and which remain hypothetical (9). Most of the current evidence relies on load-dependent functional parameters, further raising concerns about their reliability in LVAD patients, where loading conditions fluctuate dramatically (10–12).

Additionally, planned BiVAD implantation potentially improves the outcomes as mentioned previously (6), yet the definitive indication for simultaneous LV and RV support device implantation is unclear. Although numerous factors have been proposed as predictors for RHF after LVAD implantation, their reproducibility remains inconsistent.

To advance our understanding of the mechanism and possibly improve the prediction of post-LVAD RHF, this review aims to: (i) examine the recently proposed pathophysiological mechanistic evidence from the human pressure-volume (PV) loops to capture load-independent functional parameters such as RV end-systolic elastance (Ees) and end-diastolic pressure volume relation (EDPVR); (ii) evaluate existing functional assessment approaches and risk scores to predict RHF development, and consolidate the key factors; and, (iii) clarify the current knowledge gaps and future research directions. To capture the latest insights, we conducted an extensive literature search in PubMed MEDLINE, Scopus, Embase, and ClinicalTrials.gov using controlled keywords, primarily “LVAD” and “RHF.”

Figure 1 illustrates the principal concepts discussed in this review. The goal of this review is to assist clinicians in optimizing LVAD management and guiding research, ultimately to improve patient outcomes.

2 RHF definition

The Interagency Registry for Mechanically Assisted Circulatory Support (INTERMACS) and the updated Mechanical Circulatory Support—Academic Research Consortium (MCS–ARC) definitions of RHF have been widely accepted (13, 14). In the most recent consensus statement from 2020, RHF is classified into three categories based on the timing of symptom onset (Table 1) (14):

1. Early acute RHF,
   - requiring concomitant implantation of a temporary VAD or
   - requiring RVAD with an LVAD implantation
2. Early post-implantation RHF,
   - requiring a RVAD <30 days or
   - failing to wean from inotropes, vasopressors or nitric oxide within 14 days, or
   - death attributable to RHF <14 days from an LVAD implantation
3. Late RHF,
   - requiring a RVAD more than 30 days or
   - requiring hospitalization for RHF >30 days after an LVAD implantation

In addition to these categories, the diagnostic criteria also include multiple clinical indicators, such as hemodynamic parameters (elevated central venous pressure, reduced cardiac index, and reduced venous oxygen saturation), right heart failure symptoms (e.g., edema, ascites), and end-organ dysfunction (e.g., kidney dysfunction, liver failure) (14). Furthermore, the statement also recommends classifying RHF incidence into three categories based on its associations: (1) patient-related (e.g., valvular heart disease, pulmonary disease, cardiorenal syndrome); (2) management-related (e.g., surgical procedures, inotrope withdrawal, volume overload); and (3) device-related (e.g., pump malfunction, outflow graft compromise). Early RHF occurs most frequently. In a recent study using the STS INTERMACS database, the prevalence of *de novo* RHF at one month (i.e., early RHF) was as high as 24% (8).

Although the overall prevalence of late RHF remains stable and less than early RHF at a rate of 8%–10% over their three-year surveillance, it cannot be underestimated (8). This is because late RHF is also associated with the least favorable outcome (8, 15). Takeda et al. demonstrated the prognostic significance of late RHF after continuous-flow LVAD implantation, with the survival of patients with RHF progressively worsening compared to that of patients without RHF (Figure 2) (16).

This definition is widely adopted in most studies and is therefore used in this review.

3 Mechanisms of RHF

This section outlines the impact of implantation of an LVAD on the RV and discusses the potential mechanisms driving RHF.

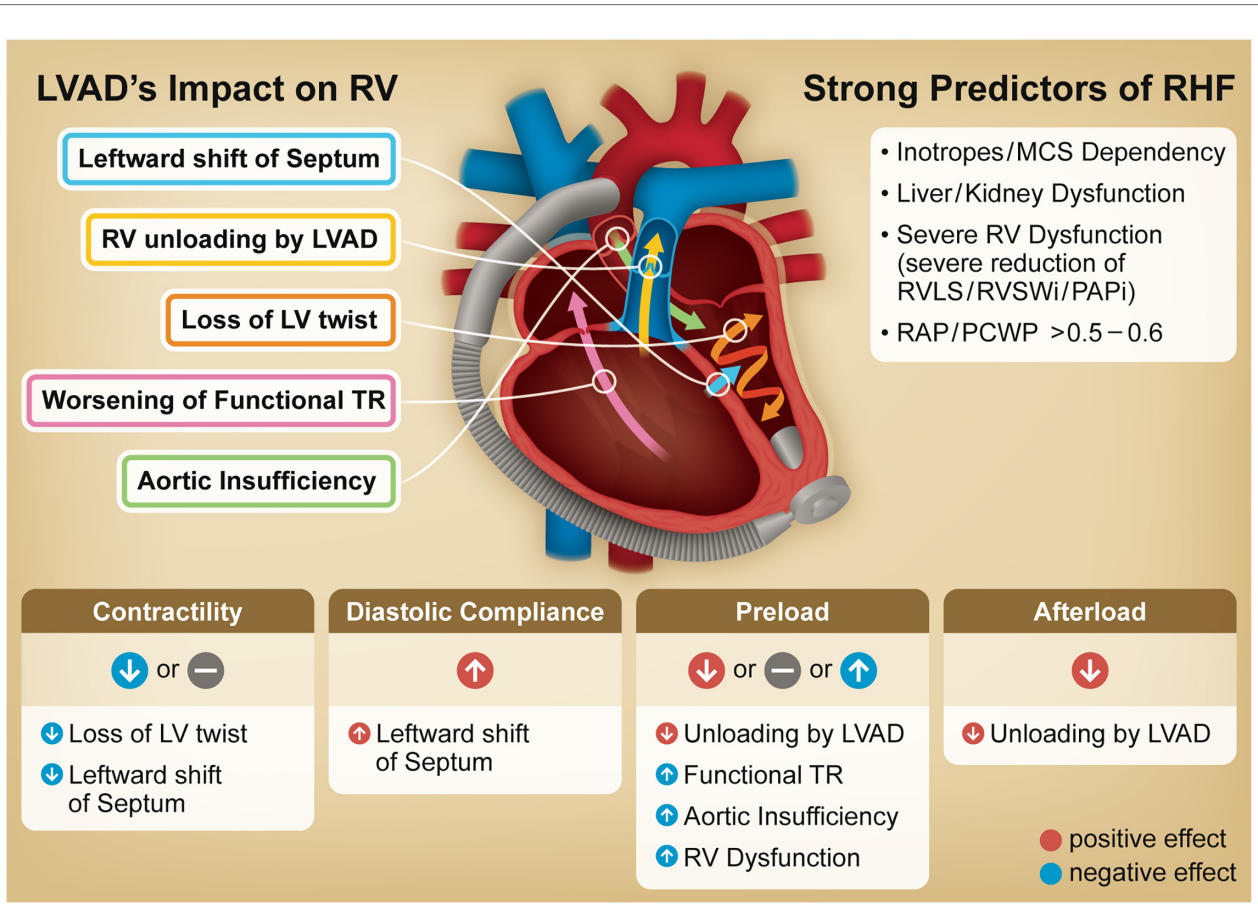

FIGURE 1
Graphical abstract. Illustration outlines the primary impact of an LVAD on the RV, including underlying mechanisms driving post-LVAD RHF. The table at the bottom summarizes changes in RV function and loading conditions following LVAD implantation. The column on the right identifies strong predictors for RHF including non-cardiac factors, all of which are incorporated into at least two representative risk scores and have been identified as significant predictors in large scale multivariable analyses. LVAD, left ventricular assist device; TR, tricuspid regurgitation; RV, right ventricle; RHF, right heart failure; MCS, mechanical circulatory support; RV LS, right ventricular longitudinal strain; RVSWi, right ventricular stroke work index; PAPi, pulmonary artery pulsatility index; RAP, right atrial pressure; PCWP, pulmonary capillary wedge pressure.

In the later part of the section, PV loop data from clinical studies are summarized, as it accurately reflects afterload and preload on RV and provide load-independent functional parameters such as Ees and EDPVR (Figure 3). Moreover, PV loops also provide pulmonary artery (PA) effective arterial elastance (Ea) and the RV Ees/Ea ratio, commonly referred to as "RV-PA coupling," which serve as valuable indices of RV contractility in relation to the afterload imposed by the PA (17). These approaches will contribute to a more comprehensive understanding of RHF mechanisms.

A fundamental understanding of interventricular interaction is essential to grasp this section, as it plays a critical role in the pathophysiology of post-LVAD RHF. The Torrent-Guasp helical model describes the entire heart as composed of two interconnected loops of the myocardium (18, 19). One loop has muscle fibers wrapping around both ventricles in parallel with a short axis at their basement, and the other loop has fibers spiraling around the left ventricle (LV), including the interventricular septum. The RV is constructed from these two fiber systems, with the free wall formed by the first (wrapping) myocardial loop and the septal wall formed by the second (helical) structure. This structure is crucial because the "helical" or "twisting" motion of the secondary loop significantly contributes to the RV systolic function. This LV "twisting" contributes to longitudinal motion of RV, while wrapping myocardium primarily facilitates "transverse (radial)" movement of RV free wall (20, 21).

According to studies in a canine model by Hoffman and colleagues, where the RV free wall was replaced with a xenograft pericardial patch, LV motion accounted for 24%–35% of RV stroke work (SW) (22). Thus, RV function can be significantly influenced by the LV through the septal wall, which is key factor in the occurrence of RHF after LVAD implantation.

3.1 LVAD-specific effects on RV

The following mechanisms can act individually or in combination: (1) Loss of LV twist, (2) Leftward shift of the interventricular septum, (3) Changes in RV Loading Conditions

TABLE 1 MCS-ARC definition of right heart failure.

RHF type	Criteria for diagnosis
Early Acute RHF	• Need for implantation of a temporary or durable RVAD (including ECMO) concomitant with LVAD implantation (i.e., the RVAD is implanted before the patient leaves the operating room).
Early post-implant RHF	• Need for implantation of a temporary or durable RVAD (including ECMO) within 30 days following LVAD implantation (for any duration of time); OR • Failure to wean from inotropes or vasopressors, or inhaled nitric oxide within 14 days following LVAD implantation; OR • Need to (re)initiate this support within 30 days of LVAD implantation for a duration of at least 14 days; OR • Death occurring within 14 days of LVAD implantation in patients who did not receive an RVAD but remained on inotropes or vasopressors at the time of death and met the diagnostic criteria for RHF (at least 2 clinical findings or 1 manifestation listed below. • Primary diagnosis of RHF (must have ≥2 of the clinical findings OR ≥1 manifestation): ○ Clinical Findings: ■ Ascites ■ Functionally limiting peripheral edema (at least moderate level of swelling in the extremities) ■ Elevated estimated JVP (at least halfway up the neck in an upright patient) ■ Elevated measured CVP or RA pressure (≥16 mm Hg) ○ Manifestations: ■ Renal failure: serum creatinine >2 × baseline ■ Liver injury: ≥2 × upper limit normal in AST/ALT, or total bilirubin >2.0 mg/dl ■ S_VO_2 < 50% ■ Cardiac index <2.2 L/min/m^2 ■ Reduction in pump flow of >30% from the previous baseline (in the absence of mechanical causes such as tamponade or ■ tension pneumothorax) ■ Elevated lactate >3.0 mmol/L. · · Pediatric Adaptation The above criteria may be modified for pediatric patients. Primary diagnosis of RHF requires ≥2 of the clinical findings OR ≥1 manifestation ○ Clinical Findings: ■ Ascites ■ Significant peripheral edema (at least moderate level of swelling in the extremities) ■ Elevated JVP (visible in an upright patient) or hepatomegaly (3 + cm below costal margin) ■ Elevated CVP or RA pressure: - Age 10–18 years: CV*P* >14 mm Hg - Age 5–10 years: CVP >12 mm Hg - Age <5 years: CVP >10 mm Hg ○ Manifestations: ■ Renal failure: serum creatinine ≥1.5 × above baseline. ■ Liver injury with an elevation of AST, ALT or total bilirubin ≥2 × upper normal. ■ Decrease in pump flow ≥30% from a recent baseline in the absence of tamponade. ■ We need to decrease the pump rate ≥20% or more from a recent baseline owing to the poor filling of LVAD in a pulsatile system. ■ Cardiac Index <2.2 L/min/m^2
Late RHF	• Need for implantation of an RVAD (including ECMO) ≥30 days after LVAD implantation. This may occur during the index hospitalization for LVAD placement or any subsequent readmission, OR • Hospitalization ≥30 days post-implant requiring intravenous diuretics or inotropic support for ≥72 h and associated with RHF by criteria below: ○ Diagnosis of RHF (must have ≥2 clinical findings OR ≥1 manifestation: ■ Clinical Findings ■ Ascites ■ Functionally limiting peripheral edema (>2+). ■ Elevated estimated JVP at least halfway up the neck in an upright patient. ■ Elevated measured CVP (>16 mm Hg). ○ Manifestations: ■ Renal failure: serum creatinine >2 × baseline value ■ Liver injury: ≥2 × upper limit normal in AST/ALT, or total bilirubin >2.0 mg/dl ■ Reduction in pump flow of >30% from the previous baseline (in the absence of tamponade) ■ S_VO_2 < 50% ■ Cardiac index <2.2 L/min/m^2 ■ Elevated lactate >3.0 mmol/L • Pediatric Adaptation ○ Requirement for intravenous diuretics or inotropic support of ≥72 h due to new onset right heart failure (i.e., not present continuously since implantation, with a period of ≥7 consecutive days off intravenous support) ■ Diagnosis of RHF requires ≥2 of the following clinical findings, or ≥1 manifestations (as above, adjusting for pediatric CVP thresholds and definitions of ascites, edema, and hepatomegaly)

Above definition of RHF is extracted from the MCS-ARC consensus statement (14). RHF, right heart failure; LVAD, left ventricular assist device; RVAD, right ventricular assist device; ECMO, extracorporeal membrane oxygenator; AST, aspartate aminotransferase; ALT, alanine aminotransferase; SvO_2, venous oxygen saturation; JVP, jugular venous pressure; CVP, central venous pressure; RA, right atrium.

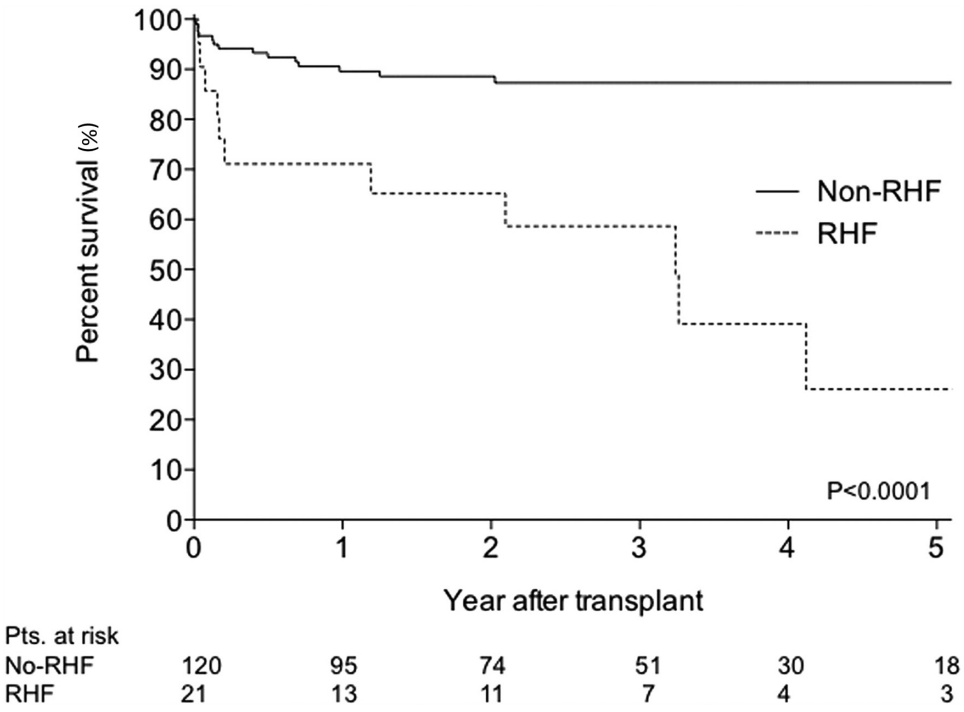

FIGURE 2
Comparison of survival rate between patients with and without right heart failure five-year kaplan-meier curve between patients with and without RHF.. RHF was defined as rehospitalization and medical treatment because of recurrent RHF or patients who required continuous inotropic support because of persistent RHF >4 weeks after implantation. The survival curve gap between the two groups widens year by year. Reproduced with permission from "Comparison of survival: non-RHF group versus RHF group. RHF, right heart failure" by Koji Takeda, Hiroo Takayama, Paolo C. Colombo, Ulrich P. Jorde, Melana Yuzefpolskaya, Shinichi Fukuhara, Donna M. Mancini and Yoshifumi Naka, licensed under CC-BY-NC-ND.

Due to LVAD, (4) Worsening of functional tricuspid regurgitation (TR), (5) Aortic insufficiency (AI). Notably, these mechanisms remain incompletely characterized in the literature, as studying the mechanisms of RHF in patients is challenging presumably due to the heterogeneity of LVAD candidates' pathophysiology and the lack of accurate human data.

3.1.1 Loss of LV twist

- Decrease in RV contractility

In LVAD patients, LV twisting motion is primarily impaired due to two factors: (1) loss of constraint following pericardiotomy, and (2) constraining of the LV apex and septum.

The relationship between pericardial constraint and LV twist has been frequently discussed in the past. A preclinical study demonstrated a decline in LV twist, measured by LV speckle tracking, following pericardiotomy—due to the loss of pericardial constraint, suggesting that this constraint plays a significant role in LV twist. This study was specifically designed to investigate the role of the pericardium and further revealed that the decline in LV twist was restored after pericardial closure (23). Additionally, impaired longitudinal motion of the RV after pericardiotomy has been reported in clinical settings including mitral valve surgery, heart transplantation and coronary artery bypass graft (CABG) surgery, whereas other thoracic surgeries, such as lung transplantation, did not demonstrate a similar effect. Given that LV twist plays a significant role in the longitudinal movement of the RV, RHF after LVAD implantation may be attributable to the loss of LV twist. Long-term follow-up studies have reported that this reduction in longitudinal motion persists for more than one month even after chest closure (23–26). Clinical data linking the loss of LV twist to pericardiotomy specifically in LVAD implantation remain sparse, highlighting the need for further data accumulation to support this explanation.

Additionally, the LVAD replacement to the LV apex can also constrain the LV apex and septum, potentially impairing LV twisting movement (Figure 1). This deformation is considered to negatively affect RV outflow although clinical research on this impact remain limited (20). However, data directly supporting this mechanism also remain scarce, making this impact somewhat speculative. More detailed data on LV twist in LVAD patients are needed.

3.1.2 Leftward shift of interventricular septum

- Decrease in RV contractility

- Improvement in RV diastolic compliance

In an LVAD configuration, suction within the LV displaces the interventricular septum leftward, altering its geometry, reducing septal motion, and consequently diminishing RV contractility, while simultaneously improving RV diastolic compliance (9).

A decline in RV contractility by leftward shift of the interventricular septum is the subject of debate (27), and

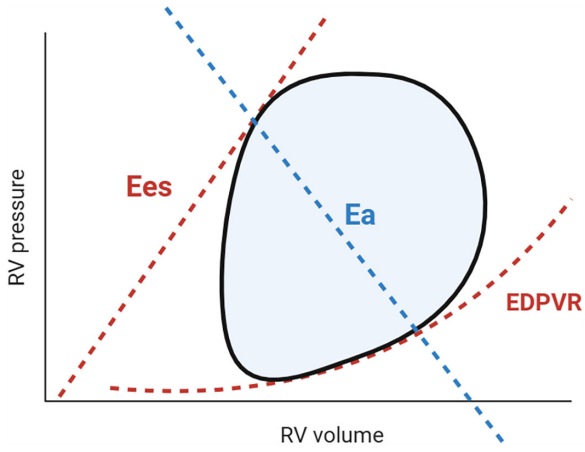

FIGURE 3
Pressure-Volume loop and right ventricular and pulmonary artery coupling. The steady-state RV PV loop (black line) illustrates the relationship between pressure and volume during a cardiac cycle. The enclosed area by the PV loop represents RV stroke work. By reducing preload (e.g., via inferior vena cava occlusion or the Valsalva maneuver), multiple PV loops can be generated, from which Ees and EDPVR can be derived. Effective pulmonary arterial elastance (Ea; blue) is a determinant of RV afterload. The RV Ees/Ea ratio describes RV-PA coupling, assessing contractility relative to load. An optimal ratio (1.5–2.0) ensures cardiac efficiency, whereas uncoupling (0.6–1.0) signifies RV decompensation (17, 20). RV, right ventricle; PV, pressure volume; Ees, end-systolic elastance; EDPVR, end-diastolic pressure volume relationship; Ea, effective arterial elastance.

preclinical studies support this expectation (28, 29). Since the interventricular septum plays a pivotal role in RV systolic function, as previously mentioned, excessive LVAD suction can impair septal wall motion, thereby compromising RV function. A study on PV loops and septal strain for RV contractility assessment in LVAD patients found that alterations in RV Ees during ramp test were significantly correlated with RV septal strain ($r = 0.78$, $p = 0.02$) but not with free wall strain ($r = 0.45$, $p = 0.26$), highlighting the critical role of the interventricular septum in RV contractility (30). Impaired septal movement can be compensated by the RV free wall; however, this mechanism fails in patients with a high afterload. In this context, contractile impairment significantly affects RV SV, resulting in RV-PA uncoupling (20).

In contrast to contractility, leftward septal deformation can enhance RV compliance. Left-sided suction allows the RV to expand further, even under low end-diastolic pressure, thereby increasing diastolic compliance, a mechanism that will be discussed later in the PV loop part (3–2. PV loop in patients with LVAD). This effect is beneficial to the RV, and does not directly contribute to RHF (31).

3.1.3 Changes in RV loading conditions due to LVAD

- Decrease(/Increase) in RV afterload

- Decrease/Increase in RV preload

To avoid confusion, this paper defines afterload/preload as end-systolic pressure (ESP) and end-diastolic pressure (EDP), respectively as per Guyton and Hall Textbook (32). LVAD unloading generally relieves the load on the RV. However, preload can increase in specific conditions, such as RV dysfunction, TR, and LVAD-induced AI. Since claims especially regarding changes in preload after LVAD implantation vary depending on review papers (33, 34), we present actual hemodynamic data of ESP and EDP to support our discussion.

RV afterload

Since an LVAD relieves congestion on the left side of the heart and in the pulmonary circulation, RV afterload is generally expected to decrease following device placement. Below, we have listed three papers that report a reduction in RV afterload (ESP) or related components, including pulmonary capillary wedge pressure (PCWP) and mean PA pressure.

1. Data from Brener and colleagues demonstrated a slight but significant decrease in RV afterload during a temporary increase in LVAD speed (RV ESP 31.58 ± 9.75–29.58 ± 9.41 mmHg: $p = 0.02$) (35).
2. Regarding factors related to RV afterload, Masri and colleagues reported pulmonary artery catheter (PAC) data showing a significant reduction in PCWP (23.2 ± 7.6–14.9 ± 7.3 mmHg; $p < 0.01$) and mean PA pressure (from 35.9 ± 9.9 to 23.3 ± 7.7 mmHg; $p < 0.01$) within 72 h after LVAD implantation with a volume displacement pump (63%), axial pump (26%), and centrifugal pumps (11%) (36).
3. This trend generally continues over the long-term, as another study reported sustained decreases in PCWP (from 23 [1st and 3rd interquartile 17, 30] to 12 [7, 17] mmHg) and in effective arterial elastance (Ea; from 1.31 [0.7, 1.62] to 0.59 [0.42, 0.9] mmHg/ml) over six months after implantation of axial pumps (28%) and centrifugal pumps (72%) (37).

However, specifically in cases of AI, afterload may increase. Hemodynamic data comparing pressure parameters showed that patients who developed AI had higher mean PA pressure and PCWP compared to those without AI (38, 39).

RV preload

Preload, or RV end-diastolic pressure (EDP), decreases or remains stable immediately after LVAD implantation because of LVAD suction.

Below, we have listed three papers that report a reduction or stabilization in RV preload.

1. PV loop data from Brener and colleagues also demonstrated a slight decrease in preload (RV EDP 7.95 ± 3.55–7.42 ± 3.29 mmHg: $p = 0.04$).
2. Right atrial pressure (RAP) also generally decreases or stabilizes in the short term (RAP: 11.8 ± 6.5–10.1 ± 5.4 mmHg) after LVAD implantation with volume displacement pump, axial pump, and centrifugal pumps (36)
3. This trend generally continues over the long-term (RAP: 11 [1st and 3rd interquartile 5, 16], 10 [5, 15] mmHg) after implantation of axial pump and centrifugal pump (37).

Changes aforementioned are slight and biologically insignificant, suggesting that RV preload remains unchanged after LVAD

implantation. However, in the presence of RV dysfunction, functional TR, or AI, preload may increase (40). The impact of AI and TR on the RV is discussed later in sections "3-1-4. Worsening of Functional Tricuspid Regurgitation" and "3-1-5. Aortic Insufficiency".

Notably, there is an explanation suggesting that RV preload increases due to LVAD flow (34), probably based on data showing an increase in RV EDV (41). However, the studies examining changes in RV EDP, RAP, or CVP, not EDV, immediately after LVAD implantation or during ramp test, generally demonstrate either a decrease or stability in these values (35, 42, 43). An increase in RV EDV may result from improved RV compliance due to LVAD-induced suction; therefore, careful interpretation of these parameters is necessary to accurately assess true RV preload following LVAD implantation.

However, excessive LVAD speed remains a potential concern in LVAD management, because excessive LVAD speed may significantly impair RV contractility by disrupting LV twist and septal motion. In this dysfunctional RV, increased preload may be required to maintain stroke volume and circulatory equilibrium (41).

3.1.4 Worsening of functional tricuspid regurgitation

- Increase in preload

Leftward shift of the septal wall can enlarge the tricuspid annulus, potentially inducing functional TR (44, 45). However, the real-world data has shown that over 50% of moderate-severe TR improves following LVAD implantation, attributed to the reduction in afterload (46–48). A particular proportion of patients (30%) still have persistent TR, and 6%–20% develops significant TR following surgery (46–48), both of which are associated with RHF development (44). Nakanishi and colleagues identified preprocedural tricuspid valve annular diameter as a predictor of persistent or worsening TR (49) and atrial fibrillation (AF) has also been reported as a potential predictor (48, 50). However, a large registry study from INTERMACS did not demonstrate a prognostic benefit of tricuspid valve procedures at the time of LVAD implantation, suggesting that the extent to which TR contributes to the development of right heart failure (RHF) remains unclear. Rather, TR may be a consequence of right heart enlargement secondary to RHF (51).

3.1.5 Aortic insufficiency

- Increase in preload and afterload

AI increases preload on the LV and, ultimately RV (52). Indeed, AI has been linked to worsening mitral regurgitation following LVAD implantation, further supporting significant volume overload on the LV and subsequent negative effects on RV (53). Given its gradual progression, AI may contribute to late RHF.

Aortic insufficiency (AI) can develop over time due to LVAD outflow into the aorta. According to the STS INTERMACS registry, 15% of patients developed AI ≥moderate at 2 years after LVAD implantation, which was associated with poor outcomes (53). Importantly, this percentage gradually rose after LVAD implantation, having reached 37.6% within three years (54, 55).

At the time of LVAD implantation, it is reasonable to consider concomitant procedures on the aortic valve for more than mild AI and the outflow graft anastomosis should be oriented downstream to prevent the development of or progression of AI. However, outcome data on these interventions remain conflicting, and the effectiveness has not been clearly demonstrated (56). Following implantation, optimizing LVAD flow is also required to avoid excessive output to the aorta (54).

3.2 PV loop in patients with LVAD

This section summarizes data on the RV PV loop during a ramp test in patients with an LVAD, to capture true or intrinsic change of RV function due to LVAD suctioning.

Brener et al. published data in HeartMate3 recipients ($n = 19$) recruited from two sites (35). Based on the statistical analysis of ramp tests including all patients, they concluded the impact of an LVAD on the RV is as follows:

1. No significant decline in RV contractility
2. Improvement in RV diastolic compliance
3. Reduction in RV afterload

Notably, contractility did not significantly change, which contradicts the commonly held view that RV contractility declines due to loss of LV twist and impaired septum motion. In their study population, as pump speed was increased from 5,000 to 5,800 rpm, the RV PV loop expanded rightward and shifted downward, indicating an increase in SV and SW in response to higher pump speed. This change is attributed to "an improvement in diastolic compliance (EDPVR), also referred to as adaptive diastolic compliance in response to LVAD suctioning," as well as "a reduction in afterload" (Figure 4A). From this perspective, therefore, the RV may accommodate the increased flow generated by the LVAD through enhanced diastolic function. In contrast, part of RVs in their study show inability to improve EDPVR, referred to inadaptive diastolic compliance, and only afterload is decreased in response to increased LVAD flow (Figure 4B), where PV loop shifts only downwards without rightward shift. These RVs failing to increase RV diastolic compliance, may be unable to generate a comparable SV, which may result in compromised hemodynamics and RHF.

Although the authors (35) concluded that contractility did not change, this interpretation should be treated with caution given the study limitation: (1) all patients were stable outpatients in a late postoperative phase, with a median of 144.5 days (interquartile range: 53.5–357 days) after LVAD implantation; (2) the small sample size ($n = 19$) limits the generalizability of the findings: and (3) only temporary changes were considered in this study, leaving uncertainty regarding the chronic impact of LVAD support. Further research with a larger, more heterogeneous cohort and longitudinal assessments is needed to draw more definitive conclusions about systolic function.

Besides, Scheel et al. also reported the measurement of RV Ees using conductance catheters in HeartMate 3 (Abbott, Chicago, IL)

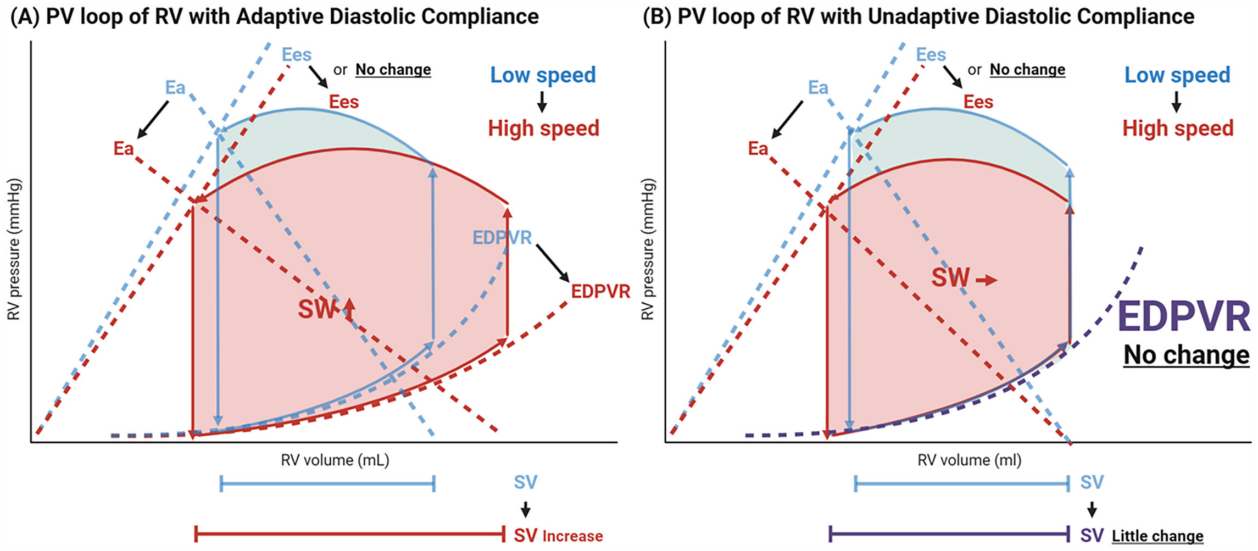

FIGURE 4
Transformation in right ventricular pressure-volume loop during ramp test. Depicted is the schematic illustration of RV PV loop transformation based on the current study (35). With the increase in LVAD pump speed, the EDPVR curve leans downwards, and the inclination of Ea line gets smaller (rightward/downward shift in RV PV loop), meaning that diastolic compliance improves, and afterload decreases **(A)** However, they identified certain recipients whose EDPVR does not improve and only RV afterload decreases (only downward shift) in response to pump speed, susceptive of inadaptive diastolic compliance, which may compromise hemodynamics and causes RHF **(B)** RV, right ventricle; PV, pressure-volume; Ea, effective arterial elastance; Ees, end-systolic elastance; EDPVR, end-diastolic pressure-volume relationship; SW, stroke work; SV, stroke volume; LVAD, left ventricular assist device; RVSWi, right ventricular stroke work index; RHF, right heart failure.

and HeartWare (Medtronic, Minneapolis, MN) recipients ($n = 13$) (30). During their ramp test (low, intermediate, and high speeds, increased by 100–200 rpm), RV Ees declined in specific cases. These findings differ from those reported by Brener et al., suggesting a heterogeneous impact on a case-by-case basis and underscoring that the negative effect of LVAD pump suction on RV contractility still cannot be overlooked.

Of note, all cases studied in the above reports were stable outpatients from 1 to 12 months after LVAD implantation, and thus their RVs may have been stable and managed well. Based on these results and previous data, we summarized the impact of LVAD on RV in the table on Figure 1.

3.3 RHF mechanism and knowledge gaps

Based on the latest evidence, we propose the following LVAD-specific mechanisms of RHF:

1. Inadequate Adaptation of Diastolic Function to Increased Flow: While diastolic compliance generally improves to accommodate the increased flow and generate more SV comparable to LVAD-generated SV, some RVs with unchanged diastolic compliance fail to provide the necessary SV, possibly leading to RHF (Figure 4B).
2. Reduced Contractility: RV contractility declines due to the loss of LV twist and reduced mobility of the septal wall caused by LVAD suction. Compromised contractility leads to RV-PA uncoupling and RHF, particularly in patients with high afterload, where the RV free wall fails to compensate for impaired septal movement.
3. Elevation of Preload: Dysfunctional RV and other factors (e.g., functional TR and AI) can increase preload chronically and result in RHF.

This represents the simplest scenario; however, other factors—such as the progression of underlying RV or pulmonary vessel diseases and *de novo* AF—can further compromise RV function and hemodynamic conditions. HF is invariably heterogenous.

The knowledge gap identified from the literature search is the scarcity of firm clinical evidence on proposed mechanisms, particularly on LV twist, and load-independent functional assessments using PV loop derived parameters such as Ees, EDPVR and Ees/Ea in real-world LVAD recipients. These limitations restrict the understanding of RHF within the expected range. Further data from human studies, including heterogenous patients are required to achieve a more definitive understanding.

4 Functional parameters and predictive value

Functional assessment of RV is essential to predict the likelihood of RHF following LVAD implantation (6). Severely depressed RV function prior to LVAD placement is one of the most significant predictors [odds ratio [OR] 1.60; 95% confidence interval [CI] 1.17–2.20; $p = 0.004$] in the multivariable analysis of STS–INTERMACS database (5–8). However, accurately assessing

TABLE 2 Performance of systolic function parameters.

Study (population)	Performance	Cut off	Outcome	Comparison
TAPSE				
Raymer et al. (2019) (*n*=) (96)	AUC 0.67		RHF[a]	PAPi (AUC 0.63)
Patil et al. (2015) (*n* = 152) (97)	AUC 0.85	12.5 mm (Sens 84% Spec 75%)	RVAD implantation	
RV S'				
Kato et al. (2013) (*n* = 68) (67)	AUC 0.81	4.4 cm/s (Sens 87.5% Spec 68.2%)	RHF[a]	E/e' (AUC 0.72) RV LS (AUC 0.75)
Dandel et al. (2010) (*n* = 205) (98)	AUC 0.90	8 cm/s (Sens 84% Spec 90%)	RHF[b]	
RV FAC				
Morita et al. (2018) (*n* = 80) (99)	AUC 0.80	15.9% (Sens 77.3% Spec 54.5%)	RVAD implantation	
Raina et al. (2013) (*n* = 55) (100)	AUC 0.67	31% (Sens 82% Spec 52%)		LAVI (AUC 0.71)
RV LS				
Liang et al. (2022) (*n* = 55) (101)	RVGLS OR 1.44	GLS −9.7% (Sens 0.89 Spec 0.78)	RHF[a]	FWLS (OR 1.23) TAPSE (OR 0.37) FAC (OR 0.91)
Dufendach et al. (2021) (*n* = 137) (102)	RVFWLS C-index 0.65 OR 1.14		1-year mortality	TAPSE (OR 0.44) PVR (OR 1.03)
Gumus et al. (2018) (*n* = 54) (77)	FWLS AUC 0.94	FWLS −15.5% (Sens 86.4% Spec 95.2%)	RHF[3]	RVSWI (AUC 0.82) FAC (AUC 0.72) RV EF (AUC 0.71)
Magunia et al. (2018) (*n* = 26) (103)	FWLS AUC 0.91		RVAD or inotropes >14 days	RVEF (AUC 0.88)
Comeli et al. (2013) (*n* = 10) (104)	FWLS AUC 0.93		RHF[a]	GLS (AUC 0.81) FAC (AUC 0.61) RV S' (AUC 0.43) TAPSE (AUC 0.33)
Grant et al. (2012) (*n* = 177) (105)	FWLS AUC 0.70	FWLS −9.6% Sens 68%/Spec 76%	RVAD or Inotropes >14 days	RVFRS (AUC 0.66) (14)

TAPSE, tricuspid annular plane systolic excursion; AUC, area under the curve; RHF, right heart failure; PAPi, pulmonary artery pulsatility index; RVAD, right ventricular assist device; RV S', right ventricular tissue Doppler S' wave; RV LS, right ventricular longitudinal strain; FAC, fractional area change; FWLS, free wall longitudinal strain; RVGLS, right ventricular global longitudinal strain; GLS, global longitudinal strain; E/e', ratio of early mitral inflow velocity to mitral annular early diastolic velocity; LAVI, left atrial volume index; RVEF, right ventricular ejection fraction; RVSWI, right ventricular stroke work index; PVR, pulmonary vascular resistance; RVFRS, University of Michigan right ventricular failure risk score.

[a]Post-implant inotropic support >14 days, RVAD implantation for intra-operative or post-operative RHF, or death within 14 days due to RHF.

[b]Need for the previously unplanned insertion of a RVAD after LVAD implantation or the necessity of both prolonged reduction of PVR by nitric oxide or iloprost inhalation and intravenous inotrope therapy for >10 consecutive days to increase the cardiac index >2 L/min per m^2.

[c]The mean arterial pressure <55 mmHg, central venous pressure or right atrial pressure >16 mmHg, cardiac index <2 L/min/m^2, requirement of prolonged postimplant inotropes (inotropic score >20 units), or inhaled nitric oxide or intravenous vasodilators continued beyond postoperative day 14 following LVAD implant or requiring RVAD or extracorporeal membrane oxygenation support.

RV function remains a long-standing challenge. In end-stage HF, loading conditions fluctuate dramatically, undermining the reliability of functional parameters. To enhance the prediction of post-LVAD RHF, this section summarizes the relevant functional parameters, highlighting their utility and identifying the existing knowledge gaps.

The latest consensus statement recommends evaluating tricuspid annular plane systolic excursion (TAPSE), systolic tissue Doppler velocity of the tricuspid annulus (RV S'), right ventricular fractional area change (RV FAC), and right ventricular longitudinal strain (RV LS) prior to LVAD implantation (57). Echocardiography is the initial imaging modality of choice accessible for severely ill patients, with CT and MRI considered if echocardiographic findings remain inconclusive. Beyond these imaging modalities, right heart catheterization (RHC) parameters provide incremental value for assessing RV function in a load-independent manner, such as RVSWi, and pulmonary artery pulsatility index (PAPi) (58, 59). Although RAP/PCWP does not typically reflect RV function, it is included in this section as it is also derived from a RHC. This section highlights the predictive value (Tables 2–6), and limitations of these indices.

4.1 Systolic function

TAPSE, RV S', RV FAC, and RV LS are the most commonly used parameters for measuring RV systolic function. A meta-analysis demonstrated that TAPSE, RV FAC, and RV global longitudinal strain (GLS) reliably distinguish between patients who do and do not develop RHF (60). Among these parameters, RV free-wall longitudinal strain (FWLS) is specifically

TABLE 3 Performance of diastolic function parameters.

Study (population)	Performance	Cut off	Outcome	Comparison
Trans tricuspid E/e'				
Kato et al. (2013) ($n = 68$) (67)	OR 1.32		RVAD or inotropes >14 days	TAPSE (OR 0.32) S' (0.22) RV GLS (OR 1.26)
RA reservoir strain				
Charisopoulo et al. (2019) ($n = 70$) (68)	AUC 0.91 OR 2.5	10.5% (Sens 94% Spec 65%)	RVAD	FWLS (AUC 0.62; OR 1.3)
Catheter-derived RA waveform				
Samura et al. (2019) ($n = 71$) (69)	Deep Y descent OR 10.5		RVAD or inotropes >14 days	CVP/PCWP(OR2.02) PAPi (OR 1.13) RVSWi (OR 0.95)

RVAD, right ventricular assist device; TAPSE, tricuspid annular plane systolic excursion; S', myocardial tissue Doppler systolic velocity; RV GLS, right ventricular global longitudinal strain; FWLS, free wall longitudinal strain; CVP, central venous pressure; PCWP, pulmonary capillary wedge pressure; PAPi, pulmonary artery pulsatility index; RWSWi, right ventricular stroke work index.

recommended for evaluating subclinical RV dysfunction in LVAD candidates (57). Indeed, RV LS generally demonstrates superior performance in predicting RHF and adverse events, in comparison to TAPSE, RV FAC (Table 2).

Limitations: However, it is important to note that these parameters represent geographic or volumetric changes in the RV, rather than "contractility" or "Ees" derived from the PV loop, strictly speaking (61). Consequently, they have load-dependency, which is a critical limitation in capturing intrinsic RV function data in severe heart failure, where afterload and preload can dramatically fluctuate (10–12). Although Ees derived from the PV loop is considered the gold standard for assessing contractility independently of loading conditions, its routine use in daily clinical practice is limited by the invasiveness, analytical complexity, and high cost (62).

Additionally, all these assess only regional function, and TAPSE and RV S' have angle dependency, thus requiring clinicians to be cautious when interpreting actual values (61). Given the complex structure of the RV, three-dimensional ejection fraction would be ideal to capture more global motion (63), yet this approach is technically challenging to accurately visualize and is not widely available in real-world clinical settings, as indicated in current guidelines (64).

Moreover, the median values of TAPSE (1.03–1.61 cm), RV FAC (18.7%–40.4%), and RV GLS (6.7%–12.6%) in patients who developed RHF vary widely across studies (60), suggesting their unreliability as definitive predictors of RHF. Therefore, careful consideration of simultaneous loading conditions, or other load-dependent indices is highly recommended.

4.2 Diastolic function

Given the discussion in the previous section of pathophysiology, the adaptability of diastolic function can be a key contributor to post-LVAD RHF development, yet the data remains particularly scarce (65). In echocardiography or MRI, trans-tricuspid E/A ratio, deceleration time of peak E velocity, E/e', RV diastolic strain rate (DSR), or right atrial (RA) strain are used to assess RV diastolic function (66). E/e' is associated with RV filling pressure, and E/e' > 10 may be helpful in predicting post-LVAD RHF. However, the supporting evidence is limited to univariable analysis, and further investigation is warranted (67). In addition, impaired peak RA strain, which also reflects RV filling pressure or RA reservoir function, was reported as another independent predictor of subsequent RVAD implantation (68). Their analysis demonstrated excellent predictive values of diastolic functional parameters including peak RA strain and late diastolic strain rate, outperforming RV LS.

Furthermore, catheter-derived RA waveforms show better predictive values for RHF. A deeper Y descent compared to X descent, indicative of impaired RV diastolic compliance, demonstrated a high OR of 10.5 (95% CI 1.75–63.5), surpassing other catheter-derived parameters such as central venous pressure (CVP)/PCWP, PAPi, and RVSWi (69).

Limitations: As a significant knowledge gap, evidence pertaining to diastolic function remains extremely limited, and even studies investigating systolic function often do not compare their findings to diastolic function parameters (Table 3). However, the data on diastolic function parameters identified thus far have demonstrated excellent utility in predicting post-LVAD RHF or mortality, comparable or even superior to RV LS, and further studies are strongly warranted.

4.3 RV-PA coupling

RV Ees/Ea, or RV-PA coupling, serves as a mediator of RV contractility while accounting for PA elastance or afterload, and is primarily measured using a conductance catheter and PV loop. Scheel and colleagues demonstrated that a lower RV Ees/Ea (below 0.35) was associated with more frequent heart failure symptoms compared to a RV Ees/Ea ≥0.35 (71% vs. 17%, $p = 0.048$), suggesting that this parameter effectively captures an uncoupled, abnormal RV state by incorporating loading conditions (30, 42). However, as previously mentioned, data

obtained using conductance catheters and PV loops remains limited.

Recently, the ratio of echocardiographic systolic parameters, such as TAPSE, RV S', RV LS, and approximated pulmonary artery systolic pressure (PASP), have been employed as a surrogate of RV Ees/Ea (61). This echocardiographic surrogate has been adopted across various patient populations (70), yet the utility in LVAD population is unclear, with studies indicating that this parameter lacks predictive value for RHF development (71–73).

Limitations: A few limitations should be considered: (1) PASP estimation is challenging in cases of severe or greater TR due to the widened regurgitant orifice, which hinders the accurate capture of the pressure gradient; (2) TAPSE, RV S', and RV LS do not fully capture global RV systolic function, as they provide only regional assessments, which is problematic in an enlarged, dysfunctional RV; (3) in end-stage RV dysfunction, PASP may not increase as expected due to the RV's inability to generate sufficient flow and pressure, being critical to use PASP as a surrogate of Ea (66, 70). Although RV-PA coupling is reliable indices, adoption of echocardiography estimate in LVAD is not clearly explored.

4.4 RVSWi

The right ventricular stroke work index (RVSWi) reflects the RV external workload, representing the area enclosed by the PV loop. It is obtained from PV loops using a conductance catheter or estimated using RHC-derived parameters based on the following formula:

$$\text{RVSWI} = (\text{mean PA pressurendashCVP}) \times \text{SVindex} (\times 0.0136)$$

RVSWi is considered a load-independent parameter and is particularly useful in evaluating complex pathophysiology, where loading conditions are highly variable (74). In general, RVSWi decreases in dysfunctional RV because low Ees and impaired EDPVR are unable to generate sufficient external workload (74). Specifically, RVSWi <250, 300, or 400 mmHg L/m^2 are used for cut-off points for predicting post-LVAD RHF (75–77).

The recent meta-analysis demonstrated the highest standard mean difference of RVSWI (0.58) among various RV hemodynamic and functional parameters such as TAPSE, RV FAC, and RV LS, although PAPi and RAP/PCWP were not included in this analysis (7).

Limitations: RVWSi is frequently used in LVAD populations (Table 4), yet most RVSWi measurements used in clinical, or research settings are derived from RHC-derived parameters. These estimations do not necessarily capture true workload as measured from PV loops and are susceptible to errors in hemodynamic measurements (77). Moreover, there are also some studies that have shown limited predictive capacity of RVSWi in multivariable analyses (78). The specific situation or population where its performance becomes unreliable is still unclear, it should be noted that functional assessment should be multifaceted.

4.5 PAPi

The pulmonary artery pulsatility index (PAPi) is a measure initially developed for use in MI and MCS conditions and it has demonstrated a good predictive value for RHF development or mortality after LVAD implantation either (79). PAPi is calculated using the following formula:

$$\text{PAPi} = (\text{systolic - diastolic PA pressure}) / \text{RA pressure},$$

where PA pulse pressure provides an estimate of RV pulsatile load and contractile strength, and RA pressure acts as a mediator of preload (80). Lower PAPi indicates impaired RV function. A systematic review incorporating 32 studies found that patients who developed RHF had a significantly lower preoperative PAPi than those who did not (2.17 vs. 2.87; $p < 0.001$) (79) (Table 5).

In analysis on PAPi, the utility of simulation test has been proposed in addition to the resting value. Cacioli and colleagues

TABLE 4 Performance of RVSWi.

Study (population)	Performance	Cut off	Outcome	Comparison
RVSWI				
Gumus et al. (2019) ($n = 57$) (77)	AUC 0.82	400 mmHg[a]ml/m^2	RHF[a]	FWLS (AUC 0.94) FAC (AUC 0.72) RV EF (AUC 0.71)
Bellavia et al. (2017) ($n = 4428$) (7)	SMD 0.58		Depends on the paper	CVP (SMD 0.47) TAPSE(SMD 0.29) FAC (SMD 0.29)
Kormos et al. (2010) ($n = 484$) (75)	OR 2.9	300 mmHg[a]ml/m^2	RVAD or inotropes >14 days	RAP/PCWP(OR 2.5)

RWSWi, right ventricular stroke work index; AUC, area under the curve; SMD, standardized mean difference; RHF, right heart failure; FWLS, free wall longitudinal strain; FAC, fractional area change; RV EF, right ventricular ejection fraction; CVP, central venous pressure; TAPSE, tricuspid annular plane systolic excursion; RAP, right atrial pressure; PCWP, pulmonary capillary wedge pressure.

[a]The mean arterial pressure <55 mmHg, CVP or RAP >16 mmHg, cardiac index <2 L/min/m^2, requirement of prolonged postimplant inotropes (inotropic score >20 units), or inhaled nitric oxide or intravenous vasodilators continued beyond postoperative day 14 following LVAD implant or requiring RVAD or extracorporeal membrane oxygenation support.

TABLE 5 Performance of PAPi.

Study (population)	Performance	Cut off	Outcome	Comparison
PAPi				
Akamkam et al. (2024) ($n = 170$) (95)	AUC 0.68	2.84	3-month mortality	
Sheel et al. (2024) ($n = 33$) (106)	AUC 0.80		RV Ees/Ea <0.35	RVSWI (AUC 0.51) RAP/PCWP (AUC 0.52) CI (AUC 0.77)
Cacioli et al. (2022) ($n = 54$) (81)	Post NTP AUC 0.95	Post NTP PAPi 3.2	RHF[a]	CRITT score (AUC 0.72) EUROMACS (AUC 0.72)
Morine et al. (2016) ($n = 132$)	AUC 0.94	1.85	RVAD or inotropes >14 days	RAP/PCSP (AUC 0.84) RVSWI (AUC 0.69)

PAPi, pulmonary artery pulsatility index; AUC, area under the curve; RAP, right atrial pressure; PCWP, pulmonary capillary wedge pressure; CI, cardiac index; RWSWi, right ventricular stroke work index; NTP, normalized transpulmonary pressure; RHF, right heart failure; CRITT, cardiac risk, inflammatory response, timing of support, technical difficulty score; EUROMACS, European registry for patients with mechanical circulatory support; RVAD, right ventricular assist device; PCSP, pulmonary capillary systolic pressure; RV, right ventricular; Ees/Ea, end-systolic elastance to arterial elastance ratio.
[a]Post-implant inotropic support >14 days, right ventricular assist device (RVAD) implantation for intra-operative or post-operative RV failure, or death within 14 days due to RV failure.

TABLE 6 Performance of RAP (CVP)/PCWP.

Study (population)	Performance	Cut off	Outcome	Comparison
RAP (CVP)/PCWP				
Beneyto et al. (2024) ($n = 224$) (73)	HR 1.35 AUC 0.62	0.33	6-month mortality	TR (HR 5.13) PVR (HR 1.11)
Mehra et al. (2022) ($n = 1312$) (93)	HR 1.57	0.60	1-year mortality	LVEDD <5.5 cm (HR 1.86)
Ruiz-Cano et al. (2020) ($n = 80$) (107)	OR 4.0	0.55	RHF[a]	TAPSE ($p = 0.17$) Severe TR ($p = 0.34$)
Akin et al. (2020) ($n = 2,689$) (108)	OR 1.46		90-day mortality	PAPi (OR 0.88; $p < 0.001$) RVSWI (OR 0.91; $p < 0.001$) TAPSE (OR 0.99; $p = 0.48$)
Samura et al. (2019) ($n = 115$) (88)	OR 2.02		RVAD or inotropes >14 days	RVSWI (OR 0.95) PAPi (OR 1.13)

RAP, right atrial pressure; CVP, central venous pressure; PCWP, pulmonary capillary wedge pressure; HR, hazard ratio; OR, odds ratio; AUC, area under the curve; RHF, right heart failure; RVAD, right ventricular assist device; TR, tricuspid regurgitation; PVR, pulmonary valve resistance; TAPSE, tricuspid annular plane systolic excursion; PASP, pulmonary artery systolic pressure; PAPi, pulmonary artery pulsatility index; LVEDD, left ventricular end-diastolic dimension; RWSWi, right ventricular stroke work index.
[a]Evidence of CVP >16 mm Hg with a CI <2.3 L $min^{-1}m^{-2}$ (in the absence of elevated PCWP, tamponade, ventricular arrhythmias or pneumothorax) after LVAD implantation requiring previously unplanned temporary RVAD) or the necessity of nitric oxide (iNO) and intravenous inotropes beyond postoperative day 14.

reported PAPi measured after administering sodium nitroprusside (NTP) had the potential to predict RHF development. By administrating the vasodilator and reducing pulmonary vascular resistance, post-NTP PAPi was considered capable of assessing (1) reversibility of pulmonary hypertension and (2) the reserve in RV function. Indeed, the post-NTP PAPi improved predictive value, and when combined with RV FAC and systolic PA pressure, the area under the curve (AUC) increased up to 0.95 in their study (81). Hsi and colleagues also reported the efficacy of PAPi measured in a micro-axial flow pump (mAFP) test to predict RHF before LVAD implantation (82). These dynamic changes in parameters during simulation testing may help capture the intrinsic adaptability of the RV and improve the prediction of RHF (83). Although this was also suggested in the study by Brener and colleagues where they proposed RVSWi (35), available data remains limited.

Limitations: A concern regarding PAPi is that pulmonary circulation factors—including resistance and compliance—can significantly affect its value. Not only RV dysfunction but also pulmonary embolism and PA diseases can diminish PAPi value since pulse pressure declines in these conditions (84).

Another concern is the variable cutoff value reported in literature. From 0.88 to 3.3 have been reported as an effective cutoffs, and median values also vary across studies (85). Even small changes in RA pressure can significantly affect PAPi, precise measurement of catheter parameters is essential.

4.6 RAP (CVP)/PCWP

RAP (or CVP)/PCWP includes the LV component when evaluating the RV preload, thereby reflecting right-sided preload relative to the left side and implying RV's adaptability towards certain volume condition, not representing RV function (86). With respect to prediction, RAP/PCWP ratio shows excellent predictive values (87, 88). A higher RAP/PCWP ratio indicates excessively accumulated preload in the RV, suggesting inadequate adaptation of RV to certain volume

conditions or afterloads. In general, 0.55–0.6 are considered as cutoff values (58) (Table 6).

Regarding this parameter, data are available not only for its resting value at a single time point but also from a simulation test of LVAD suctioning. In terms of this parameter, there is a data of utility by simulation test of LVAD, not only rest value at one point. Hsi and colleagues reported the efficacy of a simulation test with mAFP in assessing the RAP/PCWP ratio either (82). In their study, the ratio decreased significantly after mAFP insertion in patients who did not develop RHF, compared to those who did (non-RHF group: 0.61 → 0.38; RHF group: 0.46 → 0.40) (82). Simulation test performed before implantation may further improve the predictive value of this parameter as PAPi. RAP/PCWP is simple to obtain and has a high predictive reliability; therefore, its assessment is reasonable and recommended.

Limitations: As a limitation, this ratio can be low when PCWP is particularly high. Amsallem and colleagues reported that 43% of patients with a low RAP/PAWP ratio (≤0.54) and high RAP (≥15 mmHg) developed RHF after LVAD implantation, suggesting that the absolute value of RAP itself should also be considered (89).

5 Risk sores and significant items for prediction

Various scoring models, many of which do not focus solely on RV factors, have been developed to predict the incidence of post-LVAD RHF. Although incorporating the non-RV-centered factors helps further identify high-risk patients for developing RHF prior to LVAD implantation, comprehensive validation of these models and comparisons of their performance remains limited.

This section outlines several risk scores validated externally (Table 7). Components of these scores can be classified as follows: (1) baseline characteristics/presentation; (2) treatment-related factors (e.g., vasopressors, inotropes, MCS); (3) right heart conditions (hemodynamics, and RV function); (4) laboratory data. Most scores define RHF as the need for MCS or RVAD, iNO ≥48h, or inotropes ≥14 days, same as MCS-ARC early RHF definition (14).

As summarized in Table 7, the discrimination performances of most scores are generally "fair" or "moderate," with C-index or AUC values less than 0.7, and comparable results observed in external validations. Scores relatively recently developed, including STOP-RVF Score, EUROMACS Score, and CRITT, are derived from cohort all with continuous flow pump, whereas that for other scores included pulsatile flow pump. Kalogeropoulos and colleagues compared six existing risk scores in their cohort who were all recipients of continuous flow LVAD, with the Michigan Right Ventricular Failure Risk Score (RVFRS) achieving the highest C-index of 0.62 (Figure 5). They attribute the limited performance to: (1) Variability in RHF definitions, (2) The inclusion of non-RV markers as surrogates for RV dysfunction, and (3) Differences in the cohorts used for model derivation, as older scoring systems included fewer patients receiving destination therapy and continuous-flow pumps (90).

The most recent risk prediction model, called "STOP-RVF score", derived using a machine learning approach, has demonstrated superior performance, achieving a C-statistic of 0.75 even in external validation, outperforming other scores such as the Kormos et al. score [C statistic, 0.5 (75)] and score from the University of Utah [C statistic, 0.627 (91)] (87).

Noticeably, four items—(1) liver/renal dysfunction, (2) MCS/catecholamine dependency (or INTERMACS profile 1/2) before implantation, (3) pre-existing severe RV dysfunction, and (4) high RAP/PCWP—are included in at least two scoring models and thus, should be incorporated certainly when evaluating the RHF risk (Figure 1). Meta-analysis or large-scale registry studies ($n > 1{,}000$) conducting multivariable analysis for the incidence of post-LVAD RHF, also demonstrated the statistical significance of the aforementioned four factors (7, 8, 92, 93).

Unfortunately, "severe RV dysfunction" is not clearly defined in most studies including risk score deviation paper (76, 88, 94), yet, given their superior predictive capacities discussed in previous section, RV LS, RVSWi, and PAPi should be evaluated. Considering preimplantation RV LS ≥16% (77), RVSWi <250–300 mmHg L/m^2 (75–77), or PAPi <2.0–3.0 (95) as a critical factor strongly indicative of RV dysfunction, patients with additional risk factors—such as liver/renal dysfunction, MCS/catecholamine dependency, or high RAP/PCWP (0.5–0.6)—should be strongly considered for RVAD implantation.

6 Conclusion

This review consolidates the latest insights into the pathophysiology of and predictive models for RHF following LVAD implementation.

As highlighted in Figure 1, both the loss of LV twist and LVAD suction on the septal wall are LVAD-specific factors that negatively impact RV contractility. Although LVAD suction improves diastolic compliance, insufficient adaptation to increased flow may contribute to RHF. Furthermore, functional TR and AI can additionally promote congestion.

To predict this unfavorable outcome, guidelines and expert consensus recommend several RV functional parameters from imaging modalities or RHC. Among these, RV LS, RVSWi, and PAPi, exhibit strong predictive value in large-scale studies. Since none of these parameters alone provide definitively high predictive accuracy, and each reflects different aspects of RV function, considering multiple parameters in combination may enhance the prediction of RHF.

Although several risk scores have been developed for prediction, most have demonstrated only "fair" performance in discriminating RHF during external validation. Across these score models, four specific factors recur and have demonstrated consistent performance in meta-analysis either, thereby we propose multiparametric approach for RHF prediction, specifically focusing on four factors—(1) liver/renal dysfunction,

TABLE 7 Summary of existing risk scores.

Risk score	Included Risk factors (weight)	Performance	Definition of RHF	Performance in validation (comparison)
STOP-RHF Score ($n = 798$) Taleb et al. (2024) (87)	Baseline background/presentation: • NICM (Yes/No) • INTERMACS 1–2 (Yes/No) Therapy: • IABP (Yes/NO) • Impella/VA-ECMO (Yes/No) • LVAD configuration (Centrifugal/ axial) • ACEi (Yes/No) Right heart: • RAP/PCWP (value) Laboratory data: • Albumin (value) • Creatinine (value) • Platelet (value) Serum sodium (value)	C-index 0.75 AUC 0.75	1) and/or 2) within 30 days 1. Right-side circulatory support 2. inotropes therapy for ≥14 days	1) C-index 0.73 (University of Utah: C-index 0.62) (87)
EUROMACS-RHF ($n = 2,000$) Soliman et al. (2018) (88)	Baseline background/presentation: • INTERMACS class 1–3 (2 points) • ≥3 intravenous inotropes (2.5 points) Right heart: • Severe RV dysfunction (2 points) • RAP/PCWP > 0.54 (2 points) Laboratory data: haemoglobin ≤10 g/dl (1 point)	C-index 0.70 (cut off 2.5 pts Sens 74%/Spec 57%)	At least one of three 1. need for right side MCS 2. inotropic support for ≥14 days iNO for ≥48 h	1) C-index 0.67 (88) 2) AUC 0.64 (CRIIT: AUC 0.64/ University of Utah: AUC 0.57/ RVFRS: AUC 0.58) (109) 3) AUC 0.67 (110) 4) AUC 0.59 (111)
CRIIT score ($n = 218$) Alturi et al. (2013) (94)	Baseline background/presentation: • Pre-operative intubation (1 point) • Tachycardia >100 (1 point) Right heart: • Severe RV dysfunction (1 point) • CVP >15 mmHg (1 point) Severe tricuspid regurgitation (1 point)	C-index 0.8 AUC 0.80 (95% CI 0.72–0.88) sens 84%/spec 63% (cut off 2 pts)	Need for biventricular support	1) C-index 0.60 (University of Utah: C-index 0.59/ University of Pennsylvania: C-index 0.56) (90) 2) AUC 0.64 (109)
University of Utah ($n = 175$) Drakos et al. (2010) (91)	Baseline background/presentation: • Destination therapy (3.5 points) • Obesity (2 points) Therapy: ➢ IABP (4 points) ➢ Inotrope dependency (2.5 points) • ACEi/RAS (2.5 points) • β blocker (2 points) Right heart: Increased PVR (1–4 points)	Points and RHF (%) ≤5.0 (11%) 5.5–8 (37%) 8.5–12 (56%) ≥12.5 (83%)	At least one of the three 1. iNO for ≥48 h 2. Iinotropes for >14 days RVAD implantation	1) C-index 0.59 (90) 2) AUC 0.57 (109) 3) C-index 0.62 (87)
RVFRS ($n = 197$) Matthews et al. (2008) (112)	Therapy: • Vasopressor (4 points) Laboratory data: • AST ≥80 IU/L (2 points) • Bilirubin ≥2.0 mg/dl (2.5 points) Creatinine ≥2.3 mg/dl (3 points)	AUC 0.73	At least one of the four 1. Inotropes for >14 days; 2. iNO for ≥48 h; 3. right-sided circulatory support 4. hospital discharge with inotrope	1) C-index 0.62 (90) 2) AUC 0.61 (90) 3) AUC 0.58 (109)
University of Pennsylvania ($n = 266$) Fitzpatrick et al. (2008) (76)	Baseline background/presentation: • SBP ≤96 mm Hg (13 points) • Cardiac index ≤2.2 L/min/m^2 (18 points) Right heart: • RVSWI ≤0.25 mm Hg L/m^2 (18 points) • Severe pre-VAD RV dysfunction (16 points) Laboratory data: • Creatinine ≥1.9 mg/dl (17 points)	Sens 83%/spec80% (cut off 50 pts)	Need for MCS	C-index 0.56 (90)

Discrimination performance generally ranges from "fair (AUC 0.5–0.7)" to "acceptable (AUC 0.7–0.8)". Of them, liver/renal dysfunction, MCS/catecholamine dependency, and high RAP/PCWP are factors used in at least two scoring models and thus should be incorporated certainly to evaluate the risk of RV development.

AST, aspartate aminotransferase; AUC, area under curve; BiVAD, biventricular assist device; CVP, central venous pressure; IABP, intra-aortic ballon pumping; INR, international normalised ratio; INTERMACS, Interagency Registry for Mechanically Assisted Circulatory Support; LVAD, left ventricular assist device; NICM, non-ischaemic cardiomyopathy; RA/PCWP, right atrium to pulmonary capillary wedge pressure ratio; RHF, right heart failure; RV, right ventricle; RVSWI, right ventricular stroke work index; SBP, systolic blood pressure; VAD, ventricular assist device.

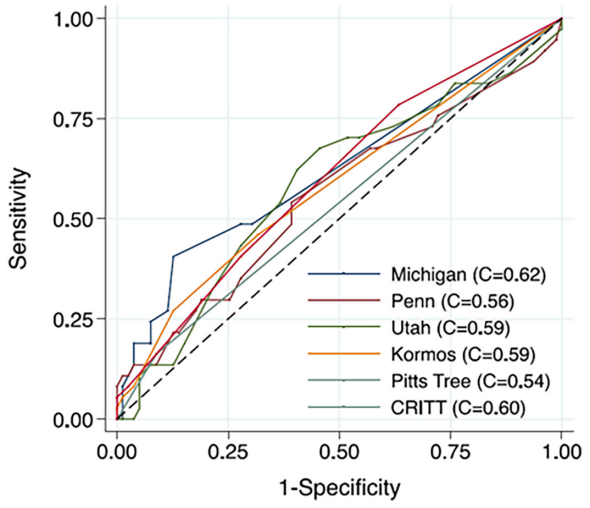

FIGURE 5
Comparison of discrimination of risk scores. Kalogeropoulos et al. compared existing risk scores in 116 patients with continuous-flow LVAD, either the HeartMate II (Thoratec, Inc.) or the HeartWare HVAD (Heart-Ware, Inc.), in single center. Although the Michigan score showed the highest value, the C-indexes of all scores remained around 0.6. Reproduced with permission from "Comparative Receiver Operating Characteristic Curve Plots with Right Ventricular Failure Prediction as the Outcome of Interest for the Scores Evaluated" by Andreas P. Kalogeropoulos, Anita Kelkar, Jeremy F. Weinberger, Alanna A. Morris, Vasiliki V. Georgiopoulou, David W. Markham, Javed Butler, J. David Vega and Andrew L. Smith, licensed under CC-BY-NC-ND.

(2) MCS/catecholamine dependency (or INTERMACS profile 1/2), (3) pre-existing severe RV dysfunction (impairment in RV LS, RVSWi, and PAPi), and (4) high RAP/PCWP (Figure 1).

We identified the following knowledge gaps and future directions:

1. Incomplete Clinical Evidence on RV Pathophysiology in LVAD Candidates

The proposed pathophysiological mechanisms are largely derived from preclinical studies or estimations based on imaging modalities or RHC, where contractility and diastolic compliance cannot be accurately assessed. More robust evidence on proposed mechanisms, particularly the loss of LV twist, along with comprehensive, larger-scale evaluations of the RV PV loop in human patients, is needed.

2. Evaluation of Diastolic Compliance

Although diastolic compliance may significantly influence how the RV adapts to the increased flow from an LVAD, standard assessment methods via imaging modality or RHC for diastolic function remain limited. Further research is required to collect data on current diastolic function metrics and develop reliable parameters.

3. Simulation and Intraoperative Testing

Simulation studies that replicate LVAD hemodynamics, as well as short-term intraoperative tests just before LVAD implantation, could enhance predictive accuracy by providing more precise assessments of RV functional reserve. However, comprehensive and refined data are still needed.

Addressing these gaps is crucial for improving LVAD management and enhancing quality of life for patients reliant on LVAD support.

Author contributions

HN: Conceptualization, Investigation, Visualization, Writing – original draft, Writing – review & editing. LL: Conceptualization, Data curation, Methodology, Writing – original draft, Writing – review & editing. NO: Supervision, Writing – review & editing. JS: Supervision, Writing – review & editing. DM: Supervision, Visualization, Writing – original draft, Writing – review & editing. JPF: Conceptualization, Methodology, Resources, Supervision, Writing – original draft, Writing – review & editing. JFF: Supervision, Writing – original draft, Writing – review & editing.

Funding

The author(s) declare that financial support was received for the research and/or publication of this article. HN is supported by The Prince Chales Hospital Foundation through his PhD scholarship (2024-01).

Acknowledgments

Figure 1 was created by illustrator Nick Valmas. We thank him for his cooperation.

Conflict of interest

The authors declare that the research was conducted in the absence of any commercial or financial relationships that could be construed as a potential conflict of interest.

Generative AI statement

The author(s) declare that no Generative AI was used in the creation of this manuscript.

Publisher's note

References

1. Lippi G, Sanchis-Gomar F. Global epidemiology and future trends of heart failure. *AME Med J*. (2020) 5:15. doi: 10.21037/amj.2020.03.03

2. Members ATF, McMurray JJ, Adamopoulos S, Anker SD, Auricchio A, Böhm M, et al. ESC Guidelines for the diagnosis and treatment of acute and chronic heart failure 2012: the task force for the diagnosis and treatment of acute and chronic heart failure 2012 of the European Society of Cardiology. Developed in collaboration with the heart failure association (HFA) of the ESC. *Eur Heart J*. (2012) 33(14):1787–847. doi: 10.1093/eurheartj/ehs104

3. de By TM, Mohacsi P, Gummert J, Bushnaq H, Krabatsch T, Gustafsson F, et al. The European registry for patients with mechanical circulatory support (EUROMACS): first annual report. *Eur J Cardiothorac Surg*. (2015) 47(5):770–7. doi: 10.1093/ejcts/ezv096

4. Lam KM-T, Ennis S, O'Driscoll G, Solis JM, MacGillivray T, Picard MH. Observations from non-invasive measures of right heart hemodynamics in left ventricular assist device patients. *J Am Soc Echocardiogr*. (2009) 22(9):1055–62. doi: 10.1016/j.echo.2009.06.006

5. Baumwol J, Macdonald PS, Keogh AM, Kotlyar E, Spratt P, Jansz P, et al. Right heart failure and "failure to thrive" after left ventricular assist device: clinical predictors and outcomes. *J Heart Lung Transplant*. (2011) 30(8):888–95. doi: 10.1016/j.healun.2011.03.006

6. Takeda K, Naka Y, Yang JA, Uriel N, Colombo PC, Jorde UP, et al. Outcome of unplanned right ventricular assist device support for severe right heart failure after implantable left ventricular assist device insertion. *J Heart Lung Transplant*. (2014) 33(2):141–8. doi: 10.1016/j.healun.2013.06.025

7. Bellavia D, Iacovoni A, Scardulla C, Moja L, Pilato M, Kushwaha SS, et al. Prediction of right ventricular failure after ventricular assist device implant: systematic review and meta-analysis of observational studies. *Eur J Heart Fail*. (2017) 19(7):926–46. doi: 10.1002/ejhf.733

8. Kapelios CJ, Lund LH, Wever-Pinzon O, Selzman CH, Myers SL, Cantor RS, et al. Right heart failure following left ventricular device implantation: natural history, risk factors, and outcomes: an analysis of the STS INTERMACS database. *Circ Heart Fail*. (2022) 15(6):e008706. doi: 10.1161/CIRCHEARTFAILURE.121.008706

9. Moon MR, Bolger AF, DeAnda A, Komeda M, Daughters GT, Nikolic SD, et al. Septal function during left ventricular unloading. *Circulation*. (1997) 95(5):1320–7. doi: 10.1161/01.CIR.95.5.1320

10. Ho SY, Nihoyannopoulos P. Anatomy, echocardiography, and normal right ventricular dimensions. *Heart*. (2006) 92 Suppl 1(Suppl 1):i2–13. doi: 10.1136/hrt.2005.077875

11. Schlangen J, Petko C, Hansen JH, Michel M, Hart C, Uebing A, et al. Two-Dimensional global longitudinal strain rate is a preload independent Index of systemic right ventricular contractility in hypoplastic left heart syndrome patients after fontan operation. *Circ Cardiovasc Imaging*. (2014) 7(6):880–6. doi: 10.1161/CIRCIMAGING.114.002110

12. Yuchi Y, Suzuki R, Kanno H, Saito T, Teshima T, Matsumoto H, et al. Influence of heart rate on right ventricular function assessed by right heart catheterization and echocardiography in healthy anesthetized dogs. *BMC Vet Res*. (2022) 18(1):166. doi: 10.1186/s12917-022-03271-y

13. STS-INTERMACS. Appendix A—adverse event definitions.: UAB School of Medicine).

14. Kormos RL, Antonides CF, Goldstein DJ, Cowger JA, Starling RC, Kirklin JK, et al. Updated definitions of adverse events for trials and registries of mechanical circulatory support: a consensus statement of the mechanical circulatory support academic research consortium. *J Heart Lung Transplant*. (2020) 39(8):735–50. doi: 10.1016/j.healun.2020.03.010

15. Rame JE, Pagani FD, Kiernan MS, Oliveira GH, Birati EY, Atluri P, et al. Evolution of late right heart failure with left ventricular assist devices and association with outcomes. *J Am Coll Cardiol*. (2021) 78(23):2294–308. doi: 10.1016/j.jacc.2021.09.1362

16. Takeda K, Takayama H, Colombo PC, Jorde UP, Yuzefpolskaya M, Fukuhara S, et al. Late right heart failure during support with continuous-flow left ventricular assist devices adversely affects post-transplant outcome. *J Heart Lung Transplant*. (2015) 34(5):667–74. doi: 10.1016/j.healun.2014.10.005

17. Brener MI, Masoumi A, Ng VG, Tello K, Bastos MB, Cornwell WK, et al. Invasive right ventricular pressure-volume analysis: basic principles, clinical applications, and practical recommendations. *Circ Heart Fail*. (2022) 15(1):e009101. doi: 10.1161/CIRCHEARTFAILURE.121.009101

18. Torrent-Guasp FF, Whimster WF, Redmann K. A silicone rubber mould of the heart. *Technol Health Care*. (1997) 5(1-2):13–20. doi: 10.3233/THC-1997-51-202

19. Buckberg GD, RESTORE Group. The ventricular septum: the lion of right ventricular function, and its impact on right ventricular restoration. *Eur J Cardiothorac Surg*. (2006) 29(Supplement_1):S272–S8. doi: 10.1016/j.ejcts.2006.02.011

20. Houston BA, Shah KB, Mehra MR, Tedford RJ. A new "twist" on right heart failure with left ventricular assist systems. *J Heart Lung Transplant*. (2017) 36(7):701–7. doi: 10.1016/j.healun.2017.03.014

21. Surkova E, Kovács A, Tokodi M, Lakatos BK, Merkely B, Muraru D, et al. Contraction patterns of the right ventricle associated with different degrees of left ventricular systolic dysfunction. *Circ Cardiovasc Imaging*. (2021) 14(10):e012774. doi: 10.1161/CIRCIMAGING.121.012774

22. Hoffman D, Sisto D, Frater RW, Nikolic SD. Left-to-right ventricular interaction with a noncontracting right ventricle. *J Thorac Cardiovasc Surg*. (1994) 107(6):1496–502. doi: 10.1016/S0022-5223(12)70150-2

23. Chang SA, Kim HK, Kim YJ, Cho GY, Oh S, Sohn DW. Role of pericardium in the maintenance of left ventricular twist. *Heart*. (2010) 96(10):785–90. doi: 10.1136/hrt.2009.182345

24. Wranne B, Pinto FJ, Hammarström E, St Goar FG, Puryear J, Popp RL. Abnormal right heart filling after cardiac surgery: time course and mechanisms. *Br Heart J*. (1991) 66(6):435–42. doi: 10.1136/hrt.66.6.435

25. Raina A, Vaidya A, Gertz ZM, Susan C, Forfia PR. Marked changes in right ventricular contractile pattern after cardiothoracic surgery: implications for post-surgical assessment of right ventricular function. *J Heart Lung Transplant*. (2013) 32(8):777–83. doi: 10.1016/j.healun.2013.05.004

26. Unsworth B, Casula RP, Kyriacou AA, Yadav H, Chukwuemeka A, Cherian A, et al. The right ventricular annular velocity reduction caused by coronary artery bypass graft surgery occurs at the moment of pericardial incision. *Am Heart J*. (2010) 159(2):314–22. doi: 10.1016/j.ahj.2009.11.013

27. Damiano RJ Jr, La Follette P Jr, Cox JL, Lowe JE, Santamore WP. Significant left ventricular contribution to right ventricular systolic function. *Am J Physiol*. (1991) 261(5 Pt 2):H1514–24. doi: 10.1152/ajpheart.1991.261.5.H1514

28. Park CH, Nishimura K, Kitano M, Matsuda K, Okamoto Y, Ban T. Analysis of right ventricular function during bypass of the left side of the heart by afterload alterations in both normal and failing hearts. *J Thorac Cardiovasc Surg*. (1996) 111(5):1092–102. doi: 10.1016/S0022-5223(96)70386-0

29. Apitz C, Honjo O, Humpl T, Li J, Assad RS, Cho MY, et al. Biventricular structural and functional responses to aortic constriction in a rabbit model of chronic right ventricular pressure overload. *J Thorac Cardiovasc Surg*. (2012) 144(6):1494–501. doi: 10.1016/j.jtcvs.2012.06.027

30. Scheel PJ, III C, Salazar IM, Friedman S, Haber L, Mukherjee M, et al. Occult right ventricular dysfunction and right ventricular-vascular uncoupling in left ventricular assist device recipients. *J Heart Lung Transplant*. (2024) 43(4):594–603. doi: 10.1016/j.healun.2023.11.015

31. Sack KL, Dabiri Y, Franz T, Solomon SD, Burkhoff D, Guccione JM. Investigating the role of interventricular interdependence in development of right heart dysfunction during LVAD support: a patient-specific methods-based approach. *Front Physiol*. (2018):9:520. doi: 10.3389/fphys.2018.00520

32. Khonsary SA. Guyton and Hall: textbook of medical physiology. *Surg Neurol Int*. (2017) 8:275. doi: 10.4103/sni.sni_327_17 eCollection 2017.

33. Ali HR, Kiernan MS, Choudhary G, Levine DJ, Sodha NR, Ehsan A, et al. Right ventricular failure post-implantation of left ventricular assist device: prevalence, pathophysiology, and predictors. *Asaio J*. (2020) 66(6):610–9. doi: 10.1097/MAT.0000000000001088

34. Bravo CA, Navarro AG, Dhaliwal KK, Khorsandi M, Keenan JE, Mudigonda P, et al. Right heart failure after left ventricular assist device: from mechanisms to treatments. *Front Cardiovasc Med*. (2022) 9:1023549. doi: 10.3389/fcvm.2022.1023549

35. Brener MI, Kanwar MK, Lander MM, Hamid NB, Raina A, Sethi SS, et al. Impact of interventricular interaction on ventricular function: insights from right ventricular pressure-volume analysis. *JACC Heart Fail*. (2024) 12(7):1179–92. doi: 10.1016/j.jchf.2023.12.001

36. Masri SC, Tedford RJ, Colvin MM, Leary PJ, Cogswell R. Pulmonary arterial compliance improves rapidly after left ventricular assist device implantation. *Asaio J*. (2017) 63(2):139–43. doi: 10.1097/MAT.0000000000000467

37. Houston BA, Kalathiya RJ, Hsu S, Loungani R, Davis ME, Coffin ST, et al. Right ventricular afterload sensitivity dramatically increases after left ventricular assist device implantation: a multi-center hemodynamic analysis. *J Heart Lung Transplant*. (2016) 35(7):868–76. doi: 10.1016/j.healun.2016.01.1225

38. Sayer G, Sarswat N, Kim GH, Adatya S, Medvedofsky D, Rodgers D, et al. The hemodynamic effects of aortic insufficiency in patients supported with continuous-flow left ventricular assist devices. *J Card Fail*. (2017) 23(7):545–51. doi: 10.1016/j.cardfail.2017.04.012

39. Rubinstein GAL, Moeller CM, Lotan DOR, Slomovich S, Fernandez-Valledor A, Ranard LS, et al. The hemodynamic effects of aortic regurgitation in patients supported by a HeartMate 3 left ventricular assist device. *J Card Fail*. (2024) 30(1):95–9. doi: 10.1016/j.cardfail.2023.08.010

40. Haddad F, Hunt SA, Rosenthal DN, Murphy DJ. Right ventricular function in cardiovascular disease, part I. *Circulation*. (2008) 117(11):1436–48. doi: 10.1161/CIRCULATIONAHA.107.653576

41. Moon MR, Castro LJ, DeAnda A, Tomizawa Y, Daughters GT, Ingels NB, et al. Right ventricular dynamics during left ventricular assistance in closed-chest dogs. *Ann Thorac Surg*. (1993) 56(1):54–67. doi: 10.1016/0003-4975(93)90402-4

42. McCarthy PM, Savage RM, Fraser CD, Vargo R, James KB, Goormastic M, et al. Hemodynamic and physiologic changes during support with an implantable left ventricular assist device. *J Thorac Cardiovasc Surg*. (1995) 109(3):409–17. discussion 17-8. doi: 10.1016/S0022-5223(95)70271-7

43. Uriel N, Sayer G, Addetia K, Fedson S, Kim GH, Rodgers D, et al. Hemodynamic ramp tests in patients with left ventricular assist devices. *JACC Heart Fail*. (2016) 4(3):208–17. doi: 10.1016/j.jchf.2015.10.001

44. Mitra A, Siddique A. Tricuspid regurgitation in the setting of LVAD support. *Front Cardiovasc Med*. (2023) 10:1090150. doi: 10.3389/fcvm.2023.1090150

45. Piacentino V III, Williams ML, Depp T, Garcia-Huerta K, Blue L, Lodge AJ, et al. Impact of tricuspid valve regurgitation in patients treated with implantable left ventricular assist devices. *Ann Thorac Surg*. (2011) 91(5):1342–7. doi: 10.1016/j.athoracsur.2011.01.053

46. Veen KM, Mokhles MM, Soliman O, de By T, Mohacsi P, Schoenrath F, et al. Clinical impact and 'natural' course of uncorrected tricuspid regurgitation after implantation of a left ventricular assist device: an analysis of the European registry for patients with mechanical circulatory support (EUROMACS). *Eur J Cardiothorac Surg*. (2021) 59(1):207–16. doi: 10.1093/ejcts/ezaa294

47. Mulzer J, Mueller M, Knierim J, Lanmueller P, Potapov E. Myocardial function recovery interventional assessment and surgical pump removal. *Ann Cardiothorac Surg*. (2021) 10(3):402–4. doi: 10.21037/acs-2020-cfmcs-12

48. Itzhaki Ben Zadok O, Ben-Avraham B, Barac YD, Hammer Y, Rubachevski V, Shaul A, et al. Natural history and prognosis of patients with unrepaired tricuspid regurgitation undergoing implantation of left ventricular assist device. *Asaio J*. (2022) 68(4):508–15. doi: 10.1097/MAT.0000000000001521

49. Nakanishi K, Homma S, Han J, Takayama H, Colombo PC, Yuzefpolskaya M, et al. Prevalence, predictors, and prognostic value of residual tricuspid regurgitation in patients with left ventricular assist device. *J Am Heart Assoc*. (2018) 7(13):e008813. doi: 10.1161/JAHA.118.008813

50. Anwer LA, Tchantchaleishvili V, Poddi S, Daly RC, Joyce LD, Kushwaha SS, et al. Atrial fibrillation should guide prophylactic tricuspid procedures during left ventricular assist device implantation. *ASAIO Journal*. (2018) 64(5):586–93. doi: 10.1097/MAT.0000000000000698

51. Mullan C, Caraballo C, Ravindra NG, Miller PE, Mori M, McCullough M, et al. Clinical impact of concomitant tricuspid valve procedures during left ventricular assist device implantation. *J Heart Lung Transplant*. (2020) 39(9):926–33. doi: 10.1016/j.healun.2020.05.007

52. Boulet J, Nayak A, Mehra MR. Hemodynamic aberrancies in left ventricular assist device-associated heart failure syndromes. *J Card Fail*. (2022) 28(12):1738–40. doi: 10.1016/j.cardfail.2022.09.007

53. Truby LK, Garan AR, Givens RC, Wayda B, Takeda K, Yuzefpolskaya M, et al. Aortic insufficiency during contemporary left ventricular assist device support: analysis of the INTERMACS registry. *JACC Heart Failure*. (2018) 6(11):951–60. doi: 10.1016/j.jchf.2018.07.012

54. Jorde UP, Uriel N, Nahumi N, Bejar D, Gonzalez-Costello J, Thomas SS, et al. Prevalence, significance, and management of aortic insufficiency in continuous flow left ventricular assist device recipients. *Circ Heart Fail*. (2014) 7(2):310–9. doi: 10.1161/CIRCHEARTFAILURE.113.000878

55. Cowger J, Pagani FD, Haft JW, Romano MA, Aaronson KD, Kolias TJ. The development of aortic insufficiency in left ventricular assist device-supported patients. *Circ Heart Fail*. (2010) 3(6):668–74. doi: 10.1161/CIRCHEARTFAILURE.109.917765

56. Acharya D, Kazui T, Al Rameni D, Acharya T, Betterton E, Juneman E, et al. Aortic valve disorders and left ventricular assist devices. *Front Cardiovasc Med*. (2023) 10:1098348. doi: 10.3389/fcvm.2023.1098348

57. Cameli M, Aboumarie HS, Pastore MC, Caliskan K, Cikes M, Garbi M, et al. Multimodality imaging for the evaluation and management of patients with long-term (durable) left ventricular assist devices: a clinical consensus statement of the European association of cardiovascular imaging of the European Society of Cardiology. *Eur Heart J Cardiovasc Imaging*. (2024) 25(10):e217–e40. doi: 10.1093/ehjci/jeae165

58. Adamopoulos S, Bonios M, Ben Gal T, Gustafsson F, Abdelhamid M, Adamo M, et al. Right heart failure with left ventricular assist devices: preoperative, perioperative and postoperative management strategies. A clinical consensus statement of the heart failure association (HFA) of the ESC. *Eur J Heart Fail*. (2024) 26(11):2304–22. doi: 10.1002/ejhf.3323

59. Saeed D, Feldman D, Banayosy AE, Birks E, Blume E, Cowger J, et al. The 2023 international society for heart and lung transplantation guidelines for mechanical circulatory support: a 10- year update. *J Heart Lung Transplant*. (2023) 42(7):e1–e222. doi: 10.1016/j.healun.2022.12.004

60. Chriqui L-E, Monney P, Kirsch M, Tozzi P. Prediction of right ventricular failure after left ventricular assist device implantation in patients with heart failure: a meta-analysis comparing echocardiographic parameters. *Interact Cardiovasc Thorac Surg*. (2021) 33(5):784–92. doi: 10.1093/icvts/ivab177

61. Nonaka H, Rätsep I, Obonyo NG, Suen JY, Fraser JF, Chan J. Current trends and latest developments in echocardiographic assessment of right ventricular function: load dependency perspective. *Front Cardiovasc Med*. (2024) 11:1365798. doi: 10.3389/fcvm.2024.1365798

62. Hsu S. Coupling right ventricular-pulmonary arterial research to the pulmonary hypertension patient bedside. *Circ Heart Fail*. (2019) 12(1):e005715.

63. Tanaka T, Sugiura A, Kavsur R, Öztürk C, Vogelhuber J, Wilde N, et al. Right ventricular ejection fraction assessed by computed tomography in patients undergoing transcatheter tricuspid valve repair. *Eur Heart J Cardiovasc Imaging*. (2023) 24(11):1501–8. doi: 10.1093/ehjci/jead102

64. Stainback RF, Estep JD, Agler DA, Birks EJ, Bremer M, Hung J, et al. Echocardiography in the management of patients with left ventricular assist devices: recommendations from the American society of echocardiography. *J Am Soc Echocardiogr*. (2015) 28(8):853–909. doi: 10.1016/j.echo.2015.05.008

65. Rodenas-Alesina E, Brahmbhatt DH, Rao V, Salvatori M, Billia F. Prediction, prevention, and management of right ventricular failure after left ventricular assist device implantation: a comprehensive review. *Front Cardiovasc Med*. (2022) 9:1040251. doi: 10.3389/fcvm.2022.1040251

66. Rudski LG, Lai WW, Afilalo J, Hua L, Handschumacher MD, Chandrasekaran K, et al. Guidelines for the echocardiographic assessment of the right heart in adults: a report from the American society of echocardiography endorsed by the European association of echocardiography, a registered branch of the European Society of Cardiology, and the Canadian society of echocardiography. *J Am Soc Echocardiogr*. (2010) 23(7):685–713. quiz 86-8. doi: 10.1016/j.echo.2010.05.010

67. Kato TS, Jiang J, Schulze PC, Jorde U, Uriel N, Kitada S, et al. Serial echocardiography using tissue Doppler and speckle tracking imaging to monitor right ventricular failure before and after left ventricular assist device surgery. *JACC Heart Failure*. (2013) 1(3):216–22. doi: 10.1016/j.jchf.2013.02.005

68. Charisopoulou D, Banner NR, Demetrescu C, Simon AR, Rahman Haley S. Right atrial and ventricular echocardiographic strain analysis predicts requirement for right ventricular support after left ventricular assist device implantation. *Eur Heart J Cardiovasc Imaging*. (2019) 20(2):199–208. doi: 10.1093/ehjci/jey065

69. Samura T, Yoshioka D, Asanoi H, Toda K, Miyagawa S, Yoshikawa Y, et al. Right atrial pressure waveform predicts right ventricular failure after left ventricular assist device implantation. *Ann Thorac Surg*. (2019) 108(5):1361–8. doi: 10.1016/j.athoracsur.2019.04.050

70. Li Q, Zhang M. Echocardiography assessment of right ventricular-pulmonary artery coupling: validation of surrogates and clinical utilities. *Int J Cardiol*. (2024) 394:131358. doi: 10.1016/j.ijcard.2023.131358

71. Amsallem M, Aymami M, Hiesinger W, Zeigler S, Moneghetti K, Marques M, et al. Right ventricular load adaptability metrics in patients undergoing left ventricular assist device implantation. *J Thorac Cardiovasc Surg*. (2019) 157(3):1023–33.e4. doi: 10.1016/j.jtcvs.2018.08.095

72. Shah H, Maharaj V, Kenny B, Kalra R, Rafei AE, Duval S, et al. Non-Invasive TAPSE/PASP ratio is not predictive of early right ventricular failure post LVAD implantation. *J Heart Lung Transplant*. (2020) 39(4):S427–S8. doi: 10.1016/j.healun.2020.01.218

73. Beneyto M, Martins R, Galand V, Kindo M, Schneider C, Sebestyen A, et al. Right ventriculoarterial coupling surrogates and long-term survival in LVAD recipients: results of the ASSIST-ICD multicentric registry. *J Card Fail* (2025) 31(2):388–96. doi: 10.1016/j.cardfail.2024.05.007

74. Sanz J, Sánchez-Quintana D, Bossone E, Bogaard HJ, Naeije R. Anatomy, function, and dysfunction of the right ventricle: JACC State-of-the-Art Review. *J Am Coll Cardiol*. (2019) 73(12):1463–82. doi: 10.1016/j.jacc.2018.12.076

75. Kormos RL, Teuteberg JJ, Pagani FD, Russell SD, John R, Miller LW, et al. Right ventricular failure in patients with the HeartMate II continuous-flow left ventricular assist device: incidence, risk factors, and effect on outcomes. *J Thorac Cardiovasc Surg*. (2010) 139(5):1316–24. doi: 10.1016/j.jtcvs.2009.11.020

76. Fitzpatrick JR III, Frederick JR, Hsu VM, Kozin ED, O'Hara ML, Howell E, et al. Risk score derived from Pre-operative data analysis predicts the need for biventricular mechanical circulatory support. *J Heart Lung Transplant*. (2008) 27(12):1286–92. doi: 10.1016/j.healun.2008.09.006

77. Gumus F, Durdu MS, Cakici M, Kurklu TST, Inan MB, Dincer I, et al. Right ventricular free wall longitudinal strain and stroke work index for predicting right heart failure after left ventricular assist device therapy. *Interact Cardiovasc Thorac Surg*. (2018) 28(5):674–82. doi: 10.1093/icvts/ivy328

78. Frankfurter C, Molinero M, Vishram-Nielsen JKK, Foroutan F, Mak S, Rao V, et al. Predicting the risk of right ventricular failure in patients undergoing left ventricular assist device implantation. *Circ Heart Fail*. (2020) 13(10):e006994. doi: 10.1161/CIRCHEARTFAILURE.120.006994

79. Essandoh M, Kumar N, Hussain N, Dalia AA, Wang D, Al-Qudsi O, et al. Pulmonary artery pulsatility index as a predictor of right ventricular failure in left ventricular assist device recipients: a systematic review. *J Heart Lung Transplant*. (2022) 41(8):1114–23. doi: 10.1016/j.healun.2022.04.007

80. Kapur NK, Esposito ML, Bader Y, Morine KJ, Kiernan MS, Pham DT, et al. Mechanical circulatory support devices for acute right ventricular failure. *Circulation*. (2017) 136(3):314–26. doi: 10.1161/CIRCULATIONAHA.116.025290

81. Cacioli G, Polizzi V, Ciabatti M, Cristiano E, Pergolini A, Distefano G, et al. Prediction of right ventricular failure after left ventricular assist device implantation: role of vasodilator challenge. *Eur Heart J Acute Cardiovasc Care*. (2022) 11(8):629–39. doi: 10.1093/ehjacc/zuac085

82. Hsi B, Joseph D, Trachtenberg B, Bhimaraj A, Suarez EE, Xu J, et al. Degree of change in right ventricular adaptation measures during axillary impella support informs risk stratification for early, severe right heart failure following durable LVAD implantation. *J Heart Lung Transplant*. (2022) 41(3):279–82. doi: 10.1016/j.healun.2021.11.007

83. Tadokoro N, Koyamoto T, Tonai K, Yoshida Y, Hirahsima K, Kainuma S, et al. The outcomes of a standardized protocol for extracorporeal mechanical circulatory support selection-left ventricular challenge protocol. *J Artif Organs*. (2024) 27(4):358–67. doi: 10.1007/s10047-023-01427-7

84. Iannaccone M, Gamardella M, Fumarola F, Mangione R, Botti G, Russo F, et al. Pulmonary artery pulsatility index evaluation in intermediate-to-high and high-risk pulmonary embolism patients underwent transcatheter intervention. *Eur Heart J*. (2024) 45(Supplement_1). doi: 10.1093/eurheartj/ehae666.2324

85. Yim IHW, Khan-Kheil AM, Drury NE, Lim HS. A systematic review and physiology of pulmonary artery pulsatility index in left ventricular assist device therapy. *Interdisciplin Cardiovasc Thorac Surg*. (2023) 36(5):ivad068. doi: 10.1093/icvts/ivad068

86. Rajagopalan N, Borlaug Barry A, Bailey Alison L, Eckman Peter M, Guglin M, Hall S, et al. Practical guidance for hemodynamic assessment by right heart catheterization in management of heart failure. *JACC Heart Fail*. (2024) 12(7):1141–56. doi: 10.1016/j.jchf.2024.03.020

87. Taleb I, Kyriakopoulos CP, Fong R, Ijaz N, Demertzis Z, Sideris K, et al. Machine learning multicenter risk model to predict right ventricular failure after mechanical circulatory support: the STOP-RVF score. *JAMA Cardiol*. (2024) 9(3):272–82. doi: 10.1001/jamacardio.2023.5372

88. Soliman OI, Akin S, Muslem R, Boersma E, Manintveld OC, Krabatsch T, et al. Derivation and validation of a novel right-sided heart failure model after implantation of continuous flow left ventricular assist devices: the EUROMACS (European registry for patients with mechanical circulatory support) right-sided heart failure risk score. *Circulation*. (2018) 137(9):891–906. doi: 10.1161/CIRCULATIONAHA.117.030543

89. Amsallem M, Aymami M, Hiesinger W, Zeigler S, Moneghetti K, Marques M, et al. Right ventricular load adaptability metrics in patients undergoing left ventricular assist device implantation. *J Thorac Cardiovasc Surg*. (2019) 157(3):1023–33.e4. doi: 10.1016/j.jtcvs.2018.08.095

90. Kalogeropoulos AP, Kelkar A, Weinberger JF, Morris AA, Georgiopoulou VV, Markham DW, et al. Validation of clinical scores for right ventricular failure prediction after implantation of continuous-flow left ventricular assist devices. *J Heart Lung Transplant*. (2015) 34(12):1595–603. doi: 10.1016/j.healun.2015.05.005

91. Drakos SG, Janicki L, Horne BD, Kfoury AG, Reid BB, Clayson S, et al. Risk factors predictive of right ventricular failure after left ventricular assist device implantation. *Am J Cardiol*. (2010) 105(7):1030–5. doi: 10.1016/j.amjcard.2009.11.026

92. Bahl A, Qureshi B, Zhang K, Bravo C, Mahr C, Li S. Explainable machine learning analysis of right heart failure after left ventricular assist device implantation. *ASAIO J*. (2023) 69(5):417–23.

93. Mehra MR, Nayak A, Morris AA, Lanfear DE, Nemeh H, Desai S, et al. Prediction of survival after implantation of a fully magnetically levitated left ventricular assist device. *JACC Heart Fail*. (2022) 10(12):948–59. doi: 10.1016/j.jchf.2022.08.002

94. Atluri P, Goldstone AB, Fairman AS, MacArthur JW, Shudo Y, Cohen JE, et al. Predicting right ventricular failure in the modern, continuous flow left ventricular assist device era. *Ann Thorac Surg*. (2013) 96(3):857–64. doi: 10.1016/j.athoracsur.2013.03.099

95. Akamkam A, Galand V, Jungling M, Delmas C, Dambrin C, Pernot M, et al. Association between pulmonary artery pulsatility and mortality after implantation of left ventricular assist device. *ESC Heart Fail*. (2024) 11(4):2100–12. doi: 10.1002/ehf2.14716

96. Raymer DS, Moreno JD, Sintek MA, Nassif ME, Sparrow CT, Adamo L, et al. The combination of tricuspid annular plane systolic excursion and HeartMate risk score predicts right ventricular failure after left ventricular assist device implantation. *Asaio J*. (2019) 65(3):247–51. doi: 10.1097/MAT.0000000000000808

97. Patil NP, Mohite PN, Sabashnikov A, Dhar D, Weymann A, Zeriouh M, et al. Preoperative predictors and outcomes of right ventricular assist device implantation after continuous-flow left ventricular assist device implantation. *J Thorac Cardiovasc Surg*. (2015) 150(6):1651–8. doi: 10.1016/j.jtcvs.2015.07.090

98. Dandel M, Potapov E, Krabatsch T, Stepanenko A, Löw A, Vierecke J, et al. Load dependency of right ventricular performance is a Major factor to be considered in decision making before ventricular assist device implantation. *Circulation*. (2013) 128(11_suppl_1):S14–23. doi: 10.1161/CIRCULATIONAHA.112.000335

99. Morita Y, Lencho T, Gunasekaran S, Modak R. Modified tricuspid annular plane systolic excursion using transesophageal echocardiography and its utility to predict postoperative course in heart transplantation and left ventricular assist device implantation. *J Cardiothorac Vasc Anesth*. (2018) 32(3):1316–24. doi: 10.1053/j.jvca.2017.11.024

100. Raina A, Seetha Rammohan HR, Gertz ZM, Rame JE, Woo YJ, Kirkpatrick JN. Postoperative right ventricular failure after left ventricular assist device placement is predicted by preoperative echocardiographic structural, hemodynamic, and functional parameters. *J Card Fail*. (2013) 19(1):16–24. doi: 10.1016/j.cardfail.2012.11.001

101. Liang LW, Jamil A, Mazurek JA, Urgo KA, Wald J, Birati EY, et al. Right ventricular global longitudinal strain as a predictor of acute and early right heart failure post left ventricular assist device implantation. *ASAIO J*. (2022) 68(3). doi: 10.1097/MAT.0000000000001467

102. Dufendach KA, Zhu T, Diaz Castrillon C, Hong Y, Countouris ME, Hickey G, et al. Pre-implant right ventricular free wall strain predicts post-LVAD right heart failure. *J Card Surg*. (2021) 36(6):1996–2003. doi: 10.1111/jocs.15479

103. Magunia H, Dietrich C, Langer HF, Schibilsky D, Schlensak C, Rosenberger P, et al. 3D Echocardiography derived right ventricular function is associated with right ventricular failure and mid-term survival after left ventricular assist device implantation. *Int J Cardiol*. (2018) 272:348–55. doi: 10.1016/j.ijcard.2018.06.026

104. Cameli M, Lisi M, Righini FM, Focardi M, Lunghetti S, Bernazzali S, et al. Speckle tracking echocardiography as a new technique to evaluate right ventricular function in patients with left ventricular assist device therapy. *J Heart Lung Transplant*. (2013) 32(4):424–30. doi: 10.1016/j.healun.2012.12.010

105. Grant ADM, Smedira NG, Starling RC, Marwick TH. Independent and incremental role of quantitative right ventricular evaluation for the prediction of right ventricular failure after left ventricular assist device implantation. *J Am Coll Cardiol*. (2012) 60(6):521–8. doi: 10.1016/j.jacc.2012.02.073

106. Scheel PJ III, Cubero Salazar IM, Friedman S, Haber L, Mukherjee M, Kauffman M, et al. Occult right ventricular dysfunction and right ventricular-vascular uncoupling in left ventricular assist device recipients. *J Heart Lung Transplant*. (2024) 43(4):594–603. doi: 10.1016/j.healun.2023.11.015

107. Ruiz-Cano MJ, Morshuis M, Koster A, Lauenroth V, Prashovikj E, Gummert J, et al. Risk factors of early right ventricular failure in patients undergoing LVAD implantation with intermediate intermacs profile for advanced heart failure. *J Card Surg*. (2020) 35(8):1832–9. doi: 10.1111/jocs.14696

108. Akin S, Soliman O, de By T, Muslem R, Tijssen JGP, Schoenrath F, et al. Causes and predictors of early mortality in patients treated with left ventricular assist device implantation in the European registry of mechanical circulatory support (EUROMACS). *Intensive Care Med*. (2020) 46(7):1349–60. doi: 10.1007/s00134-020-05939-1

109. Rivas-Lasarte M, Kumar S, Derbala MH, Ferrall J, Cefalu M, Rashid SMI, et al. Prediction of right heart failure after left ventricular assist implantation: external validation of the EUROMACS right-sided heart failure risk score. *Eur Heart J Acute Cardiovasc Care*. (2021) 10(7):723–32. doi: 10.1093/ehjacc/zuab029

110. Kumar S, Rivas-Lasarte M, Rashid S, Scatola A, Rochlani Y, Murthy S, et al. External validation and comparison of the EUROMACS and right ventricular failure risk score for right ventricular failure prediction after left ventricular assist device. *J Heart Lung Transplant*. (2020) 39(4):S38. doi: 10.1016/j.healun.2020.01.1196

111. Shah H, Murray T, Schultz J, John R, Martin CM, Thenappan T, et al. External assessment of the EUROMACS right-sided heart failure risk score. *Sci Rep*. (2021) 11(1):16064. doi: 10.1038/s41598-021-94792-3

112. Matthews JC, Koelling TM, Pagani FD, Aaronson KD. The right ventricular failure risk score: a pre-operative tool for assessing the risk of right ventricular failure in left ventricular assist device candidates. *J Am Coll Cardiol*. (2008) 51(22):2163–72. doi: 10.1016/j.jacc.2008.03.009

frontiers | Frontiers in Cardiovascular Medicine

TYPE Original Research
PUBLISHED 23 May 2025
DOI 10.3389/fcvm.2025.1566021

OPEN ACCESS

EDITED BY
Leonard Y. Lee,
The State University of New Jersey,
United States

REVIEWED BY
Paul C. Tang,
Mayo Clinic, United States
Masahiro Yamamoto,
Kumamoto University, Japan

*CORRESPONDENCE
Kei Sato
✉ sato.kei@ncvc.go.jp
Keita Saku
✉ saku.keita@ncvc.go.jp

RECEIVED 24 January 2025
ACCEPTED 30 April 2025
PUBLISHED 23 May 2025

CITATION
Sato K, Yoshida Y, Yokota S, Matsushita H, Morita H, Fukumitsu M, Nishikawa T, Uemura K, Kawada T and Saku K (2025) Pressure-strain product reflects left ventricular stroke work under a wide range of left ventricular assist device support levels.
Front. Cardiovasc. Med. 12:1566021.
doi: 10.3389/fcvm.2025.1566021

Pressure-strain product reflects left ventricular stroke work under a wide range of left ventricular assist device support levels

Kei Sato[1]*, Yuki Yoshida[1], Shohei Yokota[1], Hiroki Matsushita[1], Hidetaka Morita[1], Masafumi Fukumitsu[1], Takuya Nishikawa[2], Kazunori Uemura[1,3], Toru Kawada[1] and Keita Saku[1,3]*

[1]Department of Cardiovascular Dynamics, National Cerebral and Cardiovascular Center Research Institute, Suita, Japan, [2]Department of Research Promotion and Management, National Cerebral and Cardiovascular Center, Suita, Japan, [3]Bio Digital Twin Center, National Cerebral and Cardiovascular Center, Suita, Japan

Introduction: Assessment of native cardiac function is vital in patients with cardiogenic shock supported by a left ventricular assist device (LVAD), as it is directly related to the critical decision of LVAD management. Left ventricular stroke work (LVSW) can be useful for cardiac assessment to predict survival in cardiogenic shock patients; however, this measurement cannot necessarily be obtained under LVAD support, especially in cases where the aortic valve is closed (i.e., total support). Therefore, we propose a novel echocardiographic parameter named the pressure-strain product (PSP), the product of left ventricular (LV) pressure and LV myocardial strain, as this measurement can be calculated even under LV total support. This study aimed to investigate whether PSP was correlated with pressure-volume (PV) loop-based LVSW and myocardial oxygen consumption under LVAD support.

Method: We used 15 adult goats. An LVAD system was established during open chest surgery by draining blood from the left ventricle and returning it to the carotid artery. LV PV loops were analyzed by measuring LV pressure and volume using sonomicrometry. PV loop-based LVSW was defined as the area surrounded by PV loops. The PSP was defined as the product of the peak LV pressure and global circumferential strain (GCS) using speckle-tracking echocardiography. LVAD support levels were divided into three groups: control, and partial (with residual native cardiac output) and total (without native cardiac output) support. Myocardial oxygen consumption was measured using coronary flow and blood gas analyses. The correlation coefficient was measured using linear regression analysis.

Results: According to each LVAD support level at control, partial support, and total support, LVSW was $1{,}748 \pm 867$, 840 ± 467, and 290 ± 262 mmHg·ml, while PSP was $2{,}341 \pm 507$, $1{,}836 \pm 768$, and 539 ± 269 mmHg·%, respectively. PSP ($r = 0.54$) showed the strongest correlation with PV loop-based LVSW among other echocardiographic parameters, including LV end-diastolic volume ($r = 0.37$), GCS ($r = 0.40$), and echo-based LVSW ($r = 0.50$). PSP level was significantly associated with myocardial oxygen consumption ($r = 0.55$).

Conclusion: PSP significantly correlated with PV loop-based LVSW at various LVAD support levels. PSP can be a non-invasive parameter for assessing myocardial metabolism under LVAD support, potentially reflecting myocardial oxygen consumption.

KEYWORDS

speckle-tracking echocardiography, left ventricular stroke work, myocardial oxygen consumption, left ventricular assist device, left ventricular unloading, coronary flow regulation

Introduction

For patients with cardiogenic shock, assessment of cardiac function is imperative to judge the native heart recovery. A percutaneous left ventricular (LV) unloading device (i.e., Impella) can decrease LV end-diastolic pressure and volume, which reduces the myocardial workload and oxygen demand of the LV myocardium (1, 2). This LV unloading can contribute to myocardial protection and recovery (3); thus, accurate assessment of LV workload has been gaining increasing attention among clinicians (4). However, there is a knowledge gap regarding the accurate measurement of LV workload under device support. In particular, this is challenging with total LV support where the aortic valve constantly closes without LV ejection. Under these conditions, conventional parameters such as cardiac power output cannot be calculated. Therefore, a substitute is needed to evaluate the cardiac workload, indicating LV protection and recovery under LV unloading.

Echocardiographic myocardial strain captures myocardial deformation, indicating cardiac contractility. This measurement can sensitively detect subtle changes in cardiac function and can be useful even with mechanical circulatory support (5). Furthermore, the product of echocardiographic strain and blood pressure, named the pressure-strain product (PSP), has been reported to correlate with LV stroke work (LVSW) in a few animal models (6–8). Considering that LVSW can predict survival better than conventional cardiac parameters, including LV ejection fraction, in the cardiac intensive care unit (9), it is worth investigating whether PSP can estimate LVSW reflecting myocardial oxygen consumption under left ventricular assist device (LVAD) support.

This study aimed to evaluate whether PSP can be correlated with pressure-volume (PV) loop-based LVSW using a large animal model supported by an open-chest LVAD system across various LVAD support levels. Additionally, the relationship of PSP with myocardial oxygen consumption and coronary perfusion were investigated to evaluate LV protection.

Materials and methods

Ethics for animal experiments

Animal care strictly adhered to the Guiding Principles for the Care and Use of Animals in the Field of Physiological Sciences, approved by the Physiological Society of Japan. All the experiments were approved by the Animal Subjects Committee of the National Cerebral and Cardiovascular Center.

Experimental preparation

We used 15 adult goats (Saanen breed of *Capra aegagrus hircus*), weighing 36–54 kg, with a sex distribution of three males and twelve females. Anesthesia was induced using intramuscular xylazine (2 mg/kg), pentazocine (15 mg), and midazolam (10 mg), followed by endotracheal intubation. A laryngotracheal separation was performed to avoid aspiration pneumonia. Separate ventilation for each lung was applied using a double-lumen endotracheal tube to apply different levels of positive end-expiratory pressure (i.e., 15 mmHg for the right lung and 10 mmHg for the left lung). This procedure prevented severe atelectasis of the right lung during left thoracotomy in the right lateral position. Eight and 10 Fr sheaths were inserted into the bilateral femoral artery and vein, respectively (one artery for the measurement of arterial pressure, another artery for collecting blood samples, one vein for the fluid line, and another vein for continuous infusion of muscle relaxant). A 10 Fr long sheath was inserted into the right carotid vein to access the right atrium for a 6 Fr catheter to measure coronary sinus blood gas. Heparin (100 IU/kg) was prophylactically administered to avoid catheter thrombosis and subsequent pulmonary embolism. A 5 Fr pressure catheter (Millar Instruments, Houston, TX, USA) was inserted through the 8 Fr femoral artery catheter into the ascending aorta to measure the aortic pressure.

Sedation and ventilation settings

An appropriate level of anesthesia was maintained by continuous inhalation of sevoflurane (1%–2%) and rocuronium (10 mg/h) drop infusion. Additional intravenous fentanyl and propofol were administered when required. Ventilation was performed using volume control with a fraction of inspired oxygen ranging from 0.6 to 1.0 to maintain PaO_2 >80 mmHg. The tidal volume was set at 8–10 ml/kg and the respiratory rate was adjusted to 12–20 breaths per minute to maintain $PaCO_2$ at approximately 40 mmHg.

Open chest surgery

Left thoracotomy was performed in the left fourth intercostal space in the right lateral position. Following the cut of the pericardium, four ultrasound crystals for sonomicrometry (Sonometrics Corporation, London, Ontario, Canada) were inserted into the myocardium and secured with a tourniquet: one pair at the base and apex of the LV wall and another pair at the middle part of the posterior and anterior LV wall. A 5 Fr pressure catheter (Millar Instruments, Houston, TX, USA) was inserted into the LV cavity from the LV free wall to continuously monitor the LV pressure. A 6 Fr catheter (Judkins Right 3.5, Medtronic, Minneapolis, MN, USA) was inserted into the coronary sinus to measure blood gas. Three (3PSB2171, Transonic Systems, Ithaca, NY) and 20 mm flow probes (20PAX1232, Transonic Systems) were attached to the left main trunk and pulmonary artery to evaluate coronary artery flow and pulmonary artery flow, respectively. The stroke volume measured using the pulmonary artery flow probe was used to correct the volume measured using sonomicrometry.

LVAD system

Following heparinization with 300 IU/kg, a 25 Fr drainage cannula and 19 Fr returning cannula were inserted into LV and left carotid artery, respectively, with the support of fluoroscopy. The tip of the return cannula was placed into the aortic arch. A centrifugal pump (Senko Medical Instrument Mfg. Co., Tokyo, Japan) was used for the LVAD support. Partial support was defined as the maximum support that allowed residual native cardiac output, whereas total support was defined as the support that eliminated native cardiac output.

Echocardiography

Epicardial echocardiography was performed using an E95 ultrasound machine (GE Healthcare, Chicago, IL, USA) with a 6Sc echo probe. All images were transferred to a separate workstation and analyzed offline by an experienced cardiologist using the Echopac software (GE Healthcare, Chicago, IL, USA). A speckle-tracking echocardiography parameter, the global circumferential strain (GCS) at the LV mid-papillary level, was calculated, and automated measurement was applied to the appropriate echo loops. PSP was calculated as the product of GCS (absolute value) and peak LV pressure (Supplementary Figure S1). The appropriate image quality was selected when the software approved the quality of the speckle tracking as well as a visual assessment by an investigator. End-diastolic and end-systolic timing markers were manually adjusted, if required. A frame rate of 43/s was applied for strain assessment.

Measurement of LVSW and pressure-volume area using PV loop

LVSW, the area enclosed by the PV loop, was calculated using Green's theorem and the formula embedded in the LabChart 8 software (AD Instruments, Dunedin, New Zealand) (6):

$$\sum_{i=a}^{b} \{(v_i p_{i+1}) - (v_{i+1} p_i)\}$$

where a and b denote the start and end positions of the loop, respectively. The loop is "closed" by setting v_{i+1} and p_{i+1} to v_a and p_a when i = b.

Multiple PV loops were generated by altering the preload through inferior vena cava balloon occlusion, and the end-systolic pressure-volume relationship (ESPVR), end-diastolic pressure-volume relationship (EDPVR), and V_0 (i.e., the intersection of ESPVR with the LV volume axis) were calculated. The area enclosed by the ESPVR, EDPVR, and PV loop was defined as the pressure-volume area (PVA). The PVA was measured using an in-house program (MATLAB R2018b; Mathworks, Natick, MA, USA).

Measurement of myocardial oxygen consumption and coronary vascular resistance

Myocardial oxygen consumption (MVO_2) was measured using the following formula:

$$MVO_2 = \{1.36 \times Hb \times (S_aO_2 - S_{cs}O_2) \times (\text{coronary flow})\} / \{(\text{heart rate}) \times \text{LV weight (per 100 mg)}\}$$

where Hb is the hemoglobin concentration (g/dl) and S_aO_2 and $S_{cs}O_2$ are the oxygen saturations of the artery and coronary sinus, respectively. Coronary vascular resistance (CVR) was calculated using the following formula:

$$CVR = CPP/(\text{coronary flow})$$

where CPP is coronary perfusion pressure defined as MAP-mean LV pressure.

Experimental protocol

Following experimental preparation (Figure 1), hemodynamic parameters (i.e., LV pressure and PV loop-based LVSW), blood gas (i.e., one from the femoral artery and another from the coronary sinus), and an echocardiographic image of the LV short-axis view were assessed after 5 min stabilization at the control and partial and total support of the LVAD (Figure 2).

Statistics

Friedman test was conducted to compare the hemodynamic or echocardiographic parameters during the three different LVAD support levels. The Bonferroni *post hoc* test was applied for inter-group comparisons. The correlation coefficient was measured using linear regression analysis. $p < 0.05$ was considered statistically significant. Statistical tests were conducted using EZR (version 1.68) (10) in R Commander (version 2.9-1) and Microsoft Excel (Microsoft Corp., Redmond, WA, USA).

Results

Representative hemodynamic waveforms based on LVAD support levels

Baseline characteristics of animals are described in the Table 1. Representative hemodynamic waveforms are shown in Figure 3. As the LVAD support level increased, LV pressure and volume decreased and the PV loop shifted left and downward. In addition, as the aortic pressure gradually increased, the coronary flow in the left main trunk showed a decreasing trend.

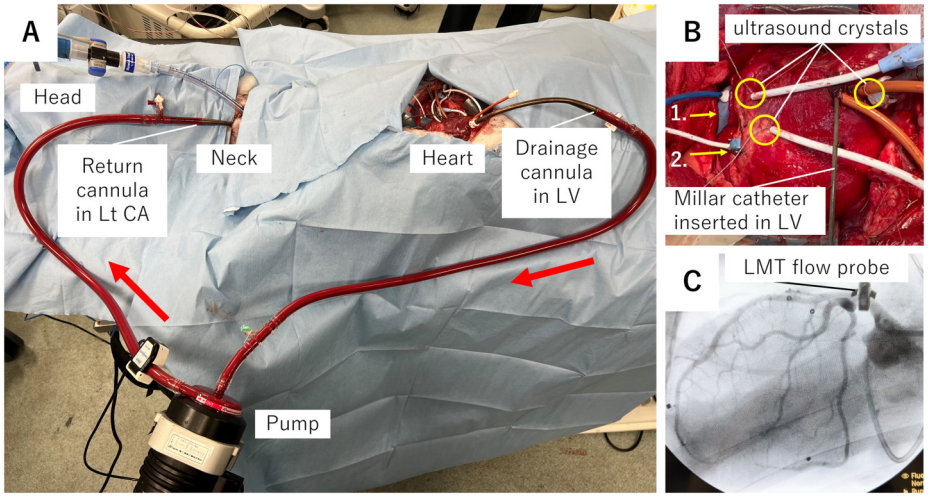

FIGURE 1
Overview of experimental setup. **(A)** Picture describing LVAD system. Blood sucked from a drainage cannula at the left ventricle flows through a pump to the carotid artery via the return cannula. Red arrows show the direction of blood flow. **(B)** Picture showing the location of ultrasound crystals and flow probe. (1) A flow probe at pulmonary artery; (2) a flow probe at left main trunk of coronary artery. **(C)** Cine film showing the left coronary arteries and the flow probe at the left main trunk. CA, carotid artery; LMT, left main trunk; Lt, left; LVAD, left ventricular assist device.

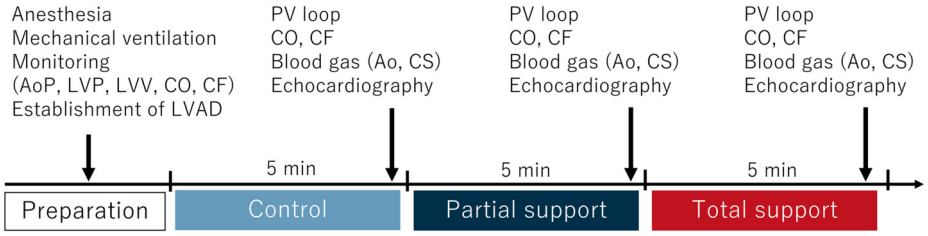

FIGURE 2
Study protocol. Following the preparation, PV loop, hemodynamic parameters, blood gas, and echocardiographic parameters were assessed after 5 min stabilization at control, partial, and total support of LVAD. Ao, aorta; AoP, aortic pressure; CF, coronary flow; CO, cardiac output; CS, coronary sinus; LVAD, left ventricular assist device; LVP, left ventricular pressure; LVV, left ventricular volume; PV, pressure-volume.

Representative echocardiographic images and PSP based on LVAD support levels

Representative ultrasound images (LV short axis view) and speckle-tracking analyses are shown in Figure 4. As LVAD support level increased, GCS, LV systolic pressure, and subsequent PSP decreased.

Trends in hemodynamic and echocardiographic parameters based on LVAD support levels

Hemodynamic parameters, including heart rate, mean arterial pressure, and LV systolic pressure, are shown in Figure 5. As LVAD support levels increased, the heart rate and mean arterial pressure increased significantly, whereas LV systolic pressure decreased significantly. Similarly, the LV end-diastolic volume (EDV), GCS, and PSP significantly declined when LVAD support increased.

Correlation analysis between PV loop-based LVSW and echo/hemodynamic parameters

Scatter plots of PV loop-based LVSW vs. echo-based LV EDV, echo-based LVSW, GCS, and PSP are shown in Figure 6. PSP showed the strongest correlation ($r = 0.54$, $p < 0.01$) with the PV loop-based LVSW among other parameters.

Trends in cardiac energetics and coronary perfusion based on LVAD support levels

MVO_2 and PVA were significantly reduced as LVAD support level increased (Figure 7). MVO_2 and PVA were significantly

TABLE 1 Baseline characteristics including hemodynamics and echocardiographic parameters.

Parameters	Median (IQR)
BW (kg)	47 (45–50)
HR (/min)	79 (68–97)
MAP (mmHg)	73 (58–77)
Peak LVP (mmHg)	87 (70–92)
LVEDP (mmHg)	11 (10–13)
Hb (g/dl)	9.4 (8.5–10.5)
SaO_2 (%)	99 (98–100)
$ScsO_2$ (%)	52 (49–69)
LVEDV (ml)	63 (53–73)
LVESV (ml)	21 (15–29)
LVSV (ml)	40 (34–44)
LVEF (%)	68 (61–71)
GCS (absolute) (%)	27.6 (26.5–31.7)
PSP (mmHg·%)	2,427 (2,252–2,699)
LVSW (based on PV-loop) (mmHg·ml)	1,728 (1,052–2,183)
LV mass (g)	115 (110–119)

BW, body weight; GCS, global circumferential strain; Hb, hemoglobin; HR, heart rate; IQR, interquartile range; LVEDP, left ventricular end-diastolic pressure; LVEDV, left ventricular end-diastolic volume; LVEF, left ventricular ejection fraction; LVESV, left ventricular end-systolic volume; LVP, left ventricular pressure; LVSV, left ventricular stroke volume; LVSW, left ventricular stroke work; MAP, mean arterial pressure; PSP, pressure-strain product; SaO2, arterial oxygen saturation; ScsO2, coronary sinus oxygen saturation.

correlated ($r = 0.68$, $p < 0.01$). Coronary perfusion pressure, $S_{CS}O_2$, and coronary vascular resistance significantly increased, whereas coronary flow at the left main trunk showed a decreasing trend as LVAD support increased (Figure 8).

Correlation analysis of PSP with both cardiac energetics and coronary perfusion

Pressure-strain product were significantly correlated with LV MVO_2 ($r = 0.55$, $p < 0.01$), PVA ($r = 0.40$, $p < 0.01$), $S_{CS}O_2$ ($r = 0.38$, $p = 0.011$), and coronary vascular resistance (CVR) ($r = 0.42$, $p < 0.01$) (Figure 9).

Discussion

Pressure-strain product showed the strongest correlation with PV loop-based LVSW among other echocardiographic parameters, including echo-based LV EDV, echo-based LVSW, and GCS. PSP is also related to myocardial oxygen consumption, which can be a reasonable parameter reflecting LV unloading and protection.

Rationale of correlation between PSP and LVSW

Pressure-strain product was conceptualized using a pressure-strain loop, where the volume was replaced with the myocardial strain in the pressure-volume loop (Supplementary Figure S1) (6–8). Russell et al. reported that the area surrounded by the LV pressure-strain loop, called myocardial work, was significantly correlated with PV loop-based LVSW (11). In addition, regional myocardial work could reflect myocardial glucose metabolism, as measured by positron emission tomography. While myocardial work requires vendor-dependent software and uses global longitudinal strain (GLS), we propose a vendor-independent PSP that can be calculated as the product of mean arterial pressure and GCS. Previous studies have shown that PSP calculated using mean arterial pressure (MAP) correlates well with LVSW in various settings, including the ovine model of septic cardiomyopathy (8), brain stem death (7) and cardiogenic shock supported by V-A ECMO (6). The crucial difference between previous studies and the present study is that we examined whether PSP could be measured even under total LV unloading,

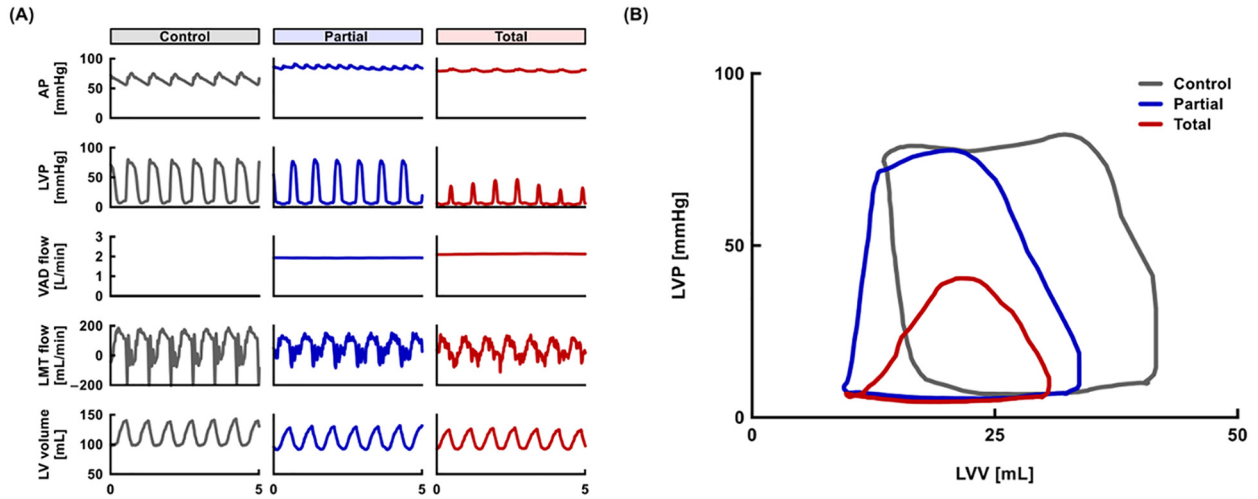

FIGURE 3
Representative hemodynamics. (A) Wave forms of AP, LVP, VAD flow, LMT flow, and LV volume at control, partial, and total support. (B) Pressure-volume loops at control, partial, and total support. AP, aortic pressure; LMT, left main trunk; LV, left ventricular; LVP, left ventricular pressure; LVV, left ventricular volume; VAD, ventricular assist device.

10.3389/fcvm.2025.1566021

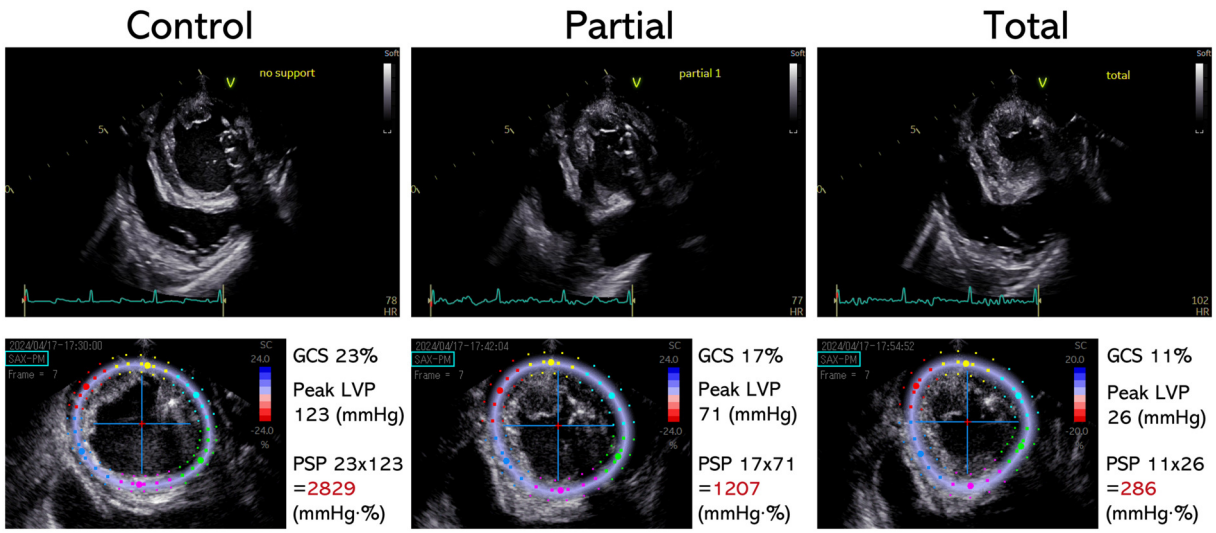

FIGURE 4
Representative echocardiographic images and PSP calculation. Upper pictures: Echocardiographic images of left ventricular short axis view at the mid-papillary level. Lower pictures: Speckle-tracking echocardiographic analysis corresponding to the upper pictures. PSP at each LVAD support level is shown as the product of GCS and peak LV pressure. GCS, global circumferential strain; LVAD, left ventricular assist device; LVP, left ventricular pressure; PSP, pressure-strain product.

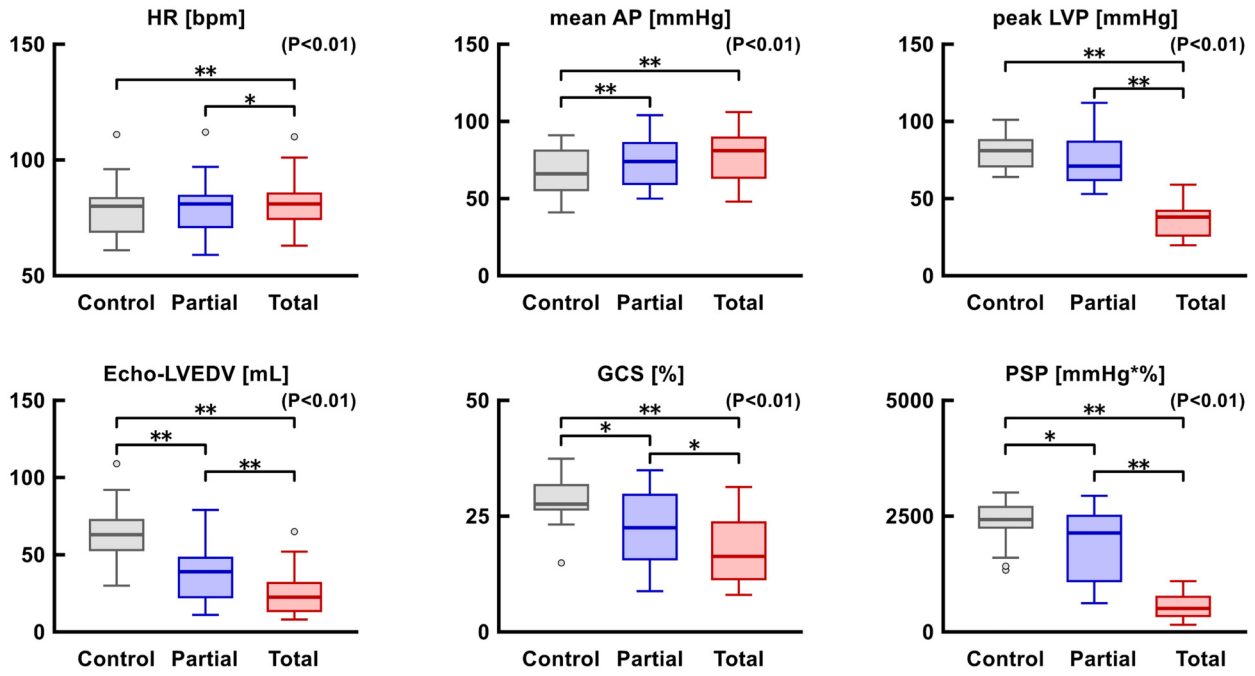

FIGURE 5
Trends in hemodynamic (upper row) and echocardiographic (lower row) parameters. *$p < 0.05$, **$p < 0.01$. AP, arterial pressure; GCS, global circumferential strain; HR, heart rate; LVEDV, left ventricular end-diastolic volume; LVP, left ventricular pressure; PSP, pressure-strain product.

where significant gap exists between MAP and LVSP. Therefore, we redefined PSP from MAP × GCS as used in previous reports, to peak LVP × GCS to appropriately express LV workload during total LV unloading. Thus, the novelty of our study lies in measuring PSP using a different definition from previous reports and analyzing its correlation with LVSW.

Potential benefits to use GCS rather than stroke volume or global longitudinal strain in estimating LVSW

To obtain the value of LVSW, measurement of the stroke volume (SV) is essential. As an invasive method, the Swan-Gantz catheter can

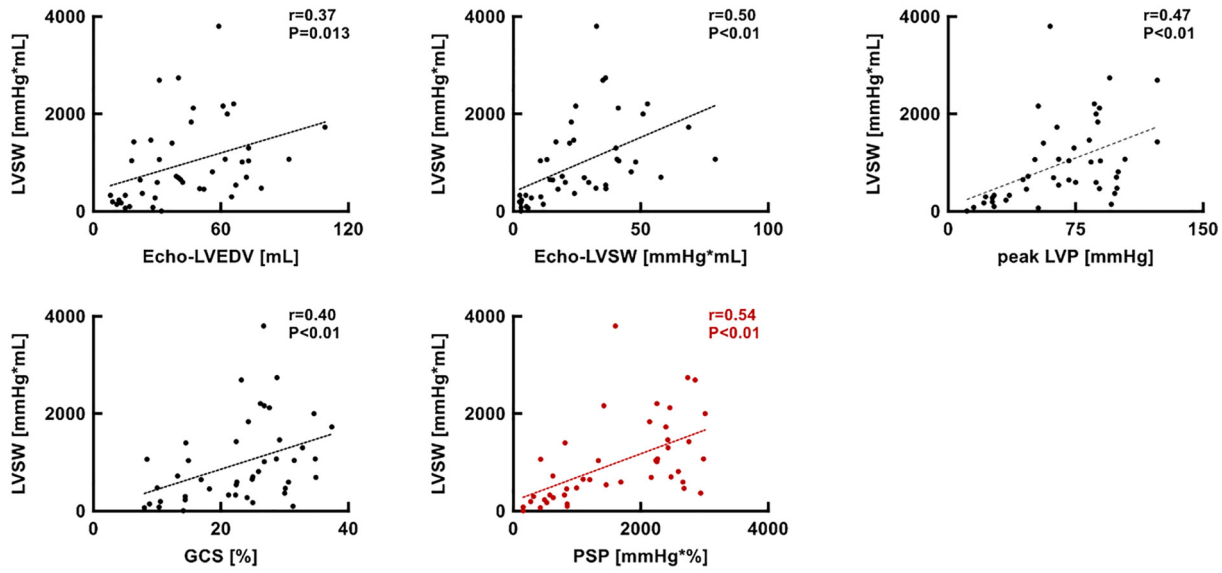

FIGURE 6
Scatter plots showing the relationship between PV loop-based LVSW and echo-LVEDV, echo-LVSW, peak LVP, GCS, and PSP. GCS, global circumferential strain; LVEDV, left ventricular end-diastolic volume; LVP, left ventricular pressure; LVSW, left ventricular stroke work; PSP, pressure-strain product; PV, pressure-volume.

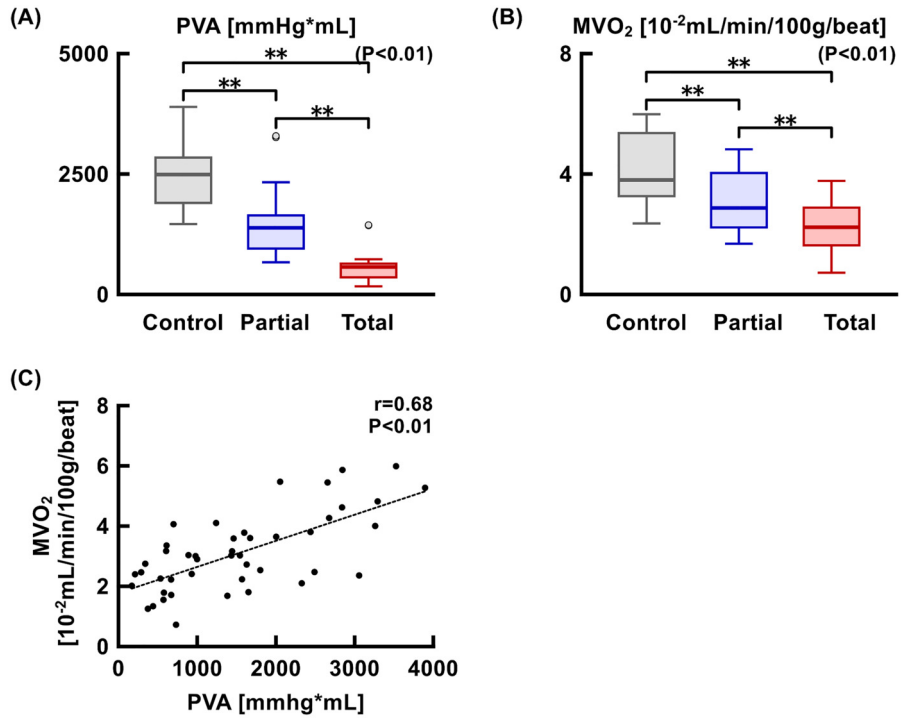

FIGURE 7
Trends in PVA (A) and MVO_2 (B) at each LVAD support level and the correlation between the two parameters (C) MVO_2, myocardial oxygen consumption; PVA, pressure-volume area.

accurately measure SV as the gold standard; however, this method is not routinely recommended in clinical settings because of its invasive nature and subsequent complications (12). Echocardiography can be applied as a non-invasive method to evaluate SV; however, significant pitfalls regarding variations among sonographers have been reported (13). Speckle-tracking echocardiography-based myocardial work can overcome this limitation by applying automated methods to evaluate myocardial strain, achieving high reproducibility (14). The limitation

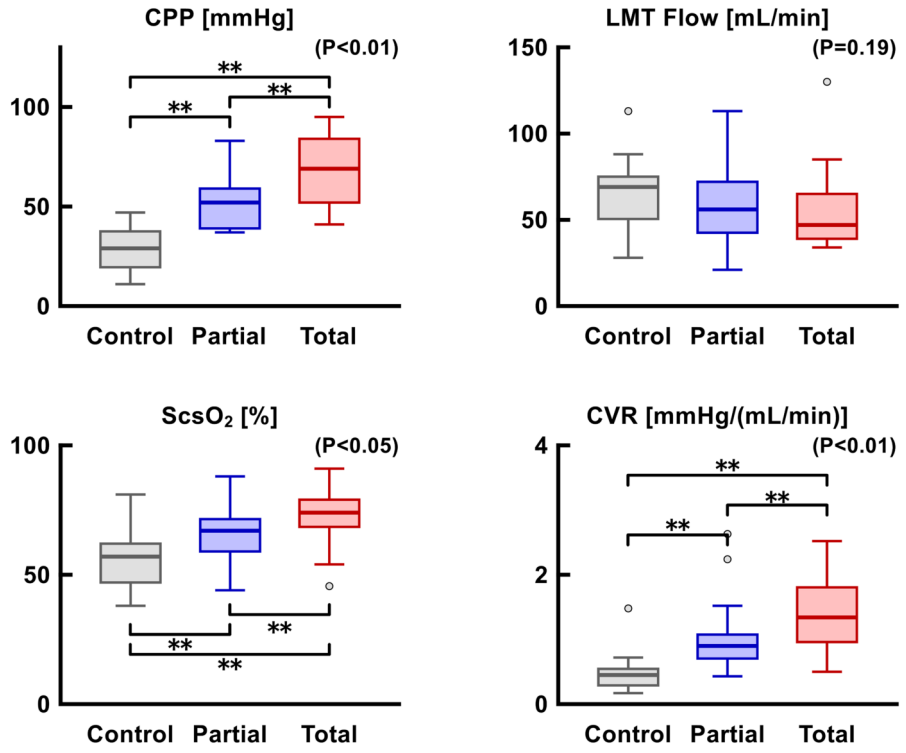

FIGURE 8
Trends in CPP, LMT flow, $S_{CS}O_2$, and CVR according to LVAD support. CPP, coronary perfusion pressure; CVR, coronary vascular resistance; LMT, left main trunk; $ScsO_2$, oxygen saturation of coronary sinus blood.

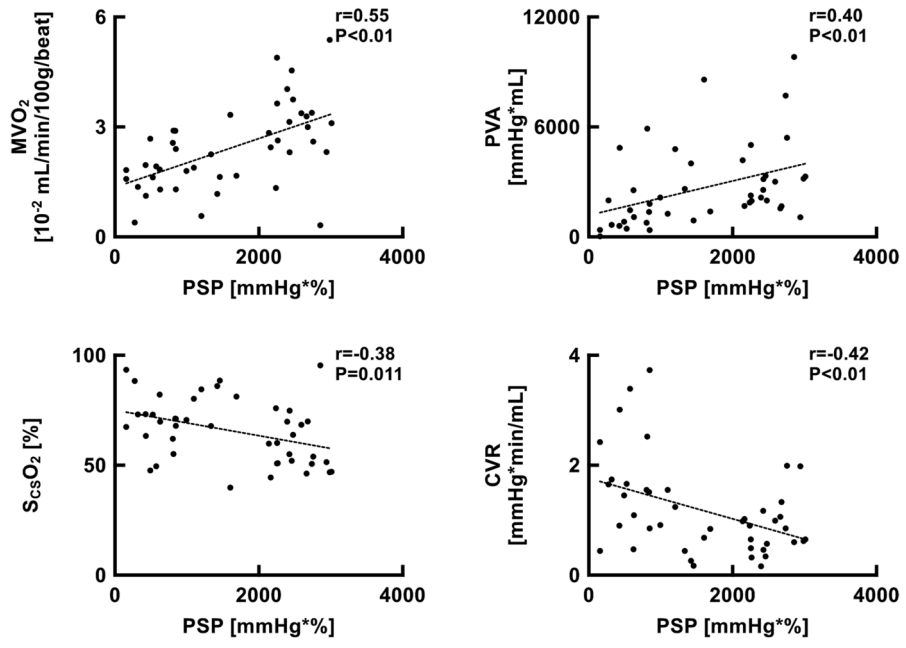

FIGURE 9
Scatter plots showing the relationship between PSP and MVO_2, PVA, $S_{CS}O_2$, and CVR. CVR, coronary vascular resistance; MVO_2, myocardial oxygen consumption; PSP, pressure-strain product; PVA, pressure-volume area; $ScsO_2$, oxygen saturation of coronary sinus blood.

of this method is the difficulty in obtaining three appropriate echo images (2-, 3-, and 4-chamber views from the LV apex) to calculate GLS (14), especially in ICU settings where patients cannot cooperate with echo sonographers to adjust respiratory timing. In contrast, GCS can be obtained using the LV short axis view alone, which is simpler than obtaining the GLS. Therefore, PSP consisting of GCS can be a user-friendly measurement for clinicians to estimate LVSW.

The significance of PSP for the cardiac assessment and the optimization of LVAD support

Left ventricular stroke work was calculated using echocardiography as follows: LVSV × MAP × 0.0134 (9). However, the LVSV does not exist under the condition of total LV support, where the aortic valve constantly closes. In this situation, we cannot measure LVSV and subsequent LVSW using the LV outflow tract velocity-time integral, which is one of the most common parameters in clinical settings. Although the value of LVSV, defined as the gap between LV EDV and end-systolic volume, can be obtained under LV total support, the LVSW estimated using this method was less correlated with PV loop-based LVSW than PSP (Figure 6). Given that LV myocardial strain can be obtained even under the condition of aortic valve closure, PSP has an advantage over echo-based LVSW and potentially evaluates the LV workload in patients with cardiogenic shock, even under LV total support.

With the emergence of percutaneous LVAD (i.e., Impella®), clinicians need to consider LV workload and myocardial oxygen metabolism as well as hemodynamic stability to optimally utilize the device. Considering that PSP was significantly correlated with MVO_2 and PVA (Figure 9), PSP can be utilized for the LVAD optimization by potentially reflecting myocardial oxygen metabolism. In the present study, although coronary perfusion pressure increased with higher levels of LVAD support, coronary flow remained limited, and coronary vascular resistance was elevated (Figure 8). This may be attributed to the reduced myocardial oxygen demand under LVAD support, which limits coronary flow by increasing coronary vascular resistance. This phenomenon has also been reported in a previous study (15), suggesting a mechanism of optimization known as coronary vascular autoregulation.

Validity of the model

The present study aimed to evaluate the physiological relationships between the pressure-strain product (PSP) and myocardial oxygen consumption. This objective necessitated highly invasive procedures, including the implantation of sonomicrometry probes within the left ventricular myocardium under open-chest conditions, placement of a flow probe around the coronary artery, and insertion of a catheter into the coronary sinus. Considering the experimental duration and procedural success rate, a normal heart model was employed. Further investigation using an appropriate model is required to determine whether the present findings are applicable to failing hearts. Nevertheless, PSP may represent a valuable tool for assessing native cardiac function during LVAD weaning in the recovery phase.

A future perspective

Because the current Impella (e.g., Impella 5.5) has a system called Smart Assist, which is equipped with a catheter to estimate LV pressure, our method can be immediately applied in clinical settings to evaluate LVSW without additional catheters. Considering that a centrifugal pump rather than an Impella was used under normal heart model in this study, we are currently conducting experiments using an Impella 5.5 in a failed heart model to investigate whether the results observed in the current study can be applicable. Future clinical studies are required to investigate whether PSP can be useful for optimizing Impella support level and to clarify the optimal threshold of PSP to predict cardiac recovery.

Limitations

Our study had a few limitations. First, we applied epicardial echocardiography, which is different from clinical practice. Pressure from the echo probe might affect echocardiographic parameters, including the GCS. Second, peak LV pressure, rather than mean arterial pressure, was used in this study for the calculation of PSP, which might have overestimated the LVSW. However, considering the significant gap between MAP and peak LV pressure in LVAD total support, the method applied in this study is reasonable compared to the previously reported method using MAP. Third, since hemodynamic assessments were performed following 5-min stabilization after changing the LVAD flow settings, longer-term effects were not considered. Finally, the model of normal hearts rather than deteriorated hearts was used in the current study. In the condition of cardiogenic shock, LV contractility is reduced, LV afterload is increased, and LV preload is elevated compared to a normal heart. These conditions can affect LV strain, LV pressure and subsequent PSP. In addition, the impact of coronary vascular autoregulation on the results may differ in failed hearts. Therefore, future studies applying a cardiogenic shock model are necessary to validate our findings under these distinct physiological conditions.

Conclusions

Echocardiography-based PSP significantly correlated with PV loop-based LVSW under various LVAD support levels, including total LV support. PSP can be useful in the noninvasive monitoring of myocardial metabolism by potentially reflecting myocardial oxygen consumption. Future clinical studies are required to investigate whether PSP can contribute to the optimization of Impella support and the prediction of cardiac recovery using the Impella device.

Data availability statement

The original contributions presented in the study are included in the article/Supplementary Material, further inquiries can be directed to the corresponding authors.

Ethics statement

The animal studies were approved by The Animal Subjects Committee of the National Cerebral and Cardiovascular Center. The studies were conducted in accordance with the local legislation and institutional requirements. Written informed consent was obtained from the owners for the participation of their animals in this study.

Author contributions

KS: Conceptualization, Data curation, Formal analysis, Investigation, Methodology, Project administration, Validation, Visualization, Writing – original draft, Writing – review & editing. YY: Data curation, Formal analysis, Investigation, Methodology, Writing – original draft, Writing – review & editing. SY: Data curation, Methodology, Writing – original draft, Writing – review & editing. HMa: Data curation, Methodology, Writing – original draft, Writing – review & editing. HMo: Data curation, Methodology, Writing – original draft, Writing – review & editing. MF: Writing – original draft, Writing – review & editing. TN: Writing – original draft, Writing – review & editing. KU: Writing – original draft, Writing – review & editing. TK: Writing – original draft, Writing – review & editing. KS: Conceptualization, Data curation, Formal analysis, Funding acquisition, Investigation, Methodology, Project administration, Resources, Supervision, Writing – original draft, Writing – review & editing.

Funding

The author(s) declare that financial support was received for the research and/or publication of this article. This work was partly supported by grants from the Grant-in-Aid for Scientific Research (JSPS KAKENHI 24K19018, 24K23422, 24K11283, 24K23449, 24K00885, 22K08222), the research program of the Japan Agency for Medical Research and Development (24hk0102085h0003 and 24ama121050j0003), the research program of the Ministry of Internal Affairs and Communications (SCOPE: JP225006004), the Intramural Research Fund for Cardiovascular Diseases of the National Cerebral and Cardiovascular Centre (24-B-7), JST (JPMJPF2018), Abiomed Inc., and Neuroceuticals Inc. The study design, article content, and journal selection were not influenced by any of these funding parties.

Acknowledgments

We thank the staff of the Department of Cardiovascular Dynamics at the National Cerebral and Cardiovascular Center for their assistance with animal experiments. We would like to thank Editage (https://www.editage.jp) for English language editing.

Conflict of interest

TK received a consulting fee from NTT Research, Inc. KS received research funding from Abiomed Inc., NTT Research, Inc., Asahi Kasei ZOLL Medical Corporation, Neuroceuticals Inc., and Zeon Medical Inc., and honoraria from Abiomed Japan K.K. and Mallinckrodt Pharma K.K.

The remaining authors declare that the research was conducted in the absence of any commercial or financial relationships that could be construed as a potential conflict of interest.

Generative AI statement

The author(s) declare that no Generative AI was used in the creation of this manuscript.

Publisher's note

Supplementary material

The Supplementary Material for this article can be found online at: https://www.frontiersin.org/articles/10.3389/fcvm.2025.1566021/full#supplementary-material

SUPPLEMENTARY FIGURE S1
Schematic of PSP. PSP was measured as the area of a rectangle consisting of the LV pressure and LV strain. The PSP of control (light blue), partial support (dark blue), and total support (red) are illustrated based on each LV systolic pressure and global circumferential strain. PSP, pressure-strain product.

References

1. Combes A, Price S, Slutsky AS, Brodie D. Temporary circulatory support for cardiogenic shock. *Lancet*. (2020) 396(10245):199–212. doi: 10.1016/S0140-6736(20)31047-3

2. Saito S, Okubo S, Matsuoka T, Hirota S, Yokoyama S, Kanazawa Y, et al. Impella—current issues and future expectations for the percutaneous, microaxial flow left ventricular assist device. *J Cardiol*. (2024) 83(4):228–35. doi: 10.1016/j.jjcc.2023.10.008

3. Lemaire A, Anderson MB, Lee LY, Scholz P, Prendergast T, Goodman A, et al. The impella device for acute mechanical circulatory support in patients in cardiogenic shock. *Ann Thorac Surg*. (2014) 97(1):133–8. doi: 10.1016/j.athoracsur.2013.07.053

4. Hammoudi N, Watanabe S, Bikou O, Ceccaldi A, Fish K, Yamada KP, et al. Speckle-tracking echocardiographic strain analysis reliably estimates degree of acute LV unloading during mechanical LV support by impella. *J Cardiovasc Transl Res*. (2019) 12(2):135–41. doi: 10.1007/s12265-018-9812-2

5. Sato K, Chan J, Appadurai V, Obonyo N, Hoe S, Suen L, et al. Exploration of the utility of speckle-tracking echocardiography during mechanical ventilation and mechanical circulatory support. *Crit Care Explor*. (2022) 4(4):e0666. doi: 10.1097/CCE.0000000000000666

6. Sato K, Heinsar S, Chan J, Farah SM, Wildi K, Obonyo NG, et al. A novel echocardiographic parameter considering left ventricular afterload during V-A ECMO support. *Eur J Clin Invest*. (2024) 54(10):e14263. doi: 10.1111/eci.14263

7. Sato K, Hoe LS, Chan J, Obonyo NG, Wildi K, Heinsar S, et al. Echocardiographic surrogate of left ventricular stroke work in a model of brain stem death donors. *Eur J Clin Invest*. (2024) 54(10):e14259. doi: 10.1111/eci.14259

8. Sato K, Wildi K, Chan J, Palmieri C, Obonyo NG, Heinsar S, et al. A novel speckle-tracking echocardiography parameter assessing left ventricular afterload. *Eur J Clin Invest*. (2024) 54(2):e14106. doi: 10.1111/eci.14106

9. Jentzer JC, Anavekar NS, Burstein BJ, Borlaug BA, Oh JK. Noninvasive echocardiographic left ventricular stroke work Index predicts mortality in cardiac intensive care unit patients. *Circ Cardiovasc Imaging*. (2020) 13(11):E011642. doi: 10.1161/CIRCIMAGING.120.011642

10. Kanda Y. Investigation of the freely available easy-to-use software "EZR" for medical statistics. *Bone Marrow Transplant*. (2013) 48(3):452–8. doi: 10.1038/bmt.2012.244

11. Russell K, Eriksen M, Aaberge L, Wilhelmsen N, Skulstad H, Remme EW, et al. A novel clinical method for quantification of regional left ventricular pressurestrain loop area: a non-invasive index of myocardial work. *Eur Heart J*. (2012) 33(6):724–33. doi: 10.1093/eurheartj/ehs016

12. Youssef N, Whitlock RP. The routine use of the pulmonary artery catheter should be abandoned. *Can J Cardiol*. (2017) 33(1):135–41. doi: 10.1016/j.cjca.2016.10.005

13. Sattin M, Burhani Z, Jaidka A, Millington SJ, Arntfield RT. Stroke volume determination by echocardiography. *Chest*. (2022) 161(6):1598–605. doi: 10.1016/j.chest.2022.01.022

14. Ilardi F, D'andrea A, D'ascenzi F, Bandera F, Benfari G, Esposito R, et al. Myocardial work by echocardiography: principles and applications in clinical practice. *J Clin Med*. (2021) 10(19):4521. doi: 10.3390/jcm10194521

15. Ando M, Takewa Y, Nishimura T, Yamazaki K, Kyo S, Ono M, et al. Coronary vascular resistance increases under full bypass support of centrifugal pumps–relation between myocardial perfusion and ventricular workload during pump support. *Artif Organs*. (2012) 36(1):105–10. doi: 10.1111/j.1525-1594.2011.01298.x

frontiers | Frontiers in Cardiovascular Medicine

TYPE Original Research
PUBLISHED 13 June 2025
DOI 10.3389/fcvm.2025.1580599

OPEN ACCESS

EDITED BY
Fabio Guarracino,
Azienda Ospedaliero Universitaria Pisana, Italy

REVIEWED BY
Minghao Luo,
Heidelberg University, Germany
Miguel Alvarez Villela,
Lenox Hill Hospital, United States

*CORRESPONDENCE
Naoki Tadokoro
naoki.tadokoro87@gmail.com

RECEIVED 20 February 2025
ACCEPTED 29 May 2025
PUBLISHED 13 June 2025

CITATION
Tadokoro N, Saku K, Tonai K, Tadokoro Y, Kutsuzawa R and Fukushima S (2025) Rapid-onset postoperative acute kidney injury is associated with mortality in patients with postcardiotomy cardiogenic shock. Front. Cardiovasc. Med. 12:1580599. doi: 10.3389/fcvm.2025.1580599

Rapid-onset postoperative acute kidney injury is associated with mortality in patients with postcardiotomy cardiogenic shock

Naoki Tadokoro[1*], Keita Saku[2], Kohei Tonai[1], Yuki Tadokoro[1], Reiko Kutsuzawa[1] and Satsuki Fukushima[1]

[1]Department of Cardiac Surgery, National Cerebral and Cardiovascular Center, Suita, Osaka, Japan, [2]Department of Cardiovascular Dynamics, National Cerebral and Cardiovascular Center Research Institute, Suita, Osaka, Japan

Background: Post-cardiotomy cardiogenic shock (PCCS) is a serious condition that necessitates veno-arterial extracorporeal membrane oxygenation (VA-ECMO). Although acute kidney injury (AKI) often complicates PCCS, its specific effects on patient outcomes remain unclear. This study seeks to evaluate the impact of AKI on 90-day mortality.

Methods: This retrospective study included 91 patients with postoperative cardiogenic shock requiring venoarterial extracorporeal membrane oxygenation following cardiac surgery between 2013 and 2023. Rapid-onset AKI was defined as KDIGO Stage 2 or higher within 24 h of ICU admission. Survival was analyzed using Kaplan–Meier and Cox regression methods to assess its association with 90-day mortality.

Results: Twenty-four patients (26.4%) were classified as rapid-onset AKI. The median age, primary diagnosis, and preoperative serum creatinine levels were similar between groups. However, the rapid-onset AKI group had a preoperative lower left ventricular ejection fraction (42.5% vs. 60.0%, $p = 0.006$), longer cardiopulmonary bypass time (332 vs. 245 min, $p = 0.009$), and a longer duration of mechanical circulatory support (6.0 vs. 2.0 days, $p = 0.001$). The success rate of weaning from mechanical circulatory support was lower (61.1% vs. 93.3%, $p = 0.002$), and the 90-day cumulative survival probability was lower in the rapid-onset AKI group (29.1% [95% confidence interval (CI): 15.6–54.4 vs. 79.1% [95% CI: 69.9–89.4], $p < 0.001$). Cox regression analysis confirmed an independent association between rapid-onset AKI and 90-day mortality (adjusted hazard ratio: 3.15, 95% CI: 1.38–7.19, $p = 0.006$).

Conclusion: Rapid-onset AKI was significantly associated with increased 90-day mortality in patients with PCCS who required V-A ECMO.

KEYWORDS

postcardiotomy cardiogenic shock, acute kidney injury, mechanical circulatory support, veno-arterial extracorporeal membrane oxygenation, extracorporeal life support, ventricular assist device

1 Introduction

Postoperative cardiogenic shock (PCCS) is characterized as a low cardiac output syndrome accompanied by impaired peripheral perfusion. Although its incidence is relatively low, ranging from 0.5% to 1.5%, the in-hospital mortality rate remains extremely high, between 60% and 80% (1). Mechanical circulatory support devices, such as veno-arterial extracorporeal membrane oxygenation (V-A ECMO), are commonly employed in its management (2–4). Circulatory failure has been identified as a critical determinant of survival outcomes, underscoring the importance of prompt hemodynamic stabilization.

Another critical complication is Cardiac surgery-associated acute kidney injury (CSA-AKI), which is also one of the most significant postoperative complications affecting patient prognosis (5, 6). It typically arises from renal hypoperfusion and systemic inflammatory responses triggered during and after surgery (7, 8). Both PCCS and AKI are severe postoperative complications, and they can exacerbate each other's pathophysiology. Renal hypoperfusion caused by PCCS can precipitate AKI, while the progression of AKI can further worsen circulatory status through fluid overload and inflammation (9, 10).

Among these, the development of Stage 2 or higher AKI within 24 h after surgery is likely to reflect acute hemodynamic and inflammatory changes and may serve as an early warning sign of systemic deterioration. This is based on evidence indicating that the severity of renal tubular injury strongly reflects the degree of inflammatory response, and that early recognition of AKI may be useful in predicting the prognosis of CSA-AKI (11–13).

In patients with PCCS, who are already at high risk for profound circulatory instability and multi-organ dysfunction, the prognostic implications of early AKI may be particularly significant. Therefore, identifying whether AKI occurs within the first 24 h following surgery and clarifying its impact on subsequent survival is a critical clinical issue.

This study focuses on the occurrence of AKI within 24 h after cardiac surgery in patients with PCCS and investigates its association with 90-day postoperative survival. By elucidating the prognostic significance of perioperative AKI, the aim is to provide insights that may contribute to risk stratification and early therapeutic decision-making in patients with PCCS.

2 Materials and methods

2.1 Study design, cohort, and data collection

This study was a single-center retrospective analysis conducted between January 2013 and December 2023, with data collection carried out in October 2024. A total of 6,208 patients underwent cardiothoracic surgery using cardiopulmonary bypass. 110 patients required postoperative V-A ECMO. After excluding patients who were dialysis-dependent preoperatively ($n = 3$), received V-A ECMO for non-cardiac indications ($n = 2$), underwent heart transplantation ($n = 8$), or had missing postoperative clinical data ($n = 2$), 95 patients remained for analysis as those experiencing postoperative cardiogenic shock requiring V-A ECMO (Figure 1). No major changes were made to the overall surgical techniques employed at our institution during the study period. The basic composition of the cardioplegia solution was consistently extracellular type, mixed with blood at a ratio of either 1:1 or 3:1. Cardioplegia was administered under hypothermia at 14°C for aortic procedures, while tepid cardioplegia at 29°C was used for other cases during the study period. AKI was defined according to the KDIGO criteria.

Previous studies on mortality risk and acute kidney injury (AKI) in patients supported with V-A ECMO have demonstrated that the risk is particularly elevated in those with KDIGO Stage 2 or higher (14). Therefore, to specifically evaluate the impact of hyperacute kidney injury in this study, we defined patients who met the criteria for KDIGO Stage 2 or higher within 24 h after ICU admission—either a serum creatinine level more than twice the preoperative value or urine output less than 0.5 ml/kg/h for more than 12 h—as the rapid-onset AKI group (15). Based on these criteria, 24 patients developed rapid-onset AKI, while the remaining 71 patients did not.

The primary outcome was mortality from all causes within 90 days post-surgery. Secondary outcomes included the duration and successful weaning from mechanical circulatory support.

2.2 Criteria and hemodynamic assessment for V-A ECMO initiation in PCCS patients

The criteria for initiating V-A ECMO in PCCS patients included an inability to wean from cardiopulmonary bypass or a cardiac index of less than 2.2 L/min/m^2, as well as a systolic blood pressure below 90 mmHg (or a mean arterial pressure below 60 mmHg), despite optimal treatment with inotropic or vasopressor agents and/or intra-aortic balloon pumping (IABP) (2, 16). Heart failure was diagnosed based on Swan-Ganz catheter data obtained immediately before V-A ECMO initiation and transesophageal echocardiography (TEE) performed by anesthesiologists. Left ventricular failure occurs when the pulmonary artery wedge pressure (PAWP) exceeds 18 mmHg, and the ratio of right atrial pressure to pulmonary capillary wedge pressure (RAP/PCWP) falls below 0.63, or when TEE confirms preserved right ventricular function alongside a reduction in RV fractional area change (RVFAC) of less than 20%. Right ventricular failure is diagnosed when inhaled nitric oxide is administered, PAWP remains below 18 mmHg, and TEE indicates an RVFAC reduction of 20% or more. Biventricular failure is identified when PAWP exceeds 18 mmHg, the RAP/PCWP ratio is greater than 0.63, and TEE reveals an RVFAC reduction of less than 20%.

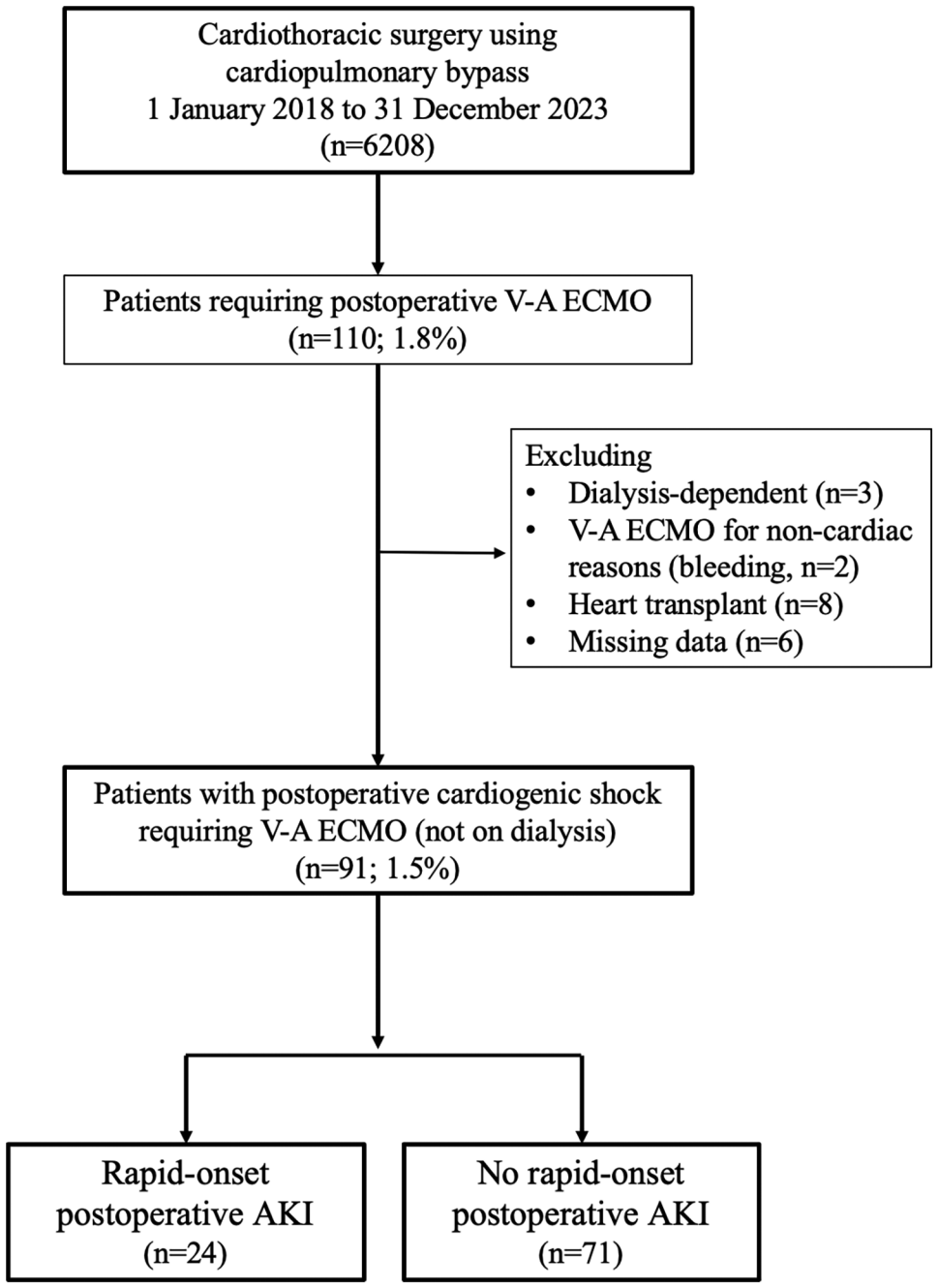

FIGURE 1
Study population and inclusion criteria for postoperative cardiogenic shock requiring veno-arterial extracorporeal membrane oxygenation.

2.3 Mechanical circulatory system selection

In ECMO management, the choice between peripheral and central cannulation, as well as the decision to introduce LV venting, was made intraoperatively through discussions between the surgeons and anesthesiologists. The Heart Team determined the postoperative selection of mechanical circulatory support modalities, which included cardiologists, surgeons, and other relevant specialists. Before the Impella (Abiomed, Danvers, MA, USA) device was introduced in Japan in 2018, left ventricular unloading was achieved using either IABP or left atrial/ventricular venting. In Japan, upgrading to an extracorporeal ventricular assist device (Ex-VAD) was generally indicated for patients under 65, while those aged 65 years or older continued to be managed with V-A ECMO. This study was conducted at a high-volume tertiary referral center capable of advanced cardiac surgery, including heart transplantation and the implantation of durable left ventricular assist device (LVAD), where approximately 1,000 adult cardiothoracic surgeries are performed annually.

2.4 Hemodynamic and AKI management

In our institution, hemodynamic management was guided by cardiac function in conjunction with specific targets, including a mean arterial pressure (MAP) above 60 mmHg, arterial oxygen saturation above 90%, and venous oxygen saturation above 60% (17).

In cases where CSA-AKI was identified, efforts were made to correct hypotension and low cardiac output, and to optimize fluid balance (10, 18). Loop diuretics were the first-line treatment used to prevent or manage fluid overload in patients with AKI; however, when diuretic response was poor and rapid correction of fluid overload was necessary, renal replacement therapy (RRT) was initiated (19).

2.5 Weaning protocols for MCS

The decannulation process from V-A ECMO was guided by hemodynamic stability, defined as a MAP >60 mmHg with minimal inotropic support, V-A ECMO flow <3 L/min, and sustained arterial pulsatility with a pulse pressure >20 mmHg for more than 24 h (20, 21). V-A ECMO flow was reduced in 1 L/min increments with 10-minute assessments at each level, down to a minimum of 0.5 L/min. Final evaluation at 0.5 L/min focused on cardiac function. LVAD weaning followed modified Berlin criteria, including a left ventricular ejection fraction (LVEF) >45% and left ventricular end-diastolic diameter (LVDd) <55 mm; however, elective explantation was considered in selected patients with LVEF >30% and no hemodynamic deterioration during the pump-off test (22).

2.6 Statistical analysis

Descriptive statistics were reported as the median [interquartile range] for continuous variables, as normality was not confirmed through histograms. Categorical variables were presented as counts (percentages). The Kruskal–Wallis test was applied to compare continuous variables between groups, while Fisher's exact test was employed for categorical variables. An unadjusted survival analysis comparing the two groups based on the occurrence of rapid-onset AKI was conducted using the Kaplan–Meier method. A multivariable Cox regression analysis was conducted to explore the association between rapid-onset AKI and 90-day survival. Factors included in the Cox model were determined based on previous studies. The factors included in the Cox models are as follows: age (per 10-year increase), primary diagnosis of aortic disease, lactate levels at 24 h after ICU admission, CPB duration (per hour increase), and postoperative LVEF (per 10-% increase) (1–3, 7, 23, 24). The hazard ratio (HR) is presented with 95% confidence intervals (95% CIs). Statistical analyses were conducted at a two-sided 5% significance level. Although this study had a small sample size, a multivariable Cox analysis was conducted while acknowledging the potential risks of multicollinearity and overfitting. All statistical analyses were performed using R version 4.4.2 (The R Foundation for Statistical Computing, Vienna, Austria).

3 Result

3.1 Patients' characteristics

The median age of the patients was 71.0 years [IQR, 57.0–79.0], including 55 males (60.4%) (Table 1). The preoperative left ventricular ejection fraction (LVEF) was 59.0% [IQR, 40.0–65.0], with 19 patients (20.9%) exhibiting an LVEF of less than 35%. A history of cardiac surgery was reported in 28 patients (30.8%), while 34 patients (37.4%) underwent emergency surgery. The primary indications for surgery included valvular disease in 30 patients (33.0%), aortic aneurysm in 15 patients (16.5%), aortic dissection in 13 patients (14.3%) and ischemic heart disease in 26 patients (28.6%). The European System for Cardiac Operative Risk Evaluation (EuroSCORE) II was 11.6 [IQR, 4.9–25.7].

When comparing the rapid-onset AKI group with the non-rapid-onset group, the median age was similar between the two groups (74.0 years [IQR, 62.5–80.2] vs. 71.0 years [IQR, 57.0–8.5], $p = 0.430$), and there were no significant differences in primary diagnosis or type of surgery. Preoperative serum creatinine levels (1.08 mg/dl [IQR, 0.81–1.39] vs. 0.95 mg/dl[IQR, [0.78–1.21], $p = 0.222$) and estimated glomerular filtration rate (eGFR; 44.0 ml/min/1.73 m^2 [IQR, 29.3–63.2] vs. 50.0 ml/min/1.73 m^2 [IQR, 37.5–65.2], $p = 0.242$) were also comparable. However, LVEF was significantly lower in the rapid-onset AKI group (42.5% [IQR, 28.8–58.5] vs. 60.0% [IQR, 45.0–65.0], $p = 0.006$).

For the overall cohort, the median durations of surgery, CPB, and cardiac arrest were 518 min [IQR, 354–634], 258 min [IQR, 176–362], and 141 min [IQR, 87–176], respectively. Unplanned intraoperative additional coronary artery bypass grafting was conducted in 20 cases (22.0%). The primary indications for V-A ECMO included failure to wean from CPB in 42 cases (46.2%), post-CPB heart failure in 34 cases (37.4%), and arrhythmias in 15 cases (16.5%). All arrhythmias occurred following failure to wean from cardiopulmonary bypass and were associated with cardiac arrest. These events were managed in the operating room, where all cardiac arrests were promptly treated with the initiation of V-A ECMO.

Peripheral V-A ECMO was employed in 76 patients (83.5%). 45 patients (49.5%) did not undergo any LV unloading. In comparison, 39 patients (42.9%) were supported with an IABP, two patients (2.2%) with an Impella device, and another five patients (5.5%) with left atrial (LA) or LV unloading. V-A ECMO was used as the primary modality of mechanical circulatory support in all patients. No patients were treated with IABP or Impella alone prior to V-A ECMO initiation.

When comparing the two groups, the rapid-onset AKI group showed longer operative time (604 min [IQR, 488–707] vs. 503 min[IQR, 315–598], $p = 0.012$) and CPB time (332 min [IQR, 240–420] vs. 245 min [IQR, 170–323], $p = 0.009$).

10.3389/fcvm.2025.1580599

TABLE 1 Patient characteristics and presentation.

Variable	Category	Overall	Rapid-onset postoperative AKI	No rapid-onset postoperative AKI	*P* value
n		91	24	67	
Age, years		71.0 [57.0, 79.0]	74.0 [62.5, 80.2]	71.0 [57.0, 78.5]	0.430
Age > 65 years		58 (63.7)	42 (62.7)	16 (66.7)	0.920
Gender					0.145
	Male	55 (60.4)	18 (75.0)	37 (55.2)	
	Female	36 (39.6)	6 (25.0)	30 (44.8)	
Body surface area, m^2		1.67 [1.50, 1.79]	1.67 [1.53, 1.79]	1.67 [1.50, 1.79]	0.811
Hypertension		49 (53.8)	16 (66.7)	33 (49.3)	0.219
Hyperlipidemia		29 (31.9)	10 (41.7)	19 (28.4)	0.344
Insulin-dependent diabetes		6 (6.6)	2 (8.3)	4 (6.0)	1.000
Past Smoker		28 (30.8)	7 (29.2)	21 (31.3)	1.000
Chronic lung disease		11 (12.1)	3 (12.5)	8 (11.9)	1.000
Preoperative Creatinine, mg/dl		0.97 [0.79, 1.29]	1.08 [0.81, 1.39]	0.95 [0.78, 1.21]	0.222
Estimated Glomerular Filtration Rate, ml/min/1.73 m^2		49.0 [34.7, 65.0]	44.0 [29.3, 63.2]	50.0 [37.5, 65.2]	0.242
Recent myocardial infarction		22 (24.2)	3 (12.5)	19 (28.4)	0.201
LVEF, %		59.0 [40.0, 65.0]	42.5 [28.8, 58.5]	60.0 [45.0, 65.0]	0.006
LVEF < 30%		19 (20.9)	9 (37.5)	10 (14.9)	0.041
NYHA class					0.785
	Class I	15 (16.5)	5 (20.8)	10 (14.9)	
	Class II	33 (36.3)	8 (33.3)	25 (37.3)	
	Class III	23 (25.3)	7 (29.2)	16 (23.9)	
	Class IV	20 (22.0)	4 (16.7)	16 (23.9)	
History of Previous Cardiac Surgery		28 (30.8)	11 (45.8)	17 (25.4)	0.108
Urgency					0.405
	Elective	48 (52.7)	11 (45.8)	37 (55.2)	
	Urgent	9 (9.9)	4 (16.7)	5 (7.5)	
	Emergency	34 (37.4)	9 (37.5)	25 (37.3)	
Primary diagnosis					
	Valve-related cardiac disease	30 (33.0)	7 (29.2)	23 (34.3)	0.835
	Aortic aneurysm	15 (16.5)	6 (25.0)	9 (13.4)	0.322
	Aortic dissection	13 (14.3)	6 (25.0)	7 (10.4)	0.159
	Ischemic heart disease	26 (28.6)	5 (20.8)	21 (31.3)	0.475
	Thromboembolic Pulmonary disease	4 (4.4)	0 (0.0)	4 (6.0)	0.520
	Cardiac tumor	3 (3.3)	0 (0.0)	3 (4.5)	0.698
Type of surgery					0.127
	Graft Replacement for aortic disease	28 (30.8)	12 (50.0)	16 (23.9)	
	Valve surgery	24 (26.4)	4 (16.7)	20 (29.9)	
	AMI complication repair	15 (16.5)	2 (8.3)	13 (19.4)	
	Coronary surgery	10 (11.0)	3 (12.5)	7 (10.4)	
	Coronary and Valve surgery	7 (7.7)	3 (12.5)	4 (6.0)	
	Pulmonary thrombectomy	4 (4.4)	0 (0.0)	4 (6.0)	
	Tumor resection	3 (3.3)	0 (0.0)	3 (4.5)	
EuroSCORE II		11.6 [4.9, 25.7]	14.8 [6.7, 42.1]	9.9 [3.7, 21.4]	0.081
Operation time, min		518 [354, 634]	604 [488, 707]	503 [314, 598]	0.012
Cardiopulmonary bypass time, min		258 [176, 362]	332 [240, 420]	245 [170, 323]	0.009
Arrest time, min		141 [87, 176]	156 [117, 192]	127 [85 172]	0.214
Unplanned additional CABG		20 (22.0)	6 (25.0)	14 (20.9)	0.897

Data are presented as medians [interquartile ranges] or numbers (%). AKI, acute kidney injury; AMI, Acute myocardial infarction; CABG, coronary artery bypass grafting; EuroScore, European system for cardiac operative risk evaluation; LVEF, left ventricular ejection fraction; NYHA, New York heart association.

10.3389/fcvm.2025.1580599

TABLE 2 Early postoperative results: types of PCCS and hemodynamic parameters.

Variable	Category	Overall	Rapid-onset postoperative AKI	No rapid-onset postoperative AKI	*p* value
n		91	24	67	
Reasons for ECMO					0.327
	Unable to wean CPB	42 (46.2)	9 (37.5)	33 (49.3)	
	HF after CPB	34 (37.4)	12 (50.0)	22 (32.8)	
	Arrythmia	15 (16.5)	3 (12.5)	12 (17.9)	
Type of heart failure					0.256
	LV failure	51 (56.0)	12 (50.0)	39 (58.2)	
	RV failure	13 (14.3)	3 (12.5)	10 (14.9)	
	Biventricular failure	12 (13.2)	6 (25.0)	6 (9.0)	
VIS Score Just Before ECMO Initiation		21.0 [9.5, 35.0]	31.9 [13.0, 59.0]	17.0 [8.0, 31.2]	0.028
VIS score >24 just before ECMO initiation		42 (46.2)	15 (62.5)	27 (40.3)	0.102
ECMO selection					0.103
	Peripheral ECMO	76 (83.5)	17 (70.8)	59 (88.1)	
	Central ECMO	15 (16.5)	7 (29.2)	8 (11.9)	
Primary LV unloading device					0.019
	None	45 (49.5)	14 (58.3)	31 (46.3)	
	IABP	39 (42.9)	7 (29.2)	32 (47.8)	
	Impella	2 (2.2)	2 (8.3)	0 (0.0)	
	LA drainage	1 (1.1)	1 (4.2)	0 (0.0)	
	LV drainage	4 (4.4)	0 (0.0)	4 (6.0)	
ECMO parameters					
At ICU admission	ECMO flow, L/min	3.5 [2.6, 4.1]	3.1 [2.4, 4.3]	3.5 [3.0, 4.0]	0.586
	ECMO flow index, L/min/m2	2.1 [1.7, 2.5]	2.1 [1.5, 2.4]	2.2 [1.7, 2.5]	0.402
At 24 h after ICU admission	ECMO flow, L/min	3.4 [2.5, 4.1]	3.5 [2.4, 3.8]	3.3 [2.5, 4.2]	0.850
	ECMO flow index, L/min/m2	2.0 [1.6, 2.5]	2.0 [1.8, 2.2]	2.0 [1.6, 2.5]	0.931
Hemodynamic parameters					
At ICU admission	Mixed venous oxygen saturation	81.2 [75.0, 87.0]	81.2 [75.7, 85.3]	81.2 [74.2, 87.2]	0.736
	Lactate level, mmol/L	5.3 [3.5, 7.5]	5.6 [4.0, 7.5]	5.3 [3.5, 7.3]	0.753
	hemoglobin, g/dl	9.9 [9.2, 10.8]	9.7 [8.7, 11.0]	9.9 [9.3, 10.8]	0.463
	VIS score	8.0 [5.0, 18.4]	12.3 [7.1, 27.2]	6.0 [4.0, 13.2]	0.007
At 24 h after ICU admission	Mixed venous oxygen saturation, %	78.1 [73.0, 84.0]	79.0 [71.0, 87.0]	78.0 [73.8, 82.2]	0.668
	Lactate level	2.4 [1.6, 3.5]	3.3 [1.8, 4.3]	2.0 [1.6, 3.3]	0.020
	Hemoglobin	10.6 [10.0, 11.0]	10.5 [9.9, 10.8]	10.6 [10.1, 11.1]	0.087
	VIS score	8.8 [4.9, 15.0]	8.7 [5.2, 15.1]	9.8 [4.3, 14.6]	0.528
LVEF at 24 h after ICU admission		35.0 [25.0, 45.0]	25.0 [25.0, 35.0]	35.0 [25.0, 45.0]	0.007
LVEF < 30% at 24 h after ICU admission		43 (47.3)	16 (66.7)	27 (40.3)	0.047
Total Bilirubin	At ICU admission	1.7 [1.1, 2.2]	1.8 [1.1, 2.3]	1.7 [1.2, 2.1]	0.853
	At 24 h after ICU admission	2.5 [2.0, 3.7]	2.3 [2.0, 3.7]	2.5 [2.0, 3.7]	0.586

Data are presented as medians [interquartile ranges] or numbers (%). AKI, acute kidney injury; CPB, cardiopulmonary bypass; ECMO, extracorporeal membrane oxygenation; HF, heart failure; ICU, intensive care unit; LA, left atrium; LV, left ventricle; LVEF, left ventricular ejection fraction; RV, right ventricle; VIS, vasoactive inotropic score.

3.2 Postoperative clinical outcomes

The results at ICU admission and 24 h after ICU admission are presented in Table 2. The V-A ECMO flow index at ICU admission was 2.1 L/min/m^2 [IQR, 1.7–2.5], with 42 patients (46.2%) receiving a V-A ECMO flow index greater than 2.4 L/min/m^2. RRT was initiated within 24 h after surgery for four patients (4.4%) and at 24 h after ICU admission. The median postoperative LVEF at 24 h after ICU admission was 35.0 [IQR, 25.0–45.0], and 43 patients (47.3%) had an LVEF of 30% or less.

The two groups showed no significant differences in V-A ECMO flow, flow index, mixed venous oxygen saturation, or lactate levels at ICU admission. However, the VIS was higher in the rapid-onset AKI group (12.3 [IQR, 7.1–27.2] vs. 6.0 [IQR,

10.3389/fcvm.2025.1580599

TABLE 3 Clinical outcome.

Variable	Category	Overall	Rapid-onset postoperative AKI	No rapid-onset postoperative AKI	*p* value
n		91	24	67	
Incidence of AKI at 24 h after ICU admission		57 (62.6)	24 (100.0)	33 (49.3)	<0.001
AKI stage at 24 h after ICU admission					<0.001
	Stage 1	33 (57.9)	0 (0.0)	33 (100.0)	
	Stage 2	9 (15.8)	9 (37.5)	0 (0.0)	
	Stage 3	15 (26.3)	15 (62.5)	0 (0.0)	
Initiation of RRT within 24 h		4 (4.4)	4 (16.7)	0 (0.0)	0.005
Total Urine Output in the First 24 h		2,270 [1,244, 3,606]	621 [244, 1,410]	2,917 [1,956, 4,193]	<0.001
Urine output, ml/kg/hr.		1.6 [0.8, 2.6]	0.4 [0.2, 0.8]	1.9 [1.3, 2.9]	<0.001
Use of Lasix		28 (30.8)	4 (16.7)	24 (35.8)	0.137
Overall initiation of RRT		32 (35.2)	20 (83.3)	12 (17.9)	<0.001
ECMO outcomes					
Up-grade to Ex-VAD		10 (11.0)	5 (20.8)	5 (7.5)	0.157
Add Impella		4 (4.4)	2 (8.3)	2 (3.0)	0.606
MCS weaning (ECMO/Impella/Ex-VAD)		78 (85.7)	18 (75.0)	60 (89.6)	0.159
Successful weaning		67 (85.9)	11 (61.1)	56 (93.3)	0.002
Conversion to durable LVAD		2 (2.2)	0 (0.0)	2 (3.0)	0.964
Total MCS support duration, days		3.0 [2.0, 7.0]	6.0 [3.0, 20.2]	2.0 [1.5, 5.5]	0.001
Incidence of complication on MCS support		19 (20.9)	10 (41.7)	9 (13.4)	0.009
Type of complication	Neurological complications	8 (8.8)	4 (16.7)	4 (6.0)	0.243
	Hemorrhage	6 (6.6)	5 (20.8)	1 (1.5)	0.005
	Vascular injury	2 (2.2)	1 (4.2)	1 (1.5)	1.000
	LA thrombosis	3 (3.3)	0 (0.0)	3 (4.5)	0.698
In-hospital mortality		30 (33.0)	17 (70.8)	13 (19.4)	<0.001
Mortality on MCS		11 (12.1)	6 (25.0)	5 (7.5)	0.058
Mortality on MCS or death within 30 days after decannulation		22 (24.2)	13 (54.2)	9 (13.4)	<0.001
90-days mortality		31 (34.1)	17 (70.8)	14 (20.9)	<0.001
Cause of Mortality	Multiple Organ Dysfunction Syndrome	15 (16.5)	7 (29.2)	8 (11.9)	0.103
	Sepsis	6 (6.6)	3 (12.5)	3 (4.5)	0.379
	Hemorrhagic event	4 (4.4)	4 (16.7)	0 (0.0)	0.005
	Neurological event	5 (5.5)	2 (8.3)	3 (4.5)	0.850
	Other event	1 (1.1)	1 (4.2)	0 (0.0)	0.590

Data are presented as medians [interquartile ranges] or numbers. AKI, Acute kidney injury; ECMO, Extracorporeal membrane oxygenation; ex-VAD, Extracorporeal ventricular assist device; LVAD, Left ventricular assist device; MCS, Mechanical circulatory support; RRT, Renal replacement therapy.

4.0–13.2], $p = 0.007$). At 24 h after ICU admission, lactate levels were significantly elevated in the rapid-onset AKI group (3.3 mmol/L [IQR, 1.8–4.3] vs. 2.0 mmol/L [IQR, 1.6–3.3], $p = 0.02$).

A total of nine patients (15.8%) were classified as Stage 2 and fifteen (26.3%) as Stage 3 AKI within 24 h postoperatively and were therefore categorized into the rapid-onset AKI group (Table 3). Ten patients (11.0%) were upgraded to an Ex-VAD and four (4.4%) received Impella in a delayed fashion within one week after the initiation of V-A ECMO. The weaning process from mechanical circulatory support (MCS), including V-A ECMO, Impella, and Ex-VAD, was completed in 78 patients (85.7%). Of these, 67 patients (85.9%) met the criteria for successful weaning, defined as survival for at least 30 days following device removal. In addition, two patients were transitioned to a durable LVAD. The median duration of MCS was 3.0 days [IQR, 2.0–7.0].

The success rate of MCS weaning was lower in the rapid-onset AKI group compared to the non-rapid-onset group (61.1% vs. 93.3%, $p = 0.002$), and the duration of MCS support was significantly longer (6.0 days vs. 2.0 days, $p = 0.001$). Complications during MCS support occurred in 19 patients (20.9%).

Ninety-day mortality was observed in 31 patients (34.1%) overall and was significantly higher in the rapid-onset AKI group (70.8% vs. 20.9%, $p < 0.001$).

During MCS management, bleeding events were more frequent in the rapid-onset AKI group (20.8% vs. 1.5%, $p = 0.005$), and the mortality rate during MCS support or within 30 days after weaning from MCS was higher (54.2% vs. 13.4%, $p = 0.058$). The most common cause of death was multiorgan failure (29.2% vs. 11.9%, $p = 0.103$), followed by bleeding-related events (16.7% vs. 0%, $p = 0.005$).

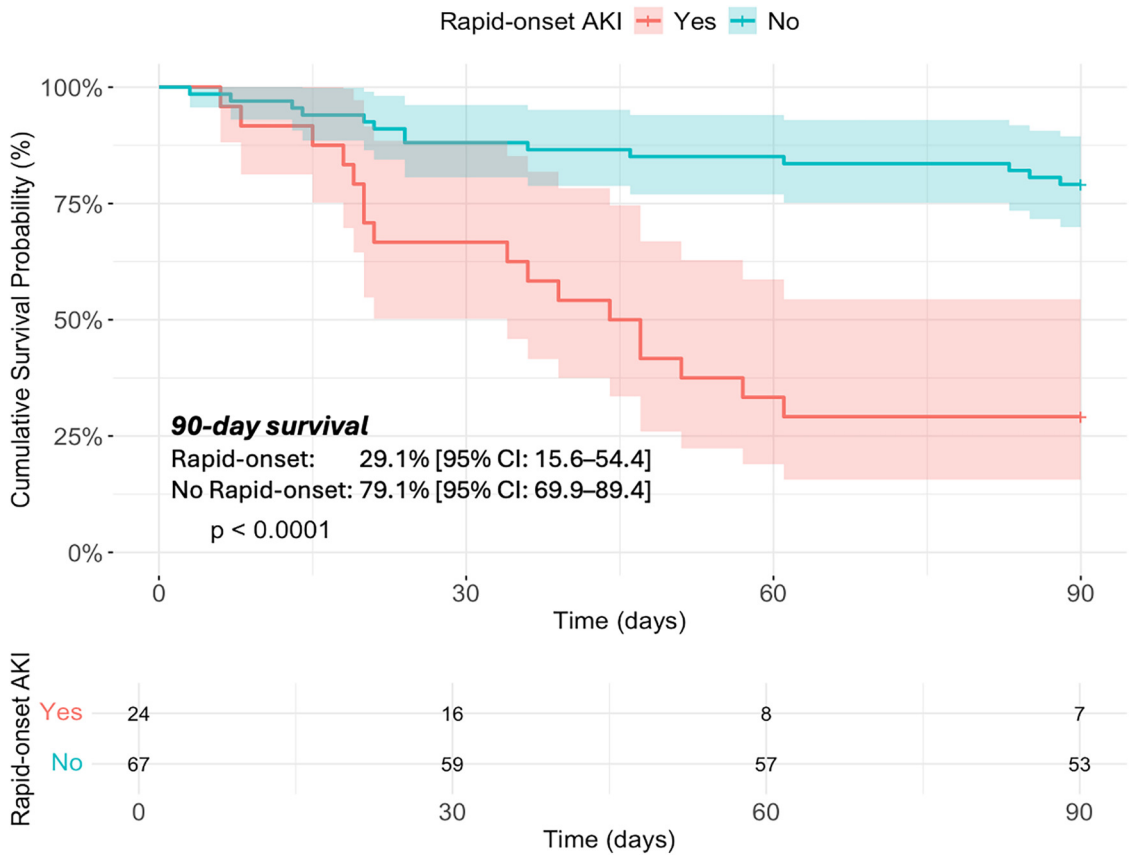

FIGURE 2
90-day survival in patients with post-cardiotomy cardiogenic shock stratified by incidence of rapid-onset AKI.

TABLE 4 Cox multivariate analysis between rapid-onset postoperative kidney injury and 90-day mortality.

Variable	Hazard ratio (95% CI)	*p* value
Incidence of Rapid-onset postoperative AKI	**3.15 (1.38, 7.19)**	**0.006**
Age (per 10 years)	**1.32 (1.00, 1.73)**	**0.048**
Primary diagnosis of aortic dissection	**2.72 (1.18, 6.27)**	**0.019**
Cardiopulmonary bypass time (per 1 h)	1.05 (0.92, 1.21)	0.465
Lactate level at 24 h after ICU admission	1.16 (0.91, 1.48)	0.232
LVEF at 24 h postoperatively (for every 10% increase)	**0.49 (0.30, 0.79)**	**0.004**

AKI, acute kidney injury; LVEF, left ventricular ejection fraction.
Bold values indicate statistical significance ($p < 0.05$).

3.3 Survival analysis

Kaplan–Meier analysis showed a significantly lower 90-day cumulative survival probability in the rapid-onset AKI group (29.1% [95% confidence interval (CI): 15.6–54.4]) compared to the non-rapid-onset AKI group (79.1% [95% CI: 69.9–89.4], $p < 0.001$) (Figure 2). Multivariate Cox regression analysis identified the occurrence of rapid-onset AKI (adjusted hazard ratio [aHR]: 3.15, 95% CI: 1.38–7.19, $p = 0.006$) (Table 4). Other factors associated with 90-day mortality included age (per 10-year increase, adjusted hazard ratio [aHR]: 1.32, 95% CI: 1.00–1.73, $p = 0.048$), a primary diagnosis of aortic dissection (aHR: 2.72, 95% CI: 1.18–6.27, $p = 0.019$), and postoperative LVEF (per 10% increase, aHR: 0.49, 95% CI: 0.30–0.79, $p = 0.004$).

4 Discussion

In our study, patients with rapid-onset AKI—defined as KDIGO Stage 2 or higher within 24 h of ICU admission—had lower preoperative cardiac function, longer CPB times, and required prolonged MCS compared to those without AKI. Although mortality during MCS support did not differ significantly between groups, the 30-day survival rate after weaning was significantly lower in the rapid-onset AKI group. Multivariate Cox analysis confirmed rapid-onset AKI as an independent predictor of 90-day mortality. The leading causes of death were multiorgan failure and bleeding.

It is well-known that increases in creatinine levels and the incidence of AKI after cardiac surgery negatively impact both short-term and long-term prognosis. Approximately 80% of patients undergoing V-A ECMO for cardiogenic shock develop AKI, with in-hospital mortality rates around 26% for AKI stage 1 and exceeding 60% for AKI stage 2 or higher. Moreover, reports suggest that combining the Society for Cardiovascular

Angiography and Interventions (SCAI) shock stage with the AKI stage can effectively predict in-hospital mortality (14).

In this study, we focused on cases in which stage 2 or higher AKI developed within 24 h after cardiac surgery and identified an association with reduced 90-day survival. AKI occurring within this early postoperative window likely reflects systemic stress responses such as intraoperative and immediate postoperative hypoperfusion, ischemia-reperfusion injury, and acute inflammation (25). These processes suggest that Rapid-onset AKI represents not only a change in renal function but also an early indicator of systemic deterioration and multiorgan dysfunction.

Although the use of additional MCS devices, including Ex-VAD and Impella, was comparable between groups, the rapid-onset AKI group exhibited a significantly longer duration of MCS support and a lower successful weaning rate of only 61.1%. The combined effects of AKI-associated multiorgan failure, MCS-related hemorrhagic events, and postoperative low cardiac output may explain these findings. The presence or absence of AKI within 24 h postoperatively may serve as a valuable predictor of short-term outcomes and support early postoperative risk stratification. It may also provide a rationale for timely interventions, including enhanced bleeding risk management and organ failure prevention. Recent studies have proposed revising the definition of AKI specifically for cardiac surgery patients, suggesting that using a higher threshold for serum creatinine change (0.55 mg/dl) than the conventional criteria may improve the accuracy of prognostic prediction (26). This raises the possibility that, in the context of postcardiotomy syndrome (PCS), both the timing of AKI onset and its severity should be reconsidered to better reflect patient outcomes.

In the present study, postoperative cardiac dysfunction was also associated with poor prognosis. In this patient population, the use of MCS is intended not only to promote the recovery of multiple organ dysfunction but also to serve as a bridge to long-term therapies such as durable LVAD or heart transplantation. Our findings showed a high mortality rate following MCS weaning, suggesting that the ability to discontinue MCS does not necessarily indicate sufficient recovery from organ dysfunction. Moreover, this may imply that, in some patients, MCS did not adequately fulfill its role as a bridge-to-bridge (BTB) strategy.

When recovery from organ failure is inadequate at the time MCS weaning criteria are met, the decision to proceed with weaning often requires careful discussion among the clinical team. In elderly patients or those with MCS-related complications, weaning may be selected despite incomplete recovery, potentially leading to deterioration of organ function and subsequent death. This context may also explain why multiple organ failure and bleeding events were frequently identified as causes of death in our cohort.

Although early recovery from multiorgan failure is desirable and higher flow support might be beneficial, achieving this can be challenging in patients with PCCS, V-A ECMO may increase afterload, potentially leading to complications such as pulmonary congestion and left ventricular thrombus formation. Management strategies for such cases include using direct left ventricular venting methods, such as Impella or central V-A ECMO combined with LA/LV venting (27). However, these approaches carry risks of bleeding and hemolysis, which may further worsen AKI, requiring careful consideration (28–32). Furthermore, a unique aspect of clinical practice in Japan is that durable LVAD and heart transplantation are generally not indicated for patients aged 65 years or older, or for those with significant organ dysfunction. As a result, aggressive treatment, including the use of MCS as a bridge-to-bridge (BTB) strategy, may not be pursued in such cases. In our study, 63.7% of the patients were aged ≥65 years, and a significant number of deaths occurred within 30 days after MCS weaning, which may have influenced the overall outcomes. Nevertheless, the increased use of devices such as Impella in Japan since 2019 suggests that treatment strategies combining multiple MCS modalities will likely play an increasingly important role in improving survival rates.

Additionally, in patients with organ dysfunction such as AKI and those aged ≥65 years, durable LVADs are not indicated in Japan, and in some cases, aggressive treatment may not be pursued. In the present study, 63.7% of the patients were aged ≥65 years, and many deaths occurred within 30 days after MCS weaning, which likely influenced the outcomes. Nevertheless, with the increased use of devices such as Impella in Japan since 2019, treatment strategies that combine various MCS modalities are expected to become increasingly important in improving survival.

5 Limitations

This study has several limitations. First, as a single-center retrospective observational study, the generalizability of the findings is limited. It remains unclear whether similar trends would be observed in patient populations from other institutions or regions; therefore, further multicenter studies are needed to confirm the external validity of the results. Although multivariate analysis was used to adjust for confounding factors, the potential influence of unmeasured confounders cannot be ruled out. Additionally, the sample size of this study was limited, and due to its inherent nature, a comprehensive evaluation of all relevant factors was challenging. Thus, it is important to consider that unknown factors may also affect the prognosis. Furthermore, this study could not investigate the impact of rapid left ventricular unloading on prognosis. Given these limitations, careful interpretation of the study findings is warranted, and future multicenter collaborative studies and prospective research are needed to provide higher-quality evidence.

6 Conclusion

Rapid-onset AKI, defined as KDIGO Stage 2 or higher within 24 h of ICU admission, was significantly associated with increased 90-day mortality in patients with postcardiotomy cardiogenic shock requiring V-A ECMO.

Data availability statement

The raw data supporting the conclusions of this article will be made available by the authors, without undue reservation.

Ethics statement

The studies involving humans were approved by Ethics Committee of the National Cerebral and Cardiovascular Center. The studies were conducted in accordance with the local legislation and institutional requirements. The participants provided their written informed consent to participate in this study.

Author contributions

NT: Conceptualization, Investigation, Methodology, Visualization, Writing – original draft, Writing – review & editing. KS: Conceptualization, Funding acquisition, Project administration, Resources, Supervision, Writing – review & editing. KT: Data curation, Formal analysis, Investigation, Writing – original draft. YT: Conceptualization, Data curation, Methodology, Writing – original draft. RK: Data curation, Investigation, Writing – original draft. SF: Conceptualization, Data curation, Supervision, Validation, Writing – review & editing.

Funding

The author(s) declare that financial support was received for the research and/or publication of this article. This work was partly supported by the Intramural Research Fund for Cardiovascular Diseases of National Cerebral and Cardiovascular Center (24-B-7) and the research grant from JST (JPMJPF2018). The authors confirm that these parties did not influence the study design, article contents, or journal selection.

Conflict of interest

KS received research funding from Abiomed Inc., NTT Research, Inc., Asahi Kasei ZOLL Medical Corporation, Neuroceuticals Inc., and Zeon Medical Inc., and honoraria from Abiomed Japan K.K. and Mallinckrodt Pharma K.K.

The remaining authors declare that the research was conducted in the absence of any commercial or financial relationships that could be construed as a potential conflict of interest.

Generative AI statement

The author(s) declare that Generative AI was used in the creation of this manuscript. English editing of this manuscript was performed using ChatGPT-4.0 (OpenAI), which was employed solely for the purpose of language correction and refinement. No content generation or interpretation of scientific results was conducted using AI tools. All scientific content was created and validated by the authors.

Publisher's note

References

1. Wang L, Wang H, Hou X. Clinical outcomes of adult patients who receive extracorporeal membrane oxygenation for postcardiotomy cardiogenic shock: a systematic review and meta-analysis. *J Cardiothorac Vasc Anesth*. (2018) 32:2087–93. doi: 10.1053/j.jvca.2018.03.016

2. Fux T, Holm M, Corbascio M, Lund LH, van der Linden J. Venoarterial extracorporeal membrane oxygenation for postcardiotomy shock: risk factors for mortality. *J Thorac Cardiovasc Surg*. (2018) 156:1894–1902.e3. doi: 10.1016/j.jtcvs.2018.05.061

3. Formica F, D'Alessandro S, Sangalli F. Arterial lactate level: a simple and effective tool during extracorporeal membrane oxygenation. *J Thorac Cardiovasc Surg*. (2019) 157:e265–6. doi: 10.1016/j.jtcvs.2018.11.120

4. Papadopoulos N, Marinos S, El-Sayed Ahmad A, Keller H, Meybohm P, Zacharowski K, et al. Risk factors associated with adverse outcome following extracorporeal life support: analysis from 360 consecutive patients. *Perfusion*. (2015) 30:284–90. doi: 10.1177/0267659114542458

5. Van Diepen S, Katz JN, Albert NM, Henry TD, Jacobs AK, Kapur NK, et al. Contemporary management of cardiogenic shock: a scientific statement from the American heart association. *Circulation*. (2017) 136:e232–68. doi: 10.1161/CIR.0000000000000525

6. Ghionzoli N, Sciaccaluga C, Mandoli G, Vergaro G, Gentile F, D'Ascenzi F, et al. Cardiogenic shock and acute kidney injury: the rule rather than the exception. *Heart Fail Rev*. (2021) 26:487–96. doi: 10.1007/s10741-020-10034-0

7. Bouisset B, Pozzi M, Ruste M, Varin T, Vola M, Rodriguez T, et al. Cardiopulmonary bypass blood flow rates and major adverse kidney events in cardiac surgery: a propensity score-adjusted before-after study. *J Cardiothorac Vasc Anesth*. (2024) 38:2213–20. doi: 10.1053/j.jvca.2024.07.019

8. Lankadeva YR, Cochrane AD, Marino B, Iguchi N, Hood SG, Bellomo R, et al. Strategies that improve renal medullary oxygenation during experimental cardiopulmonary bypass may mitigate postoperative acute kidney injury. *Kidney Int*. (2019) 95:1338–46. doi: 10.1016/j.kint.2019.01.032

9. Jentzer JC, Bihorac A, Brusca SB, Del Rio-Pertuz G, Kashani K, Kazory A, et al. Contemporary management of severe acute kidney injury and refractory cardiorenal syndrome: JACC council perspectives. *J Am Coll Cardiol*. (2020) 76:1084–101. doi: 10.1016/j.jacc.2020.06.070

10. Scurt FG, Bose K, Mertens PR, Chatzikyrkou C, Herzog C. Cardiac surgery–associated acute kidney injury. *Kidney360*. (2024) 5:909. doi: 10.34067/KID.0000000000000466

11. Chawla LS, Eggers PW, Star RA, Kimmel PL. Acute kidney injury and chronic kidney disease as interconnected syndromes. *N Engl J Med*. (2014) 371:58–66. doi: 10.1056/NEJMra1214243

12. Molitoris BA. Therapeutic translation in acute kidney injury: the epithelial/endothelial axis. *J Clin Invest*. (2014) 124:2355–63. doi: 10.1172/JCI72269

13. Neyra JA, Hu MC, Minhajuddin A, Nelson GE, Ahsan SA, Toto RD, et al. Kidney tubular damage and functional biomarkers in acute kidney injury following cardiac surgery. *Kidney Int Rep*. (2019) 4:1131–42. doi: 10.1016/j.ekir.2019.05.005

14. Li C, Wang Y, Wang X, Shao C, Xin M, Xu B, et al. Acute kidney injury and cardiogenic shock severity for mortality risk stratification in patients supported with VA ECMO. *ESC Heart Fail.* (2024) 11:3872. doi: 10.1002/EHF2.14967

15. Kellum JA, Lameire N, Aspelin P, Barsoum RS, Burdmann EA, Goldstein SL, et al. KDIGO clinical practice guideline for acute kidney injury. *Kidney Int Suppl (2011).* (2012) 2:1–138. doi: 10.1038/KISUP.2012.1

16. Rao P, Khalpey Z, Smith R, Burkhoff D, Kociol RD. Venoarterial extracorporeal membrane oxygenation for cardiogenic shock and cardiac arrest. *Circ Heart Fail.* (2018) 11:e004905. doi: 10.1161/CIRCHEARTFAILURE.118.004905

17. Richardson ASC, Tonna JE, Nanjayya V, Nixon P, Abrams DC, Raman L, et al. Extracorporeal cardiopulmonary resuscitation in adults. Interim guideline consensus statement from the extracorporeal life support organization. *ASAIO J.* (2021) 67:221–8. doi: 10.1097/MAT.0000000000001344

18. Rangaswami J, Bhalla V, Blair JEA, Chang TI, Costa S, Lentine KL, et al. Cardiorenal syndrome: classification, pathophysiology, diagnosis, and treatment strategies: a scientific statement from the American heart association. *Circulation.* (2019) 139:E840–78. doi: 10.1161/CIR.0000000000000664

19. Costanzo MR, Ronco C, Abraham WT, Agostoni P, Barasch J, Fonarow GC, et al. Extracorporeal ultrafiltration for fluid overload in heart failure: current Status and prospects for further research. *J Am Coll Cardiol.* (2017) 69:2428–45. doi: 10.1016/j.jacc.2017.03.528

20. Keller SP. Management of peripheral venoarterial extracorporeal membrane oxygenation in cardiogenic shock. *Crit Care Med.* (2019) 47:1235–42. doi: 10.1097/CCM.0000000000003879

21. Koziol KJ, Isath A, Rao S, Gregory V, Ohira S, Van Diepen S, et al. Extracorporeal membrane oxygenation (VA-ECMO) in management of cardiogenic shock. *J Clin Med.* (2023) 12:5576. doi: 10.3390/jcm12175576

22. Drakos SG, Mehra MR. Clinical myocardial recovery during long-term mechanical support in advanced heart failure: insights into moving the field forward. *J Heart Lung Transplant.* (2016) 35:413–20. doi: 10.1016/j.healun.2016.01.001

23. Karim H, Yunus M, Saikia M, Kalita J, Mandal M. Incidence and progression of cardiac surgery-associated acute kidney injury and its relationship with bypass and cross clamp time. *Ann Card Anaesth.* (2017) 20:22. doi: 10.4103/0971-9784.197823

24. Kowalewski M, Zieliński K, Brodie D, Maclaren G, Whitman G, Raffa GM, et al. Venoarterial extracorporeal membrane oxygenation for postcardiotomy shock—analysis of the extracorporeal life support organization registry∗. *Crit Care Med.* (2021) 49:1107–17. doi: 10.1097/CCM.0000000000004922

25. Yang X, Zhu L, Pan H, Yang Y. Cardiopulmonary bypass associated acute kidney injury: better understanding and better prevention. *Ren Fail.* (2024) 46:2331062. doi: 10.1080/0886022X.2024.2331062

26. Zeng J, Su X, Lin S, Li Z, Zhao Y, Zheng Z. Cardiac surgery-specific subtle perioperative serum creatinine change in defining acute kidney injury after coronary surgery. *JACC Adv.* (2024) 3:101326. doi: 10.1016/J.JACADV.2024.101326

27. Ezad SM, Ryan M, Donker DW, Pappalardo F, Barrett N, Camporota L, et al. Unloading the left ventricle in venoarterial ECMO: in whom, when, and how? *Circulation.* (2023) 147:1237–50. doi: 10.1161/CIRCULATIONAHA.122.062371

28. Thiele H, Jobs A, Ouweneel DM, Henriques JPS, Seyfarth M, Desch S, et al. Percutaneous short-term active mechanical support devices in cardiogenic shock: a systematic review and collaborative meta-analysis of randomized trials. *Eur Heart J.* (2017) 38:3523–31. doi: 10.1093/eurheartj/ehx363

29. Biancari F, Kaserer A, Perrotti A, Ruggieri VG, Cho SM, Kang JK, et al. Central versus peripheral postcardiotomy veno-arterial extracorporeal membrane oxygenation: systematic review and individual patient data meta-analysis. *J Clin Med.* (2022) 11:7406. doi: 10.3390/jcm11247406

30. Vetrovec GW, Kaki A, Dahle TG. A review of bleeding risk with impella-supported high-risk percutaneous coronary intervention. *Heart Int.* (2020) 14:92. doi: 10.17925/HI.2020.14.2.92

31. Djordjevic I, Eghbalzadeh K, Sabashnikov A, Deppe AC, Kuhn E, Merkle J, et al. Central vs peripheral venoarterial ECMO in postcardiotomy cardiogenic shock. *J Card Surg.* (2020) 35:1037–42. doi: 10.1111/jocs.14526

32. Van Edom CJ, Gramegna M, Baldetti L, Beneduce A, Castelein T, Dauwe D, et al. Management of bleeding and hemolysis during percutaneous microaxial flow pump support: a practical approach. *Cardiovasc Interv.* (2023) 16:1707–20. doi: 10.1016/j.jcin.2023.05.043

frontiers | Frontiers in Cardiovascular Medicine

TYPE Case Report
PUBLISHED 27 June 2025
DOI 10.3389/fcvm.2025.1587383

OPEN ACCESS

EDITED BY
Fabio Guarracino,
Azienda Ospedaliero Universitaria Pisana, Italy

REVIEWED BY
Audrey Adji,
Victor Chang Cardiac Research Institute, Australia
Adam Gottula,
University of Michigan, United States

*CORRESPONDENCE
Kenichiro Sawada
✉ sawada.kenichiro@ncvc.go.jp

RECEIVED 04 March 2025
ACCEPTED 10 June 2025
PUBLISHED 27 June 2025

CITATION
Ota I, Sawada K, Saku K and Noguchi T (2025) Case Report: Intra-aortic balloon pump in a patient with refractory cardiogenic shock complicating severe aortic stenosis—enhanced hemodynamic response with low aortic compliance.
Front. Cardiovasc. Med. 12:1587383.
doi: 10.3389/fcvm.2025.1587383

Case Report: Intra-aortic balloon pump in a patient with refractory cardiogenic shock complicating severe aortic stenosis—enhanced hemodynamic response with low aortic compliance

Issei Ota[1], Kenichiro Sawada[1]*, Keita Saku[2] and Teruo Noguchi[1]

[1]Division of Cardiovascular Intensive Care, Department of Cardiovascular Medicine, National Cerebral and Cardiovascular Center, Suita, Osaka, Japan, [2]Department of Cardiovascular Dynamics, National Cerebral and Cardiovascular Center, Suita, Osaka, Japan

Intra-aortic balloon pump (IABP) counterpulsation generates pressure changes that are primarily influenced by aortic compliance, an index of arterial elasticity that varies widely among patients with cardiovascular disease. However, the potential role of aortic compliance in determining IABP efficacy remains poorly understood. We present the case of an 80-year-old man with severe aortic stenosis and pneumonia who was admitted with generalized fatigue and worsening dyspnea. He developed refractory Society for Cardiovascular Angiography & Interventions stage D cardiogenic shock despite multiple vasopressors. In this patient, who had low aortic compliance (0.62–0.81 ml/mmHg), IABP initiation resulted in immediate hemodynamic improvement through enhanced diastolic augmentation and systolic unloading, leading to rapid reversal of both hypoperfusion and pulmonary congestion. Following successful weaning from vasopressors and IABP removal, the patient underwent transcatheter aortic valve replacement without temporary mechanical circulatory support-related complications. The notable hemodynamic improvement observed in this case highlights the potential importance of aortic compliance as a key determinant of IABP efficacy in elderly patients with cardiogenic shock, suggesting that aortic compliance may help optimize patient selection for IABP support.

KEYWORDS

intra-aortic balloon pump, cardiogenic shock, older adults, aortic compliance, hemodynamics

Introduction

The clinical role of the intra-aortic balloon pump (IABP) remains controversial. While the IABP-SHOCK II trial showed no survival benefit in patients with acute myocardial infarction-related cardiogenic shock (AMI-CS) (1), recent large-scale studies have shown non-inferior clinical outcomes with IABP compared to percutaneous ventricular assist devices (pVADs) (2–5). Nonetheless, IABP remains the most widely used temporary mechanical circulatory support (tMCS) device in Japan, accounting for 65.3% of cases compared to venoarterial extracorporeal membrane oxygenation (VA-ECMO, 29.6%) and pVADs (5.0%) (6). This discrepancy in clinical outcomes

suggests potential heterogeneity in treatment response among patients receiving IABP support.

The hemodynamic benefits of IABP are achieved through counterpulsation, which involves systolic unloading and diastolic augmentation. During systolic unloading, rapid balloon deflation just before systole (QRS-T interval) lowers peak systemic blood pressure, thereby decreasing left ventricular (LV) afterload. During diastolic augmentation, balloon inflation in diastole (T-P interval) enhances systemic diastolic blood pressure and coronary perfusion pressure (CPP). These IABP-induced pressure changes are fundamentally determined by aortic compliance, an index of arterial elastic properties, which can be approximated clinically by dividing stroke volume by pulse pressure. Aortic compliance decreases with age and the progression of cardiovascular disease, although it varies significantly among individuals (7). Prior studies suggest that lower compliance may amplify IABP-induced pressure changes (8, 9).

Despite its critical role in IABP hemodynamics, the influence of aortic compliance on IABP efficacy remains underexplored, with limited supporting clinical evidence. A better understanding of this relationship could explain the heterogeneous treatment responses and help optimize patient selection for IABP support. Here, we present a case that demonstrates the potential importance of aortic compliance in determining IABP effectiveness in an elderly patient with refractory cardiogenic shock.

Case description

An 80-year-old man with a history of hypertension and chronic kidney disease stage (CKD) 3b presented to the emergency department with generalized fatigue. His initial vital signs included a blood pressure (BP) of 109/49 mmHg and a heart rate (HR) of 77 beats per min. Despite receiving oxygen of 10 L/min via reservoir mask, he remained tachypneic with a respiratory rate of 28 breaths per min and hypoxic with an oxygen saturation of 89%. His body temperature was 36.2°C.

Physical examination revealed bilateral pulmonary crackles and a grade 4/6 systolic ejection murmur at the right second intercostal space. Additional findings included jugular vein distention, mild peripheral edema, and warm extremities. Laboratory results showed metabolic acidosis (pH 7.275, pCO_2 31.3 mmHg, HCO_3 14.1 mmol/L, lactate 3.3 mmol/L), hemoglobin 11.1 g/dl, white blood cell count of 9,590/μl, c-reactive protein concentration (CRP) of 2.23 mg/dl, and elevated B-type natriuretic peptide (BNP) at 4,301 pg/ml. Electrocardiography demonstrated sinus rhythm with T-wave inversion in the precordial and inferior leads. Chest radiograph showed increased pulmonary vascular markings and right lower lung field infiltration. Echocardiography revealed newly reduced LV ejection fraction (LVEF 30%, down from 60%) and severe aortic stenosis (AS) with a peak velocity of 4.4 m/s, mean pressure gradient of 50 mmHg, and an aortic valve area of 0.7 cm^2 as calculated using the continuity equation. Subsequent coronary angiography showed no significant coronary artery stenosis. Right heart catheterization showed a pulmonary capillary wedge pressure (PCWP) of 18 mmHg, pulmonary artery pressure (PAP) of 30/20 mmHg, right atrial pressure (RAP) of 7 mmHg, cardiac index (CI) of 1.91 L/min/m^2 obtained from thermodilution cardiac output, and systemic vascular resistance (SVR) of 1,548 dyne·s/cm^5. In this case, the estimated aortic compliance range was 0.62–0.81 ml/mmHg, calculated by dividing the stroke volume obtained from thermodilution cardiac output by pulse pressure. Given that the normal range is 1.2–2.4 ml/mmHg (8), these values indicate a substantial reduction in aortic compliance in this patient. During hospitalization, PCWP was estimated from diastolic PAP, which measured 20 mmHg and corresponded with the directly measured PCWP of 18 mmHg (10). Pulmonary vascular resistance (PVR) was calculated to be 133 dyne·s/cm^5, indicating no significant elevation.

The patient was diagnosed with Society for Cardiovascular Angiography and Interventions (SCAI) stage B cardiogenic shock complicated by severe respiratory failure with a PaO_2/FiO_2 (P/F) ratio of 76 mmHg due to pulmonary congestion and pneumonia. Initial management included invasive mechanical ventilation, hemodynamic support with dobutamine at 3 μg/kg/min and norepinephrine at 0.02 μg/kg/min, and antimicrobial therapy using ampicillin/sulbactam at 3 grams every 8 h. After 9 h, peripheral hypoperfusion improved (lactate 0.7 mmol/L); however, norepinephrine requirements increased, and elevated PCWP and low CI persisted. Following a heart team conference to discuss definitive treatment for severe AS, contrast-enhanced computed tomography was performed to assess candidacy for transcatheter aortic valve replacement (TAVR). Following the computer tomography scan, the patient developed progressive hypotension and peripheral hypoperfusion. Despite escalating vasopressor support (dobutamine at 3 μg/kg/min, norepinephrine at 0.2 μg/kg/min, vasopressin at 3 U/h, and epinephrine at 0.05 μg/kg/min), mean arterial pressure (MAP) remained at 51 mmHg. Peripheral hypoperfusion worsened (lactate increased from 0.7 to 3.8 mmol/L) and severe pulmonary congestion developed (P/F ratio declined from 186 to 84; PCWP increased from 16 to 41 mmHg) (Figure 1).

Given the refractory wet-cold profile based on the Nohria-Stevenson classification and SCAI stage D, tMCS was indicated. Upon arrival in the catheterization laboratory, MAP was stable at 51 mmHg. Considering the patient's advanced age and risk-benefit profile, IABP was selected as the initial support strategy. Intra-aortic balloon pump initiation resulted in immediate hemodynamic improvements, with MAP increasing from 51 to 63 mmHg and end-systolic pressure (ESP) decreasing from 49 to 45 mmHg (Figure 2). Pulmonary capillary wedge pressure decreased substantially from 41 to 21 mmHg. Cardiac index improved to 2.0 L/min/m^2, comparable to pre-deterioration values, demonstrating effective systolic unloading and diastolic augmentation.

At 18 h after post-IABP initiation, all vasopressors were successfully discontinued. Dobutamine was maintained at 3 μg/kg/min. Hemodynamics showed sustained improvement: MAP of 61 mmHg, HR of 64 bpm, PAP of 25/14 mmHg, right atrial pressure of 3 mmHg, CI of 2.4 L/min/m^2, and SVR of 1,221 dyne·s/cm^5 (Figure 1). The IABP was successfully removed

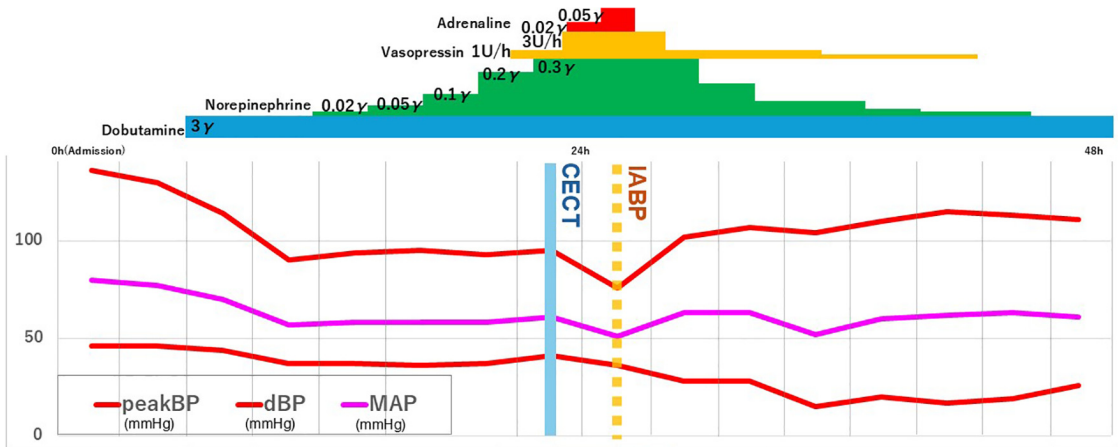

HR (bpm)	69	· · · ·	81	91	94	· · · · ·	64
MAP (mmHg)	70	· · · ·	61	51	63	· · · · ·	61
PCWP (mmHg)	18	· · · ·	19	41	21	· · · · ·	14
CI (L/min/m^2)	1.9	· · · ·	2.0	↓↓	2.0	· · · · ·	2.4
SV (mL)	45	· · · ·	39	↓↓	34	· · · · ·	59
SVR (dyne·sec/cm^5)	1548	· · · ·	1340	↑	1325	· · · · ·	1221
Lactate (mmol/L)	1.0	· · · ·	1.9	3.8	1.4	· · · · ·	0.7

FIGURE 1
The hemodynamic course over the first 48 h following admission. Following contrast-enhanced computed tomography, further hemodynamic deterioration was observed, necessitating increased catecholamine doses. Directional arrows (↓↓severe reduction, ↑elevation) indicate clinical trajectory based on physical examination and available pressure data. However, significant improvement was achieved with the initiation of IABP. CECT, contrast-enhanced computed tomography; CI, cardiac index; dBP, diastolic blood pressure; HR, heart rate; MAP, mean arterial pressure; PCWP, pulmonary capillary wedge pressure; peakBP, peak blood pressure; SV, stroke volume; SVR, systemic vascular resistance.

	Pre – IABP	Post - IABP
Aortic Pressure Waveform	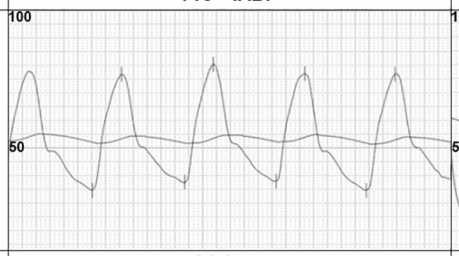	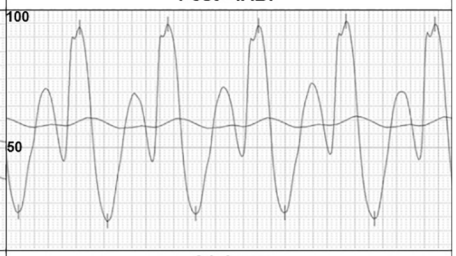
HR	91 bpm	94 bpm
ABP (s/d/m)	77/35/51 mmHg	96/27/63 mmHg
Augmentation pressure	-	96 mmHg
End systolic pressure	49 mmHg	45 mmHg
PCWP	41 mmHg	21 mmHg
RAP	11 mmHg	10 mmHg
Cardiac Index	↓↓	2.0 L/min/m^2
Stroke Volume	↓↓	34 mL
SVR	↑	1325 dyne·sec/cm^5
Ea	↑	1.32 mmHg/mL

FIGURE 2
Hemodynamic changes before and after IABP initiation. The initiation of IABP resulted in a rapid increase in blood pressure and a significant reduction in PCWP. The middle line in the aortic pressure waveform represents mean arterial pressure. Directional arrows are as described in Figure 1. ABP (s/d/m), arterial blood pressure (systolic/diastolic/mean); Ea, effective arterial elastance; HR, heart rate; PCWP, pulmonary capillary wedge pressure; RAP, right atrial pressure; SVR, systemic vascular resistance.

after 52 h of support. On hospital day 8, the patient underwent uncomplicated trans-femoral TAVR under strict infection precautions. Following TAVR, dobutamine was weaned, and guideline-directed medical therapy was initiated. A pre-discharge echocardiography revealed improvement in LVEF from 30% to 44%. The patient was discharged to rehabilitation on postoperative day 24 and maintains function mobility during ongoing outpatient follow-up.

Discussion

We describe an elderly patient with severe AS and pneumonia who developed refractory SCAI stage D cardiogenic shock despite multiple vasopressors. The patient exhibited low aortic compliance (0.62–0.81 ml/mmHg) and demonstrated notable hemodynamic improvement following IABP support. Previous observational studies have characterized potential IABP responders in hypoperfused acute decompensated heart failure as those with elevated SVR, isolated LV or biventricular dysfunction, pulmonary congestion, and absence of excessive tachycardia (11–13). Although our patient exhibited several of these favorable characteristics, importantly, the shock had progressed to SCAI stage D, where IABP is generally considered insufficient (14, 15). Nevertheless, the immediate and substantial improvement in both hypoperfusion and pulmonary congestion led us to consider the role of the patient's low aortic compliance as a potential determinant of IABP efficacy, particularly in older adult patients.

The hemodynamic effects of IABP fundamentally depend on the interaction between balloon inflation/deflation and the mechanical properties of the arterial system (8). Aortic compliance is a major determinant of the degree of systolic unloading and diastolic augmentation. During diastole, the lower the compliance, the greater the increase in diastolic augmentation pressure. This effect contributes to an increase in MAP and CPP, thereby improving peripheral hypoperfusion and coronary blood flow. During systole, the lower the compliance, the greater the decrease in ESP. This, in turn, leads to a greater reduction in LV afterload, which results in an increase in stroke volume and a decrease in PCWP.

Previous studies have demonstrated that lower aortic compliance amplifies the hemodynamic effects of IABP, as pressure changes are determined by the ratio of balloon volume to aortic compliance. Papaioannou et al. demonstrated greater pressure augmentation with decreased compliance *in vitro* (8), and observed similar findings in patients with AMICS (9). Although low aortic compliance is generally considered disadvantageous in cardiovascular disease (16), it may enhance IABP effectiveness throughout the cardiac cycle. While this physiological relationship has been shown, our case uniquely demonstrates its clinical significance in SCAI stage D shock. This observation suggests that aortic compliance assessment might help identify patients who could benefit from IABP support, even in refractory cardiogenic shock.

In our case, the patient exhibited lower-than-normal aortic compliance (0.62–0.81 ml/mmHg) during the acute phase. Intra-aortic balloon pump support resulted in immediate hemodynamic improvement as evidenced by increased diastolic augmentation without increasing afterload (MAP rising from 51 to 63 mmHg and lactate levels decreasing from 3.8 to 1.4 mmol/L). Additionally, ESP decreased from 49 to 45 mmHg), and pulmonary congestion improved (PCWP reduced from 41 to 21 mmHg). Given the reduced LVEF (30%), this enhanced afterload reduction was particularly effective in improving stroke volume and reducing PCWP, consistent with previously reported benefits of afterload reduction in severe AS with LV dysfunction (17). The benefits of IABP-mediated afterload reduction specifically in patients with severe AS have been previously demonstrated (18). In addition, the enhanced CPP (increased from 35 to 96 mmHg) (19) may have contributed to LV systolic functional recovery through improved coronary perfusion in severe AS with impaired coronary microcirculation (20). Figure 3 shows the hemodynamic effects of IABP in our patient with low aortic compliance.

Sustained hemodynamic improvements were observed at 24 h post-initiation (MAP: 64 mmHg, lactate: 0.7 mmol/L, CI: 2.4 L/min/m^2, and PCWP: 14 mmHg), facilitating rapid withdrawal of catecholamines and suggesting improved LV function.

Finally, compared to pVADs and VA-ECMO, IABP use has been associated with significantly lower rates of adverse events such as bleeding, stroke, acute kidney injury, limb ischemia, hemolysis, and sepsis, partly due to its smaller sheath size (7.5 Fr to 8 Fr) (21). Given that tMCS-related complications are associated with poor prognosis (21), IABP may be a preferable option when sufficient hemodynamic improvement is anticipated with this less invasive approach, as demonstrated in our case where successful circulatory support was achieved without MCS-related complications. Therefore, this case highlights aortic compliance as a potential key predictor of IABP efficacy, particularly in older adult patients at high risk for tMCS-related complications.

Limitations

Several important limitations should be noted. First, although we observed significant hemodynamic improvement with IABP, we could not directly evaluate changes in myocardial contractility during the period when the patient was deteriorating. Second, although we observed enhanced CPP following IABP support, we could not definitively attribute the improved LV function to recovery from myocardial ischemia, as there were no ischemic electrocardiogram changes before or after IABP insertion. Third, this is a single case observation, and the relationship between aortic compliance and IABP efficacy requires validation in larger studies including comparisons with other tMCS devices. Fourth, while our findings suggest a relationship between low aortic compliance and an enhanced IABP response, we acknowledge that multiple conditions, including severe AS, reduced LV function, and pneumonia, may have created hemodynamics interactions that prevent attributing the observed IABP benefits solely to aortic compliance. Finally, the potential increased risk of vascular complications such as limb ischemia and peripheral embolization in patients with low aortic compliance needs to be

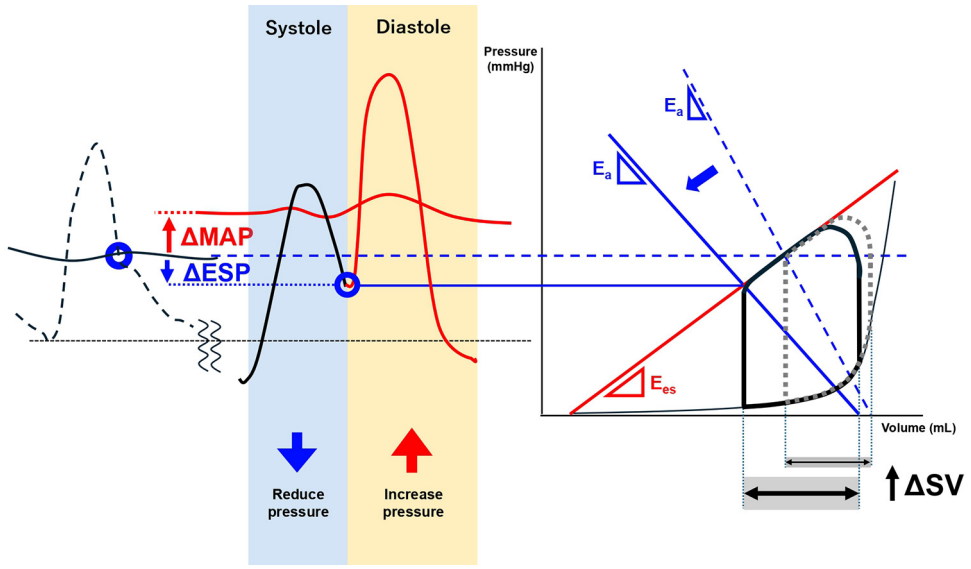

FIGURE 3
Hemodynamic effects of IABP in A patient with Low aortic compliance. This figure illustrates the hemodynamic changes induced by intra-aortic balloon pump (IABP) support in a patient with low aortic compliance, severe aortic stenosis, and left ventricular dysfunction. The dotted line (...) represents the state before IABP insertion, while the solid line (—) represents the state after IABP insertion. The pressure-dynamic effects of IABP are achieved through balloon deflation just before systole (systolic unloading), which lowers end-systolic pressure (Ea), increases stroke volume, and reduces left ventricular end-diastolic pressure, as shown in the pressure-volume (PV) loop on the right. These effects improve ventriculo-arterial coupling through reduced Ea, which is particularly beneficial in the presence of impaired contractility (Ees). During diastole, balloon inflation (diastolic augmentation) increases augmentation pressure without imposing additional left ventricular afterload, thereby enhancing coronary perfusion pressure and maintaining or increasing mean arterial pressure, as shown in the pressure waveform on the left. The pressure changes become greater as compliance decreases, resulting in enhanced hemodynamic response. Ea, effective arterial elastance; Ees, end-systolic elastance; ESP, end-systolic pressure; MAP, mean arterial pressure; SV, stroke volume. Ea represents left ventricular afterload. Ees represents left ventricular contractility.

evaluated, as reduced compliance often reflects underlying arterial disease and poor vascular integrity.

Conclusion

This case demonstrates successful management of an older adult with SCAI stage D cardiogenic shock with IABP support in the context of low aortic compliance. Our findings suggest that aortic compliance might be a key determinant of IABP efficacy and could potentially guide patient selection for this less invasive tMCS approach.

Data availability statement

The original contributions presented in the study are included in the article/Supplementary Material, further inquiries can be directed to the corresponding author.

Ethics statement

Written informed consent was obtained from the individual(s) for the publication of any potentially identifiable images or data included in this article.

Author contributions

IO: Writing – original draft. KenS: Writing – original draft, Writing – review & editing. KeiS: Supervision, Writing – review & editing. TN: Supervision, Writing – review & editing.

Funding

The author(s) declare that no financial support was received for the research and/or publication of this article.

Conflict of interest

KS received research funding from Abiomed Inc., NTT Research, Inc., Asahi Kasei ZOLL Medical Corporation, Neuroceuticals Inc., and Zeon Medical Inc., and honoraria from Abiomed Japan K.K. and Mallinckrodt Pharma K.K.

The remaining authors declare that the research was conducted in the absence of any commercial or financial relationships that could be construed as a potential conflict of interest.

Generative AI statement

The author(s) declare that no Generative AI was used in the creation of this manuscript.

Publisher's note

All claims expressed in this article are solely those of the authors and do not necessarily represent those of their affiliated organizations, or those of the publisher, the editors and the reviewers. Any product that may be evaluated in this article, or claim that may be made by its manufacturer, is not guaranteed or endorsed by the publisher.

Supplementary material

The Supplementary Material for this article can be found online at: https://www.frontiersin.org/articles/10.3389/fcvm.2025.1587383/full#supplementary-material

References

1. Thiele H, Zeymer U, Neumann FJ, Ferenc M, Olbrich HG, Hausleiter J, et al. Intraaortic balloon support for myocardial infarction with cardiogenic shock. *N Engl J Med*. (2012) 367:1287–96. doi: 10.1056/NEJMoa1208410

2. Miller PE, Bromfield SG, Ma Q, Crawford G, Whitney J, DeVries A, et al. Clinical outcomes and cost associated with an intravascular microaxial left ventricular assist device vs intra-aortic balloon pump in patients presenting with acute myocardial infarction complicated by cardiogenic shock. *JAMA Intern Med*. (2022) 182:926–33. doi: 10.1001/jamainternmed.2022.2735

3. Schrage B, Ibrahim K, Loehn T, Werner N, Sinning JM, Pappalardo F, et al. Impella support for acute myocardial infarction complicated by cardiogenic shock. *Circulation*. (2019) 139:1249–58. doi: 10.1161/CIRCULATIONAHA.118.036614

4. Ouweneel DM, Eriksen E, Sjauw KD, van Dongen IM, Hirsch A, Packer EJS, et al. Percutaneous mechanical circulatory support versus intra-aortic balloon pump in cardiogenic shock after acute myocardial infarction. *J Am Coll Cardiol*. (2017) 69:278–87. doi: 10.1016/j.jacc.2016.10.022

5. Watanabe A, Miyamoto Y, Ueyama H, Gotanda H, Tsugawa Y, Kuno T. Percutaneous microaxial ventricular assist device versus intra-aortic balloon pump for nonacute myocardial infarction cardiogenic shock. *J Am Heart Assoc*. (2024) 13: e034645. doi: 10.1161/JAHA.123.034645

6. Nishimoto Y, Ohbe H, Matsui H, Nakata J, Takiguchi T, Nakajima M, et al. Trends in mechanical circulatory support use and outcomes of patients with cardiogenic shock in Japan, 2010 to 2020 (from a nationwide inpatient database study). *Am J Cardiol*. (2023) 203:203–11. doi: 10.1016/j.amjcard.2023.06.082

7. Chirinos JA, Segers P, Hughes T, Townsend R. Large-Artery stiffness in health and disease: JACC state-of-the-art review. *J Am Coll Cardiol*. (2019) 74(9):1237–63. doi: 10.1016/j.jacc.2019.07.012

8. Papaioannou TG, Mathioulakis DS, Nanas JN, Tsangaris SG, Stamatelopoulos SF, Moulopoulos SD. Arterial compliance is a main variable determining the effectiveness of intra-aortic balloon counterpulsation: quantitative data from an *in vitro* study. *Med Eng Phys*. (2002) 24:279–84. doi: 10.1016/s1350-4533(02)00013-9

9. Papaioannou TG, Mathioulakis DS, Stamatelopoulos KS, Gialafos EJ, Lekakis JP, Nanas J, et al. New aspects on the role of blood pressure and arterial stiffness in mechanical assistance by intra-aortic balloon pump: *in vitro* data and their application in clinical practice. *Artif Organs*. (2004) 28:717–27. doi: 10.1111/j.1525-1594.2004.00080.x

10. Lappas D, Lell WA, Gabel JC, Civetta JM, Lowenstein E. Indirect measurement of left-atrial pressure in surgical patients—pulmonary-capillary wedge and pulmonary-artery diastolic pressures compared with left-atrial pressure. *Anesthesiology*. (1973) 38:394–7. doi: 10.1097/00000542-197304000-00017

11. Scheidt S, Wilner G, Mueller H, Summers D, Lesch M, Wolff G, et al. Intra-aortic balloon counterpulsation in cardiogenic shock. Report of a co-operative clinical trial. *N Engl J Med*. (1973) 288:979–84. doi: 10.1056/NEJM197305102881901

12. Annamalai SK, Buiten L, Esposito ML, Paruchuri V, Mullin A, Breton C, et al. Acute hemodynamic effects of intra-aortic balloon counterpulsation pumps in advanced heart failure. *J Card Fail*. (2017) 23:606–14. doi: 10.1016/j.cardfail.2017.05.015

13. Sintek MA, Gdowski M, Lindman BR, Nassif M, Lavine KJ, Novak E, et al. Intra-aortic balloon counterpulsation in patients with chronic heart failure and cardiogenic shock: clinical response and predictors of stabilization. *J Card Fail*. (2015) 21:868–76. doi: 10.1016/j.cardfail.2015.06.383

14. Mehta A, Vavilin I, Nguyen AH, Batchelor WB, Blumer V, Cilia L, et al. Contemporary approach to cardiogenic shock care: a state-of-the-art review. *Front Cardiovasc Med*. (2024) 11:1354158. doi: 10.3389/fcvm.2024.1354158

15. Luo D, Huang R, Wang X, Zhang J, Cai X, Liu F, et al. Intra-aortic balloon pump reduces 30-day mortality in early-stage cardiogenic shock complicating acute myocardial infarction according to scai classification. *Shock*. (2023) 60(3):385–91. doi: 10.1097/SHK.0000000000002184

16. Lilly SM, Jacobs D, Bluemke DA, Duprez D, Zamani P, Chirinos J. Resistive and pulsatile arterial hemodynamics and cardiovascular events: the multiethnic study of atherosclerosis. *J Am Heart Assoc*. (2014) 3:e001223. doi: 10.1161/JAHA.114.001223

17. Khot UN, Novaro GM, Popović ZB, Mills RM, Thomas JD, Tuzcu EM, et al. Nitroprusside in critically ill patients with left ventricular dysfunction and aortic stenosis. *N Engl J Med*. (2003) 348:1756–63. doi: 10.1056/NEJMoa022021

18. Aksoy O, Yousefzai R, Singh D, Agarwal S, O'Brien B, Griffin BP, et al. Cardiogenic shock in the setting of severe aortic stenosis: role of intra-aortic balloon pump support. *Heart*. (2011) 97(10):838–43. doi: 10.1136/hrt.2010.206367

19. Sorcher JL, Santos PT, Adams S, Kulikowicz E, Vaidya D, Lee JK, et al. Association of diastolic blood pressure with coronary perfusion pressure during resuscitation in pediatric swine. *Pediatr Res*. (2025) 97:827–34. doi: 10.1038/s41390-024-03308-y

20. McConkey HZR, Marber M, Chiribiri A, Pibarot P, Redwood SR, Prendergast BD. Coronary microcirculation in aortic stenosis. *Circ Cardiovasc Interv*. (2019) 12: e007547. doi: 10.1161/CIRCINTERVENTIONS.118.007547

21. Kapur NK, Whitehead EH, Thayer KL, Pahuja M. The science of safety: complications associated with the use of mechanical circulatory support in cardiogenic shock and best practices to maximize safety. *F1000Res*. (2020) 9:F1000 Faculty Rev-794. doi: 10.12688/f1000research.25518.1.eCollection

Frontiers in
Cardiovascular Medicine

Innovations and improvements in cardiovascular treatment and practice

Focuses on research that challenges the status quo of cardiovascular care, or facilitates the translation of advances into new therapies and diagnostic tools.

Discover the latest Research Topics

See more →

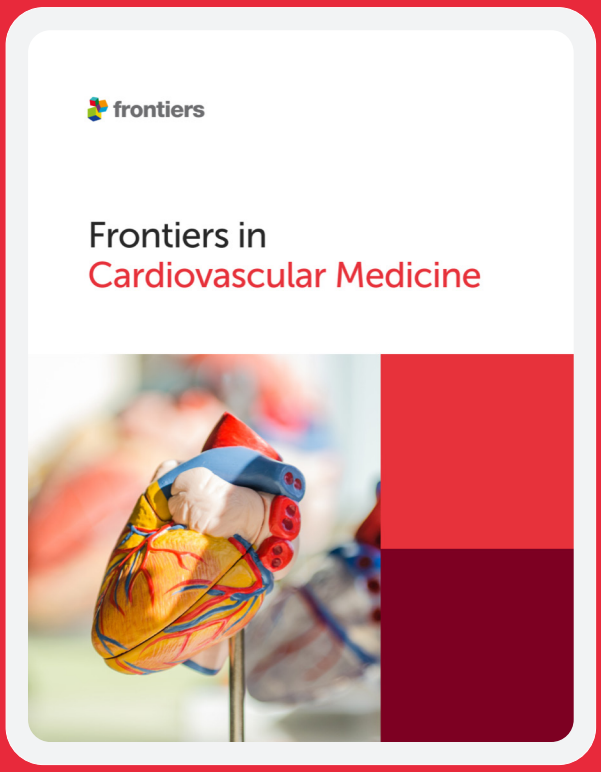

Frontiers

Avenue du Tribunal-Fédéral 34
1005 Lausanne, Switzerland
frontiersin.org

Contact us

+41 (0)21 510 17 00
frontiersin.org/about/contact